

The Connectivity of the Mammalian Prefrontal Cortex

Stacey Ann Bedwell

A thesis submitted in partial fulfillment of the requirements of
Nottingham Trent University for the degree of Doctor of
Philosophy

April 2015

This work is the intellectual property of the author. You may copy up to 5% of this work for private study, or personal, non-commercial research. Any re-use of the information contained within this document should be fully referenced, quoting the author, title, university, degree level and pagination. Queries or requests for any other use, or if a more substantial copy is required, should be directed in the owner(s) of the Intellectual Property Rights.

Acknowledgements

I would like to thank my supervisory team, Dr. Chris Tinsley, Dr. Jonathan Crofts and Prof. Ellen Billett, for their guidance and supervision throughout my PhD. I would also like to thank Andy Marr and Danielle McDonald for their assistance in the biomedical services facility. Finally, my gratitude goes to my fellow PhD students and family for their support and encouragement.

Table of Contents

Table of figures.....	6
List of Abbreviations	17
Abstract.....	18
Chapter 1: Introduction	20
1 Prefrontal cortex.....	20
2 Function	22
3 Structure.....	25
4 Organisation.....	27
5 Connectivity.....	31
6 Aims.....	37
Chapter 2: Organisation of Prefrontal Cortex – Temporal Cortex Connections .	39
2.1 Introduction.....	39
2.2 Aims.....	39
2.3 Methodology.....	40
2.4 Results.....	45
2.5 Discussion.....	55
Chapter 3: Organisation of Connections to Temporal Cortex from Anterior, Central and Posterior Prefrontal Cortex.....	59
3.1 Introduction.....	59
3.2 Aims.....	60
3.3 Methodology.....	60
3.4 Results.....	63
3.5 Discussion.....	92
Chapter 4: The Fine Scale Organisation of Prefrontal Cortex – Temporal Cortex Connections	96
4.1 Introduction.....	96
4.2 Aims.....	97
4.3 Methodology.....	97
4.4 Results.....	100
4.5 Discussion.....	108
Chapter 5: Organisation of Prefrontal Cortex – Sensory-Motor Cortex Connections	117
5.1 Introduction.....	117
5.2 Aims.....	118
5.3 Methodology.....	118
5.4 Results.....	122
5.5 Discussion.....	133
Chapter 6: Organisation of Connections to Sensory-Motor Cortex from Anterior, Central and Posterior Prefrontal Cortex.....	139
6.1 Introduction.....	139
6.2 Aims.....	140
6.3 Methodology.....	140
6.4 Results.....	142
6.5 Discussion.....	171

Chapter 7: The Fine Scale Organisation of Prefrontal Cortex – Sensory-Motor Cortex Connections.....	177
7.1 Introduction.....	177
7.2 Aims.....	178
7.3 Methodology.....	179
7.4 Results.....	181
7.5 Discussion.....	190
Chapter 8: The Organisation of Frontal Association Cortex - Temporal Cortex Connections	200
8.1 Introduction.....	200
8.2 Aims.....	201
8.3 Methodology.....	201
8.4 Results.....	204
8.5 Discussion.....	213
Chapter 9: Discussion.....	217
9.1 Organisation of Prefrontal Cortex – Temporal Cortex Connections.....	217
9.2 Organisation of Prefrontal Cortex – Sensory-Motor Cortex Connections.....	220
9.3 Organisation of Frontal Association Cortex – Temporal Cortex Connections.....	223
9.4 Conclusions.....	223
References.....	225
Appendices.....	237
Table of Contents	233
Table of Figures	238
Appendix A: Preliminary Experiments.....	242
Appendix B: Organisation of Prefrontal Cortex – Temporal Cortex Connections, Resultant from Separate Retrograde and Anterograde Injections	248
Appendix C: Hemispheric Effect of Injection Site and Resultant Labelling in Temporal Cortex.....	254
Appendix D: Anterograde Properties of Biotinylated Dextran Amines (BDA)	256
Appendix E: Comparison of Labelling in Temporal Cortex from Single and Co-injections of Fluoro-Gold and BDA	257
Appendix F: Analysis of Biotinylated Dextran Amine Labelling using Darkfield Microscopy.....	258
Appendix G: Anterograde properties of Fluoro-Ruby.....	262
Appendix H: Statistical Evidence for Organisation of Input and Output Connections Resultant from Separate Injections of Fluoro-Gold and Fluoro-Ruby in Central Prefrontal Cortex.....	269
Appendix I: Labelling in Temporal Cortex from Co-injection of Retrograde (Fluoro-Gold) and Anterograde (Fluoro-Ruby) Tracers in Central Prefrontal Cortex	271
Appendix J: Organisation of Connections from Central Prefrontal Cortex – Temporal Cortex, using Fluoro-Gold and Fluoro-Emerald.....	276
Appendix K: Statistical Comparison Between Central Prefrontal Cortex Connections to Temporal Cortex using BDA & Fluoro-Gold and Fluoro-Ruby & Fluoro-Gold.....	279
Appendix L: Preliminary Small (20-30nl) Tracer Injection Volumes	280
Appendix M: Organisation of Connections from Prefrontal Cortex - Sensory-Motor Cortex Resultant from Separate Injections of Fluoro-Gold (100nl) and BDA (100nl).....	282
Appendix N: Hemispheric Effect of Injection Site and Resultant Labelling in Sensory-Motor Cortex.....	289
Appendix O: Comparison of Labelling in Sensory-Motor Cortex from Single and Co-injections of Fluoro-Gold and BDA.....	291

Appendix P: Statistical Evidence for Organisation of Input and Output Connections Resultant from Separate Injections of Fluoro-Gold and Fluoro-Ruby in Central Prefrontal Cortex.....	292
Appendix Q: Labelling in Sensory-Motor Cortex from Co-injection of Retrograde (Fluoro-Gold) and Anterograde (Fluoro-Ruby) Tracers in Central Prefrontal Cortex.....	294
Appendix R: Statistical Comparison between Central Prefrontal cortex connections to Sensory-Motor Cortex using BDA & Fluoro-Gold and Fluoro-Ruby & Fluoro-Gold	298
Published Articles	299

Table of Figures

Figure 1.1. Coronal sections showing the cytoarchitectural sub-divisions of PFC in (i) rats, according to Van de Werd & Uylings (2008) and (ii) humans, according to Ongur et al (2003) 22

Figure 2.1. Coronal section of PFC (A-P 4.2mm from Bregma) showing the cytoarchitectural boundaries of PFC sub-regions according to Van de Werd & Uylings (2008), depicting sites of tracer injections; Prelimbic (PL):A, ventral orbital (VO):B, ventrolateral orbital(VLO):C and dorsolateral orbital(DLO):D, with 1mm separation.42

Figure 2.2. (A) Coronal cross section of temporal cortex at -3.3mm posterior to bregma, depicting the three dimensions in which the locations of labelled cells were recorded (Anterior-Posterior (A-P), Medial-Lateral (M-L) and Dorsal-Ventral (D-V)). (B) Retrogradely labelled cells (blue cells) in temporal cortex produced by an injection of Fluoro-Gold (100nl) into VO. Arrows indicate measurements of labelled cell location in the medial-lateral dimension (distance to lateral cortical surface) and dorsal-ventral dimension (distance from rhinal sulcus). (C) Anterogradely labelled area (Brown) in temporal cortex produced by an injection of BDA (100nl) into PL. Crosses indicate the four points on the perimeter at which measurements were taken. Arrows indicate measurements of labelled area location in the medial-lateral dimension (distance to lateral cortical surface) and dorsal-ventral dimension (distance from rhinal sulcus). Scale bars = 200µm.....44

Figure 2.3. (i) Coronal section of PFC showing location and spread of (100nl) Fluoro- Gold and (100nl) Fluorescein at injection site in VO. (ii) Coronal section of PFC showing location and spread of (100nl) Fluoro-Gold and (100nl) Fluorescein at injection site in DLO. (iii) Representations of Fluoro-Gold and Fluorescein co- injection site in VLO (R41) in the right hemisphere. (iv) Representations of Fluoro- Gold and Fluorescein co-injection sites in PL (R42), VO (R37), and DLO (R38) in the left hemisphere.. Scale bars = 200µm.46

Figure 2.4. Diagram representing the amalgamated dual-injection sites of Fluoro-Gold and BDA, and the projection sites in temporal cortex for both retrograde (Fluoro- Gold) and anterograde (BDA) tracer injections from 4 rats. (i) The locations of injection sites A (PL: R42), B (VO: R37), C (VLO:R41) and D (DLO:R38) in PFC. (ii) The locations of retrogradely labelled cells in temporal cortex, resultant from 100nl Fluoro-Gold injections into PFC sites A-D (R37, R38, R41, R42). (iii) The locations of anterogradely labelled areas in temporal cortex, resultant from 100nl BDA (Fluorescein) injections into PFC sites A-D (R37, R38, R41, R42).48

Figure 2.5. (i) Coronal section of temporal cortex showing retrogradely labelled cells (Fluoro-Gold, blue) resultant from co-injection of Fluoro-Gold and BDA (Fluorescein) into DLO. (ii) Retrogradely labelled cells in temporal cortex (blue, Fluoro-Gold) resultant from co-injection of Fluoro-Gold and BDA (Fluorescein) into DLO. (iii) Coronal section of temporal cortex showing area of anterogradely labelled axon terminals (brown, BDA) resultant from co-injection of BDA and Fluoro-Gold into VLO (injection C). Scale bars = 200µm. (iv) Anterograde labelling of axon terminals (green) resultant from co-injection of BDA and Fluoro-Gold into DLO Scale bar = 100µm.....50

Figure. 2.6. The mean effect of injection site on the (i) dorsal-ventral ,(ii) anterior- posterior and (iii) medial-lateral location of retrogradely labelled cells (n=425 arising from 4 rats: PL=77, VO=160, VLO=89, DLO=99 (cases R37, R38, R41, R42)) and anterogradely labelled areas (n=40 arising from 4 rats: PL=12, VO=12, VLO=12, DLO=4 (cases R37, R38, R41, R42)) within temporal cortex. Error bars = standard error. (iv) Coronal cross section of PFC showing the position of 4 injection sites; PL (A), VO (B), VLO (C) and DLO (D). Coronal cross section of temporal cortex showing the three dimensions in which the locations of labels were recorded.53

Figure 2.7. The effect of PFC injection site (PL:A, VO:B, VLO:C, DLO:D) on the three dimensional mean location of retrogradely labelled cells (blue) and anterogradely labelled areas (red) in temporal cortex. Error bars = standard error.54

Figure 3.1. Coronal sections of PFC ((i) A-P 4.7mm , (ii) 3.7mm and (iii) 4.2mm from Bregma) showing the cytoarchitectural boundaries of PFC sub-regions according to Van de Werd & Uylings (2008), depicting sites of tracer injections; PL (Aa, A, Ap), VO (Ba, B, Bp), VLO (Ca, C, Cp) and DLO (Da, D, Dp), with 1mm separation.61

Figure 3.2. (i) Confocal image of temporal cortex showing Fluoro-Ruby labelling (red) and Fluorescein labeled alpha tubulin (green) resultant from Fluoro-Ruby (100nl) injection into DLO (R39). (ii) Confocal image of temporal cortex showing Fluoro-Ruby labelling (red) and Fluorescein labeled alpha tubulin (green) resultant from Fluoro-Ruby (100nl) injection into (R39). Note that Fluororuby occurs both separate to and in the same place as Fluorescein, with the majority of cases being separate (anterograde). Scale bars = 20 µm.62

Figure 3.3. (i) Coronal section of anterior PFC (AP 4.7mm from Bregma) showing the cytoarchitectural boundaries of the prelimbic (PL), medial orbital (MO), ventral orbital (VO), ventrolateral orbital (VLO), lateral orbital (LO) and dorsolateral orbital (DLO) cortices (according to Van de Werd & Uylings, 2008), depicting sites of injections; Prelimbic: Aa, Ventral orbital: Ba, Ventrolateral orbital: Ca and dorsolateral orbital: Da, with 1mm spread. (ii) Coronal section of prefrontal cortex showing location and spread of (100nl) Fluoro-Gold at injection site in VO (R24). (iii) Coronal section of prefrontal cortex showing location and spread of (100nl) Fluoro-Ruby at injection site in PL (R32). (iv) Representations of Fluoro-Ruby (100nl) (R21, R23, R24, R32 (broken line)) injection sites in PL (R32), VO (R23), VLO (R21) and DLO (R24) in the right hemisphere. (v) Representations of Fluoro-Gold (100nl) (R17, R23, R24, R28 (solid line)) injection sites in PL (R28), VO (R24), VLO (R17) and DLO (R23) in the left hemisphere. Fluoro-Ruby injection sites were predominantly within the boundaries of Fluoro-Gold injection sites. There is minimal overlap between Fluoro-Gold injection sites (R28 & R24, R24 & R17). Fluoro-Gold and Fluoro-Ruby injection sites are mostly limited to the cytoarchitectural boundaries of PFC regions, and span the majority of the region (PL, VO/MO, VLO, DLO), injections into VO spread into MO. Scale bars = 100µm.65

Figure 3.4. Diagram representing the injection sites of Fluoro-Gold and Fluoro-Ruby, and the projection sites to temporal cortex for both retrograde (Fluoro-Gold) and anterograde (Fluoro-Ruby) tracer injections. (i) The locations of injection sites Aa (PL: R28, R32), Ba (R23, R24), Ca (R17, R21) and Da (R23, R24) in anterior PFC. (ii) The locations of retrogradely labeled cells in temporal cortex, resultant from 100nl Fluoro-Gold injections into anterior PFC injection sites Aa-Da (R17, R23, R24, R28). (iii) The locations of anterogradely labeled axon terminals in temporal cortex, resultant from 100nl Fluoro-Ruby injections into anterior PFC injection sites Aa-Da (R21, R23, R24, R32).67

Figure 3.5. (i) Coronal section showing retrogradely labeled cells (blue) in temporal cortex produced by injection of Fluoro-Gold (100nl) into VO (R24). (ii) Coronal section showing retrogradely labeled cells (blue) in temporal cortex produced by injection of Fluoro-Gold into DLO (R23). (iii) Retrogradely labeled cells (blue) in temporal cortex. (iv) Coronal section showing anterogradely labeled axon terminals (red) in temporal cortex produced by injection of Fluoro-Ruby (100nl) into DLO (R24). (v) Coronal section showing anterogradely labeled axon terminals (red) in temporal cortex produced by injection of Fluoro-Ruby (100nl) into VLO (R21). (vi) Anterograde labelling (red) in temporal cortex. Scale bars = 100µm.69

Figure 3.6. The mean effect of injection site in anterior PFC on the (i) dorsal-ventral, (ii) anterior-posterior and (iii) medial-lateral location of retrogradely labelled cells (n=578 arising from 4 rats: PL=75, VO=102, VLO=334, DLO=67) and anterogradely labelled axon terminals (n=220 arising from 4 rats: PL=47, VO=29, VLO=113, DLO=31) within temporal cortex. Error bars = standard error. (iv) Coronal cross section of PFC showing the position of 4 injection sites; Prelimbic (Aa), Ventral orbital (Ba), Ventrolateral orbital (Ca) and Dorsolateral orbital (Da). Coronal cross section of temporal cortex showing the three dimensions in which the locations of labels were recorded.71

Figure 3.7 (i) Coronal section of PFC (AP 4.2mm from Bregma) showing the cytoarchitectural boundaries of the prelimbic (PL), infralimbic (IL), medial orbital (MO), ventral orbital (VO), ventrolateral orbital (VLO) and dorsolateral orbital (DLO) cortices (according to Van de Werd & Uylings, 2008), depicting sites of injections; prelimbic:A, ventral orbital:B, ventrolateral orbital:C and dorsolateral orbital:D, with 1mm spread. (ii) Coronal section of prefrontal cortex

showing location and spread of (100nl) Fluoro-Gold (blue) at injection site in VO. (iii) Coronal section of prefrontal cortex showing location and spread of (100nl) Fluoro-Ruby (red) at injection site in VLO. (iv) Representations of Fluoro-Gold (100nl) (R4, R5, R6, R7 (solid line)) and Fluoro-Ruby (100nl) (R9, R19, R20, R29 (broken line)) injection sites in PL (R7, R29), VO (R6, R20), VLO (R4, R9) and DLO (R5, R19), in the right hemisphere. Scale bars = 100µm. 73

Figure 3.8. Diagram representing the injection sites of Fluoro-Gold and Fluoro-Ruby, and the projection sites to temporal cortex for both retrograde (Fluoro-Gold) and anterograde (Fluoro-Ruby) tracer injections. (i) The locations of injection sites A (PL: R7, R29), B (VO:R6, R20), C (VLO:R4, R9) and D (DLO: R5, R19) in central PFC. (ii) The locations of retrogradely labeled cells in temporal cortex, resultant from 100nl Fluoro-Gold injections into central PFC injection sites A-D (R4, R5, R6, R7). (iii) The locations of anterogradely labeled axon terminals in temporal cortex, resultant from 100nl Fluoro-Ruby injections into central PFC injection sites A-D (R9, R19, R20, R29). 75

Figure 3.9. (i) Coronal section showing retrogradely labelled cells (blue) in temporal cortex produced by injection of Fluoro-Gold (100nl) into VO (R6). (ii) Coronal section showing retrogradely labelled cells (blue) in temporal cortex produced by injection of Fluoro-Gold (100nl) into DLO (R5). (iii) Retrogradely labelled cells in temporal cortex produced by injection of Fluoro-Gold (100nl) into DLO (R5). (iv) Coronal section showing anterogradely labelled axon terminals (red) in temporal cortex produced by injection of Fluoro-Ruby into VO (R20). (v) Anterogradely labelled axon terminals in temporal cortex produced by injection of Fluoro-Ruby into VLO (R9). (vi) Anterogradely labelled axon terminals in temporal cortex produced by injection of Fluoro-Ruby into PL (R29). Arrows denote the location of the rhinal sulcus. Scales bars = 100µm 77

Figure 3.10. The mean effect of central PFC injection site on the (i) dorsal-ventral, (ii) anterior-posterior and (iii) medial-lateral location of retrogradely labelled cells (n=1412 arising from 4 rats: PL=253, VO=677, VLO=131, DLO=351) and anterogradely labelled axon terminals (n=444 arising from 4 rats: PL=63, VO=144, VLO=97, DLO=140) within temporal cortex. Error bars=standard error. (iv) Coronal cross section of prefrontal cortex showing the position of 4 injection sites; prelimbic (A), ventral-orbital (B), ventrolateral orbital (C) and dorsolateral orbital (D). Coronal cross section of temporal cortex showing the three dimensions in which the locations of labels were recorded..... 78

Figure 3.11 (i) Coronal section of PFC (AP 3.7mm from Bregma) showing the cytoarchitectural boundaries of the prelimbic (PL), infralimbic (IL), ventral orbital (VO) ventrolateral orbital (VLO) and dorsolateral orbital (DLO) cortices (according to Van de Werd & Uylings, 2008), depicting sites of injections; Prelimbic: Ap, Ventral orbital: Bp, Ventrolateral orbital: Cp and Dorsolateral orbital: Dp, with 1mm spread. (ii) Coronal section of prefrontal cortex showing location and spread of (100nl) Fluoro-Gold (blue) at injection site in PL (R27). (iii) Coronal section of prefrontal cortex showing location and spread of (100nl) Fluoro-Ruby (red) at injection site in PL (R28). (iv) Representations of Fluoro-Ruby (100nl) (R25, R26, R27, R28 (broken line) injection sites in PL (R28), VO (R26), VLO (R25) and DLO (R27), in the right hemisphere. (v) Representations of Fluoro-Gold (100nl) (R11, R22, R26, R27 (solid line)) injection sites in PL (R27), VO (R22), VLO (R11) and DLO (R26), in the left hemisphere. Fluoro-Ruby injection sites were consistently within the boundaries of corresponding Fluoro-Gold injection sites. There is minimal overlap between Fluoro-Gold injection sites (R27 & R22). Scale bars = 100µm..... 80

Figure 3.12. Diagram representing the injection sites of Fluoro-Gold and Fluoro-Ruby, and the projection to temporal cortex for both retrograde (Fluoro-Gold) and anterograde (Fluoro-Ruby) tracer injections. (i) The locations of injection sites Ap (PL:R27,R28), Bp (VO:R22,R26), Cp (VLO:R11,R25) and Dp (DLO:R26,R27) in posterior PFC. (ii) The locations of retrogradely labelled cells in temporal cortex, resultant from 100nl Fluoro-Gold injections into posterior PFC injection sites Ap-Dp (R11, R22, R26, R27). (iii) The locations of anterogradely labelled axon terminals in temporal cortex, resultant from 100nl Fluoro-Ruby injections into posterior PFC injection sites Ap-Dp (R25, R26, R27, R28). 82

Figure 3.13. (i) Coronal section showing retrogradely labelled cells (blue) in temporal cortex produced by injection of Fluoro-Gold (100nl) into posterior VO (R22). (ii) Retrogradely labelled

cells (blue) in PRh, resultant from injection of Fluoro-Gold (100nl) into posterior VO (R22). (iii) Retrogradely labelled cells (blue) in PRh, resultant from injection of Fluoro-Gold into posterior PL (R27). (iv) Coronal section showing anterogradely labelled axon terminals (red) in temporal cortex produced by injection of Fluoro-Ruby (100nl) in posterior VLO (R25). (v) Anterogradely labelled axon terminals in PRh, resultant from injection of Fluoro-Ruby (100nl) in posterior VLO (R25). (vi) Anterogradely labelled axon terminals in PRh, resultant from injection of Fluoro-Ruby (100nl) in posterior DLO (R27). Scale bars = 100µm. 84

Figure 3.14. The mean effect of posterior PFC injection site location on the (i) dorsal-ventral (ii) anterior-posterior and (iii) medial-lateral location of retrogradely labeled cells (n=269 arising from 4 rats: PL=114, VO=25, VLO=85, DLO=45) and anterogradely labeled axon terminals (n=261 arising from 4 rats: PL=51, VO=36, VLO=113, DLO=61) within temporal cortex. Error bars = standard error. (iv) Coronal cross section of PFC showing the position of 4 injection sites; prelimbic (Ap), ventral orbital (Bp), ventrolateral orbital (Cp) and dorsolateral orbital (Dp). Coronal cross section of temporal cortex showing the three dimensions in which the locations of labels were recorded. 86

Figure 3.15. Diagram representing the projections to temporal cortex for both retrograde (Fluoro-Gold) and anterograde (Fluoro-Ruby) tracer injections, from anterior, central and posterior PFC. Retrograde labelling in temporal cortex produced by Fluoro-Gold injections into (i) anterior PFC. (ii) central PFC and (iii) posterior PFC. Anterograde labelling in temporal cortex produced by Fluoro-Gold injections into (iv) central PFC and (vi) Anterograde labelling in sensory-motor cortex produced by Fluoro-Gold injections into posterior PFC. 89

Figure 3.16. The mean effect of PFC injection site on the location of retrograde and anterograde labels in temporal cortex. (i) The effect of anterior PFC injection sites (Aa (PL), Ba (VO), Ca (VLO), Da (DLO)) on the mean anterior-posterior distance of retrograde and anterograde labels from Bregma. (ii) The effect of central PFC injection sites (A (PL), B (VO), C (VLO), D (DLO)) on the mean anterior-posterior distance of retrograde and anterograde labels from Bregma. (iii) The effect of posterior PFC injection sites (Ap (PL), Bp (VO), Cp (VLO), Dp (DLO)) on the mean anterior-posterior distance of retrograde and anterograde labels from Bregma. (iv) The effect of anterior PFC injection sites (Aa (PL), Ba (VO), Ca (VLO), Da (DLO)) on the mean dorsal-ventral distance of retrograde and anterograde labels from the rhinal sulcus. (v) The effect of central PFC injection sites (A (PL), B (VO), C (VLO), D (DLO)) on the mean dorsal-ventral distance of retrograde and anterograde labels from the rhinal sulcus. (vi) The effect of posterior PFC injection sites (Ap (PL), Bp (VO), Cp (VLO), Dp (DLO)) on the mean dorsal-ventral distance of retrograde and anterograde labels from the rhinal sulcus. (vii) The effect of anterior PFC injection sites (Aa (PL), Ba (VO), Ca (VLO), Da (DLO)) on the mean medial-lateral distance of retrograde and anterograde labels from the cortical surface. (viii) The effect of central PFC injection sites (A (PL), B (VO), C (VLO), D (DLO)) on the mean medial-lateral distance of retrograde and anterograde labels from the cortical surface. (ix) The effect of posterior PFC injection sites (Ap (PL), Bp (VO), Cp (VLO), Dp (DLO)) on the mean medial-lateral distance of retrograde and anterograde labels from the cortical surface. 90

Fig. 3.17. The effect of the anterior-posterior location of PFC injection site on the average 3 dimensional distance between anterograde and retrograde labelling produced by (100nl) injections of Fluoro-Gold and Fluoro-Ruby into anterior, central and posterior PFC in temporal cortex Error bars = standard error. 91

Figure 4.1. Coronal section of PFC (A-P 3.7mm from Bregma) showing the cytoarchitectural boundaries of PFC sub-regions according to Van de Werd & Uylings (2008), depicting sites of tracer injections; PL (A, B), IL/MO (C), VO/VLO (D), VLO/LO (E), LO/DLO (F) and DLO (G), with 0.5mm separation. 98

Figure 4.2. (i) Coronal section of PFC (AP 4.2mm from Bregma) showing the cytoarchitectural boundaries of the prelimbic (PL), infralimbic (IL), medial orbital (MO), ventral orbital (VO), ventrolateral orbital (VLO), lateral orbital (LO) and dorsolateral orbital (DLO) cortices (according to Van de Werd & Uylings, 2008), depicting amalgamated sites of Fluoro-Gold and Fluoro-Ruby injections; Prelimbic: A & B, Infralimbic/Medial orbital: C, Ventral orbital/Ventrolateral orbital: D, Ventrolateral orbital/Lateral orbital: E, Lateral orbital/Dorsolateral orbital: F and Dorsolateral orbital: G, with 0.5mm spread. (ii) Coronal section of PFC showing location and spread of

(20nl) Fluoro-Ruby at injection site in VLO/LO (R11). (iii) Coronal section of PFC showing location and spread of (30nl) Fluoro-Gold at injection site in PL (R21). (iv) Representations of Fluoro-Ruby (20nl) (R13, R17, R16, R15, R11, R12, R8 (broken line)) injection sites in PL (R13, R17), IL/MO (R16), VO/VLO (R15), VLO/LO (R11), LO/DLO (R12) and DLO (R8) in the right hemisphere. (v) Representations of Fluoro-Gold (30nl) (R13, R21, R19, R20, R16, R12, R9 (solid line)) injection sites in PL (R13, R21), IL/MO (R19) VO/VLO (R20), VLO/LO (R16), LO/DLO (R12) and DLO (R9) in the left hemisphere. Fluoro-Ruby injection sites were predominantly within the boundaries of Fluoro-Gold injection sites. There is some overlap between retrograde injection sites into PL, IL and VO (R13 & R21, R21 & R19, R21 & R20). There is minimal overlap between anterograde injection sites into DLO (R8 & R12). Scale bars = 100µm. 101

Figure 4.3 (i) Coronal section showing retrogradely labelled cells (blue) in temporal cortex produced by injection of Fluoro-Gold (30nl) into PL (B: R21). (ii) Coronal section showing retrogradely labelled cells (blue) in temporal cortex produced by injection of Fluoro-Gold (30nl) into DLO (F: R12). (iii) Retrogradely labelled cells in temporal cortex (blue) produced by injection of Fluoro-Gold (30nl) into DLO (F: R12). (iv) Coronal section showing anterogradely labelled axon terminals (red) in temporal cortex produced by injection of Fluoro-Ruby (20nl) into PL (B: R17). (v) Coronal section showing anterogradely labelled axon terminals (red) in temporal cortex produced by injection of Fluoro-Ruby (20nl) into DLO (G: R8). (vi) Anterogradely labelled axon terminals (red) in temporal cortex produced by injection of Fluoro-Ruby (20nl) into IL/MO (C: R16). Arrows denote the location of the rhinal sulcus. Scales bars = 100µm. 102

Figure 4.4. Diagram representing the amalgamated injection sites of Fluoro-Gold and Fluoro-Ruby, and the projection sites to temporal cortex for both retrograde (Fluoro-Gold) and anterograde (Fluoro-Ruby) tracer injections. (i) The locations of injection sites A (PL: R13), B (PL: R17, R21), C (IL/MO: R16, R19), D (VO/VLO: R15, R20), E (VLO/LO: R11, R16), F (LO/DLO: R12) and G (DLO: R8, R9). (ii) The locations of retrogradely labelled cells in temporal cortex, resultant from 30nl Fluoro-Gold injections into PFC injection sites A-G (R13, R21, R19, R20, R16, R12, R9). (iii) The locations of anterogradely labelled axon terminals in temporal cortex resultant from 20nl Fluoro-Ruby injections into PFC injection sites A-D (R13, R17, R16, R15, R11, R12, R8). 104

Figure 4.5. The mean effect of PFC injection site on the (i) dorsal-ventral, (ii) anterior-posterior and (iii) medial-lateral location of retrogradely labeled cells (n=1122 arising from 7 rats: A(PL:R13)=59, B(PL:R21)=184, C(IL/MO:R19)=360, D(VO/VLO:R20)=92, E(VLO/LO:R16)=39, F(LO/DLO:R12)=194, G(DLO:R9)=194) and anterogradely labeled axon terminals (n=167 arising from 7 rats: A(PL:R13)=27, B(PL:R17)=24, C(IL/MO:R16)=19, D(VO/VLO:R15)=21, E(VLO/LO:R11)=45, F(LO/DLO:R12)=19, G(DLO:R8)=12) within temporal cortex. Error bars = standard error. (iv) Coronal cross section of PFC showing the position of 7 injection sites; PL (A, B), IL/MO (C), VO/VLO (D), VLO/LO (E), LO/DLO (F) and DLO (G). Coronal cross section of temporal cortex showing the three dimensions in which the locations of labels were recorded. 107

Figure 4.6. Connectivity matrix showing the relationship between input and output connections from PFC to temporal cortex. X = Retrograde and anterograde labelling found in the same cytoarchitectural regions of temporal cortex. X = Reciprocal connection: Retrograde and anterograde labelling from the same PFC injection site is found in the same cytoarchitectural region of temporal cortex. E.g. Retrograde projection site A is found in the same cytoarchitectural region as anterograde projections A, B and E. 114

Figure 4.7. (i) The effect of PFC retrograde (Fluoro-Gold) injection site on the reciprocity index, derived from connectivity matrix (Fig.4.6): median distance between Fluoro-Gold and Fluoro-Ruby PFC injection sites of retrograde and anterograde labelling found in the same cytoarchitectural regions of temporal cortex. A distance of 1 PFC injection site is given a value of 1 (e.g. the distance between retrograde site A and anterograde site B = 1). The absolute value is taken, regardless of direction. Regions where no anterograde projections were found in the same cytoarchitectural region as the retrograde connection (e.g. injection site G:DLO) were not included, as a value of zero here represent an entirely reciprocal connection. Where a retrograde projection is found in the same region as multiple anterograde projections a median distance is calculated. Fluoro-Gold injection sites made into the same PFC sub-regions (i.e. PL) are

combined. Injection G (DLO) is excluded due to having no return connections. PL = A & B, MO = C, VO = D, VLO = E, LO = F. Error bars = standard error. (ii) The connectivity matrix from which the graph (i) is produced..... 115

Figure 5.1. Coronal section of PFC (A-P 4.2mm from Bregma) showing the cytoarchitectural boundaries of PFC sub-regions according to Van de Werd & Uylings (2008), depicting sites of amalgamated anterograde and retrograde tracer injections; Prelimbic (PL):A, ventral orbital (VO):B, ventrolateral orbital(VLO):C and dorsolateral orbital(DLO):D, with 1mm separation. 119

Figure 5.2. (A) Coronal cross section of sensory-motor cortex at 2.2mm posterior to bregma, depicting the three dimensions in which the locations of labelled cells were recorded (Anterior-Posterior (A-P), Medial-Lateral (M-L) and Dorsal-Ventral (D-V)). (B) Retrogradely labelled cells (blue cells) in sensory-motor cortex produced by a co-injection of Fluoro-Gold (100nl) and BDA (Fluorescein, 100nl (green cells)) into VO. Arrows indicate measurements of labelled cell location in the medial-lateral dimension (distance to lateral cortical surface) and dorsal-ventral dimension (distance from rhinal sulcus). (C) Anterogradely labelled area (Brown) in sensory-motor cortex produced by an injection of BDA (100nl) into PL. Crosses indicate the four points on the perimeter at which measurements were taken. Arrows indicate measurements of labelled area location in the medial-lateral dimension (distance to medial cortical surface) and dorsal-ventral dimension (distance from dorsal surface: laminar). Scale bars = 200µm. 121

Figure 5.3. (i) Coronal section of PFC showing location and spread of (100nl) Fluoro-Gold and (100nl) Fluorescein at injection site in VO. (ii) Coronal section of PFC showing location and spread of (100nl) Fluoro-Gold and (100nl) Fluorescein at injection site in DLO. (iii) Representations of Fluoro-Gold and Fluorescein co-injection sites in PL (R42), VO (R37), VLO (R41) and DLO. Scale bars = 200µm..... 123

Figure 5.4. Diagram representing the injection sites of Fluoro-Gold and BDA, and the projection sites to sensory motor cortex for both retrograde (Fluoro-Gold) and anterograde (BDA) tracer injections. (i) The locations of injection sites A (PL: R3, R7), B (VO:R6, R7), C (VLO:R1, R4) and D (DLO:R5, R8) in PFC. (ii)The locations of retrogradely labelled cells in sensory-motor cortex, resultant from 100nl Fluoro-Gold injections into PFC injection sites A-D (R4, R5, R6, R7). (iii) The locations of anterogradely labelled areas in sensory-motor cortex, resultant from 100nl BDA injections into PFC injection sites A-D (R1, R3, R7, R8). 125

Figure 5.5. (i) Coronal section of sensory-motor cortex showing retrograde labelling (blue) and anterograde labelling (green) resultant from co-injection of Fluoro-Gold and BDA (Fluorescein) into VO (injection site B, R37). (ii) Retrograde (blue) and anterograde (green) labelling in motor cortex resultant from co-injection of Fluoro-Gold and BDA (Fluorescein) into VO (injection site B, R37). (iii) Coronal section of sensory-motor cortex showing area of anterograde labelling (brown (fluorescein visualised with DAB)) resultant from co-injection of Fluoro-Gold and BDA into DLO (injection site D, R38). (iv) Retrograde (blue) and anterograde (green (fluorescein visualised with fluorescence)) labelling in motor cortex resultant from co-injection of Fluoro-Gold and BDA (fluorescein) into VLO (injection site C, R41). Scale bars = 100µm. 128

Figure. 5.6. The mean effect of PFC co-injection site location on the mean location of retrogradely labelled cells (n= 307; PL (A:R42)=77, VO (B:R37)=121, VLO (C:R41)=80, DLO (D:R38)=29) and anterogradely labeled axon terminals (n=24; PL (A:R42)=4, VO (B:R37)=4, VLO (C:R41)=4, DLO (D:R38)=12) within temporal cortex, in the (i) dorsal-ventral (ii) anterior-posterior and (iii) medial-lateral axes. Error bars = standard error. (iv) Coronal cross section of PFC showing the position of 4 injection sites; Prelimbic (A), ventral orbital (B), ventrolateral orbital (C), dorsolateral orbital (D). Coronal cross section of temporal cortex showing the three dimensions in which the locations of labels were recorded. 131

Figure 5.7. The effect of PFC injection site (PL:A, VO:B, VLO:C, DLO:D) on the three dimensional mean location of retrogradely labelled cells (blue) and anterogradely labelled areas (red) in sensory-motor cortex. Error bars = standard error. 132

Figure 6.1. Coronal sections of PFC ((i) A-P 4.7mm, (ii) 3.7mm and (iii) 4.2mm from Bregma) showing the cytoarchitectural boundaries of PFC sub-regions according to Van de Werd & Uylings (2008), depicting the amalgamated sites of

tracer injections; PL (Aa, A, Ap), VO (Ba, B, Bp), VLO (Ca, C, Cp) and DLO (Da, D, Dp), with 1mm separation. 141

Figure 6.2. (i) Coronal section of anterior PFC (AP 4.7mm from Bregma) showing the cytoarchitectural boundaries of the prelimbic (PL), medial orbital (MO), ventral orbital (VO), ventrolateral orbital (VLO), lateral orbital (LO) and dorsolateral orbital (DLO) cortices (according to Van de Werd & Uylings, 2008), depicting sites of injections; Prelimbic: Aa, Ventral orbital: Ba, Ventrolateral orbital: Ca and dorsolateral orbital: Da, with 1mm spread. (ii) Coronal section of PFC showing location and spread of (100nl) Fluoro-Gold at injection site in VO (R24). (iii) Coronal section of PFC showing location and spread of (100nl) Fluoro-Ruby at injection site in PL (R32). (iv) Representations of Fluoro-Ruby (100nl) (R21, R23, R24, R32 (broken line)) injection sites in PL (R32), VO (R23), VLO (R21) and DLO (R24) in the right hemisphere. (v) Representations of Fluoro-Gold (100nl) (R17, R23, R24, R28 (solid line)) injection sites in PL (R28), VO (R24), VLO (R17) and DLO (R23) in the left hemisphere. Fluoro-Ruby injection sites were predominantly within the boundaries of Fluoro-Gold injection sites. There is minimal overlap between Fluoro-Gold injection sites (R28 & R24, R24 & R17). Fluoro-Gold and Fluoro-Ruby injection sites are mostly limited to the cytoarchitectural boundaries of PFC regions, and span the majority of the region (PL, VO/MO, VLO, DLO), injections into VO spread into MO. Scale bars = 100µm..... 143

Figure 6.3. (i) Coronal section showing retrogradely labeled cells (blue) in sensory-motor cortex produced by injection of Fluoro-Gold (100nl) into VO (R24). (ii) Retrogradely labeled cells (blue) in sensory-motor cortex produced by injection of Fluoro-Gold into VO (R24). (iii) Coronal section showing anterogradely labeled axon terminals (red) in sensory-motor cortex produced by injection of Fluoro-Ruby (100nl) into PL (R32). (iv) Anterograde labelling (red) in sensory-motor cortex produced by injection of Fluoro-Ruby (100nl) into DLO (R24). Scale bars = 100µm..... 145

Figure 6.4 Diagram representing the amalgamated injection sites of Fluoro-Gold and Fluoro-Ruby in anterior PFC, and the projection sites to sensory-motor cortex for both retrograde (Fluoro-Gold) and anterograde (Fluoro-Ruby) tracer injections. (i) The locations of injection sites Aa (PL: R28, R32), Ba (R23, R24), Ca (R17, R21) and Da (R23, R24) in anterior PFC. (ii) The locations of retrogradely labeled cells in sensory-motor cortex, resultant from 100nl Fluoro-Gold injections into anterior PFC injection sites Aa-Da (R17, R23, R24, R28). (iii) The locations of anterogradely labeled axon terminals in sensory-motor cortex, resultant from 100nl Fluoro-Ruby injections into anterior PFC injection sites Aa-Da (R21, R23, R24, R32)..... 147

Figure 6.5. The mean effect of injection site in *anterior* PFC on the (i) dorsal-ventral, (ii) anterior-posterior and (iii) medial-lateral location of retrogradely labelled cells (n=208 arising from 4 rats: PL=20, VO=77, VLO=39, DLO=72) and anterogradely labelled axon terminals (n=244 arising from 4 rats: PL=87, VO=91, VLO=30, DLO=36) within sensory-motor cortex. Error bars = standard error. (iv) Coronal cross section of PFC showing the position of 4 injection sites; Prelimbic (Aa), Ventral orbital (Ba), Ventrolateral orbital (Ca) and Dorsolateral orbital (Da). Coronal cross section of sensory-motor cortex showing the three dimensions in which the locations of labels were recorded..... 149

Figure 6.6 (i) Coronal section of central PFC (AP 4.2mm from Bregma) showing the cytoarchitectural boundaries of the prelimbic (PL), infralimbic (IL), medial orbital (MO), ventral orbital (VO), ventrolateral orbital (VLO) and dorsolateral orbital (DLO) cortices (according to Van de Werd & Uylings, 2008), depicting sites of injections; prelimbic:A, ventral orbital:B, ventrolateral orbital:C and dorsolateral orbital:D, with 1mm spread. (ii) Coronal section of PFC showing location and spread of (100nl) Fluoro-Gold (blue) at injection site in VO (R6). (iii) Coronal section of PFC showing location and spread of (100nl) Fluoro-Ruby (red) at injection site in VLO (R9). (iv) Representations of Fluoro-Gold (100nl) (R4, R5, R6, R7 (solid line)) and Fluoro-Ruby (100nl) (R9, R19, R20, R29 (broken line)) injection sites in PL (R7, R29), VO (R6, R20), VLO (R4, R9) and DLO (R5, R19), in the right hemisphere. 151

Figure 6.7.(i) Coronal section showing retrogradely labelled cells (blue) in cingulate cortex produced by 100nl injection of Fluoro-gold into VLO (R4). (ii) Coronal section showing retrogradely labelled cells (blue) in cingulate cortex produced by 100nl injection of Fluoro-gold into VO (R6). (iii) Coronal section showing anterograde labelling (red) produced by injection of

Fluoro-Ruby into DLO (R19). Anterograde labelling in sensory-motor cortex produced by injection of Fluoro-Ruby into DLO (R19). Scale bars = 100µm. 152

Figure 6.8. Diagram representing the amalgamated injection sites of Fluoro-Gold and Fluoro-Ruby, and the projection sites to sensory-motor cortex for both retrograde (Fluoro-Gold) and anterograde (Fluoro-Ruby) tracer injections. (i) The locations of injection sites A (PL: R7, R29), B (VO:R6, R20), C (VLO:R4, R9) and D (DLO: R5, R19) in central PFC. (ii) The locations of retrogradely labeled cells in sensory-motor cortex, resultant from 100nl Fluoro-Gold injections into central PFC injection sites A-D (R4, R5, R6, R7). (iii) The locations of anterogradely labeled axon terminals in sensory-motor cortex, resultant from 100nl Fluoro-Ruby injections into central PFC injection sites A-D (R9, R19, R20, R29). 154

Figure 6.9. The mean effect of central PFC injection site on the (i) dorsal-ventral, (ii) anterior-posterior and (iii) medial-lateral location of retrogradely labelled cells (n=494 arising from 4 rats: PL=143, VO=156, VLO=83, DLO=112) and anterogradely labelled axon terminals (n=224 arising from 4 rats: PL=138, VO=29, VLO=19, DLO=38) within sensory-motor cortex. Error bars=standard error. (iv) Coronal cross section of PFC showing the position of 4 injection sites; prelimbic (A), ventral-orbital (B), ventrolateral orbital (C) and dorsolateral orbital (D). Coronal cross section of sensory-motor cortex showing the three dimensions in which the locations of labels were recorded. 156

Figure 6.10 (i) Coronal section of PFC (AP 3.7mm from Bregma) showing the cytoarchitectural boundaries of the prelimbic (PL), infralimbic (IL), ventral orbital (VO) ventrolateral orbital (VLO) and dorsolateral orbital (DLO) cortices (according to Van de Werd & Uylings, 2008), depicting sites of injections; Prelimbic: Ap, Ventral orbital: Bp, Ventrolateral orbital: Cp and Dorsolateral orbital: Dp, with 1mm spread. (ii) Coronal section of PFC showing location and spread of (100nl) Fluoro-Gold (blue) at injection site in PL (R27). (iii) Coronal section of PFC showing location and spread of (100nl) Fluoro-Ruby (red) at injection site in PL (R28). (iv) Representations of Fluoro-Ruby (100nl) (R25, R26, R27, R28 (broken line) injection sites in PL (R28), VO (R26), VLO (R25) and DLO (R27), in the right hemisphere. (v) Representations of Fluoro-Gold (100nl) (R11, R22, R26, R27 (solid line)) injection sites in PL (R27), VO (R22), VLO (R11) and DLO (R26), in the left hemisphere. Fluoro-Ruby injection sites were consistently within the boundaries of corresponding Fluoro-Gold injection sites. There is minimal overlap between Fluoro-Gold injection sites (R27 & R22). Scale bars = 100µm. 158

Figure 6.11. (i) Coronal section showing retrogradely labelled cells (blue) in sensory-motor cortex produced by injection of Fluoro-Gold (100nl) into *posterior* VO (R22). (ii) Retrogradely labelled cells (blue) in sensory-motor cortex, resultant from injection of Fluoro-Gold (100nl) into posterior VLO (R11). (iii) Coronal section showing anterogradely labelled axon terminals (red) in sensory-motor cortex produced by injection of Fluoro-Ruby (100nl) in posterior DLO (R27). (iv) Anterograde labelling (red) in sensory-motor cortex, resultant from injection of Fluoro-Ruby (100nl) in posterior VO(R26). Scale bars = 100µm. 160

Figure 6.12. Diagram representing the amalgamated injection sites of Fluoro-Gold and Fluoro-Ruby, and the projection to sensory-motor cortex for both retrograde (Fluoro-Gold) and anterograde (Fluoro-Ruby) tracer injections. (i) The locations of injection sites Ap (PL:R27,R28), Bp (VO:R22,R26), Cp (VLO:R11,R25) and Dp (DLO:R26,R27) in posterior PFC. (ii) The locations of retrogradely labelled cells in sensory-motor cortex, resultant from 100nl Fluoro-Gold injections into posterior PFC injection sites Ap-Dp (R11, R22, R26, R27). (iii) The locations of anterogradely labelled axon terminals in sensory-motor cortex, resultant from 100nl Fluoro-Ruby injections into posterior PFC injection sites Ap-Dp (R25, R26, R27, R28). 162

Figure 6.13. The mean effect of posterior PFC injection site location on the (i) dorsal-ventral (ii) anterior-posterior and (iii) medial-lateral location of retrogradely labeled cells (n=586 arising from 4 rats: PL=152, VO=268, VLO=136, DLO=30) and anterogradely labeled axon terminals (n=243 arising from 4 rats: PL=124, VO=44, VLO=35, DLO=40) within sensory-motor cortex. Error bars = standard error.(iv) Coronal cross section of PFC showing the position of 4 injection sites; prelimbic (Ap), ventral orbital (Bp), ventrolateral orbital (Cp) and dorsolateral orbital (Dp). Coronal cross section of sensory-motor cortex showing the three dimensions in which the locations of labels were recorded. 164

Fig. 6.14 Diagram representing the projections to sensory-motor cortex for both retrograde (Fluoro-Gold) and anterograde (Fluoro-Ruby) tracer injections, from anterior, central and posterior PFC. (i) Retrograde labelling in sensory-motor cortex produced by Fluoro-Gold injections into anterior PFC. (ii) Retrograde labelling in sensory-motor cortex produced by Fluoro-Gold injections into central PFC. (iii) Retrograde labelling in sensory-motor cortex produced by Fluoro-Gold injections into posterior PFC. (iv) Anterograde labelling in sensory-motor cortex produced by Fluoro-Gold injections into anterior PFC. (v) Anterograde labelling in sensory-motor cortex produced by Fluoro-Gold injections into central PFC. (vi) Anterograde labelling in sensory-motor cortex produced by Fluoro-Gold injections into posterior PFC. 166

Figure 6.15. The mean effect of PFC injection site on the location of retrograde and anterograde labels in sensory-motor cortex. (i) The effect of anterior PFC injection sites (Aa (PL), Ba (VO), Ca (VLO) , Da (DLO)) on the mean anterior-posterior distance of retrograde and anterograde labels from Bregma. (ii) The effect of central PFC injection sites (A (PL), B (VO), C (VLO), D (DLO)) on the mean anterior-posterior distance of retrograde and anterograde labels from Bregma. (iii) The effect of posterior PFC injection sites (Ap (PL), Bp (VO), Cp (VLO), Dp (DLO)) on the mean anterior-posterior distance of retrograde and anterograde labels from Bregma. (iv) The effect of anterior PFC injection sites (Aa (PL), Ba (VO), Ca (VLO) , Da (DLO)) on the mean dorsal-ventral distance of retrograde and anterograde labels from the cortical surface. (v) The effect of central PFC injection sites (A (PL), B (VO), C (VLO), D (DLO)) on the mean dorsal-ventral distance of retrograde and anterograde labels from the cortical surface. (vi) The effect of posterior PFC injection sites (Ap (PL), Bp (VO), Cp (VLO), Dp (DLO)) on the mean dorsal-ventral distance of retrograde and anterograde labels from the cortical surface. (vii) The effect of anterior PFC injection sites (Aa (PL), Ba (VO), Ca (VLO) , Da (DLO)) on the mean medial-lateral distance of retrograde and anterograde labels from the medial surface. (viii) The effect of central PFC injection sites (A (PL), B (VO), C (VLO), D (DLO)) on the mean medial-lateral distance of retrograde and anterograde labels from the medial surface. (ix) The effect of posterior PFC injection sites (Ap (PL), Bp (VO), Cp (VLO), Dp (DLO)) on the mean medial-lateral distance of retrograde and anterograde labels from the medial surface. 169

Fig. 6.16. The effect of the anterior-posterior location of PFC injection site on the mean 3 dimensional distance (E) between anterograde and retrograde labels in sensory-motor cortex. Error bars = standard error. 171

Figure 7.1. Coronal section of PFC (A-P 3.7mm from Bregma) showing the cytoarchitectural boundaries of PFC sub-regions according to Van de Werd & Uylings (2008), depicting sites of tracer injections; PL (A, B), IL/MO (C), VO/VLO (D), VLO/LO (E), LO/DLO (F) and DLO (G), with 0.5mm separation. 179

Figure 7.2. (i) Coronal section of PFC (AP 4.2mm from Bregma) showing the cytoarchitectural boundaries of the prelimbic (PL), infralimbic (IL), medial orbital (MO), ventral orbital (VO), ventrolateral orbital (VLO), lateral orbital (LO) and dorsolateral orbital (DLO) cortices (according to Van de Werd & Uylings, 2008), depicting sites of injections; Prelimbic: A & B, Infralimbic/Medial orbital: C, Ventral orbital/Ventrolateral orbital: D, Ventrolateral orbital/Lateral orbital: E, Lateral orbital/Dorsolateral orbital: F and Dorsolateral orbital: G, with 0.5mm spread. (ii) Coronal section of prefrontal cortex showing location and spread of (20nl) Fluoro-Ruby at injection site in VLO/LO (R11). (iii) Coronal section of prefrontal cortex showing location and spread of (30nl) Fluoro-Gold at injection site in PL (R21). (iv) Representations of Fluoro-Ruby (20nl) (R13, R17, R16, R15, R11, R12, R8 (broken line)) injection sites in PL (R13, R17), IL/MO (R16), VO/VLO (R15), VLO/LO (R11), LO/DLO (R12) and DLO (R8) in the right hemisphere. (v) Representations of Fluoro-Gold (30nl) (R13, R21, R19, R20, R16, R12, R9 (solid line)) injection sites in PL (R13, R21), IL/MO (R19) VO/VLO (R20), VLO/LO (R16), LO/DLO (R12) and DLO (R9) in the left hemisphere. Fluoro-Ruby injection sites were predominantly within the boundaries of Fluoro-Gold injection sites. There is some overlap between retrograde injection sites into PL, IL and VO (R13 & R21, R21 & R19, R21 & R20). There is minimal overlap between anterograde injection sites into DLO (R8 & R12). Scale bars = 100µm. 182

Figure 7.3. (i) Coronal section showing retrogradely labelled cells (blue) in sensory-motor cortex produced by injection of Fluoro-Gold (30nl) into VO/VLO (D: R20). (ii) Coronal section showing retrogradely labelled cells (blue) in sensory-motor cortex produced by injection of

Fluoro-Gold (30nl) into PL (B: R21). Arrow denotes location of retrogradely labeled cells. (iii) Retrogradely labelled cells in sensory-motor cortex (blue) produced by injection of Fluoro-Gold (30nl) into PL (B: R20). (iv) Coronal section showing anterogradely labelled axon terminals (red) in sensory-motor cortex produced by injection of Fluoro-Ruby (20nl) into PL (B: R17). (v) Anterograde labelling (red) in sensory-motor cortex produced by injection of Fluoro-Ruby (20nl) into DLO (G: R8). (vi) Anterograde labelling (red) in temporal cortex produced by injection of Fluoro-Ruby (20nl) into VLO/LO (E: R11). Scales bars = 100µm. 184

Figure 7.4. Diagram representing the amalgamated injection sites of Fluoro-Gold and Fluoro-Ruby, and the projection sites to sensory-motor cortex for both retrograde (Fluoro-Gold) and anterograde (Fluoro-Ruby) tracer injections. (i) The locations of injection sites A (PL: R13), B (PL: R17, R21), C (IL/MO: R16, R19), D (VO/VLO: R15, R20), E (VLO/LO: R11, R16), F (LO/DLO: R12) and G (DLO: R8, R9). (ii) The locations of retrogradely labelled cells in sensory-motor cortex, resultant from 30nl Fluoro-Gold injections into PFC injection sites A-G (R13, R21, R19, R20, R16, R12, R9). Note the concentration of retrograde labelling in layers V and VI, with laminar ordering present. (iii) The locations of anterogradely labelled axon terminals in sensory-motor cortex resultant from 20nl Fluoro-Ruby injections into PFC injection sites A-D (R13, R17, R16, R15, R11, R12, R8). 186

Figure 7.5. The mean effect of PFC injection site on the (i) dorsal-ventral, (ii) anterior-posterior and (iii) medial-lateral location of retrogradely labeled cells (n= 597 arising from 7 rats: A(PL:R13)=119, B(PL:R21)=52, C(IL/MO:R19)=91, D(VO/VLO:R20)=85, E(VLO/LO:R16)=22, F(LO/DLO:R12)=71, G(DLO:R9)=157) and anterogradely labeled axon terminals (n=305 arising from 7 rats: A(PL:R13)=34, B(PL:R21)=138, C(IL/MO:R19)=63, D(VO/VLO:R20)=24, E(VLO/LO:R16)=22, F(LO/DLO:R12)=10, G(DLO:R9)=14) within sensory-motor cortex. Error bars = standard error. (iv) Coronal cross section of PFC showing the position of 7 injection sites; PL (A, B), IL/MO (C), VO/VLO (D), VLO/LO (E), LO/DLO (F) and DLO (G). Coronal cross section of sensory-motor cortex showing the three dimensions in which the locations of labels were recorded. 189

Figure 7.6. Connectivity matrix showing the relationship between input and output connections from PFC to sensory-motor cortex. X = Retrograde and anterograde labelling found in the same cytoarchitectural regions of sensory or motor cortex. X = Reciprocal connection: Retrograde and anterograde labelling from the same PFC injection site is found in the same cytoarchitectural region of sensory or motor cortex. E.g. Retrograde injection site A receives input connections from a region of sensory-motor cortex which injection site E sends output connections to. 195

Figure 7.7. The effect of retrograde PFC injection site on the number of return anterograde connections from the same cytoarchitectural region of sensory-motor cortex, constructed using the connectivity matrix in Fig. 7.6. Error bars = standard error. 196

Figure 7.8. (i) The effect of PFC retrograde (Fluoro-Gold) injection site on the median distance between Fluoro-Gold and Fluoro-Ruby PFC injection sites of retrograde and anterograde labelling found in the same cytoarchitectural regions of sensory-motor cortex. A distance of 1 PFC injection site is given a value of 1 (e.g. the distance between retrograde site A and anterograde site B = 1). Where a retrograde projection is found in the same region as multiple anterograde projections a median distance is calculated. Fluoro-Gold injection sites made into the same PFC sub-regions (i.e. PL) are combined. PL = A & B, VO= D, LO=F, DLO=G. Injection G (DLO) is excluded due to having no return connections. Error bars = standard error. Error bars = standard error. (ii) The connectivity matrix from which the graph (i) is produced. 198

Figure 8.1. Coronal section of PFC (A-P 4.7mm from Bregma) showing the cytoarchitectural boundaries of PFC sub-regions according to Van de Werd & Uylings (2008) and FrA according to Paxinos & Watson (1998), depicting sites of tracer injections, with 1mm separation. 202

Figure 8.2. (i) Coronal section of PFC (AP 4.7mm from Bregma) showing the cytoarchitectural boundaries of the prelimbic (PL), infralimbic (IL), medial orbital (MO), ventral orbital (VO), ventrolateral orbital (VLO), lateral orbital (LO) and dorsolateral orbital (DLO) cortices (according to Van de Werd & Uylings, 2008) and FrA (according to Paxinos & Watson, 1998). (ii) Coronal section of frontal association cortex showing location and spread of (100nl) Fluoro-Gold at injection site in medial FrA (R33). (iii) Coronal section of frontal association cortex showing location and spread of (100nl) Fluoro-Ruby at injection site in lateral FrA (R38). (iv) Representations of Fluoro-Ruby (100nl) ((R37, R38) (broken line)) injection sites in central

(R37) and lateral FrA (R38) and Fluoro-Gold (100nl) ((R33) solid line) injection site in medial FrA, in the right hemisphere. (v) Representations of Fluoro-Ruby (100nl) ((R41)(broken line)) injection site in medial FrA, and Fluoro-Gold (100nl) ((R29, R36)(solid line)) injection sites in central (R29) and lateral FrA (R36), in the left hemisphere. Scale bars = 100µm.205

Figure 8.3. (i) Coronal section (-4.52mm from Bregma) showing retrogradely labeled cells (blue) in temporal cortex produced by injection of Fluoro-Gold (100nl) into medial FrA (injection site A:R33). (ii) Coronal section (-4.16mm from Bregma) showing retrogradely labeled cells (blue) in temporal cortex produced by injection of Fluoro-Gold (100nl) into lateral FrA (injection site C:R36). (iii) Coronal section (-4.3mm from Bregma) showing anterogradely labeled axon terminals (red) in temporal cortex produced by injection of Fluoro-Ruby (100nl) into central FrA (injection site B:R37). Arrows denote the location of the rhinal sulcus. Scale bars = 100µm.206

Figure 8.4. Diagram representing the injection sites of Fluoro-Gold and Fluoro-Ruby, and the projection sites to temporal cortex for both retrograde (Fluoro-Gold) and anterograde (Fluoro-Ruby) tracer injections. (i) The locations of injection sites in FrA (A:R33 & R41, B:R29 & R37, C:R36 & R38). (ii)The locations of retrogradely labelled cells in temporal cortex, resultant from 100nl Fluoro-Gold injections into FrA injection sites A (R33), B (R29) and C (R36) (iii) The locations of anterogradely labelled areas in temporal cortex, resultant from 100nl Fluoro-Ruby injections into FrA injection sites A (R41), B (R37) and C (R38).208

Figure. 8.5. The mean effect of FrA injection site location on the mean location of retrogradely labelled cells (n=32: medial(R 33)=8, central(R29)=11, lateral (R36)=13) and anterogradely labeled axon terminals (n=93: medial (R41)=39, central (R37)=18, lateral (R38)=36) within temporal cortex, in the (i) dorsal-ventral (ii) anterior-posterior and (iii) medial-lateral axes. Error bars = standard error. (iv) Coronal cross section of PFC showing the position of 3 injection sites; medial, central and lateral FrA. Coronal cross section of temporal cortex showing the three dimensions in which the locations of labels were recorded.210

Figure 8.6. The effect of FrA injection site (medial, central and lateral FrA) on the three dimensional mean location of retrogradely labelled cells (blue) and anterogradely labelled axon terminals (red) in temporal cortex. Error bars = standard error.211

Figure 8.7. The mean distance between Fluoro-Gold and Fluoro-Ruby labelling in temporal cortex, resultant from tracer injections (100nl) into FrA, anterior regions of PL, VO, VLO & DLO, central regions of PL, VO, VLO & DLO and posterior regions of PL, VO, VLO & DLO. Note that the distance becomes greater in more anterior regions. Note that the A-P distance from Bregma of FrA and anterior PFC injection sites were equal.212

List of Abbreviations

PFC - Prefrontal cortex

OMPFC - Orbital medial prefrontal cortex

DLPFC - Dorsolateral prefrontal cortex

dmPFC - Dorsomedial prefrontal cortex

mPFC - Medial prefrontal cortex

PrL - Prelimbic cortex

PL - Prelimbic cortex

IL - Infralimbic cortex

MO - Medial orbital cortex

VO - Ventral orbital cortex

VLO - Ventrolateral orbital cortex

LO - Lateral orbital cortex

DLO - Dorsolateral orbital cortex

M1 - Primary motor cortex

M2 - Secondary motor cortex

S1 - Primary somatosensory cortex

S2 - Secondary somatosensory cortex

PRh - Perirhinal cortex

Ect - Ectorhinal cortex

Te - Visual area Te

Ent - Entorhinal cortex

Au1 - Primary auditory cortex

S1J - Primary somatosensory cortex, jaw region

S1BF - Primary somatosensory cortex, barrel field

Cg1 - Cingulate cortex, area 1

Pir - Piriform cortex

AID - Agranular insular cortex, dorsal part

AuV - Secondary auditory cortex, ventral area

BDA - Biotinylated dextran amine

FrA - Frontal association cortex

AM - Anteromedial nucleus of the thalamus

FPm - Medial frontal polar cortex

AGm - Medial frontal agranular cortex

AC - Anterior cingulate cortex

Abstract

The fine scale connections of prefrontal cortex (PFC) were investigated in the rat brain, in order to determine organizational properties of PFC pathways which were previously undefined. Neuroanatomical tract tracers (Fluro-Gold, Fluoro-Ruby, Fluoro-Emerald, Biotinylated dextran amines; Fluorescein and Texas red) were injected (20 -100 nl) into subdivisions of PFC (prelimbic, infralimbic, medial-orbital, ventral-orbital, ventrolateral-orbital, lateral-orbital and dorsolateral-orbital) and their projections studied. Tracer studies identified clear evidence of significantly ordered projections from PFC to temporal and sensory-motor cortices in three axes of orientation ($p < 0.001$), showing differential ordering of input and output connections ($p < 0.001$). Ordered connections were consistent across PFC (from anterior to posterior) and showed evidence of changes in organisation in anterior compared to posterior PFC, in both the PFC-temporal and PFC-sensory-motor cortex pathways. Detailed analysis revealed evidence for an organizational gradient in the relationship between inputs and outputs from anterior to posterior PFC, in which retrograde and anterograde labelling become increasingly differentiated as PFC injection site is moved from posterior to anterior. Analysis of fine scale tracer injections (20-30 nl) revealed evidence to show underlying complex organizational properties of connections from PFC to temporal and sensory-motor cortices. Taken together, the findings show that PFC displays ordered arrangements of connections to temporal and sensory-motor cortex, input and output connections are consistently not found in the same locations and the relationship between inputs and outputs differs in relation to the anterior-posterior location in PFC.

Introduction

Contents

1. Prefrontal cortex.....	20
1.1 Prefrontal cortex across species.....	21
1.2 Prefrontal cortex in rats	21
2. Function	22
2.1 Cerebral cortex.....	22
2.2 Prefrontal cortex.....	23
3. Structure.....	25
3.1 Cerebral cortex.....	25
3.2 Prefrontal cortex.....	26
4. Organisation.....	27
4.1 Cerebral cortex.....	27
4.2 Prefrontal cortex.....	28
5. Connectivity.....	31
5.1 Cerebral cortex.....	31
5.2 Prefrontal cortex.....	33
6. Aims.....	37
6.1 Broad scale prefrontal cortex connections	37
6.2 Fine scale prefrontal cortex connections.....	38

Often described as the final frontier in understanding human cognition and behaviour, prefrontal cortex (PFC) is a vital brain region in the execution of a range of complex processes (Shallice, 2001). Despite its established functional importance, there remains relatively little knowledge in contemporary neuroscience regarding prefrontal cortex organisation. The current lack of structural knowledge poses difficulties in developing our understanding of PFC function, and to a great extent prevents progress in the understanding, prevention and treatment of its associated neurological deficits.

Mapping the connections of the human brain has become a major focus in recent neuroscience research. Brain mapping, both structural and functional, has so far proven to be of great practical use, particularly in neurosurgery, allowing for safer and more successful surgeries. Detailed ordered maps have been described for multiple brain regions in humans and cats including motor, sensory, visual and auditory cortex (Penfield & Rasmussen, 1950; Tootell, 1998; Sereno et al, 2001; Hagler & Sereno, 2006; Merzenich et al, 1975), providing us with a greater level of understanding of these areas. For instance, the well-known topographic map of primary motor cortex (Penfield, 1951) provided an important basis for explaining previously unexplained phenomena such as phantom limbs and enabled neurologists to pinpoint the location of specific motor deficits in the cerebral cortex. Many regions, like the primary motor cortex, have been clearly mapped. However, some cortical regions remain to be defined in such a way, perhaps most notably the prefrontal cortex.

1. Prefrontal Cortex

The most anterior region of the frontal lobe of the mammalian brain is known as the prefrontal cortex. The area of cortex defined as prefrontal was often defined by a granular layer IV. Rose & Woolsey (1948) defined PFC as the projection target of the mediodorsal nucleus of the thalamus in the rabbit, sheep and cat. More recent findings have expanded this definition to PFC having stronger connections with the mediodorsal thalamic nucleus than other nuclei of the thalamus (Uylings et al, 2003); this is a definition which remains in use in the recognition of PFC across mammalian species.

In evolutionary terms, PFC is thought to be the newest mammalian brain region. Evidence shows that throughout phylogenetic development the prefrontal region increases in size considerably, both in volume and relative size to the rest of the brain, reaching its largest in primates, most notably constituting 29% of cortex in humans (Brodmann, 1909, 1912). It has also increased in size through evolution more than any other cortical region (Preuss, 2000). Evolution states that natural selection acts on specific brain regions that are advantageous to the particular species. With this in mind, the disproportionate size of PFC in humans and other primates suggests that its function is advantageous

to us as a species. The prefrontal cortex is the last human cortical region to develop fully, reaching full maturity after approximately 20 years. This could be a result of highly complex connectivity, which takes longer to develop than the structural connectivity patterns of other cortical regions, suggesting a more complex organisation than is currently known. Despite obvious interests in PFC in terms of its contribution to advanced brain function, there remains relatively little understanding about it as a functional cortical region.

1.1 Prefrontal Cortex Across Species

The prefrontal cortex has been recognised in a range of species; however, without a single clear definition of PFC there remains some controversy in the presence of PFC in non-primates. Brodmann's (1909) representation of PFC in monkeys greatly resembles that of the human (although some homologies are unclear). There is a consistent opinion that the architecture of human PFC is largely similar to that of other primates (Petrides and Pandya, 1994; Semendeferi, 1998). Rose and Woolsey (1948) described orbital prefrontal cortical regions in rats, cats and rabbits based on the connections identified and their similarity to the orbital medial PFC (OMPFC) described in primates. More recent studies confirmed similarities in both OMPFC and dorsolateral PFC (DLPFC) between primates and rats (Goldman-Rakic, 1988; Uylings and Van Eden, 1990). There is also thought to be functional similarities between specific PFC regions across species, for example dmPFC in rats is thought to represent similar functions to PFC regions in primates (Groenewegen and Uylings, 2000; Uylings et al, 2003).

These similarities in PFC between mammalian species are of great importance in the study of PFC organisation and allows for the investigation of PFC in non-human species to be projected onto humans.

1.2 Prefrontal Cortex in Rats

Rat DLPFC shares homologies with that of the human (Fig.1.1), in terms of inputs and outputs it receives. Areas of rat PFC have been linked in similarity of function to regions of primate PFC e.g. prelimbic cortex (PL) is said to be implicated in anxiety, learned helplessness, emotive control and goal directed behaviour across species (Holmes and Wellman, 2009). It has been suggested that infralimbic cortex (IL) in rats is homologous to Brodmann area 25 and prelimbic cortex (PrL) to

Brodmann area 32 (Gabbott, 2003, Uylings & Van Eden, 1990). This is supported by findings of similar anatomical connections (Barbas et al, 2003; Vertes, 2004).

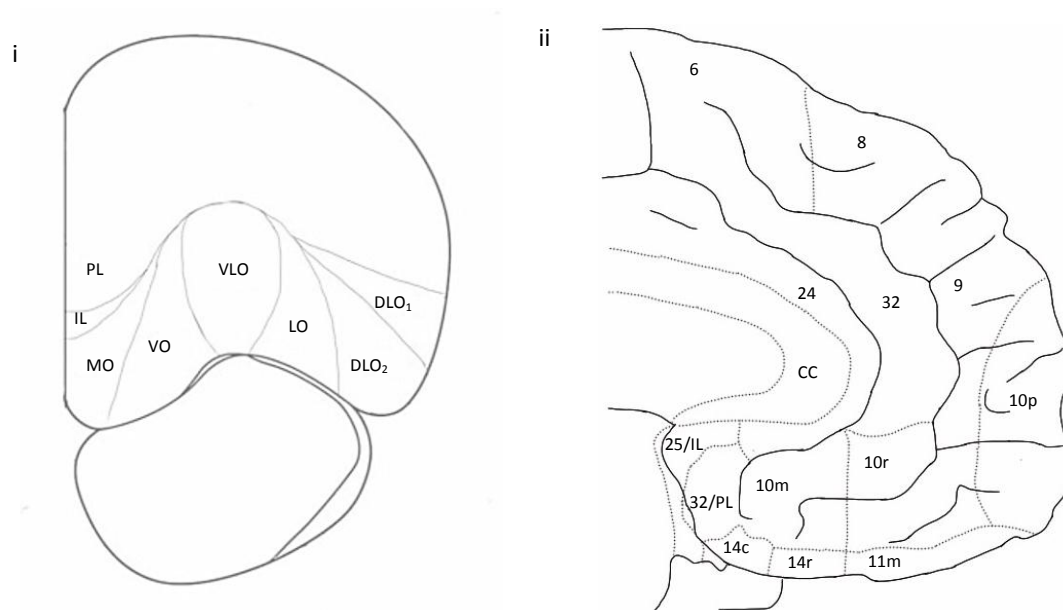


Figure 1.1. Coronal sections showing the cytoarchitectural sub-divisions of PFC in (i) rats, according to Van De Werd & Uylings (2008) and (ii) humans, according to Ongur et al (2003).

It is clear that rats possess much of the PFC properties found in primates and humans. However, there is no dispute that rats lack the granular PFC found in primates, thought to be a product of evolution. Despite this, neuroscientists have claimed, based on similarities in the effects of lesions, anatomical and physiological similarities, that the medial aspect of frontal cortex in rats is homologous to the granular lateral PFC in primates (Kolb, 2007; Seamans et al, 2008). The medial PFC of the rat is said to be most likely comparable to human PFC regions associated with psychopathology, psychosis, sociopathy, depression and addiction. This makes the rat a useful model on which to build an understanding of PFC organisation, which is comparable to areas of interest in humans. Based on such comparisons it is reasonable to assume that findings from rat PFC connectivity are largely comparable to that in primates, including humans.

2. Function

2.1 Cerebral Cortex

The localisation of function is a recurring interest in neuroscience research, not only of the complex functions of PFC but for numerous processes carried out across the entire brain. The desire to

understand individual functions in increasingly fine detail has inevitably led to the need to understand brain structure and connectivity at a greater resolution.

It is understood that the cerebral cortex as a whole is the most highly developed part of the brain. On a broad scale, the cortex is divided into lobes, each of which is further divided into sub-regions according to function. The parietal lobe includes visual, auditory and somatosensory cortex and is involved in processing sensory information. The temporal lobe is associated with memory retention, emotion, auditory processing and language. The occipital lobe is involved in vision and memory, and the frontal lobe (including prefrontal cortex) is involved in executive functions, decision-making, problem solving, abstract thinking and forward planning. All cortical regions can generally be divided into either sensory, motor or association regions.

2.2 Prefrontal Cortex

Once assumed to hold no real function, it is now understood that the prefrontal cortex is one of the most highly connected regions within the human cerebral cortex (Fuster, 1999). Connections to PFC have been reported from brain regions associated with attention, cognition, action, emotion, reward expectation, processing of outcomes, arousal, sleep, memory, movement, inhibition, distractions (Stuss & Benson, 1986; Schnider et al, 2005; Gehring & Willoughby, 2002; Stuss & Levine, 2002; Goldman-Rakic, 1996).

Early human neuroscience studies soon identified function associated with PFC, demonstrating that removal of the PFC resulted in a reduction in anxiety, emotional outbursts and impaired ability in complex tasks, specifically those requiring a delayed spatial response (Golz, 1890; Jacobsen et al, 1935). These early findings formed an important basis for our understanding of the involvement of PFC in emotion, reward and complex functions. The anterior location and volume of PFC in humans makes it vulnerable to damage and injury, resulting in impairment of its complex processes and functions. Case studies of PFC injury have revealed the importance of the region in personality and emotion, as well as its involvement in anxiety, empathy, ambition and social control (Goldman – Rakic, 1995, Fuster, 2008). Despite our increased knowledge of PFC as an integrative association area and our growing knowledge of PFC connectivity, the fine detail of underlying physiological and anatomical mechanisms remains largely unknown.

PFC is widely recognised in having the ability to represent information which is not currently available in reality i.e. abstract representation (Fuster, 2000; Goldman-Rakic 1996). It is proposed that abstract representation of information and events in PFC enables the region to guide us in thought,

action and emotion. Working memory serves as an important aspect of the integration of information in PFC and allows for the combination of information from past and present events for decision making (Fuster, 2000). It is understood that PFC integrates information received from several other brain regions including the thalamus, amygdala and hippocampus as well as cortical regions.

Current observations in neuroscience research have revealed PFC to be highly associated with executive functions in humans such as forward planning, decision making and goal directed behaviour (Alvarez and Emory, 2006; Miller and Cohen, 2001) as well as temporal processing and autonomic functions (Kolb, 1984; Neafsey, 1990; Schoenbaum & Esber, 2010). PFC in rats is known to be linked functionally to motor cortex, involving it in motor processing (Narayanan & Laubach, 2006; Vertes, 2006; Kim et al 2013), PFC is also associated with cognitive processing and emotional control (Fryszak & Neafsey, 1994; Vertes, 2006). The prefrontal cortex of rats has been implicated in autonomic control, working memory, attention, response initiation and emotion (Fryszak & Neafsey, 1994; Vertes, 2006; Shoenbaum & Esber, 2010; Neafsey, 1990; Kolb, 1984; Alvarez & Emory, 2006).

It is understood that working memory processing and retrieval play an important role in the abstract processes of PFC in primates (Fuster, 1990; Goldman-Rakic, 1990; Cohen et al, 1997). The dynamic filtering theory suggests that PFC acts as a filtering region, allowing the high level control of various processes; filtering information from across the cortex and allowing for the regulation of emotion (Shimamura, 2000). Further to this, Miller and Cohen's (2001) integrative theory of PFC function expands on the earlier observations of Goldman-Rakic (1996) and Fuster (2000), stating that PFC guides input connections, integrates information from different cortical regions and mediates our actions. Miller and Cohen suggest that PFC is able to integrate information in order to create rules and goals, as well as providing guidance to other cortical regions by means of top-down processing.

The importance of PFC in working memory is undisputed; however, the functional organisation of PFC in terms of working memory remains unclear, meaning that a definitive explanation of working memory has yet to be produced. Courtney et al (1998) suggest that the different PFC regions may contribute specific functions within working memory tasks, the organisation of which could be important in successful task performance. The same review concludes that different PFC regions may be involved in different aspects of working memory, indicating that some level of ordered organisation must be present.

There have been great advances in our understanding of PFC, however there remains a level of controversy and a lot to be explained in finer detail, especially in comparison to other areas of the brain that are much more clearly defined. Critical to advanced human function, PFC is described as being regulatory in the thought processes that drive decision-making responses. Our complex prefrontal functions allow us as humans to implement strategic forward planning and change our

actions according to environmental cues, in order to carry out goal directed behaviours. It is also our prefrontal cortex processing that allows us to evaluate events or concepts based on our prior knowledge, using our working memory (Fuster, 2000). This requires complex circuitry between PFC and multiple cortical and subcortical brain regions.

PFC has been implicated in a number of neurological disorders in humans such as autism and psychosis (Courchesne et al, 2001; Perlstein et al, 2001; Cohen, 1999; Goldman-Rakic, 1991). It is thought that abnormal connectivity in PFC pathways may be a contributing factor to their manifestation. However, the precise neuronal circuitry of PFC regions remains largely undefined, meaning the functional connectivity cannot yet be fully understood.

Neuropsychological research has implicated different PFC regions in an equally wide range of high order functions. DLPFC has been associated with top-down functions such as working memory processes thought to mediate higher order functions and inhibition, whereas mPFC is directly involved in higher order functions and integrates goal directed behaviour in rats (Hoover and Vertes, 2007). Dorsomedial PFC (dmPFC) regions hold functional connections with motor cortex and have been found to be involved in motor and temporal processing (Narayanan and Laubach, 2006). Infralimbic (IL) and prelimbic (PL) mPFC regions in rats are known to have separate functions, dorsal areas are associated more with motor functions and ventral mPFC is involved in emotive responses (Vertes, 2006; Narayanan and Laubach, 2006; Kim et al 2013). Orbital PFC in rats is thought to be involved in associative learning and decision making (Schoenbaum and Esber, 2010; Schoenbaum and Roesch, 2005). Evidence shows that the agranular insular region of PFC has an involvement in sensory processing (Fujita et al, 2011; Gallagher et al, 1999).

3. Structure

3.1 Cerebral Cortex

The mammalian brain is divided into multiple differentiated regions and sub-regions. On a basic level all of these regions, which carry out very different processes, are fundamentally the same in their structure. All cortical regions of the brain contain neurons, and each of these neurons is connected to others by synapses. It is evident that the processes that a particular brain region is involved in are dependent largely on the way in which the neurons that make it up are connected in a structural network in the human brain (Honey et al, 2010). The most widely used classification of cortical regions based on architectural differences was produced by Brodmann (1909), who divided the human

cortex into 51 distinct areas. Many regions described by Brodmann have since been identified with their own individual complex structural organisations and functions.

3.2 Prefrontal Cortex

The prefrontal cortex in mammals, much like other cortical regions, has traditionally been defined by cytoarchitectural features. It is thought that the cytoarchitectural subdivisions of prefrontal cortex in humans (described by Brodmann, 1909) correspond to distinct functions. In the rat, PFC is typically divided into medial prefrontal cortex (occupying the medial wall of the region), orbital prefrontal cortex (dorsal to the olfactory bulb and rhinal sulcus) and agranular insular regions (anterior of the rhinal sulcus) (Van De Werd & Uylings, 2008). Each of these regions is said to hold distinct functions, which correspond to a large extent to those found in primates and humans. Medial PFC is associated with rule switching, attention shifting (Furuyashiki & Gallagher, 2007), fear response (Morgan & LeDoux, 1995), working memory and behavioural flexibility (Heidbreder & Groenewegen, 2003). Orbital PFC has been found to be involved in reversal learning (McAlonan & Brown, 2003; Chudasama & Robbins, 2003). Agranular insular cortex and OFC as a whole are thought to have a role in the anticipation of reward and working memory (Kesner & Gilbert, 2007; Schoenbaum et al, 1998). However, there is no clear definition of unique functions belonging to each subdivision.

Prefrontal cortex architecture follows the same characteristic pattern of development, in terms of expansion, cell migration and lamination, as the rest of the cerebral cortex (Angevine, 1970; Sidman & Rakic, 1973). This basic architecture is established by genetics, however further development continues for 20 years in humans. Perhaps it is the fine detailed changes in structure that continue for this time that result in such a highly complex cortical region. The anatomical architecture of PFC is not known to be significantly dissimilar to other brain regions. With this in mind, there is no clear anatomical reason why the connectivity of PFC should be significantly different to that seen elsewhere in the cerebral cortex. However, it is clear that PFC is involved in some of the most complex and evolutionary advanced cognitive processes; therefore it is reasonable to suggest that something must be different in its anatomy for PFC to be able to carry out such complex tasks.

4. Organisation

4.1 Cerebral Cortex

Topographic Organisation of Cerebral Cortex

The organisation of cortical connections is highly complex. However, despite vast differences in function and connectivity between brain regions, there is a recurring theme in organisation throughout the brain. Topographic organisation has been described as a hallmark feature of cortical organisation among vertebrates (Thivierge & Marcus, 2007) and is widely regarded as necessary for complex brain function (Thivierge & Marcus, 2007; Kaas, 1997). Topographic connectivity refers to point-to-point mappings, which preserve the spatial arrangements of information; nearby locations in a source region connect to nearby locations in the target region, maintaining the same spatial organisation. Topographic maps allow for efficient local computations by grouping together neurons that interact the most, or are consistently activated at the same time. This reduces metabolic costs in terms of wiring and efficiently deals with the allocation of resources (Serenio & Huang, 2006; Kaas, 1997).

The existence of ordered representations of sensory processes has long been known. Topographically ordered physiological and anatomical organisation has been described for multiple regions of cerebral cortex including motor, sensory, auditory, visual and temporal cortex in rodents, primates, cats and humans (Arcaro, 2009; Albright, 1987; Lemon, 2008; Penfield, 1937; Merzenich, 1975; Welker, 1971; Woolsey, 1967; Hafting et al, 2005). Many physiologically topographic cortical regions are also known to contain topographically ordered anatomical connections in primates (Perkel et al, 1986; Albright & Desimone, 1987; He et al, 1995; Suzuki and Amaral, 1994; Arcaro et al, 2009), giving a strong indication of underlying anatomical topography of ordered functional maps in rodents (Porter and White, 1983; Aronoff et al, 2010; Henry and Catania, 2006). There are multiple topographic maps described within the visual cortex. Retinotopic maps, in which the image received by the retina is maintained in terms of spatial order when projected to V1, were amongst the earliest described topographic cortical representations. The clear physiological topographic ordering, on which visual cortex relies, is dependent on underlying anatomical connections (Perkel et al, 1986). This is thought to be the case throughout the cerebral cortex.

Hierarchical Organisation of Cerebral Cortex

In a traditional model of hierarchical organisation, PFC is positioned at the top of a processing hierarchy (Botvinick, 2008; Fuster, 2001; Alexander et al, 1986). In a hierarchical model, connections would travel from primary sensory cortex, followed by secondary sensory cortex and association areas, then reaching the top of the processing hierarchy e.g. PFC. This is followed by return connections travelling to secondary motor cortex followed by primary motor cortex (e.g. S1 → S2 → Association areas → PFC → M2 → M1), it is understood that reciprocal connections exist between source and target regions at each level of the hierarchy. Based on this understanding of cortical connectivity, it is thought that all cortical networks must contain a significant level of reciprocity in order to function, making it a fundamental structural component.

4.2 Prefrontal Cortex

Topographic Organisation of Prefrontal Cortex

In comparison to cortical regions such as motor and sensory cortex, there have been relatively few descriptions of detailed ordered organisation in PFC. However, what has been found can offer a great deal of insight into the organisation of its structure. It has been suggested that association and prefrontal cortex may not be as specific in terms of the information represented as other regions. It is understood that neurons in PFC possess the unique capability of encoding different types of information (Duncan, 2001). Duncan's (2001) adaptive coding model proposes that all PFC neurons are recruited in all tasks, resulting in little functional specialisation of individual neurons. This may be a large contributing factor to the relatively few ordered maps found in this region to date, along with obvious difficulties raised in deciphering abstract topographies. This is in comparison to the more easily detectable motor and sensory representations.

Many early studies identified the PFC connection to the subcortical medio-dorsal thalamic nucleus as being highly topographically ordered (Walker, 1940; Rose and Woolsey, 1948; Leonard, 1969; Uylings and Van Eden, 1990). This consistent finding of topography implies that PFC cortical connections may also be topographically and reciprocally organised, much like the rest of the mapped cerebral cortex. However, the fine scale organisation remains relatively unclear and the presence of sub-cortical topography does not necessarily infer cortico-cortical topographic connections. As well as prominent subcortical networks, PFC is known to hold connections with a vast number of cortical regions. It is the organisation of these cortical connections that hold the key to understanding complex

PFC functions. Adrianov (1978) described cortico-cortical connections as a distinctive trait of primate evolution. Therefore defining the detailed organisation of PFC cortico-cortical connections can provide a great insight into high order functioning. Recent advances in anatomical neuroscience have enabled the visualisation of these connections in greater detail than ever before.

Funahashi (1989) found that prefrontal neurons possess information about the location of visual cues. Although only demonstrated for a subset of neurons, the findings established that different neurons code for different cue locations, implying a topographic map. Sawaguchi (2001) reported a gross topographic map in DLPFC in monkeys, identifying specific sites responsible for the working memory process of specific visuospatial co-ordinates, to guide goal directed behaviour. As there is evidence for topographic maps in DLPFC, and therefore associated topographic connections, there is reason to propose that a similar organisation exists elsewhere in the PFC. Evidence of spatially ordered maps within human frontal cortex was described by Hagler and Sereno (2006); the use of a facial recognition task revealed reproducible topographic maps within several frontal areas. Although organised in some manner, the described map requires the attention to objects in specific spatial locations. Topographic maps were revealed in dorsolateral prefrontal cortex. The study identified clear representations of visual space in areas of PFC, indicating the presence of ordered topographic maps.

The use of fMRI in humans has revealed topographic maps in frontal cortex regions (Kastner et al, 2007), spatial working memory tasks indicated two distinct topographic maps covering pre-central cortex. The topographic maps identified were described as different in terms of their representation of visual space, in comparison to the organisation found in visual and parietal cortex (Kastner et al, 2007). Notably, Kastner et al (2007) reported no evidence of topographic organisation in dmPFC and described high levels of individual variation, only in frontal cortical regions. This suggests that prefrontal organisation may not be as systematic and consistent as the topographic maps identified elsewhere. Contrary to Kastner's (2007) findings, Taren et al (2011) proposed a model of parallel ordered organisation in both DLPFC and DMPFC. Taren et al (2011) identified a posterior to anterior connectivity gradient in DLPFC, indicating evidence of a topographically ordered organisation of connections. The parallel topographic map was reproduced from posterior to anterior DLPFC regions during resting state fMRI, and showed increasingly diffuse connections towards more lateral regions. A similar ordered hierarchical organisation of DLPFC connections has been described in primates (Petrides and Pandya, 1999). This suggests hierarchical ordered organisation across DLPFC, which according to Taren (2011) could represent the dynamic processing and adaptability of PFC functions. Christoff (2009) described a similar phenomenon of dynamic organisation in which PFC is topographically organised according to levels of abstraction, where PFC becomes more anterior its representations become increasingly abstract. fMRI has revealed evidence of topographic maps in

human parietal and frontal cortex in which visual field representations are reproduced (Hagler, Riecke and Sereno, 2007; Silver and Kastner, 2009).

Electrophysiological findings show that different types of demands revealed the same PFC co-recruitment in monkeys (Miller, 2002). Just et al (2001) demonstrated that humans cannot carry out two tasks which are considered to involve complex processing simultaneously, this indicates that the same neurons must be required for these different tasks, putting them in multiple functional maps. This may be a large contributing factor to the relatively few anatomical and functional maps established in this region to date. It may be possible that PFC areas possess the ability to express different topographic representations at different times. Such phenomena have been described in parietal cortex in monkeys (Heider, 2005). Interestingly, this is a region in which many established topographic maps are representative of the visual field, similar to those that have been observed in DLPFC. This gives an indication that PFC is likely to be organised in a similar way.

Rapid advances in neuroimaging are constantly improving our ability to visualise and localise brain function. However, the results of functional neuroimaging studies cannot be fully understood and interpreted until the underlying structural anatomy is understood. Based on the evidence discussed here, functional connections of PFC appear to be organised similarly to other brain regions, in a topographic order. Therefore it is reasonable to propose that the anatomical connectivity is no different. With this in mind, it is also clear that the functional capabilities of PFC are more complex than other cortical regions, so it is plausible that the underlying anatomical connectivity may be more complex.

Hierarchical Organisation of Prefrontal Cortex

Traditional models of hierarchical organisation indicate that PFC must be arranged in some kind of logical order to enable it to successfully connect with other cortical regions, as do historical theories of reciprocal connectivity. Hebb (1949) states that an ordered map is guaranteed as long as the initial projection is ordered. If the initial input projection from a secondary sensory region is topographically ordered (which previous findings state they are), then according to Hebb's law PFC cortical connections would also have to be topographically ordered.

5. Connectivity

5.1 Cerebral Cortex

The anatomical connectivity of a given cortical region is often a strong indicator of the overlying physiological organisation. That is, how a region is connected anatomically can often provide us with important detailed information about how it works in terms of function (Zeki & Shipp, 1988). For instance, in human somatosensory cortex, ordered representations correspond to the physical spatial layout of structures on the surface of the body (Penfield, 1951). The functional organisation of a given cortical region is thought to be highly dependent upon underlying structural organisation (Honey et al, 2010; Bullmore and Sporns, 2009). Clear relationships between structure and function are common across biological systems, with structural organisation providing the basis and physiological constraints of function (Honey et al, 2010). It is suggested that the ability of a group of neurons to synchronise their activity depends on their ordered structural connectivity (Buzsaki and Draguhn, 2004).

The ordered structural arrangement identified in projections from primate visual cortex (Nakamura et al, 1993; Zeki, 1980; Ungerleider et al 1986a) is thought to be a direct product of the visual processing requirements of different regions (Gattass, 2005). Similar relationships between structural and physiological connectivity patterns have been described throughout the cerebral cortex. Gattass et al (2005) proposed that the functional topographic maps described within visual processes are largely consequences of topographically ordered anatomical connections within the associated visual pathways (Perkel et al, 1986).

Structural connectivity data has proven invaluable in connectivity research. For instance, functional connectivity studies have defined unique input and output connections to cytoarchitecturally distinct PFC regions with the implementation of anatomical connection data. Passingham et al (2002) identified unique connectional fingerprints associated with different cortical regions, in which no two regions produced the same pattern of cortico-cortical connections. Similar studies have used neuroinformatics to demonstrate the unique connectivity patterns of functionally distinct frontal regions (Averbeck & Seo, 2008). The clear relationship between functional and structural connectivity patterns throughout the cerebral cortex demonstrates the advantages of defining anatomical connectivity to gain an understanding of functional organisation.

Topographic Cortical Connections

Topographic, reciprocal and aligned organisation of connections is clearly abundant in the mammalian brain; however it remains unclear why this type of organisation is so prevalent. Topographic mapping is not present in all cortical connections. However, all of the most highly studied cortical regions contain considerable ordered anatomical mapping of some kind. Goldman-Rakic (1988) stated that topography may be of vital importance in successful cognition, implying it would be necessary for all cortical regions. A common assumption is that topographic connections serve primarily to preserve sensory information. Hebb (1949) claimed that topography actually provides no functional advantage, arguing that topographic organisation in associative regions (such as PFC) would not make sense if the primary role of the region is to integrate and merge information, not to preserve it in a spatial order. Topography may not be functionally advantageous at all, but an evolutionary by-product of minimising neural wiring costs (Buzsaki, 2004). This means that even if not for functional efficiency, we would expect PFC to possess topographically ordered connections as a result of evolutionary reductions in wiring costs. Although topographic organisation is a common feature in the mammalian brain, some argue that prevalence does not mean necessity (Buzsaki, 2004). It has been suggested that information processing in complex centres, such as PFC requires a combination of different types of connectivity patterns, for example, a complex combination of topographic, convergent and divergent maps (Montagini and Treves, 2003).

Notably, many regions known to have strong connections to areas of PFC are consistently largely topographically organised. Topographically ordered and reciprocal connections have been described in the pathway between visual cortex and areas of sensory and motor cortex in rats (Miller and Vogt, 1984). Miller and Vogt (1984) suggest that the ordered reciprocal connections of visual cortex provide a means for integration and visually guided behaviour, thus implying that reciprocal, ordered (and therefore also aligned) connectivity is an important basis for complex processing. However, the authors also reported a large number of non-reciprocal connections from perirhinal to visual cortex, whereby input connections are found considerably posterior in comparison to output connections. This shows some evidence for non-alignment of input and output connections within the perirhinal - visual cortex pathway (where alignment refers to input and output connections projecting to the same location). Topographically ordered reciprocal connections have also been described within somatosensory cortex in monkeys (Coq et al, 2004), and from M1 to S2 in cats (Burton and Kopf, 1984), in which a uniform ordered pattern of connections from S2 was reported. Interestingly, the same study observed areas of somatosensory cortex which exhibited no topographic organisation of connections. Despite there being clear evidence for non-topographic and non-reciprocal connections occurring in these regions, they are relatively small instances compared to the much more reproduced

reported topography. It appears that the regions described are mostly highly reciprocal and topographically organised. Further evidence for topographic organisation of cortical connections has been reported between temporal and visual cortex in marmosets (Spatz, 1977). Clear ordered and aligned connections have been described in the projection from S1 to S2 in monkeys (Pons and Kaas, 1986). Anterograde tracing studies have identified reciprocal topographic connections from perirhinal (PRh), postrhinal and Ect in rats, although the degree of reciprocity was reported to vary across these regions (Agster and Burwell, 2009).

Reciprocity and Alignment of Cortical Connections

Along with topographic ordering of connections, reciprocity and alignment of input and output connections is a common attribute in the cerebral cortex. Observations of perirhinal, entorhinal and parahippocampal regions in primates (Suzuki and Amaral, 1994; Canto et al, 2008) identified reciprocal connections to be a recurring property. Similarly, reciprocal cortical connections, most notably in the well-defined visual cortex, are widely described and are shown to maintain clear alignment between inputs and outputs from V1 (Triplett, 2009; Tigges et al, 1973), V2 (Nascimento-Silva et al, 2014) and MT (Spatz, 1977; Maunsell & Van Essen, 1983).

5.2 Prefrontal Cortex

Based on evidence from other cortical regions, the identification of an ordered functional organisation within PFC implies the existence of an underlying ordered arrangement of anatomical connections. To date there is no widely accepted organisational pattern of PFC connections, and there have been few detailed anatomical studies of the arrangement of PFC projections. Research has attempted to establish how prefrontal cortex is organised in terms of processes and information. Johnson (2003) proposed that PFC organisation is dependent upon a specific combination of information and processes e.g. a specific neuron is not always activated by specific information, it is only activated by that information when a certain process is also present. Johnson et al (2003) found different regions to be activated when the same information was processed differently. Similarly, Kargo (2007) demonstrated that PFC neurons in mice varied their discharge patterns depending on the action choice and specific rewards received. It has been reported that pharmacological blockade of monkey DLPFC can induce topographically mapped memory impairments (Sawaguchi and Iba, 2001); however this observation has not been reproduced by similar more recent reports.

To date there is no commonly accepted structural organisation of PFC, particularly in terms of cortico-cortical connections. There have been few detailed and systematic anatomical studies of the organisation of its projections. The current literature has identified evidence for an ordered organisation of PFC in terms of physiology; however the precise circuitry is evidently more complex than the more clearly understood cortical regions (e.g. visual and motor cortex) and is yet to be fully defined. In order to clearly establish the nature of physiological organisation within PFC, it is necessary to first gain a more detailed picture of the underlying anatomical connectivity.

Topographic Prefrontal Connections

Topographic organisation is so prominent throughout the mammalian brain that it is often viewed as a fundamental component of cortical connectivity (Kaas, 1997). PFC has in fact often been described as being topographically organised and is considered to be established as reciprocal in nature (Pandya et al, 1971). Goldman-Rakic (1989) suggests that PFC is part of a complex and integrated network of cortical regions, and described a substantial topographic ordering between PFC and posterior cortical regions in monkeys. However, it should be noted that these observations are based primarily on broad scale findings, which did not allow for the highly detailed examination of anatomical connections that is possible with modern technologies. Therefore, although PFC may appear to be organised in the same manner as other more clearly understood cortical regions in terms of topology, more recent findings show us a different, more contradictory picture of PFC organisation.

Diffusion tractography in monkeys and humans has revealed ordered organisation in the pathway between PFC and mediodorsal thalamus, in which two distinct networks associated with distinct aspects of reward-guided behavior were identified (Klein et al, 2010). This gives a clear indication of broad PFC topography. In addition, an ordered shift in anatomical connections has been described from dorsal to ventral PFC in rats (Heidbreder & Groenewegen, 2003), meaning that the locations of labels follow an ordered arrangement, maintaining the spatial representation of PFC origins. Schilman (2008) used tracers to identify a similar topographic arrangement in anatomical connections, from dorsal to ventral as well as from medial to lateral, in connections between PFC sub-regions and the caudate-putamen in rats. These relatively broad scale studies all point towards a topographically ordered PFC expected based on other cortical regions.

Advances in neuroanatomical tracing methodology over recent years has allowed for the visualisation of cortical connections in increasing detail, resolution and accuracy. Connection studies using neuroanatomical tracers indicate that PFC displays gross-level topologically organised connections. PFC forms part of large scale topologically arranged (in terms of anterior-posterior) cortico-cortical

pathways, and ordered projections from lateral and medial PFC regions to the posterior cingulate area have been reported in cats (Olson & Musil, 1992). Tracer studies have demonstrated a broad medial-lateral topographic organisation of connections from PFC sub-regions to sub-cortical structures (Berendse, 1992; Schilman, 2008). A medial-lateral shift in injection sites in PFC produced a corresponding medial-lateral shift in anterogradely labelled projections in striatum and caudate putamen in rats (Schilman, 2008). However, this ordered arrangement has only been reported in subcortical PFC projections, and is described only between cytoarchitecturally distinct PFC sub-regions. Gross topographic organisation of both input and output connections of the orbital prefrontal cortex to temporal cortex (notably perirhinal cortex) has recently been reported in monkeys (Saleem et al, 2008). The same study also reports two distinct organisational networks within PFC, in which some areas overlap and can be assigned to both networks. Anatomically distinct networks connecting to PFC sub-regions have also been described in human diffusion tractography studies (Klein et al, 2010). This provides evidence of complex, but ordered, organisational patterns of connectivity within PFC and supports ideas of prefrontal neurons being able to carry out multiple processes (proposed by Duncan, 2001), in which they adapt their processes to current demands.

Anterograde tract tracing findings have revealed spatially ordered projections from the medial prefrontal cortex (mPFC), both within and across different cytoarchitectural areas. There are clear ordered projections from adjacent areas of insular cortex to adjacent regions (PL and IL) in mPFC (Sesack, 1989). There is clear evidence that the pattern of connections from IL differs significantly to that from PL (Vertes, 2003), which is consistent with evidence to suggest different roles for PL and IL (Hoover and Vertes, 2007). Similarly, retrograde tracing has produced evidence for ordered organisation of connections from the different sub-regions of mPFC in rats, with each region receiving substantially different projections (Hoover and Vertes, 2007). Hoover and Vertes (2007) identified a clear shift in the pattern of connections in mPFC, where dorsal regions received projections from sensorimotor cortex and the thalamus in contrast to limbic cortical and midline thalamus inputs to more ventral regions of mPFC. The same study described a topographically ordered connection between insular cortex and mPFC, consistent with that reported by Gabbott et al (2003).

Further, retrograde tracers reveal projections of medial orbital (MO) and ventral orbital (VO) cortices in the rat (Schilman, 2008; Berendse, 1992). The findings showed that within orbital PFC, MO is more involved in a medial prefrontal network than VO, implying a specificity of organisation. The prominent cortical targets (orbital fields) of MO and VO were found to be adjacent. The findings demonstrated a topographical organisation of MO and VO projections to medial dorsal striatum. They also revealed convergent organisation of projections from MO and VO, e.g. to the thalamus.

Retrograde tracer studies have reported a topologically organised projection from rat lateral prefrontal cortex to perirhinal cortex and area TE in rats (Hoover and Vertes, 2011), in which MO and VO in PFC project to the same broad regions, with MO labels being observed ventrally to VO labels. There was a significant overlap between labels from MO and VO. MO connections were described as more widely distributed in the target region compared to VO projections. Similarly, dual tracer studies have indicated evidence of ordered organisation of projections from PFC to subcortical structures in rats (Kim and Lee, 2012) and from prefrontal cortex to dorsal premotor cortex in monkeys (Takahara et al, 2012). Similarly, pathways arranged in parallel organisations have been described from PFC to rhinal cortices (Bunce et al, 2013). Miyachi (2013) demonstrated a topographically ordered projection between monkey prefrontal cortex and representations in primary motor cortex. However, these findings often report PFC connectivity on a relatively large scale and from specific sub-regions, lacking the detail and systematic approach required to determine PFC structural organisation as a whole. Recent findings from Kondo and Witter (2014) described topographic organisation of the projection from orbitofrontal cortex to the parahippocampal region in rats. They demonstrated an ordered arrangement of output connections from PFC sub-regions (MO, VO, LO) to areas of perirhinal, postrhinal and entorhinal cortex. This ordered arrangement is however limited to the output projection, meaning that the organisation of connectivity in terms of reciprocity, alignment and the relationship between input and output connections remains unknown.

Reciprocity and Alignment of Prefrontal Cortex

PFC connections are often assumed to be reciprocal, as this appears to be a common attribute elsewhere in the cortex. Although the evidence is clear for the existence of reciprocity in PFC, there is also emerging evidence for the existence of non-reciprocal connections. There have been reported cases of input and output connections within motor and sensory cortex ‘missing each other’ (Flaherty and Graybiel, 1994), resulting in topographically mismatched pairs; some labelled projections between striatum and motor/sensory cortex demonstrated that regions did not receive inputs from the same area they sent outputs to. However, the same study reported a general rule of strong alignment and assigned instances of mis-matching of inputs and outputs to uncontrolled variances. MacFarland and Haber (2002) identified non-reciprocal connections in pathways between frontal cortex and the basal ganglia with anterograde and bidirectional tracers. Evidence that not all cortical connections are reciprocal gives rise to the possibility that it may not be necessary for PFC to be reciprocally connected in order to function efficiently.

It is clear from the current literature that there remains a level of controversy surrounding the organisation of the prefrontal cortex, especially in terms of its cortical connections. In order to enable a clearer understanding of functional organisation, it is necessary to first build upon the current knowledge surrounding anatomical organisation. Developing an anatomical map has the ability to offer great advances in our understanding of how this relatively little understood brain region works.

6. Aims

This PhD established the organisation of prefrontal cortex connections, providing a clearer understanding of prefrontal cortex structure. The project defined the anatomical organisation of input and output connections from PFC at a level of detail and precision which has not previously been described.

The following thesis describes a series of experiments, which tackle the current problem of a limited structural understanding of PFC. The goal of this PhD was to systematically identify the structural organisational pattern of PFC connections in such detail that has not previously been described. We began the project by investigating the fine scale connections of two distinct pathways from the same region of prefrontal cortex. This study formed a basis on which to build a more complex investigation, and revealed previously unexplored structural properties of prefrontal cortex connections. We expanded our analysis of connections across a wide area of PFC, allowing us to develop a connectivity model for the whole region. We then proceeded to examine the connectivity patterns of these PFC pathways at a greater resolution, allowing us to define novel fine scale structural and connectional properties of two PFC pathways.

6.1 Broad Scale Prefrontal Cortex Connections

The initial study established the broad scale input and output connections of PFC, in order to determine the ordered connectivity. This provided an important basis on which to build the proceeding studies into fine scale connectivity, as well as enabling the development of a connectivity pattern across the whole of PFC.

Retrograde and anterograde neuronal tracers were injected into regions of medial and lateral prefrontal cortex (prelimbic (PrL), ventral orbital (VO), lateral orbital (LO) and dorsolateral orbital cortex (DLO) and their projections studied. We employed an extensive numerical analysis of the retrograde and anterograde labels in target regions in order to create an accurate 3 dimensional

representation of where projections were in the brain. We then applied statistical analyses to determine the ordered organisation of PFC connections in two pathways, as well as the relationship between input and output connections. We also examined how the connectivity pattern changed across the whole area of the prefrontal cortex.

6.2 Fine Scale Prefrontal Cortex Connections

The fine scale connectivity aspect of this project examined PFC connectivity on a finer scale, enabling us to determine properties of two PFC pathways (temporal and posterior-frontal cortex), which cannot be seen at a greater resolution. We achieved this by using the smallest possible injected anterograde and retrograde tracer volumes that we were able to visualise, enabling us to investigate the connections from PFC injection sites placed only 0.5mm apart.

By numerically analysing the projections to two target regions (temporal and sensory-motor cortex), and applying statistical analyses we were able to identify properties of ordered organisation, reciprocity and alignment of input and output connections which could not have been observed on a larger scale.

Chapter 2.

Organisation of Prefrontal Cortex – Temporal Cortex Connections

In contrast to other regions of the cerebral cortex, the structural organisation of PFC remains relatively little understood, and lacks a clear definition. There have been reports of ordered arrangements of connections within PFC (Goldman-Rakic 1988; Giguere and Goldman-Rakic 1988; Schilman et al. 2008; Hoover and Vertes 2011; Berendse et al. 1992; Sesack et al. 1989; Kondo and Witter 2014). Functional studies have also identified maps in the frontal cortex (Sawaguchi and Iba 2001; Hagler and Sereno 2006; Kastner et al. 2007; Christoff et al. 2009; Klein et al. 2010; Taren et al. 2011; Venkatraman et al. 2009), however there is currently no accepted fine-scale functional organisational pattern of PFC.

Reciprocity and a high degree of alignment between input and output connections is apparent throughout the cerebral cortex, both in terms of anatomy (Triplett et al, 2012) and physiology (Wang et al. 2006; (Cantone et al. 2005; Nascimento-Silva et al. 2014). The alignment of prefrontal cortex inputs and outputs is relatively undefined. Studies of the temporal cortex have shown that its connections with the prefrontal cortex and elsewhere are largely reciprocal (Agster and Burwell 2009). There is also evidence that these connections are not always clearly aligned when viewed at high resolution (Agster and Burwell 2009).

Aims

The intention of the initial study was to identify the ordered arrangement of broad scale PFC connections, as well as the alignment of input and output connections. This would provide an important basis on which to build a further investigation into the fine scale arrangement of PFC connections. Co-injections of retrograde and anterograde neuroanatomical tracers were made into rat medial and lateral prefrontal cortex (prelimbic (PL), ventral orbital (VO), lateral orbital (VLO) and dorsolateral orbital cortex (DLO).

Methodology

Animals

Data was collected from 18 adult male Sprague-Dawley CD rats (294-371g, Charles River, UK). Animal procedures were carried out in accordance with the UK Animals scientific procedures act (1986), EU directive 2010/63 and were approved by the Nottingham Trent University ethical committee. On receipt the rats were examined for signs of ill-health or injury. The rats were acclimatised for ten days during which time their health status was assessed. Prior to surgery the animals were housed together in individually ventilated cages (IVC) (Techniplast double decker Greenline rat cages). The animals were allowed free access to food and water. Mains drinking water was supplied from polycarbonate bottles attached to the cage. The diet and drinking water were considered not to contain any contaminant at a level that might have affected the purpose or integrity of the study. Bedding was supplied by IPS Product Supplies Ltd in form of 8/10 corncob. Environmental enrichment was provided in the form of wooden chew blocks and cardboard fun tunnels (Datesand Ltd., Cheshire, UK). Post- surgery the animals were individually housed in the same conditions. The animals were housed in a single air-conditioned room within a barrier unit. The rate of air exchange was at least fifteen air changes per hour and the low intensity fluorescent lighting was controlled to give twelve hours continuous light and twelve hours darkness. The temperature and relative humidity controls were set to achieve target values of $21 \pm 2^{\circ}\text{C}$ and $55 \pm 15\%$ respectively. Individual bodyweights were recorded on Day -10 (prior to the start of dosing) and daily thereafter. All animals were examined for overt signs of ill-health or behavioural change immediately prior to surgery dosing, during surgery and the period following surgery. There were no observed clinical signs/ symptoms of toxicity or infection. There was no significant effect on body weight development detected.

Surgical and Experimental Procedures

Rats were anaesthetised with isoflurane (Merial, Harlow, UK) and placed in a stereotaxic frame with the incisor bar set so as to achieve a flat skull. Craniotomies (< 1mm diameter) were made at predetermined stereotaxic coordinates (according to Paxinos & Watson, 1998). Sterile tracer solution was deposited into the prefrontal cortex by injection, via a 0.5µl Neuro-syringe (Hamilton, Germany). Injections of anterograde (biotinylated dextran amines; Fluorescein (catalog #: SP-1130) and Texas red (catalog #: SP-1140), Vector Laboratories, CA) and/or retrograde tracer (4% Fluoro-Gold in distilled water, Fluorochrome, Denver, Colorado) were made into the prelimbic (PL), ventral orbital (VO), lateral orbital (VLO) or dorsolateral orbital cortex (DLO), with the intention of revealing the broad scale anatomical connections to and from prefrontal regions. The distance between craniotomy co-ordinates (1mm) was based on the measured spread of tracers in preliminary studies (<1mm in diameter) (see Appendix A). The tracer injections were all made with the injection needle orientated vertically.

In the experiments reported here, each rat received a co-injection of retrograde (Fluoro-Gold) and anterograde (Fluorescein; BDA) into the same craniotomy (R37, R38, R41, R42). In earlier experiments (Appendix B) each rat received an injection of retrograde tracer (Fluoro-Gold) into one hemisphere and an injection of anterograde tracer (BDA) into the other hemisphere to allow accurate identification of the tracers injected. In all experiments rats received injections of Fluorescein (100nl) or Texas red (100nl) at a rate of 100nl/min and/or Fluoro-Gold (100nl) at a rate of 100nl/min into the various subdivisions of PFC (Fig.2.1). Additional and equivalent Fluoro-Gold injections were made into the left hemisphere in later studies; this was used to verify whether the location and ordering of projections differed on either side of the brain (Appendix C). No difference was found.

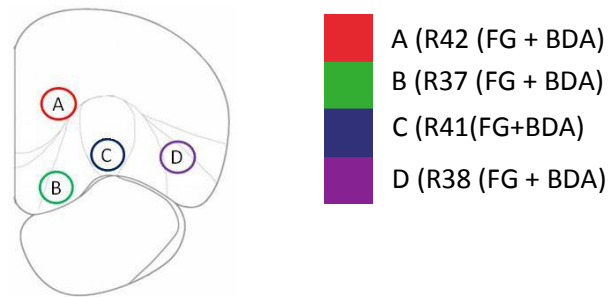


Figure 2.1. Coronal section of PFC (A-P 4.2mm from Bregma) showing the cytoarchitectural boundaries of PFC sub-regions according to Van de Werd & Uylings (2008), depicting sites of tracer injections; prelimbic (PL):A, ventral orbital (VO):B, ventrolateral orbital(VLO):C and dorsolateral orbital(DLO):D, with 1mm separation.

The coordinates used were all at +4.2mm with respect to bregma, injection A (PL) was 1.2mm from the midline and 2.4mm below the cortical surface. Injections B (VO), C (VLO) and D (DLO) were 3.2mm below the cortical surface and 1.2, 2.2 and 3.3mm from the midline. Therefore injections A (PL) and B (VO) were spaced at a distance of 0.8mm and injections B (VO), C (VLO) and D (DLO) were positioned 1mm apart. After each injection a diffusion time of 2 minutes was allowed. The positioning of tracer injections was altered (-0.5mm in the AP axis) from the coordinates provided in Paxinos and Watson (1998), based on my findings from preliminary experiments (Appendix A).

Following a survival time of 7-8 days, the rats were deeply anesthetised with pentobarbital (Sigma-Aldrich, UK), and transcardially perfused with 0.1M phosphate buffered saline (PBS) (~200ml) followed by 4% paraformaldehyde (PFA) (~200ml) in PBS. The brain was subsequently removed and stored for 24 hours in 4% PFA in 0.1M PBS, followed by cryoprotection in 30% sucrose in 0.1M PBS.

Anatomical Processing

For analysis of labelling produced by co-injections of BDA and Fluoro-Gold, two series of 40µm coronal sections were taken (3 in 6) on a freezing microtome (CM 1900, Leica, Germany). Sections were mounted directly onto gelatin coated slides (shown to be preferable for maintaining vibrancy of tracers in my preliminary experiments, and reduced the formation of air bubbles in finished slides (Appendix A). The first series was coverslipped with

Vectashield® Mounting medium with PI (Vector Laboratories, CA), for visualisation of Fluoro-Gold labelled cells and Fluorescein labelled axon terminals. The second series was processed by implementing the standard avidin-biotin method (Vectastain® ABC, Vector Laboratories, CA). Labelling was detected with DAB, incubated at room temperature for 1-3 minutes. This series was counterstained with thionin, for bright field imaging of Fluorescein labelled axon terminals visualised by the brown precipitate formed by the DAB reaction.

Microscopic Analysis

Sections were examined using either brightfield (BDA) or fluorescent microscopy (BDA, Fluoro-Gold). Fluorescent photos were captured of BDA and Fluoro-Gold injection sites, retrogradely labelled cells (Fluoro-Gold) and fluorescein labelled axon terminals. Brightfield photos were captured of anterogradely (BDA) labelled areas (Fluorescein). All photos were captured using an Olympus DP-11 system microscope with an x4, x10 and x20 objective lens, as with subsequent studies.

The entire forebrain was examined for labelling. Areas of temporal cortex were found to contain the strongest and most consistent labelling of connections; therefore a more detailed analysis was carried out on this region to examine the organisation of connections.

Statistical Analysis of the Arrangement of Connections Between Prefrontal and Temporal Cortex

I implemented a statistical analysis to determine whether prefrontal cortex connections displayed an ordered arrangement. ImageJ (Wayne Rasband, NIH) was used to determine numerical values representing the location of retrogradely labelled cells in temporal cortex. The three dimensional location of each retrogradely labelled cell (Fluoro-Gold) was calculated by measuring the distance of each labelled cell or axon terminal from (in temporal cortex) the rhinal sulcus (Dorsal-ventral and Medial- lateral), the anterior-posterior location of each labelled cell/axon terminal was recorded in terms of distance from Bregma (according to Paxinos and Watson, 1998) (Fig.2.2). The same analysis was repeated for fluorescent labelling of axon terminals (BDA; Fluorescein). A similar acquisition of data was

implemented for the anterograde BDA labelling produced by DAB staining of BDA, whereby four data points were recorded from the perimeter of each anterogradely labelled area, denoting its distance (mm) from the rhinal sulcus in dorsoventral and medial-lateral directions (Fig.2.2iii). The anterior–posterior location of each labelled area was also recorded.

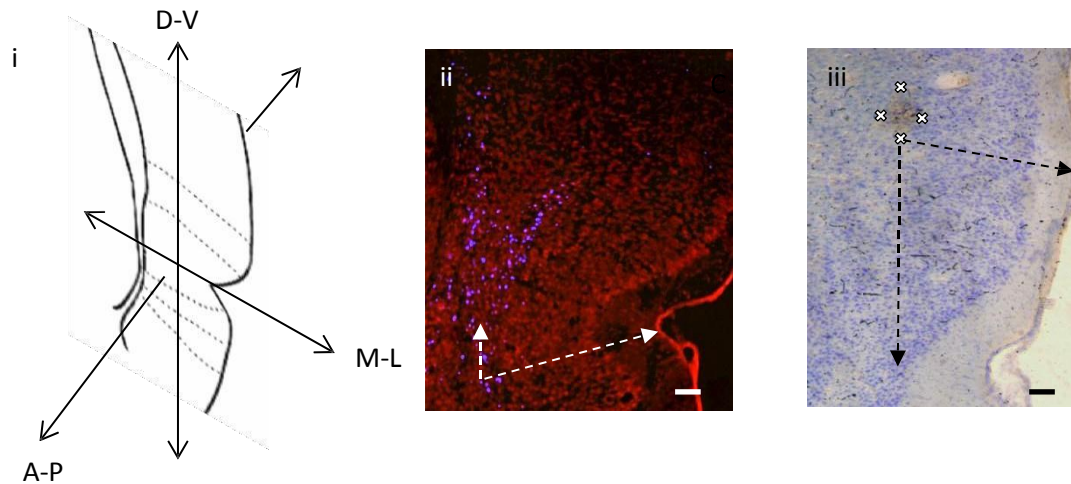


Figure 2.2. (i) Coronal cross section of temporal cortex at -3.3mm posterior to bregma, depicting the three dimensions in which the locations of labelled cells were recorded (Anterior-Posterior (A-P), Medial-Lateral (M-L) and Dorsal-Ventral (D-V)). (ii) Retrogradely labelled cells (blue cells) in temporal cortex produced by an injection of Fluoro-gold (100nl) into VO. Arrows indicate measurements of labelled cell location in the medial-lateral dimension (distance to lateral cortical surface) and dorsal-ventral dimension (distance from rhinal sulcus). (iii) Anterogradely labelled area (Brown) in temporal cortex produced by an injection of BDA (100nl) into PL. Crosses indicate the four points on the perimeter at which measurements were taken. Arrows indicate measurements of labelled area location in the medial-lateral dimension (distance to lateral cortical surface) and dorsal-ventral dimension (distance from rhinal sulcus). Scale bars = 200 μ m.

Labelled cells were grouped according to injection site location. These data sets were analysed in SPSS by way of a factorial ANOVA, in order to establish the existence of an effect of injection location on positioning of labelled cells in anterior-posterior, dorsoventral and medial-lateral dimensions. The relationship between anterograde and retrograde label locations was examined by means of a 2 factor ANOVA. Further statistical analyses were applied in the form of paired samples t-tests, in order to compare the results from separate tracer injections and co-injections of retrograde and anterograde tracer, confirming consistency between them (Appendix D). Paired samples T-tests were applied to the Euclidean distance between labels from left and right hemisphere injections in order to

establish if a hemispheric difference in labelling was present (Appendix C). All statistical tests were applied with a significance level of .05 and confidence intervals of 95%.

Results

Injection sites in PFC from co-injections of (100nl) Fluoro-Gold and (100nl fluorescein) BDA were positioned in the intended regions, comparable to separate Fluoro-Gold and BDA injection sites (Appendix A). A similar spread of both tracers (BDA and Fluoro-Gold) was seen at co-injection sites to that which had been observed at single injection sites (Fig.2.3i, ii). Co-injection sites spanned layers I/II – VI and covered the majority of the intended cytoarchitectural region. Injection sites into PL (A) and VO (B) overlapped to some extent, however the majority of the spread of tracers was confined to separate cytoarchitectural regions. The majority of the spread of tracers from co-injection sites was limited to the cytoarchitectural borders of PFC sub-regions. The co-injection sites in PL, VLO and DLO were similar in position and spread of tracer to the separate Fluoro-Gold and BDA injection sites. The co-injection into VO was positioned dorsally to the equivalent separate injections of Fluoro-Gold and BDA (Appendix A); however the majority of the spread of tracers were in the same location (Fig.2.3iii).

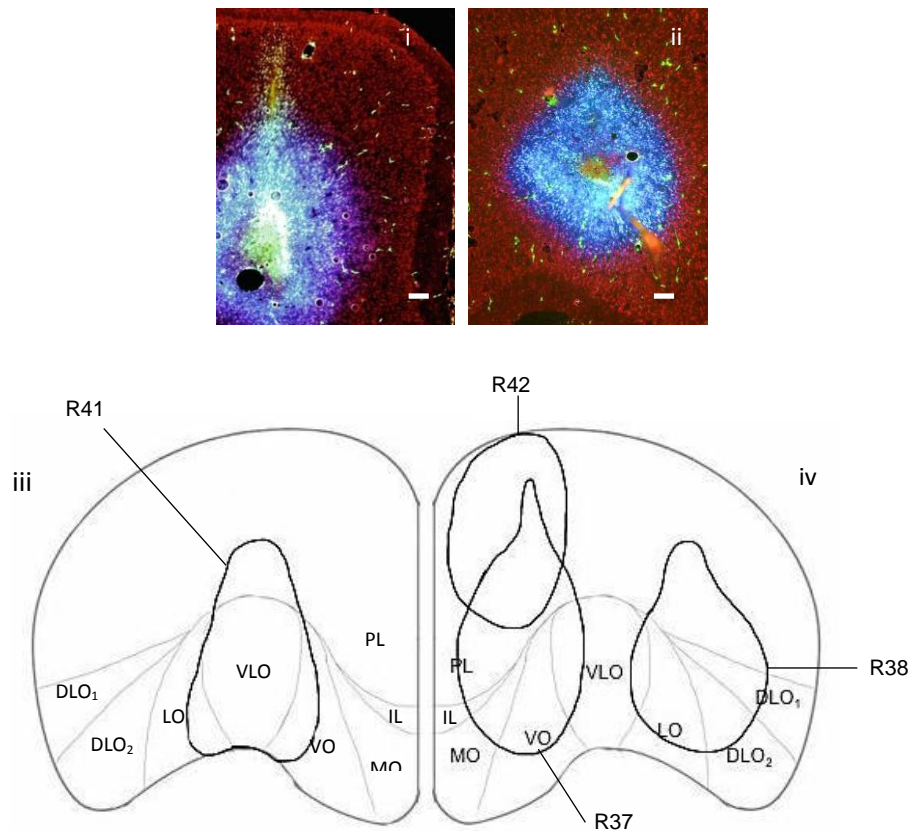


Figure 2.3. (i) Coronal section of PFC showing location and spread of (100nl) Fluoro-Gold and (100nl) Fluorescein at injection site in VO. (ii) Coronal section of PFC showing location and spread of (100nl) Fluoro-Gold and (100nl) Fluorescein at injection site in DLO. (iii) Representations of Fluoro-Gold and Fluorescein co-injection site in VLO (R41) in the right hemisphere. (iv) Representations of Fluoro-Gold and Fluorescein co-injection sites in PL (R42), VO (R37), and DLO (R38) in the left hemisphere. Scale bars = 200µm.

patterns of labelling were observed throughout the brain following co-injections of anterograde and retrograde tracer into prefrontal cortex (PL, VO, VLO and DLO) using light/fluorescent microscopy. Retrogradely labelled cells were seen in perirhinal cortex (areas 35v, 35d, 36d, 36v), entorhinal cortex (Ent), area Te (Te), secondary auditory cortex (AuV), primary auditory cortex (Au1), secondary motor cortex (M2), primary motor cortex (M1), primary somatosensory cortex (S1J, S1BF), cingulate cortex (Cg1) and piriform cortex (Pir) (Fig.2.4ii). Anterograde labelling was seen in PRh (areas 35d, 36v) (Fig.2.5), Te, Ent, M2, Cg1, S1J, secondary somatosensory cortex (S2), agranular insular cortex (AID), and prefrontal cortex regions (Fig. 2.4iii). Similar patterns of labelling were observed from co-injections of Fluoro-Gold and BDA into PL, VO, VLO and DLO. The strongest labelling in both cases was present in temporal (PRh, Ent, Te) regions; therefore a statistical analysis was

applied to this area to determine whether there was evidence for an organised arrangement of connections. Labelling produced by separate injections of BDA and Fluoro-Gold confirmed observations that input and output projections from PFC did not occur in the same places in temporal cortex (Appendix A). Anterograde and retrograde labels were furthest apart from one another in temporal cortex from an injection into DLO (D).

i



ii

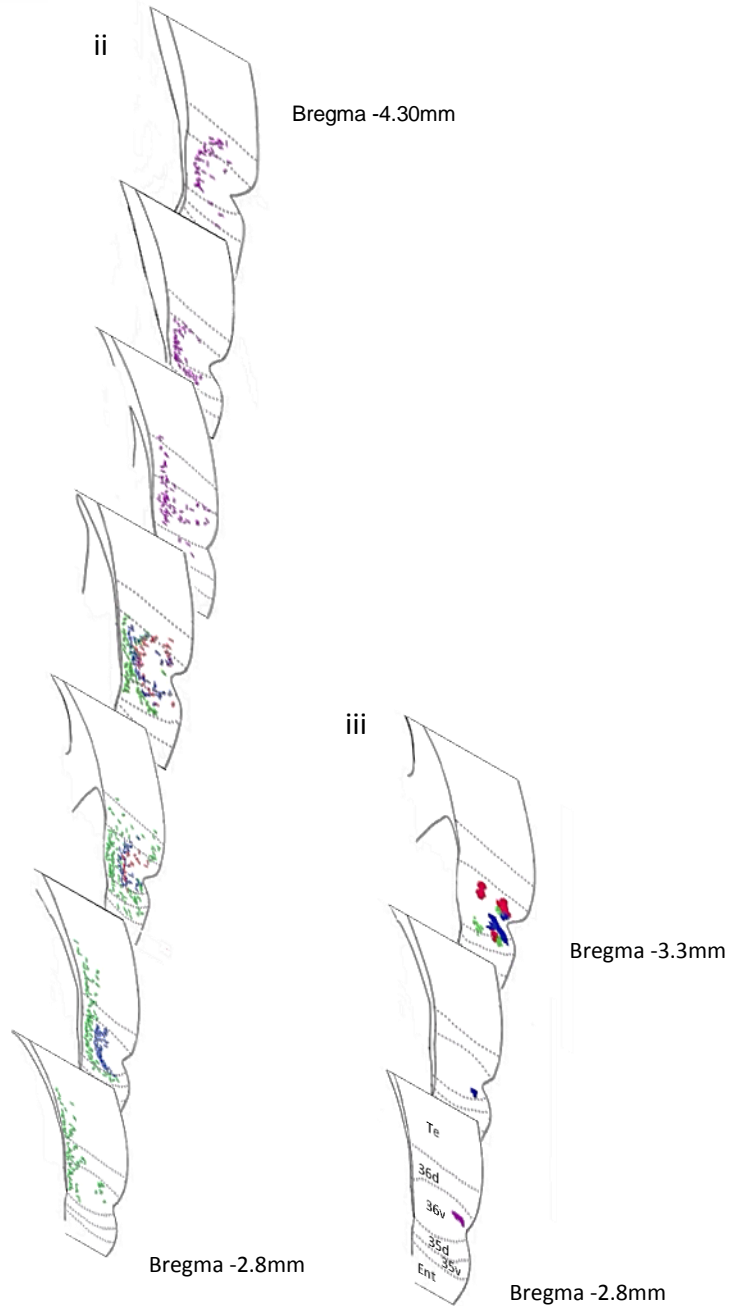


Figure 2.4. Diagram representing the amalgamated dual-injection sites of Fluoro-Gold and BDA, and the projection sites in temporal cortex for both retrograde (Fluoro- Gold) and anterograde (BDA) tracer injections from 4 rats. (i) The locations of injection sites A (PL:

R42), B (VO: R37), C (VLO:R41) and D (DLO:R38) in PFC and the location of labelling in temporal cortex. (ii) The locations of retrogradely labelled cells in temporal cortex, resultant from 100nl Fluoro-Gold injections into PFC sites A-D (R37, R38, R41, R42). (iii) The locations of anterogradely labelled areas in temporal cortex, resultant from 100nl BDA (Fluorescein) injections into PFC sites A-D (R37, R38, R41, R42).

Organisation of Input Connections from Temporal to Prefrontal Cortex

Labelled input (retrograde) projections to PFC from temporal cortex were seen in PRh (areas 35v, 35d, 36v, 36d), Ent and Te (Fig.2.4). Labelled cells from each injection location were distributed across several cytoarchitecturally distinct regions (according to Burwell, 2008). The distribution of retrogradely labelled cells within temporal cortex maintained a spatial order according to the corresponding PFC injection sites. Moving laterally in PFC from VO to DLO: projections to VO (PRh, Te) were seen dorsally to those from VLO. An overlap of VO and LO projections is present. Projections to VLO are present only in PRh regions. Projections to DLO (PRh, Ent) are situated ventrally to those from VLO. An overlap of projections to VLO and DLO was seen. A factorial ANOVA revealed a significant main effect of PFC injection site location on the dorsal-ventral distance of retrogradely labelled cells from the rhinal sulcus ($F(3, 421)=6.491$ $p<0.001$ $r=0.123$). Post-hoc analyses (Tukey HSD) revealed no significant differences between retrograde injection sites. Distance of retrograde labelled cells from the rhinal sulcus increases as the injection site moves from lateral (DLO) to medial (VO) and decreases when the injection site reaches PL, indicating a change in pattern.

In addition, there was an ordered organisation present in the anterior- posterior axis. VO projections were seen more anteriorly to VLO projections. DLO projections are more posterior within perirhinal cortex to VLO projections. An overlap of projections to VO and VLO as well as VLO and DLO is present on the anterior-posterior axis. A factorial ANOVA revealed a significant main effect of injection site on the anterior-posterior location of retrogradely labelled cells ($F(3,421)=467.804$ $p<0.001$ $r=0.726$). Post hoc analyses (Tukey HSD) indicated significant differences between retrograde injection sites A*B ($p=0.001$), A*D, B*C, B*D and C*D ($p<0.001$). Fig.2.6ii shows the anterior-posterior ordered arrangement of VLO, DLO and VO. A-P location of retrogradely labelled cells becomes more anterior as the injection site is moved from lateral (DLO) to medial (VO), with A-P location becoming more posterior as the injection site moves from VO to PL.

A factorial ANOVA also revealed a significant main effect of injection site on medial-lateral location of retrogradely labelled cells in temporal cortex ($F(3, 421)=185.795$ $p<0.001$ $r=0.553$). As the injection site is moved from medial to lateral PFC, the labelled cells in temporal cortex become more lateral. Post hoc analyses (Tukey HSD) indicated significant differences between retrograde injection sites A*B, A*D, B*C, B*D and C*D ($p<0.001$).

The labelling from co-injections of Fluoro-Gold and BDA shows evidence of ordered arrangements of both input and output connections from PFC to temporal cortex, as well as clear evidence of non-alignment of connections. Some co-labelling of cells with BDA and Fluoro-Gold was seen, with the majority of Fluorescein and Fluoro-Gold labels seen in different locations to one another (Fig.2.5). The co-injection of retrograde (100nl Fluoro-Gold) and anterograde (100nl Fluorescein) tracers revealed similar results to those produced from separate retrograde and anterograde injections (Appendix A).

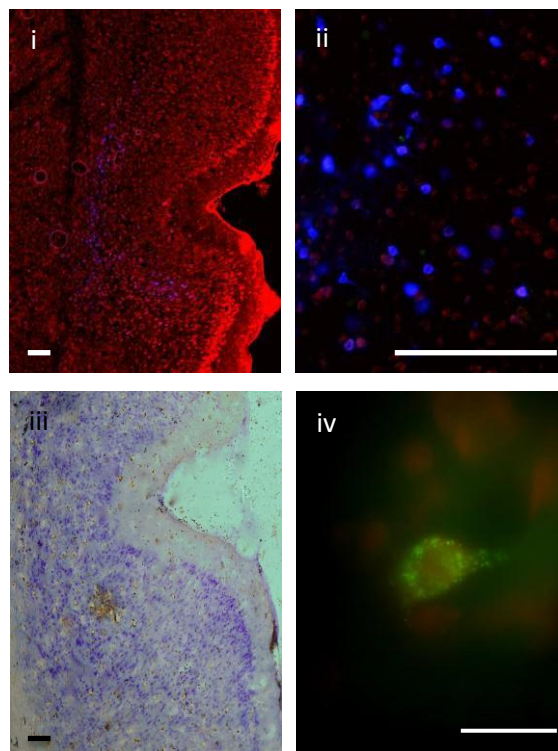


Figure 2.5. (i) Coronal section of temporal cortex showing retrogradely labelled cells (Fluoro-Gold, blue) resultant from co-injection of Fluoro-Gold and BDA (Fluorescein) into DLO. (ii) Retrogradely labelled cells in temporal cortex (blue, Fluoro-Gold) resultant from co-injection of Fluoro-Gold and BDA (Fluorescein) into DLO. (iii) Coronal section of temporal cortex showing area of anterogradely labelled axon terminals (brown, BDA) resultant from co-injection of BDA and Fluoro-Gold into VLO (injection C). Scale bars =

200µm. (iv) Anterograde labelling of axon terminals (green) resultant from co-injection of BDA and Fluoro-Gold into DLO Scale bar = 100µm.

Organisation of Output Projections from Prefrontal to Temporal Cortex

In comparison to earlier experiments (Appendix A), labelling of output projections from PFC to temporal cortex resultant from injections of BDA;Fluorescein (100nl) was seen with both fluorescence and DAB staining. Labelled axon terminals were numerically analysed from both visualisation methods (fluorescent and bright field). The locations of areas of DAB stained axon terminals were measured in order to directly compare findings. Individual fluorescently labelled axon terminals were measured in terms of their 3-dimensional location, consistent with the methodology used to quantify retrograde (Fluoro-Gold) labelling.

Labelled output (anterograde) projections from PFC to temporal cortex were seen in regions of PRh (35d, 36v). The distribution of anterogradely labelled areas within temporal cortex maintained a spatial order in accordance with their corresponding BDA injection sites in PFC, specifically from VO, VLO and DLO. Injections of anterograde tracer into central regions of PFC produced a clear ordered organisational pattern within PRh (35d, 36v).

A factorial ANOVA revealed a significant main effect of PFC injection site location on the dorsal-ventral distance of anterogradely labelled axon terminals from the rhinal sulcus (Fluorescent labelling: $F(3,301)= 8.181p<0.001$ $r=0.163$; DAB staining: $F(3,36)=5.786$ $p=0.002$ $r=0.372$). Post-hoc analyses (Tukey HSD) revealed significant differences between anterograde injection sites (based on fluorescent labelling) A*B ($p=0.012$), B*D ($p<0.001$) and C*D ($p=0.011$). Three of the PFC regions tested (VLO, VO and DLO) exhibited an ordered arrangement in terms of dorsoventral location of retrograde labels (Fig. 2.6i). Consistent with input connections, anterograde labels from VO, VLO and DLO also display an ordered arrangement, as injection site moves from lateral to medial the mean location of labels decrease in distance from the rhinal sulcus. These results are consistent with those from separate Fluoro-Gold and BDA injections.

A factorial ANOVA revealed a significant main effect of injection site on the anterior-posterior location of anterogradely labelled axon terminals in temporal cortex (Fluorescent labelling: $F(3,301)=151.566$ $p<0.001$ $r=0.579$; DAB staining: $F(3,36)=151.153$ $p<0.001$

$r=0.899$). Post hoc analyses (Tukey HSD) indicated significant differences between anterograde injection sites (fluorescent labelling) A*C, A*D, B*C, B*D and C*D ($p<0.001$). As anterograde injection sites move from lateral (DLO) to medial (VO) PFC, the anterior-posterior location of anterogradely labelled areas becomes more posterior (Fig.2.6ii). This is not the case between VO and PL, where the anterior- posterior location of labelled areas becomes more anterior, indicating a change in the ordered arrangement of connections. In contrast to input connections to PFC, the effect of injection location on the anterior-posterior location of anterogradely labelled areas was only found to be significant between two pairs of PFC sub-regions (VO*DLO, VO*PL). Projections from VO are most greatly affected within the organisational pattern of connections to temporal cortex. As the injection site is moved from medial to lateral PFC, the labelled areas in temporal cortex become more medial.

There was clear convergence of prefrontal-temporal cortex connections; injections into cytoarchitecturally distinct PFC regions (1mm apart) produced anterograde labelling much closer together in the same cytoarchitectural area of temporal cortex. This is not the case with temporal-prefrontal input connections from the same PFC injection sites.

A 2 factor ANOVA revealed a significant interaction effect of PFC injection site location between input and output connections to temporal cortex in the dorsal-ventral axis ($F(3,722)=9.505$ $p<0.001$), in the anterior- posterior axis ($F(3,722)=541.788$ $p<0.001$) and in the medial-lateral axis ($F(3,722)=15.841$ $p<0.001$). These results indicate differences in the ordering of input and output connections and non-alignment between input and output connections in three axes of orientation.

This analysis indicates an ordered organisation of connections between prefrontal and temporal cortex. As the prefrontal cortex is traversed in the mediolateral direction (VO to DLO; B to D), the pattern of input projections moves in an anterior-posterior direction across temporal cortex, whilst simultaneously moving in a dorsoventral direction. In addition, there is a linear structure of organisation in which the pattern of input projections moves in a mediolateral direction across temporal cortex as the prefrontal cortex is traversed in the mediolateral direction (PL to VLO; from A to C). These two structures overlap within VLO (B) and VO (C).

Similarly to the organisational pattern found in retrograde projections, an organisation of

prefrontal–temporal cortex connections is seen. However, the organisational pattern here appears to move in a different direction to that seen in temporal- prefrontal connections. As retrograde injection sites move from lateral to medial (DLO, VLO, VO; D, C, B) the locations of labelled cells in temporal cortex move from ventral to dorsal and posterior to anterior. In comparison, as anterograde injection sites move from lateral to medial (DLO, VLO, VO; D, C, B), the location of labelled cells in temporal cortex move from dorsal to ventral and anterior to posterior. A further linear organisational structure appears to exist on the medial-lateral axis, from PL (A) to VLO (C). This overlaps with the first structure within VO (B) and VLO (C). In comparing the organisation of connections labelled from anterograde and retrograde injections, corresponding input and output connections are not aligned with one another.

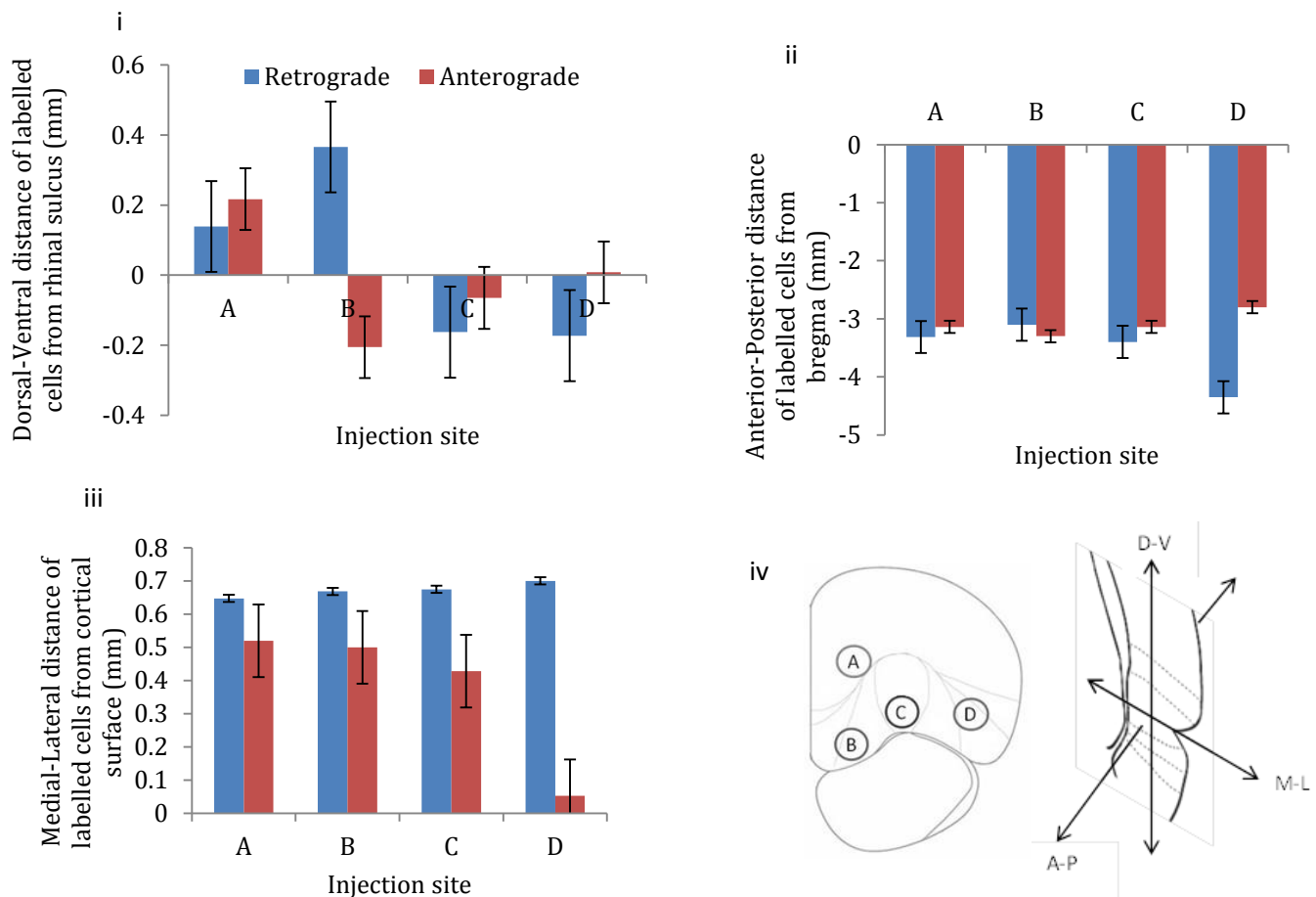


Figure. 2.6. The mean effect of injection site on the (i) dorsal-ventral ,(ii) anterior- posterior and (iii) medial-lateral location of retrogradely labelled cells (n=425 arising from 4 rats: PL=77, VO=160, VLO=89, DLO=99 (cases R37, R38, R41, R42)) and anterogradely labelled areas (n=40 arising from 4 rats: PL=12, VO=12, VLO=12, DLO=4 (cases R37, R38, R41, R42)) within temporal cortex. Error bars = standard error. (iv) Coronal cross section of PFC

showing the position of 4 injection sites; PL (A), VO (B), VLO (C) and DLO (D). Coronal cross section of temporal cortex showing the three dimensions in which the locations of labels were recorded.

The calculation of a 3 dimensional mean location (E) for the labelling produced by each retrograde and anterograde injection site,

$$E = \sqrt{(DV)^2 + (AP)^2 + (ML)^2}$$

where DV =dorsal-ventral location, AP =anterior-posterior location and ML =medial-lateral location, allowed for the visualisation of the 3-dimensional locations of input and output connections in comparison to one another (Fig. 2.7).

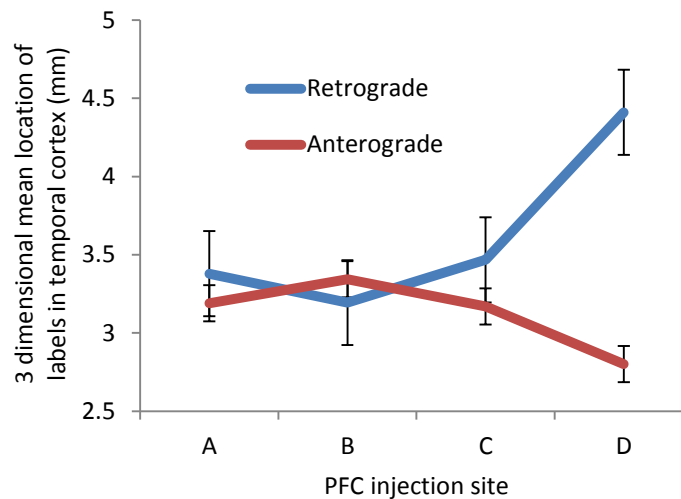


Figure 2.7. The effect of PFC injection site (PL:A, VO:B, VLO:C, DLO:D) on the three dimensional mean location of retrogradely labelled cells (blue) and anterogradely labelled areas (red) in temporal cortex. Error bars = standard error.

The results of the analysis show that input and output connections follow different orders of arrangement as injection sites move from PL (A) to DLO (D). These findings indicate that the ordered arrangement of input and output connections are affected by one another in terms of the medial-lateral and anterior- posterior axis, however they do not appear to interact to such an extent on the dorsal- ventral axis. Further to this, we have demonstrated that the location of retrogradely labelled cells is directly associated with the location of anterogradely labelled cells (in the anterior-posterior axis), in that one becomes increasingly posterior as the other

becomes increasingly anterior. This finding is consistent across multiple studies.

The results from co-injections of retrograde and anterograde tracer injections showed no difference in the location of temporal cortex labelling in comparison to separate injections. Statistical evidence for this is shown by paired samples t-tests. No significant difference in the mean location of retrograde labelling in temporal cortex was found: in the dorsal-ventral axis ($t(3)=0.766$ $p=0.500$), anterior-posterior axis ($t(3)=-0.003$ $p=0.998$) and medial-lateral axis ($t(3)=-0.753$ $p=0.506$). No significant difference in the mean location of anterograde labelling in temporal cortex was found: in the dorsal-ventral axis ($t(3)=-1.071$ $p=0.363$), anterior-posterior axis ($t(3)=2.004$ $p=0.128$) and medial-lateral axis ($t(3)=-1.602$ $p=0.207$). These findings demonstrate the consistency of labelling between co-injections and separate injections of Fluoro-Gold and BDA, as well as the reproducibility of my findings.

Discussion

Broad scale connections of PFC – Temporal Cortex Pathway

This study investigated the organisation of connections from adjacent prefrontal regions with the use of neuroanatomical tracers. The findings have revealed evidence for ordered patterns of organisation within prefrontal-temporal cortex connections. I have revealed a clear ordered arrangement of PFC connections as well as evidence for differential ordering of input and output projections from PFC to regions of temporal cortex.

Input connections to prefrontal cortex

Following the administration of the retrograde tracer, Fluoro-Gold, to the prefrontal cortical areas PL (A), VO (B), VLO (C) and DLO (D), I found labelling of neuronal cell bodies in medial frontal cortex, temporal cortex, auditory cortex, somatosensory cortex, cingulate cortex and piriform cortex. The projections arising from the temporal cortex (including area TE, perirhinal cortex and entorhinal cortex) displayed the most labelled cells (as well as regions of motor and sensory cortices; investigated separately). These findings are comparable with previous studies (Hoover and Vertes, 2011), which outlined extensive input

connections from temporal cortex to prefrontal cortex, as well as projections from prefrontal to temporal and medial-frontal cortex (Sesack, 2004). I found similar retrograde labelling produced by co-injections of Fluoro-Gold with BDA.

Output connections from prefrontal cortex

Following the administration of the anterograde tracers, biotinylated dextran amines to the prefrontal cortical areas PL, VO, VLO and, DLO I found labelling of axon terminals in several cortical regions. The projections going to the temporal cortex (including area TE, perirhinal cortex and entorhinal cortex) displayed the most prominent labelling. This was broadly consistent with previous studies, which outlined extensive output connections from prefrontal cortex to temporal cortex (Hoover and Vertes, 2011). In contrast to the large numbers of labelled cells in MO and VO following Fluoro-Gold injection in perirhinal cortex observed by Hoover and Vertes (2011); I found there to be more specific, small areas of anterograde labelling in perirhinal cortex following BDA injections into VO, VLO and DLO. It should be noted that the slight overlap in injection sites may have had an impact on the observed convergence. The resultant location of labelling within perihinal cortex from BDA injection sites was also broadly consistent with previous findings, in that my labelled connections were seen between the same cortical regions as Fluoro-Gold labelled connections from VO to PRh (Hoover and Vertes, 2011) and anterogradely labelled connections from PFC to PRh (Sesack, 2004). I identified similar anterograde labelling in temporal cortex resultant from co-injections of BDA with Fluoro-Gold, supporting my findings of differential anterograde and retrograde labelling. Similar anterograde labelling and findings of ordered arrangement were observed with both brightfield imaging of DAB stained labeled axon terminals and fluorescent imaging of fluorescein labeled axon terminals.

Organisation and alignment of connections between PFC and Temporal cortex

The analysis of temporal cortex connections revealed an ordered arrangement of input and output connections to prefrontal cortex occurring in anterior-posterior, dorsal-ventral and medial-lateral (laminar) axes. Most prominently in the anterior-posterior dimension, tracer injections in sites B (VO), C (VLO) and D (DLO) revealed an ordered arrangement of both

input and output connections. This was observed with both separate and dual-injections. This ordered arrangement was observed in opposing orders for the input and output connections (Fig. 2.4, 2.6), indicating differential organisation of inputs and outputs. This opposing order can also be seen in the dorsal-ventral axis. In the medial-lateral axis, tracer injections in sites A (PL), B (VO) and C (VLO) produced an ordered arrangement of connections (Fig. 2.4, 2.6, 2.7). This arrangement consistently occurred in different orders for the input and output connections from PFC to temporal cortex.

When observed in separate axes of orientation (anterior-posterior, dorsal-ventral and medial-lateral), there appears to be different and overlapping maps of connections between prefrontal and temporal cortex (i.e. PL→VO→VLO for ordered mediolateral distributions and VO→VLO→DLO for anterior-posterior and dorsoventral distributions).

There are some indications for an ordered arrangement of output connections from PFC to temporal cortex from previous studies. For instance, moving mediolaterally in PFC, previous findings (Hoover and Vertes, 2011) have shown evidence for an ordered arrangement of PFC output connections in the dorsal-ventral axis, in the same direction shown by my results here. Similar studies have shown consistent evidence of an ordered arrangement of connections from medial to lateral. Studies of PFC outputs have shown an ordered arrangement of connections to the striatum (Berendse, 1992; Schilman, 2008). Our study did not produce any strong projections to the striatum following injections of anterograde tracers into the PFC.

These findings show that prefrontal cortex displays an ordered arrangement of connections to temporal cortex. The connections between prefrontal cortex and temporal cortex are highly ordered and indicate evidence for topological mapping between these two cortical regions. The temporal cortex region labelled here includes area Te, perirhinal cortex and entorhinal cortex. There is existing evidence that these temporal regions exhibit functional mapping in terms of responses (Boussaoud et al 1991, de Beek et al 2008, Hafting et al 2005; Killian et al 2012), based on this it may be functionally important to preserve an ordered arrangement in terms of the connections linking these two regions. My findings indicate an ordered arrangement of connections between PFC and temporal cortex. However these results do not yet provide the highly detailed analysis of connections required for a complete understanding of prefrontal organisation.

An unexpected observation in the organisation of connections between PFC and temporal cortex was the non-alignment of input and output connections; whereby input and output labels from the same PFC injection sites were not found in the same target locations. For example, anterograde labelling from injections into DLO (injection site D) are seen significantly posterior in temporal cortex in comparison to retrograde labels from the same injection site. This was apparent with both separate and co-injections of retrograde and anterograde tracers. This is an arrangement which has not been described in cortical connections previously. There have been instances of reported non-alignment in cortical connections (Flaherty & Graybiel, 1994), whereby normally highly reciprocal inputs and outputs were described as on occasion “missing each other”. The same study however concluded this observation to be an experimental artifact. Previous observations in terms of organisation, specifically of the connections from temporal (entorhinal and perirhinal) cortex, suggest alignment in connections to be a common property (Suzuki and Amaral, 1994; Canto et al, 2008). In addition, recent dual-tracer studies into prefrontal projections give no indication of non-alignment within input and output connections (Kim and Lee, 2012; Takahara et al, 2012). My findings indicate that this is not the case for PFC-temporal cortex connections. The observed non-alignment of input and output connections was seen with both separate injections and co-injections of retrograde and anterograde tracers. This consistency in observations of differential ordering indicates that my findings are not a product of comparing injections from different animals and are reproducible. Further studies were carried out to enable us to determine if this is a common property throughout prefrontal cortex.

In summary, I have shown evidence for an ordered arrangement of connections between prefrontal and temporal cortex. The ordering of these connections appears across anatomical orientations and shows a consistent non-alignment between input and output connections.

Chapter 3.

Organisation of Connections to Temporal Cortex from Anterior, Central and Posterior Prefrontal Cortex

It is understood that PFC forms part of a large scale cortico-cortical pathway, organised from anterior to posterior (Olson & Musil, 1992). Differences in function between anterior and posterior PFC have been described. Taren et al (2011) described a posterior to anterior connectivity gradient in DLPFC. This provides evidence for a topographically ordered organisation of connections, as well as differences in the organisation of connections between anterior and posterior PFC. The first studies described in Chapter 2 established an ordered arrangement of connections in the PFC – temporal cortex pathway, and produced evidence of non-alignment between input and output connections. However this study only examined the central area of PFC (in terms of its anterior-posterior dimension), further investigation into the anterior-posterior connectivity of PFC will provide a greater insight into its detailed structural organisation.

Based on the understanding that functional organisation is often a product of underlying anatomical organisation, we would expect the anatomical organisation of PFC connections to differ between anterior and posterior regions. Taren (2011) suggests that the organisational gradient observed in PFC could be representational of a dynamic processing ability and a level of adaptability in PFC function. This is similar to the ability of PFC neurons in rodents to process different types of information (Duncan, 2001; Kargo, 2007) and Duncan's (2001) adaptive coding model. There is less known about the function of anterior PFC in comparison to more posterior regions. Ramnani & Owen (2004) suggest that anterior PFC has a specific purpose, to integrate the information from multiple cognitive processes, in which information is transferred between multiple processes with the outcome of reaching a predetermined goal. These processes identified with anterior PFC are much more abstract in nature than many of the processes associated with more posterior regions of PFC in rats e.g. autonomic function, temporal processing and motor processing (Kolb, 1984; Neafsey, 1990; Schoenbaum & Esber, 2010; Narayanan & Laubach, 2006; Vertes, 2006; Kim et al 2013). Anterior regions of

PFC are reportedly unique in terms of hierarchical organisation, and are thought not to have clear connections to lower cortical regions in the same sense as other higher order cortical regions identified in rats (Ramnani & Owen, 2004). This gives reason to suggest that the anatomical organisation of anterior regions of PFC differ to that found in posterior PFC.

Aims

The aim of this study was to expand on my earlier work and determine the connectivity pattern of a wider area of prefrontal cortex, from anterior to posterior, in terms of ordered connections as well as alignment between input and output connections.

Methodology

For detailed methodology and surgical procedures, see Chapter 2.

The anterograde tracer Fluoro-Ruby (FR) was introduced to this study, replacing the previously used BDA. The fluorescence of Fluoro-Ruby proved to be more vibrant, and provided more detailed images of labelled projections, allowing for more detailed investigations and analysis.

Data was collected from 19 adult male CD rats (296-367g, Charles River, UK). Craniotomies (<1mm) were repeated at 3 A-P locations (Bregma 4.7mm, 4.2mm, 3.7mm) (Fig.3.1). The medial-lateral co-ordinates and depth of injections at each AP location were identical to injection sites A, B, C and D (PL, VO, VLO and DLO) described in Chapter 2. Injections of anterograde (100nl 10% Fluoro-Ruby in distilled water, Fluorochrome, Denver, Colorado) and retrograde tracer (100nl 4% Fluoro-Gold in distilled water, Fluorochrome, Denver, Colorado) were made into PL, VO, VLO and DLO (Fluro-Gold:100nl/min, 2 mins diffusion time; Fluoro-Ruby 10nl/min, 2 mins diffusion time).

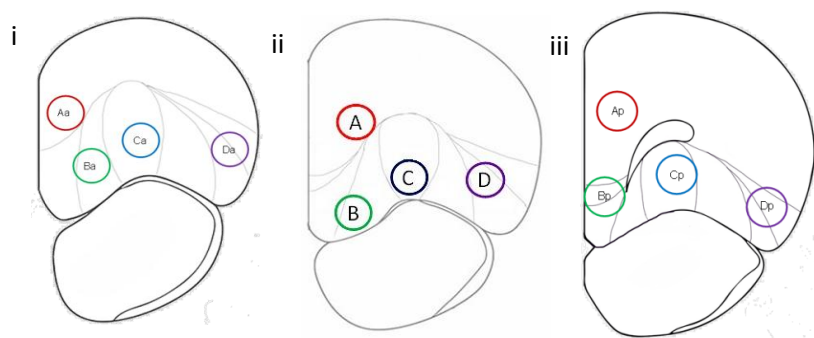


Figure 3.1. Coronal sections of PFC ((i) A-P 4.7mm, (ii) 4.2mm and (iii) 3.7mm from Bregma) showing the cytoarchitectural boundaries of PFC sub-regions according to Van de Werd & Uylings (2008), depicting sites of tracer injections; PL (Aa, A, Ap), VO (Ba, B, Bp), VLO (Ca, C, Cp) and DLO (Da, D, Dp), with 1mm separation between injection sites.

Additional co-injections of (100nl) Fluoro-Gold and (100nl) Fluoro-Ruby were made into the same central PFC co-ordinates (Appendix F). Further anterograde (100nl Fluoro-Emerald) injections were made into central PFC (PL, VO, VLO and DLO), in the same co-ordinates as previous injection sites in order to provide confirmation of anterograde labelling (Appendix H).

Anatomical Processing, Imaging and Microscopic Analysis

For details of anatomical processing, see Chapter 2 and Appendix B. Areas of temporal cortex were known from earlier studies to contain strong connections with PFC, therefore a detailed analysis was carried out on labelling found in temporal cortex to examine the organisation of a wider area of prefrontal cortex. *For details of microscopic analysis see Chapter 2.*

Statistical Analysis of the Arrangement of Connections Between Prefrontal and Temporal Cortex

I applied the same numerical and statistical analysis to that which had been used in the previous experiments (Chapter 2), in order to determine whether connections between prefrontal cortex and temporal cortex displayed an ordered arrangement similar to that which I had observed previously, and how that ordered arrangement differed as the anterior-

posterior location of PFC injection sites changed. The replacement of BDA with Fluoro-Ruby allowed for a more precise measuring of anterograde labelling, in which the 3-dimensional location of each individually labeled axon terminal could be recorded.

The anterograde tracer Fluoro-Ruby is reported to hold retrograde properties (Zelev et al, 2010; Hainec et al, 2012) and is thought by some to be a bi-directional tracer. In order to approach the possibility of retrograde labelling from the anterograde injections in this study, the labelling properties of Fluoro-Ruby were investigated (detailed analysis can be seen in Appendix F). Through detailed visualisation and comparison with other tracers, the findings conclude Fluoro-Ruby to be primarily anterograde (~70%).

The labelling produced by Fluoro-Ruby injections was investigated for its retrograde and anterograde properties. High resolution confocal microscopy allowed for detailed imaging of Fluoro-Ruby labelling (images in Appendix F). High resolution images revealed Fluoro-Ruby to produce labelling with both anterograde and retrograde properties. In addition to confocal imaging, I also visualised Fluoro-Ruby alongside fluorescently labeled (with fluorescein) alpha tubulin. Similar results were found, ~70% of Fluoro-Ruby labelling was determined to be anterograde.

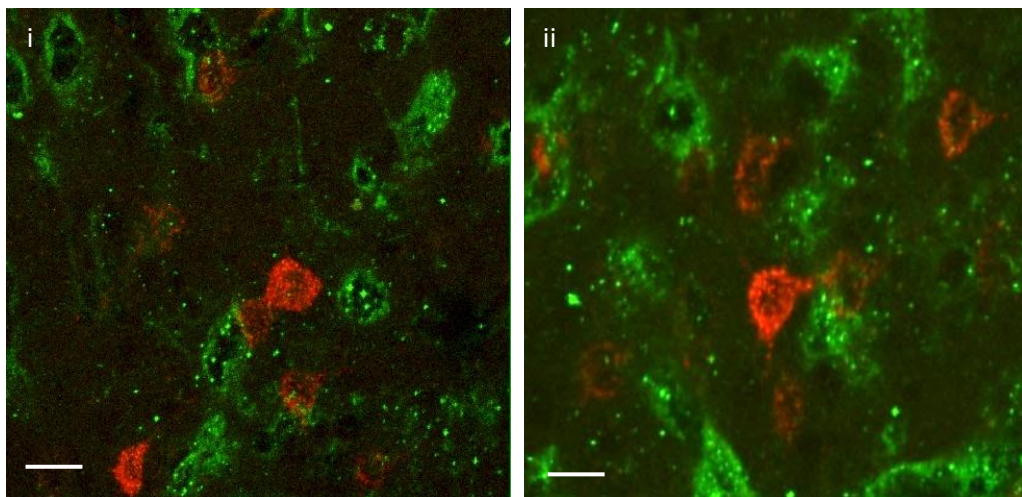


Figure 3.2 (i) Confocal image of temporal cortex showing Fluoro-Ruby labelling (red) and Fluorescein labeled alpha tubulin (green) resultant from Fluoro-Ruby (100nl) injection into DLO (R39). (ii) Confocal image of temporal cortex showing Fluoro-Ruby labelling (red) and Fluorescein labeled alpha tubulin (green) resultant from Fluoro-Ruby (100nl) injection into (R39). Note that Fluororuby occurred both separate to and in the same place as Fluorescein, with the majority of cases being separate (anterograde). Scale bars = 20 μ m.

Figure 3.2 shows that Fluoro-Ruby labelling was mostly seen separate to the labeled alpha tubulin, meaning the labelling was outside of the cell body and therefore considered anterograde. However, there were instances in which Fluoro-Ruby and labeled alpha tubulin was seen in the same locations. This implies retrograde labelling. Quantification of the labelling found in temporal cortex showed the majority of the labelling I observed (~70%) to show anterograde properties, therefore the labelling produced in this experiment was treated as anterograde.

It should be noted that the analyses reported in the results of this study assume all Fluoro-Ruby labelling to be anterograde. The error produced by this assumption is considered to be relatively low due to the high percentage of anterograde labelling present, and therefore should not have a significant effect on the findings. Further details of the anterograde and retrograde properties of Fluoro-Ruby I observed can be seen in Appendix F.

To determine the organisation of connections across PFC from anterior to posterior, a factorial ANOVA was applied. Post hoc analyses revealed the presence of differences in ordering between anterior, middle and posterior PFC. The alignment of connections from anterior, middle and posterior PFC were compared by applying a further statistical analysis: The mean Euclidean distance between retrograde and anterograde labels from 4 injection sites was calculated. Paired samples T-tests were used to compare the distance between retrograde and anterograde labels at each anterior-posterior location in PFC. All statistical tests were applied at a significance level of .05 and confidence intervals of 95%.

Results

Retrograde labelling was found in areas of M2, M1, S1J, S1BF, Cg1, Pir, PRh, Ent, AuV and Au1 and prefrontal regions. Anterograde labelling was found in areas of M2, S1J, Cg1, S2, PRh, Ent, AID and prefrontal regions. To investigate the PFC – temporal cortex pathway I had already established in Chapter 2, the statistical analysis was applied to labelling found in PRh. The organisation of input and output connections were initially investigated at three A-P

PFC locations separately (anterior, middle, posterior). I then proceeded to examine the connectivity across the whole investigated PFC region.

Anterior Prefrontal Cortex

Retrograde injection sites into the anterior aspect of PFC (R28, R24, R17, R23) were observed in PL, VO, VLO and DLO (Fig. 3.2). Retrograde injection sites were mostly confined to cytoarchitectural boundaries of PFC regions and covered layers I-V/VI. There is some overlap seen between the retrograde injection sites in PL (R28) and VO (R24). There was some minimal overlap between the retrograde injections into VO and VLO (R24 and R17). Anterograde injection sites into the anterior aspect of PFC (R32, R23, R21, R24) were observed in the subdivisions of PL, VO, VLO and DLO (according to Van de Werd & Uylings, 2008). The spread of tracer at anterograde injection sites was confined to the cytoarchitectural boundaries of PFC regions. No overlapping occurred between anterograde PFC injection sites. Anterograde injection sites were observed in similar regions to the equivalent retrograde injection sites, the spread of anterograde injections was consistently contained within the boundary of retrograde counterparts.

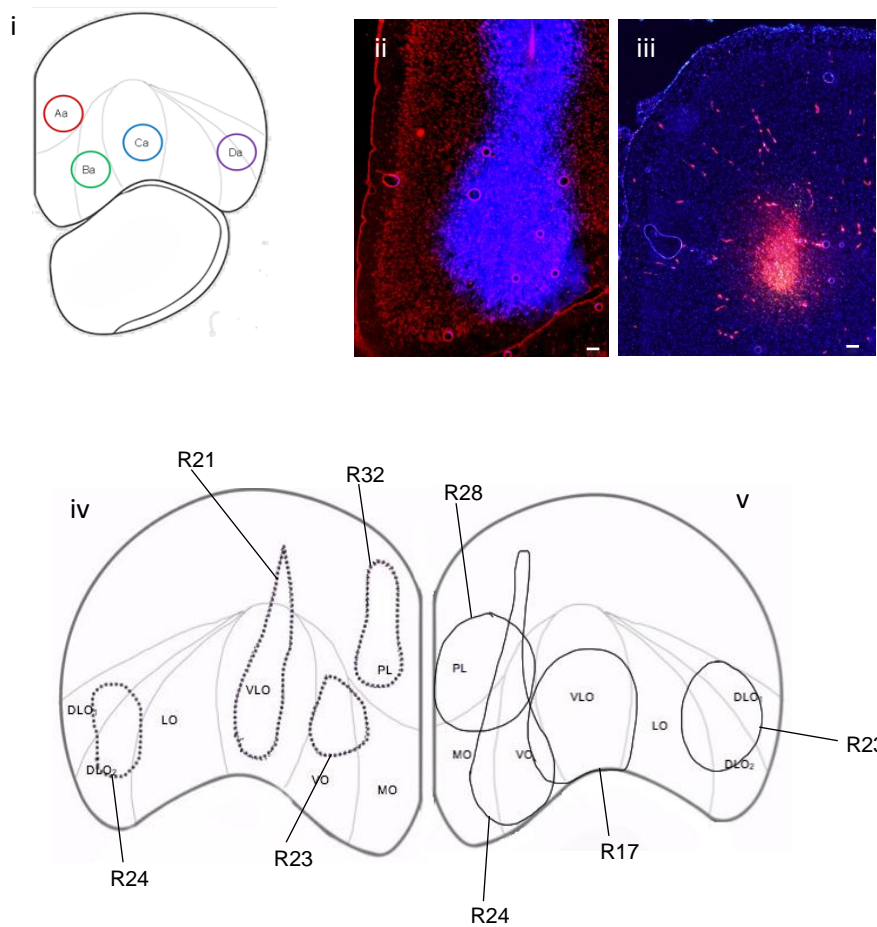
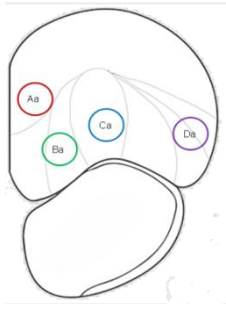


Figure 3.3. (i) Coronal section of anterior PFC (AP 4.7mm from Bregma) showing the cytoarchitectural boundaries of the prelimbic (PL), medial orbital (MO), ventral orbital (VO), ventrolateral orbital (VLO), lateral orbital (LO) and dorsolateral orbital (DLO) cortices (according to Van de Werd & Uylings, 2008), depicting sites of injections; Prelimbic: Aa, Ventral orbital: Ba, Ventrolateral orbital: Ca and dorsolateral orbital: Da, with 1mm spread. (ii) Coronal section of prefrontal cortex showing location and spread of (100nl) Fluoro-Gold at injection site in VO (R24). (iii) Coronal section of prefrontal cortex showing location and spread of (100nl) Fluoro-Ruby at injection site in PL (R32). (iv) Representations of Fluoro-Ruby (100nl) (R21, R23, R24, R32 (broken line)) injection sites in PL (R32), VO (R23), VLO (R21) and DLO (R24) in the right hemisphere. (v) Representations of Fluoro-Gold (100nl) (R17, R23, R24, R28 (solid line)) injection sites in PL (R28), VO (R24), VLO (R17) and DLO (R23) in the left hemisphere. Fluoro-Ruby injection sites were consistently within the boundaries of Fluoro-Gold injection sites. There is minimal overlap between Fluoro-Gold injection sites (R28 & R24, R24 & R17). Fluoro-Gold and Fluoro-Ruby injection sites are mostly limited to the cytoarchitectural boundaries of PFC regions, and span the majority of the region (PL, VO/MO, VLO, DLO), injections into VO spread into MO. Scale bars = 100µm.

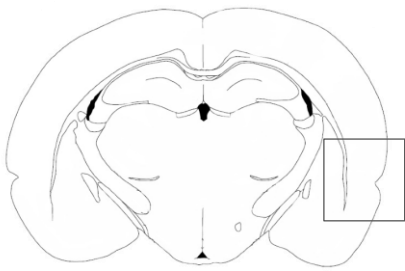
Retrograde labelling, resultant from Fluoro-Gold injections into anterior PFC (PL, VO, VLO and DLO) was found in regions of PRh, Ent, AuV, Cg1, M2, M1, S1J, Te and prefrontal

regions (Fig. 3.3. ii). Anterograde labelling resultant from Fluoro-Ruby injections into anterior PFC (PL, VO, VLO and DLO) was found in regions of PRh, Ect, Cg1, M2 and M1, as well as prefrontal regions (Fig. 3.3. iii). In order to further investigate the pathway between PFC and temporal cortex, which I had already identified, I initially analysed the labelling within areas of PRh and Ent.

i



- Aa (PL: R28(FG), R32(FR))
- Ba (VO: R24(FG), R23(FR))
- Ca (VLO: R17(FG), R21(FR))
- Da (DLO: R23(FG), R24(FR))



ii

Bregma -4.52mm

iii

Bregma -4.52mm

Bregma -2.8mm

Bregma -2.8mm

2mm

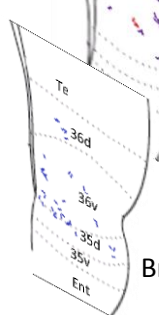


Figure 3.4 Diagram representing the injection sites of Fluoro-Gold and Fluoro-Ruby, and the projection sites to temporal cortex for both retrograde (Fluoro-Gold) and anterograde (Fluoro-Ruby) tracer injections. (i) The locations of injection sites Aa (PL: R28, R32), Ba (R23, R24), Ca (R17, R21) and Da (R23, R24) in anterior PFC. (ii) The locations of retrogradely labeled cells in temporal cortex, resultant from 100nl Fluoro-Gold injections into anterior PFC injection sites Aa-Da (R17, R23, R24, R28). (iii) The locations of anterogradely labeled axon terminals in temporal cortex, resultant from 100nl Fluoro-Ruby injections into anterior PFC injection sites Aa-Da (R21, R23, R24, R32).

Organisation of input connections from temporal to *anterior* prefrontal cortex

Projections to anterior PFC from temporal cortex were seen in PRh, Ent and Te (Fig. 3.3ii, Fig. 3.4). Retrogradely labelled cells from each each PFC injection site were distributed across several cytoarchitecturally distinct regions. The distribution of retrogradely labelled cells in temporal cortex maintained a spatial order according to the corresponding (Fluoro-Gold) PFC injection sites (PL, VO, VLO and DLO). Moving laterally in PFC from VO to DLO, projections from VO were seen dorsally compared to those from VLO (Fig. 3.3ii). There is an overlap between VO and VLO projections. Further, projections from DLO are seen ventrally to projections from VLO (Fig. 3.3 ii), indicating an ordered arrangement in the dorsal-ventral axis. A Factorial ANOVA revealed a significant main effect of anterior PFC injection site location on the dorsal-ventral distance from the rhinal sulcus of retrogradely labelled neuronal cells in temporal cortex ($F(3,648)=8.009$ $p<0.001$ $r=0.11$). Post hoc comparisons (Tukey HSD) revealed significant differences between retrograde injection sites into anterior Aa*Ca ($p=0.006$), Aa*Da ($p<0.001$) and VO*DLO ($p=0.003$). These results show evidence for an ordered arrangement of input connections from temporal cortex to anterior PFC (Fig. 3.5i).

Additionally, an ordered organisation can be seen in the anterior-posterior axis; projections from VO are present more anterior to VLO and projections from VLO anterior compared to DLO. There is an overlap in the anterior-posterior axis of projections from VO and VLO. A Factorial ANOVA revealed a significant main effect of anterior PFC injection site location on the anterior-posterior location of retrogradely labelled cells in temporal cortex ($F(3,648)=1008.089$ $p<0.001$ $r=0.78$). Post hoc comparisons (Tukey HSD) revealed significant differences between all of the four retrograde injection sites ($p<0.001$). These

findings indicate an ordered arrangement of input connections from PFC to temporal cortex in this axis of orientation (Fig. 3.5ii).

A Factorial ANOVA also revealed a significant main effect of anterior PFC injection site location on the medial-lateral distance from the cortical surface of retrogradely labelled cells in temporal cortex ($F(3,648)=39.076$ $p<0.001$ $r=0.24$). Post hoc comparisons (Tukey HSD) revealed significant differences between retrograde injection sites Aa*Ba, Aa*Ca and Aa*Da ($p<0.001$). This results show evidence for an ordered arrangement of input connections from anterior PFC to temporal cortex in this axis of orientation (Fig. 3.5iii).

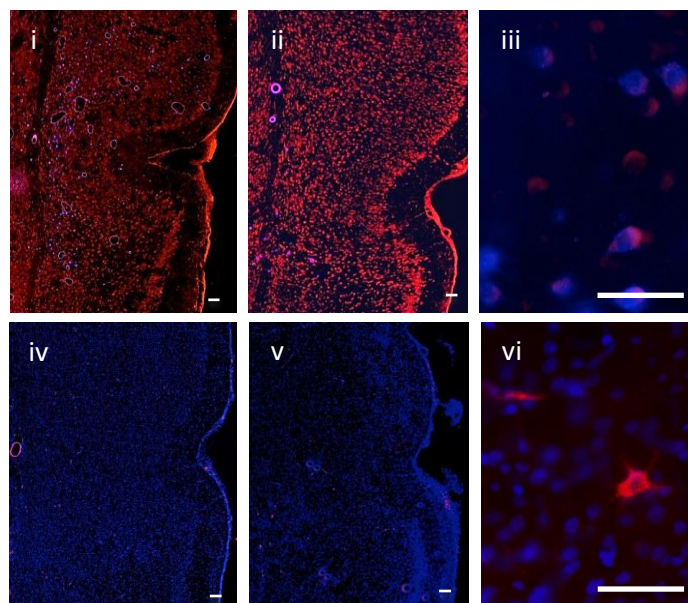


Figure 3.5. (i) Coronal section showing retrogradely labeled cells (blue) in temporal cortex produced by injection of Fluoro-Gold (100nl) into VO (R24). (ii) Coronal section showing retrogradely labeled cells (blue) in temporal cortex produced by injection of Fluoro-Gold into DLO (R23). (iii) Retrogradely labeled cells (blue) in temporal cortex. (iv) Coronal section showing anterogradely labeled axon terminals (red) in temporal cortex produced by injection of Fluoro-Ruby (100nl) into DLO (R24). (v) Coronal section showing anterogradely labeled axon terminals (red) in temporal cortex produced by injection of Fluoro-Ruby (100nl) into VLO (R21). (vi) Anterograde labelling (red) in temporal cortex. Scale bars = 100µm.

Organisation of Output Connections from *Anterior Prefrontal Cortex* to *Temporal Cortex*

Output projections from anterior PFC to temporal cortex were seen in PRh (36d, 36v, 35d) and Ent. The distribution of anterogradely labelled axon terminals in temporal cortex resultant from anterior PFC tracer injections is less widespread than the corresponding retrograde labelling. The distributions of anterogradely labelled axon terminals in temporal cortex maintain a spatial order in terms of the corresponding Fluoro-Ruby PFC injection site. Moving laterally in PFC from VO to DLO, projections from VO are seen more ventral in temporal cortex than projections from VLO, projections from DLO are seen more ventral to projections from VLO (Fig. 3.3 iii.). However, a Factorial ANOVA revealed no significant effect of anterior PFC injection site location on the dorsal-ventral distance from the rhinal sulcus of anterogradely labelled axon terminals in temporal cortex ($F(3,215)=2.053$ $p=0.107$ $r=0.10$).

Similarly, in the anterior-posterior axis, output projections from VO are located posterior to projections from VLO, projections from VLO are posterior to those from DLO. There is little overlapping in the output projections from anterior PFC to temporal cortex. : A Factorial ANOVA revealed a significant main effect of anterior PFC injection site location on the anterior-posterior location of anterogradely labelled axon terminals in temporal cortex ($F(3, 215)=99.042$ $p<0.001$ $r=0.56$). Post hoc comparisons (Tukey HSD) revealed significant differences between anterograde injection sites Aa*Ba, Aa*Ca, Ba*Ca, Ba*Da ($p<0.001$) and Aa*Da ($p=0.001$). These findings indicate an ordered arrangement of output connections from PFC to temporal cortex in this axis of orientation (Fig. 3.5ii).

A Factorial ANOVA also revealed a significant main effect of anterior PFC injection site location on the medial-lateral distance from the cortical surface of anterogradely labelled axon terminals in temporal cortex ($F(3,215)=40.627$ $p<0.001$ $r=0.40$). Post hoc comparisons (Tukey HSD) revealed significant differences between anterograde injection sites Aa*Ba, Aa*Da, Ba*Ca and Ca*Da ($p<0.001$). This results show evidence for an ordered arrangement of output connections from anterior PFC to temporal cortex in this axis of orientation (Fig. 3.5iii).

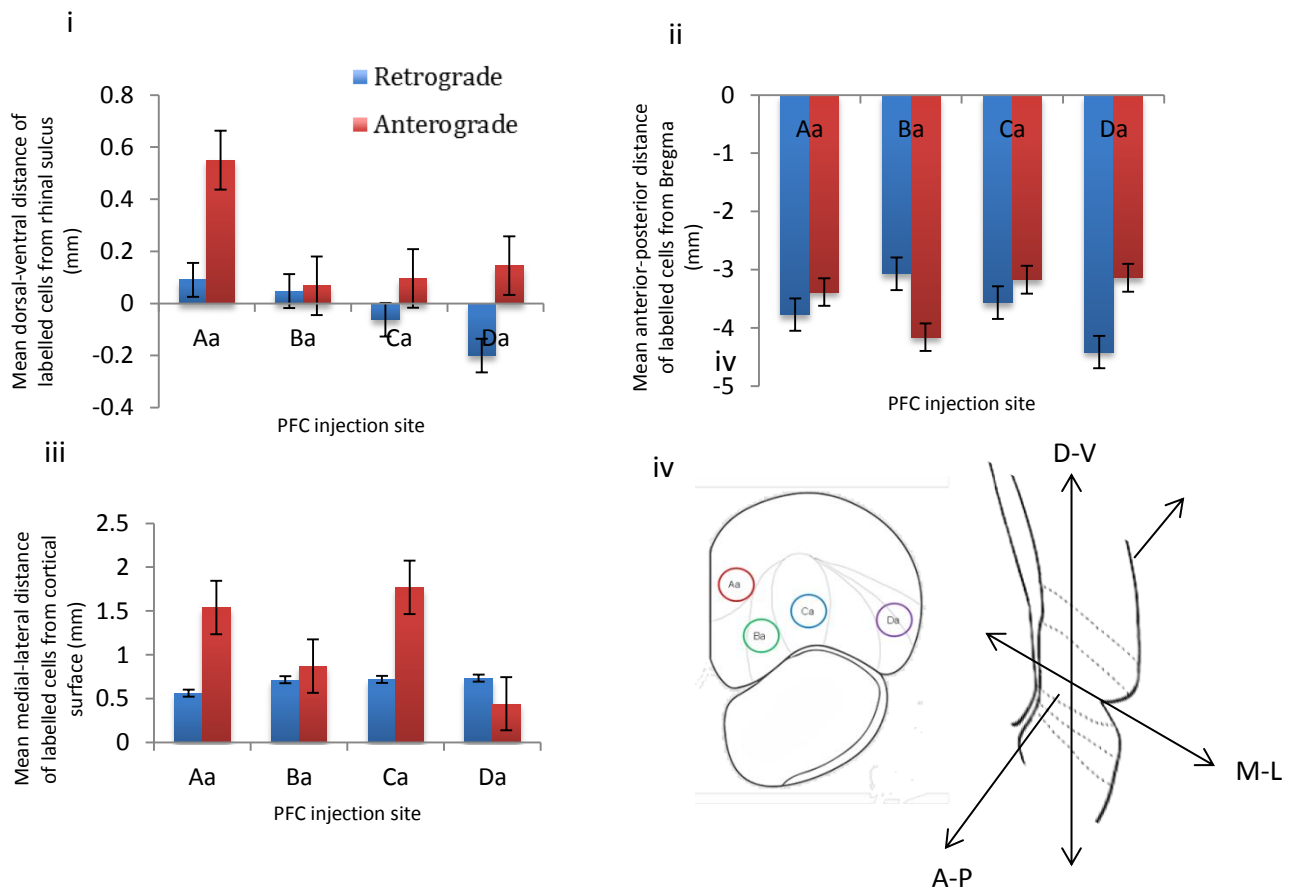


Figure 3.6. The mean effect of injection site in anterior PFC on the (i) dorsal-ventral, (ii) anterior-posterior and (iii) medial-lateral location of retrogradely labelled cells ($n=578$ arising from 4 rats: PL=75, VO=102, VLO=334, DLO=67) and anterogradely labelled axon terminals ($n=220$ arising from 4 rats: PL=47, VO=29, VLO=113, DLO=31) within temporal cortex. Error bars = standard error. (iv) Coronal cross section of PFC showing the position of 4 injection sites; Prelimbic (Aa), Ventral orbital (Ba), Ventrolateral orbital (Ca) and Dorsolateral orbital (Da). Coronal cross section of temporal cortex showing the three dimensions in which the locations of labels were recorded.

This analysis shows evidence for an ordered organisation of connections between anterior PFC and temporal cortex. As PFC injection sites move in the mediolateral direction (VO to DLO; Ba to Da), the pattern of input projections moves in a dorsal-ventral direction across temporal cortex, whilst simultaneously moving in an anterior-posterior direction. In addition, there is a linear structural organisation in terms of the mediolateral direction. Similarly, an organisational pattern of output projections can be observed, however this occurs in a different direction to input projections. As anterograde injection sites move mediolaterally in PFC from VO to DLO, the projections in temporal cortex move from posterior to anterior.

A two factor ANOVA revealed no significant interaction effect of input and output connections ($F(3,789)=2.227$ $p=0.084$). This indicates some similarity in the ordered arrangement of input and output connections in this axis of orientation (Fig. 3.5i).

A two factor ANOVA revealed a significant interaction effect of input and output connections in the anterior-posterior axis ($F(3,789)=505.379$ $p<0.001$ $r=0.390$) and medial-lateral axis ($F(3,789)=95.321$ $p<0.001$ $r=0.107$). These results show a clear difference in the ordered arrangement of input and output connections in these axes of orientation, indicating non-alignment (Fig. 3.5ii). No significant interaction between input and output connections was seen in the dorsal-ventral axis ($F(3,789)=2.227$ $p=0.084$). This indicates some similarity in the ordered arrangement of input and output connections in this axis of orientation (Fig. 3.5i). It is evident from these results that the input and output connections from anterior PFC to temporal cortex are not aligned with one another.

Central Prefrontal Cortex

The retrograde injection sites and labelling used in this part of the investigation uses the same data as in earlier studies (Appendix B;R4, R5, R6, R7). Additional co-injections of Fluoro-Gold and Fluoro-Ruby were made into the same central PFC co-ordinates as shown here to eliminate the possibility of an effect of separate injections on the results (Appendix G). Further central PFC injections of the anterograde tracer Fluoro-Emerald were made into the same co-ordinates as shown here to assist in the confirmation of anterograde labelling from Fluoro-Ruby (Appendix H).

Retrograde injections made into central PL, VO, VLO and DLO occurred in the intended PFC regions (Fig. 3.7). The majority of retrograde injection sites spanned layers I-VI, covered most of the cytoarchitectural region and were principally confined to cytoarchitectural boundaries of PFC sub-regions. The retrograde injection made into VO covered both VO and MO. There was some overlap between PL and VO injection sites and some spread into infralimbic cortex (IL) (Fig.3.7iv). Anterograde injection sites were mostly confined to the same region as counterpart retrograde injection sites, with anterograde injection sites consistently showing a smaller area of spread and predominantly covering layers III – VI.

Some minimal overlap can be seen between the anterograde injection into VO (R20) and the retrograde injection into PL (R29), however the majority of the anterograde VO injection site falls within the boundaries of the retrograde VO injection site.

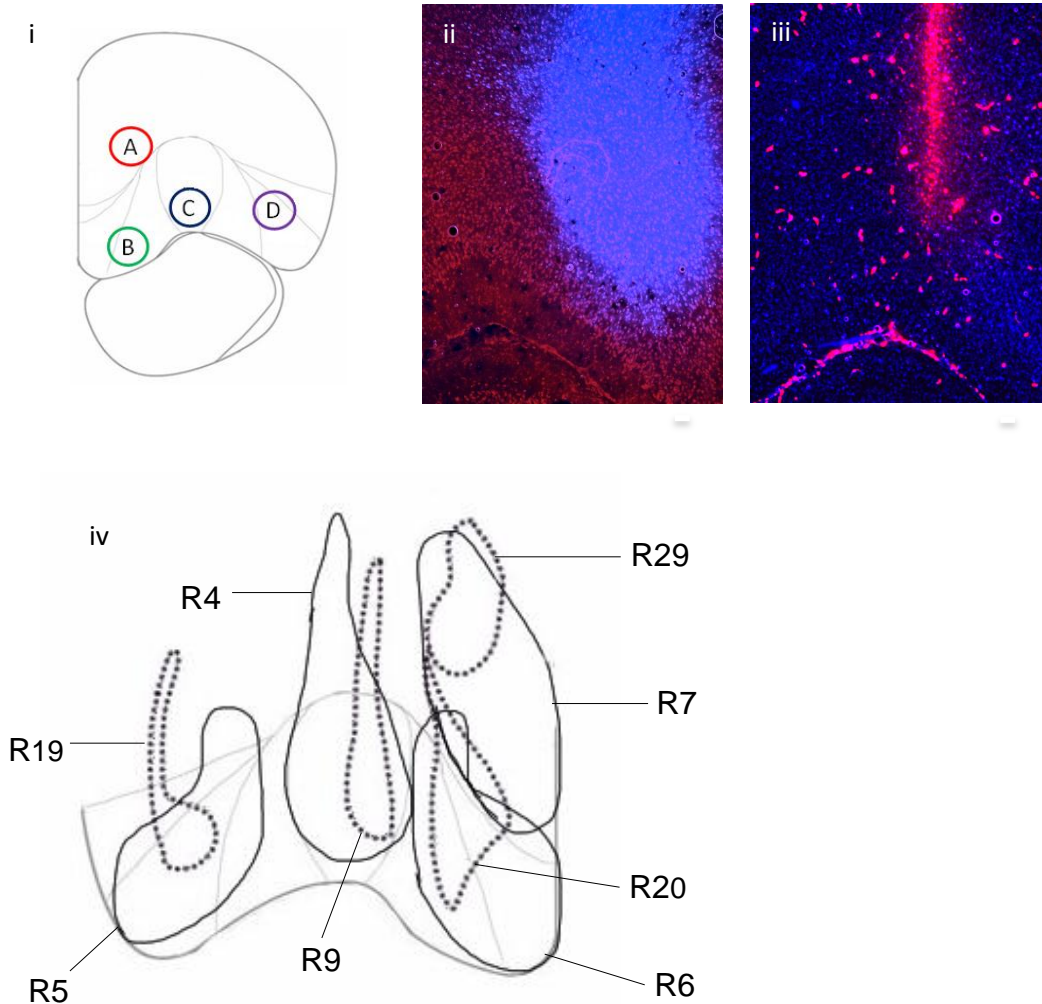


Figure 3.7 (i) Coronal section of PFC (AP 4.2mm from Bregma) showing the cytoarchitectural boundaries of the prelimbic (PL), infralimbic (IL), medial orbital (MO), ventral orbital (VO), ventrolateral orbital (VLO) and dorsolateral orbital (DLO) cortices (according to Van de Werd & Uylings, 2008), depicting sites of injections; prelimbic:A, ventral orbital:B, ventrolateral orbital:C and dorsolateral orbital:D, with 1mm spread. (ii) Coronal section of prefrontal cortex showing location and spread of (100nl) Fluoro-Gold (blue) at injection site in VO. (iii) Coronal section of prefrontal cortex showing location and spread of (100nl) Fluoro-Ruby (red) at injection site in VLO. (iv) Representations of Fluoro-Gold (100nl) (R4, R5, R6, R7 (solid line)) and Fluoro-Ruby (100nl) (R9, R19, R20, R29 (broken line)) injection sites in PL (R7, R29), VO (R6, R20), VLO (R4, R9) and DLO (R5, R19), in the right hemisphere. Scale bars = 100µm.

Anterograde labelling, resultant from Fluoro-Ruby injections into central PFC (PL, VO, VLO, DLO) was seen in regions of temporal cortex similar to that which I previously identified with BDA injections in the same region (Chapter 2). Anterograde labelling was seen in areas of PRh, Ect and Ent. The locations of both input and output connections observed in central PFC was similar to that seen in anterior PFC. Similar locations of retrograde and anterograde labelling were seen as a result of co-injections of Fluoro-Gold and Fluoro-Ruby (Appendix G) and anterograde labelling from injections of Fluoro-Emerald (Appendix H).

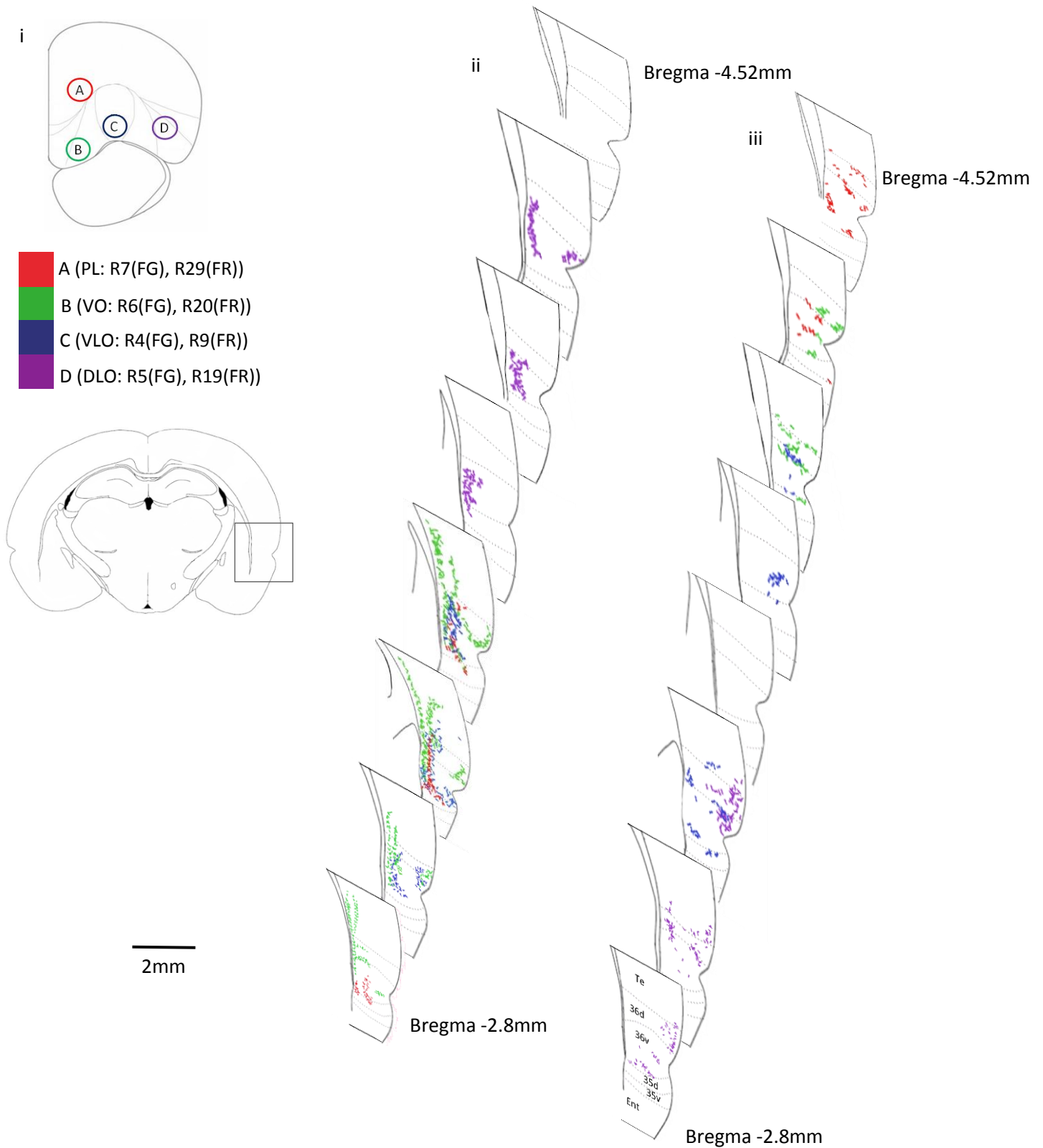


Figure 3.8. Diagram representing the injection sites of Fluoro-Gold and Fluoro-Ruby, and the projection sites to temporal cortex for both retrograde (Fluoro-Gold) and anterograde (Fluoro-Ruby) tracer injections. (i) The locations of injection sites A (PL: R7, R29), B (VO:R6, R20), C (VLO:R4, R9) and D (DLO: R5, R19) in central PFC. (ii) The locations of

retrogradely labeled cells in temporal cortex, resultant from 100nl Fluoro-Gold injections into central PFC injection sites A-D (R4, R5, R6, R7). (iii) The locations of anterogradely labeled axon terminals in temporal cortex, resultant from 100nl Fluoro-Ruby injections into central PFC injection sites A-D (R9, R19, R20, R29).

Organisation of Input Connections to *Central Prefrontal Cortex* from Temporal Cortex

Projections to central PFC from temporal cortex were seen in PRh, Ent and Te (Fig. 3.7.ii). Labelled cells from each injection location were distributed across several cytoarchitecturally distinct regions. The distribution of retrogradely labelled cells within temporal cortex maintained a spatial order according to the corresponding Fluoro-Gold injection sites. Moving laterally in PFC from VO to DLO: projections to VO (PRh, Te) were seen dorsally to those from VLO. An overlap of VO and LO projections is present. Projections to VLO are present only in PRh. Projections to DLO (PRh, Ent) are situated ventrally to those from VLO. An overlap of projections to VLO and DLO was seen. In addition, there was an ordered organisation present in the anterior-posterior axis. VO projections were seen more anteriorly to VLO projections. DLO projections are more posterior within perirhinal cortex to VLO projections. An overlap of projections to VO and VLO as well as VLO and DLO is present on the anterior-posterior axis. These findings are consistent with those described in Chapter 2.

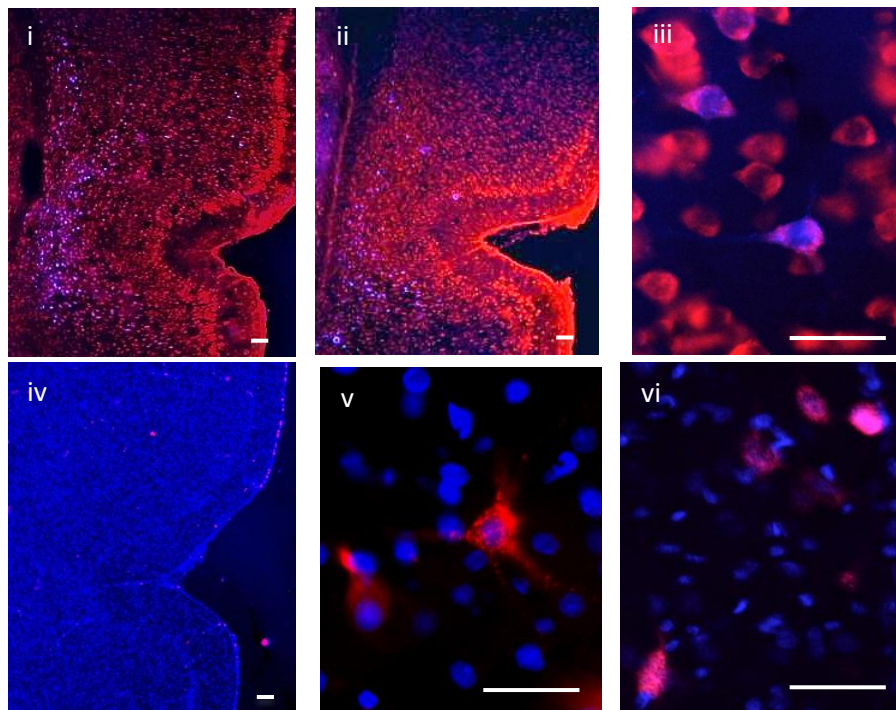


Figure 3.9. (i) Coronal section showing retrogradely labelled cells (blue) in temporal cortex produced by injection of Fluoro-Gold (100nl) into VO (R6). (ii) Coronal section showing retrogradely labelled cells (blue) in temporal cortex produced by injection of Fluoro-Gold (100nl) into DLO (R5). (iii) Retrogradely labelled cells in temporal cortex produced by injection of Fluoro-Gold (100nl) into DLO (R5). (iv) Coronal section showing anterogradely labelled axon terminals (red) in temporal cortex produced by injection of Fluoro-Ruby into VO (R20). (v) Anterogradely labelled axon terminals in temporal cortex produced by injection of Fluoro-Ruby into VLO (R9). (vi) Anterogradely labelled axon terminals in temporal cortex produced by injection of Fluoro-Ruby into PL (R29). Arrows denote the location of the rhinal sulcus. Scales bars = 100 μ m

Organisation of Output Connections to *Central Prefrontal Cortex* from Temporal Cortex

Output projections from central PFC to temporal cortex were seen in PRh (35d, 36v, 36d) and Te. The distribution of anterogradely labelled axon terminals in temporal cortex maintained a spatial order corresponding to Fluoro-Ruby central PFC injection sites (Fig. 3.7iii). As PFC injection sites move from medial to lateral (VO to DLO) projections in temporal cortex move from ventral to dorsal, whilst simultaneously moving from posterior to anterior. In addition, an ordered organisation of projections can be seen in the medial-lateral axis, with projections moving from medial to lateral as PFC injection sites move mediolaterally from VO to DLO. VO projections are seen more ventral, posterior and medial to VLO, VLO projections are seen more ventral, posterior and medial to DLO. Some overlap in VLO and DLO projections can be seen in the anterior-posterior axis, as well as between VO and VLO, and between PL and VO. The extent of the overlap is less than with equivalent retrograde labelling. The

distribution of anterograde labelling in temporal cortex is consistently less than retrograde labelling from the same central PFC injection sites (Fig. 3.8).

Statistical evidence for this ordered arrangement is consistent with that described in Chapter 2 and can be seen in detail in Appendix F. A Factorial ANOVA revealed a significant main effect of central PFC injection location on the location of retrogradely labeled cells in temporal cortex (in the dorsal-ventral axis ($p < 0.001$), anterior-posterior axis ($p < 0.001$) and medial-lateral axis ($p < 0.001$) and anterogradely labeled axon terminals in temporal cortex (in the dorsal-ventral axis ($p < 0.001$), anterior-posterior axis ($p < 0.001$) and medial-lateral axis ($p < 0.001$) (Fig. 3.9). A two factor ANOVA also revealed evidence of differential ordering of inputs and outputs in the anterior-posterior, dorsal-ventral and medial-lateral axes ($p < 0.001$). These results show clear evidence of ordering for both input and output connections from prefrontal to temporal cortex, as well as clear non-alignment between inputs and outputs.

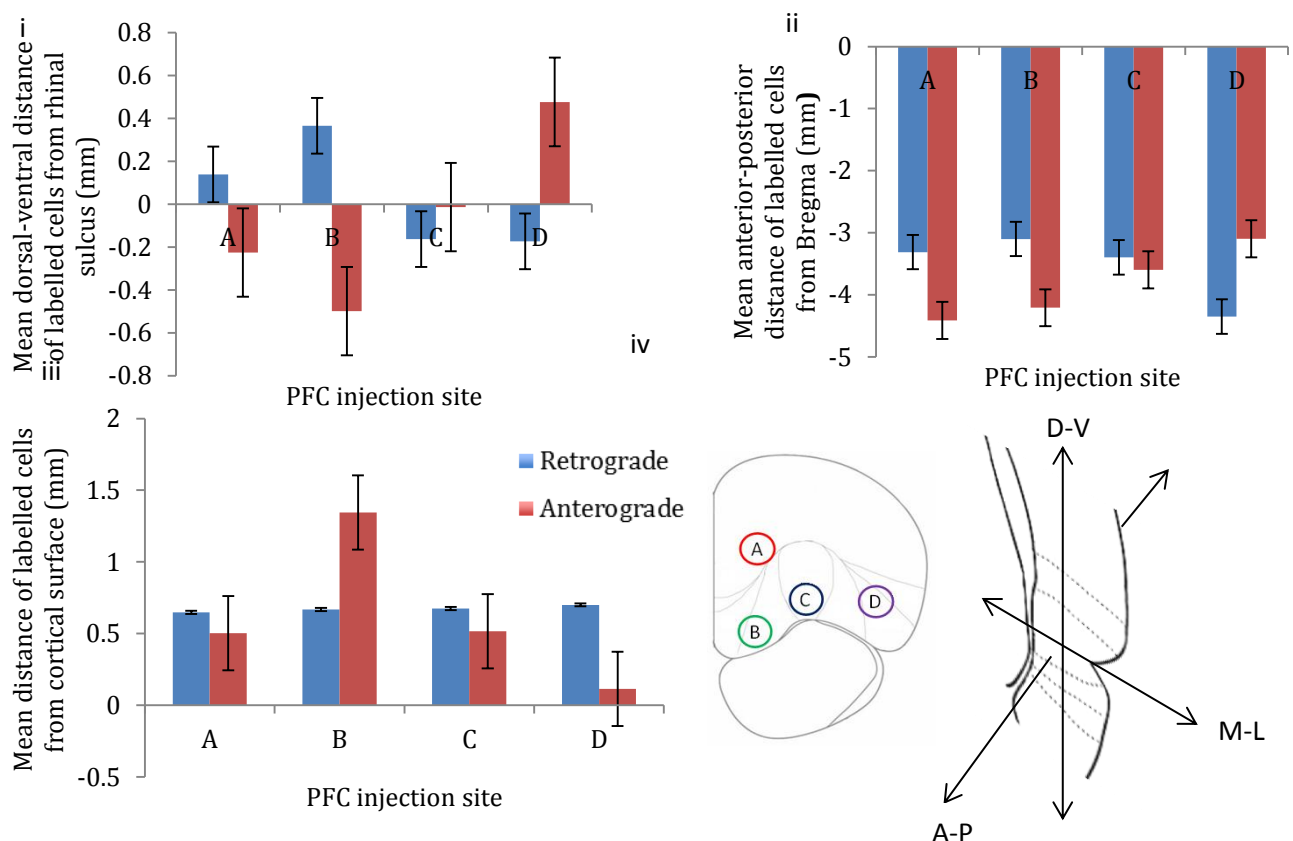


Figure 3.10. The mean effect of central PFC injection site on the (i) dorsal-ventral, (ii) anterior-posterior and (iii) medial-lateral location of retrogradely labeled cells ($n=1412$ arising from 4 rats: PL=253, VO=677, VLO=131, DLO=351) and anterogradely labeled axon terminals ($n=444$ arising from 4 rats: PL=63, VO=144, VLO=97, DLO=140) within temporal cortex. Error bars=standard error. (iv) Coronal cross section of prefrontal cortex

showing the position of 4 injection sites; prelimbic (A), ventral-orbital (B), ventrolateral orbital (C) and dorsolateral orbital (D). Coronal cross section of temporal cortex showing the three dimensions in which the locations of labels were recorded.

A statistical comparison between central PFC labelling seen here and that produced by BDA and Fluoro-Gold injections (Chapter 2) revealed no significant difference ($p=0.272$), indicating consistency in my findings of ordering and non-alignment (Appendix I).

Posterior Prefrontal Cortex

Retrograde injections made into posterior PL, VO, VLO and DLO (R11, R22, R26, R27) occurred in the intended PFC regions. All retrograde injections covered the majority of the intended PFC cytoarchitectural regions, covered layers I-VI and were for the most part separate from one another, minimal overlapping between injection sites was observed. The injection into PL (R27) spread across layers II-VI and overlapped slightly with the injections into VO and VLO. The injection into VO (R22) overlapped with the PL injection and spread into the PL region, however the majority of injected tracer was seen within the intended regions of VO and MO. The VLO injection site also spread beyond the intended region, however the majority of injected tracer remained within the boundaries of VLO and covered layers I-VI. The DLO injection site did not overlap with any other retrograde injection sites and remained mostly within the cytoarchitectural region of DLO.

Anterograde injections made into posterior PL, VO, VLO and DLO (R25, R26, R27, R28) occurred in the intended PFC regions. All anterograde injections remained within the cytoarchitectural boundaries of PFC sub-regions. All of the anterograde injection sites produced a smaller spread of tracer than the corresponding retrograde injection sites. All of the anterograde injection sites were positioned mostly within the boundaries of the corresponding retrograde injection sites. There was no overlapping between anterograde posterior PFC injection sites.

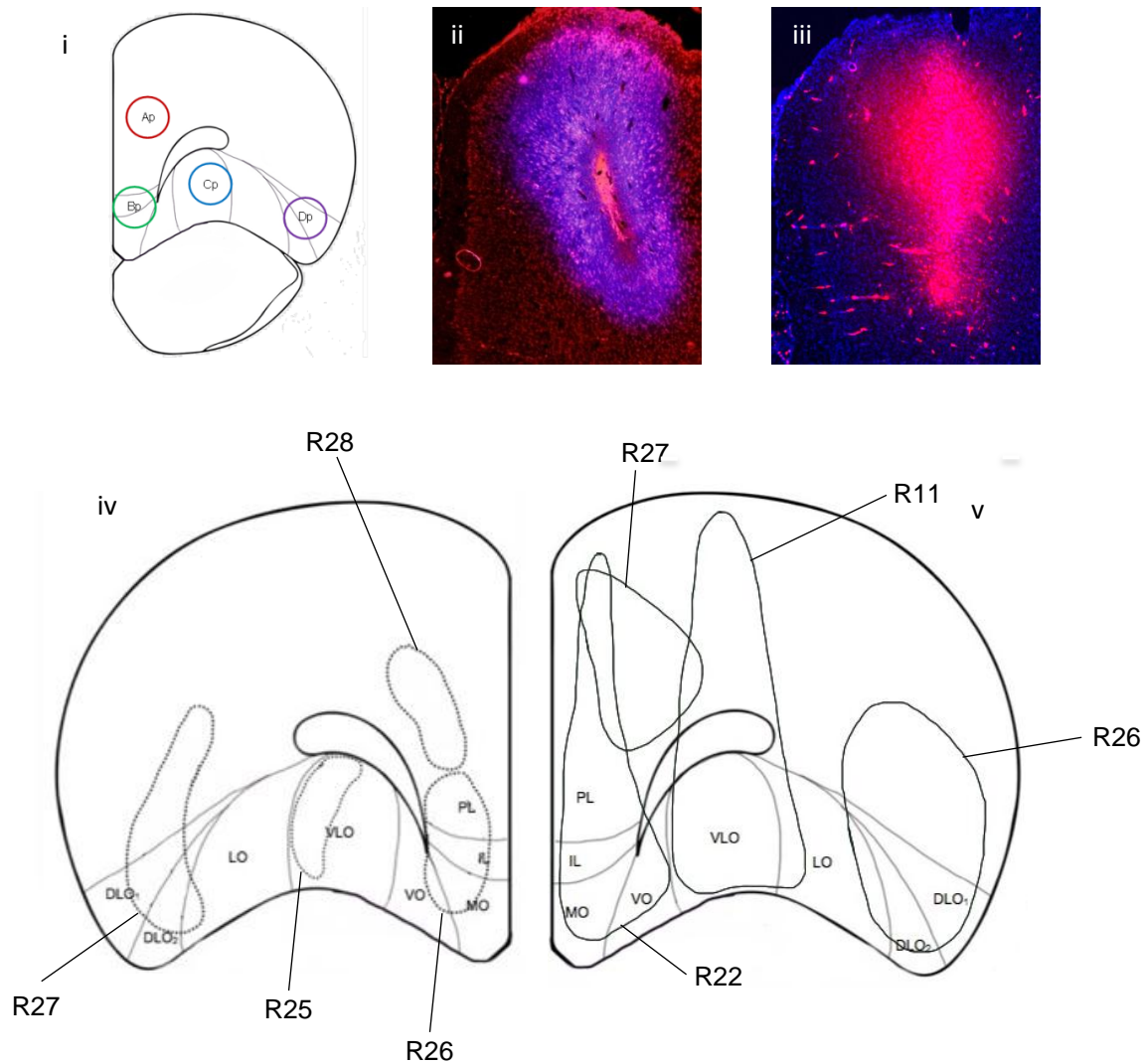


Figure 3.11 (i) Coronal section of PFC (AP 3.7mm from Bregma) showing the cytoarchitectural boundaries of the prelimbic (PL), infralimbic (IL), ventral orbital (VO) ventrolateral orbital (VLO) and dorsolateral orbital (DLO) cortices (according to Van de Werd & Uylings, 2008), depicting sites of injections; Prelimbic: Ap, Ventral orbital: Bp, Ventrolateral orbital: Cp and Dorsolateral orbital: Dp, with 1mm spread. (ii) Coronal section of prefrontal cortex showing location and spread of (100nl) Fluoro-Gold (blue) at injection site in PL (R27). (iii) Coronal section of prefrontal cortex showing location and spread of (100nl) Fluoro-Ruby (red) at injection site in PL (R28). (iv) Representations of Fluoro-Ruby (100nl) (R25, R26, R27, R28 (broken line) injection sites in PL (R28), VO (R26), VLO (R25) and DLO (R27), in the right hemisphere. (v) Representations of Fluoro-Gold (100nl) (R11, R22, R26, R27 (solid line)) injection sites in PL (R27), VO (R22), VLO (R11) and DLO (R26), in the left hemisphere. Fluoro-Ruby injection sites were consistently within the boundaries of corresponding Fluoro-Gold injection sites. There is minimal overlap between Fluoro-Gold injection sites (R27 & R22). Scale bars = 100 μ m.

Retrograde labelling, resultant from Fluoro-Gold injections into posterior PFC (PL, VO, VLO and DLO) was found in regions of PRh, Ent, AuV, Cg1, M2, M1, S1J and prefrontal regions (Fig.3.11i, ii. Fig. 6.12ii). Anterograde labelling resultant from Fluoro-Ruby injections into posterior PFC (PL, VO, VLO and DLO) was found in regions of PRh, Ent, Cg1, M2 and M1, as well as prefrontal regions (Fig. 3.11iii, iv. 3.12iii). In order to investigate the pathway between posterior PFC and temporal cortex, the labelling within areas of Cg1, M1, M2 and S1J was analysed.

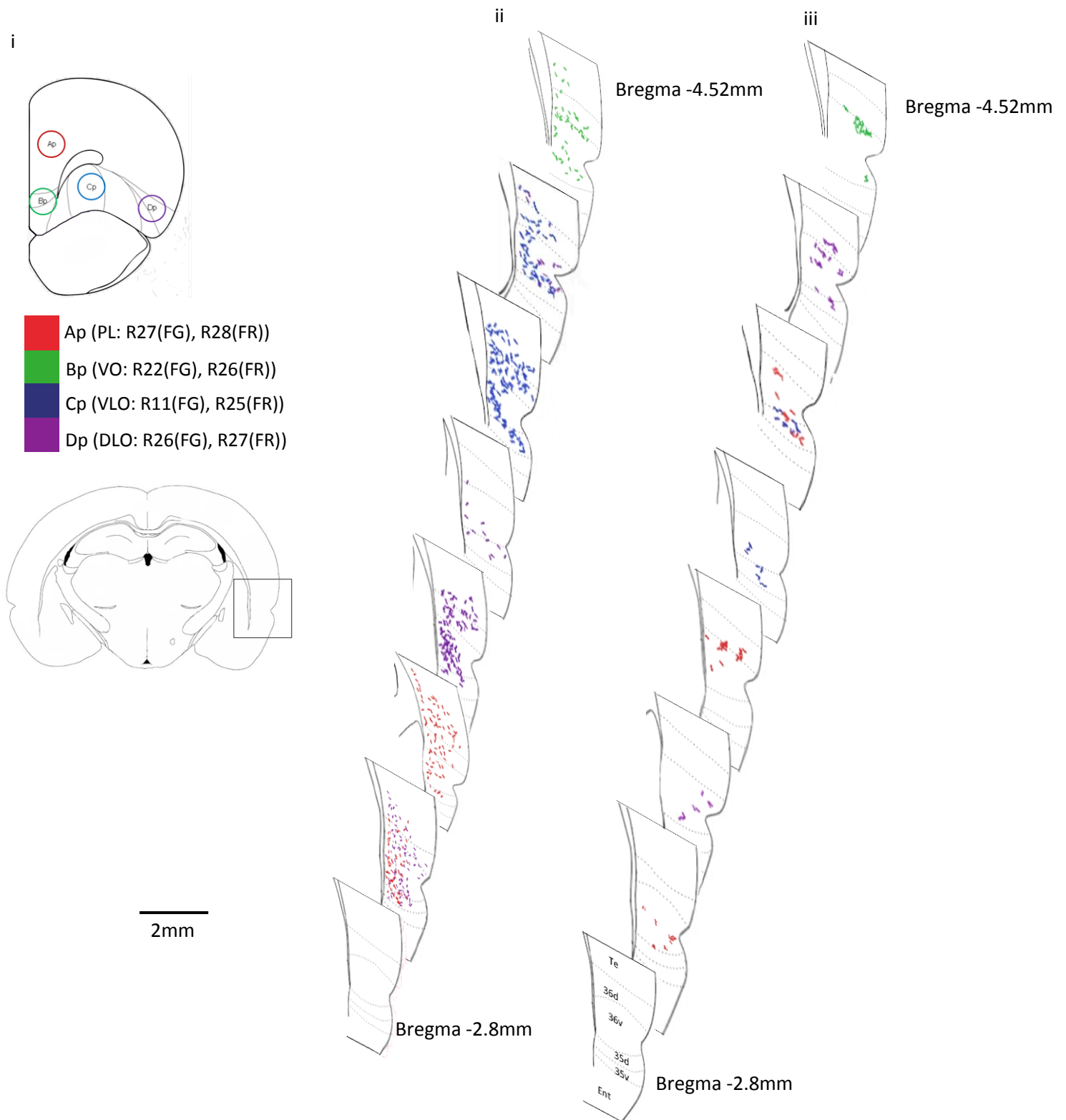


Figure 3.12. Diagram representing the injection sites of Fluoro-Gold and Fluoro-Ruby, and the projection to temporal cortex for both retrograde (Fluoro-Gold) and anterograde (Fluoro-Ruby) tracer injections. (i) The locations of injection sites Ap (PL:R27,R28), Bp (VO:R22,R26), Cp (VLO:R11,R25) and Dp (DLO:R26,R27) in posterior PFC. (ii) The locations of retrogradely labelled cells in temporal cortex, resultant from 100nl Fluoro-Gold

injections into posterior PFC injection sites Ap-Dp (R11, R22, R26, R27). (iii) The locations of anterogradely labelled axon terminals in temporal cortex, resultant from 100nl Fluoro-Ruby injections into posterior PFC injection sites Ap-Dp (R25, R26, R27, R28).

Organisation of Input Connections to *Posterior Prefrontal Cortex* from Temporal Cortex

Projections to posterior PFC from temporal cortex were seen in PRh and Te (Fig. 3.11ii) Labelled cells from each injection location were distributed across several cytoarchitecturally distinct regions of temporal cortex. The distribution of retrogradely labelled cells with temporal cortex maintained a spatial order according to the corresponding Fluoro-Gold posterior PFC injection sites. Moving from medial to lateral in posterior PFC from VO to DLO, projections to VO were seen more posterior to projections to VLO, projections to VLO were seen more posterior compared to projections to DLO. A Factorial ANOVA revealed a significant main effect of posterior PFC injection site location on the anterior-posterior location of retrogradely labelled cells in temporal cortex ($F(3,265)=648.369$ $p<0.001$ $r=0.84$). Post hoc comparisons (Tukey HSD) revealed significant differences between all retrograde injection sites ($p<0.001$). These results provide evidence for ordering of input connections from posterior PFC to temporal cortex in this axis of orientation (Fig.3.13ii).

Additionally, VO projections could be seen dorsally to VLO projections and VLO projections dorsally to DLO. An overlap in temporal cortex projections can be seen between VLO and DLO. However, a Factorial ANOVA revealed no significant main effect of posterior PFC injection site location on the dorsal-ventral distance from the rhinal sulcus of retrogradely labelled cells in temporal cortex ($F(3,265)=0.535$ $p=0.659$), showing no significant evidence for ordering of input or output connections from posterior PFC to temporal cortex in this axis of orientation (Fig.3.13i).

A Factorial ANOVA also revealed a significant main effect of posterior PFC injection site location on the medial-lateral distance from the cortical surface of retrogradely labelled cells in temporal cortex ($F(3, 265)=267.195$ $p<0.001$ $r=0.71$). Post hoc comparisons (Tukey HSD) revealed significant differences between retrograde injection sites Ap*Bp, Bp*Cp, Bp*Dp

($p < 0.001$) and Cp*Dp ($p = 0.045$). These results show evidence for clear ordering of input connections in this axis of orientation (Fig. 3.13iii).

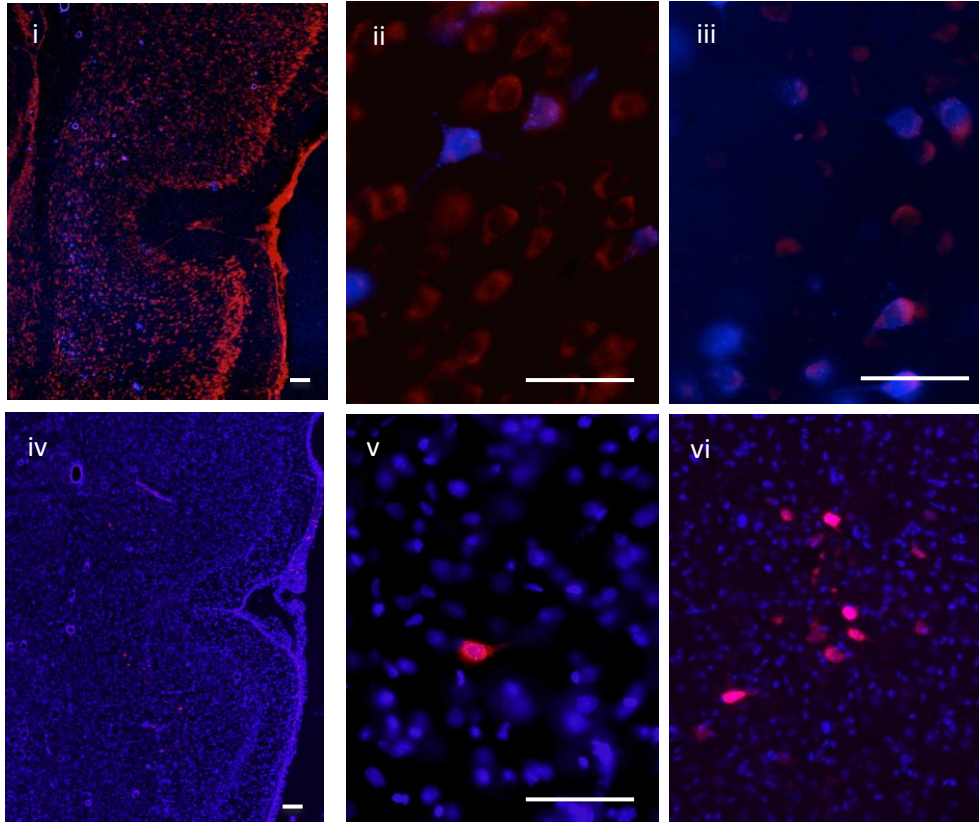


Figure 3.13. (i) Coronal section showing retrogradely labelled cells (blue) in temporal cortex produced by injection of Fluoro-Gold (100nl) into posterior VO (R22). (ii) Retrogradely labelled cells (blue) in PRh, resultant from injection of Fluoro-Gold (100nl) into posterior VO (R22). (iii) Retrogradely labelled cells (blue) in PRh, resultant from injection of Fluoro-Gold into posterior PL (R27). (iv) Coronal section showing anterogradely labelled axon terminals (red) in temporal cortex produced by injection of Fluoro-Ruby (100nl) in posterior VLO (R25). (v) Anterogradely labelled axon terminals in PRh, resultant from injection of Fluoro-Ruby (100nl) in posterior VLO (R25). (vi) Anterogradely labelled axon terminals in PRh, resultant from injection of Fluoro-Ruby (100nl) in posterior DLO (R27). Scale bars = 100 μ m.

Organisation of output connections from *posterior* prefrontal to temporal cortex

Projections from posterior PFC to temporal cortex were seen in PRh (Fig. 3.11iii). The distribution of anterogradely labelled axon terminals maintained a spatial order according to

Fluoro-Ruby posterior PFC injection sites. Moving from medial to lateral in posterior PFC (VO to DLO), anterograde labels in temporal cortex move from posterior to anterior. A Factorial ANOVA revealed a significant main effect of posterior PFC injection site location on the anterior-posterior location of anterogradely labelled axon terminals in temporal cortex ($F(3,257)=59.249$ $p<0.001$ $r=0.43$). Post hoc comparisons (Tukey HSD) revealed significant differences between anterograde injection sites Ap*Bp, Ap*Cp, Ap*Dp, Bp*Cp and Bp*Dp ($p<0.001$). These results provide evidence for ordering of output connections from posterior PFC to temporal cortex in this axis of orientation (Fig.3.13ii).

No clear order of output connections from posterior PFC can be seen in the dorsal-ventral axis. A Factorial ANOVA revealed no significant effect of posterior PFC injection site on the dorsal-ventral distance from the rhinal sulcus of anterogradely labelled axon terminals in temporal cortex ($F(3,257)=0.717$ $p=0.543$). Similarly, no clear ordering can be seen in the medial-lateral axis. However, A Factorial ANOVA revealed a significant main effect of posterior PFC injection site location on the medial-lateral distance from the cortical surface of anterogradely labelled axon terminals in temporal cortex ($F(3,257)=78.813$ $p<0.001$ $r=0.49$). Post hoc comparisons (Tukey HSD) revealed significant differences between anterograde injection sites Ap*Cp, Bp*Cp and Cp*Dp ($p<0.001$). These results show evidence for clear ordering of output connections in this axis of orientation (Fig. 3.13iii).

This analysis provides evidence for an ordered organisation of connections between posterior prefrontal and temporal cortex. As posterior PFC is moved from medial to lateral (VO to DLO: Bp to Dp), the pattern of input projections moves in a posterior to anterior direction. At the same time, the pattern of output projections also moves from posterior to anterior. The resultant labelling of input and output connections from posterior PFC show that inputs and outputs are aligned with one another. A two factor ANOVA revealed no significant interaction effect of input and output connections in the dorsal-ventral ($F(3,522)=0.921$ $p=0.430$) axis. Significant interactions were observed in the anterior-posterior ($F(3,522)=49.350$ $p<0.001$ $r=0.086$) and medial-lateral ($F(3,522)=131.903$ $p<0.001$ $r=0.202$) axes. These findings provide evidence to suggest a difference in the organisation of input and output connections in these axes of orientation (Fig. 3.13ii, iii).

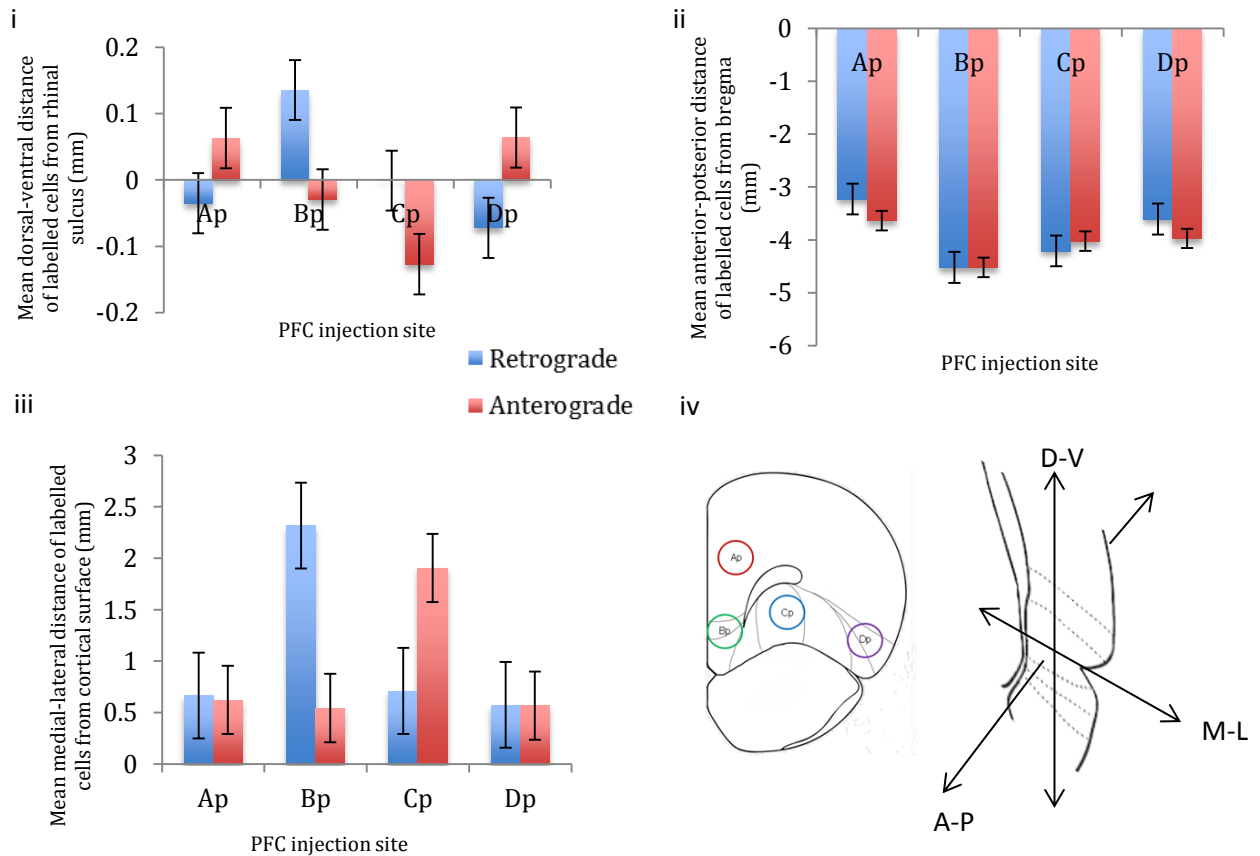


Figure 3.14. The mean effect of posterior PFC injection site location on the (i) dorsal-ventral (ii) anterior-posterior and (iii) medial-lateral location of retrogradely labeled cells ($n=269$ arising from 4 rats: PL=114, VO=25, VLO=85, DLO=45) and anterogradely labeled axon terminals ($n=261$ arising from 4 rats: PL=51, VO=36, VLO=113, DLO=61) within temporal cortex. Error bars = standard error. (iv) Coronal cross section of PFC showing the position of 4 injection sites; prelimbic (Ap), ventral orbital (Bp), ventrolateral orbital (Cp) and dorsolateral orbital (Dp). Coronal cross section of temporal cortex showing the three dimensions in which the locations of labels were recorded.

Organisation of Connections from Anterior to Posterior Prefrontal Cortex

A factorial ANOVA was applied to determine if there was an effect of the anterior-posterior location of PFC injection sites on the location of retrograde and anterograde labels in temporal cortex. The analysis revealed evidence for a gradient in terms of alignment of input and output connections from PFC to temporal cortex.

Statistical evidence for this alignment gradient came from the following analysis:

In the dorsal-ventral axis: A factorial ANOVA revealed a significant effect of the anterior-posterior location of PFC injection site on the dorsal-ventral location of retrogradely labelled cells ($F_{(2,2255)}=13.238$ $p<0.001$ $r=0.08$) and anterogradely labelled axon terminals in temporal cortex ($F_{(2,924)}=3.381$ $p=0.034$). Post hoc comparisons (Tukey HSD) revealed significant differences between anterior and central retrograde PFC injection sites ($p<0.001$) as well as central and posterior retrograde PFC injection sites ($p=0.012$). Post hoc comparisons (Tukey HSD) revealed significant differences between anterior and central anterograde PFC injection sites ($p=0.035$) and no significant difference between central and posterior anterograde PFC injection sites ($p=0.987$). These findings show evidence for ordering of input and output connections from anterior to posterior PFC.

In the anterior-posterior axis: A factorial ANOVA revealed a significant effect of the A-P location of PFC injection site on the anterior-posterior location of retrogradely labelled cells in temporal cortex ($F_{(2,2255)}=31.354$ $p<0.001$ $r=0.12$) and anterogradely labelled axon terminals in temporal cortex ($F_{(2,924)}=112.043$ $p<0.001$). Post hoc comparisons (Tukey HSD) revealed significant differences between anterior and central retrograde PFC injection sites as well as central and posterior retrograde PFC injection sites ($p<0.001$). Post hoc comparisons (Tukey HSD) revealed significant differences between anterior, central and posterior anterograde PFC injection sites ($p<0.001$). These findings show evidence for ordering of input and output connections from anterior to posterior PFC.

In the medial-lateral axis: A factorial ANOVA revealed a significant effect of the A-P location of PFC injection site on the medial-lateral location of retrogradely labelled cells in temporal cortex ($F_{(2,2255)}=42.146$ $p<0.001$ $r=0.14$) and anterogradely labelled axon terminals in temporal cortex ($F_{(2,924)}=288.179$ $p<0.001$). Post hoc comparisons (Tukey HSD) revealed significant differences between anterior and central retrograde PFC injection sites ($p=0.002$) as well as between central and posterior retrograde PFC injection sites ($p<0.001$). Post hoc comparisons (Tukey HSD) revealed significant differences between anterior, central and posterior anterograde PFC injection sites ($p<0.001$). These findings show evidence for ordering of input and output connections from anterior to posterior PFC.

These results show that an anterior-posterior change in the location of PFC injection sites substantially changes the location of labelled targets in temporal cortex, indicating evidence of ordered organisation occurring from anterior to posterior PFC (Fig. 3.14).

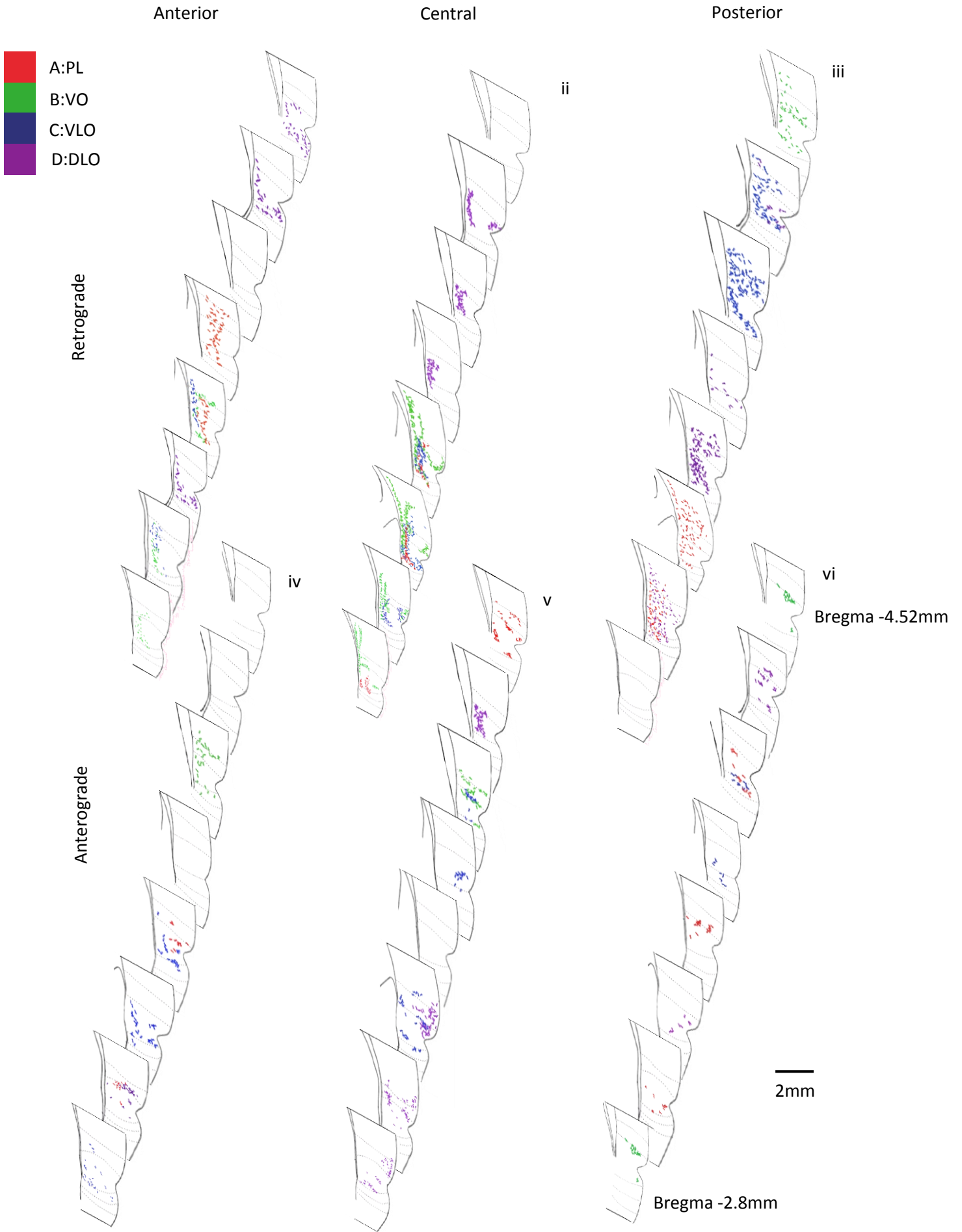


Figure 3.15. Diagram representing the projections to temporal cortex for both retrograde (Fluoro-Gold) and anterograde (Fluoro-Ruby) tracer injections, from anterior, central and posterior PFC. Retrograde labelling in temporal cortex produced by Fluoro-Gold injections into (i) anterior PFC. (ii) central PFC and (iii) posterior PFC. Anterograde labelling in temporal cortex produced by Fluoro-Gold injections into (iv) central PFC and (vi) Anterograde labelling in sensory-motor cortex produced by Fluoro-Gold injections into posterior PFC.

Figure 3.15 shows a substantial change in the organisational pattern of both input and output connections as the PFC source region (injection site) moves from anterior to posterior. Most notably in the anterior-posterior and dorsal-ventral axes, the organisation of input and output connections become considerably more aligned with one another in posterior PFC compared to central and anterior PFC.

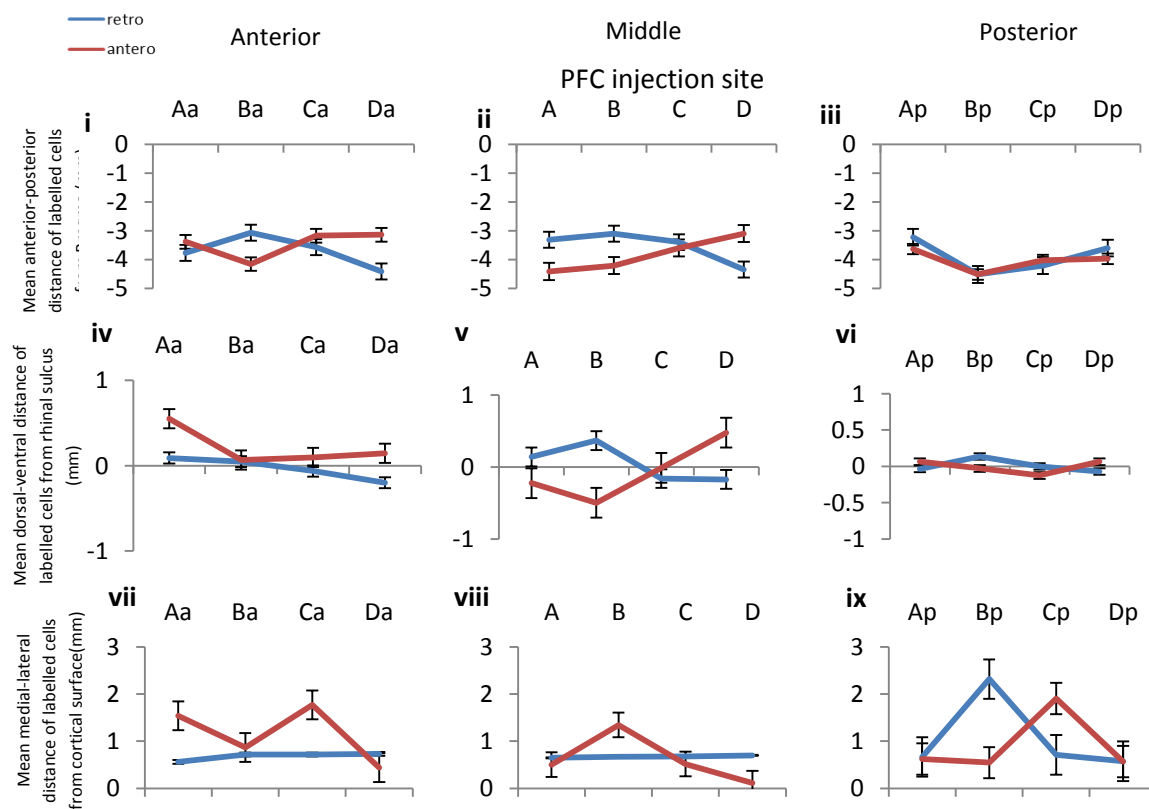


Figure 3.16. The mean effect of PFC injection site on the anterior-posterior, dorsal-ventral and medial-lateral location of retrograde and anterograde labels in temporal cortex from (i, ii, iii) anterior PFC injection sites, (iv, v, vi) central PFC injection sites and (vii, viii, ix) posterior PFC injection sites (PL, VO, VLO and DLO).

Alignment of input and output connections to temporal cortex from anterior – posterior PFC

To clearly visualise the relationship between input and output connections to temporal cortex across anterior – posterior PFC, the mean Euclidean distance (E) between retrograde and anterograde labels from each injection site was calculated. Paired samples T-tests revealed a significant difference in the distance between anterograde and retrograde labels in temporal cortex from anterior PFC injections ($t(3)=-3.154$ $p=0.05$), compared to no significant difference following posterior PFC injections ($t(3)=-2.226$ $p=0.112$). Fig. 3.15 shows that as PFC injection sites become more posterior, the distance between retrograde and anterograde labels becomes smaller, meaning that input and output connections become more aligned with one another.

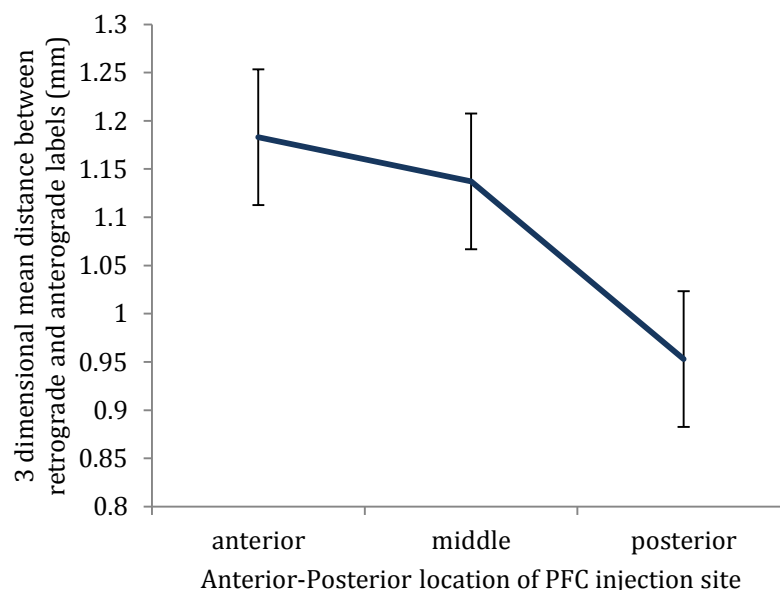


Figure. 3.17. The effect of the anterior-posterior location of PFC injection site on the average 3 dimensional distance between anterograde and retrograde labelling produced by (100nl) injections of Fluoro-Gold and Fluoro-Ruby into anterior, central and posterior PFC in temporal cortex Error bars = standard error.

Discussion

This study investigated connections to temporal cortex from the most anterior region of PFC (4.7mm from Bregma) to the most posterior region of PFC (3.7mm from Bregma). The findings support my earlier observations of an ordered arrangement of projections from PFC to regions of temporal cortex (Chapter 2) and provides additional insights into the alignment of PFC connections. The findings revealed a clear ordered arrangement of connections from central PFC (Bregma 4.2mm) to temporal cortex, from both anterograde and retrograde labelling, similar to that seen with Fluoro-Gold and BDA in my previous study and consistent with the findings of Kondo & Witter (2014), Hoover & Vertes (2011) and Sesack (1989). The results also revealed evidence of a similar ordered organisation of both input and output connections occurring in the pathways between anterior PFC (Bregma 4.7mm) and temporal cortex and posterior PFC (Bregma 3.7mm) to temporal cortex; where the ordering in posterior PFC differs to that seen in anterior and central PFC. This provides evidence to suggest differential organisational patterns within PFC. These findings have shown consistent evidence for non-alignment in the input and output connections from PFC to temporal cortex. In addition this study has shown evidence for changes in the degree of alignment in anterior compared to posterior PFC, whereby anterior PFC is highly non-aligned and posterior PFC is considerably aligned. This demonstrates an organisational gradient of connections, consistent with reported functional organisational gradients observed in terms of abstraction (Christoff, 2009).

Anterior Prefrontal Cortex

Following administration of the anterograde tracer Fluoro-Ruby to the anterior PFC regions PL, VO, VLO and DLO, labelling of axon terminals was found in areas of prefrontal cortex, temporal cortex, motor cortex, cingulate cortex, piriform cortex and somatosensory cortex.

The retrograde labelling found in temporal cortex resultant from anterior PFC tracer injections differed to that which was identified from central PFC injections, in that labelling was more ventral and posterior than that produced from central PFC injections. The pattern of

ordered organisation of input connections from temporal cortex to PFC was very similar in anterior and central PFC.

My results show clear evidence of ordering of both input and output connections in the anterior PFC – temporal cortex pathway in multiple orientations. There is strong evidence of non-alignment of inputs and outputs, in that anterograde and retrograde labelling from the same PFC injection sites are not found in the same locations. Despite the clear non-alignment, there remains to be evidence of broad scale reciprocity of connections, similar to that identified in the earlier experiments (Chapter 2).

Central Prefrontal Cortex

Injection of the retrograde tracer Fluoro-Gold and the anterograde tracer Fluoro-Ruby to central PFC regions of PL, VO, VLO and DLO resulted in similar retrograde and anterograde labelling to that described in Chapter 2. Retrograde labelling was seen more widespread in temporal cortex (and elsewhere in the cortex) than anterograde counterparts. Large amounts of retrograde and anterograde labelling from the same PFC injection site was found in different regions of temporal cortex. The findings from this study show the same ordered organisation of input and output connections described for anterior PFC, however my analysis shows a significant increase in alignment between inputs and outputs from anterior to central PFC (although they remain non-aligned).

There was some co-labelling of cells with Fluoro-Gold and Fluoro-ruby observed (<50%) from co-injection sites, indicating some possible retrograde labelling from Fluoro-Ruby (for details see Appendix E), however the majority of Fluoro-Ruby labelling was considered anterograde and separate from equivalent retrograde labelling.

The resultant labelling in temporal cortex from central PFC tracer injections shows clear evidence for ordered arrangements of both input and output connections, with differential ordering of inputs and outputs. This is most prominent in the anterior-posterior axis, where moving mediolaterally in PFC (from VO to DLO) retrograde labelling in temporal cortex becomes more posterior, whereas anterograde labelling becomes more anterior. This finding

of non-alignment has been replicated with three different anterograde tracers and has been found using both separate and co-injections.

Posterior Prefrontal Cortex

Following administration of the anterograde tracer Fluoro-Ruby to the posterior PFC regions PL, VO, VLO and DLO, labelling of axon terminals was found in areas of prefrontal cortex, temporal cortex, motor cortex, cingulate cortex, piriform cortex and somatosensory cortex. Anterograde labelling resultant from posterior PFC injections was seen in more posterior and dorsal regions of temporal cortex than the anterograde labelling produced by central PFC injections. The ordering of output connections from posterior PFC differed to the ordering seen in anterior and central PFC, this is clearest in the anterior-posterior axis where output connections follow an opposing order to those from anterior and central PFC; moving mediolaterally in PFC (from VO to DLO), output connections from posterior PFC become more anterior, whereas the output connections from anterior and central PFC become more posterior. The output projections from posterior PFC to temporal cortex follow the same ordered arrangement as the input projections. As well as following the same order, the input and output connections from posterior PFC to temporal cortex are aligned with one another.

The retrograde labelling produced from posterior PFC injections was seen in more posterior and ventral regions of temporal cortex to that identified in central PFC. The ordering of input connections to posterior PFC differed to the order observed from anterior and central PFC, specifically in the anterior-posterior and dorsal-ventral axes where the ordering was opposite to that seen in anterior and central PFC. The retrograde labelling resultant from injections into posterior PFC was consistently found to be more widespread than that produced by anterior and central PFC injection sites, indicating less specificity of the connections from this region of PFC.

Alignment of Input and Output Connections Across Prefrontal Cortex, from Anterior to Posterior

The findings presented here clearly show that as PFC connections become more anterior, the inputs and outputs become less aligned with one another. The distance between labelled input and output connections from the same PFC injection site becomes greater moving from posterior to anterior PFC, across three axes of orientation simultaneously. It was also observed that connections become more widespread in temporal cortex as injection sites in PFC become more posterior. This is the case for both anterograde and retrograde connections. Such a change in the convergence/divergence pattern of connections indicates a change in the specificity of connections to temporal cortex from anterior compared to posterior PFC. The differential organisation of anterior PFC compared to more posterior regions, and other cortical regions, is consistent with the conclusions of Ranmani & Owen (2004) that anterior PFC holds a specific purpose in the complex integration of multiple cognitive operations, different to that of other prefrontal regions.

Together these findings show that alignment of PFC connections to temporal cortex follows a gradient from anterior to posterior. The observed change in the ordering connections along the A-P axis of PFC (anterior → central → posterior) implies that there may be two functional maps between PFC and temporal cortex. These findings provide evidence to support claims of differential functional organisation from anterior to posterior PFC, in terms of an organisational gradient (Taren et al, 2011) and observations of differences in the level of abstraction between anterior and posterior PFC (Christoff, 2009). Christoff (2009) proposed increased abstract processing in anterior PFC, the findings reported here imply that increased abstract and complex processing is associated with a different ordered arrangement of connections to that required by less abstract PFC regions. This means that anterior regions of PFC function differently compared to more posterior regions. Based on these observations, it is reasonable to suggest that the increased abstract processing associated with anterior regions of PFC requires anatomical connections to be non-aligned in terms of inputs and outputs.

Chapter 4.

The Fine Scale Organisation of Prefrontal Cortex – Temporal Cortex Connections

There is evidence for ordered connections between prefrontal cortex (PFC) and temporal cortex. Chapters 2 and 3 identified clear ordered arrangements of both input and output connections and have established there is differential ordering between inputs and outputs, most prominently in anterior and central regions of PFC. These findings of ordering are consistent with those described by Hoover & Vertes (2011), in that there are ordered connections from prefrontal regions to PRh. Similar ordered connections have also been described by Kondo & Witter (2014). There is evidence of differential ordering in cortical connections (Flaherty & Graybiel, 1994) similar to that identified by my studies, however this is not a property which has been explored in great detail.

In order to gain a clear understanding of prefrontal organisation, it is necessary to establish an understanding of the organisation of connections on a fine scale. The findings from earlier studies (Chapter 2 and 3) provided an important basis from which to expand the experiments and investigate the organisation of prefrontal – temporal cortex connections at a greater resolution, revealing the fine scale topographic organisation of connections in comparison to the topological organisation which has been explored so far.

Conde et al (1995) described ordered connections from regions within medial PFC to areas of temporal cortex. This fine scale study investigated multiple PFC injection sites within a single cytoarchitectural region, providing a description of ordering which is overlooked on a larger scale. For instance, the findings from Chapter 2 and 3 show ordering from VO to DLO, resulting in the medial area of PFC (PL, IL, MO) being excluded from the observed pattern. Only finer scale analysis, such as that carried out by Conde et al (1995) can reveal the smaller organisational properties underlying the largescale arrangement already identified. Similar studies investigating only lateral PFC (VO, LO) have identified ordering within specific regions (Hoover & Vertes, 2011).

This study sought to address whether these relationships could be seen at a finer scale and in the same pathway. By using smaller injection volumes of tracers (20nl Fluoro-Ruby, 30nl Fluoro-Gold) it was possible to establish that there is a more detailed ordering of both input and output connections and that the ordering seen usually reflects that observed at a broader level. In addition, the findings established that the alignment of the connections is unaligned, again in agreement with the earlier work. Following the initial findings of an ordered arrangement within broad scale PFC projections, the investigation was continued using smaller volumes of tracer (retrograde: Fluoro-Gold and anterograde: Fluoro-Ruby). These smaller injections were positioned along the same medial-lateral line in central PFC as the previous 100nl injections (Chapters 2 and 3). Use of the anterograde tracer Fluoro-Ruby rather than the previously used BDA allowed for fine scale visualisation, which would otherwise not have been possible. This is due to its increased sensitivity and ability to be easily visualised with fluorescence.

Aims

This study determined if the organisational pattern identified on a broad scale is present when examined in finer detail, and if the properties of the underlying fine scale organisation of connections differed. This study sought to establish if the non-alignment in the order of arrangement between input and output connections which had been observed at 100nl injection volumes was repeated at a finer scale, or whether the underlying fine scale connectivity pattern differs to that seen at a broad level revealing a more reciprocal organisation typical of complex brain regions.

Methodology

Animals and Surgical Procedures

Data was collected from eleven male CD rats, weighing 302-371g (Charles River, UK). Animal procedures were carried out in accordance with the UK Animals scientific procedures act (1986), EU directive 2010/63 and were approved by the Nottingham Trent University Animal Welfare and Ethical review body. Details of animals and surgical procedures can be seen in Chapter 2.

Injections of anterograde (20nl 10% Fluoro-Ruby in distilled water, Fluorochrome, Denver, Colorado) and retrograde tracer (30nl 4% Fluoro-Gold in distilled water, Fluorochrome, Denver, Colorado) were made into the prelimbic (PL), ventral orbital (VO), ventrolateral orbital (VLO) or dorsolateral orbital cortex (DLO), with the intention of revealing the fine scale anatomical connections of PFC (Fig.4.1). The distance between craniotomy coordinates (0.5mm) and optimum volume for visualisation of each tracer (Fluoro-Gold:30nl, Fluoro-Ruby:20nl) was based on the measured spread of tracers in preliminary studies (Appendix J). A smaller volume of tracer injection, allowing for a smaller distance between injection sites, allowed for the investigation of connections with PFC cytoarchitectural regions as well as between them. Each rat received an injection of retrograde tracer into one hemisphere and an injection of anterograde tracer into the other hemisphere to allow accurate identification of the tracers injected. All Fluoro-Gold injections were made in the left hemisphere in this experiment, and Fluoro-Ruby injections made into the right hemisphere. Equivalent Fluoro-Gold injections made into the right hemisphere were used to verify whether the location and ordering of projections differed on either side of the brain (Appendix C). No difference was found.

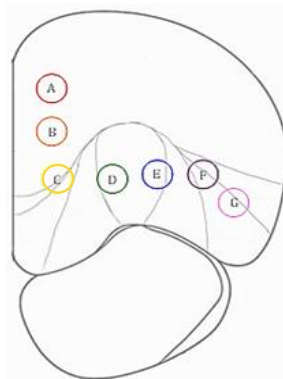


Figure 4.1. Coronal section of PFC (A-P 3.7mm from Bregma) showing the cytoarchitectural boundaries of PFC sub-regions according to Van de Werd & Uylings (2008), depicting sites of tracer injections; PL (A, B), IL/MO (C), VO/VLO (D), VLO/LO (E), LO/DLO (F) and DLO (G), with 0.5mm separation.

Anatomical Processing, Imaging and Microscopic Analysis

For the analysis of both anterograde and retrograde connections, two series of 40µm coronal sections were taken (2 in 6 sections) on a freezing microtome (CM 1900, Leica, Germany).

Sections were mounted onto gelatin coated slides. One series of sections was cover slipped with Vectashield® (Vector laboratories) mounting medium (with DAPI), for fluorescent imaging of Fluoro-Ruby injection sites and labeled projections. The second series was cover slipped with Vectashield® (Vector laboratories) mounting medium (with propidium iodide) for fluorescent imaging of Fluoro-Gold injection sites and labeled projections. Sections were examined using fluorescent microscopy. Fluorescent photos were captured of injection sites, retrogradely labeled cells (Fluoro-Gold) and anterogradely labeled axon terminals (Fluoro-Ruby) using an Olympus DP-11 system microscope with a x4, x10 and x20 objective lens.

Statistical Analysis of the Fine Scale Connections Between Prefrontal and Temporal Cortex

A statistical analysis was implemented similar to that used in my previous studies (see Chapter 2). The three dimensional location of each retrogradely labeled cell (Fluoro-Gold) or anterogradely labeled axon terminal (Fluoro-Ruby) was determined. ImageJ (Wayne Rasband, NIH) was used to measure the distance of each label from the rhinal sulcus in the dorsal-ventral and medial-lateral axes. The anterior-posterior location of each retrogradely labelled cell was also recorded, in terms of distance (mm) from Bregma (according to Paxinos and Watson, 1998).

Labelled cells were grouped according to injection site location. The resultant data was analysed in SPSS by way of a factorial ANOVA, in order to establish the existence of an effect of injection site location on positioning of labeled cells in temporal cortex (in dorsal-ventral, anterior-posterior and medial-lateral axes). The relationship between anterograde and retrograde labelling was determined from a two factor ANOVA.

A statistical comparison of the results obtained here from injections of small tracer volumes and the results obtained earlier from larger tracer injections enabled confirmation that the observations made were reliable representations of the underlying fine scale structure of the same ordered organisation identified in Chapter 2. By calculating the Euclidean distance between anterograde and retrograde labels from large and small tracer volumes it was possible to produce a valid comparison between the two datasets. A t-test was applied to

determine if there was any significant difference in the broad scale organisation produced from the two experiments.

By constructing a connectivity matrix, in which an anterograde and retrograde injection site were connected to one another if they produced labelling in the same region of temporal cortex, it was possible to investigate the connectional organisation of PFC to temporal cortex projections further.

Results

Injection sites from PFC injections of (30nl) Fluoro-Gold were positioned in the intended regions. Retrograde injection sites spanned layers II - VI. There was some minimal overlap between retrograde injection sites; there was overlapping between injections into PL, IL, MO and VO (A & B, B&C, B&D), there was also a small overlap of the spread of tracer at injection sites into LO and DLO₂ (F&G). The majority of the spread of tracer at retrograde injection sites was confined to the intended cytoarchitectural region and the seven injection sites were evenly spaced from one another.

Fluoro-Ruby injection sites were found in the intended regions of PFC. The spread of Fluoro-Ruby at 20nl injection sites was comparably smaller than equivalent Fluoro-Gold injection sites, due to the smaller injection volume as well as the consistent smaller spread of Fluoro-Ruby (identified in Chapter 3). Fluoro-Ruby injection sites were predominantly confined to the intended cytoarchitectural regions of PFC and were found to be mostly within the borders of the equivalent 30nl Fluoro-Gold injection sites. There is some overlap between injection sites into LO and DLO (F&G). The Fluoro-Ruby injection sites spanned layers III-VI and were found to be equally spaced from one another.

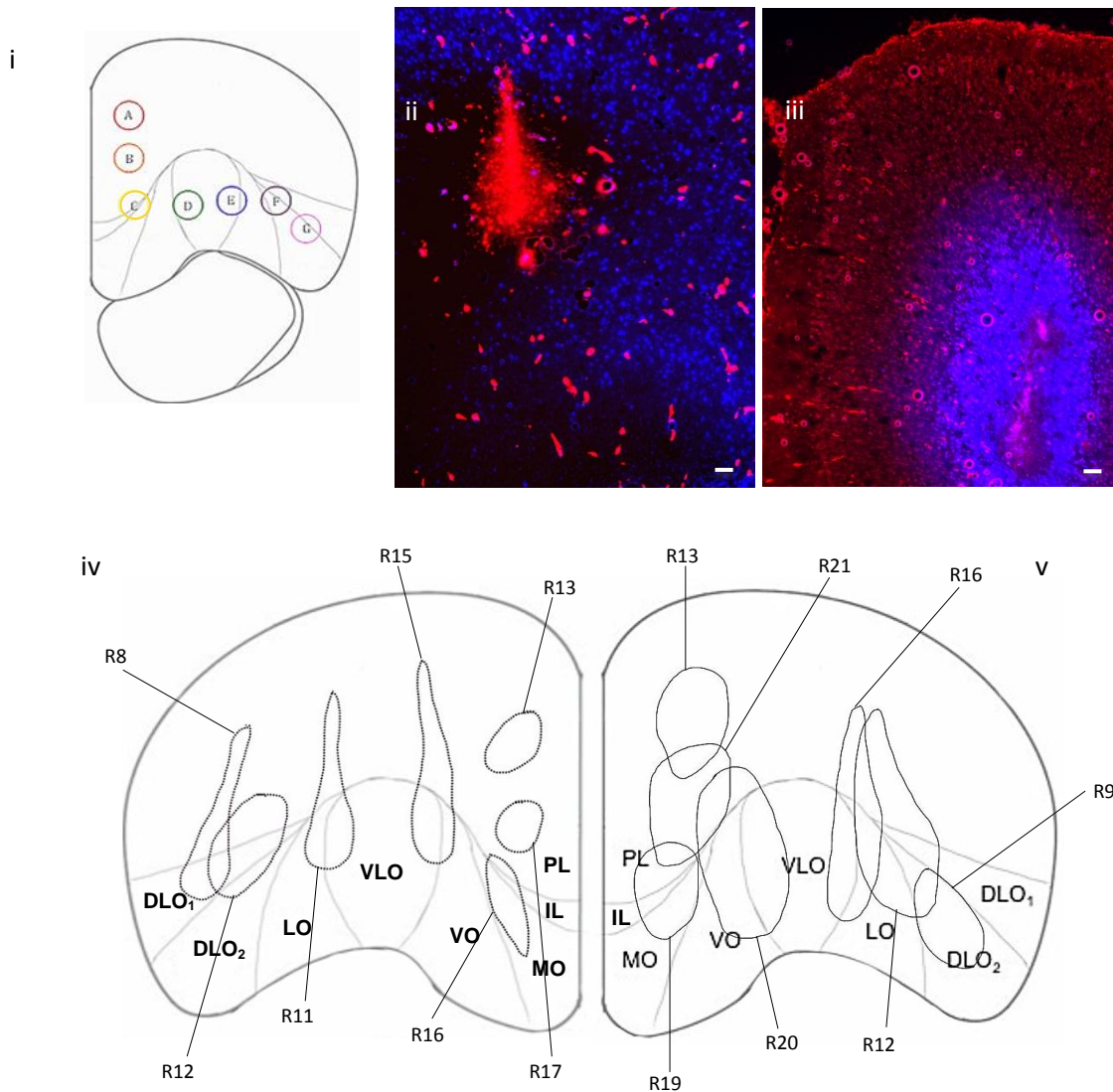


Figure 4.2. (i) Coronal section of PFC (AP 4.2mm from Bregma) showing the cytoarchitectural boundaries of the prelimbic (PL), infralimbic (IL), medial orbital (MO), ventral orbital (VO), ventrolateral orbital (VLO), lateral orbital (LO) and dorsolateral orbital (DLO) cortices (according to Van de Werd & Uylings, 2008), depicting amalgamated sites of Fluoro-Gold and Fluoro-Ruby injections; Prelimbic: A & B, Infralimbic/Medial orbital: C, Ventral orbital/Ventrolateral orbital: D, Ventrolateral orbital/Lateral orbital: E, Lateral orbital/Dorsolateral orbital: F and Dorsolateral orbital: G, with 0.5mm spread. (ii) Coronal section of PFC showing location and spread of (20nl) Fluoro-Ruby at injection site in VLO/LO (R11). (iii) Coronal section of PFC showing location and spread of (30nl) Fluoro-Gold at injection site in PL (R21). (iv) Representations of Fluoro-Ruby (20nl) (R13, R17, R16, R15, R11, R12, R8 (broken line)) injection sites in PL (R13, R17), IL/MO (R16), VO/VLO (R15), VLO/LO (R11), LO/DLO (R12) and DLO (R8) in the right hemisphere. (v) Representations of Fluoro-Gold (30nl) (R13, R21, R19, R20, R16, R12, R9 (solid line)) injection sites in PL (R13, R21), IL/MO (R19) VO/VLO (R20), VLO/LO (R16), LO/DLO (R12) and DLO (R9) in the left hemisphere. Fluoro-Ruby injection sites were predominantly within the boundaries of Fluoro-Gold injection sites. There is some overlap between retrograde injection sites into PL, IL and VO (R13 & R21, R21 & R19, R21 & R20). There is minimal overlap between anterograde injection sites into DLO (R8 & R12). Scale bars = 100 μ m.

Retrograde labelling, resultant from Fluoro-Gold injections into PFC (PL, IL, MO VO, VLO, LO and DLO) was found in regions of PRh, Ent, Te, AuV, Cg1, M2, M1, S1J and prefrontal regions (Fig.4.4ii). Anterograde labelling resultant from Fluoro-Ruby injections into PFC (PL, IL, MO VO, VLO, LO and DLO) was found in regions of PRh, Ent, Cg1, M2 and M1, as well as prefrontal regions (Fig.4.4iii). In order to further investigate the pathway between PFC and temporal cortex in fine detail, which had already been identified in Chapter 2, the labelling within areas of PRh, Ent and Te was analysed.

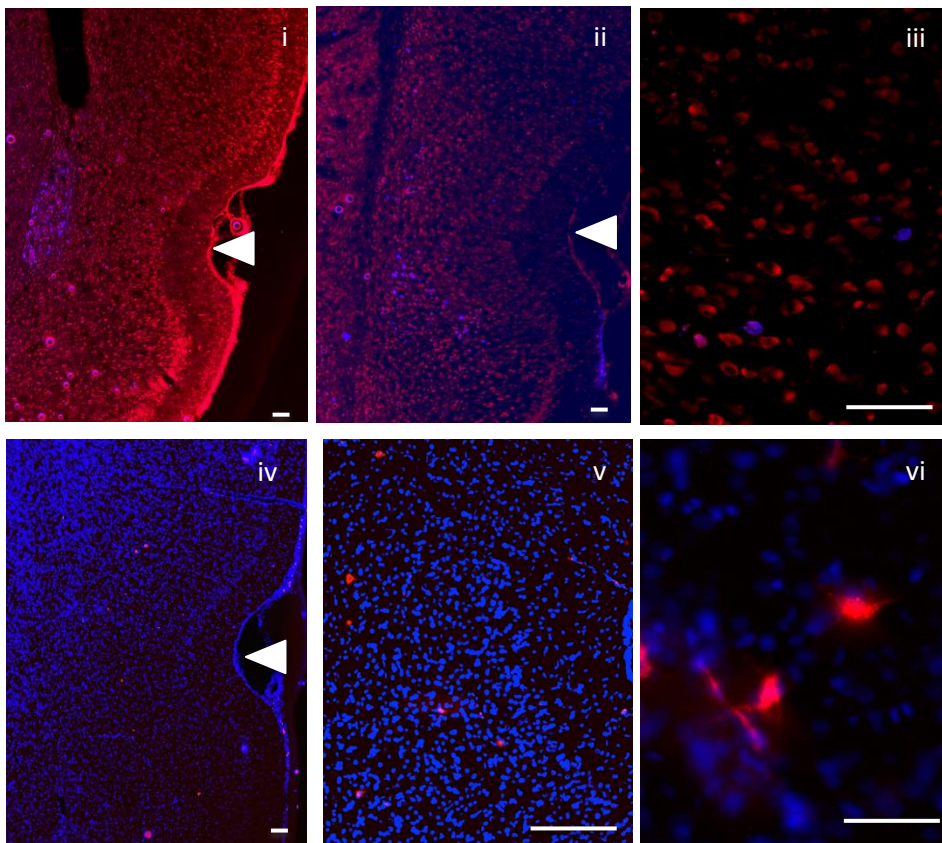


Figure 4.3 (i) Coronal section showing retrogradely labelled cells (blue) in temporal cortex produced by injection of Fluoro-Gold (30nl) into PL (B: R21). (ii) Coronal section showing retrogradely labelled cells (blue) in temporal cortex produced by injection of Fluoro-Gold (30nl) into DLO (F: R12). (iii) Retrogradely labelled cells in temporal cortex (blue) produced by injection of Fluoro-Gold (30nl) into DLO (F: R12). (iv) Coronal section showing anterogradely labelled axon terminals (red) in temporal cortex produced by injection of Fluoro-Ruby (20nl) into PL (B: R17). (v) Coronal section showing anterogradely labelled axon terminals (red) in temporal cortex produced by injection of Fluoro-Ruby (20nl) into DLO (G: R8). (vi) Anterogradely labelled axon terminals (red) in temporal cortex produced by injection of Fluoro-Ruby (20nl) into IL/MO (C: R16). Arrows denote the location of the rhinal sulcus. Scales bars = 100µm.

Organisation of Input Connections from Prefrontal Cortex to Temporal Cortex

Projections to PFC from temporal cortex were seen in PRh, Ent and Te (Fig.4.3, Fig.4.4). All temporal cortex areas were defined according to (Burwell, 2001). The distribution of retrogradely labelled cells is seen across several cytoarchitectural regions within temporal cortex (Fig.4.3i, ii, Fig.4.4ii) and maintains a spatial order in accordance with the corresponding Fluoro-Gold injection sites in PFC (PL, IL, MO, VO, VLO, LO and DLO). Moving from medial to lateral in PFC from PL to VLO/LO, projections to IL/MO (injection site C) were seen dorsally to those from PL (injection site B) (Fig.4.4ii). This dorsal-ventral ordering continues laterally across PFC; projections to VO/VLO (injection site D) are seen dorsally to those to IL/MO (injection site C) and projections to VLO/LO (injection site E) are seen dorsally to projections to VO/VLO (injection site D). An additional order of input connections can be seen in the anterior-posterior axis; labelling from lateral PFC injection sites (VO to DLO) is seen in more posterior regions of temporal cortex compared to medial PFC injection sites (PL – VO) (Fig.4.4ii). Clear anterior – posterior ordering can be seen from injection sites B – G (PL – DLO). Fluoro-Gold labelling was seen in the same cytoarchitectural regions as Fluoro-Gold labelling from the previous 100nl injections (Chapter 2, Appendix B).

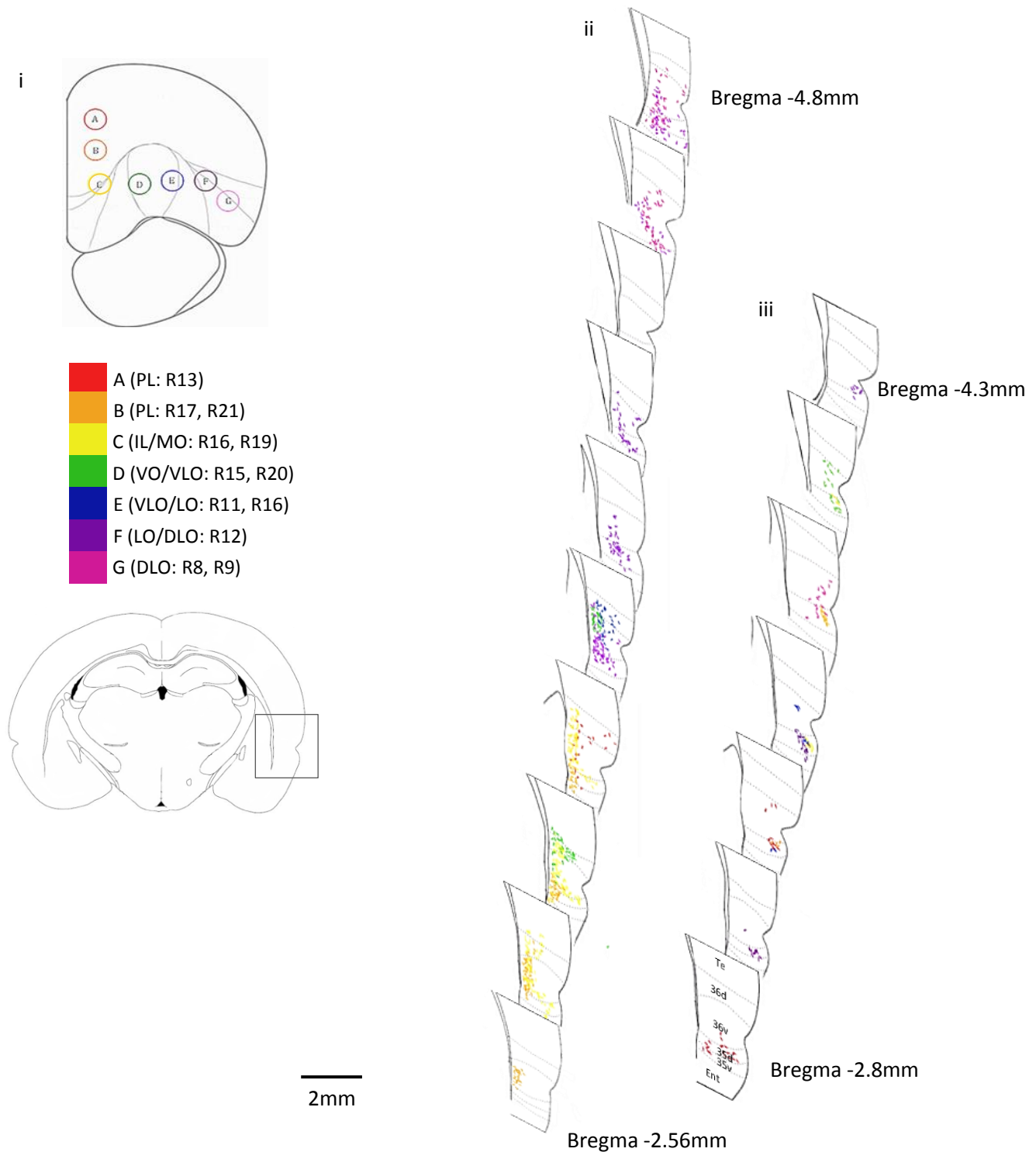


Figure 4.4. Diagram representing the amalgamated injection sites of Fluoro-Gold and Fluoro-Ruby, and the projection sites to temporal cortex for both retrograde (Fluoro-Gold) and anterograde (Fluoro-Ruby) tracer injections. (i) The locations of injection sites A (PL: R13), B (PL: R17, R21), C (IL/MO: R16, R19), D (VO/VLO: R15, R20), E (VLO/LO: R11, R16), F (LO/DLO: R12) and G (DLO: R8, R9) and the location of labelling in temporal cortex. (ii) The locations of retrogradely labelled cells in temporal cortex, resultant from 30nl Fluoro-Gold injections into PFC injection sites A-G (R13, R21, R19, R20, R16, R12, R9). (iii) The locations of anterogradely labelled axon terminals in temporal cortex resultant from

20nl Fluoro-Ruby injections into PFC injection sites A-D (R13, R17, R16, R15, R11, R12, R8).

Organisation of Output Connections from Prefrontal Cortex to Temporal Cortex

Projections from PFC to temporal cortex were seen in PRh (areas 35 and 36), Te and Ent (Fig.4.4, Fig. 4.4iii). The distribution of anterogradely labelled cells within temporal cortex maintained an overall spatial order in accordance with their corresponding Fluoro-Ruby injection sites in PFC (Fig.4.4iii). In comparison to a relatively large number of cells labelled by Fluoro-Gold injections, Fluoro-Ruby injections into the same PFC sites produced anterograde labelling in PFC of a small number of cells, showing a high degree of convergence (Fig.4.4iv, v, VI, Fig.4.4iii). Moving laterally in PFC from PL to VO/VLO, projections from PL were seen more ventral in temporal cortex than projections from IL/MO, projections from IL/MO were seen more ventral to VO/VLO. Similarly, ordering can be seen in the anterior-posterior axis. Output projections from PL were seen anterior to IL/MO, IL/MO are anterior to VO/VLO (Fig. 4.4iii.).

Statistical evidence for this ordered arrangement came from the following analysis.

For the dorsal-ventral axis: A factorial ANOVA revealed a significant main effect of injection site on the dorsal-ventral location of retrogradely labelled cells ($F_{(6,1115)}=16.159$ $p<0.001$ $r=0.120$). Post hoc comparisons (Tukey HSD) revealed significant differences between retrograde injection sites A*B, A*C, A*F, A*G, B*D, B*E, B*G, C*E ($p<0.001$), B*F ($p=0.002$), C*D ($p=0.001$), E*F ($p=0.014$) and E*G ($p=0.029$). A factorial ANOVA revealed a significant effect of injection site on the dorsal-ventral location of anterogradely labelled axon terminals ($F_{(6,166)}=0.855$ $p<0.001$ $r=0.072$). Post hoc comparisons (Tukey HSD) between the seven groups indicated significant differences between anterograde injection sites A*D ($p<0.001$), A*G ($p=0.005$), B*D ($p=0.009$), B*G ($p=0.047$), D*E ($p<0.001$), D*F ($p=0.003$), E*G ($p=0.003$) and G*F ($p=0.017$). This indicates a broad ordered arrangement of both input and output connections from PFC to temporal cortex (Fig. 4.5i). The two factor ANOVA revealed a significant interaction effect between input and output connections ($F_{(5,1275)}=5.831$ $p<0.001$ $r=0.067$). These results indicate evidence of ordering, which is different for inputs and outputs.

For the anterior-posterior axis: A factorial ANOVA revealed a significant main effect of injection site on the anterior-posterior location of retrogradely labelled cells ($F_{(6,1115)}=1196.266$ $p<0.001$ $r=0.720$). Post hoc comparisons (Tukey HSD) revealed significant differences between retrograde injection sites A*B, A*C, A*E, A*F, A*G, B*D, B*E, B*E, B*F, B*G, C*D, C*E, C*F, C*G, D*E, D*F, D*G, E*F, E*G and F*G ($p<0.001$). A factorial ANOVA revealed a significant effect of injection site on the anterior-posterior location of anterogradely labelled axon terminals ($F_{(6,160)}=2.953$ $p<0.001$ $r=0.135$). Post hoc comparisons (Tukey HSD) between the seven groups indicated significant differences between A*B, A*C, A*D, A*E, A*F, A*G, B*D, C*D C*E, D*F, E*G ($p<0.001$), B*E ($p=0.001$) and E*F ($p=0.033$). This indicates an overall ordered arrangement, specifically of the central most PFC region (Fig.4.5ii). This indicates a clear ordered arrangement of input and output connections. The two factor ANOVA revealed a significant interaction effect between input and output connections ($F_{(5,1275)}=117.087$ $p<0.001$ $r=0.290$). These results show evidence of differential ordering for input and output connections that are not entirely opposing.

For the medial-lateral axis: A factorial ANOVA revealed a significant main effect of injection site on the medial-lateral location of retrogradely labelled cells ($F_{(6,1115)}=2678.276$ $p<0.001$ $r=0.840$). Post hoc comparisons (Tukey HSD) revealed significant differences between retrograde injection sites A*B, A*C, A*D, A*E, A*G, B*C, B*D, B*E, B*F, B*G, C*F, C*G, D*F, D*G, E*F, E*G and F*G ($p<0.001$). A factorial ANOVA revealed a significant effect of injection site on the medial-lateral location of anterogradely labelled axon terminals ($F_{(6,160)}=6.900$ $p<0.001$ $r=0.203$). Post hoc comparisons (Tukey HSD) between the seven groups indicated significant differences between anterograde injection sites B*C ($p<0.001$), C*E ($p<0.001$) and C*F ($p<0.001$). This indicates an ordered arrangement of connections in the medial-lateral axis, specifically within central areas of PFC (Fig.4.5iii). This indicates a broad ordered arrangement. The two factor ANOVA revealed a significant interaction effect between input and output connections ($F_{(5,1275)}=243.455$ $p<0.001$ $r=0.400$). These results show evidence for differential ordering of inputs and outputs.

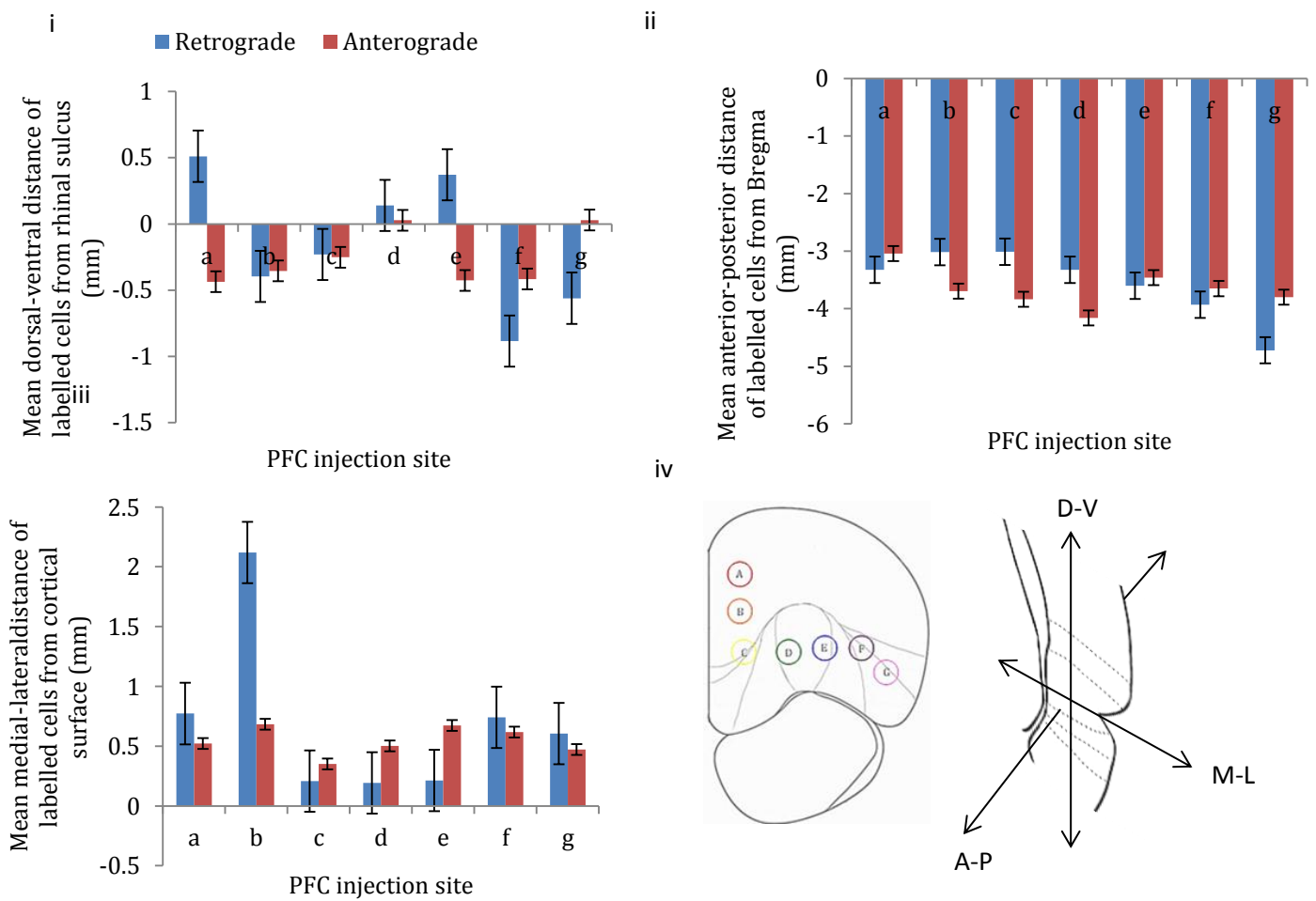


Figure 4.5. The mean effect of PFC injection site on the (i) dorsal-ventral, (ii) anterior-posterior and (iii) medial-lateral location of retrogradely labeled cells ($n=1122$ arising from 7 rats: A(PL:R13)=59, B(PL:R21)=184, C(IL/MO:R19)=360, D(VO/VLO:R20)=92, E(VLO/LO:R16)=39, F(LO/DLO:R12)=194, G(DLO:R9)=194) and anterogradely labeled axon terminals ($n=167$ arising from 7 rats: A(PL:R13)=27, B(PL:R17)=24, C(IL/MO:R16)=19, D(VO/VLO:R15)=21, E(VLO/LO:R11)=45, F(LO/DLO:R12)=19, G(DLO:R8)=12) within temporal cortex. Error bars = standard error. (iv) Coronal cross section of PFC showing the position of 7 injection sites; PL (A, B), IL/MO (C), VO/VLO (D), VLO/LO (E), LO/DLO (F) and DLO (G). Coronal cross section of temporal cortex showing the three dimensions in which the locations of labels were recorded.

This analysis shows evidence for fine scale ordered organisation of connections between PFC and temporal cortex. As PFC injection sites move from medial to lateral (PL to VLO/LO; B to E), the pattern of input projections moves in a dorsal-ventral direction across temporal cortex, whilst simultaneously moving from anterior to posterior (from PL to DLO; B to G). A similar organisation of output projections can be observed, as anterograde injection sites

move mediolaterally from PL to VO/VLO (A to D), the pattern of projections becomes more dorsal and posterior in temporal cortex. It is evident from these findings that input and output connections do not show exactly the same ordering, but do show similar organisational properties. Both inputs and outputs show evidence of ordering from the same regions of PFC to the same regions of temporal cortex, however they do not follow the same patterns of organisation.

A direct comparison of broad and fine scale connectivity patterns, using a comparison of Euclidean distances between corresponding retrogradely and anterogradely labelled cells ($E = \sqrt{(\langle DVr \rangle - \langle DVa \rangle)^2 + (\langle APr \rangle - \langle APa \rangle)^2 + (\langle MLr \rangle - \langle MLa \rangle)^2}$), indicates similar orders of organisation in regards to the relationship between input and output connections; a paired samples T-test indicated no significant difference between the organisational pattern found from 100nl injections and 20-30nl injections ($t(2)=-0.310$, $p=0.786$). This shows that although PFC – temporal cortex connections are ordered on a broad scale, the underlying fine scale organisation is not so clearly defined.

Discussion

Fine Scale Connections of the Prefrontal Cortex – Temporal Cortex Pathway

Despite an overall similar appearance to the ordered pattern of connectivity we see at a broad scale compared to fine scale, the more detailed visualisation and analysis of organisation at a finer scale has revealed properties within the organisation of PFC connections which could not be seen with larger injection volumes. In addition to differential ordering, these findings have shown that inputs and outputs did not move in opposing directions as it may appear at a larger scale, but that the relationship between connections is more complex. It should be noted that the previous analysis (Chapter 3 & Appendix F) showed Fluoro-Ruby to be approximately 70% anterograde (30% retrograde). The bidirectional properties of Fluoro-Ruby should be taken into account when interpreting these findings.

These findings have demonstrated that when analysed in greater detail the interaction between input and output connections is more complex than the ordering that can be seen on

a larger scale. At this finer scale it becomes clearer that changes in the arrangement of connections differ to varying degrees in labelling produced by Fluoro-Gold and Fluoro-Ruby, i.e. retrograde connections change at a greater rate.

Input Connections to Prefrontal Cortex from Temporal Cortex

Following the administration of the retrograde tracer Fluoro-Gold to the prefrontal cortical areas PL (A: R13, B:R21), IL/MO (C: R19) VO/VLO (D: R20), VLO/LO (E: R16) , LO/DLO (F:R12) and DLO (G:R9), labelling of neuronal cell bodies was found in temporal cortex, sensory-motor cortex, cingulate cortex, somatosensory cortex and piriform cortex. The labelling found in areas of temporal cortex (PRh, Ent, Te) was amongst the most prominent. This is consistent with the findings from larger tracer injection volumes (Chapter 2 & 3) and with labelling reported in previous studies (Hoover and Vertes, 2011; Sesack, 1989). Evidence was found for fine scale ordering of input connections from temporal cortex to PFC. This ordering is most clear in the anterior-posterior axis; moving from medial to lateral in PFC from VO to DLO (injection site C to G), retrograde labelling in temporal cortex becomes more posterior. Injection sites into PL and IL do not follow the same organisation. These findings are consistent with the previous studies (Chapter 2 and 3). There is also evidence of ordering in the dorsal-ventral axis, however this is not as clear as it appears at a lower resolution (from larger injections). Moving mediolaterally in PFC, the location of retrograde labels in temporal cortex become more dorsal, however this is only apparent between PL and VLO (injection site B – E), the ordering appears to change direction when injection sites reach DLO.

Output Connections from Prefrontal Cortex to Temporal Cortex

Following administration of the anterograde tracer Fluoro-Ruby to the prefrontal cortical regions PL (A:R13, B:R17), IL/MO(C:R16), VO/VLO (D:15), VLO/LO (E:R11), LO/DLO (F:R12) and DLO (G:R8), anterograde labelling was found (Fluoro-Ruby) in several cortical regions. The projections arising from regions of temporal cortex (PRh, Ent, Te) were amongst

the most prominent and consistent with the findings from larger injection volumes (Chapter 2, Chapter 3 and Appendix B).

Organisation and Alignment of Fine Scale Connections Between Prefrontal Cortex and Temporal Cortex

The findings of this study indicate a clear ordered arrangement of fine scale PFC-temporal cortex connections. When considered as an overall pattern, this is consistent with the previous findings of broad scale organisation, and the previously identified evidence of ordering and differential labelling from PL and IL (Sesack, 1989; Vertes, 2004), ordering from MO, VO and LO (Kondo & Witter, 2014) and ordered connections from areas of lateral PFC to perirhinal cortex and area Te (Hoover and Vertes, 2011). Hoover & Vertes (2011) described a dorsal to ventral ordering in temporal cortex resultant from a lateral to medial change in retrograde PFC injections (VO to MO). The findings show a similar ordering between VO and MO; retrograde labelling from injection C (IL/MO) is seen ventrally in temporal cortex to retrograde labelling from injection D (VO/VLO). The findings show that this dorsal-ventral organisation expands into PL and LO (Fig. 4.5i). A similar ordering can be seen in the output connections from PL to LO, moving from medial to lateral in PFC (from PL (injection site B) to VLO/LO (injection site E), anterograde labelling in temporal cortex becomes more dorsal. This observation shows that as well as showing clear evidence of differential ordering, the inputs and outputs from PFC to temporal cortex also show instances of similar fine scale organisation.

When viewed at this fine scale, the ordered arrangement continues to show evidence for differential ordering in the input and output connections; anterograde labelling is consistently found in different regions of temporal cortex to the retrograde labelling from equivalent injection sites in PFC. For example, anterograde labelling from the injection into VLO (injection D) is seen in areas 35d and 35v, whereas the retrograde labelling from the same injection site is seen in areas 36d and 36v. There does remain to be a broad sense of reciprocity, in that anterograde and retrograde labels are found in the same general cytoarchitectural regions. For instance, both anterograde and retrograde labels from the injections into DLO₁ (injection F) are found in PRh. When interpreting the reciprocity of

connections it should be considered that some labelling from Fluoro-Ruby injections (30%) is retrograde, therefore some of the reciprocal connections identified may be a resultant of retrograde Fluoro-Ruby labelling.

The observations of the fine scale connections between prefrontal and temporal cortex indicate a complex relationship between the organisation of input and output connections. Similar to the earlier broad scale analysis of the same circuit, there is strong evidence for non-alignment of these connections. On a broad scale, there is a general theme of reciprocity between input and output connections from PFC to temporal cortex, in that both inputs and outputs from the same PFC injection site are found in regions of temporal cortex (PRh, Ent, Te). However, when visualised at a fine scale (enabled here by small tracer injection volumes) it is clear that there is less reciprocity present than was observed on a larger scale. Here very few retrograde labels are found in the same cortical column, or even specific cytoarchitectural region as anterograde labels from the same injection site. For example, both retrograde and anterograde labels from injection site D (VO) are found in area 35, but the observed anterograde labelling is considerably posterior to the equivalent retrograde labelling. A similar observation can be made for labelling from injection site B (PL) and C (MO). In many cases the dorsal-ventral distribution of retrograde and anterograde labels differs greatly. This indicates differential organisation of the inputs and outputs to a greater extent to that which can be observed on a broader scale.

Labelling from injections sites in PL was identified in the earlier studies as being relatively reciprocal in comparison to more lateral regions of PFC. Similarly, the findings from this study show a greater level of reciprocity for connections from a medial PFC injection sites in PL. The findings here show evidence for an anatomical separation between medial and orbital PFC regions, whereby medial regions are much more reciprocal in their connectivity to temporal cortex. This is consistent with previous findings of ordered and highly reciprocal connections between adjacent medial PFC regions (Conde et al, 1995). Retrograde and anterograde labelling from injection site A (PL) is found in the same region of area 36. However, there is also evidence of non-reciprocal connections from PL; there was anterograde labelling from injection site A (PL) in an anterior region of area 36, where no equivalent retrograde labelling was seen. This shows that although there is evidence for general reciprocity when viewed on a relatively large scale, more detailed investigation is able to show that PFC – temporal cortex connections are not highly reciprocal.

Connections from Prefrontal Cortex to Temporal Cortex

In order to investigate the fine scale relationship between input and output connections from prefrontal to temporal cortex further, and visualise the fine scale connectivity, a connectivity matrix was constructed (Fig.4.6). The connectivity matrix demonstrates the spatial relationship between input and output connections from PFC to temporal cortex, whereby a retrograde and anterograde injection site are connected if they produce labelling in the same cytoarchitectural region of temporal cortex. The rows of the matrix represent retrograde projections to temporal cortex from injection sites in PFC (A-G), the columns represent anterograde projections to temporal cortex from injection sites in PFC (A-G). Fig. 4.6 shows the retrograde and anterograde projections which occur in the same cytoarchitectural regions of temporal cortex. A retrograde and anterograde projection are said to be connected if they occur in the same cytoarchitectural region of temporal cortex, indicating the return anterograde projections to each retrograde projection.

Figure 4.6. shows a clear difference in the connections between anterograde and retrograde labelling. Retrograde injection sites A, B, E and F produced labelling in cytoarchitectural regions that received anterograde projections from the same PFC injection sites, i.e. they show reciprocal connectivity. Retrograde projections from C, D and G do not show this level of reciprocity, labelling from injection G was found in regions of temporal cortex containing no anterograde labelling. Figure 4.6 shows that some retrograde injection sites produced labelling in temporal regions that received a large amount anterograde labelling (>3), whereas others received less anterograde labelling (<3). Retrograde projection sites B, C and F were found in cytoarchitectural regions of temporal cortex which received anterograde labelling from >3 PFC injection sites. Interestingly, the retrograde labelling in sites B, C and F was predominantly ventral in temporal cortex, whereas the retrograde labelling found in regions with more anterograde labels (A, D and E) was predominantly dorsal to the rhinal sulcus in temporal cortex. Retrograde projections A, C, D, E, F and G were all found dorsal to the rhinal sulcus in temporal cortex (area 36 and Te), however very few of these labeled regions received return anterograde labelling in the dorsal part of temporal cortex. The majority of return anterograde labelling was found in the ventral aspect of temporal cortex (area 35). This is with the exception of retrograde labelling in projection site F, labelling from here was found in the same regions of area 36 as anterograde labelling from injection sites D and G.

This gives further evidence for differential organisation between medial and lateral PFC, indicating clearer reciprocity of connections in more lateral regions (this is excluding injection site G, which may receive return connections from areas not studied).

Additionally, figure 4.6. shows that retrograde labelling in temporal cortex produced by PFC injections A, B and C (medial PFC) was found in cytoarchitectural regions also containing anterograde labelling from from medial and lateral PFC. In contrast, retrograde labelling in temporal cortex produced by PFC injections D, E and F (lateral PFC) was found in cytoarchitectural regions containing anterograde labelling from only lateral PFC. This shows that the areas of temporal cortex from which medial PFC regions receive inputs receives outputs from medial as well as lateral PFC. Whereas the areas of temporal cortex from which lateral PFC regions receive inputs, receives outputs from only lateral regions of PFC. This observation may indicate the existence of two organisational maps, which overlap substantially with one another; one across medial PFC including injection sites A, B and C, the other across the whole region including A, B, C, D, E and F.

The connectivity matrix shows that VLO/LO (inj E) is very highly connected. Labelling from every retrograde projection site (excluding G (DLO)) was found in the same cytoarchitectural region of temporal cortex as the anterograde labelling from projection E (VLO/LO). Anterograde labelling from sites C and D was found in the same cytoarchitectural region as labelling from only one retrograde projection (F).

Figure 4.6. clearly shows two distinct areas of return anterograde connections. For the most part, labelling from every retrograde injection site receives return anterograde connections from the area of PFC covered by injection sites A and B (PL) and/or the area of PFC covered by injection sites E and F (VLO/LO/DLO). The clear separation of these regions of return connections is consistent with evidence of differential functions of medial, and orbital and PFC (Furuyashiki & Gallagher, 2007; Heidbreder & Groenewegen, 2003; McAlonan & Brown, 2003; Chudasama & Robbins, 2003). These findings may indicate differential organisation for medial and lateral regions of PFC. These two distinct patterns of ordered organisation exist within the overall ordering from medial to lateral identified on a larger scale (Chapter 2 and 3).

		Anterograde projection						
		A	B	C	D	E	F	G
Retrograde projection	A	X	X			X		
	B	X	X			X	X	
	C	X	X			X	X	
	D					X	X	
	E					X	X	
	F			X	X	X	X	
	G							

Figure 4.6. Connectivity matrix showing the relationship between input and output connections from PFC to temporal cortex. X = Retrograde and anterograde labelling found in the same cytoarchitectural regions of temporal cortex. **X** = Reciprocal connection: Retrograde and anterograde labelling from the same PFC injection site is found in the same cytoarchitectural region of temporal cortex. E.g. Retrograde projection site A is found in the same cytoarchitectural region as anterograde projections A, B and E.

To further investigate the relationship between Fluoro-Gold and Fluoro-Ruby labelled connections, the source regions (in PFC) of return anterograde connections to retrograde projections from PL, VO, LO and DLO was analysed (retrograde projection sites with 0 return anterograde projections were excluded from this analysis to prevent false findings). A numerical distance of each return anterograde PFC source region from the retrograde PFC source regions (found in the same area of temporal cortex) was measured, based on the connectivity matrix (Fig. 4.6). Each adjacent PFC injection site was given a distance of 1. A greater assigned value for return anterograde projection = a greater distance (in PFC) of anterograde projection from retrograde projection, therefore a retrograde injection site with a large median distance would be more widely connected, a distance of 0 represents a 100% reciprocal connection (e.g. if retrograde labelling from PL (A, B) were to be found in a temporal cortex region with anterograde labelling from only PL (A, B) and no other PFC region).

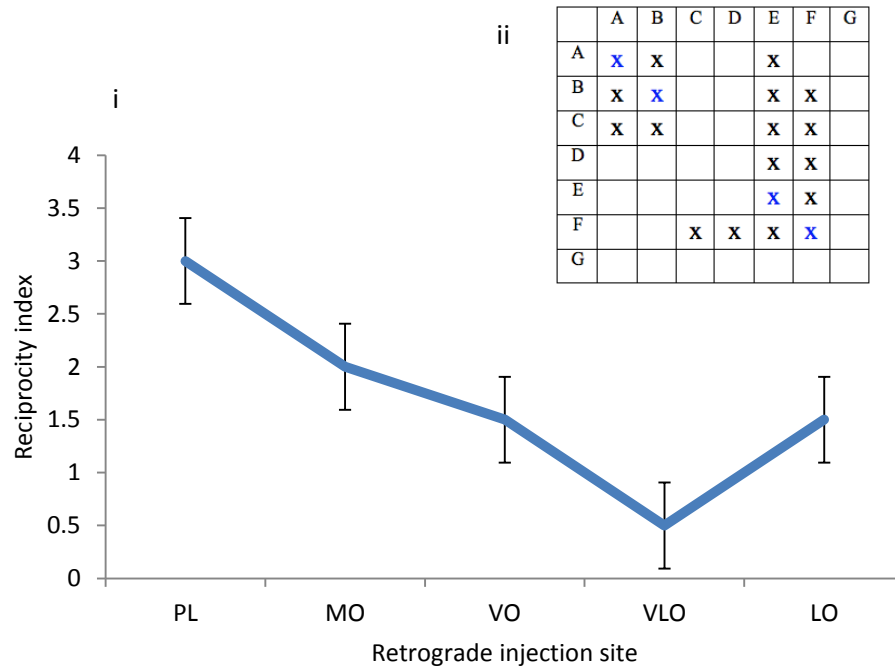


Figure 4.7. (i) The effect of PFC retrograde (Fluoro-Gold) injection site on the reciprocity index, derived from connectivity matrix (Fig.4.6): median distance between Fluoro-Gold and Fluoro-Ruby PFC injection sites of retrograde and anterograde labelling found in the same cytoarchitectural regions of temporal cortex. A distance of 1 PFC injection site is given a value of 1 (e.g. the distance between retrograde site A and anterograde site B = 1). The absolute value is taken, regardless of direction. Regions where no anterograde projections were found in the same cytoarchitectural region as the retrograde connection (e.g. injection site G:DLO) were not included, as a value of zero here represent an entirely reciprocal connection. Where a retrograde projection is found in the same region as multiple anterograde projections a median distance is calculated. Fluoro-Gold injection sites made into the same PFC sub-regions (i.e. PL) are combined. Injection G (DLO) is excluded due to having no return connections. PL = A & B, MO = C, VO = D, VLO = E, LO = F. Error bars = standard error. (ii) The connectivity matrix from which the graph (i) is produced.

Figure 4.7 shows that as retrograde injection site moves from medial to lateral in PFC, the median distance between the source retrograde and anterograde PFC injection sites of labeled inputs and outputs found in the same cytoarchitectural regions of temporal cortex decreases (from PL to VLO). This analysis shows that although PL is the most reciprocal of the PFC regions represented here (Fig. 4.4), it has the most widespread connections. The area with the closest connections, in that retrograde and anterograde connections are found close together (with little anterograde labelling far from the retrograde projections) is VLO.

This result shows that as retrograde injection site is moved from medial to lateral in PFC (increasing in distance from injection A and B (PL)), the distance between the source injection site of retrograde labelling in temporal cortex, and the source injection sites of anterograde labels found in the same cytoarchitectural regions of temporal cortex decreases (from PL to VLO). Much like the alignment gradient from anterior to posterior PFC discussed in Chapter 3 and the ordered shift in anatomical connections from PFC described by Heidbreder & Groenewegen (2003), figure 4.7 shows an ordered changes in the relationship between input and output connections, following a gradient. For input and output connections to follow different ordered arrangements, there must be some level of underlying order in the relationship between them, this gradient relationship may be an important factor in the fine detail of PFC to temporal cortex organisation. These findings give an insight into the detailed arrangement of PFC connections to temporal cortex and the complex relationship between input and output projections.

Chapter 5.

Organisation of Prefrontal Cortex – Sensory-Motor Cortex Connections

Prefrontal cortex (PFC) is known to be associated with executive functions, complex cognitive processes, temporal ordering and autonomic function (Kolb, 1984; Neafsey, 1990; Alvarez and Emory, 2006; Schoenbaum and Esber, 2010) and has been implicated in a number of neurological disorders (Goldman-Rakic, 1991; Perlstein et al, 2001; Courchesne et al, 2011). Functional differentiation of PFC regions has been observed in rats; dorsal mPFC is involved in motor and temporal processing (Narayanan & Laubach, 2006; Vertes, 2006; Kim et al, 2013), ventral mPFC is involved in cognition and emotion (Fryszak & Neafsey, 1994; Vertes, 2006), orbital cortex is described as being involved in making predictions based on the environment, as well as associative learning (Schoenbaum & Roesch, 2005; Schoenbaum & Esber, 2010). However, despite advances in understanding prefrontal function there remains relatively little detailed understanding of the anatomical connectivity and organisation of PFC. Without a clear understanding of anatomical organisation, the functional connectivity of PFC cannot be fully defined.

Recent studies into PFC organisation indicate ordered connectivity (Hoover & Vertes, 2011; Kondo & Witter, 2014). These studies have described topographic organisation between PFC and the parahippocampal region in rats. Chapters 2, 3 and 4 have explored the organisation of PFC connections to areas of temporal cortex.

Studies in rats have shown evidence of projections for connections from PFC to a number of subcortical and cortical targets (Vertes, 2004; Gabbott et al, 2005; Hoover & Vertes, 2007). Studies have also shown rat PFC to exhibit broad scale topological ordering; ordered projections from lateral and posterior regions of PFC to the posterior cingulate have been described (Olsen & Musil, 1992). The findings in

chapters 2 and 3 were consistent with reports of ordered connections to PRh and Te (Hoover & Vertes, 2011) and a medial-lateral topographic organisation previously only reported in subcortical connections from PFC (Berendse et al, 1992; Schilman et al, 2008).

PFC is known to have connections to multiple cortical regions, therefore a clear understanding of PFC organisation requires the investigation of multiple PFC connections. The earlier studies (Chapters 2, 3 and 4) identified prominent labelling in areas of sensory-motor cortex as well as the temporal cortex labelling which has been investigated already. In order to clearly establish the nature of physiological organisation within PFC, it is necessary to gain a detailed understanding of multiple PFC pathways.

Aims

This study aimed to reveal the broad scale ordered arrangement of connections from PFC to regions of motor and sensory cortex, as well as the relationship between input and output connections in this pathway. This study provides an important basis on which to build further investigations into the fine scale organisation of this pathway. Retrograde and anterograde neuroanatomical tracers (co-injections) were injected into rat medial and lateral PFC (prelimbic (PL), ventral orbital (VO), lateral orbital (VLO) and dorsolateral orbital cortex (DLO).

Methodology

For detailed methodology and surgical procedures, see Chapter 2.

Data was collected from 18 male CD rats (294-371g, Charles River, UK). Animal procedures were carried out in accordance with the UK Animals scientific procedures act (1986), EU directive 2010/63 and were approved by the Nottingham Trent University ethical committee. The data used in the experiments reported here is derived from the same PFC injection sites used in Chapter 2: Co-injections of Fluoro-Gold (100nl) and BDA (Fluorescein, 100nl) were made into predetermined co-ordinates in PFC (R37, R38, R41, R42). In this experiment three of the injections

were made into the left hemisphere (R37, R38, and R42) and one injection was made in the right hemisphere (R41). Additional single injections of Fluoro-Gold (100nl) and BDA (Fluorescein or Texas Red, 100nl), in which rats received an injection of Fluoro-Gold into the right hemisphere (R4, R5, R6, R7) and BDA into the left (R1, R3, R7, R8) were administered in a separate study (Bedwell et al, 2014), the findings of which are reported in Appendix L. Additional and equivalent Fluoro-Gold injections were made into the left hemisphere in later studies (Chapter 6: R9, R12, R13, R16, R19, R20, R21). This data was used to verify whether the location and ordering of projections differed on either side of the brain. No difference was found (Appendix M).

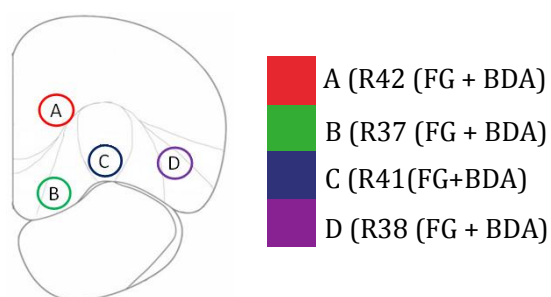


Figure 5.1. Coronal section of PFC (A-P 4.2mm from Bregma) showing the cytoarchitectural boundaries of PFC sub-regions according to Van de Werd & Uylings (2008), depicting sites of amalgamated anterograde and retrograde tracer injections; Prelimbic (PL):A, ventral orbital (VO):B, ventrolateral orbital(VLO):C and dorsolateral orbital(DLO):D, with 1mm separation.

The volume and location of PFC injection sites was based on the findings of preliminary experiments (reported in Appendix A). The co-ordinates used were all at 3.7mm with respect to Bregma, injection site A (PL) was 1.2mm from the midline and 2.4mm below the cortical surface. Injection sites B (VO), C (VLO) and D (DLO) were all positioned 3.2mm below the cortical surface and 1.2mm (B), 2.2mm (C) and 3.2mm (D) from the midline. The spread of tracer at each injection site was less than 1mm.

Anatomical Processing and Microscopic Analysis

The anatomical and microscopic analysis used in this study is described in detail in Chapter 2. The entire forebrain was examined for labelling. Areas of sensory-motor cortex were identified as containing strong and consistent labelling, therefore a detailed analysis was carried out on this region.

Statistical Analysis of the Arrangement of Connections Between Prefrontal and Sensory-Motor Cortex

The numerical and statistical analysis used in this study was similar to that used in the previous temporal cortex studies (Chapters 2 and 3). Image J (Wayne Rasband, NIH) was used to determine numerical values representing the location of each retrogradely labeled cell in sensory-motor cortex. The three dimensional location of each retrogradely labeled cell (Fluoro-Gold) was calculated by measuring the distance of each labeled cell from the medial surface (medial-lateral) and the dorsoventral distance from the most dorsal aspect of the cortical surface (dorsal-ventral). The anterior-posterior location of labeled cells was recorded in terms of distance from Bregma (according to Paxinos and Watson, 1998). The same analysis was repeated for fluorescent BDA labelling. A similar acquisition of data was implemented for the anterograde BDA labelling, whereby four data points were recorded from the perimeter of each anterogradely labeled area, denoting its distance from the medial and dorsal surfaces. The anterior-posterior location of each labeled area was also recorded.

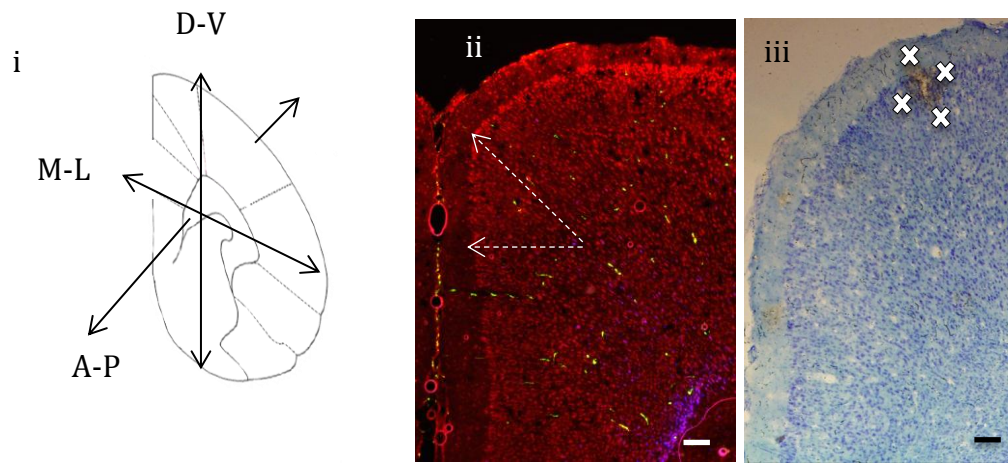


Figure 5.2. (i) Coronal cross section of sensory-motor cortex at 2.2mm posterior to bregma, depicting the three dimensions in which the locations of labelled cells were recorded (Anterior-Posterior (A-P), Medial-Lateral (M-L) and Dorsal-Ventral (D-V)). (ii) Retrogradely labelled cells (blue cells) in sensory-motor cortex produced by a co-injection of Fluoro-Gold (100nl) and BDA (Fluorescein, 100nl (green cells)) into VO. Arrows indicate measurements of labelled cell location in the medial-lateral dimension (distance to lateral cortical surface) and dorsal-ventral dimension (distance from cortical surface). (iii) Anterogradely labelled area (Brown) in sensory-motor cortex produced by an injection of BDA (100nl) into PL. Crosses indicate the four points on the perimeter at which measurements were taken. Arrows indicate measurements of labelled area location in the medial-lateral dimension (distance to medial cortical surface) and dorsal-ventral dimension (distance from dorsal surface: laminar). Scale bars = 200µm.

Labelled cells/areas were grouped according to PFC injection site location. These data sets were analysed in SPSS by way of a factorial ANOVA, in order to establish the existence of an effect of injection site location on the positioning of labels in sensory-motor cortex (in dorsal-ventral, anterior-posterior and medial-lateral axes). The relationship between input (retrograde) and output (anterograde) connections was examined by a two factor ANOVA. Anterograde DAB labelling is reported in the results section and shown in figures 5.4 and 5.6, with the exception of where fluorescent labelling is clearly stated.

Further statistical analyses were applied in the form of paired samples t-tests, in order to compare the results produced from separate tracer injections and co-injections of retrograde (Fluoro-Gold) and anterograde (BDA) tracer, confirming consistency in the findings (Appendix N). Paired samples t-tests were applied to the Euclidean distance between labels from left and right hemisphere injections in order to establish

if a hemispheric difference in labelling was present (Appendix M). All statistical tests were applied with a significance level of 0.05 and confidence intervals of 95%.

Results

The data used in this study was produced from the same co-injections of Fluoro-Gold (100nl) and BDA (Fluorescein, 100nl) described in Chapter 2. Labelling in sensory-motor cortex from additional separate injections of Fluoro-Gold and BDA (injection sites described in Appendix L), in the same PFC co-ordinates as used here, was investigated prior to this study and produced similar results (Bedwell et al, 2014; for findings see Appendix L).

Co-injections of Fluoro-Gold (100nl) and BDA (100nl Fluorescein) made into PL, VO, VLO and DLO (R42, R37, R41, R38) occurred in the intended PFC regions. Details of these co-injection sites were described in Chapter 2. The co-injection sites (Fluoro-Gold & BDA) spanned layers I/II – VI and covered the majority of the intended cytoarchitectural region. Injection sites into PL (A) and VO (B) overlapped, however the majority of the spread of tracers was confined to separate PFC sub-regions. The positioning of co-injections of Fluoro-Gold and BDA was considered to be comparable to the positioning of separate injection sites of Fluoro-Gold, BDA, Fluoro-Ruby and Fluoro-Emerald described elsewhere (Appendix A, Appendix F, Appendix H). The co-injection site into VO (B) was positioned dorsally in comparison to the separate Fluoro-Gold and BDA injection sites described in Appendix A, despite this the majority of the spread of tracers at this injection site was in the same location as that seen with separate injection sites (Fig.5.3).

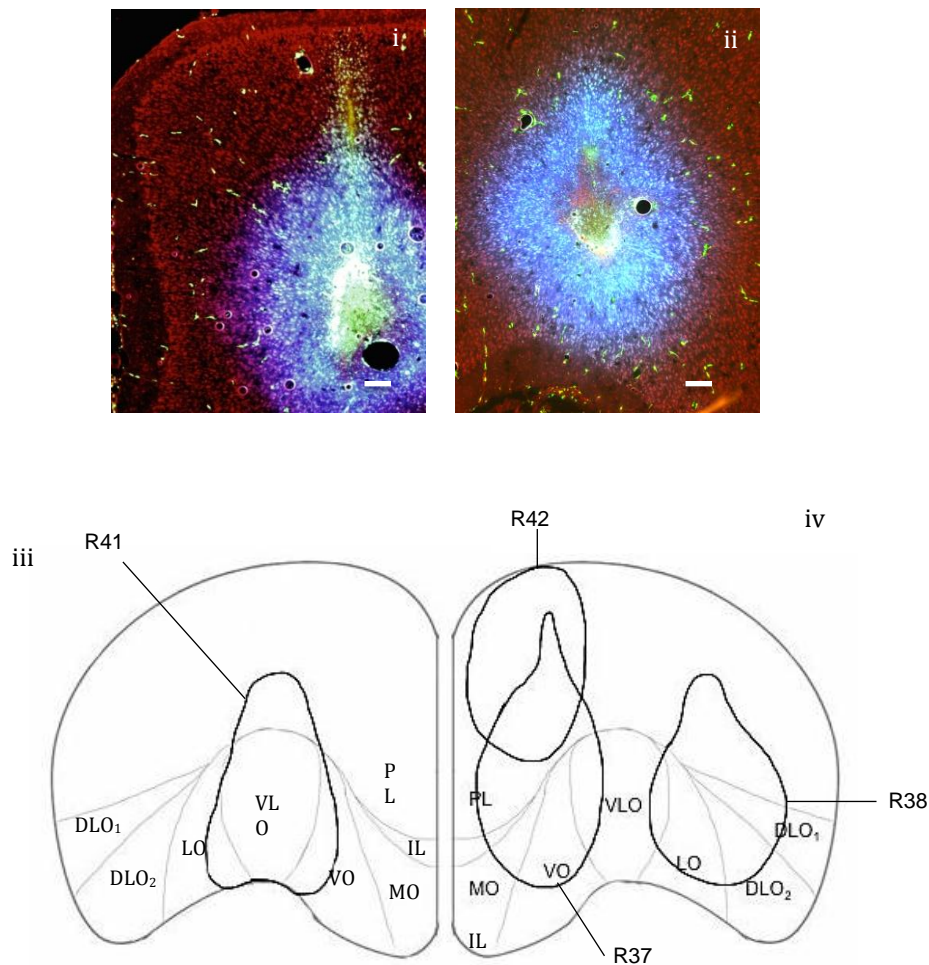


Figure 5.3. (i) Coronal section of PFC showing location and spread of (100nl) Fluoro-Gold and (100nl) Fluorescein at injection site in VO. (ii) Coronal section of PFC showing location and spread of (100nl) Fluoro-Gold and (100nl) Fluorescein at injection site in DLO. (iii) Representations of Fluoro-Gold and Fluorescein co-injection sites in PL (R42), VO (R37), VLO (R41) and DLO. Scale bars = 200 μ m.

We observed locations of labelling throughout the brain following co-injections of anterograde (BDA; Fluorescein) and retrograde (Fluoro-Gold) tracer into PFC (PL, VO, VLO and DLO) using light and fluorescent microscopy. Retrogradely labelled cells were seen in secondary motor cortex (M2), primary motor cortex (M1), primary somatosensory cortex (S1J, S1BF), cingulate cortex (Cg1), piriform cortex (Pir), perirhinal cortex (PRh), entorhinal cortex (Ent), secondary auditory cortex (AuV) and primary auditory cortex (Au1). Anterograde labelling was seen in M2, S1J, secondary

somatosensory cortex (S2), Cg1, PRh, Ect, LEnt, agranular insular cortex (AID) and PFC regions. Labelling was most prominent in temporal (analysed in Chapters 2, 3 and 4) and sensory-motor cortex (M1, M2, SIJ and Cg1). Therefore a statistical analysis was applied to this region to determine whether there was evidence for an ordered arrangement of prefrontal to sensory-motor cortex connections. Labelling from separate injections of BDA and Fluoro-Gold in the same PFC co-ordinates as those described here, confirmed observations that labeled inputs and outputs occurred in different locations.

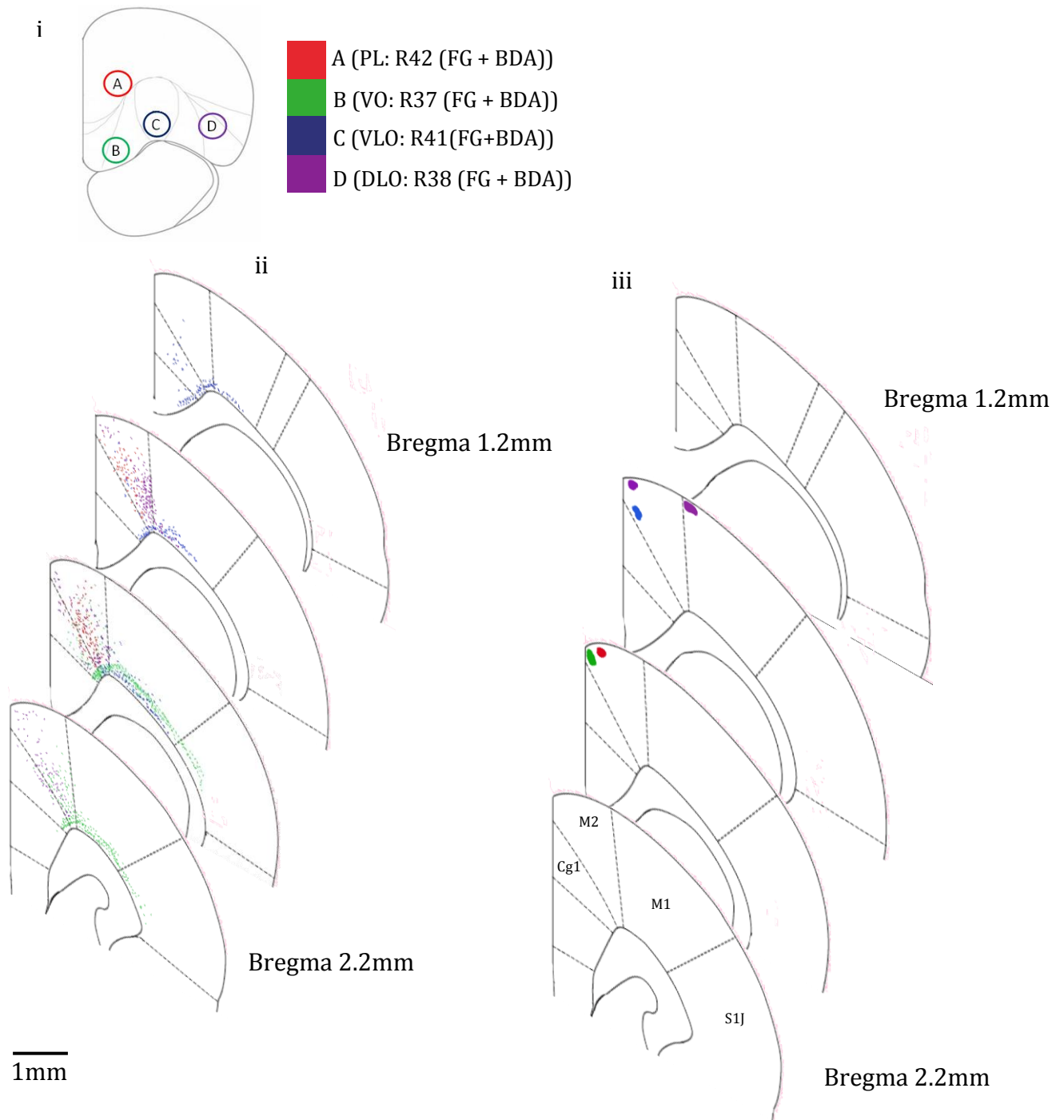


Figure 5.4. Diagram representing the injection sites of Fluoro-Gold and BDA, and the projection sites to sensory motor cortex for both retrograde (Fluoro-Gold) and anterograde (BDA) tracer injections. (i) The locations of injection sites A (PL: R3, R7), B (VO:R6, R7), C (VLO:R1, R4) and D (DLO:R5, R8) in PFC. (ii)The locations of retrogradely labelled cells in sensory-motor cortex, resultant from 100nl Fluoro-Gold injections into PFC injection sites A-D (R4, R5, R6, R7). (iii) The locations of anterogradely labelled areas in sensory-motor cortex, resultant from 100nl BDA injections into PFC injection sites A-D (R1, R3, R7, R8).

Organisation of Input Connections to Prefrontal Cortex from Sensory-Motor Cortex

Labelled input (retrograde) projections to PFC from areas of sensory-motor cortex were seen in secondary motor (M2), primary motor (M1) and primary somatosensory cortex (S1J) (Fig.5.4ii). Retrogradely labelled cells from each injection location were distributed across several cytoarchitecturally distinct regions. The distribution of retrogradely labelled cells within temporal cortex maintained a spatial order according to the corresponding PFC injection sites. Retrogradely labelled cells in the sensory-motor region showed an ordered arrangement in terms of cortical layers (Fig.5.4ii). Labelled cells produced by an injection of retrograde tracer (Fluoro-Gold) into VLO appear in layer VI, whereas those produced by an injection of tracer into VO appear in layer V in the same region. Cells labelled following an injection of retrograde tracer into DLO appear across layers II to VI. In addition, retrogradely labelled cells were consistently seen in deeper cortical layers (VI, V) than anterogradely labelled areas (I, II) (Fig. 5.4ii & iii.). The factorial ANOVA revealed a significant main effect of injection site on dorsoventral (i.e. laminar) location of retrogradely labeled cells ($F(3,303)=176.557$ $p<0.001$ $r=0.607$). Post hoc comparisons (Tukey HSD) revealed significant differences between retrograde injection sites A*B, B*C and B*D ($p<0.001$). This indicates an ordered arrangement of input projections from sensory-motor regions to medial sub-regions of PFC (PL, VO, VLO).

An ordered organisation of input connections can be seen in the anterior-posterior axis; moving mediolaterally in PFC, specifically from VO to DLO, labeled cells in sensory-motor cortex become more posterior. A factorial ANOVA revealed a significant main effect of injection site on anterior-posterior location of retrogradely labelled cells ($F(3,303)=81.301$ $p<0.001$ $r=0.460$). Post hoc comparisons (Tukey HSD) revealed significant differences between retrograde injection sites A*B, B*C, B*D ($p<0.001$) and C*D ($p=0.001$). A factorial ANOVA also revealed a significant main effect of injection site on medial-lateral location of retrogradely labeled cells ($F(3,303)=415.149$ $p<0.001$ $r=0.760$). Post hoc comparisons (Tukey HSD) revealed significant differences between retrograde injection sites A*B, B*C and B*D ($p<0.001$). Retrogradely labelled cells were found in additional regions to those in

which corresponding anterograde labels were seen, indicating non-alignment of connections.

In comparison to earlier single injection experiments (Bedwell et al, 2014; Appendix L), labelling of output projections from PFC to sensory-motor cortex resultant from injections of BDA; Fluorescein (100nl) was seen with both fluorescence and DAB staining. Labelled axon terminals were numerically analysed from both visualisation methods (fluorescent and brightfield). The locations of areas of DAB stained axon terminals were measured in order to directly compare findings. Individual fluorescently labelled axon terminals were measured in terms of their 3-dimensional location, consistent with the methodology used to quantify retrograde (Fluoro-Gold) labelling.

The labelling seen in sensory-motor cortex from co-injections of Fluoro-Gold and BDA shows evidence of ordered arrangements of both input and output connections from PFC to sensory-motor cortex, as well as clear evidence of non-alignment of connections. Some co-labelling of cells with BDA and Fluoro-Gold was seen, with the majority of Fluorescein and Fluoro-Gold labels seen in different locations to one another (Fig.5.4). The co-injection of retrograde (100nl Fluoro-Gold) and anterograde (100nl Fluorescein) tracers revealed similar results to those produced from separate retrograde and anterograde injections (Bedwell et al, 2014; Appendix L).

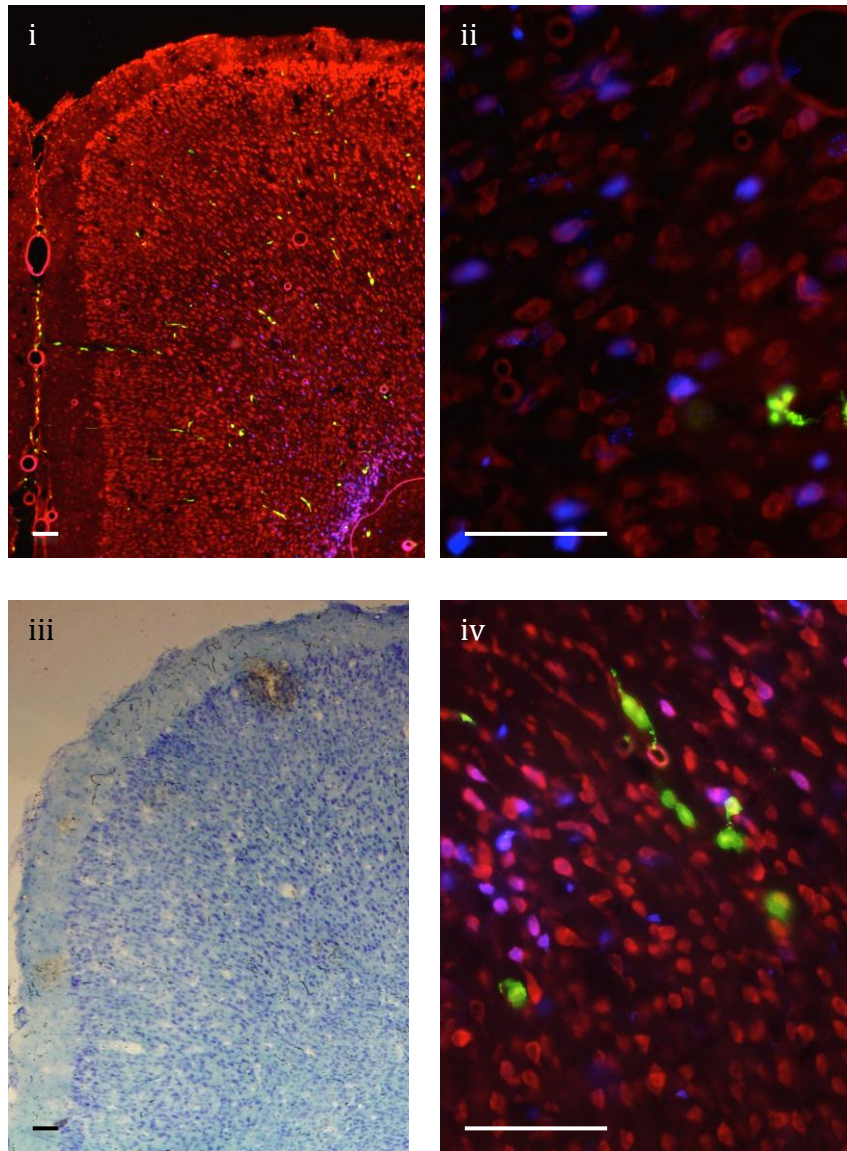


Figure 5.5. (i) Coronal section of sensory-motor cortex showing retrograde labelling (blue) and anterograde labelling (green) resultant from co-injection of Fluoro-Gold and BDA (Fluorescein) into VO (injection site B, R37). (ii) Retrograde (blue) and anterograde (green) labelling in motor cortex resultant from co-injection of Fluoro-Gold and BDA (Fluorescein) into VO (injection site B, R37). (iii) Coronal section of sensory-motor cortex showing area of anterograde labelling (brown (fluorescein visualised with DAB)) resultant from co-injection of Fluoro-Gold and BDA into DLO (injection site D, R38). (iv) Retrograde (blue) and anterograde (green (fluorescein visualised with fluorescence)) labelling in motor cortex resultant from co-injection of Fluoro-Gold and BDA (fluorescein) into VLO (injection site C, R41). Scale bars = 100µm.

Organisation of Output Connections from Sensory-Motor Cortex to Prefrontal Cortex

Labelled output (anterograde) projections from PFC to sensory-motor cortex were seen in M1, M2 and cingulate cortex (cg1). The distribution of anterogradely labelled areas within motor cortex (M1, M2) maintained a relatively clear spatial order in accordance with their corresponding injection sites in PFC (VO, LO and DLO). An ordered arrangement of output connections can be seen in the dorsal-ventral axis. Moving from lateral to medial in PFC (from DLO to VO), anterograde labelling in sensory-motor cortex becomes more ventral. The factorial ANOVA revealed a significant main effect of injection site on dorsoventral (i.e. laminar) location of anterogradely labeled areas (Fluorescent labelling: $F(3,408)=14.112$ $p<0.001$ $r=0.183$, DAB staining: $F(3,20)=4.248$ $p=0.018$ $r=0.419$) in sensory-motor cortex. Post hoc comparisons (Tukey HSD) revealed significant differences between anterograde injection sites A*C ($p=0.003$), A*D ($p<0.001$), B*C ($p=0.011$) and B*D ($p<0.001$).

There is also evidence of ordering in the anterior-posterior and medial-lateral axes. A factorial ANOVA revealed a significant main effect of injection site on anterior-posterior location of anterogradely labelled areas (Fluorescent labelling: $F(3,408)=107.054$ $p<0.001$ $r=0.456$, DAB staining: $F(3,20)=4.167$ $p=0.019$ $r=0.415$) in sensory motor cortex. Post hoc comparisons (Tukey HSD) revealed significant differences between anterograde injection sites A*D, B*D and C*D ($p<0.001$). A factorial ANOVA revealed a significant main effect of injection site on medial-lateral location of anterogradely labeled areas (Fluorescent labelling: $F(3,408)=54.016$ $p<0.001$ $r=0.342$, DAB staining: $F(3,20)=11.938$ $p<0.001$ $r=0.611$) in sensory-motor cortex. Post hoc comparisons (Tukey HSD) revealed significant differences between anterograde injection sites A*D, B*D and C*D ($p<0.001$). These results show evidence for ordering of output connections from PFC to sensory-motor cortex in three axes of orientation.

Anterograde labelling in sensory-motor cortex seen here shows a convergent organisation of connections; PFC injections separated by 1mm produce labelling much closer together e.g. injections made into separate PFC cytoarchitectural regions produced anterograde labelling close together in M2.

The anterograde labelling of connections from PFC to sensory-motor cortex shows evidence of broad scale reciprocity. Anterogradely labeled output connections are consistently seen in the same cytoarchitectural regions as corresponding retrogradely labeled neuronal cell bodies from the same PFC injection site e.g. in M2. Reciprocity on this scale is present for connections from VO, LO and DLO. This is the case both with the co-injections of retrograde and anterograde tracers described here and separate injections described in Appendix L (Bedwell et al, 2014).

The two factor ANOVA revealed a significant interaction effect between input and output connections in the dorsal-ventral ($F(3,323)=22.089$ $p<0.001$ $r=0.253$), anterior-posterior ($F(2,323)=4.177$ $p=0.006$ $r=0.113$) and medial-lateral ($F(3,323)=48.494$ $p<0.001$ $r=0.361$) axes. This shows that the location of anterogradely and retrogradely labelled cells vary in respect to one another, meaning that the input and output connections follow differential ordering.

The analysis indicates an ordered organisation of connections between prefrontal and sensory-motor cortex. As the PFC injection site moves from medial to lateral (VO to DLO), the pattern of input projections moves in a dorsal-ventral direction, indicating laminar organisation. Similarly, moving mediolaterally from VO to DLO, output projections move from ventral to dorsal (in the opposite direction to input connections), whilst simultaneously moving from posterior to anterior. Ordering of output connections can also be seen in the medial-lateral axis, as PFC injection site moves from medial to lateral (VO to VLO), sensory-motor cortex projections become more lateral. In comparing the organisation of connections labeled from anterograde and retrograde co-injections, the findings indicate differential organisation of input and output connections between prefrontal and sensory-motor cortex.

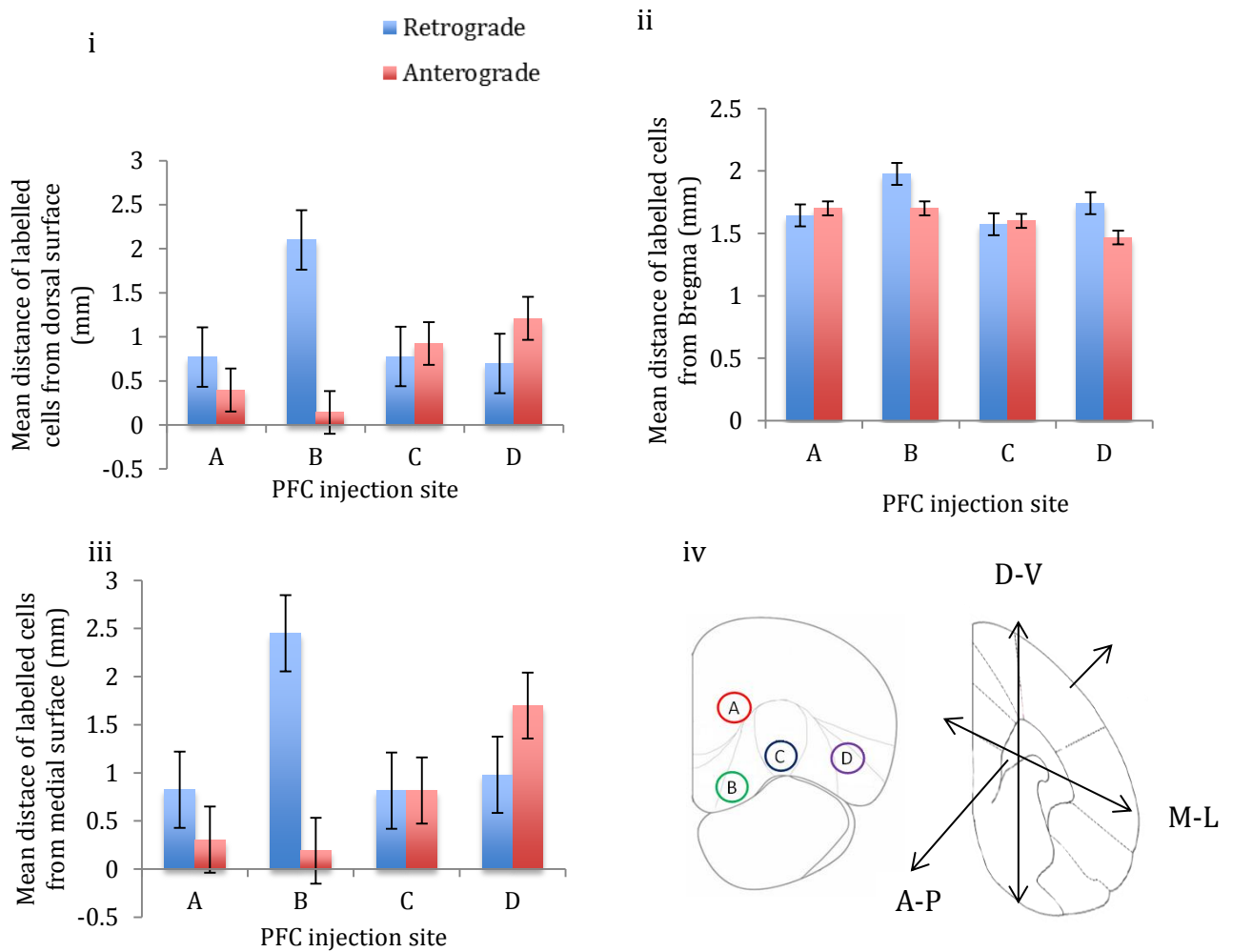


Figure. 5.6. The mean effect of PFC co-injection site location on the mean location of retrogradely labelled cells ($n= 307$; PL (A:R42)=77, VO (B:R37)=121, VLO (C:R41)=80, DLO (D:R38)=29) and anterogradely labeled axon terminals ($n=24$; PL (A:R42)=4, VO (B:R37)=4, VLO (C:R41)=4, DLO (D:R38)=12) within temporal cortex, in the (i) dorsal-ventral (ii) anterior-posterior and (iii) medial-lateral axes. Error bars = standard error. (iv) Coronal cross section of PFC showing the position of 4 injection sites; Prelimbic (A), ventral orbital (B), ventrolateral orbital (C), dorsolateral orbital (D). Coronal cross section of temporal cortex showing the three dimensions in which the locations of labels were recorded.

The calculation of a 3 dimensional mean location (E) for the labelling produced by each retrograde and anterograde injection site,

$$E = \sqrt{(DV)^2 + (AP)^2 + (ML)^2}$$

allowed for the visualisation of the 3-dimensional locations of input and output connections in comparison to one another (Fig.5.7).

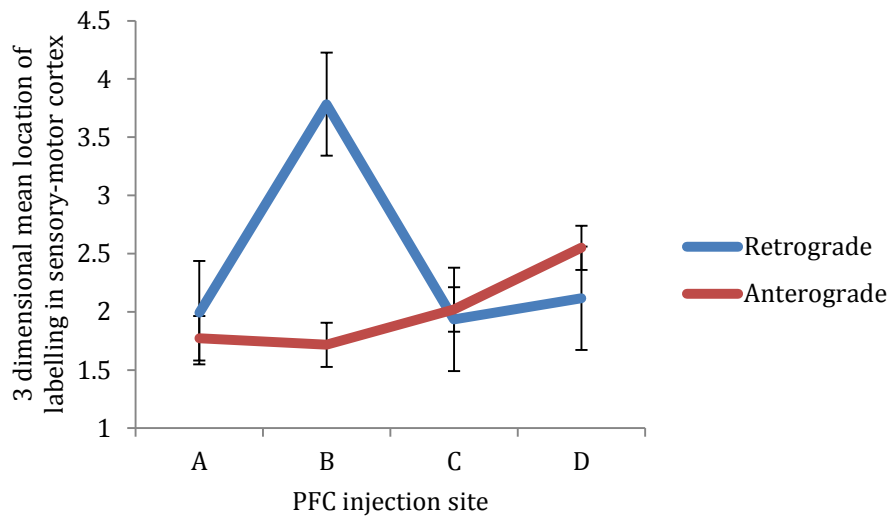


Figure 5.7. The effect of PFC injection site (PL:A, VO:B, VLO:C, DLO:D) on the three dimensional mean location of retrogradely labelled cells (blue) and anterogradely labelled areas (red) in sensory-motor cortex. Error bars = standard error.

The results of the analysis show that input and output connections follow different orders of arrangement as injection sites move from PL (injection A) to DLO (injection D). Figure 5.7. shows that connections from injection site C (VLO) show the most similarity between inputs and outputs, therefore connections from VLO to sensory-motor cortex show a high level of reciprocity. In comparison, connections from VO (injection site B) show the greatest difference between inputs and outputs, indicating a high degree of differential organisation between inputs and outputs from VO to sensory-motor cortex.

These findings indicate that the ordered arrangement of input and output connections are affected by one another, most prominently in the dorsal-ventral and medial-lateral axes. Further to this, I have demonstrated that the location of retrogradely labelled cells is directly associated with the location of anterogradely labelled cells. For instance, in the dorsal-ventral axis, retrograde and anterograde labels appear to move in opposite directions as the PFC injection sites is moved from medial to lateral (VO

to DLO); retrograde labelling becomes more ventral, whereas anterograde labelling becomes more dorsal. This finding is consistent across multiple studies.

The results from co-injections of retrograde and anterograde tracer showed no difference in the location of sensory-motor cortex labelling in comparison to separate injections (see Appendix N). Statistical evidence for this is shown by paired samples t-tests. No significant difference in the mean location of retrograde labelling in temporal cortex was found: in the dorsal-ventral axis ($t(3)=1.139$ $p=0.337$), anterior-posterior axis ($t(3)=-0.666$ $p=0.553$) and medial-lateral axis ($t(3)=0.353$ $p=0.747$). No significant difference in the mean location of anterograde labelling in temporal cortex was found: in the dorsal-ventral axis ($t(3)=0.571$ $p=0.608$), anterior-posterior axis ($t(3)=1.265$ $p=0.295$) and medial-lateral axis ($t(3)=1.357$ $p=0.268$). These findings demonstrate the consistency of labelling in sensory-motor cortex between co-injections and separate injections of Fluoro-Gold and BDA, as well as the reproducibility of the findings.

Discussion

Broad Scale Connections from Prefrontal Cortex to Sensory-Motor Cortex

This study investigated the organisation of connections from adjacent prefrontal regions with the use of neuroanatomical tracers. The findings have revealed evidence for an ordered arrangement within the projections from PFC to sensory-motor cortex. I revealed a clear ordered arrangement of PFC connections, most prominently arising from significant portions of motor cortex. In addition I found evidence of differential ordering of input and output connections between PFC and sensory-motor regions, most clearly in the dorsoventral and mediolateral axes. This means that labelling from Fluoro-Gold and Fluoro-Ruby were found in different columnar regions of sensory-motor cortex, similar to that seen in the PFC – temporal cortex pathway (Chapter 2).

Input Connections from Sensory-Motor Cortex to Prefrontal Cortex

Following the administration of the retrograde tracer, Fluoro-Gold, to the prefrontal cortical areas PL (A), VO (B), VLO (C) and DLO (D), labelling of neuronal cell bodies was observed in areas of motor cortex, temporal cortex, auditory cortex, somatosensory cortex, cingulate cortex and piriform cortex. Projections from areas of motor and sensory cortex (M1, M2 and SIJ) were amongst those displaying the most labelling. Retrograde labelling in sensory-motor areas showed an ordered arrangement in terms of cortical layers (Fig.5.6i) (in the dorsal-ventral axis). Labelled cells in sensory-motor cortex produced by a retrograde injection into DLO (injection site C, R41) can be seen in layer VI, whereas those produced by an injection into VLO (injection site B, R37) are seen in layer V (in the same cytoarchitectural region). The labelling seen in sensory-motor cortex resultant from retrograde PFC injection sites was considerably more widespread than the anterograde labelling produced from the same injection sites. This was the case both with co-injections and separate injections of retrograde and anterograde tracer (Bedwell et al, 2014; Appendix L). These findings are comparable with previous studies (Sesack, 1989) which outlined projections from prefrontal to areas of sensory-motor cortex.

Output Connections from Prefrontal Cortex to Sensory-Motor Cortex

Following the administration of the anterograde tracer, biotinylated dextran amines (100nl Fluorescein), to the prefrontal cortical areas PL (A), VO (B), VLO (C) and, DLO (D), labelling of axon terminals was observed in motor cortex, temporal cortex, auditory cortex, somatosensory cortex, agranular insular cortex, cingulate cortex and PFC regions. The projections arising from the motor and cingulate cortex (M1, M2 and cg1) were amongst those displaying the most labelling. This was broadly consistent with previous studies which outlined prefrontal connections to medial-frontal cortex (Sesack, 2004).

Organisation and Alignment of Connections Between Prefrontal Cortex and Sensory-Motor Cortex

The analysis of the location of input and output connections to and from prefrontal regions shows an ordered arrangement of connections occurring in and across 3 axes of orientation, most significantly so in the dorsal-ventral and medial-lateral axes. The analysis of sensory-motor cortex connections revealed a laminar ordered arrangement of input and output connections to PFC (occurring in the dorsal-ventral axis). For the dorsal-ventral axis, injections in sites B (VO), C (LO) and D (DLO) produced an ordered arrangement of PFC output connections to sensory-motor regions. There was clear ordering in terms of the input connections from sensory-motor cortex (M1 and S1) to PFC. Layers V and VI differentially project to injection sites B (VO) and C (LO) in PFC. Laminar distribution has been described previously in connections from PFC to subcortical and motor regions in rats (Gabbot, 2005). A similar laminar ordering to that seen in this study has been described elsewhere; projections from orbitofrontal and infralimbic cortices to entorhinal cortex produce labelling in deeper layers, with more posterior-medial injections (Insausti and Amaral, 2008), but such an organisational pattern has not been previously seen in sensory-motor cortex. This may be of particular significance to PFC function because both of these regions (M1 and S1) contain somatotopic maps. It appears that the same regions implicated in these maps (in layers V and VI) project to distinct regions of PFC (i.e. VO and LO). It could be functionally useful for the same ordered arrangement to be maintained within sensory-motor to PFC connections.

These results show a projection from M1, M2 and S1 to PFC, which then projects to M2. The circuit identified here is not typical of the organisation of connections we may expect. Based on a traditional model of hierarchical organisation of functional connectivity, PFC is positioned at the top of a processing hierarchy (Fuster, 2001; Botvinick, 2008). Subsequently connections would usually travel from primary sensory cortex, followed by secondary sensory cortex and association areas (e.g. PRh) before reaching PFC at the top of the hierarchy. From PFC connections would travel to secondary motor cortex followed by primary motor cortex (e.g. S1 → S2 → association areas → PFC → M2 → M1), following an order of hierarchical organisation from primary cortical regions, through secondary cortical regions, up to a

high order area and back down through secondary cortical regions to primary cortical regions. The connections observed here do not fit this hierarchical order. The connections described from PFC → M2, and M2→PFC are consistent with what would be expected based on a hierarchical model. However, the direct connection found from S1→ PFC connects a primary cortical regions directly to a high order region (PFC). This finding provides an insight into the complex functional organisation of the PFC to sensory-motor cortex pathway, indicating the way in which information travels between sensory and prefrontal cortices differ to that of other cortical pathways.

These findings show evidence of reciprocal connections between PFC and M2. Anterograde and retrograde labelling from identical PFC injection sites were consistently found in the same cytoarchitectural regions of M2. This indicates a broad reciprocal organisation. However, labelling from retrograde injections was considerably more widespread than that from anterograde injections, resulting in retrograde labels in areas of M1 and S1J. No evidence of anterograde labelling was seen in these regions, resulting in non-reciprocal connections. These results show that the PFC – sensory-motor cortex pathway contains aspects of reciprocity, but is not entirely reciprocal in its organisation. A large degree of reciprocity was seen in the connections from PL to M2 and Cg1, this is very different to the labelling seen of connections from VO, VLO and DLO, which shows inputs and outputs in different locations. This difference in reciprocity may be a product of differences in functional organisation between PL and VO, VLO and DLO. Haber (2003) suggested that cortical regions with similar functions are reciprocally connected, whereas regions with different functions are not reciprocally connected. Connectional studies of primary sensory (S1) and primary motor cortex (M1) often report reciprocity of connections (Dinopoulos, 1994; Lee et al 2011), in that inputs and outputs occupy the same precise locations. This has been described between S1 and S2 (Henry & Catania, 2006; Aronoff et al, 2010), M1 and S1 (Porter & White, 1983; Aronoff et al, 2010) and M1 and S2 (Porter & White, 1983). The same study by Porter and White reported non-reciprocal connections from M1 to the striatum, indicating that motor cortex input and output connections are not always found in the same locations.

These findings indicating different organisational patterns of input and output connections are particularly unexpected when compared with what is currently understood in terms of the connectivity of highly studied cortical regions, such as visual cortex. Retinotopic maps within visual cortex (V1) have been widely described (Wandell et al, 2007; Benson et al, 2011). The topographic organisation of input and output connections from visual cortex are aligned (Van Essen et al, 1986; Triplett, 2009). Recent fine scale tracer findings (Nascimento-Silva et al, 2014) show clear reciprocity in V2 and V4, although, similar to my findings in PFC, the results of this study show that not all input projections had a reciprocal output projection. It is suggested that topographic alignment of inputs and outputs is vital for visual attention (Tootell et al, 1998), therefore we might expect the complex cognitive functions associated with PFC to also be dependent on the anatomical alignment of input and output connections.

The findings of this study demonstrate that PFC displays an ordered arrangement of connections to regions of sensory-motor cortex. The input connections to PFC arise from distinct regions of sensory-motor cortex, notably different layers within M1 and S1. Output connections from PFC labeled by anterograde tracer injections are seen in distinct regions of sensory-motor cortex (M1 and M2), much more concentrated than the relatively widespread retrogradely labeled cells. In a broad sense, there is similarity between the labeled input and output projections from PFC to sensory-motor cortex, as they are found in the same general cytoarchitectural regions. However, at a more detailed level there is a separation in the location of inputs and outputs. Labelled input connections can be seen spreading significantly more laterally into regions of motor (M1) and sensory (S1J) cortex in comparison to the consistently medial (Cg1, M2) output labels. Although there are areas of reciprocity, this provides clear evidence of large areas of non-reciprocal connections and non-alignment of inputs and outputs. Such non-alignment has not been previously described in PFC, but was observed in the connections between PFC and temporal cortex investigated in Chapters 2-4. Previous observations in organisation suggest reciprocity of inputs and outputs to be a common attribute in perirhinal, entorhinal and parahippocampal regions in primates (Suzuki and Amaral, 1994; Canto et al, 2008). In addition, recent dual tracer studies in primates have given no indication of differential organisation between input and output connections to ventrolateral and medial PFC from premotor

cortex as well as subcortical regions (Kim and Lee, 2012; Takahara et al, 2012). However, these findings report PFC connectivity on a relatively large scale and from specific sub-regions.

In summary, this study showed evidence for an ordered arrangement of connections between PFC and sensory-motor cortex, with evidence of different organisational patterns of input and output connections. The ordering of these connections appears across anatomical orientations.

Chapter 6.

Organisation of Connections to Sensory-Motor Cortex from Anterior, Central and Posterior Prefrontal Cortex

Studies into prefrontal cortex (PFC) function have identified differential functioning of neurons (Duncan, 2001; Kargo, 2007) and changes in organisation in anterior compared to posterior PFC (Olson & Musil, 1992; Taren et al, 2011), often describing a gradient in terms of abstract processing (Taren et al, 2011).

The findings from the connections from anterior, central and posterior PFC to temporal cortex (Chapter 3) provided evidence to support a gradient of PFC connectivity. The findings in the PFC – temporal cortex pathway showed an increasing degree of non-alignment (and decrease in reciprocity of connections) towards anterior PFC. These observations were consistent with the findings in primates of increased abstraction (following a gradient) towards anterior PFC and suggestions of unique and differential ordering, separate to that identified with hierarchical organisation (Ramnani & Owen, 2004).

The studies described in Chapter 5 established an ordered arrangement of connections from PFC to areas of sensory-motor cortex. The findings revealed unusual properties in the organisation of connections, inconsistent with assumptions of the expected hierarchical organisation. This study also produced evidence for differential ordering of input and output connections, not previously described in this pathway and consistent with the findings from the PFC – temporal cortex pathway. The study described in Chapter 5 provided an important insight into the organisation of connections from PFC to regions of sensory and motor cortex, however focused only on a specific central area of PFC (in terms of its anterior-posterior axis), further experiment into the anterior-posterior connectivity of PFC to sensory and motor cortices will provide a greater insight into its detailed structural organisation.

Aims

The aim of this study was to expand on earlier work and determine the connectivity pattern of a wider area of PFC, from anterior to posterior, in terms of ordered connections as well as alignment between input and output connections.

Methodology

For detailed methodology and surgical procedures, see Chapter 2 and 3.

The anterograde tracer Fluoro-Ruby (FR) was introduced to this study, replacing the previously used BDA. The fluorescence of Fluoro-Ruby proved to be more vibrant, and provided more detailed images of labelled projections, allowing for more detailed investigations and analysis. The labelling properties of Fluoro-Ruby were investigated to establish the reliability of it as an anterograde tracer. Investigation of the labelling properties of Fluoro-Ruby (described in Chapter 3 and Appendix F) concluded the Fluoro-Ruby labelling produced in this experiment to be predominantly anterograde (~70% of labelling observed was anterograde). Based on this finding, the Fluoro-Ruby labelling observed in this study was treated as anterograde.

Craniotomies (<1mm) were repeated at 3 A-P locations (Bregma 4.7mm, 4.2mm, 3.7mm) (Fig.6.1). The medial-lateral co-ordinates and depth of injections at each A-P location were identical to injection sites A, B, C and D (PL, VO, VLO and DLO) described in Chapter 2 and 3. Injections of anterograde (100nl 10% Fluoro-Ruby in distilled water, Fluorochrome, Denver, Colorado) and retrograde tracer (100nl 4% Fluoro-Gold in distilled water, Fluorochrome, Denver, Colorado) were made into PL, VO, VLO and DLO (Fluro-Gold:100nl/min, 2 mins diffusion time; Fluoro-Ruby 10nl/min, 2 mins diffusion time). Injection sites were separated by 1mm and produced a spread of tracer at injection site of <1mm.

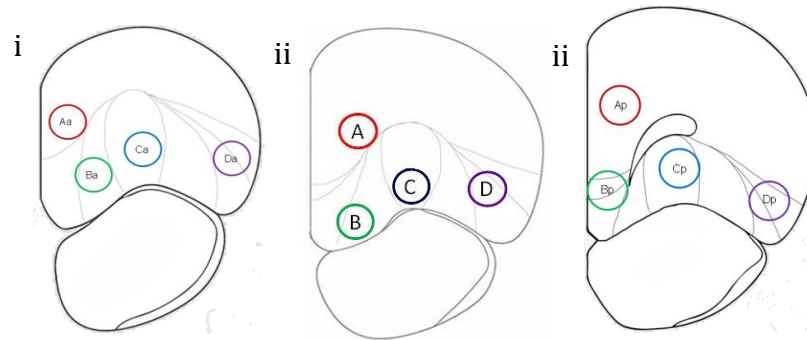


Figure 6.1. Coronal sections of PFC ((i) A-P 4.7mm, (ii) 3.7mm and (iii) 4.2mm from Bregma) showing the cytoarchitectural boundaries of PFC sub-regions according to Van de Werd & Uylings (2008), depicting the amalgamated sites of tracer injections; PL (Aa, A, Ap), VO (Ba, B, Bp), VLO (Ca, C, Cp) and DLO (Da, D, Dp), with 1mm separation.

Additional co-injections of (100nl) Fluoro-Gold and (100nl) Fluoro-Ruby were made into the same central PFC co-ordinates (Appendix Q). Further anterograde (100nl Fluoro-Emerald) injections were made into central PFC (PL, VO, VLO and DLO), in the same co-ordinates as previous injection sites in order to provide confirmation of anterograde labelling (Appendix R).

Anatomical Processing, Imaging and Microscopic Analysis

For details of anatomical processing and microscopic analysis, see Chapters 2, 3 and 5. Areas of sensory-motor cortex were known from earlier studies (Chapter 5 and Appendix L) to contain strong connections with PFC, therefore a detailed analysis was carried out on labelling found in sensory-motor cortex to examine the organisation of a wider area of PFC.

Statistical Analysis of the Arrangement of Connections Between Prefrontal and Temporal Cortex

The same numerical and statistical analysis was applied to that which had been used in the previous experiments (Chapter 5), in order to determine whether connections between PFC and sensory-motor cortex displayed an ordered arrangement similar to that which had been observed previously, and how that ordered arrangement differed

as the anterior-posterior location of PFC injection sites changed. The replacement of BDA with Fluoro-Ruby allowed for a more precise measuring of anterograde labelling, in which the 3-dimensional location of each individually labeled axon terminal could be recorded.

To determine the organisation of connections across PFC from anterior to posterior, a factorial ANOVA was applied. Post hoc analyses revealed the presence of differences in ordering between anterior, middle and posterior PFC. The alignment of connections from anterior, middle and posterior PFC were compared by applying a further statistical analysis. The mean Euclidean distance between retrograde and anterograde labels from 4 injection sites was calculated. Paired samples t-tests were used to compare the distance between retrograde and anterograde labels at each anterior-posterior location in PFC. All statistical tests were applied at a significance level of 0.05 and confidence intervals of 95%.

Results

The results presented in this study were produced from the same PFC injection sites used in Chapter 3.

Retrograde labelling was found in areas of M2, M1, S1J, S1BF, Cg1, Pir, PRh, Ent, AuV and Au1 and prefrontal regions. Anterograde labelling was found in areas of M2, S1J, Cg1, S2, PRh, Ent, AID and prefrontal regions. To investigate in detail the pathway between PFC and sensory-motor cortex, which had already been established in Chapter 5, the statistical analysis was applied to labelling found in motor and sensory regions. The organisation of input and output connections were initially investigated at three A-P PFC locations separately (anterior, middle, posterior). The connectivity to sensory-motor cortex across the whole investigated PFC region was then examined.

Anterior Prefrontal Cortex

The positioning and spread of injection sites is described in detail in Chapter 3.

Retrograde injection sites into the anterior aspect of PFC (R28, R24, R17, R23) were observed in the intended regions of PFC (according to Van de Werd & Uylings, 2008) and were mostly confined to cytoarchitectural boundaries of PFC regions (Fig.6.2v). There is some overlap seen between the retrograde injection sites in PL (R28) and VO (R24) as well VO and VLO (R24 and R17). Anterograde injection sites into the anterior aspect of PFC (R32, R23, R21, R24) were observed in the intended subdivisions of PFC and were confined to the cytoarchitectural boundaries of PFC regions. No overlapping occurred between anterograde PFC injection sites.

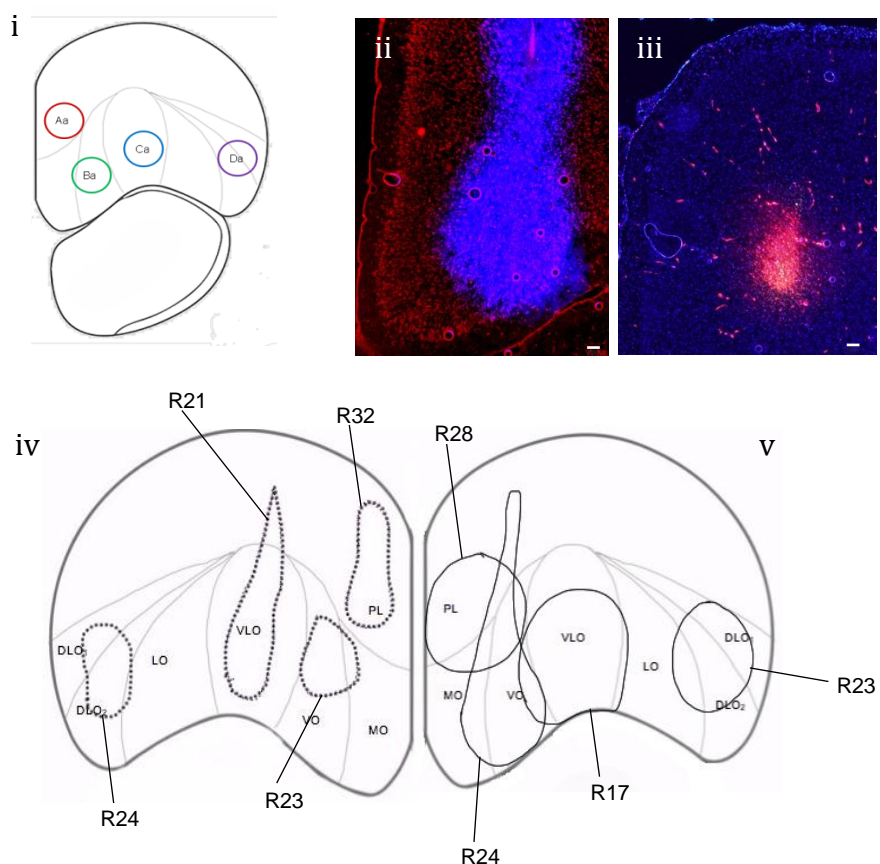


Figure 6.2. (i) Coronal section of anterior PFC (AP 4.7mm from Bregma) showing the cytoarchitectural boundaries of the prelimbic (PL), medial orbital (MO), ventral orbital (VO), ventrolateral orbital (VLO), lateral orbital (LO) and dorsolateral orbital (DLO) cortices (according to Van de Werd & Uylings, 2008), depicting sites of injections; Prelimbic: Aa, Ventral orbital: Ba, Ventrolateral orbital: Ca and dorsolateral orbital: Da, with 1mm spread. (ii) Coronal section of PFC showing

location and spread of (100nl) Fluoro-Gold at injection site in VO (R24). (iii) Coronal section of PFC showing location and spread of (100nl) Fluoro-Ruby at injection site in PL (R32). (iv) Representations of Fluoro-Ruby (100nl) (R21, R23, R24, R32 (broken line)) injection sites in PL (R32), VO (R23), VLO (R21) and DLO (R24) in the right hemisphere. (v) Representations of Fluoro-Gold (100nl) (R17, R23, R24, R28 (solid line)) injection sites in PL (R28), VO (R24), VLO (R17) and DLO (R23) in the left hemisphere. Fluoro-Ruby injection sites were predominantly within the boundaries of Fluoro-Gold injection sites. There is minimal overlap between Fluoro-Gold injection sites (R28 & R24, R24 & R17). Fluoro-Gold and Fluoro-Ruby injection sites are mostly limited to the cytoarchitectural boundaries of PFC regions, and span the majority of the region (PL, VO/MO, VLO, DLO), injections into VO spread into MO. Scale bars = 100 μ m.

Retrograde labelling, resultant from Fluoro-Gold injections into anterior PFC (PL, VO, VLO and DLO) was found in regions of PRh, Ent, AuV, Cg1, M2, M1, S1J and prefrontal regions (Fig. 6.3i, ii, 6.4ii). Anterograde labelling resultant from Fluoro-Ruby injections into anterior PFC (PL, VO, VLO and DLO) was found in regions of PRh, Ent, Cg1, M2 and M1, as well as prefrontal regions (Fig. 6.3iii, iv, 6.4iii). In order to further investigate the pathway between PFC and sensory-motor cortex, which had already been identified, the labelling within areas of M1, M2 and S1J was analysed.

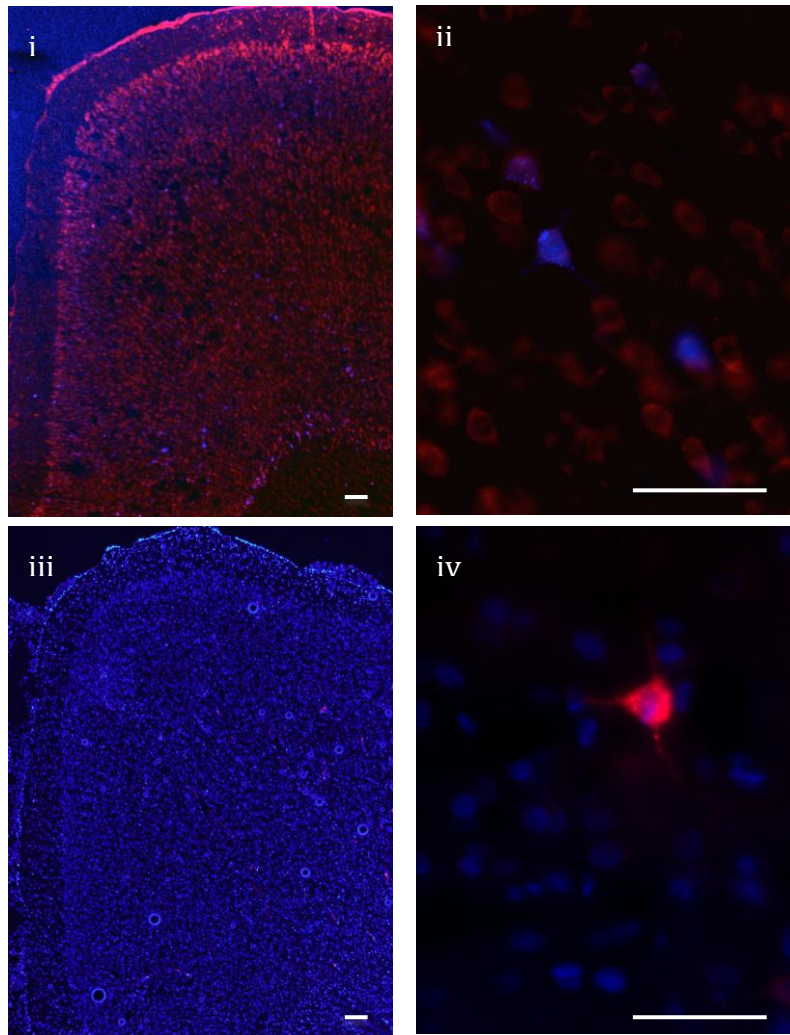


Figure 6.3. (i) Coronal section showing retrogradely labeled cells (blue) in sensory-motor cortex produced by injection of Fluoro-Gold (100nl) into VO (R24). (ii) Retrogradely labeled cells (blue) in sensory-motor cortex produced by injection of Fluoro-Gold into VO (R24). (iii) Coronal section showing anterogradely labeled axon terminals (red) in sensory-motor cortex produced by injection of Fluoro-Ruby (100nl) into PL (R32). (iv) Anterograde labelling (red) in sensory-motor cortex produced by injection of Fluoro-Ruby (100nl) into DLO (R24). Scale bars = 100µm.

Organisation of Input Connections from Sensory-Motor Cortex to *Anterior Prefrontal Cortex*

Projections to anterior PFC from temporal cortex were seen in Cg1, M2 M1 and S1J. Retrogradely labelled cells from each each PFC injection site were distributed across several cytoarchitecturally distinct regions. The distribution of retrogradely labelled cells in sensory-motor cortex maintained an overall spatial order according to the corresponding (Fluoro-Gold) PFC injection sites (PL, VO, VLO and DLO). Moving

laterally in PFC from VO to DLO (injection site Ba to Da), projections from VO were seen dorsally to those from VLO, and projections from VLO were seen dorsally to those from DLO. A factorial ANOVA revealed a significant main effect of anterior PFC injection site location on the dorsal-ventral distance from the cortical surface of retrogradely labelled cells in sensory-motor cortex ($F(3,224)=16.129$ $p<0.001$ $r=0.259$). Post hoc comparisons (Tukey HSD) revealed significant differences between retrograde PFC injection sites Aa*Ba, Ba*Da ($p<0.001$), Aa*Ca ($p=0.015$) and Ca*Da ($p=0.047$).

Additionally, an ordered organisation can be seen in the anterior-posterior axis; projections from VO are present more anterior to VLO and projections from VLO anterior compared to DLO. A factorial ANOVA revealed a significant main effect of anterior PFC injection site location on the anterior-posterior location of retrogradely labelled cells in sensory-motor cortex ($F(3,224)=70.614$ $p<0.001$ $r=0.490$). Post hoc comparisons (Tukey HSD) revealed significant differences between retrograde PFC injection sites Aa*Da, Ca*Da ($p<0.001$) and Ba*Ca ($p=0.001$).

A similar ordering can be seen between VO and DLO in the medial-lateral axis, moving from medial to lateral in PFC (VO→VLO→DLO), projections in sensory-motor cortex become more medial. A factorial ANOVA revealed a significant main effect of anterior PFC injection site location on the medial-lateral distance from the medial cortical surface of retrogradely labelled cells in sensory-motor cortex ($F(3,224)=15.020$ $p<0.001$ $r=0.251$). Post hoc comparisons (Tukey HSD) revealed significant differences between retrograde PFC injection sites Aa*Da, Ba*Da ($p<0.001$) and Ca*Da ($p=0.003$). There is considerable overlapping of projections from VO and VLO (injection sites B and C).

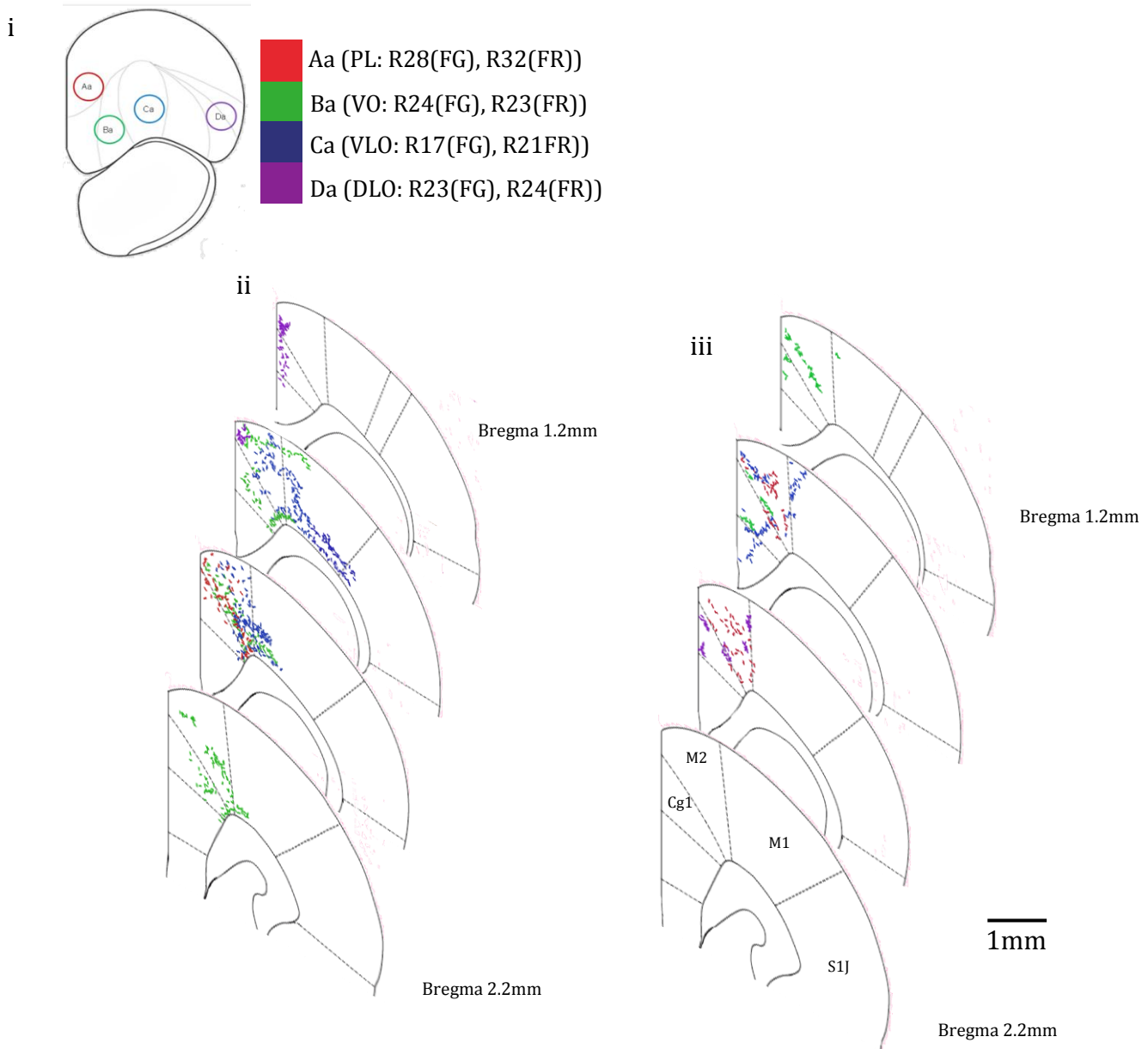


Figure 6.4 Diagram representing the amalgamated injection sites of Fluoro-Gold and Fluoro-Ruby in anterior PFC, and the projection sites to sensory-motor cortex for both retrograde (Fluoro-Gold) and anterograde (Fluoro-Ruby) tracer injections. (i) The locations of injection sites Aa (PL: R28, R32), Ba (R23, R24), Ca (R17, R21) and Da (R23, R24) in anterior PFC. (ii) The locations of retrogradely labeled cells in sensory-motor cortex, resultant from 100nl Fluoro-Gold injections into anterior PFC injection sites Aa-Da (R17, R23, R24, R28). (iii) The locations of anterogradely labeled axon terminals in sensory-motor cortex, resultant from 100nl Fluoro-Ruby injections into anterior PFC injection sites Aa-Da (R21, R23, R24, R32).

Organisation of Output Connections to Sensory-Motor Cortex from Anterior Prefrontal Cortex

Output projections from anterior PFC to temporal cortex were seen in Cg1, M2 and M1. The distribution of anterogradely labelling (from Fluoro-Ruby) in sensory-motor cortex resultant from anterior PFC tracer injections is less widespread than the corresponding retrograde labelling (from Fluoro-Gold). The distribution of anterogradely labelled axon terminals in sensory-motor cortex maintain a spatial order in terms of the corresponding Fluoro-Ruby PFC injection site. Moving from medial to lateral in PFC (from VO to DLO), projections from VO are seen more posterior to VLO. Similarly projections from VLO are seen posterior to those from DLO. A factorial ANOVA revealed a significant main effect of anterior PFC injection site location on the anterior-posterior location of anterogradely labelled axon terminals in sensory-motor cortex ($F(3,240)=178.569$ $p<0.001$ $r=0.653$). Post hoc comparisons (Tukey HSD) revealed significant differences between anterograde injection sites A*B, B*C, B*D ($p<0.001$) and C*D ($p=0.003$). No significant differences were found between anterograde injection sites Aa*Ba, Ba*Ca, Ba*Da ($p<0.001$) and Ca*Da ($p=0.003$).

The ordering of output projections seen here follows an opposing order to that seen of input connections. In contrast to labeled input projections, no clear ordering of outputs can be seen in terms of the dorsal-ventral (laminar) or medial-lateral axes, although some evidence of ordering can be seen. A factorial ANOVA revealed a significant main effect of anterior PFC injection site location on the dorsal-ventral distance from the cortical surface of anterogradely labelled axon terminals in sensory-motor cortex ($F(3,240)=79.033$ $p<0.001$ $r=0.498$). Post hoc comparisons (Tukey HSD) revealed significant differences between anterograde PFC injection sites Aa*Ba, Aa*Da, Ba*Ca and Ca*Da ($p<0.001$). A factorial ANOVA revealed a significant main effect of anterior PFC injection site location on the medial-lateral distance from the medial cortical surface of anterogradely labelled axon terminals in sensory-motor cortex ($F(3,240)=174.252$ $p<0.001$ $r=0.649$). Post hoc comparisons (Tukey HSD) revealed significant differences between anterograde injection sites Aa*Ba, Aa*Ca, Aa*Da, Ba*Ca and Ca*Da ($p<0.001$).

A two factor ANOVA revealed a significant interaction effect of input and output connections in the dorsal-ventral ($F_{(3,444)}=56.626$ $p<0.001$ $r=0.336$), anterior posterior ($F_{(3,444)}=142.386$ $p<0.001$ $r=0.493$) and medial-lateral ($F_{(3,444)}=66.212$ $p<0.001$ $r=0.360$) axes. This indicates differential organisation of input and output connections from PFC to sensory-motor cortex.

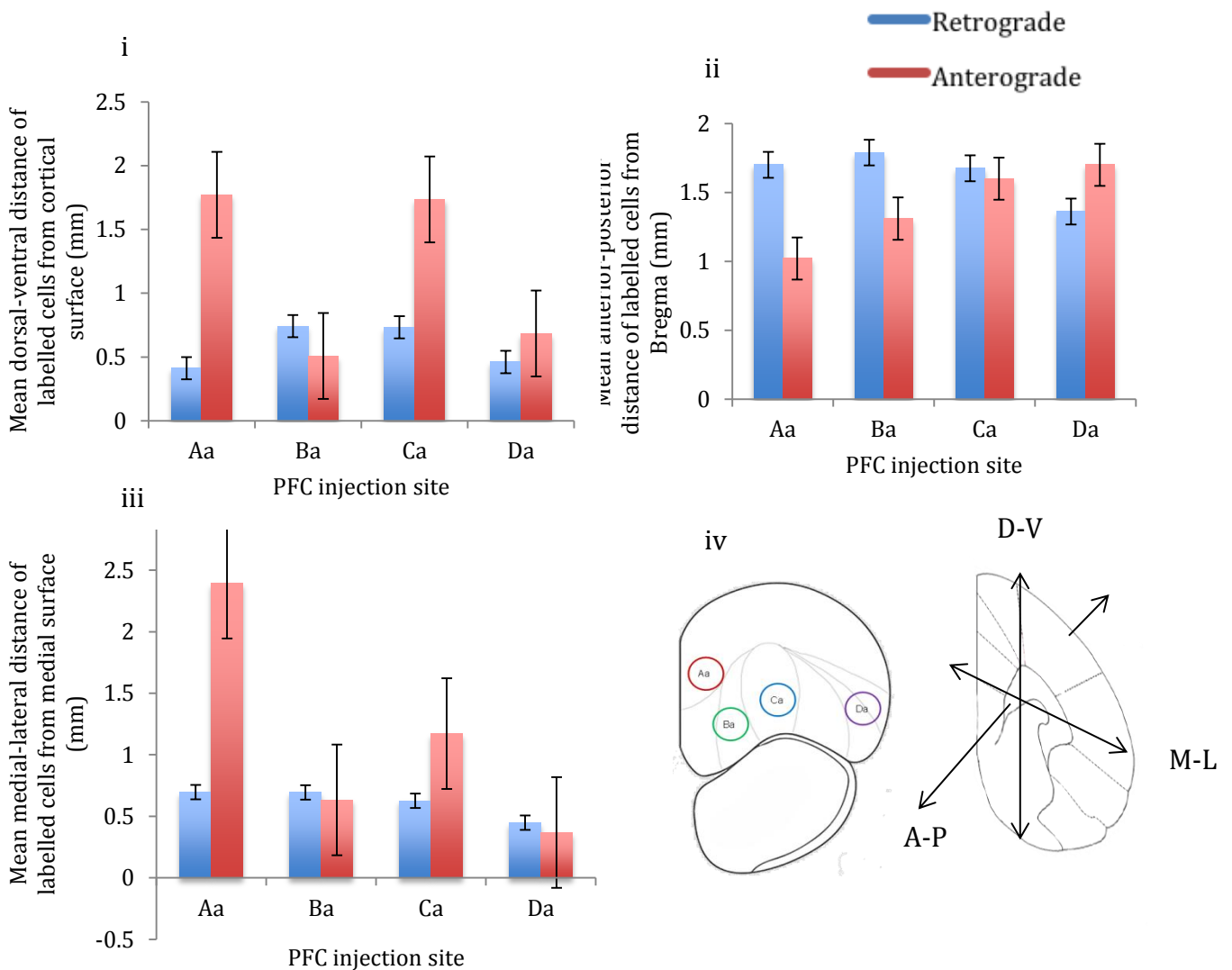


Figure 6.5. The mean effect of injection site in *anterior* PFC on the (i) dorsal-ventral, (ii) anterior-posterior and (iii) medial-lateral location of retrogradely labelled cells ($n=208$ arising from 4 rats: PL=20, VO=77, VLO=39, DLO=72) and anterogradely labelled axon terminals ($n=244$ arising from 4 rats: PL=87, VO=91, VLO=30, DLO=36) within sensory-motor cortex. Error bars = standard error. (iv) Coronal cross section of PFC showing the position of 4 injection sites; Prelimbic (Aa), Ventral orbital (Ba), Ventrolateral orbital (Ca) and Dorsolateral orbital (Da). Coronal cross section of sensory-motor cortex showing the three dimensions in which the locations of labels were recorded.

This analysis shows evidence of an ordered organisation of connections between anterior PFC and areas of sensory-motor cortex. As PFC injection sites move in the mediolateral direction (VO to DLO; Ba to Da), the pattern of input projections moves in an anterior-posterior direction across sensory-motor cortex, whilst simultaneously moving in a medial-lateral direction. Similarly, an organisational pattern of output projections can be observed, however, this occurs in a different direction to input projections. As anterograde injection sites move mediolaterally in PFC from VO to DLO, the projections in temporal cortex move from posterior to anterior. The medial-lateral organisation of output connections is not clear in comparison to input connections. It is evident from these results that the input and output connections from anterior PFC to sensory-motor cortex are organised differently.

Central Prefrontal Cortex

The positioning and spread of injection sites is described in detail in Chapter 3. Retrograde injection sites into the central aspect of PFC (R4, R5, R6, R7) were observed in the intended regions of PFC (according to Van de Werd & Uylings, 2008) and were mostly confined to cytoarchitectural boundaries of PFC regions (Fig.6.6iv). There is some overlap seen between the retrograde injection sites in PL (R7) and VO (R6). Anterograde injection sites into the central aspect of PFC (R9, R19, R20, R29) were observed in the intended subdivisions of PFC and were confined to the cytoarchitectural boundaries of PFC regions. No overlapping occurred between anterograde PFC injection sites.

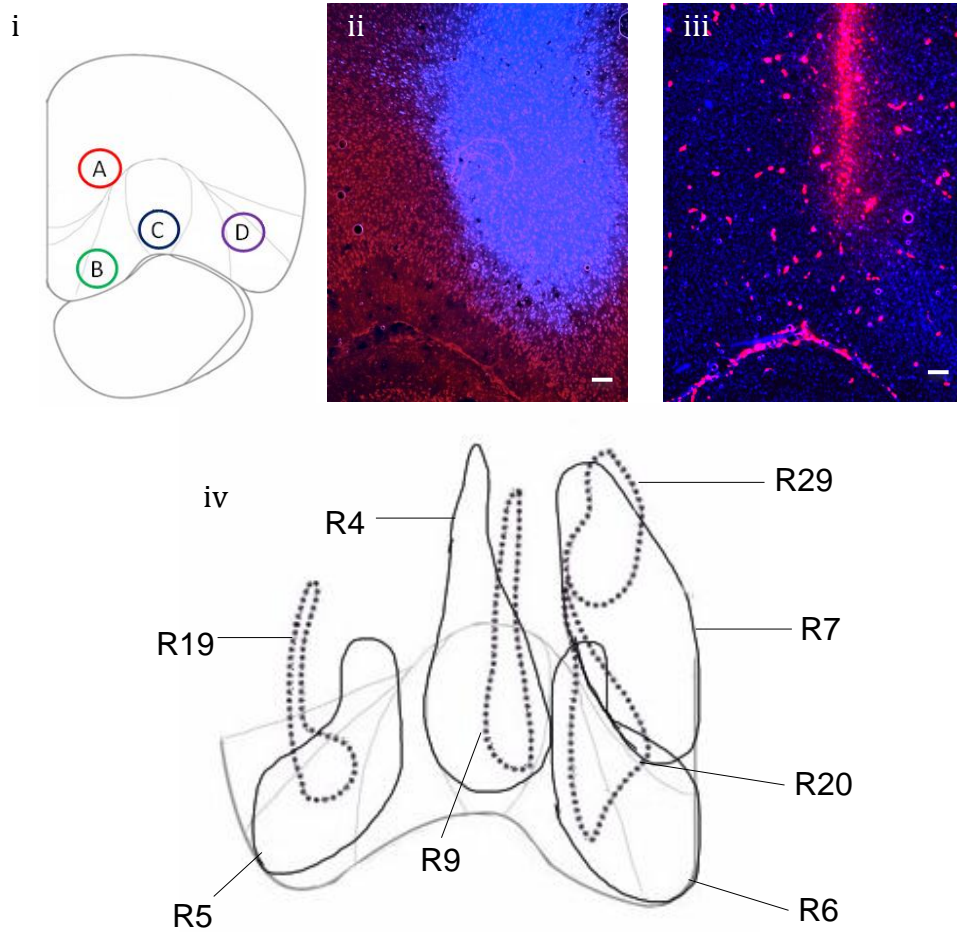


Figure 6.6 (i) Coronal section of central PFC (AP 4.2mm from Bregma) showing the cytoarchitectural boundaries of the prelimbic (PL), infralimbic (IL), medial orbital (MO), ventral orbital (VO), ventrolateral orbital (VLO) and dorsolateral orbital (DLO) cortices (according to Van de Werd & Uylings, 2008), depicting sites of injections; prelimbic:A, ventral orbital:B, ventrolateral orbital:C and dorsolateral orbital:D, with 1mm spread. (ii) Coronal section of PFC showing location and spread of (100nl) Fluoro-Gold (blue) at injection site in VO (R6). (iii) Coronal section of PFC showing location and spread of (100nl) Fluoro-Ruby (red) at injection site in VLO (R9). (iv) Representations of Fluoro-Gold (100nl) (R4, R5, R6, R7 (solid line)) and Fluoro-Ruby (100nl) (R9, R19, R20, R29 (broken line)) injection sites in PL (R7, R29), VO (R6, R20), VLO (R4, R9) and DLO (R5, R19), in the right hemisphere.

Anterograde labelling, resultant from Fluoro-Ruby injections into central PFC (PL, VO, VLO, DLO) was seen in regions of sensory and motor cortex similar to that which had previously been identified with BDA injections in the same region

(Chapter 5). Anterograde labelling was seen in areas of Cg1, M1 and M2 (fig.6.7iii, iv). The locations of both input and output connections observed in central PFC was similar to that seen in anterior PFC (Fig.6.8). Similar locations of retrograde and anterograde labelling were seen as a result of co-injections of Fluoro-Gold and Fluoro-Ruby (Appendix Q) and anterograde labelling from injections of Fluoro-Emerald (Appendix R).

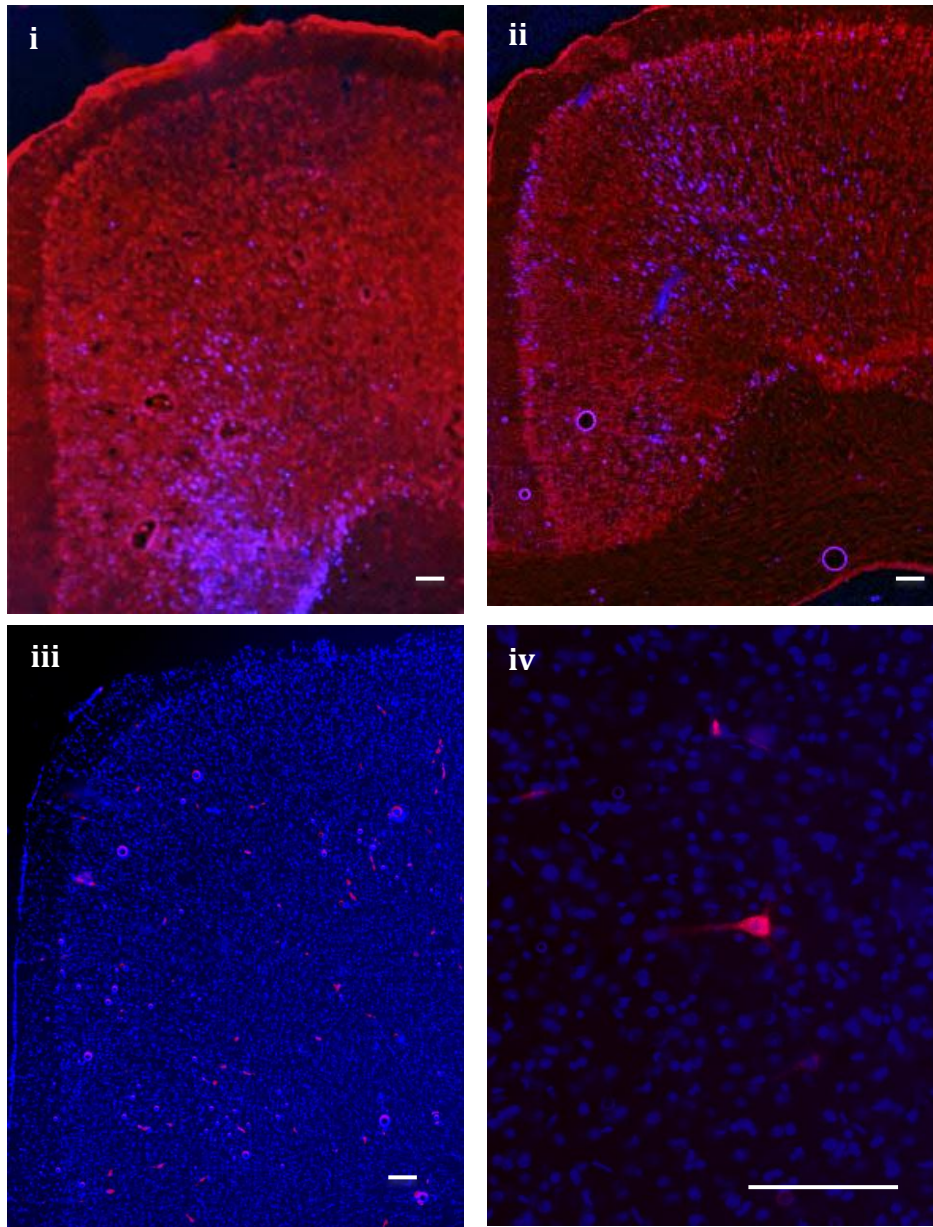


Figure 6.7.(i) Coronal section showing retrogradely labelled cells (blue) in cingulate cortex produced by 100nl injection of Fluoro-gold into VLO (R4). (ii) Coronal section showing retrogradely labelled cells (blue) in cingulate cortex produced by 100nl injection of Fluoro-gold into VO (R6). (iii) Coronal section showing anterograde labelling (red) produced by injection of Fluoro-Ruby into DLO (R19). Anterograde labelling in sensory-motor cortex produced by injection of Fluoro-Ruby into DLO (R19). Scale bars = 100µm.

Organisation of Input Connections to *Central Prefrontal Cortex* from *Sensory-Motor Cortex*

Projections to central PFC from sensory-motor cortex were seen in Cg1, M2, M1 and S1J (Fig.6.8ii). Labelled cells from each injection location were distributed across several cytoarchitecturally distinct regions. The distribution of retrogradely labelled cells within sensory-motor cortex maintained a spatial order according to the corresponding Fluoro-Gold injection sites. Moving laterally in PFC from VO to DLO: projections from VO were seen dorsally to those from VLO, and projections from DLO were seen dorsally to those from VLO. This indicates an ordered laminar organisation of connections from central PFC (VO-DLO) to sensory motor cortex, similar to that seen in anterior PFC and consistent with those described in Chapter 5. There is overlapping of projections from VO, VLO and DLO.

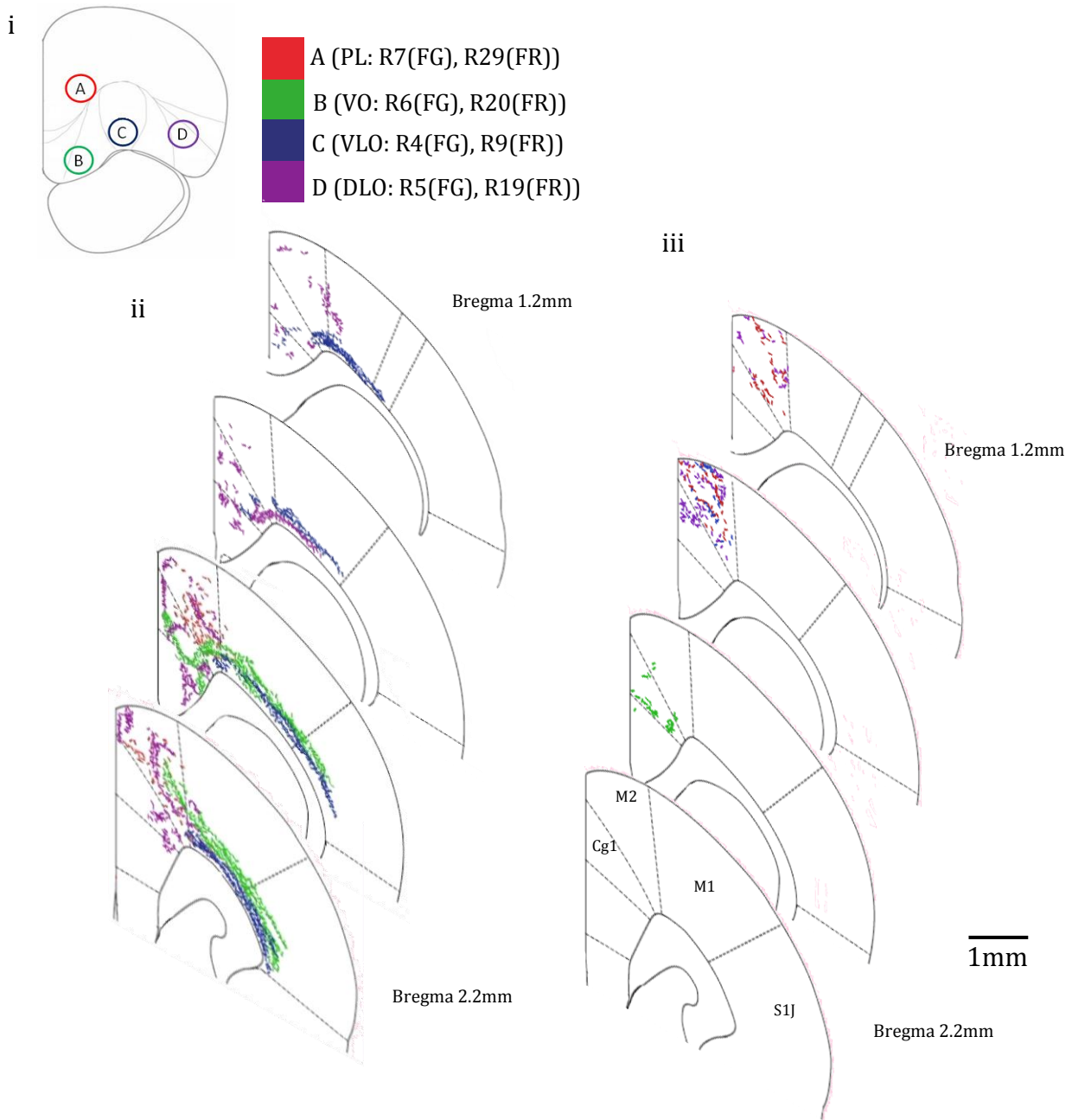


Figure 6.8. Diagram representing the amalgamated injection sites of Fluoro-Gold and Fluoro-Ruby, and the projection sites to sensory-motor cortex for both retrograde (Fluoro-Gold) and anterograde (Fluoro-Ruby) tracer injections. (i) The locations of injection sites A (PL: R7, R29), B (VO:R6, R20), C (VLO:R4, R9) and D (DLO: R5, R19) in central PFC. (ii) The locations of retrogradely labeled cells in sensory-motor cortex, resultant from 100nl Fluoro-Gold injections into central PFC injection sites A-D (R4, R5, R6, R7). (iii) The locations of anterogradely labeled axon terminals in sensory-motor cortex, resultant from 100nl Fluoro-Ruby injections into central PFC injection sites A-D (R9, R19, R20, R29).

Organisation of Output Connections to *Central Prefrontal Cortex* from Sensory-Motor Cortex

Output projections from central PFC to sensory-motor cortex were seen in Cg1 and M2 (Fig.6.8iii). The distribution of anterogradely labelled axon terminals in sensory-motor cortex maintained a spatial order corresponding to Fluoro-Ruby central PFC injection sites. As PFC injection sites move from medial to lateral (VO to DLO) projections in sensory-motor cortex move from anterior to posterior, whilst simultaneously moving from medial to lateral. This ordering is consistent with that observed with BDA injections in Chapter 5, as well as that seen with Fluoro-Emerald labelling (Appendix R) and co-injections of Fluoro-Gold and Fluoro-Ruby (Appendix Q). No clear laminar ordering (in the dorsal-ventral axis) can be seen in the output projections from central PFC to sensory-motor cortex.

Statistical evidence for this ordered arrangement is consistent with that described in Chapter 5 and can be seen in detail in Appendix P. A Factorial ANOVA revealed a significant main effect of central PFC injection location on the location of retrogradely labeled cells in sensory-motor cortex (in the dorsal-ventral axis ($p<0.001$), anterior-posterior axis ($p<0.001$) and medial-lateral axis ($p<0.001$)) and anterogradely labeled axon terminals in sensory-motor cortex (in the dorsal-ventral axis ($p<0.001$), anterior-posterior axis ($p<0.001$) and medial-lateral axis ($p<0.001$)) (Fig.6.9). A two factor ANOVA also revealed evidence of differential ordering of inputs and outputs in the anterior-posterior, dorsal-ventral and medial-lateral axes ($p<0.001$). These results show clear evidence of ordering for both input and output connections from central prefrontal to sensory-motor cortex, as well as evidence for different patterns of organisation between inputs and outputs, across 3 axes of orientation.

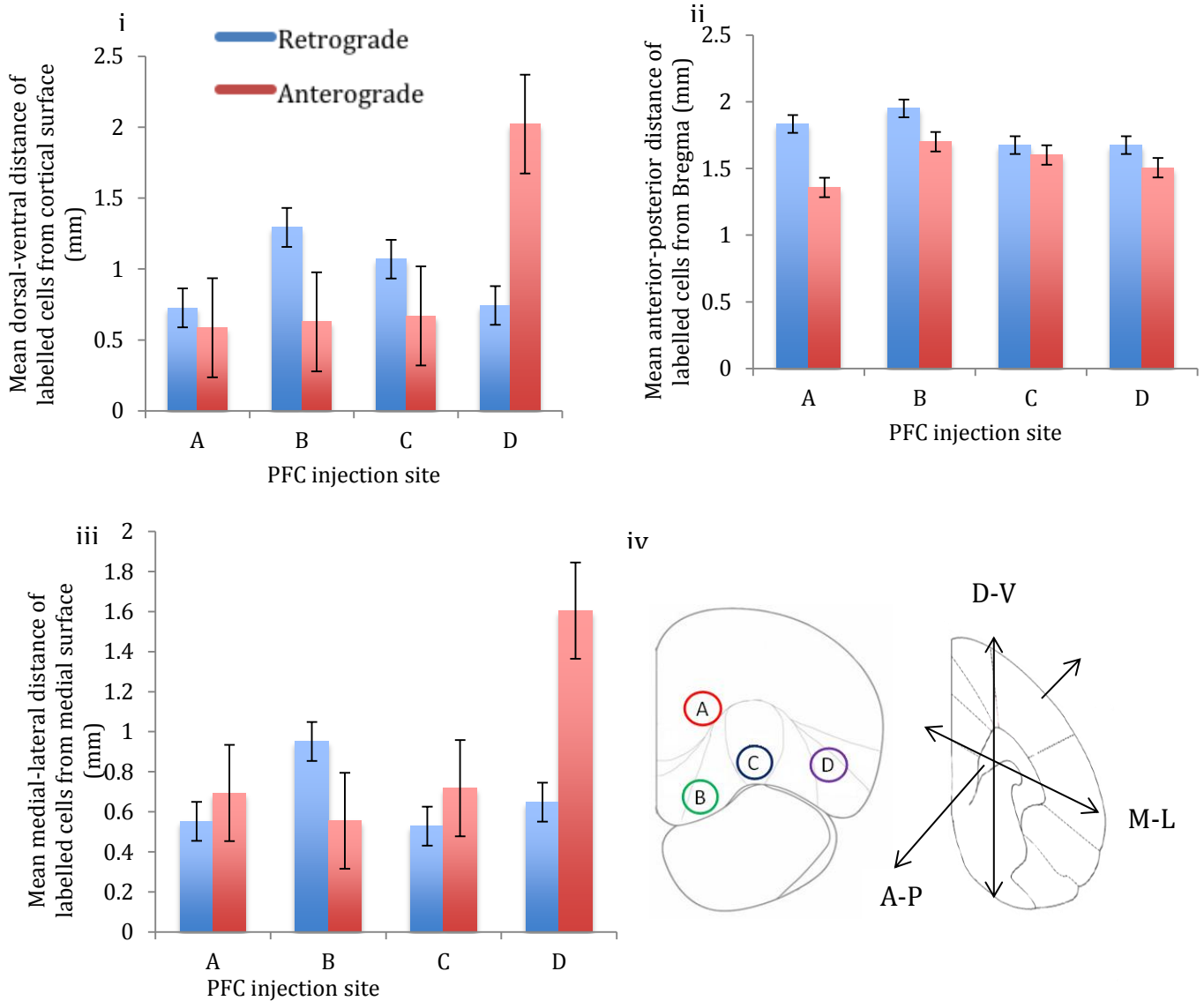


Figure 6.9. The mean effect of central PFC injection site on the (i) dorsal-ventral, (ii) anterior-posterior and (iii) medial-lateral location of retrogradely labelled cells ($n=494$ arising from 4 rats: PL=143, VO=156, VLO=83, DLO=112) and anterogradely labelled axon terminals ($n=224$ arising from 4 rats: PL=138, VO=29, VLO=19, DLO=38) within sensory-motor cortex. Error bars=standard error. (iv) Coronal cross section of PFC showing the position of 4 injection sites; prelimbic (A), ventral-orbital (B), ventrolateral orbital (C) and dorsolateral orbital (D). Coronal cross section of sensory-motor cortex showing the three dimensions in which the locations of labels were recorded.

This analysis shows evidence for an ordered organisation of connections between central PFC and sensory-motor cortex, consistent with that described in Chapter 5 and Appendix L.

Posterior Prefrontal Cortex

The positioning and spread of injection sites is described in detail in Chapter 3.

Retrograde injection sites into the posterior aspect of PFC (R27, R22, R11, R26) were observed in the intended regions of PFC (according to Van de Werd & Uylings, 2008) and were mostly confined to cytoarchitectural boundaries of PFC regions (Fig.6.10v). There is some overlap seen between the retrograde injection sites in PL (R27) and VO (R22) as well PL and VLO (R27 & R11). Anterograde injection sites into the anterior aspect of PFC (R28, R26, R25, R27) were observed in the intended subdivisions of PFC and were confined to the cytoarchitectural boundaries of PFC regions. No overlapping occurred between anterograde PFC injection sites.

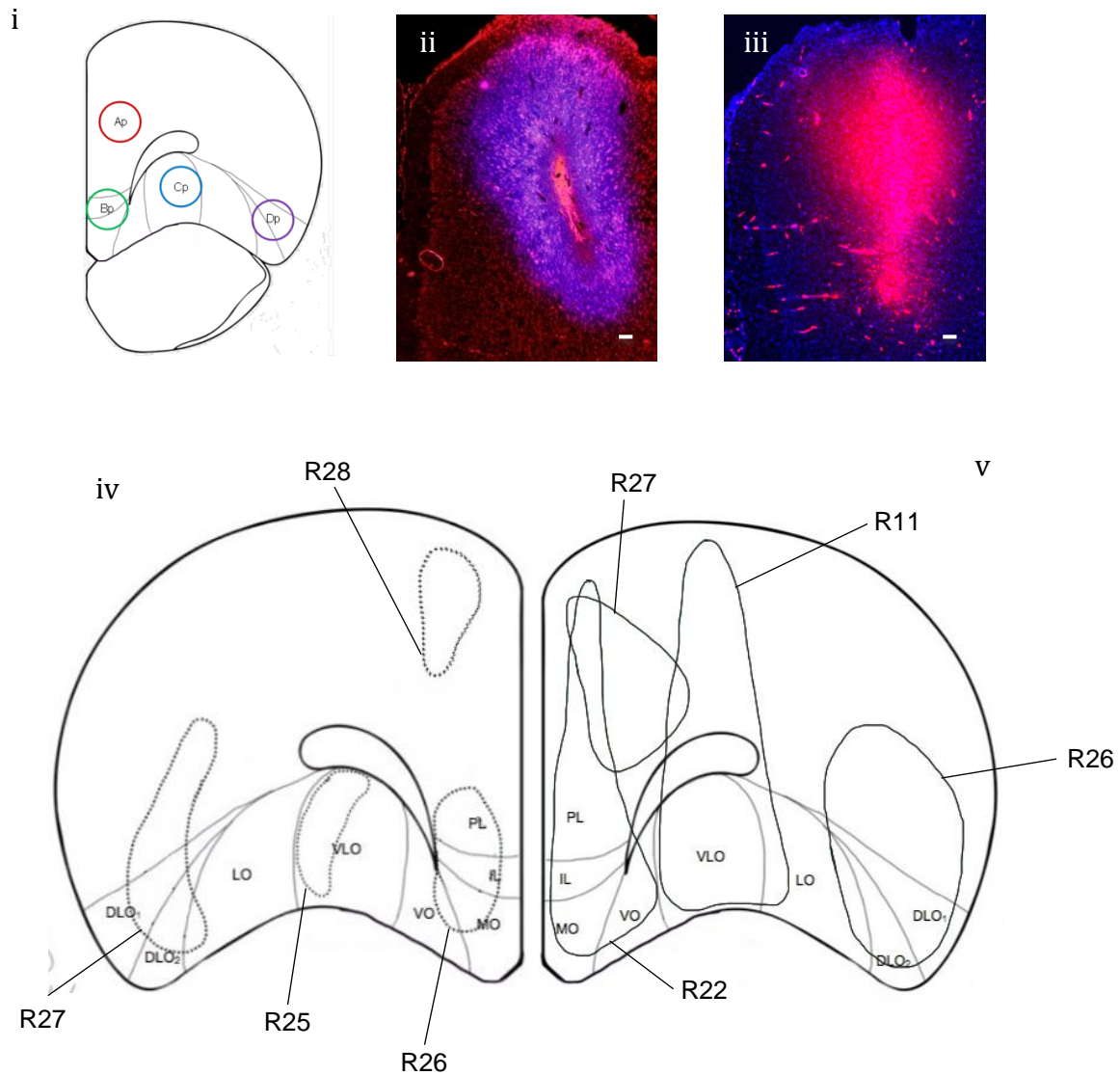


Figure 6.10 (i) Coronal section of PFC (AP 3.7mm from Bregma) showing the cytoarchitectural boundaries of the prelimbic (PL), infralimbic (IL), ventral orbital (VO) ventrolateral orbital (VLO) and dorsolateral orbital (DLO) cortices (according to Van de Werd & Uylings, 2008), depicting sites of injections; Prelimbic: Ap, Ventral orbital: Bp, Ventrolateral orbital: Cp and Dorsolateral orbital: Dp, with 1mm spread. (ii) Coronal section of PFC showing location and spread of (100nl) Fluoro-Gold (blue) at injection site in PL (R27). (iii) Coronal section of PFC showing location and spread of (100nl) Fluoro-Ruby (red) at injection site in PL (R28). (iv) Representations of Fluoro-Ruby (100nl) (R25, R26, R27, R28 (broken line) injection sites in PL (R28), VO (R26), VLO (R25) and DLO (R27), in the right hemisphere. (v) Representations of Fluoro-Gold (100nl) (R11, R22, R26, R27 (solid line)) injection sites in PL (R27), VO (R22), VLO (R11) and DLO (R26), in the left hemisphere. Fluoro-Ruby injection sites were consistently within the boundaries of corresponding Fluoro-Gold injection sites. There is minimal overlap between Fluoro-Gold injection sites (R27 & R22). Scale bars = 100 μ m.

Retrograde labelling, resultant from Fluoro-Gold injections into posterior PFC (PL, VO, VLO and DLO) was found in regions of PRh, Ent, AuV, Cg1, M2, M1, S1J and prefrontal regions (Fig.6.11i, ii. Fig.6.12ii). Anterograde labelling resultant from Fluoro-Ruby injections into posterior PFC (PL, VO, VLO and DLO) was found in regions of PRh, Ent, Cg1, M2 and M1, as well as prefrontal regions (Fig. 6.11iii, iv, 6.12iii). In order to investigate the pathway between posterior PFC and sensory-motor cortex, the labelling within areas of Cg1, M1, M2 and S1J was analysed.

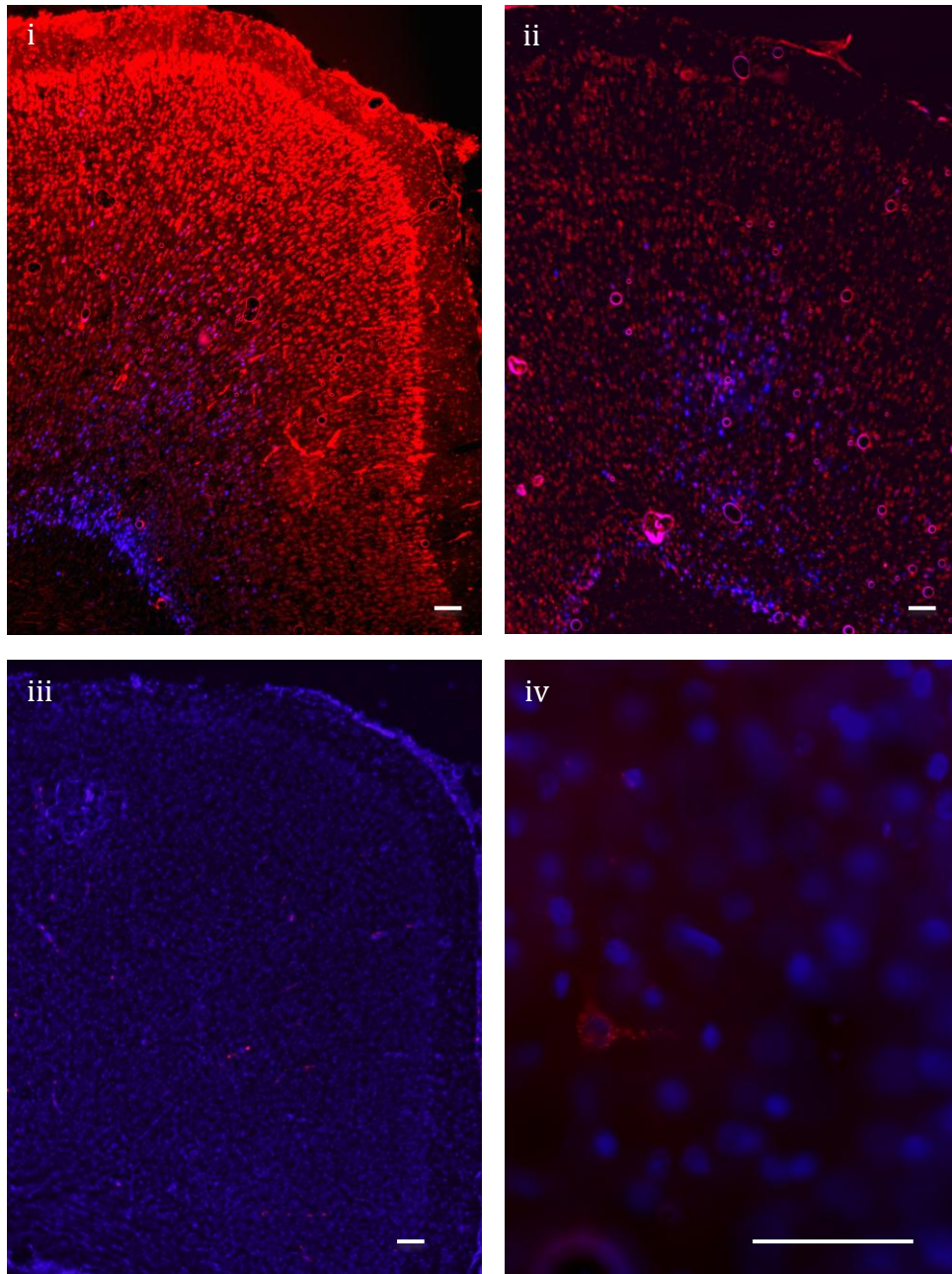


Figure 6.11. (i) Coronal section showing retrogradely labelled cells (blue) in sensory-motor cortex produced by injection of Fluoro-Gold (100nl) into *posterior* VO (R22). (ii) Retrogradely labelled cells (blue) in sensory-motor cortex, resultant from injection of Fluoro-Gold (100nl) into posterior VLO (R11). (iii) Coronal section showing anterogradely labelled axon terminals (red) in sensory-motor cortex produced by injection of Fluoro-Ruby (100nl) in posterior DLO (R27). (iv) Anterograde labelling (red) in sensory-motor cortex, resultant from injection of Fluoro-Ruby (100nl) in posterior VO(R26). Scale bars = 100µm.

Organisation of Input Connections to *Posterior Prefrontal Cortex* from *Sensory-Motor Cortex*

Projections to posterior PFC from sensory-motor cortex were seen in Cg1, M2 and M1 (6.12.ii). The distribution of retrogradely labelled cells within sensory-motor cortex maintained a spatial order according to the corresponding Fluoro-Gold injection sites in posterior PFC. Moving laterally in PFC from VO to DLO: projections from VO were seen dorsally to those from VLO, and projections from DLO were seen dorsally to those from VLO. : A factorial ANOVA revealed a significant main effect of posterior PFC injection site location on the dorsal-ventral distance from the cortical surface of retrogradely labelled cells in sensory-motor cortex ($F(3,585)=587.539$ $p<0.001$ $r=0.71$). Post hoc comparisons (Tukey HSD) revealed significant differences between all retrograde PFC injection sites; Ap*Bp, Ap*Cp, Ap*Dp, Bp*Cp, Bp*Dp ($p<0.001$) and Cp*Dp ($p=0.014$). This indicates an ordered laminar organisation of connections from central PFC (VO-DLO) to sensory motor cortex, consistent with that observed in anterior and central PFC.

An additional ordering of input connections to posterior PFC can be seen in the medial-lateral axis. As injection sites move from medial to lateral (VO – DLO), retrograde labelling in sensory-motor cortex becomes more medial; labelling from the injection into VO is seen laterally to VLO, and labelling from VLO is seen laterally to DLO. A factorial ANOVA revealed a significant main effect of posterior PFC injection site location on the medial-lateral distance from the medial cortical surface of retrogradely labelled cells in sensory-motor cortex ($F(3,585)=667.015$ $p<0.001$ $r=0.73$). Post hoc comparisons (Tukey HSD) revealed significant differences between PFC injection sites Ap*Bp, Ap*Cp, Bp*Cp, Bp*Dp and Cp*Dp ($p<0.001$). This is similar to the ordering seen in anterior and central PFC.

A factorial ANOVA also revealed a significant main effect of posterior PFC injection site location on the anterior-posterior location of retrogradely labelled cells in sensory-motor cortex ($F(3,585)=328.004$ $p<0.001$ $r=0.60$). Post hoc comparisons (Tukey HSD) revealed significant differences between retrograde PFC injection sites Ap*Bp, Bp*Cp and Bp*Dp ($p<0.001$).

i



- Ap (PL: R27(FG), R28(FR))
- Bp (VO: R22(FG), R26(FR))
- Cp (VLO: R11(FG), R25(FR))
- Dp (DLO: R26(FG), R27(FR))

ii

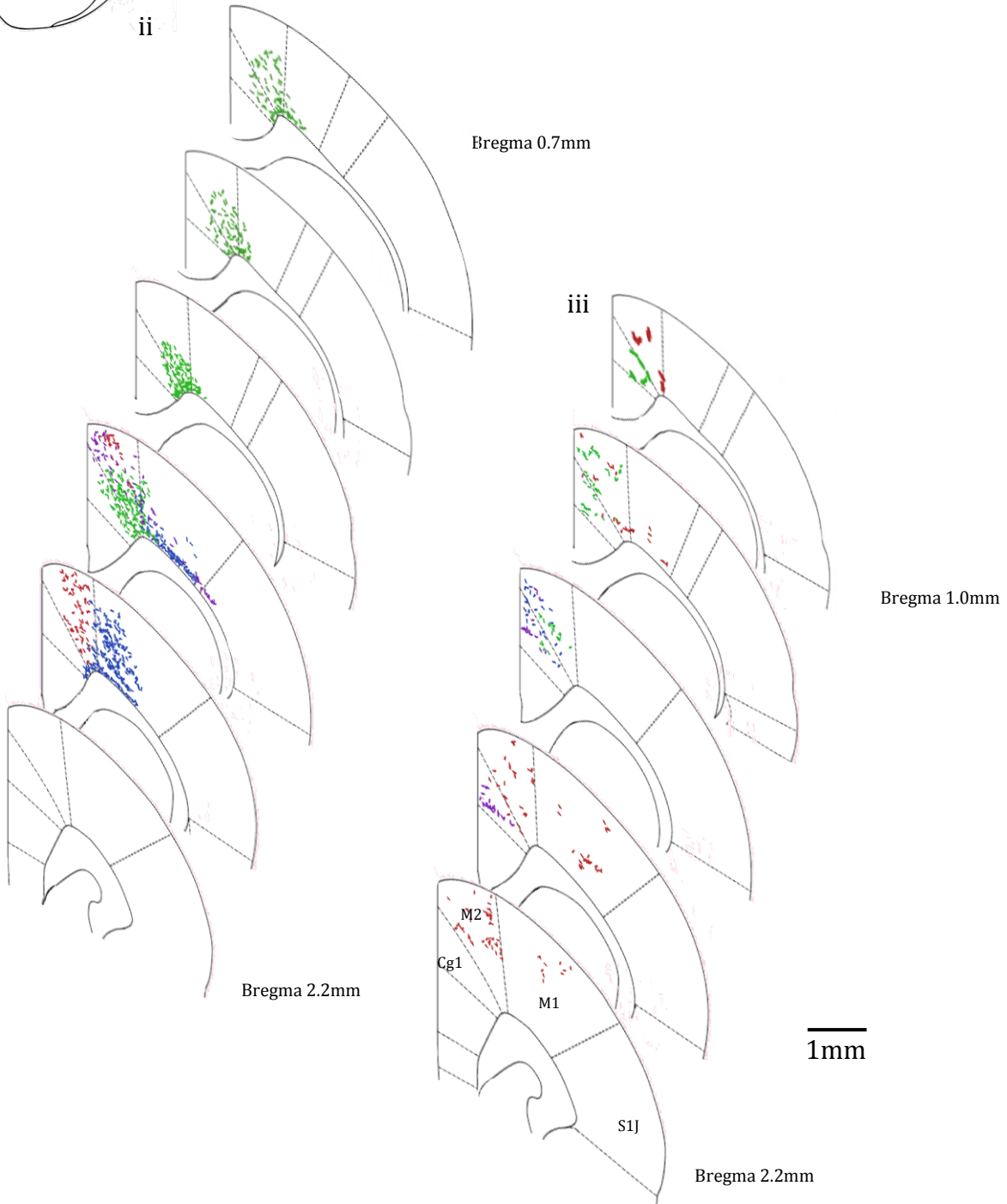


Figure 6.12. Diagram representing the amalgamated injection sites of Fluoro-Gold and Fluoro-Ruby, and the projection to sensory-motor cortex for both retrograde (Fluoro-Gold) and anterograde (Fluoro-Ruby) tracer injections. (i) The locations of injection sites Ap (PL:R27,R28), Bp (VO:R22,R26), Cp (VLO:R11,R25) and Dp (DLO:R26,R27) in posterior PFC. (ii) The locations of retrogradely labelled cells in sensory-motor cortex, resultant from 100nl Fluoro-Gold injections into posterior PFC injection sites Ap-Dp (R11, R22, R26, R27). (iii) The locations of anterogradely labelled axon terminals in sensory-motor cortex, resultant from 100nl Fluoro-Ruby injections into posterior PFC injection sites Ap-Dp (R25, R26, R27, R28).

Organisation of Output Connections to *Posterior Prefrontal Cortex* to Sensory-Motor Cortex

Output projections from posterior PFC to sensory-motor cortex were seen in Cg1, M2 and M1 (Fig.6.12iii). The distribution of anterogradely labelled axon terminals in sensory-motor cortex maintained a spatial order corresponding to Fluoro-Ruby central PFC injection sites). As PFC injection sites move from medial to lateral (VO to DLO) projections in sensory-motor cortex move from posterior to anterior, this is not consistent with the ordering of output connections seen in anterior and central PFC. A factorial ANOVA revealed a significant main effect of posterior PFC injection site location on the anterior-posterior location of anterogradely labelled axon terminals in sensory-motor cortex ($F(3,242)=41.946$ $p<0.001$ $r=0.39$). Post hoc comparisons (Tukey HSD) revealed significant differences between anterograde injection sites A*B, B*C, B*D ($p<0.001$), A*C ($p=0.002$) and A*D ($p=0.036$).

No clear ordering can be seen in the output projections from posterior PFC to sensory-motor cortex in the medial-lateral or dorsal-ventral axes, although there is evidence of ordering. A factorial ANOVA revealed a significant main effect of posterior PFC injection site location on the dorsal-ventral distance from the cortical surface of anterogradely labelled axon terminals in sensory-motor cortex ($F(3,242)=104.737$ $p<0.001$ $r=0.55$). Post hoc comparisons (Tukey HSD) revealed significant differences between anterograde injection sites A*C, B*C, C*D ($p<0.001$) and A*D ($p=0.004$). A factorial ANOVA revealed a significant main effect of posterior PFC injection site location on the medial-lateral distance from the medial cortical surface of anterogradely labelled axon terminals in sensory-motor cortex ($F(3,242)=49.475$ $p<0.001$ $r=0.41$). Post hoc comparisons (Tukey HSD) revealed significant differences

between anterograde injection sites A*C, A*D, B*C, B*D and C*D ($p<0.001$). Anterograde labelling was more widespread when resultant from posterior PFC injections than the projections seen with anterior and central PFC injections.

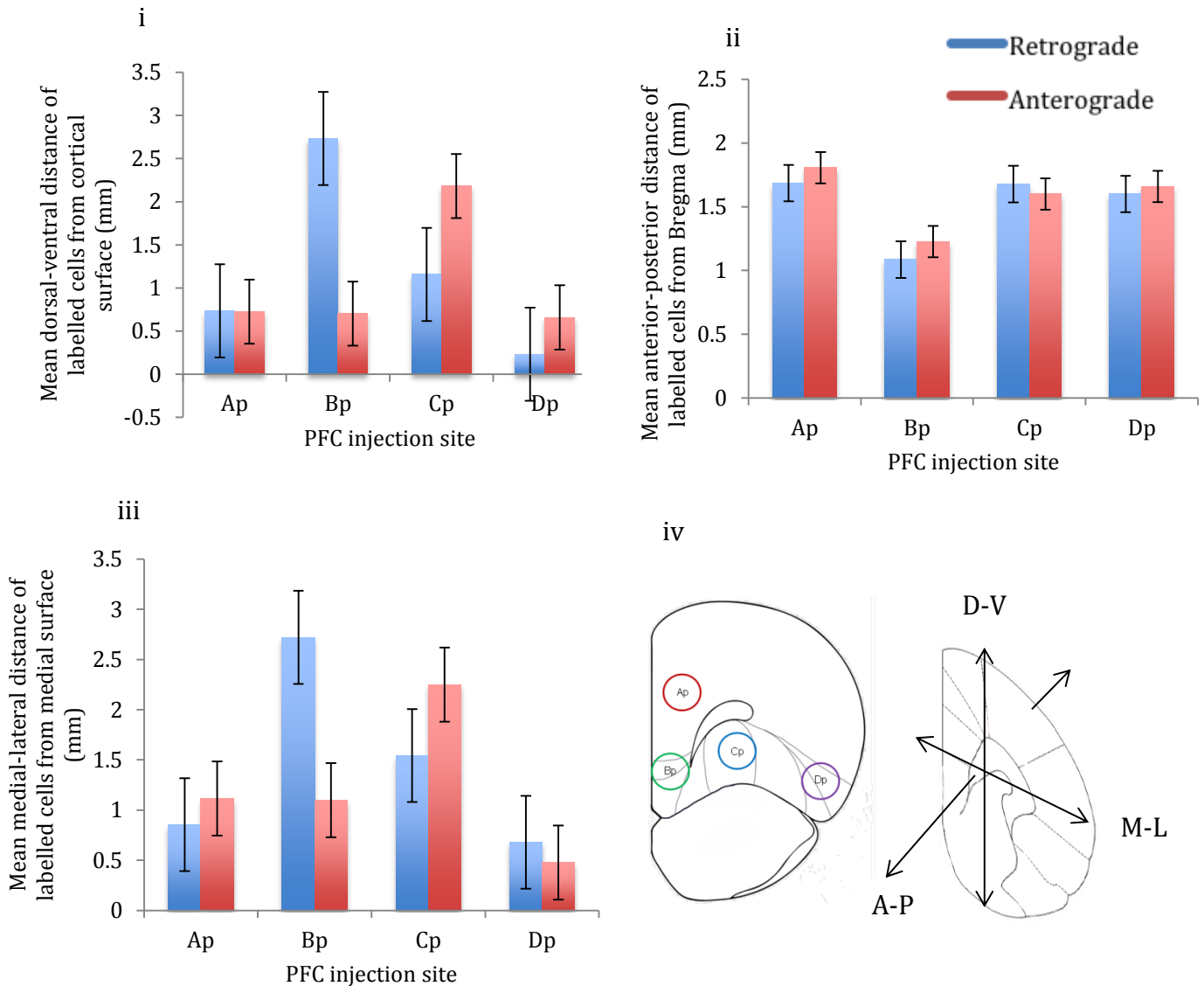


Figure 6.13. The mean effect of posterior PFC injection site location on the (i) dorsal-ventral (ii) anterior-posterior and (iii) medial-lateral location of retrogradely labeled cells ($n=586$ arising from 4 rats: PL=152, VO=268, VLO=136, DLO=30) and anterogradely labeled axon terminals ($n=243$ arising from 4 rats: PL=124, VO=44, VLO=35, DLO=40) within sensory-motor cortex. Error bars = standard error.(iv) Coronal cross section of PFC showing the position of 4 injection sites; prelimbic (Ap), ventral orbital (Bp), ventrolateral orbital (Cp) and dorsolateral orbital (Dp). Coronal cross section of sensory-motor cortex showing the three dimensions in which the locations of labels were recorded.

This analysis shows evidence for an ordered organisation of connections between posterior PFC and sensory motor cortex. As PFC injection sites move in the mediolateral direction (VO to DLO; Bp to Dp), the pattern of input projections moves in a dorsal-ventral direction across temporal cortex, whilst simultaneously moving in a lateral-medial direction. This is an opposing order compared to that seen in anterior PFC. Similarly, an organisational pattern of output projections can be observed. As anterograde injection sites move mediolaterally in PFC from VO to DLO, the projections in temporal cortex move from dorsal to ventral. It is evident from these results that the input and output connections from posterior PFC to sensory-motor cortex show more similarities in their ordering than those seen in anterior PFC.

Organisation of Connections from Anterior to Posterior Prefrontal Cortex

A factorial ANOVA was applied to determine if there was an effect of the anterior-posterior location of PFC injection sites on the location of retrograde and anterograde labels in sensory-motor cortex. The analysis revealed evidence for a gradient in terms of alignment of input and output connections from PFC to temporal cortex, with a significant change in the relationship between inputs and outputs in anterior PFC compared to central and posterior PFC.

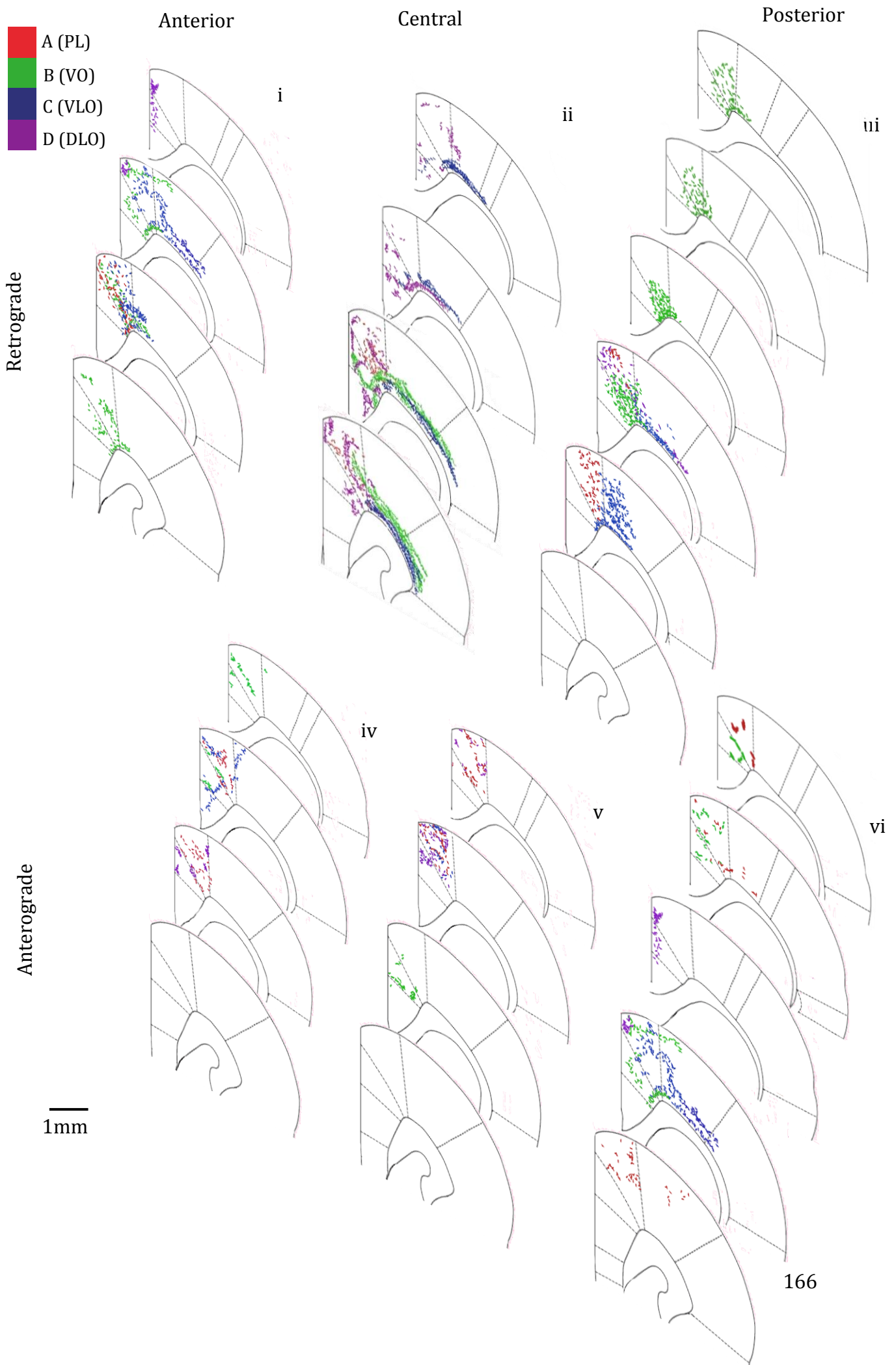


Figure 6.14 Diagram representing the projections to sensory-motor cortex for both retrograde (Fluoro-Gold) and anterograde (Fluoro-Ruby) tracer injections, from anterior, central and posterior PFC. (i) Retrograde labelling in sensory-motor cortex produced by Fluoro-Gold injections into anterior PFC. (ii) Retrograde labelling in sensory-motor cortex produced by Fluoro-Gold injections into central PFC. (iii) Retrograde labelling in sensory-motor cortex produced by Fluoro-Gold injections into posterior PFC. (iv) Anterograde labelling in sensory-motor cortex produced by Fluoro-Gold injections into anterior PFC. (v) Anterograde labelling in sensory-motor cortex produced by Fluoro-Gold injections into central PFC. (vi) Anterograde labelling in sensory-motor cortex produced by Fluoro-Gold injections into posterior PFC.

Statistical evidence for this anterior-posterior organisation came from the following analysis:

In the dorsal-ventral axis: A factorial ANOVA revealed a significant effect of the anterior-posterior location of PFC injection site on the dorsal-ventral location of retrogradely labelled cells ($F_{(2,1142)}=217.989$ $p<0.001$ $r=0.400$) and anterograde labelling ($F_{(2,708)}=8.767$ $p<0.001$ $r=0.111$) in sensory-motor cortex. Post hoc comparisons (Tukey HSD) revealed significant differences between retrograde anterior and central PFC injection sites, anterior and posterior, as well as central and posterior PFC injection sites ($p<0.001$). Post hoc comparisons (Tukey HSD) revealed significant differences between anterograde anterior and central PFC injection sites ($p<0.001$) and anterior and posterior ($p=0.009$).

In the anterior-posterior axis: A factorial ANOVA revealed a significant main effect of the anterior-posterior location of PFC injection site on the anterior-posterior location of retrogradely labelled cells ($F_{(2,1142)}=165.143$ $p<0.001$ $r=0.355$) and anterograde labelling ($F_{(2,708)}=32.715$ $p<0.001$ $r=0.210$) in sensory-motor cortex. Post hoc comparisons (Tukey HSD) revealed significant differences between retrograde anterior and central PFC injection sites, anterior and posterior PFC injection sites, as well as central and posterior PFC injection sites ($p<0.001$). Post hoc comparisons (Tukey HSD) revealed significant differences between anterograde anterior and central PFC injection sites ($p=0.005$), anterior and posterior, as well as central and posterior PFC injection sites ($p<0.001$).

In the medial-lateral axis: A factorial ANOVA revealed a significant main effect of the anterior-posterior location of PFC injection site on the medial-lateral location of retrogradely labelled cells ($F_{(2,1142)}=222.237$ $p<0.001$ $r=0.404$) and anterograde

labelling ($F_{(2,708)}=1242.129$ $p<0.001$ $r=0.798$) in sensory-motor cortex. Post hoc comparisons (Tukey HSD) revealed significant differences between retrograde anterior and central PFC injection sites, anterior and posterior injection sites and central and posterior PFC injection sites ($p<0.001$). Post hoc comparisons (Tukey HSD) revealed significant differences between anterograde anterior and central as well as central and posterior PFC injection sites ($p<0.001$).

These results show that an anterior-posterior change in the location of PFC injection sites substantially changes the location of labelled targets in sensory-motor cortex, indicating evidence of ordered organisation occurring from anterior to posterior PFC (Fig. 6.14, Fig. 6.15).

Figures 6.14 and 6.15 show a substantial change in the organisational pattern of both input and output connections as the PFC injection site moves from anterior to posterior. Most notably in the anterior-posterior axis, the organisation of input and output connections become considerably more aligned with one another in central and posterior PFC compared to anterior PFC (Fig. 6.15iii).

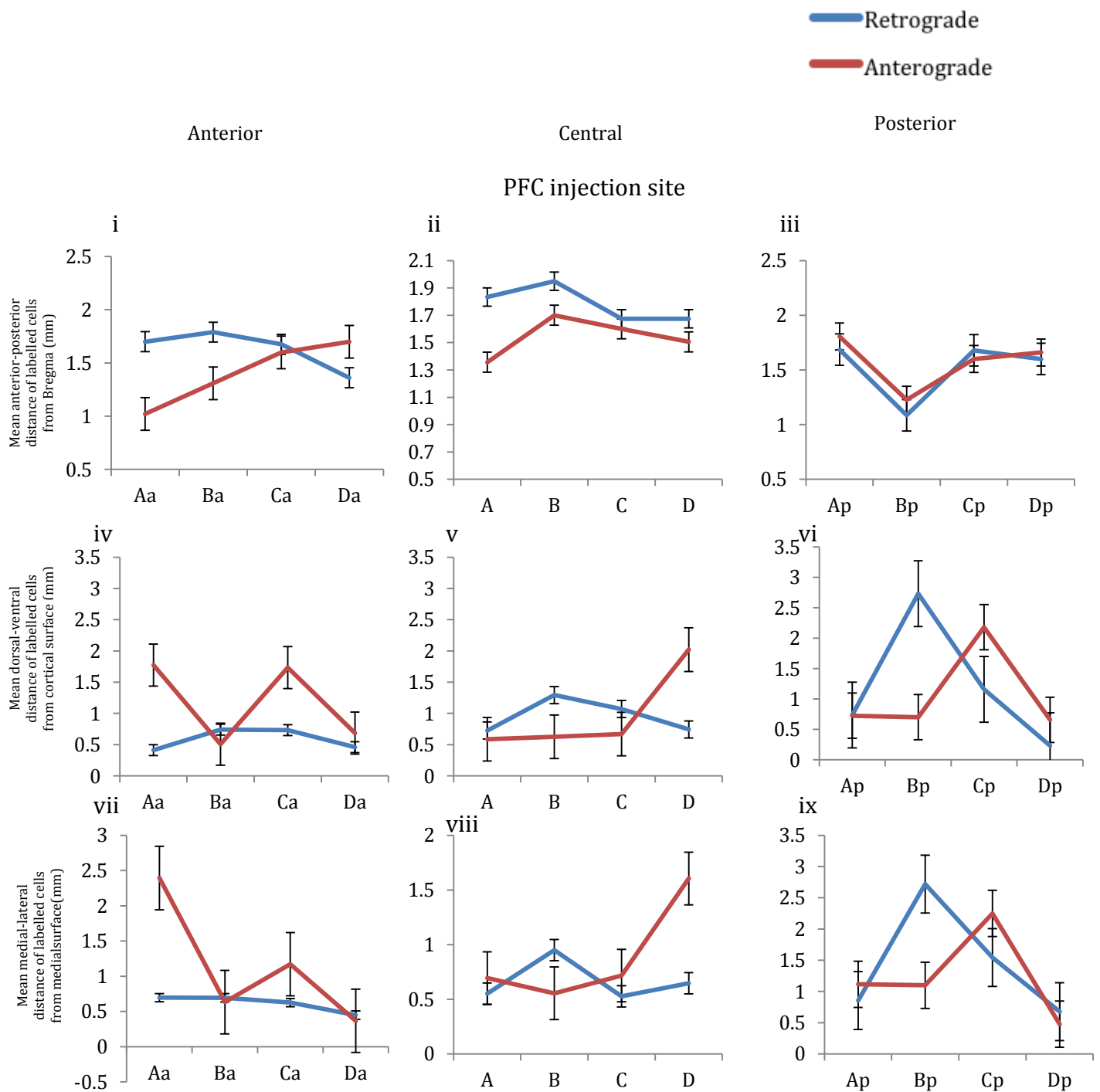


Figure 6.15. The mean effect of PFC injection site on the location of retrograde and anterograde labels in sensory-motor cortex. (i) The effect of anterior PFC injection sites (Aa (PL), Ba (VO), Ca (VLO) , Da (DLO)) on the mean anterior-posterior distance of retrograde and anterograde labels from Bregma. (ii) The effect of central PFC injection sites (A (PL), B (VO), C (VLO), D (DLO)) on the mean anterior-posterior distance of retrograde and anterograde labels from Bregma. (iii) The effect of posterior PFC injection sites (Ap (PL), Bp (VO), Cp (VLO), Dp (DLO)) on the mean anterior-posterior distance of retrograde and anterograde labels from Bregma. (iv) The effect of anterior PFC injection sites (Aa (PL), Ba (VO), Ca (VLO) , Da

(DLO))) on the mean dorsal-ventral distance of retrograde and anterograde labels from the cortical surface. (v) The effect of central PFC injection sites (A (PL), B (VO), C (VLO), D (DLO)) on the mean dorsal-ventral distance of retrograde and anterograde labels from the cortical surface. (vi) The effect of posterior PFC injection sites (Ap (PL), Bp (VO), Cp (VLO), Dp (DLO)) on the mean dorsal-ventral distance of retrograde and anterograde labels from the cortical surface. (vii) The effect of anterior PFC injection sites (Aa (PL), Ba (VO), Ca (VLO), Da (DLO)) on the mean medial-lateral distance of retrograde and anterograde labels from the medial surface. (viii) The effect of central PFC injection sites (A (PL), B (VO), C (VLO), D (DLO)) on the mean medial-lateral distance of retrograde and anterograde labels from the medial surface. (ix) The effect of posterior PFC injection sites (Ap (PL), Bp (VO), Cp (VLO), Dp (DLO)) on the mean medial-lateral distance of retrograde and anterograde labels from the medial surface.

Alignment of Input and Output Connections to Sensory-Motor Cortex from Anterior – Posterior Prefrontal Cortex

To clearly visualise the relationship between input and output connections to sensory-motor cortex across anterior – posterior PFC, the mean Euclidean distance (E) between retrograde and anterograde labels from each injection site was calculated. Paired samples t-tests revealed a greater difference in the distance between anterograde and retrograde labels in sensory-motor cortex following anterior PFC injections ($t(3)=-1.216$ $p=0.311$), compared to posterior PFC ($t(3)=0.334$ $p=0.754$). Figure 6.16 shows that as PFC injection sites become more posterior, the distance between retrograde and anterograde labels becomes smaller, meaning that input and output connections become more aligned with one another. The greatest change in the distance between inputs and outputs can be seen between anterior and central PFC, the distance does not decrease greatly from central to posterior PFC. This indicates a greater similarity in the organisation of central and posterior PFC connections to sensory-motor cortex in comparison to those in anterior PFC.

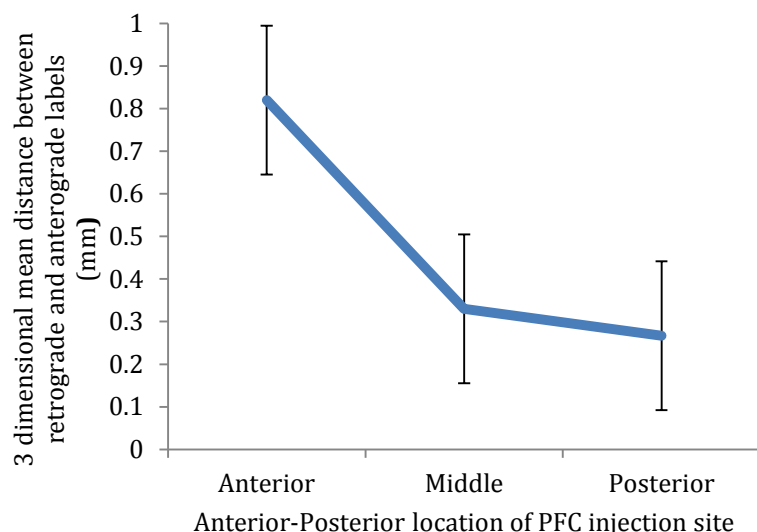


Figure 6.16. The effect of the anterior-posterior location of PFC injection site on the mean 3 dimensional distance (E) between anterograde and retrograde labels in sensory-motor cortex. Error bars = standard error.

Discussion

This study investigated connections to sensory-motor cortex from the most anterior region of PFC (4.7mm from Bregma) to the most posterior region of PFC (3.7mm from Bregma). The findings shown here support the earlier observations of an ordered arrangement of projections from PFC to regions of sensory-motor cortex (Chapter 5 and Appendix L) and provides additional insights into the alignment of PFC connections.

I revealed a clear ordered arrangement of connections from central PFC (Bregma 4.2mm) to sensory-motor cortex, resultant from both anterograde and retrograde labelling. This ordering was consistent with that seen as a result of Fluoro-Gold and BDA injections in the previous study (Chapter 5). Evidence was also revealed of a similar ordered organisation of both input and output connections occurring in the pathways between anterior PFC (Bregma 4.7mm) and sensory-motor cortex and posterior PFC (Bregma 3.7mm) to sensory-motor cortex. The ordering seen in anterior PFC showed differences in organisation compared with central and posterior PFC. This provides evidence to suggest differential organizational patterns within PFC, similar to that seen in the connections between PFC and temporal cortex

described in Chapter 3. Consistent evidence has been shown for different ordering of input and output connections from PFC to sensory-motor cortex. In addition, evidence has been shown for changes in the degree of alignment (difference between inputs and outputs) in anterior compared to posterior PFC, whereby anterior PFC is highly non-aligned and posterior PFC is considerably aligned. This is similar to the organisation seen in the PFC-temporal cortex pathway and demonstrates an organisational gradient of connections, consistent with reported functional organizational gradients observed in terms of abstraction (Christoff, 2009).

Anterior Prefrontal Cortex

The retrograde labelling found in areas of sensory and motor cortex resultant from anterior PFC tracer injections differed to that which was identified from central PFC injections, in that labelling was more ventral than that produced from central PFC injections. The pattern of ordered organisation of input connections from temporal cortex to PFC was very similar in anterior and central PFC, this is most clear in the anterior-posterior axis, where labelling becomes more posterior in sensory-motor cortex from VO to DLO. Input connections to anterior PFC showed evidence of a similar laminar organisation, specifically between VO and VLO, although this is not as clear as with central PFC connections.

The labelling of output connections found in sensory and motor regions resultant from anterior PFC tracer injections (particularly PL) was found posterior and lateral compared to those produced from central PFC injections. Labelling of input connections to anterior PFC was found to be more posterior compared to labeled input connections to central PFC. The difference between output and input connections was observed at it's greatest in anterior PFC connections, indicating the highest degree of non-alignment here. The pattern of ordered organisation of input connections from sensory-motor cortex to PFC was very similar in anterior and central PFC.

The results show clear evidence of ordering of both input and output connections in between anterior PFC and sensory-motor cortex. This ordering can be seen across multiple orientations. There is strong evidence of non-alignment of inputs and

outputs, in that anterograde and retrograde labelling from the same PFC injection sites are not found in the same locations. Despite the clear differential organisation, there remains to be evidence of broad scale reciprocity of connections, similar to that identified in earlier experiments (Chapter 5).

Central Prefrontal Cortex

Injection of the retrograde tracer Fluoro-Gold and the anterograde tracer Fluoro-Ruby to central PFC regions of PL, VO, VLO and DLO resulted in similar retrograde and anterograde labelling to that described in Chapter 5. Retrograde labelling was seen more widespread in sensory-motor cortex, spreading into areas of S1J than anterograde counterparts. Large amounts of retrograde and anterograde labelling from the same PFC injection site was found in different sensory and motor regions. The findings from this study show the same ordered organisation of input connections described for anterior PFC, however the analysis shows a change in the ordering of output connections; labelling of outputs becomes more posterior from VO to DLO, whereas in anterior PFC labelling becomes more anterior from VO to DLO. This change in ordering of output connections results in an increased alignment between inputs and outputs.

Posterior Prefrontal Cortex

The ordering of output connections from posterior PFC differed to the ordering seen in central PFC, this is clearest in the anterior-posterior axis where output connections follow an opposing order to those from central PFC; moving mediolaterally in PFC (from VO to DLO), output connections from posterior PFC become more anterior, whereas the output connections from central PFC become more posterior. This ordering of outputs is similar to that seen in anterior PFC. The output projections from posterior PFC to temporal cortex follow the same ordered arrangement as the input projections. As well as following the same order, the input and output connections from posterior PFC to temporal cortex are aligned with one another (i.e. are found in the same regions).

The retrograde labelling produced from posterior PFC injections was seen in more posterior and ventral regions of sensory-motor cortex to that observed in central and anterior PFC. The ordering of input connections to posterior PFC differed to the order observed from anterior and central PFC, specifically in the anterior-posterior axis, where the ordering was opposite to that seen in anterior and central PFC. This is clearest in the anterior-posterior axis where input connections follow an opposing order to those from anterior and central PFC; moving mediolaterally in PFC (from VO to DLO), input connections from posterior PFC become more anterior, whereas the input connections from anterior and central PFC become more posterior. The input projections from posterior PFC to sensory-motor cortex follow the same ordered arrangement as the output projections. The laminar organisation of input connections identified in anterior and central PFC (as well as Chapter 5) was not seen in the connections from posterior PFC.

The retrograde labelling resultant from injections into posterior PFC was consistently found to be more widespread than that produced by anterior and central PFC injection sites, indicating less specificity of the connections from this region of PFC.

Alignment of Input and Output Connections Across Prefrontal Cortex, from Anterior to Posterior

The findings presented here clearly show that as PFC connections become more anterior, the inputs and outputs become less aligned with one another. The distance between labelled input and output connections from the same PFC injection site becomes greater moving from posterior to anterior PFC, across three axes of orientation simultaneously. It was observed that connections become more widespread in sensory-motor cortex as injection sites in PFC become more posterior. This is the case for both anterograde and retrograde connections. Such a change in the convergence/divergence pattern of connections indicates a change in the specificity of connections to sensory-motor cortex from anterior compared to posterior PFC. The differential organisation of anterior PFC compared to more posterior regions, and other cortical regions, is consistent with the conclusions of Ranmani & Owen (2004)

that anterior PFC holds a specific purpose in the complex integration of multiple cognitive operations, different to that of other prefrontal regions. This is also consistent with the findings in the organisation of connections between PFC and temporal cortex (described in Chapter 3) and previous findings of ordered, reciprocal connections between adjacent medial PFC regions (Conde et al, 1995). McFarland & Haber (2002) identified non-reciprocal connections in frontal cortex pathways, similar to those described here. Haber (2003) suggested that cortical regions with similar functions are reciprocally connected, whereas regions with different functions are not reciprocally connected. This may mean that posterior regions of PFC, where there is greater reciprocity, are more similar to regions of sensory-motor cortex than anterior regions of PFC are.

The findings described here consistently show a circuit which is not consistent with traditional models of hierarchical organisation, in which PFC is positioned at the top of a processing hierarchy (Fuster, 2001; Botvinick, 2008) E.g. S1 → S2 → association areas → PFC → M2 → M1. The connections described from PFC → M2, and M2→PFC are consistent with what would be expected based on a hierarchical model, and are observed in anterior, central and posterior PFC. However, the direct connection found from S1→ PFC connects a primary cortical regions directly to a high order region (PFC). This connection is observed most prominently in central PFC. There are considerably fewer labels observed in S1 in posterior and anterior regions of PFC. This finding provides an insight into the complex functional organisation of the PFC – sensory-motor cortex pathway, indicating different functional organisation across PFC.

Together these findings show that the relationship between input and output connections in the pathway between PFC and sensory-motor cortex differs from anterior to posterior PFC, showing evidence of an organizational gradient from anterior to posterior (similar to that observed in PFC – temporal cortex connections in Chapter 3).

These findings provide evidence to support claims of differential functional organisation from anterior to posterior PFC, in terms of an organisational gradient (Taren et al, 2011) and observations of differences in the level of abstraction between

anterior and posterior PFC (Christoff, 2009). Christoff (2009) proposed increased abstract processing in anterior PFC in humans, the findings here imply that increased abstract and complex processing is associated with a different ordered arrangement of connections to that required by less abstract PFC regions. Based on these observations, and the similar findings described in PFC-temporal cortex connections (Chapter 3) it is reasonable to suggest that the increased abstract processing associated with anterior regions of PFC requires anatomical connections to be non-aligned in terms of inputs and outputs.

Chapter 7.

The Fine Scale Organisation of Prefrontal Cortex – Sensory-Motor Cortex Connections

There is evidence for ordered connections between prefrontal cortex and sensory-motor cortex. Chapters 5 and 6 identified clear ordered arrangements of both input and output connections and have established there is differential ordering between inputs and outputs, most prominently in anterior regions of PFC. The findings from Chapter 5 and 6 have given us an important basis in understanding the topological organisation of connections from PFC to sensory-motor cortex. In order to fully understand PFC organisation, it is necessary to establish the underlying intra-areal (topographic) connections of the topological ordering described in earlier Chapters.

The parallel arrangement of input and output projections, and therefore reciprocal connections, is a widely accepted property of cortical organisation. Such parallel arrangement of connections has been described in perirhinal, postrhinal, entorhinal, piriform, frontal, insular, temporal, cingulate, parietal and occipital cortices (Canto et al, 2008; Agster and Burwell, 2009). The structural organisation of connections described in the broad scale analysis (Chapter 5 and 6) contradicts this common property.

Previous studies have described ordered projections from PFC to areas of sensory-motor cortex (Sesack, 1989; Vertes, 2004). Connectivity studies of S1 and M1 often report reciprocal connectivity (Dinopoulos, 1994; Lee et al, 2011). Specifically, connections between M1 and S1 (Porter & White, 1983; Aronoff et al, 2010), S1 and S2 (Henry & Catania, 2006; Aronoff et al, 2010) and M1 and S2 (Porter & White, 1983) have been found to show evidence of reciprocity. However, Porter & White (1983) also reported non-reciprocal connections between M1 and Striatum. This, along with the findings from Chapter 5 and 6, indicate that motor cortex connections show considerable reciprocity, but are not always reciprocal. The

finer scale analysis allowed by small and more closely positioned tracer injections in this study allowed us to further investigate this phenomenon, allowing us to pinpoint to greater accuracy the reciprocally connected regions of PFC in the PFC – sensory-motor cortex pathway.

In order to gain a clear understanding of prefrontal organisation, it is necessary to establish an understanding of the organisation of connections on a fine scale. The findings from my earlier studies (Chapters 5 and 6) provided an important basis from which to expand the experiments and investigate the organisation of prefrontal – sensory-motor cortex connections at a greater resolution.

This study sought to address whether these relationships could be seen at a finer scale and in the same pathway. By using smaller injection volumes of tracers it was possible to establish that there is a more detailed ordering of both input and output connections and that the ordering seen usually reflects that observed at a broader level. The findings of this study established differential ordering of inputs and outputs, this is in agreement with the earlier findings. The findings of broad scale connectivity in this pathway showed evidence of a circuit not typical of the expected hierarchical organisation (see Chapter 5), by investigating these connections at a greater resolution it was possible to investigate this unexpected pathway further. Following the initial findings of an ordered arrangement within broad scale PFC projections, the investigation was continued using smaller volumes of tracer (retrograde: Fluoro-Gold and anterograde: Fluoro-Ruby). These smaller injections were positioned along the same medial-lateral line in central PFC as the previous 100nl injections (Chapters 5 and 6). Use of the anterograde tracer Fluoro-Ruby rather than the previously used BDA allowed for fine scale visualization, which would otherwise not have been possible. This is due to its increased sensitivity and ability to be easily visualised with fluorescence.

Aims

This study aimed to determine if the organisational pattern already identified on a broad scale is present when examined in finer detail, and if the properties of the

underlying fine scale organisation of connections from PFC to sensory-motor cortex differed. The earlier investigation into the fine scale organisation of connections from PFC to temporal cortex revealed a more complex organizational structure than that which could be observed at a lower resolution. The fine scale analysis provided a useful insight into the detailed organisation of connections between PFC and temporal cortex, this study enabled a similar insight into the organisation of this pathway.

Methodology

Animals and Surgical Procedures

The methodology used in this study can be seen in detail in Chapter 4. The data used in this study was obtained from the same experiments as Chapter 4.

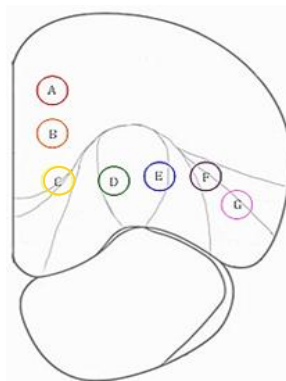


Figure 7.1. Coronal section of PFC (A-P 3.7mm from Bregma) showing the cytoarchitectural boundaries of PFC sub-regions according to Van de Werd & Uylings (2008), depicting sites of tracer injections; PL (A, B), IL/MO (C), VO/VLO (D), VLO/LO (E), LO/DLO (F) and DLO (G), with 0.5mm separation.

Anatomical Processing, Imaging and Microscopic Analysis

The anatomical and microscopic analysis used in this study is described in detail in chapters 2 and 4.

For the analysis of both anterograde and retrograde connections, two series of 40 μ m coronal sections were taken (2 in 6 sections) on a freezing microtome (CM 1900, Leica, Germany). Sections were mounted onto gelatin coated slides. One series of

sections was cover slipped with Vectashield® (Vector laboratories) mounting medium (with DAPI), for fluorescent imaging of Fluoro-Ruby injection sites and labeled projections. The second series was cover slipped with Vectashield® (Vector laboratories) mounting medium (with propidium iodide) for fluorescent imaging of Fluoro-Gold injection sites and labeled projections. Sections were examined using fluorescent microscopy. Fluorescent photos were captured of injection sites, retrogradely labeled cells (Fluoro-Gold) and anterogradely labeled axon terminals (Fluoro-Ruby) using an Olympus DP-11 system microscope with a x4, x10 and x20 objective lens.

Statistical Analysis of the Fine Scale Connections Between Prefrontal and Sensory-Motor Cortex

A statistical analysis was implemented similar to that used in previous studies (see chapters 2 and 4). The three dimensional location of each retrogradely labeled cell (Fluoro-Gold) or anterogradely labeled axon terminal (Fluoro-Ruby) was determined. ImageJ (Wayne Rasband, NIH) was used to measure the distance of each label from the cortical surface in the dorsal-ventral and medial-lateral axes. The anterior-posterior location of each retrogradely labelled cell was also recorded, in terms of distance (mm) from Bregma (according to Paxinos and Watson, 1998).

Labeled cells were grouped according to injection site location. The resultant data was analysed in SPSS by way of a factorial ANOVA, in order to establish the existence of an effect of injection site location on positioning of labeled cells in sensory-motor cortex (in dorsal-ventral, anterior-posterior and medial-lateral axes). The relationship between anterograde and retrograde labelling was determined from a two factor ANOVA.

A statistical comparison of the results obtained here from injections of small tracer volumes and the results obtained earlier from larger tracer injections enabled confirmation that the observations made were reliable representations of the underlying fine scale structure of the same ordered organisation identified in Chapter

5. By calculating the Euclidean distance between anterograde and retrograde labels from large and small tracer volumes it was possible to produce a valid comparison between the two datasets. A t-test was applied to determine if there was any significant difference in the broad scale organisation produced from the two experiments.

By constructing a connectivity matrix, in which an anterograde and retrograde injection site were connected to one another if they produced labelling in the same region of sensory or motor cortex, it was possible to investigate the connectional organisation of PFC to sensory-motor cortex projections further.

Results

The results described in this study were derived from the same injection sites as used in the fine scale investigation of PFC – temporal cortex connections (Chapter 4). Detailed descriptions of injection sites can be found in Chapter 4.

Injection sites from PFC injections of (30nl) Fluoro-Gold were positioned in the intended regions (Fig.7.2.ii, v). Retrograde injection sites spanned layers II – VI with some overlapping between injections into PL, IL, MO and VO, as well as LO and DLO₂. The majority of the spread of tracer at retrograde injection sites was confined to the intended cytoarchitectural region.

Fluoro-Ruby injection sites were found in the intended regions of PFC (Fig.7.2.iii, iv). Fluoro-Ruby injection sites were predominantly confined to the intended cytoarchitectural regions of PFC and were found to be mostly within the borders of the equivalent 30nl Fluoro-Gold injection sites. There was some overlap between injection sites into LO and DLO . The Fluoro-Ruby injection sites spanned layers III-VI.

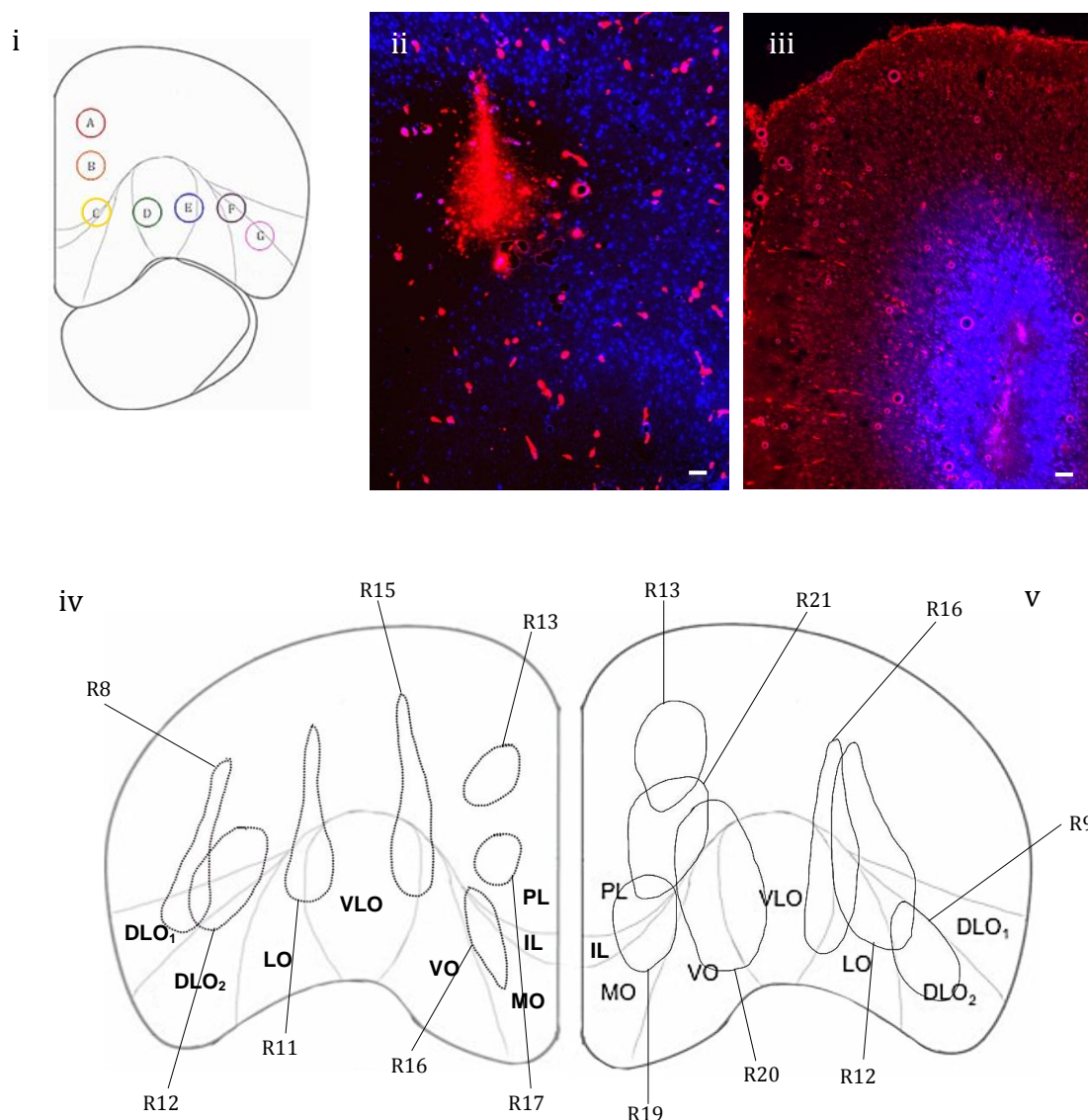


Figure 7.2. (i) Coronal section of PFC (AP 4.2mm from Bregma) showing the cytoarchitectural boundaries of the prelimbic (PL), infralimbic (IL), medial orbital (MO), ventral orbital (VO), ventrolateral orbital (VLO), lateral orbital (LO) and dorsolateral orbital (DLO) cortices (according to Van de Werd & Uylings, 2008), depicting sites of injections; Prelimbic: A & B, Infralimbic/Medial orbital: C, Ventral orbital/Ventrolateral orbital: D, Ventrolateral orbital/Lateral orbital: E, Lateral orbital/Dorsolateral orbital: F and Dorsolateral orbital: G, with 0.5mm spread. (ii) Coronal section of prefrontal cortex showing location and spread of (20nl) Fluoro-Ruby at injection site in VLO/LO (R11). (iii) Coronal section of prefrontal cortex showing location and spread of (30nl) Fluoro-Gold at injection site in PL (R21). (iv) Representations of Fluoro-Ruby (20nl) (R13, R17, R16, R15, R11, R12, R8 (broken line)) injection sites in PL (R13, R17), IL/MO (R16), VO/VLO (R15), VLO/LO (R11), LO/DLO (R12) and DLO (R8) in the right hemisphere. (v) Representations of Fluoro-Gold (30nl) (R13, R21, R19, R20, R16, R12, R9 (solid line)) injection sites in PL (R13, R21), IL/MO (R19) VO/VLO (R20), VLO/LO (R16), LO/DLO (R12) and DLO (R9) in the left hemisphere. Fluoro-Ruby injection sites were predominantly within the boundaries of Fluoro-Gold injection sites. There is some overlap between

retrograde injection sites into PL, IL and VO (R13 & R21, R21 & R19, R21 & R20). There is minimal overlap between anterograde injection sites into DLO (R8 & R12). Scale bars = 100µm.

The patterns of anterograde and retrograde labelling were observed throughout the brain using fluorescent microscopy, following tracer injections into PL, VO, VLO and DLO. Retrogradely labelled cells were found in cingulate cortex (Cg1, Cg2), secondary motor cortex (M2), primary motor cortex (M1), primary somatosensory cortex (S1J, S1JO, S1BF), piriform cortex (Pir), perirhinal cortex (PRh), entorhinal cortex (Ent), secondary auditory cortex (AuV), primary auditory cortex (Au1) and prefrontal cortex regions. Anterograde labelling was found in Cg1, Cg2, M2, PRh, Ent and prefrontal cortex regions. Both retrograde and anterograde labelling was most prominent in several areas, including the sensory-motor regions of S1J, M1, M2 and Cg1. In order to further investigate the pathway between PFC and temporal cortex in fine detail, which we had already identified in Chapter 2, the labelling within areas of Cg1, M2, M1 and S1J was analysed.

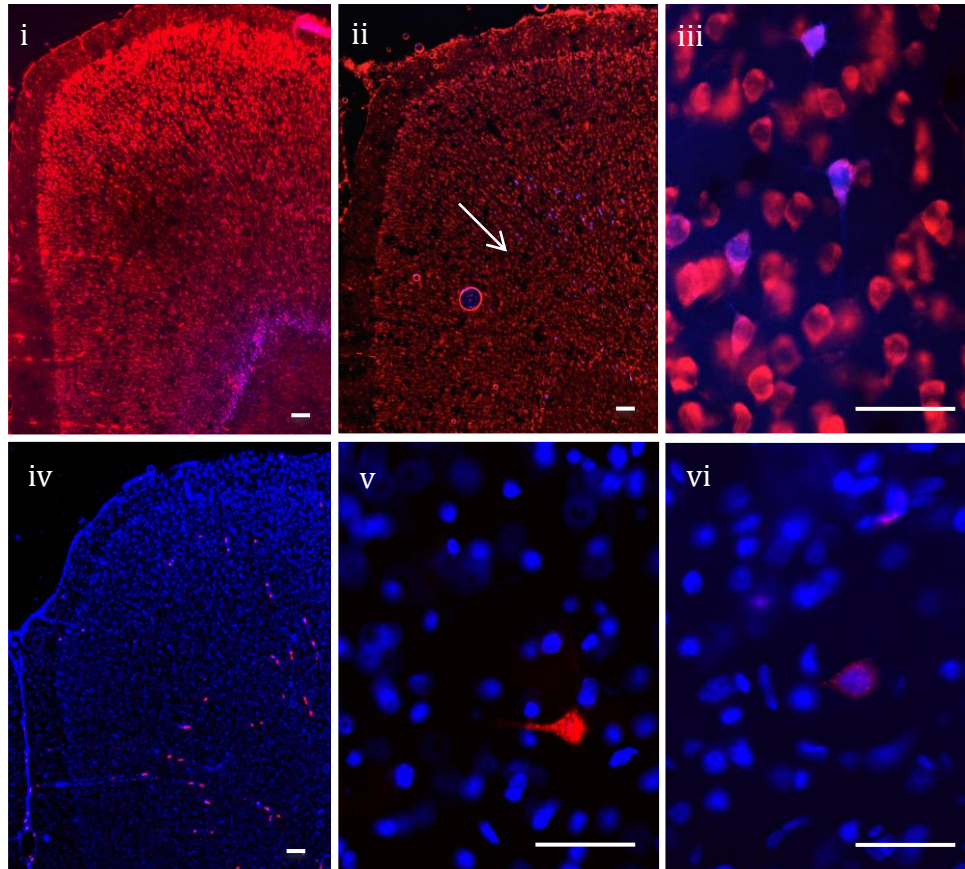


Figure 7.3. (i) Coronal section showing retrogradely labelled cells (blue) in sensory-motor cortex produced by injection of Fluoro-Gold (30nl) into VO/VLO (D: R20). (ii) Coronal section showing retrogradely labelled cells (blue) in sensory-motor cortex produced by injection of Fluoro-Gold (30nl) into PL (B: R21). Arrow denotes location of retrogradely labeled cells. (iii) Retrogradely labelled cells in sensory-motor cortex (blue) produced by injection of Fluoro-Gold (30nl) into PL (B: R20). (iv) Coronal section showing anterogradely labelled axon terminals (red) in sensory-motor cortex produced by injection of Fluoro-Ruby (20nl) into PL (B: R17). (v) Anterograde labelling (red) in sensory-motor cortex produced by injection of Fluoro-Ruby (20nl) into DLO (G: R8). (vi) Anterograde labelling (red) in temporal cortex produced by injection of Fluoro-Ruby (20nl) into VLO/LO (E: R11). Scales bars = 100µm.

Evidence of fine scale reciprocal connectivity between PFC and sensory-motor cortex was observed. Regions of sensory-motor cortex (Cg1, M2) in which anterogradely labelled axon terminals were found, also contained retrograde labelling from the same PFC injection site. E.g. anterogradely labelled axon terminals from injection B (PL) were found in M2 at AP 1.7mm from Bregma, retrogradely labelled cells from injection B (PL) were also found in M2 at AP 1.7mm from Bregma. However, for the

remaining 6 injection sites, connections which were not reciprocal were observed, where retrograde and anterograde labels from identical PFC injection sites were not found in the same region in sensory-motor cortex.

Organisation of Input Connections from Prefrontal Cortex to Sensory-Motor Cortex

Projections to PFC from sensory and motor cortex were seen in Cg1, M1, M2 and S1J (Fig. 7.3.ii., 7.4). The distribution of retrogradely labelled cells is seen across several cytoarchitectural regions within sensory-motor cortex (Fig. 7.3.ii) and maintains some spatial order in accordance with the corresponding Fluoro-Gold injection sites in PFC (PL, IL, MO, VO, VLO, LO and DLO). A factorial ANOVA revealed a significant main effect of injection site on dorsal-ventral location of retrogradely labelled cells in sensory-motor cortex ($F(6, 596) = 294.096$ $p < 0.001$). Post hoc comparisons (Tukey HSD) between the seven retrograde groups indicated significant differences between injection sites A*B, A*C, A*D, A*E, B*D, B*F, B*G, C*D, C*E, C*F, C*G, D*E, D*F, D*G, E*F, E*G ($p < 0.001$), A*G, B*E ($p = 0.001$), B*C ($p = 0.012$). A factorial ANOVA also revealed a significant main effect of injection site on anterior-posterior location of retrogradely labelled cells ($F(6, 596) = 610.057$ $p < 0.001$). Post hoc comparisons (Tukey HSD) between the seven retrograde groups indicated significant differences between injection sites A*B, A*D, A*E, A*F, A*G, B*C, B*D, B*G, C*D, C*E, C*F, C*G, D*E, D*F, D*G, E*G, F*G ($p < 0.001$).

The factorial ANOVA revealed a significant main effect of injection site on medial-lateral location of retrogradely labelled cells ($F(6, 596) = 277.002$ $p < 0.001$). Post hoc comparisons (Tukey HSD) between the seven retrograde groups indicated significant differences between injection sites A*B, A*C, A*D, A*E, A*G, B*D, B*E, B*F, B*G, C*D, C*E, C*F, C*G, D*E, D*F, D*G, E*F, E*G, F*G ($p < 0.001$).

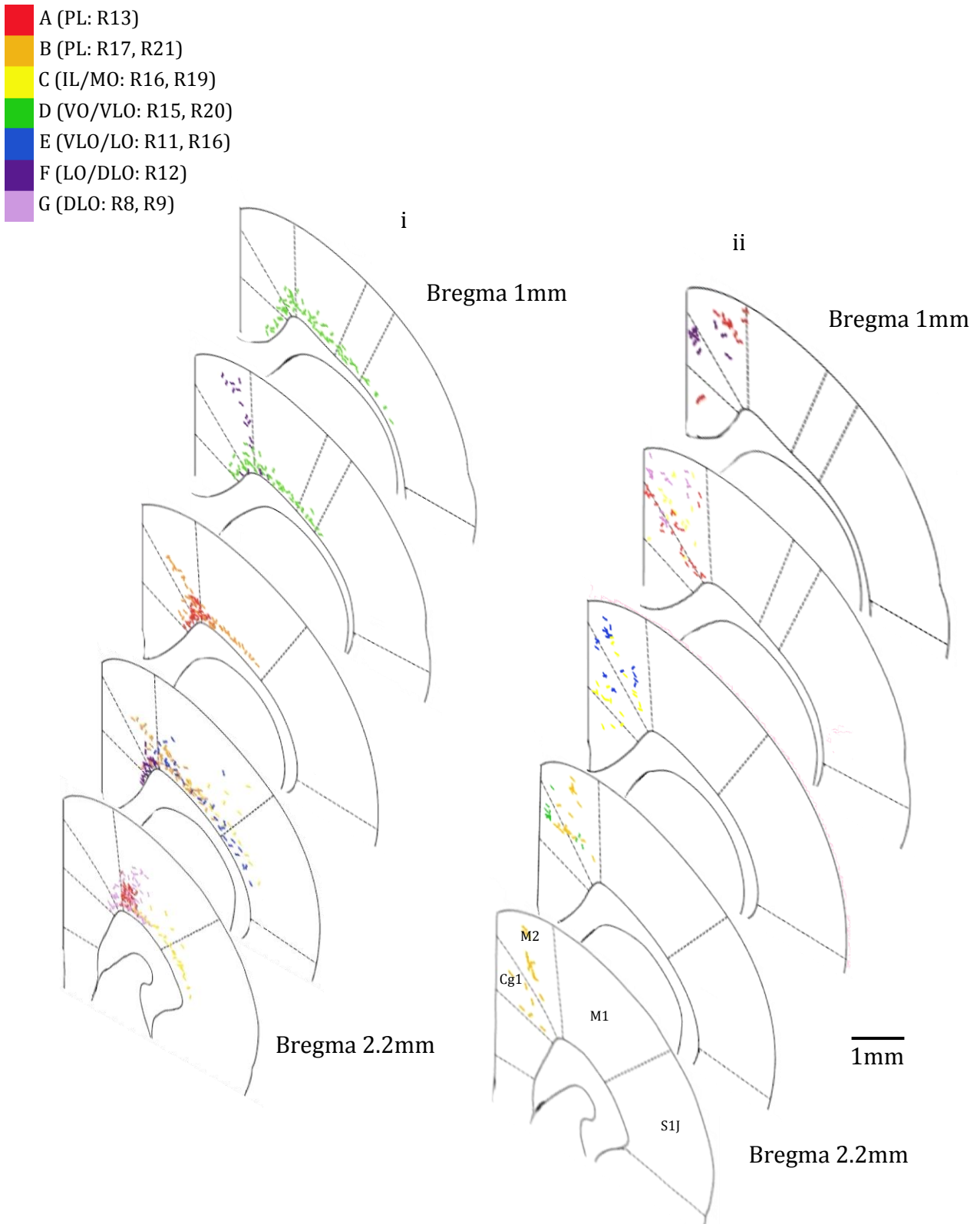


Figure 7.4. Diagram representing the amalgamated injection sites of Fluoro-Gold and Fluoro-Ruby, and the projection sites to sensory-motor cortex for both retrograde (Fluoro-Gold) and anterograde (Fluoro-Ruby) tracer injections. (i) The locations of injection sites A (PL: R13), B (PL: R17, R21), C (IL/MO: R16, R19), D (VO/VLO: R15, R20), E (VLO/LO: R11, R16), F (LO/DLO: R12) and G (DLO: R8, R9). (ii) The locations of retrogradely labelled cells in sensory-motor cortex, resultant from 30nl Fluoro-Gold injections into PFC injection sites A-G (R13, R21, R19, R20, R16, R12, R9). Note the concentration of retrograde labelling in layers V and VI, with

laminar ordering present. (iii) The locations of anterogradely labelled axon terminals in sensory-motor cortex resultant from 20nl Fluoro-Ruby injections into PFC injection sites A-D (R13, R17, R16, R15, R11, R12, R8).

Organisation of Output Connections from Prefrontal Cortex to Sensory-Motor Cortex

Projections from PFC to sensory-motor cortex were seen in Cg1 and M1 (Fig. 7.3.iii. 7.4). The distribution of anterogradely labelled cells within sensory-motor cortex maintained an overall spatial order in accordance with their corresponding Fluoro-Ruby injection sites in PFC (Fig. 7.3.iii). The factorial ANOVA revealed a significant main effect of injection site on dorsal-ventral location of anterogradely ($F(6,240)=23.233$ $p<0.001$) labelled cells in medial-frontal cortex. Post hoc comparisons (Tukey HSD) between the seven anterograde groups indicated significant differences between injection sites A*B, B*C, B*D, B*E, B*F, B*G ($p<0.001$). The results indicate an ordered arrangement of input connections in the dorsoventral axis and an ordered arrangement of output connections, specifically occurring in the medial aspect of PFC.

The factorial ANOVA revealed a significant main effect of injection site on anterior-posterior location of anterogradely ($F(6,240)=113.163$ $p<.001$) labelled cells in medial-frontal cortex. Post hoc comparisons (Tukey HSD) between the seven anterograde groups indicated significant differences between injection sites A*B, A*C, A*D, A*E, A*F, B*C, B*D, B*E, B*F, B*G, C*D, D*F, D*G, E*G ($p<0.001$), C*E, C*G ($p=0.001$). The results indicate an ordered arrangement of input and output connections in the anterior-posterior axis. Similarly, The factorial ANOVA revealed a significant main effect of injection site on medial-lateral location of anterogradely ($F(6,240)=34.959$ $p<0.001$) labelled cells in medial-frontal cortex. Post hoc comparisons (Tukey HSD) between the seven anterograde groups indicated significant differences between injection sites A*B, B*C, B*D, B*E, B*F, B*G ($p<0.001$). This indicates an ordered arrangement of input connections in the medial-lateral axis, and an ordered arrangement of output connections from the medial part of PFC.

In comparison to a relatively large number of cells labelled by Fluoro-Gold injections, Fluoro-Ruby injections into the same PFC sites produced anterograde labelling in sensory-motor cortex of a small number of cells, showing a high degree of convergence, similar to that seen on a larger scale (Chapter 5 and 6). Earlier investigations found the majority (70%) of labelling produced by Fluoro-Ruby to be anterograde. Based on this, and for the purpose of the statistical analysis, all Fluoro-Ruby labelling seen in sensory-motor cortex was assumed to be anterograde.

Statistical evidence for the ordered arrangement of Fluoro-Gold and Fluoro-Ruby labelled connections came from the following analyses.

For the dorsal-ventral axis:

The two factor ANOVA revealed a significant interaction effect between input and output connections ($F_{(6,901)}=94.900$ $p<0.001$). This shows that the dorsoventral location of anterogradely and retrogradely labelled cells vary in respect to one another, meaning that the input and output connections are not aligned. These analyses show significant ordering of both input and output connections in the dorsoventral axis. The interaction and correlation analyses show that inputs and outputs are ordered but not aligned in this axis of orientation (Fig. 7.5.i).

For the anterior-posterior axis:

The two factor ANOVA revealed a significant interaction effect between input and output connections ($F_{(6,901)}=306.116$ $p<0.001$). This shows that the anterior-posterior location of anterogradely and retrogradely labelled cells vary in respect to one another, meaning that the input and output connections are not aligned. These analyses show significant ordering of both input and output connections, and that they are not aligned with one another (Fig.7.5.ii).

For the medial-lateral axis:

The two factor ANOVA revealed a significant interaction effect between input and output connections ($F_{(6,901)}=104.511$ $p<0.001$). This shows that the mediolateral location of anterogradely and retrogradely labelled cells vary in respect to one

another, meaning that the input and output connections are not aligned. These results show ordered arrangements of input and output connections, the interaction shows that inputs and outputs are not aligned in this axis of orientation (Fig.7.5.iii).

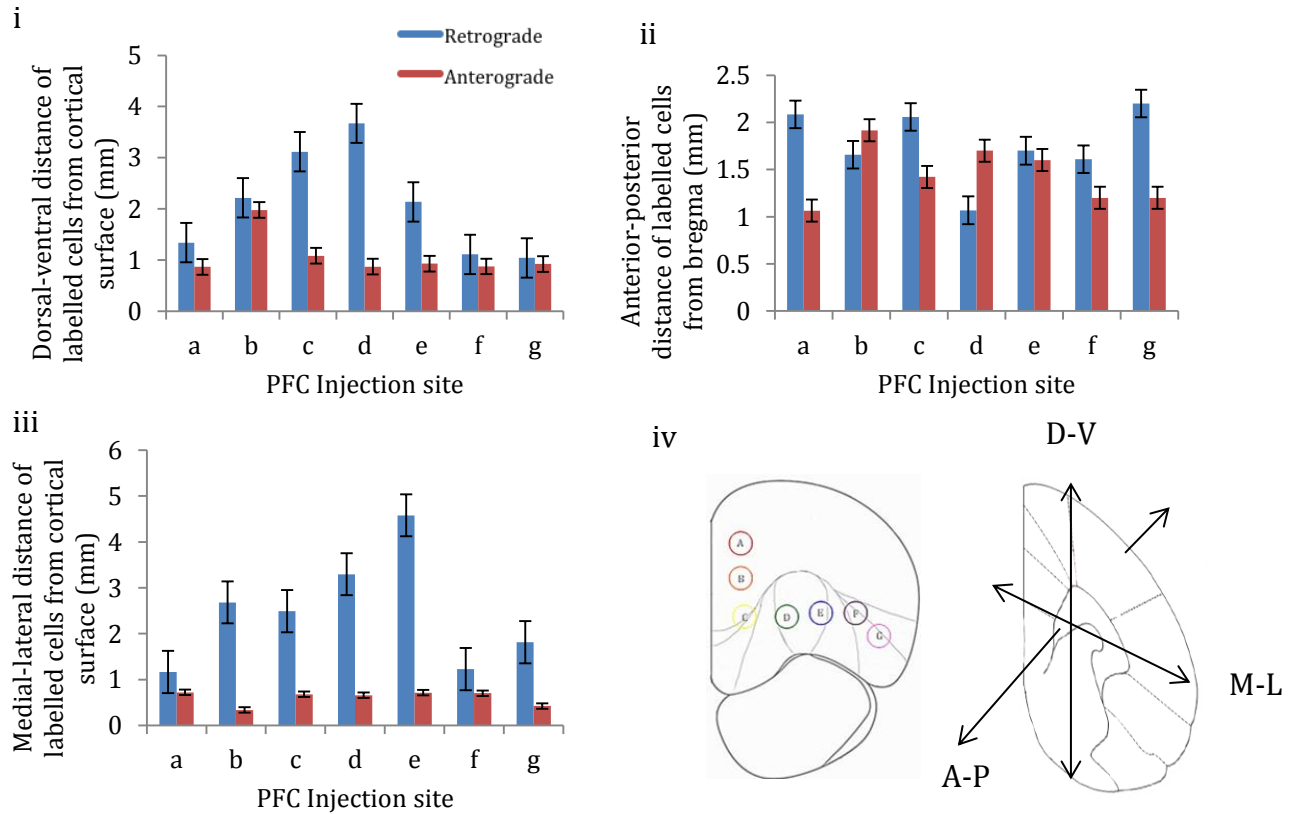


Figure 7.5. The mean effect of PFC injection site on the (i) dorsal-ventral, (ii) anterior-posterior and (iii) medial-lateral location of retrogradely labeled cells (n= 597 arising from 7 rats: A(PL:R13)=119, B(PL:R21)=52, C(IL/MO:R19)=91, D(VO/VLO:R20)=85, E(VLO/LO:R16)=22, F(LO/DLO:R12)=71, G(DLO:R9)=157) and anterogradely labeled axon terminals (n=305 arising from 7 rats: A(PL:R13)=34, B(PL:R21)=138, C(IL/MO:R19)=63, D(VO/VLO:R20)=24, E(VLO/LO:R16)=22, F(LO/DLO:R12)=10, G(DLO:R9)=14) within sensory-motor cortex. Error bars = standard error. (iv) Coronal cross section of PFC showing the position of 7 injection sites; PL (A, B), IL/MO (C), VO/VLO (D), VLO/LO (E), LO/DLO (F) and DLO (G). Coronal cross section of sensory-motor cortex showing the three dimensions in which the locations of labels were recorded.

This analysis shows evidence for fine scale ordered organisation of connections between PFC and sensory-motor cortex. As PFC injection sites move from medial to lateral (VO - DLO) input connections move from dorsal-ventral, whilst output connections (from VO - DLO) move from anterior to posterior. Output projections remain almost constant in their positioning in sensory-motor cortex from VO – DLO

in the dorsal-ventral axis; input connections change at a greater rate. Input connections from PL – VO move from ventral to dorsal in sensory-motor cortex, whilst output projections from PL – VO move from dorsal to ventral. This indicates differential ordering of Fluoro-Gold and Fluoro-Ruby labeled projections from the same PFC regions, as well as changes in ordering of input projections across PFC from PL to DLO.

A direct comparison of broad and fine scale connectivity patterns, using a comparison of Euclidean distances between corresponding retrogradely and anterogradely labelled cells

$$E = \sqrt{(\langle DVr \rangle - \langle DVa \rangle)^2 + (\langle APr \rangle - \langle APa \rangle)^2 + (\langle MLr \rangle - \langle MLa \rangle)^2}$$

indicates similar orders of organisation in regards to the relationship between input and output connections; a paired samples t-test indicated no significant difference between the organisational pattern found from 100nl injections and 20-30nl injections ($t(1)=4.541$ $p=0.138$). This shows that although PFC – sensory-motor cortex connections are ordered on a broad scale, the underlying fine scale organisation is not so clearly defined by a clear ordering from medial to lateral.

Discussion

Fine Scale Connections of the Prefrontal Cortex – Sensory-Motor Cortex Pathway

This study confirmed the earlier broad scale evidence of an ordered arrangement of projections from PFC to regions of sensory and motor cortex (M1, M2, S1J, Cg1). Despite an overall similar appearance to the ordered pattern of connectivity we see at a broad scale compared to fine scale, the more detailed visualisation and analysis of organisation at a finer scale has revealed properties within the organisation of PFC connections which could not be seen with larger injection volumes. In addition to differential ordering, this study has shown that inputs and outputs did not move in

opposing directions as it may appear at a larger scale, but that the relationship between connections is more complex, similar to that seen in fine scale PFC – temporal cortex connections (Chapter 4).

The results of this study indicate two distinct, overlapping patterns of organisation within PFC – sensory-motor cortex connections. The findings show evidence of reciprocal connectivity in the pathway between PFC and sensory-motor cortex (Cg1 & M2), consistent with that described in the earlier studies (Chapter 5, Chapter 6, Appendix L, Appendix O). Anterograde and retrograde labelling from identical PFC injection sites were found in similar areas of Cg1 and M2 resultant from injections into PL. However, from the majority of small volume injection sites it was found that connections were not reciprocal; anterograde and retrograde labels were not found in the same cytoarchitectural regions of sensory and motor cortex. In comparison to the broad scale reciprocity found from larger tracer injection volumes, the findings here indicate that the connections from PFC to sensory-motor cortex are for the most part not reciprocal.

It should be noted that the labelling produced by Fluoro-Ruby is not exclusively anterograde and is reported to hold retrograde properties (Zelevansky et al, 2010; Hainec et al, 2012). The earlier investigations into the properties of Fluoro-Ruby labelling revealed it to be 70% anterograde, with 30% of labelling produced by Fluoro-Ruby injections being retrograde (Appendix G). This should be considered when interpreting the findings. However, the majority of Fluoro-Ruby labelling is anterograde and shows no significant difference when compared to the anterograde labelling produced by BDA (Appendix G); no statistically significant difference was found in the location of labelling from the same injection sites, as well as the distance of labelling from retrograde (Fluoro-Gold) labels from the same PFC injection sites (Appendix G).

Input Connections to Prefrontal Cortex from Sensory-Motor Cortex

Following the administration of the retrograde tracer, Fluoro-Gold, to the seven equally spaced injection sites across the PFC regions PL, IL/MO VO, VLO, LO and

DLO, fluorescently labelled neuronal cell bodies were found in areas of motor cortex, temporal cortex, auditory cortex, somatosensory cortex, cingulate cortex and piriform cortex. Projections arising from regions of motor and sensory cortex were amongst the areas of most prominent labelling. These findings are consistent with the previous results from larger PFC Fluoro-Gold injections, as well as previous studies defining projections from PFC to areas of sensory-motor cortex (Sesack, 1989; Conde et al, 1995). Retrograde labelling resultant from tracer injections into PFC sub-regions (PL, IL/MO, VO, VLO, LO and DLO) was consistent with that seen at a lower resolution in my previous studies (Chapters 5 and 6) using larger tracer injection volumes. Labelling was seen in similar regions of sensory-motor cortex to that described by Sesack, (1989).

Retrogradely labelled input connections were consistently found in deeper cortical layers in comparison to anterograde labels, and show evidence of ordered laminar organisation, comparable to that identified on a broader scale. This is similar to the equivalent labelling described with larger tracer injections, and consistent with findings from Kondo and Witter (2014) of output projections from PFC terminating in superficial layers. Ordered laminar organisation of connections has been described elsewhere, but has not been reported in great detail in PFC; projections from orbitofrontal and infralimbic cortices to entorhinal cortex produce labelling in deeper layers with more posterior-medial injections (Insausti and Amaral, 2008). The laminar organisation identified on a broad scale was reproduced here at a fine scale, indicating that the organisational pattern seen across PFC regions remains broadly consistent and reproducible at a greater resolution.

Output Connections from Prefrontal Cortex to Sensory-Motor Cortex

Following the administration of the anterograde tracer, Fluoro-Ruby to the seven equally spaced injection sites across the PFC regions PL, IL, MO, VO, VLO, LO and DLO, fluorescently labelling was found in areas of motor, sensory, cingulate, perirhinal, entorhinal and piriform cortex. Projections to regions of motor and cingulate cortex were amongst the areas of most prominent labelling and were consistent with the anterograde labelling identified in earlier, larger scale studies

(Chapter 5 and 6). Anterograde labelling was consistently found to cover a smaller region of sensory-motor cortex than retrograde counterparts. This is consistent with larger scale findings and shows evidence of convergence in the PFC – sensory-motor cortex pathway.

Organisation and Alignment of Fine Scale Connections Between Prefrontal Cortex and Sensory-Motor Cortex

The comparison of labelling in sensory-motor cortex resultant from 100nl and 20-30nl tracer injections revealed no significant difference in the midpoint location of labels (for retrograde and anterograde). This indicates that the labelling of connections seen here at a fine scale gives a reliable representation of the underlying organisation of the connectivity pattern described on a broader scale (Chapter 5). The comparative analysis shows that the ordered arrangement of PFC to sensory-motor cortex connections is broadly reproduced on a finer scale, and that the non-alignment of input and output connections remains evident. However, whereas on a broader scale (100nl injections) input and output connections appear to follow opposing orders, when visualised at a finer resolution this study has shown that the relationship between input and output connections is more complex.

This fine scale analysis revealed the connectivity pattern of the PFC – sensory-motor cortex pathway in greater detail than had previously been described. Visualisation of the labelled input and output projections from the PFC injection sites shows a clear segregation of connectivity between sensory-motor regions. That is, input projections resultant from injections into PL, medial VO and DLO produce clearly defined retrograde labelling, concentrated in motor regions (M1 and M2), whereas injections into lateral VO and LO produce more widespread labelling across motor and sensory regions (Cg1, M1, M2, and S1). This shows a distinction in the organisation of connections, with the most medial and lateral regions of PFC receiving input from very specific sites, whilst connections from more central PFC regions (i.e. LO and VO) are more widespread. This is somewhat consistent with findings from Miyachi et al (2005) which identified greater motor connectivity from the most medial and ventral aspects of PFC.

The earlier studies (Chapters 5 and 6) revealed an interesting property in the circuitry of PFC – sensory-motor cortex connections, in that PFC received a direct connection from primary sensory cortex (S1J→PFC). This finding was inconsistent with theories of hierarchical organisation (S1→S2→PFC). A similar observation was made when viewed here at a greater resolution. However, here only IL/MO and VLO (injection sites C, D and E) received direct input connections from primary sensory cortex. This indicates that it is a specific region of PFC which is involved in this unexpected circuit, it is not apparent in PL, LO or DLO.

By plotting the anterograde and retrograde labels in medial-frontal cortex alongside one another it was possible to visualise how the locations of input and output connections spatially related. These results demonstrated that at a fine scale, the input and output connections are not consistently aligned with respect to one another, confirming the previous findings. This finding is of particular interest when considered in comparison to more clearly understood cortical regions, such as visual cortex, in which input and output connections are found to be consistently aligned with one another (Van Essen et al, 1986; Triplett, 2009) and considered to be important in functional organisation (Tootell et al, 1998). Additionally, topographic alignment of input and output connections has been widely described in M1 (Porter and White, 1983; Miller and Vogt, 1984). Despite the known alignment of pathways from M1 to other regions of the brain e.g. visual cortex, the findings of this study show a surprising organisational pattern in M1 – PFC connections, with a high instance of non-alignment between inputs and outputs.

Connections from Prefrontal Cortex to Sensory-Motor cortex

To visualise the connectivity of input and output connections in this circuit a connectivity matrix was constructed, demonstrating the spatial relationship of input and output connections between prefrontal and sensory-motor cortex (Fig. 7.6).

Anterograde projection

	A	B	C	D	E	F	G
Retrograde projection	A				X		
B		X		X	X		
C							
D	X		X			X	X
E							
F	X	X	X	X			X
G		X					

Figure 7.6. Connectivity matrix showing the relationship between input and output connections from PFC to sensory-motor cortex. X = Retrograde and anterograde labelling found in the same cytoarchitectural regions of sensory or motor cortex. X = Reciprocal connection: Retrograde and anterograde labelling from the same PFC injection site is found in the same cytoarchitectural region of sensory or motor cortex. E.g. Retrograde injection site A receives input connections from a region of sensory-motor cortex which injection site E sends output connections to.

The rows of the matrix represent the location of retrograde projections in sensory-motor cortex from injection sites in PFC (A-G), the columns represent anterograde projections to sensory-motor cortex from injection sites in PFC (A-G). Fig. 7.6 shows the retrograde and anterograde projections which occur in the same cytoarchitectural regions of sensory-motor cortex. X represents a retrograde and anterograde projection found in the same cytoarchitectural region of sensory-motor cortex. A retrograde and anterograde projection are said to be connected if they occur in the same cytoarchitectural region of sensory or motor cortex, indicating the return anterograde projections to each retrograde projection. Fig. 7.6 indicates two distinct patterns of connectivity between input and output connections, dependent on the number of connections between retrograde and anterograde projections (<2 or >2). Retrograde projection A is found in the same cytoarchitectural region as anterograde projection E (1 connection), retrograde projection B is found in the same cytoarchitectural region as anterograde projection B, D and E (3 connections), retrograde projection C is found

in the same cytoarchitectural region as 0 anterograde projections, retrograde projection D is found in the same region as anterograde projections A, C, F and G (4 connections), retrograde projection E is found in the same region as 0 anterograde projections, retrograde projection F is found in the same region as anterograde projections A, B, C, D, and G (5 connections) and retrograde projection G is found in the same region as anterograde projection B (1 connection). Alternate retrograde injection sites exhibited alternate connectivity patterns. This is demonstrated in Fig. 7.7.

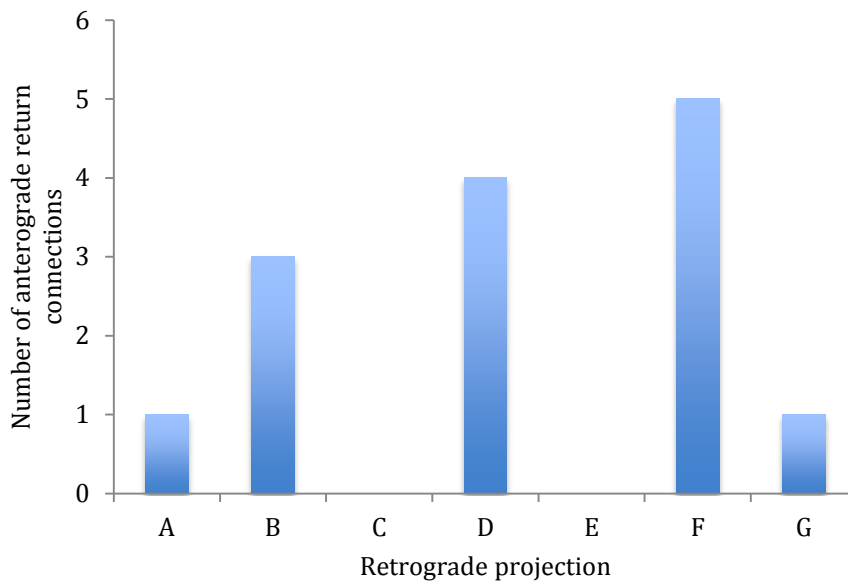


Figure 7.7. The effect of retrograde PFC injection site on the number of return anterograde connections from the same cytoarchitectural region of sensory-motor cortex, constructed using the connectivity matrix in Fig. 7.6.

Retrograde injection sites A, C, E and G produced labelling in cytoarchitectural regions of sensory-motor cortex which received relatively few anterograde projections (<2), whereas retrograde projection sites B, D and F were in cytoarchitectural regions which received a relatively large number of anterograde projections (>2). This alternation continues mediolaterally across the seven retrograde projections (A-G). In addition, it was observed that the retrograde injection sites which appear to produce different connectivity patterns project to different areas of sensory-motor cortex in terms of the anterior-posterior axis. Retrograde labelling resulting from injection sites B, D and F were all found in more posterior regions of sensory-motor cortex in comparison to the retrograde labelling resultant from injection sites A, C, E and G,

which projected to more anterior regions. Based on these findings, it is proposed that the alternating connectivity pattern between input and output connections I have described could be an indication of two distinct but overlapping organisational maps. The two organisational patterns, indicated in figure 7.7, show different ordering. The number of return connections to retrograde projection sites B, D and F increases from medial to lateral (from PL to DLO), whereas the number of return connections to PFC retrograde sites A, C, E and G remains relatively constant (0 or 1). This may indicate two different types of anatomical organisation occurring in the same pathway, implying two different types of functional organisation. In the low connectivity map, where retrograde projection sites receive <2 return connections, where there is a return connection present (injection sites A and G), it is considerably distant from the source injection site in PFC. For instance, retrograde site G receives only one return connection, from anterograde site B. This is a distance of 5. In contrast, within the highly connected map (>2 return connections) all retrograde sites receive return connections from a neighbouring anterograde site (with a distance of 1). Interestingly, the three retrograde PFC injection sites (C(IL/MO), D (VLO) and E (VLO)) which produced labelling in S1J, (showing evidence of an unusual direct connection from $S1 \rightarrow PFC$) do not appear here in the same organizational pattern. This indicates that if there are two distinct organisational maps present, this property is present in both.

To further investigate the relationship between input and output connections, the source regions (in PFC) of return anterograde connections to retrograde projections from PL, VO, LO and DLO were analysed (retrograde projection sites with 0 return anterograde projections were excluded from this analysis to prevent false findings). A linear distance of each return anterograde PFC source region from the retrograde PFC source regions (found in the same area of sensory-motor cortex) was measured, based on the connectivity matrix (Fig. 7.6). Each adjacent PFC injection site was given a distance of 1. A greater assigned value for return anterograde projection equals a greater distance (in PFC) of anterograde projection from retrograde projection, therefore a retrograde injection site with a large average distance would be more widely connected, a distance of 0 represents a 100% reciprocal connection (e.g. if retrograde labelling from PL were to be found in a sensory-motor region with anterograde labelling from only PL and no other PFC region).

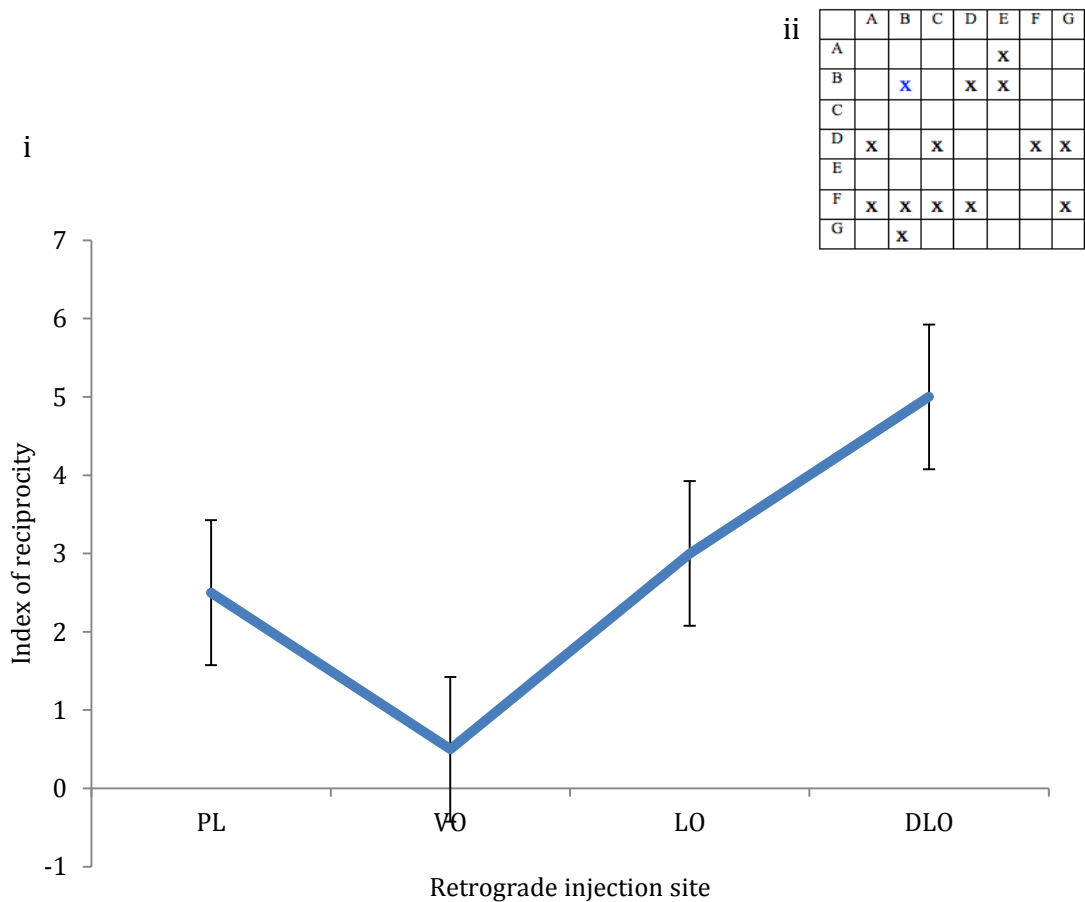


Figure 7.8. (i) The effect of PFC retrograde (Fluoro-Gold) injection site on the median distance between Fluoro-Gold and Fluoro-Ruby PFC injection sites of retrograde and anterograde labelling found in the same cytoarchitectural regions of sensory-motor cortex. A distance of 1 PFC injection site is given a value of 1 (e.g. the distance between retrograde site A and anterograde site B = 1). Where a retrograde projection is found in the same region as multiple anterograde projections a median distance is calculated. Fluoro-Gold injection sites made into the same PFC sub-regions (i.e. PL) are combined. PL = A & B, VO=D, LO=F, DLO=G. Injection G (DLO) is excluded due to having no return connections. Error bars = standard error. Error bars = standard error. (ii) The connectivity matrix from which the graph (i) is produced.

Figure 7.8 shows that as retrograde injection site moves from medial to lateral in PFC (VO-DLO), the median distance between the source retrograde and anterograde PFC injection sites of labeled inputs and outputs found in the same cytoarchitectural regions of sensory-motor cortex increases. A mean close to 0 indicates a higher degree of overall reciprocity, or a smaller spread of anterograde projections connected to a retrograde projection. This means that connections from VO are much closer

together than those from LO and DLO (Fig. 7.8). Therefore, although DLO receives a higher number of return connections (retrograde projection site F receives the greatest number), these connections are more widespread. Additionally, although PL consistently shows a high degree of reciprocity, the connections of PL are more widespread than those at neighbouring VO, because it has distant as well as reciprocal connections, the connections to VO are much closer together. It is the areas with less return anterograde projections that are more closely connected (Fig. 7.7 & 7.8), and are connected to more nearby regions (e.g.VO). Injection site B (PL) is the only injection site which shows evidence for reciprocal connections. This is consistent with the findings from larger injection volumes (Chapter 5 and 6), which identified clear reciprocal connections from PL. Notably, the injection site which shows the smallest average distance to return connection source regions (0.5), and considerably smaller than those from other regions, is injection site D (in VLO), this injection site along with E (VLO) and C (IL/MO) (which showed 0 return connections) are those which also showed input connections from S1→PFC. This may indicate that the way in which a specific region of PFC is connected, and how widespread its connections are, are related to the type of circuit which is formed. These regions may be receiving inputs from S1 in place of reciprocal connections from S2 or M2. It is not yet clear what this relationship means, however it could offer an important insight into the organisation of PFC connections to motor and sensory cortices. It should be noted that the previous analysis (Chapter 3 & Appendix F) showed Fluoro-Ruby to be approximately 70% anterograde (30% retrograde). The bidirectional properties of Fluoro-Ruby should be considered when interpreting these findings.

To conclude, this study provides further evidence to confirm previous findings of ordered arrangements of input and output connections between PFC and sensory-motor cortex, as well as differential ordering of input and output connections. These findings have also identified two possible distinct and overlapping organisations within PFC – sensory-motor cortex connections, a structural property that has not previously been described in this pathway.

Chapter 8.

The Organisation of Frontal Association Cortex - Temporal Cortex Connections

The previous chapters have established the detailed organisation of connectivity within the sub-regions of prefrontal cortex (VO, VLO, LO, VLO, DLO). The following chapter aims to investigate the connectivity of an often overlooked, and difficult to access, frontal cortex region. Frontal association cortex (FrA – Paxinos & Watson, 1998) refers to the area of cerebral cortex located in the dorsolateral frontal pole in rats (Paxinos, 2009). The same region is described as frontal polar cortex by Ray & Price (1992).

FrA has been associated with decision making, specifically having an involvement in no-go reactions (Sasaki et al, 1993). There remains little understanding about FrA compared to other cortical regions, particularly in terms of its connectivity.

Van Groen et al (1999) described connections from the anteromedial nucleus of the thalamus (AM), an area involved in spatial learning, to the frontal polar region (FrA) in rats, using tract tracers (BDA). Smaller volumes of injected tracer into AM resulted in consistent, but less dense labelling in FrA. Van Groen et al (1999) revealed an ordered shift in the pattern of labeled connections in FrA from dorsomedial – anterior - ventromedial AM, indicating topographic ordering of connections.

FrA is also known to have connections with other frontal regions. Hoover & Vertes (2007) identified strong connections between medial frontal agranular cortex (AGm) and medial frontal polar cortex (FPm, synonymous to medial FrA) in the rat. Retrograde labelling from the same AGm site was also found in MO, VO, VLO, LO, PL and IL. The same study also described connections from PL and IL to FrA. This indicates different connectivity in FrA compared to VO, VLO, LO and DLO, as well as differential organisation of PL/IL compared to MO, VO, VLO and LO, showing

consistency with the findings from chapters 2 – 4. Tracer experiments (Hoover & Vertes, 2007) showed evidence for broad scale ordering of FrA connections. Connections from anterior cingulate cortex (AC) are seen more medially in FrA than connections from AGm. Additionally, labelling in FrA from injections in PL differed to that from IL, labelling from PL was much more dense and widespread. These observations provide evidence for the topographic organisation of FrA connections. However, further, more detailed investigation is required to fully understand the connectional organisation of FrA.

There remains little evidence for the ordered organisation of cortical connections from FrA. A more detailed understanding of anatomical connectivity is required to fully appreciate the properties of FrA as a cortical region and its role in frontal cortex networks.

Aims

The intention of this study was to establish the ordered arrangement of broad scale connections from FrA, as well as the alignment of input and output connections. The understanding of FrA connections would provide a further insight into frontal cortex connectivity. Injections of retrograde and anterograde neuroanatomical tracers were made into three locations in rat FrA.

Methodology

For detailed methodology and surgical procedures, see Chapter 2.

Data was collected from 6 male CD rats (294-372g, Charles River, UK). Animal procedures were carried out in accordance with the UK Animals scientific procedures act (1986), EU directive 2010/63 and were approved by the Nottingham Trent University ethical committee.

By employing the same methodology used and optimised in the previous experiments, anterograde (Fluoro-Ruby) and retrograde (Fluoro-Gold) tracers (100nl) were injected into 3 areas of FrA, separated by 1mm (Fig.8.1). Anterograde

and retrograde injection sites were placed at three equally spaced locations, 1mm below the cortical surface, across medial to lateral FrA (4.2 mm from Bregma), according to Paxinos and Watson (1998).

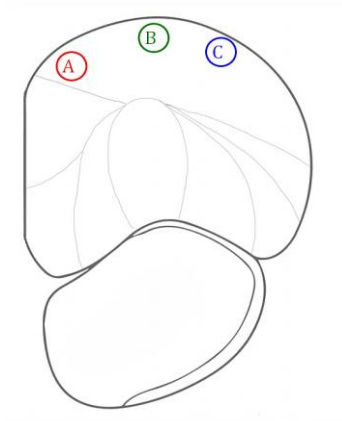


Figure 8.1. Coronal section of PFC (A-P 4.7mm from Bregma) showing the cytoarchitectural boundaries of PFC sub-regions according to Van de Werd & Uylings (2008) and FrA according to Paxinos & Watson (1998), depicting sites of tracer injections, with 1mm separation.

The volume and location of PFC injection sites was based on the findings of preliminary experiments into the spread of tracer injections (reported in Appendix A). The co-ordinates used were all at 4.2mm with respect to Bregma (altered to allow for flat skull from Paxinos & Watson, 1998). One anterograde (Fluoro-Ruby) injection site was excluded due to the injection site not being made sufficiently deep enough into the cortex, resulting in a much smaller than desired spread of tracer at the injection site.

Anatomical Processing and Microscopic Analysis

The anatomical and microscopic analysis used in this study is described in detail in Chapter 2. The entire forebrain was examined for labelling. Areas of temporal cortex were identified as containing strong and consistent labelling, therefore a detailed analysis was carried out on this region.

The previous investigations have identified Fluoro-Ruby as being 70% anterograde. For the purposes of statistical analysis, all Fluoro-Ruby labelling identified in this study was assumed to be anterograde in nature, this should be taken into consideration when interpreting the findings.

Statistical Analysis of the Arrangement of Connections Between Frontal Association Cortex and Temporal Cortex

The numerical and statistical analysis used in this study was similar to that used in the previous temporal cortex studies (Chapters 2 and 3). Image J (Wayne Rasband, NIH) was used to determine numerical values representing the location of each retrogradely labeled cell in sensory-motor cortex. The three dimensional location of each retrogradely labeled cell (Fluoro-Gold) was calculated by measuring the distance of each labeled cell from the cortical surface (medial-lateral) and rhinal sulcus (dorsal-ventral). The anterior-posterior location of labeled cells was recorded in terms of distance from Bregma (according to Paxinos and Watson, 1998). The same analysis was repeated for Fluoro-Ruby labelling.

Labelled cells/areas were grouped according to FrA injection site location. These data sets were analysed in SPSS by way of a factorial ANOVA, in order to establish the existence of an effect of injection site location on the positioning of labels in temporal cortex (in dorsal-ventral, anterior-posterior and medial-lateral axes). Where the collected data violated the assumption of equal population variance for ANOVA, rendering it inapplicable, a non-parametric Kruskal-Wallis test was applied. The relationship between input (retrograde) and output (anterograde) connections was examined by a two factor ANOVA.

Results

Injection sites from FrA injections of (100nl) Fluoro-Gold were positioned in the intended regions (Fig.8.2iv, v). Retrograde injection sites for the most part covered layers I-IV and were consistently confined to the FrA cytoarchitectural boundary (according to Paxinos and Watson, 1998). There was minimal overlapping between injection sites into central and medial FrA (R29 & R33). The three retrograde FrA injection sites were positioned separate to one another. Fluoro-Ruby (100nl) injection sites were found in the intended regions of FrA and were confined to FrA and spread across layers I-IV. There was minimal overlap between anterograde injections into central and medial FrA (R37 & R41) and central and lateral FrA (R37 & R38) (Fig.8.2).

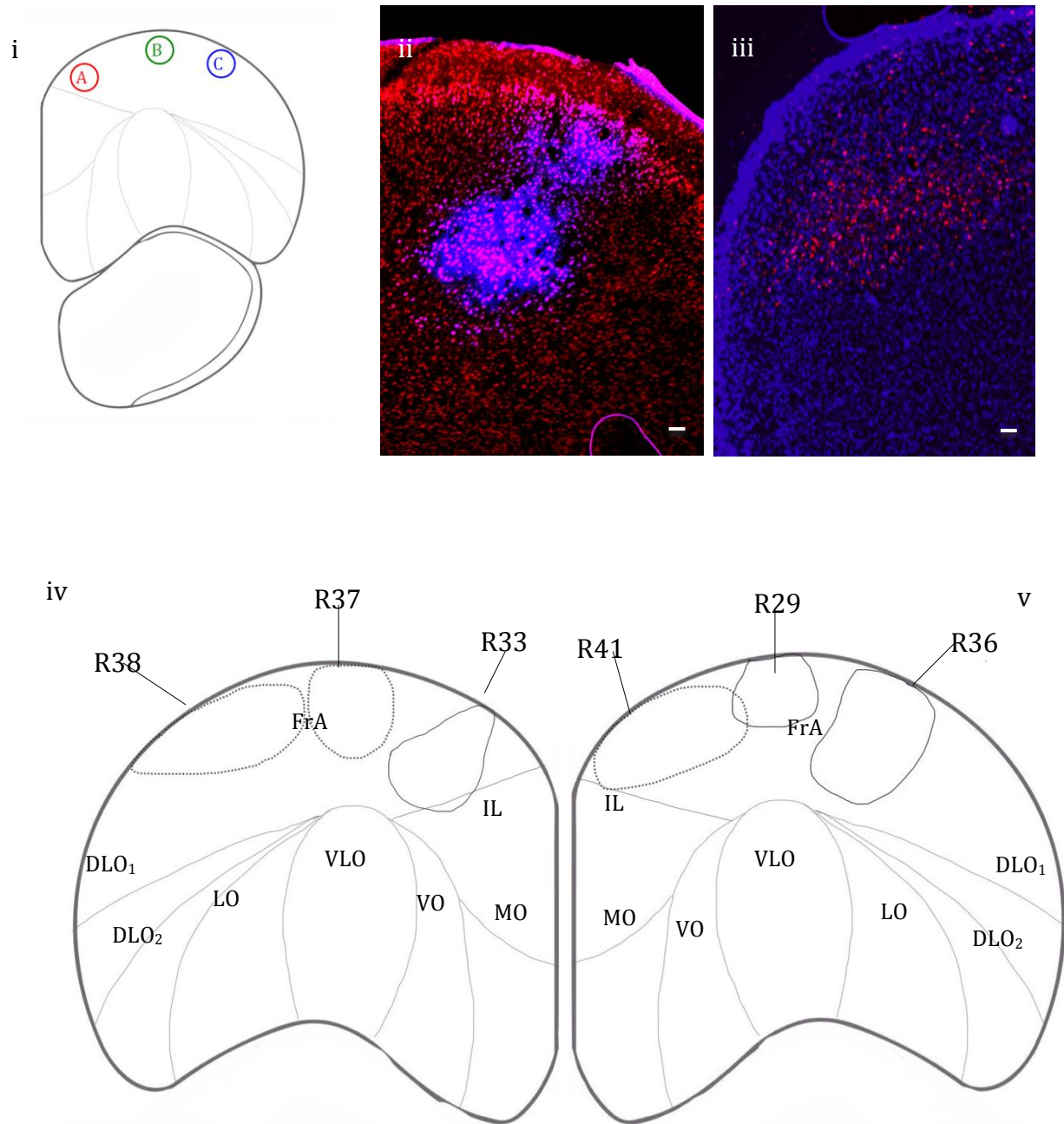


Figure 8.2. (i) Coronal section of PFC (AP 4.7mm from Bregma) showing the cytoarchitectural boundaries of the prelimbic (PL), infralimbic (IL), medial orbital (MO), ventral orbital (VO), ventrolateral orbital (VLO), lateral orbital (LO) and dorsolateral orbital (DLO) cortices (according to Van de Werd & Uylings, 2008) and FrA (according to Paxinos & Watson, 1998). (ii) Coronal section of frontal association cortex showing location and spread of (100nl) Fluoro-Gold at injection site in medial FrA (R33). (iii) Coronal section of frontal association cortex showing location and spread of (100nl) Fluoro-Ruby at injection site in lateral FrA (R38). (iv) (iv) Representations of Fluoro-Ruby (100nl) ((R37, R38) (broken line)) injection sites in central (R37) and lateral FrA (R38) and Fluoro-Gold (100nl) ((R33) solid line) injection site in medial FrA, in the right hemisphere. (v) Representations of Fluoro-

Ruby (100nl) ((R41)(broken line)) injection site in medial FrA, and Fluoro-Gold (100nl) ((R29, R36)(solid line)) injection sites in central (R29) and lateral FrA (R36), in the left hemisphere. Scale bars = 100µm.

Locations of labelling throughout the brain were observed following injections of retrograde (100nl Fluoro-Gold) and anterograde (100nl Fluoro-Ruby) into FrA (R33, R29, R36, R41, R37, R38) using fluorescent microscopy. Retrogradely labelled cells were seen in areas of temporal cortex (PRh: areas 36v, 36d) (Fig.8.3i, ii, Fig.8.4ii). Anterograde labelling was also found in temporal cortex (PRh: areas 36v, 36d, 35d) (Fig.8.3iii, Fig.8.4iii). Temporal cortex was the only area of concentrated labelling found. In order to further investigate the pathway between FrA a statistical analysis was applied to this region to determine whether there was evidence for an ordered arrangement of FrA to temporal cortex connections.

In comparison to the labelling produced by other PFC injections, labelling produced by FrA injections (both retrograde and anterograde) was much more limited (Fig.8.3), being found only in small regions of temporal cortex. This may be partially due to the smaller spread of tracers at the injection site (Fig.8.2ii, iii, iv, v). No labelling at all was found in motor or sensory cortices, in contrast to the abundant labelling seen there from other PFC connections.

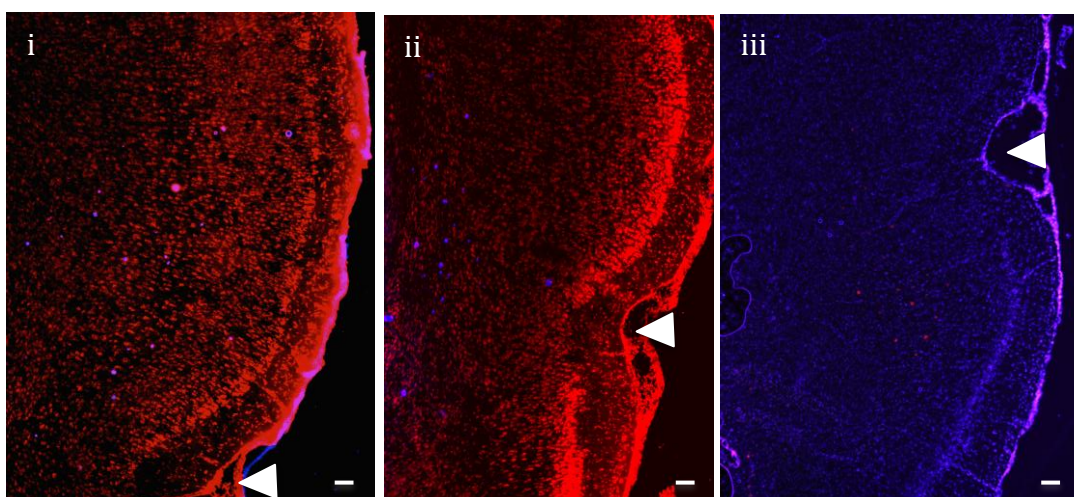


Figure 8.3. (i) Coronal section (-4.52mm from Bregma) showing retrogradely labeled cells (blue) in temporal cortex produced by injection of Fluoro-Gold (100nl) into medial FrA (injection site A:R33). (ii) Coronal section (-4.16mm from Bregma) showing retrogradely labeled cells (blue) in temporal cortex produced by injection of Fluoro-Gold (100nl) into lateral FrA (injection site C:R36). (iii) Coronal section (-4.3mm from Bregma) showing anterogradely labeled axon terminals (red) in temporal

cortex produced by injection of Fluoro-Ruby (100nl) into central FrA (injection site B:R37). Arrows denote the location of the rhinal sulcus. Scale bars = 100µm.

Organisation of Input Connections to Frontal Association Cortex from Temporal Cortex

Retrograde projections to FrA were seen in PRh (Fig.8.3i, ii, Fig.8.4ii) and areas of prefrontal cortex close to the injection site, where labelling was fairly sparse. Prefrontal labelling was not analysed due to its proximity to the injection site. The distribution of retrogradely labelled cells is seen mainly within one cytoarchitectural region (Fig.8.4ii) and maintains some spatial order in accordance with the corresponding Fluoro-Gold injection sites (medial, central and lateral). Retrograde labelling from lateral FrA is more anterior in temporal cortex to labelling from medial FrA. A factorial ANOVA revealed a significant main effect of injection site on the dorsal-ventral distance of retrogradely labeled cells from the rhinal sulcus ($F(2,29)=0.21566$ $p<0.001$ $r=0.653$). Post hoc comparisons (Tukey HSD) revealed significant differences between retrograde injection sites b*c, a*c ($p<0.001$), indicating a dorsal-ventral ordered arrangement of input projections from FrA to temporal cortex (Fig.8.5i). A factorial ANOVA also revealed a significant main effect of injection site on the medial-lateral distance of retrogradely labeled cells ($F(2,29)=53.541$ $p<0.001$ $r=0.805$). Post hoc comparisons (Tukey HSD) revealed significant differences between retrograde injection sites a*b and b*c ($p<0.001$).

The anterior-posterior data obtained from retrograde labelling violated the assumption of equality of variance for the factorial ANOVA, therefore a non-parametric alternative was applied. The Kruskal-Wallis test revealed a significant effect of FrA injection site on the anterior-posterior distance of retrogradely labeled cells from Bregma ($\chi^2(2)=31.00$ $p<0.001$). Post hoc comparisons (Mann Whitney U test) revealed significant differences between retrograde injections sites a*c and b*c ($U=0.000$ $p<0.001$). These results indicate evidence of ordering in three axes of orientation (Fig.8.5i, ii, iii).

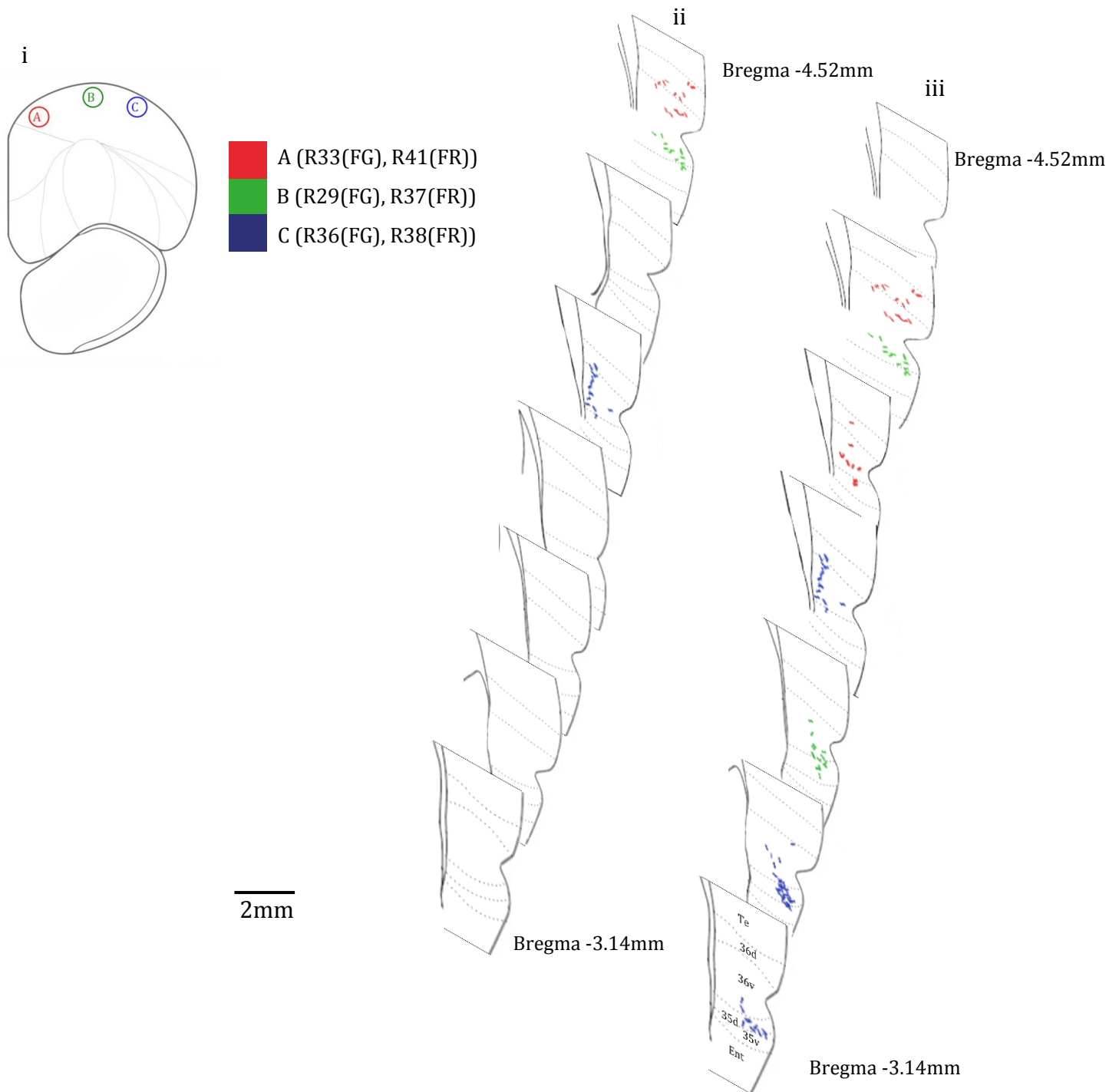


Figure 8.4. Diagram representing the injection sites of Fluoro-Gold and Fluoro-Ruby, and the projection sites to temporal cortex for both retrograde (Fluoro-Gold) and anterograde (Fluoro-Ruby) tracer injections. (i) The locations of injection sites in FrA (A:R33 & R41, B:R29 & R37, C:R36 & R38). (ii) The locations of retrogradely labelled cells in temporal cortex, resultant from 100nl Fluoro-Gold injections into FrA injection sites A (R33), B (R29) and C (R36) (iii) The locations of anterogradely labelled areas in temporal cortex, resultant from 100nl Fluoro-Ruby injections into FrA injection sites A (R41), B (R37) and C (R38).

Organisation of Output Connections from Frontal Association Cortex to Temporal Cortex

Anterograde projections to FrA were seen in PRh (Fig.8.3iii., 8.4). The distribution of anterograde labelling is seen mainly within one cytoarchitectural region (Fig.8.3iii) and maintains a spatial order in accordance with the corresponding Fluoro-Ruby injection sites in FrA (medial, central and lateral). Moving from medial to lateral in FrA, anterograde labelling in temporal cortex becomes more anterior and ventral (Fig.8.4iii). The factorial ANOVA revealed a significant main effect of FrA injection site on the anterior-posterior distance of anterogradely labeled axon terminals from Bregma ($F(2,90)=159.342$ $p<0.001$ $r=0.799$). Post hoc comparisons (Tukey HSD) revealed significant differences between anterograde injection sites a*b, a*c and b*c ($p<0.001$).

The factorial ANOVA revealed a significant main effect of injection site on the dorsal-ventral distance of anterogradely labeled axon terminals ($F(2,90)=28.405$ $p<0.001$ $r=0.490$) from the rhinal sulcus. Post hoc comparisons (Tukey HSD) revealed significant differences between anterograde injection sites a*b, b*c ($p<0.001$) and b*d ($p=0.040$).

A factorial ANOVA revealed a significant main effect of injection site on the medial-lateral distance of anterogradely labeled axon terminals ($F(2,90)=159.342$ $p<0.001$ $r=0.799$) from the cortical surface. Post hoc comparisons (Tukey HSD) revealed significant differences between anterograde injection sites a*b and a*c ($p<0.001$). These results indicate evidence for an ordered arrangement of both input and output projections from FrA to temporal cortex (Fig.8.5i,ii, iii).

In comparison to connections from PL, IL, MO, VO, VLO, LO and DLO (Chapters 2 – 7), retrograde and anterograde labelling from FrA regions was seen in a similar number of cells, covering similar areas in temporal cortex, although anterograde labelling was seen across a wider area of temporal cortex (Fig.8.4iii). Two factor ANOVAs revealed significant interaction effects between input and output connections in the dorsal-ventral ($F(2,119)=12.469$ $p<0.001$ $r=0.308$), anterior-

posterior ($F(2,119)=424.474$ $p<0.001$ $r=0.884$) and medial-lateral ($F(2,119)=95.599$ $p<0.001$ $r=0.667$) axes. This shows that the location of anterogradely and retrogradely labelled cells vary in respect to one another in three axes of orientation.

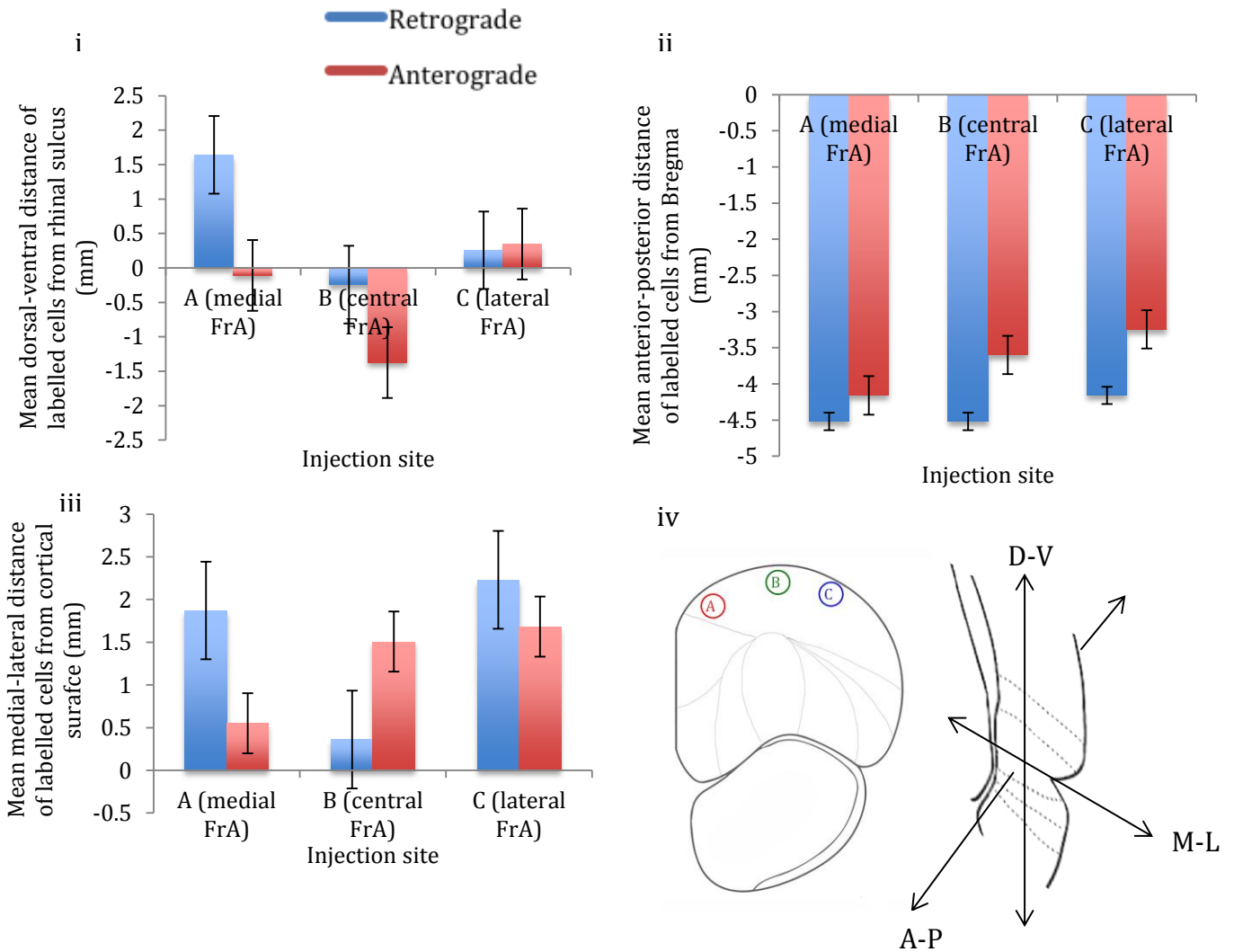


Figure 8.5. The mean effect of FrA injection site location on the mean location of retrogradely labelled cells ($n=32$: medial(R 33)=8, central(R29)=11, lateral (R36)=13) and anterogradely labeled axon terminals ($n=93$: medial (R41)=39, central (R37)=18, lateral (R38)=36) within temporal cortex, in the (i) dorsal-ventral (ii) anterior-posterior and (iii) medial-lateral axes. Error bars = standard error. (iv) Coronal cross section of PFC showing the position of 3 injection sites; medial, central and lateral FrA. Coronal cross section of temporal cortex showing the three dimensions in which the locations of labels were recorded.

The calculation of a 3 dimensional mean location (E) for the labelling produced by each retrograde and anterograde injection site,

$$E = \sqrt{(DV)^2 + (AP)^2 + (ML)^2}$$

allowed for the visualisation of the 3-dimensional locations of input and output connections in comparison to one another (Fig.8.6).

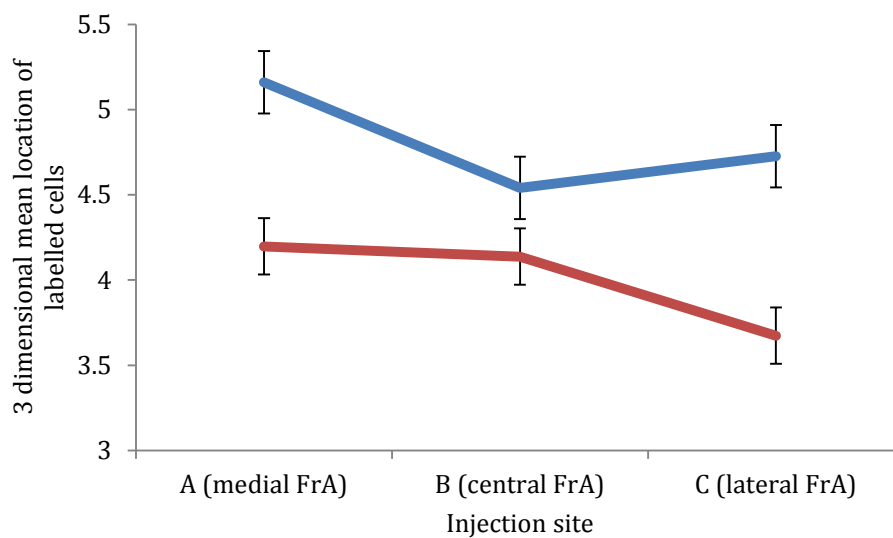


Figure 8.6. The effect of FrA injection site (medial, central and lateral FrA) on the three dimensional mean location of retrogradely labelled cells (blue) and anterogradely labelled axon terminals (red) in temporal cortex. Error bars = standard error.

The results of the analysis show that when visualized across 3 dimensions, input and output connections follow a similar order, however they occur in different places (Fig.8.6). This indicates that the ordering of inputs and outputs are overall similar, but the connections to temporal cortex from FrA are not reciprocal. The connections between FrA and PRh do not show evidence of the differential ordering seen in PFC-temporal cortex connections.

The mean distance between Fluoro-Gold and Fluoro-Ruby labelling in temporal cortex resultant from FrA injections was compared to the distances between Fluoro-

Gold and Fluoro-Ruby labelling resultant from injections into anterior, central and posterior PFC. This distance was found to be greatest for FrA (Fig.8.7).

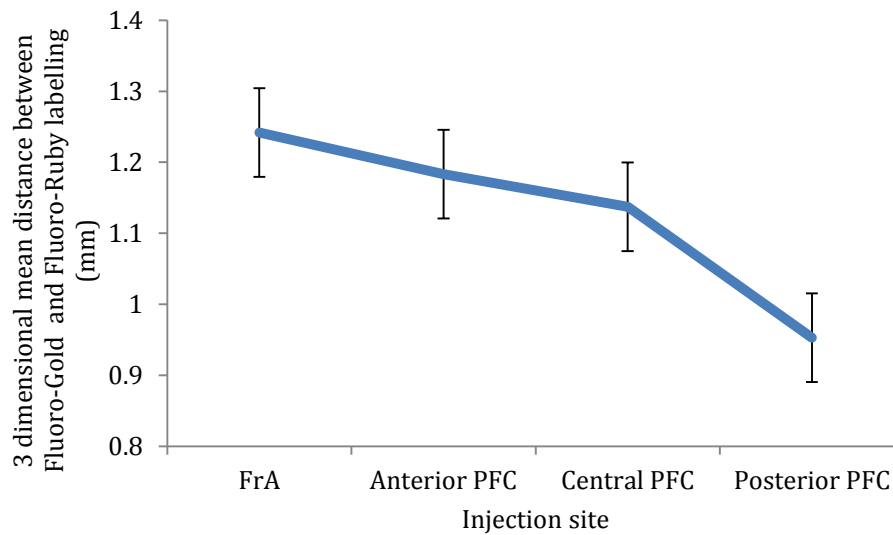


Figure 8.7. The mean distance between Fluoro-Gold and Fluoro-Ruby labelling in temporal cortex, resultant from tracer injections (100nl) into FrA, anterior regions of PL, VO, VLO & DLO, central regions of PL, VO, VLO & DLO and posterior regions of PL, VO, VLO & DLO. Note that the distance becomes greater in more anterior regions. Note that the A-P distance from Bregma of FrA and anterior PFC injection sites were equal.

When compared to connections to temporal cortex from anterior and posterior PL, VO, VLO and DLO, these results show that the distance between Fluoro-Gold and Fluoro-Ruby labelling is greatest from FrA.

These findings indicate that although input and output ordering from FrA appear much more similar to one another, in that they follow the similar order, when compared to connections from PFC to temporal cortex (Chapter 2,3 and 4) and sensory-motor cortex (Chapters 5, 6 and 7), the Fluoro-Gold and Fluoro-Ruby labelling seen here is further apart from one another. Analysis of the distance between mean locations of labels in temporal cortex (Fig.8.7) shows an increased distance in FrA compared to anterior PFC. Further investigation outside the scope of this study, with a larger number of injection sites would be required to analyse this relationship further.

Discussion

Connections from Frontal Association Cortex to Temporal Cortex

This study investigated the organisation of connections from adjacent FrA regions with the use of neuroanatomical tracers. The findings have revealed evidence for an ordered arrangement within the projections from FrA to temporal cortex. We revealed a clear ordered arrangement of FrA connections, for both inputs and outputs.

Input Connections from Temporal cortex to Frontal Association Cortex

Following the administration of the retrograde tracer, Fluoro-Gold to three FrA regions, labelling of neuronal cell bodies was observed in areas of temporal cortex (PRh). The labelling found in temporal cortex was less dense and more concentrated in a specific region to that observed from PL, VO, VLO and DLO injections.

Consistent, prominent labelling was found only in this region. Retrograde labelling in temporal cortex showed evidence of an ordered arrangement in the anterior-posterior axis. As injection sites in FrA move from medial to lateral, retrograde labelling in temporal cortex moves from posterior – anterior. This ordering is opposite to that seen in retrograde connections from VO, VLO and DLO to temporal cortex (but the same as the ordering of anterograde connections). The ordering identified here is broadly consistent with the ordering seen in the study by Hoover & Vertes (2007), in which more anterior cortical regions (anterior cingulate cortex) projected to more medial aspects of FrA.

The amount of retrograde labelling seen in temporal cortex resultant from 100nl Fluoro-Gold injections in FrA was considerably smaller than the amount of labelling seen with equivalent Fluoro-Gold injections made into PL, VO, LO and DLO (Chapter 2 and 3). The retrograde labelling seen in temporal cortex was confined to small regions of PRh and Ent, showing evidence of divergence in the circuit: temporal cortex → PFC → temporal cortex. In comparison to the pathways studied in chapters 2 – 7 (PFC – temporal cortex and PFC – sensory-motor cortex), the areas of

retrograde labelling seen here were much smaller. In contrast to PFC-temporal cortex and PFC-sensory-motor cortex connections, fewer retrograde than anterograde labels were found resultant from equivalent FrA injection sites.

The retrograde labelling (Fluoro-Gold) seen in temporal cortex was considerably more widespread than anterograde labelling (Fluoro-Ruby & BDA) in previous chapters (Chapter 2, 3 and 4). This was not the case with the labelling resultant from FrA injections. Here, Fluoro-Ruby labelling covered a much larger area in temporal cortex (anterior-posterior).

Output Connections from Frontal Association Cortex to Temporal Cortex

Following the administration of the anterograde tracer Fluoro-Ruby to three FrA regions (medial, central and lateral), anterograde labelling was observed in discrete areas of temporal cortex similar to the equivalent retrograde injections. Significant, and consistent labelling was not seen in any other major cortical region. There is clear ordering present in the anterior-posterior and dorsal-ventral axes; as injection sites move from medial to lateral in FrA, anterograde labelling in temporal cortex becomes more anterior and dorsal. Repeated ordering of output connections can be seen, specifically from central and lateral FrA injection sites (B and C) (Fig. 8.4iii). This may show evidence of fragmented mapping similar to that seen elsewhere in the cerebral cortex (Malach, 1989). The ordering seen here is the same as that seen in anterograde connections from VO, VLO and DLO – temporal cortex and is broadly consistent with the ordering of sensorimotor and limbic inputs to mPFC observed by Hoover & Vertes (2007).

Organisation and Alignment of Connections Between Frontal Association Cortex and Temporal Cortex

This study revealed a clear ordered connectivity pattern of the FrA – PRh pathway. This ordering has not been previously described in such detail. Visualisation of the labelled input and output projections from the FrA injection sites shows a clear

ordered arrangement of connections from medial to lateral. The ordered arrangement of connections is seen across FrA, however the greatest difference in labelling can be seen between medial and central regions, showing a clear difference in the connections to PRh from these two regions.

The ordering observed is similar for both inputs and outputs, demonstrating a clear difference in the organisation of FrA and the PFC regions discussed in earlier Chapters (PL, IL, MO, VO, VLO, VO, DLO). That is, input and output connections from FrA to temporal cortex show similar overall ordering as one another. When visualized in detail (Fig. 8.4), anterograde labelling (Fluoro-Ruby) appears to produce a repeating pattern of connections. This is not the case with retrograde labelling from the same FrA injection sites. Such repeated ordering may be representational of fragmented mapping similar to that described in striate cortex (Malach, 1989).

Consistent with the findings of connections to temporal cortex from VO, VLO and DLO (Chapter 2), the input and output connections labelled were not found in the same regions of temporal cortex. For both retrograde and anterograde labels, connections from lateral FrA (injection site C) are found anterior in temporal cortex compared to central and medial FrA (injection sites A and B), showing the same ordering. However, anterograde labelling from lateral FrA was seen considerably further anterior in temporal cortex compared to retrograde labelling from the same injection site in lateral FrA. Additionally, although they do show a broad consistency in location and ordering, retrograde and anterograde labelling from the same FrA injection sites was not found in the same specific cytoarchitectural region of temporal cortex. For instance, anterograde labelling from injections site C was found in PRh areas 35 and 36, whereas retrograde labelling from the same injection site was found only in area 36. The levels of reciprocity and alignment between input and output connections here is lower than that seen in connections from other PFC regions to temporal cortex (Chapters 2 and 3). Consistent with the findings described in Chapter 4, the mean distance between retrograde (Fluoro-Gold) and anterograde (Fluoro-Ruby) connections increases as injection sites become more anterior. This provides further evidence for the differential organisation of input and output connections in this pathway and an increase in distance between inputs and outputs in the most anterior regions of prefrontal cortex.

It should be noted that Fluoro-Ruby is not 100% anterograde in the labelling it produces (see Chapter 3 and Appendix F). Some of the Fluoro-Ruby labelling in temporal cortex described here may have been retrograde. However, as the level of retrograde labelling produced by Fluoro-Ruby was found to be relatively low (<30%), we can reasonably conclude that even with a 100% anterograde tracer the findings would be similar.

In conclusion, this study has shown that FrA is organised similarly to other PFC regions (VO, VLO, LO & DLO) in terms of the relationship between input and output connections. Inputs are consistently found in different regions to outputs. FrA retains properties we have come to identify with PFC connections from earlier chapters i.e. evidence of input and output connections occurring in different regions of temporal cortex. However, here the labelled input and output connections appear to follow the same overall order (although not in the same location). These findings indicate that the connections of FrA are organised in a similar way to VO, VLO, LO and DLO, and show similar properties of reciprocity as expected from previous chapters (Chapter 2 and 3). Additionally, these findings show evidence of similar ordering between inputs and outputs, however it remains clear that they show differential organisation.

Chapter 9.

Discussion

The studies carried out here have described the detailed ordered connections from the sub-regions of prefrontal cortex, in two distinct pathways. The findings have shown evidence for clear ordering of both input and output connections to areas of temporal and sensory-motor cortex. In addition to this, complex relationships between input and output connections have been revealed, in both of these pathways, which has not been previously described in such detail. The ordered connections from frontal association cortex to temporal cortex have also been revealed, along with how these differ in terms of organisation.

Organisation of Prefrontal Cortex – Temporal Cortex Connections

The investigation of the connections from PFC (PL, VO, VLO, LO, DLO) to temporal cortex (PRh, Ent, Te) consistently revealed a clear ordered arrangement of both input and output connections from VO-DLO. This ordered connectivity was broadly consistent with the findings of previous studies (Kondo & Witter, 2014; Sesack, 1989; Berendse, 1992; Schilman, 2008; Olsen & Musil, 1992), particularly the ordered output connections from PFC in the dorsal-ventral axis described by Hoover & Vertes (2011) and ordered connections from mPFC to areas of temporal cortex (Conde et al, 1995). The findings of ordered connectivity from PFC – temporal cortex are consistent with existing evidence for functional mapping in temporal regions (Boussaoud et al, 1991; De Beek et al, 2008; Hafting et al, 2005; Killian et al, 2012), this may indicate that it is functionally important to preserve an ordered arrangement in terms of connections linking these two regions. These studies revealed additional organisational properties, in terms of ordering and the relationship between inputs and outputs, previously undescribed.

The ordering of input and output connections identified here were found to differ compared to one another in terms of ordering, and were found to show little reciprocity (with the exception of PL). These properties were reliably reproduced with various tracers (BDA, Fluoro-Ruby, Fluoro-Emerald) and methods (Brightfield, Darkfield, fluorescence). There is current evidence of differential ordering in cortical connections (Flaherty & Graybiel, 1994), however this is not a property which has been investigated in great detail until now.

Reciprocity of cortical connections is a recurring characteristic throughout the brain, said to be a hallmark feature of physiological and anatomical organisation, and has been described throughout the cerebral cortex (Wang et al, 2006; Cantone et al, 2005; Agster & Burwell, 2009; Nascimento-Silva et al, 2014). Based on this, the high degree of non-reciprocal connections found between PFC and temporal cortex was a surprising observation. However, Haber (2003), described non-reciprocal connections between regions associated with different basal ganglia circuits. Haber stated that within primate basal ganglia networks there are both reciprocal and non-reciprocal connections between regions with similar functions, many of which involved PFC. This may be a recurring property throughout the cortex; Haber (2003) concluded that similarly functioning regions are connected by reciprocal connections and regions with greatly differing functions are connected with non-reciprocal connections, or a combination of reciprocal and non-reciprocal connections. This is consistent with findings of reciprocal connectivity between PL and temporal regions. Similar observations of reciprocal connections have been made elsewhere in the cortex, often between areas holding similar functions. For example, S1 & S2 (Henry & Catania, 2006; Aronoff et al, 2010) and M1 & S1 (Porter & White, 1983; Aronoff et al, 2010).

The findings of PFC – temporal cortex connections consistently showed far greater reciprocity of connections from PL (medial PFC) compared to other PFC regions (VO, VLO, LO, DLO). The reciprocity observed between PL and temporal cortex is consistent with previous findings showing that connections between temporal cortex and PFC are highly reciprocal (Agster & Burwell, 2009). The findings from VO, VLO, LO and DLO are consistent with findings from the same study (Agster & Burwell, 2009) that temporal connections are not always clearly aligned. Based on the

proposition by Haber (2003) that cortical regions with similar functions are highly reciprocal, whereas those with greatly different functions are not reciprocal, this finding suggests that PL/IL is much closer in terms of function to PRh, Ent and Te than VO, VLO, LO and DLO are. Previous studies have identified distinct functions in orbital PFC regions (Schoenbaum & Esber, 2010; Schoenbaum & Roesch, 2005) compared to mPFC (Vertes, 2006; Narayanan & Laubach, 2006; Kim et al 2013), providing further evidence to suggest they may be connected differently. This could mean that VO, VLO, LO and DLO carry out more abstract processing than PL/IL. This gives further evidence to suggest PL/IL forms part of a different PFC – temporal cortex circuit to VO, VLO, LO and DLO. The retrograde properties of Fluoro-Ruby should be considered in the interpretation of reciprocity. It is possible that a large number of Fluoro-Ruby labels identified in PL were retrograde, which would result in an over estimation of reciprocity. The possibility exists that with total anterograde labelling from Fluoro-Ruby the same level of reciprocity would not have been observed in PL. However, this could equally be the case in the connections observed from other PFC sub-regions (VO, VLO, DLO) where a much lower level of reciprocity was seen.

The analysis shows that input and output connections from PFC to temporal cortex (specifically from VO, VLO and DLO) become more similar to one another, in terms of their location, as PFC injection sites become more posterior, producing an organisational gradient. In addition to a change in ordering from anterior to posterior PFC, evidence of a gradient increase in alignment between inputs and outputs to temporal cortex from anterior to posterior PFC has been revealed. That is, labelled inputs and outputs from the same PFC injection sites became closer to one another in temporal cortex as PFC injection sites became more posterior. This organisational gradient provides further evidence of a change in connectional, and therefore also functional organisation from anterior to posterior PFC. Anterior regions of PFC are known to be associated with more abstract processes than posterior regions. Christoff (2009) identified a similar organisational gradient to that described here, in terms of levels of abstraction (abstraction increases from posterior to anterior). Based on the observations of Haber (2003), this means that posterior PFC is more similar to temporal cortex (PRh, Ent and Te) in terms of function than anterior PFC. Our findings are similar to the findings of organisation described by Haber (2003).

By examining the connections from PFC to temporal cortex across a wide area of PFC (from anterior (-4.7mm from Bregma) to posterior (-3.7mm from Bregma)), further evidence for the ordered arrangement of connections in this pathway has been provided, as well as non-reciprocal and differentially ordered inputs and outputs. The analysis of the input and output connections from anterior, central and posterior regions of PFC to temporal cortex revealed similar ordering in the anterior and central regions. Clear ordering was also found in the posterior region of PFC, however the ordering here differed to that observed in more anterior areas. Anterior PFC is known to be involved in different processes to posterior regions of PFC, this change in ordering may be a reflection of change in function between anterior and posterior regions of PFC, described in previous studies (Ramnani & Owen, 2004; Kolb, 1984; Neafsey, 1990; Schoenbaum & Esber, 2010; Narayanan & Laubach, 2006; Vertes, 2006; Kim et al 2013) and suggested by Taren (2011) to be representational of a dynamic processing ability and a level of adaptability in PFC function.

Organisation of Prefrontal Cortex – Sensory-Motor Cortex Connections

The connections identified between PFC and sensory-motor cortex showed similar organisational properties to those described in the PFC – temporal cortex pathway. However, this investigation also produced some unique observations, showing that not all PFC connections are organised in the same way.

The investigation of the connections from PFC (PL, VO, VLO, LO, DLO) to sensory-motor cortex (Cg1, M1, M2, S1J) consistently revealed a clear ordered arrangement of both input and output connections from VO-DLO (medial-lateral), this was seen in multiple axes of orientation. The ordering of input and output connection seen here were found to differ to one another, showing evidence of differential ordering similar to that seen in temporal cortex. These properties were reliably reproduced with various tracers (BDA, Fluoro-Ruby, Fluoro-Emerald) and methods (Brightfield, fluorescence).

In addition to ordering of inputs and outputs, an unusual circuit was observed when viewed in terms of a traditional model of hierarchical organisation (Fuster, 2001; Botvinick, 2008). Our studies consistently identified direct connections from S1 → PFC, which would not be expected from a traditional view of information flow (i.e. sensory cortex → higher sensory cortex → association cortex → PFC → secondary motor cortex → motor cortex). The meaning of this connection is not yet clear, however the knowledge of its existence may provide an important insight into the overall organisation of PFC.

The analysis revealed part of this circuit to show laminar organisation (VO & LO). Ordered laminar organisation has been described elsewhere in the cerebral cortex (Insausti and Amaral, 2008) as well as between PFC and motor, limbic and subcortical regions (Gabbott et al, 2005). The clear laminar organisation between VO and LO was consistently seen in multiple experiments. The laminar organisation was only seen in PFC → sensory-motor cortex (and only in specific sites), such ordering was not seen in temporal cortex connections, this could mean that in terms of PFC, laminar organisation is a specific feature of PFC – sensory-motor cortex circuit.

Although there was an overall lack of reciprocity of connections on a fine scale (as with PFC – temporal cortex), the findings show evidence of reciprocal connections between PFC and M2. A large degree of fine scale reciprocity was seen in the connections from PL to M2 and Cg1, this is very different to the labelling seen of connections from VO, VLO and DLO, which shows inputs and outputs in different locations. This gives further evidence to confirm PL and IL as part of a separate network to VO, VLO, LO and DLO.

Connectional studies of primary sensory (S1) and primary motor cortex (M1) often report reciprocity of connections (Dinopoulos, 1994; Lee et al 2011), in that inputs and outputs occupy the same precise locations. This has been described between S1 and S2 (Henry & Catania, 2006; Aronoff et al, 2010), M1 and S1 (Porter & White, 1983; Aronoff et al, 2010) and M1 and S2 (Porter & White, 1983). The same study by Porter and White reported non-reciprocal connections from M1 to the striatum, indicating that motor cortex input and output connections are not always found in the

same locations. Haber (2003) showed that areas with similar functions display high degrees of reciprocity, whereas cortical regions differing greatly in function do not possess many reciprocal connections. Based on this, the results described in both the PFC – sensory-motor cortex and PFC-temporal cortex pathway indicate that PL has functional similarities with both M2 and PRh, whereas VO, VLO, LO and DLO are not functionally similar to either region.

Previous studies suggest the reciprocity of input and output connections to be common (Suzuki & Amaral, 1994; Canto et al, 2008) and recent tracer studies have not shown evidence of non-alignment such as that described here (Kim & Lee, 2012; Takahara et al, 2012). However, these findings report PFC connectivity on a relatively large scale and from specific sub-regions and Haber's (2003) observations of differences in reciprocity imply that differences in alignment must also occur. Recent fine scale tracer findings (Nascimento-Silva et al, 2014) show clear reciprocity in V2 and V4, in which the area of labelled inputs and outputs were consistently found together. Although, on a fine scale, similar to the findings in PFC, the results of this study show that not all input projections had a reciprocal output projection. However, input and output connections were consistently centred on the same location. It is suggested that topographic alignment of inputs and outputs is vital for visual attention (Tootell et al, 1998), therefore we might expect the complex cognitive functions associated with PFC to also be dependent on the anatomical alignment of input and output connections. The findings across PFC (anterior-posterior) may indicate that PFC complex functioning is dependent on the differential ordering of inputs and outputs.

The gradient of alignment identified from anterior to posterior PFC (in both temporal and sensory-motor cortex pathways) provides an important insight into PFC anatomical organisation. The findings of this study, combined with functional observations of increased abstraction in anterior regions of PFC, indicate evidence for an association between abstract processing and non-aligned input and output connections. It is reasonable to suggest that complex abstract processes, such as executive functions, require input and output connections within PFC circuits to be ordered differently to one another, i.e. outputs from PFC → other cortical regions need

to send back inputs to a different region of PFC. This shows that although there are clear differences in the function and anatomy of different PFC sub-regions, it is necessary for them to work together as part of the overall cortical circuits. This may be a result of each individual area of PFC being highly specialised. The specialisation of every area is needed simultaneously to carry out a specific complex task.

The detailed and fine scale analysis of PFC – sensory-motor cortex connections enabled us to reveal organisational properties which have not previously been described. The fine scale analysis (chapter 7) revealed evidence for two possible overlapping connectivity maps within the PFC – sensory-motor cortex pathway.

Organisation of Frontal Association Cortex – Temporal Cortex Connections

The investigation of the connections from frontal association cortex to temporal cortex (PRh) revealed a clear ordered arrangement of both input and output connections from medial to lateral FrA. The ordering of input and output connections were found to be similar to one another, however they showed a further decrease in alignment and reciprocity than the connections seen in anterior PFC (PL, VO, VLO, LO, DLO) – temporal cortex pathway. Although connections from FrA clearly showed more similarities in the ordering of input and output connections when compared to VO, VLO, LO and DLO, the detailed analysis revealed differentiation between the 3-dimensional organisation of anterograde and retrograde labels in temporal cortex. This shows that frontal association cortex is organised in a similar way to other PFC regions, and continues the organisational gradient from posterior-anterior in terms of the relationship between inputs and outputs locations.

Conclusions

To conclude, the studies presented here have described in detail the ordered connections of three previously little understood pathways. The ordered PFC connections shown here provide clear evidence of a complex and fine scale organisational pattern different to that described in other cortical regions (e.g visual,

sensory and motor cortex). The analyses show that the organisation of PFC connections is more complex than previously understood, specifically in terms of the relationship between input and output connections.

Based on the analysis of the tracers used, it is important to note that the interpretation of the findings described in these studies is to some extent compromised by the bi-directional properties of anterograde tracers. Without a 100% anterograde tracer being available, it is not yet possible to visualise entirely anterograde labelling.

The organisational relationships between input and output connections revealed here, both in the PFC – temporal cortex and PFC – sensory-motor cortex pathway indicate an important effect of anterior-posterior PFC on reciprocity and alignment of connections. Based on functional findings of abstract processing (specifically the gradient in abstraction identified in humans by Christoff (2009)), it is reasonable to suggest that this change in organisation is an underlying cause of the change in complex processing. It is not yet clear why the anatomical organisation of connections changes with the complexity of processing/abstraction, however this provides an important insight into the structure and ultimately the organisation of function in PFC.

In summary, this project has revealed that the organisation of PFC connections changes from anterior to posterior, in two different PFC pathways. It has also demonstrated patterns of organisation in PFC connections that differ greatly to other complex cortical regions; non-reciprocal and non-aligned connections are consistently seen in PFC connections. The findings described here have identified distinct differences in how connections from PFC to different cortical regions are ordered. Further to this, the results have shown that the frontal association area shows similarities with PFC organisation. The significance of the organisational properties described here is not yet clear, however the increased understanding of prefrontal connectivity gained by these findings will provide a basis on which to build further investigations into anatomical organisation, and ultimately functional organisation.

References

- Adrianov, O. S. (1978). Principles of organization of cerebral functions. printsipakh organizatsii tserebral'nykh funktsii. Vestnik Akademii Meditsinskikh Nauk SSSR,(12), 12-20.
- Agster, K. L., and Burwell, R. D. (2009). Cortical efferents of the perirhinal, postrhinal, and entorhinal cortices of the rat. *Hippocampus*, 19(12), 1159-1186.
- Albright, T.D., and Desimone, R. (1987). Local precision of visuotopic organization in the middle temporal area (MT) of the macaque. *Experimental brain research. Experimentelle Hirnforschung* 65, 582-92.
- Alexander, G.E., DeLong, M.R. and Strick, P. (1986). Parallel organization of functionally segregated circuits linking basal ganglia and cortex *Ann. Rev. Neuroscience*, 9, 357–381
- Alvarez, J. A., and Emory, E. (2006). Executive function and the frontal lobes: A meta-analytic review. *Neuropsychology Review*, 16(1), 17-42.
- Angevine, J. B., Jr. (1970). Time of neuron origin in the diencephalon of the mouse. an autoradiographic study. *The Journal of Comparative Neurology*, 139(2), 129-187.
- Arcaro, M. J., McMains, S. A., Singer, B. D., and Kastner, S. (2009). Retinotopic organization of human ventral visual cortex. *The Journal of Neuroscience : The Official Journal of the Society for Neuroscience*, 29(34), 10638-10652.
- Aronoff, R., Matyas, F., Mateo, C., Ciron, C., Schneider, B., and Petersen, C. C. (2010). Long-range connectivity of mouse primary somatosensory barrel cortex. *The European Journal of Neuroscience*, 31(12), 2221-2233.
- Averbeck, B. B., and Seo, M. (2008). The statistical neuroanatomy of frontal networks in the macaque. *PLoS Computational Biology*, 4 (4).
- Barbas, H.S., Saha, S., Rempel-Clower, N., Ghashghaei, T. (2003). Serial pathways from primate prefrontal cortex to autonomic áreas may influence emotional expression. *BMC Neuroscience*, 4, 25.
- Bedwell, S.A., Billett, E.E., Crofts, J.J. and Tinsley, C.J. (2014). The topology of connections between rat prefrontal, motor and sensory cortices. *Frontiers in Systems Neuroscience*, 8, 177.
- Berendse, H. W., Galis-de Graaf, Y., and Groenewegen, H. J. (1992). Topographical organization and relationship with ventral striatal compartments of prefrontal corticostriatal projections in the rat. *The Journal of Comparative Neurology*, 316(3), 314-347.
- Botvinick, M. M. (2008). Hierarchical models of behavior and prefrontal function. *Trends in Cognitive Sciences*, 12, 201–208.

Brodmann, K. (1909). Beschreibung der einzelnen hirnarten IV. kapitel in vergleichende lokalisationslehre der grosshirnrinde [localisation in the cerebral cortex : The principles of comparative localisation in the cerebral cortex based on the cytoarchitectonics]. leipzig: Verlag von johann ambrosias barth. [Brodmann's Localisation in the cerebral cortex : the principles of comparative localisation in the cerebral cortex based on the cytoarchitectonics]

Brodmann, K. (1912). Neue Ergebnisse über die vergleichende histologische Localisation der Grosshirnrinde mit besonderer Berücksichtigung des Stirnhirns in Anatomischer Anzeiger, Supplement 41, 1912, pp. 157–216.

Bullmore, E., and Sporns, O. (2009). Complex brain networks: Graph theoretical analysis of structural and functional systems. *Nature Reviews Neuroscience*, 10(3), 186-198.

Bunce, J. G., Zikopoulos, B., Feinberg, M., and Barbas, H. (2013). Parallel prefrontal pathways reach distinct excitatory and inhibitory systems in memory-related rhinal cortices. *The Journal of Comparative Neurology*, 521(18), 4260-4283.

Burton, H., and Kopf, E. M. (1984). Ipsilateral cortical connections from the second and fourth somatic sensory areas in the cat. *The Journal of Comparative Neurology*, 225(4), 527-553.

Burwell, R.D. (2001). Borders and cytoarchitecture of the perirhinal and postrhinal cortices in the rat. *J Comp Neurol*.437 (1) 17-41.

Buzsaki, G., and Draguhn, A. (2004). Neuronal oscillations in cortical networks. *Science* (New York, N.Y.), 304(5679), 1926-1929.

Canto, C. B., Wouterlood, F. G., and Witter, M. P. (2008). What does the anatomical organization of the entorhinal cortex tell us? *Neural Plasticity*, 2008, 381243.

Christoff, K., Keramiatian, K., Gordon, A. M., Smith, R., and Madler, B. (2009). Prefrontal organization of cognitive control according to levels of abstraction. *Brain Research*, 1286, 94-105.

Chudasama, Y., and Robbins, T. W. (2003). Dissociable contributions of the orbitofrontal and infralimbic cortex to pavlovian autoshaping and discrimination reversal learning: Further evidence for the functional heterogeneity of the rodent frontal cortex. *The Journal of Neuroscience : The Official Journal of the Society for Neuroscience*, 23(25), 8771-8780.

Cohen, J. D., Barch, D. M., Carter, C., and Servan-Schreiber, D. (1999). Context-processing deficits in schizophrenia: Converging evidence from three theoretically motivated cognitive tasks. *Journal of Abnormal Psychology*, 108(1), 120-133.

Conde F, Maire-Lepoivre E, Audinat E and Crepel F (1995). Afferent connections of the medial frontal cortex of the rat. II. Cortical and subcortical afferents. *Journal of Comparative Neurology*, 352 (4) 567-593.

Coq, J. O., Qi, H., Collins, C. E., and Kaas, J. H. (2004). Anatomical and functional organization of somatosensory areas of the lateral fissure of the new world titi monkey (*callicebus moloch*). *The Journal of Comparative Neurology*, 476(4), 363-387.

Courchesne, E., Mouton, P. R., Calhoun, M. E., Semendeferi, K., Ahrens-Barbeau, C., Hallet, M. J., Pierce, K. (2011). Neuron number and size in prefrontal cortex of children with autism. *JAMA : The Journal of the American Medical Association*, 306(18), 2001-2010.

Courtney, S.M., Laurent, P., Haxby, J.V. and Ungerleider, L.G. (1998). The role of prefrontal cortex in working memory: examining the contents of consciousness. *Philos Trans R Soc Lond B Biol Sci*, 353 (1377).

Dinopoulos, A. (1994). Reciprocal connections of the motor neocortical area with the contralateral thalamus in the hedgehog (*Erinaceus europaeus*) brain. *Eur. J. Neuroscience*, 6, 374-380.

Duncan, J. (2001). An adaptive coding model of neural function in prefrontal cortex. *Nature Reviews. Neuroscience*, 2(11), 820-829.

Felleman, D.J. and Van Essen, D.C. (1991). Distributed hierarchical processing in the primate cerebral cortex. *Cerebral Cortex*, 1, 1-47.

Flaherty, A. W., and Graybiel, A. M. (1994). Input-output organization of the sensorimotor striatum in the squirrel monkey. *The Journal of Neuroscience : The Official Journal of the Society for Neuroscience*, 14(2), 599-610.

Fujita, S., Koshikawa, N., and Kobayashi, M. (2011). GABA(B) receptors accentuate neural excitation contrast in rat insular cortex. *Neuroscience*, 199, 259-271.

Funahashi, S., Bruce, C. J., and Goldman-Rakic, P. S. (1989). Mnemonic coding of visual space in the monkey's dorsolateral prefrontal cortex. *Journal of Neurophysiology*, 61(2), 331-349.

Furuyashiki, T., and Gallagher, M. (2007). Neural encoding in the orbitofrontal cortex related to goal-directed behavior. *Annals of the New York Academy of Sciences*, 1121, 193-215.

Fuster, J. M. (1999). Synopsis of function and dysfunction of the frontal lobe. *Acta Psychiatrica Scandinavica. Supplementum*, 395, 51-57.

Fuster JM, Bodner M, Kroger JK (May 2000). Cross-modal and cross-temporal association in neurons of frontal cortex. *Nature*, 405 (6784): 347-51.

Fuster, J. M. (2001). The prefrontal cortex – an update: time is of the essence. *Neuron*, 30, 319-333.

Fuster, Joaquin M. (2008). *The Prefrontal Cortex* (4th ed.). Boston: Academic Press. ISBN 0-12-373644-7.

Fuster, J. M. (1990) Behavioral electrophysiology of the prefrontal cortex of the primate. *Progress in brain research*, 313-323.

Fryszak, R.J. and Neafset, E.J. (1994). The effect of medial frontal cortex lesions on cardiovascular condition emotional responses in the rat. *Brain Research*, 643, 181-193.

Gabbott, P. L., Warner, T. A., Jays, P. R., Salway, P., and Busby, S. J. (2005). Prefrontal cortex in the rat: Projections to subcortical autonomic, motor, and limbic centers. *The Journal of Comparative Neurology*, 492(2), 145-177.

Gallagher, M., McMahan, R. W., and Schoenbaum, G. (1999). Orbitofrontal cortex and representation of incentive value in associative learning. *The Journal of Neuroscience : The Official Journal of the Society for Neuroscience*, 19(15), 6610-6614.

Gattass, R., Nascimento-Silva, S., Soares, J. G., Lima, B., Jansen, A. K., Diogo, A. C., Fiorani, M. (2005). Cortical visual areas in monkeys: Location, topography, connections, columns, plasticity and cortical dynamics. *Philosophical Transactions of the Royal Society of London. Series B, Biological Sciences*, 360(1456), 709-731.

Gehring, W. J., and Willoughby, A. R. (2002). The medial frontal cortex and the rapid processing of monetary gains and losses. *Science (New York, N.Y.)*, 295(5563), 2279-2282.

Goldman-Rakic, P.S. (1996). The prefrontal landscape: implications of functional architecture for understanding human mentation and the central executive. *Philosophical Transactions of the Royal Society of London. Series B, Biological Sciences* 351 (1346): 1445–5

Goldman-Rakic, Patricia S. (1995). Architecture of the Prefrontal Cortex and the Central Executive. *Annals of the New York Academy of Sciences* 769: 71–83.

Goldman-Rakic, P. S. (1991). “Prefrontal cortical dysfunction in schizophrenia: the relevance of working memory,” in *Psychopathology and the Brain*. Anonymous, (New York: Raven Press), 1–23.

Goldman-Rakic, P. S. (1990). Cellular and circuit basis of working memory in prefrontal cortex of nonhuman primates. *Progress in Brain Research*, 325-336.

Goldman-Rakic, P. S. (1988). Topography of cognition: Parallel distributed networks in primate association cortex. *Annual Review of Neuroscience*, 11, 137-156.

Hafting, T., Fyhn, M., Molden, S., Moser, M. B., and Moser, E. I. (2005). Microstructure of a spatial map in the entorhinal cortex. *Nature*, 436(7052), 801-806.

Hagler, D. J., Jr, Riecke, L., and Sereno, M. I. (2007). Parietal and superior frontal visuospatial maps activated by pointing and saccades. *Neuroimage*, 35(4), 1562-1577.

Hagler, D. J., Jr, and Sereno, M. I. (2006). Spatial maps in frontal and prefrontal cortex. *Neuroimage*, 29(2), 567-577.

He, S. Q., Dum, R. P., and Strick, P. L. (1995). Topographic organization of corticospinal projections from the frontal lobe: Motor areas on the medial surface of the hemisphere. *The Journal of Neuroscience : The Official Journal of the Society for Neuroscience*, 15(5 Pt 1), 3284-3306.

Hebb, D. O. (1949). *The Organization of Behavior: A Neuropsychological Theory*. New York: Wiley and Sons. ISBN 9780471367277.

Heidbreder, C. A., and Groenewegen, H. J. (2003). The medial prefrontal cortex in the rat: Evidence for a dorso-ventral distinction based upon functional and anatomical characteristics. *Neuroscience and Biobehavioral Reviews*, 27(6), 555-579.

Heider, B., Jando, G., and Siegel, R. M. (2005). Functional architecture of retinotopy in visual association cortex of behaving monkey. *Cerebral Cortex (New York, N.Y.: 1991)*, 15(4), 460-478.

Henry, E. C., and Catania, K. C. (2006). Cortical, callosal, and thalamic connections from primary somatosensory cortex in the naked mole-rat (*heterocephalus glaber*), with special emphasis on the connectivity of the incisor representation. *The Anatomical Record. Part A, Discoveries in Molecular, Cellular, and Evolutionary Biology*, 288(6), 626-645.

Holmes, A., and Wellman, C.L. (2009). Stress-induced prefrontal reorganization and executive dysfunction in rodents. *Neuroscience and Biobehavioral Reviews*, 33, 773-783.

Honey, C.J., Kotter, R., Breakspear, M. and Sporns, O. (2007). Network structure of cerebral cortex shapes functional connectivity on multiple time scales. *Proceedings of the National Academy of Sciences, USA*, 104, 10240-10245.

Honey, C. J., Thivierge, J. P., and Sporns, O. (2010). Can structure predict function in the human brain? *Neuroimage*, 52(3), 766-776.

Hoover, W. B., and Vertes, R. P. (2007). Anatomical analysis of afferent projections to the medial prefrontal cortex in the rat. *Brain Structure and Function*, 212(2), 149-179.

Honey, C. J., Thivierge, J. P., and Sporns, O. (2010). Can structure predict function in the human brain? *Neuroimage*, 52(3), 766-776.

Hoover, W. B., and Vertes, R. P. (2011). Projections of the medial orbital and ventral orbital cortex in the rat. *The Journal of Comparative Neurology*, 519(18), 3766-3801.

Insausti, R., and Amaral, D. G. (2008). Entorhinal cortex of the monkey: IV. topographical and laminar organization of cortical afferents. *The Journal of Comparative Neurology*, 509(6), 608-641.

Johnson, M.K., Raye, C.L., Mitchell K.J., Greene E.J. and Anderson, A.W. (2003). fMRI evidence for an organization of prefrontal cortex by both type of process and type of information. *Cerebral Cortex*, 13, 265-273.

Just, M. A., Carpenter, P. A., Keller, T. A., Emery, L., Zajac, H., and Thulborn, K. R. (2001). Interdependence of nonoverlapping cortical systems in dual cognitive tasks. *Neuroimage*, 14(2), 417-426.

Kaas, J. H., (1997). Topographic Maps are Fundamental to Sensory Processing. *Brain Research Bulletin*, 44(2): 107-112.

Kargo, W. J., Szatmary, B., and Nitz, D. A. (2007). Adaptation of prefrontal cortical firing patterns and their fidelity to changes in action-reward contingencies. *The Journal of Neuroscience : The Official Journal of the Society for Neuroscience*, 27(13), 3548-3559.

Kastner, S., DeSimone, K., Konen, C. S., Szczepanski, S. M., Weiner, K. S., and Schneider, K. A. (2007). Topographic maps in human frontal cortex revealed in memory-guided saccade and spatial working-memory tasks. *Journal of Neurophysiology*, 97(5), 3494-3507.

Kesner, R. P., and Gilbert, P. E. (2007). The role of the agranular insular cortex in anticipation of reward contrast. *Neurobiology of Learning and Memory*, 88, 82-86.

Killian, N.J., Jutras, M.J., and Buffalo, E.A. (2012). A map of visual space in the primate entorhinal cortex. *Nature*, 491, 761-764.

Kim, J., Ghim, J. W., Lee, J. H., and Jung, M. W. (2013). Neural correlates of interval timing in rodent prefrontal cortex. *The Journal of Neuroscience : The Official Journal of the Society for Neuroscience*, 33(34), 13834-13847.

Kim, U., Lee, T. (2012). Topography of descending projections from anterior insular and medial prefrontal regions to the lateral habenula of the epithalamus in the rat. *European Journal of Neuroscience*, 35, 1253-1269.

Klein, J. C., Rushworth, M. F., Behrens, T. E., Mackay, C. E., de Crespigny, A. J., D'Arceuil, H., and Johansen-Berg, H. (2010). Topography of connections between human prefrontal cortex and mediodorsal thalamus studied with diffusion tractography. *Neuroimage*, 51(2), 555-564.

Kolb, B. (2007) Do all mammals have prefrontal cortex? In *Evolution of nervous systems: Mammals*. New York. Academic Press. 443-50

Kolb B. (1984). Functions of the frontal cortex of the rat: a comparative review. *Brain Research*, 320: 1: 65-98.

Kondo, H., and Witter, M. P. (2014). Topographic organization of orbitofrontal projections to the parahippocampal region in rats. *The Journal of Comparative Neurology*, 522(4), 772-793.

Lee, T., Alloway, K.D. and Kim, U. (2011). Interconnected cortical networks between primary and somatosensory cortex septal columns and posterior parietal cortex in rat. *The Journal of Comparative Neurology*, 519, 405-419

Lemon, R. N. (2008). An enduring map of the motor cortex. *Experimental Physiology*, 93(7), 798-802.

Leonard, C. M. (1969). The prefrontal cortex of the rat. I. cortical projection of the mediodorsal nucleus. II. efferent connections. *Brain Research*, 12(2), 321-343.

Malach, R. (1989). Patterns of connections in rat visual cortex. *The Journal of Neuroscience*, 9(11), 3741-3752.

Maunsell, J. H., and van Essen, D. C. (1983). The connections of the middle temporal visual area (MT) and their relationship to a cortical hierarchy in the macaque monkey. *The Journal of Neuroscience : The Official Journal of the Society for Neuroscience*, 3(12), 2563-2586.

- McFarland, N. R., and Haber, S. N. (2002). Thalamic relay nuclei of the basal ganglia form both reciprocal and nonreciprocal cortical connections, linking multiple frontal cortical areas. *The Journal of Neuroscience : The Official Journal of the Society for Neuroscience*, 22(18), 8117-8132.
- McAlonan, K., and Brown, V. J. (2003). Orbital prefrontal cortex mediates reversal learning and not attentional set shifting in the rat. *Behavioural Brain Research*, 146, 97–103.
- Merzenich, M. M., Knight, P. L., and Roth, G. L. (1975). Representation of cochlea within primary auditory cortex in the cat. *Journal of Neurophysiology*, 38(2), 231-249.
- Miller, E. K., and Cohen, J. D. (2001). An integrative theory of prefrontal cortex function. *Annual Review of Neuroscience*, 24, 167-202.
- Miller, E. K., Freedman, D. J., and Wallis, J. D. (2002). The prefrontal cortex: Categories, concepts and cognition. *Philosophical Transactions of the Royal Society of London. Series B, Biological Sciences*, 357(1424), 1123-1136.
- Miller, M. W., and Vogt, B. A. (1984). Direct connections of rat visual cortex with sensory, motor, and association cortices. *The Journal of Comparative Neurology*, 226(2), 184-202.
- Miyachi, S., Hirata, Y., Inoue, K., Lu, X., Nambu, A., and Takada, M. (2013). Multisynaptic projections from the ventrolateral prefrontal cortex to hand and mouth representations of the monkey primary motor cortex. *Neuroscience Research*, 76(3), 141-149.
- Miyachi, S., Lu, X., Inoue, S., Iwasaki, T., Koike, S., Nambu, A., and Takada, M. (2005). Organization of multisynaptic inputs from prefrontal cortex to primary motor cortex as revealed by retrograde transneuronal transport of rabies virus. *The Journal of Neuroscience : The Official Journal of the Society for Neuroscience*, 25(10), 2547-2556.
- Montagnini, A., and Treves, A. (2003). The evolution of mammalian cortex, from lamination to arealization. *Brain Research Bulletin*, 60(4), 387-393.
- Morgan, M. A., and LeDoux, J. E. (1995). Differential contribution of dorsal and ventral medial prefrontal cortex to the acquisition and extinction of conditioned fear in rats. *Behavioral Neuroscience*, 109(4), 681-688.
- Nakamura, H., Gattass, R., Desimone, R., and Ungerleider, L. G. (1993). The modular organization of projections from areas V1 and V2 to areas V4 and TEO in macaques. *The Journal of Neuroscience : The Official Journal of the Society for Neuroscience*, 13(9), 3681-3691.
- Narayanan, N. S., and Laubach, M. (2006). Top-down control of motor cortex ensembles by dorsomedial prefrontal cortex. *Neuron*, 52(5), 921-931.
- Nascimento-Silva, S., Pinon, C., Soares, J. G., and Gattass, R. (2014). Feedforward and feedback connections and their relation to the CytOx modules of V2 in cebus monkeys. *The Journal of Comparative Neurology*.

- Neafsey, E. J. (1990). Prefrontal cortical control of the autonomic nervous system: Anatomical and physiological observations. *Prog. Brain Res.* 85, 147–165; discussion 165–166.
- Olson, C. R., and Musil, S. Y. (1992). Topographic organization of cortical and subcortical projections to posterior cingulate cortex in the cat: Evidence for somatic, ocular, and complex subregions. *The Journal of Comparative Neurology*, 324(2), 237-260.
- Ongur, D., and Price, J. L. (2000). The organization of networks within the orbital and medial prefrontal cortex of rats, monkeys and humans. *Cerebral Cortex (New York, N.Y.: 1991)*, 10(3), 206-219.
- Ongur, D., Ferry, A. T. and Price, J. L. (2003). Architectonic subdivision of the human orbital and medial prefrontal cortex. *Journal of Comparative Neurology*, 460 (3), 425-449.
- Pandya, D. N., Dye, P., and Butters, N. (1971). Efferent cortico-cortical projections of the prefrontal cortex in the rhesus monkey. *Brain Research*, 31(1), 35-46.
- Passingham, R. E., Stephan, K. E., and Kotter, R. (2002). The anatomical basis of functional localization in the cortex. *Nature Reviews. Neuroscience*, 3(8), 606-616.
- Paxinos, G., and Watson, C. (1998). *The rat brain in stereotaxic coordinates* (4th ed.). London: Academic press.
- Penfield, W. and Boldrey, E. (1937). Somatic and sensory representation in the cerebral cortex of man as studied by electrical stimulation. *Brain*, 60, 389-443.
- Penfield, W. and Rasmussen, T. (1950). *The cerebral cortex of man*. The Macmillan Company, New York, N.Y. 1950. 248 pp. *Am. J. Phys. Anthropology*, 11: 441–444.
- Penfield, W., and Welch, K. (1951). The supplementary motor area of the cerebral cortex; a clinical and experimental study. *A.M.A. Archives of Neurology and Psychiatry*, 66(3), 289-317.
- Perkel, D. J., Bullier, J., and Kennedy, H. (1986). Topography of the afferent connectivity of area 17 in the macaque monkey: A double-labelling study. *The Journal of Comparative Neurology*, 253(3), 374-402.
- Perlstein, W. M., Carter, C. S., Noll, D. C., and Cohen, J. D. (2001). Relation of prefrontal cortex dysfunction to working memory and symptoms in schizophrenia. *The American Journal of Psychiatry*, 158(7), 1105-1113.
- Petrides, M. (2005). Lateral prefrontal cortex: Architectonic and functional organization. *Philosophical Transactions of the Royal Society of London. Series B, Biological Sciences*, 360(1456), 781-795.
- Petrides M. and Pandya D. N. (1994). Comparative architectonic analysis of the human and the macaque frontal cortex. In: Boller F, Grafman J, editors. *Handbook of neuropsychology*. vol. 9. Elsevier; Amsterdam. 17–58.

Petrides, M., and Pandya, D. N. (1999). Dorsolateral prefrontal cortex: Comparative cytoarchitectonic analysis in the human and the macaque brain and corticocortical connection patterns. *The European Journal of Neuroscience*, 11(3), 1011-1036.

Pons, T. P., and Kaas, J. H. (1986). Corticocortical connections of area 2 of somatosensory cortex in macaque monkeys: A correlative anatomical and electrophysiological study. *The Journal of Comparative Neurology*, 248(3), 313-335.

Porter, L. L., and White, E. L. (1983). Afferent and efferent pathways of the vibrissal region of primary motor cortex in the mouse. *The Journal of Comparative Neurology*, 214(3), 279-289.

Preuss, T.M. (2000) What's human about the human brain? In: *The New Cognitive Neurosciences. Second Edition* (Gazzaniga MS, ed), pp 1219-1234. Cambridge, MA: MIT Press.

Ramnani, N. and Owen, A.M. (2004). Anterior prefrontal cortex: Insights into function from anatomy and neuroimaging. *Nature*, 5, 184-194.

Rose, J. E., and Woolsey, C. N. (1948). The orbitofrontal cortex and its connections with the mediodorsal nucleus in rabbit, sheep and cat. *Research Publications - Association for Research in Nervous and Mental Disease*, 27 (1 vol.)(1 vol.), 210-232.

Saleem, K. S., Kondo, H., and Price, J. L. (2008). Complementary circuits connecting the orbital and medial prefrontal networks with the temporal, insular, and opercular cortex in the macaque monkey. *The Journal of Comparative Neurology*, 506(4), 659-693.

Sasaki, K., Gemba, H., Nambu, A. and Matsuzaki, R. (1993). No-go activity in the frontal association cortex of human subjects. *Neuroscience Research*, 18 (3), 249-252.

Sawaguchi, T. (2001). The effects of dopamine and its antagonists on directional delay-period activity of prefrontal neurons in monkeys during an oculomotor delayed-response task. *Neuroscience Research*, 41(2), 115-128.

Sawaguchi, T., and Iba, M. (2001). Prefrontal cortical representation of visuospatial working memory in monkeys examined by local inactivation with muscimol. *Journal of Neurophysiology*, 86(4), 2041-2053.

Schilman, E. A., Uylings, H. B., Galis-de Graaf, Y., Joel, D., and Groenewegen, H. J. (2008). The orbital cortex in rats topographically projects to central parts of the caudate-putamen complex. *Neuroscience Letters*, 432(1), 40-45.

Schleicher, A., Amunts, K., Geyer, S., Morosan, P., and Zilles, K. (1999). Observer-independent method for microstructural parcellation of cerebral cortex: A quantitative approach to cytoarchitectonics. *Neuroimage*, 9(1), 165-177.

Schnider, A., Treyer, V., and Buck, A. (2005). The human orbitofrontal cortex monitors outcomes even when no reward is at stake. *Neuropsychologia*, 43(3), 316-323.

Schoenbaum, G., and Esber, G. R. (2010). How do you (estimate you will) like them apples? integration as a defining trait of orbitofrontal function. *Current Opinion in Neurobiology*, 20(2), 205-211.

Schoenbaum, G., and Roesch, M. (2005). Orbitofrontal cortex, associative learning, and expectancies. *Neuron*, 47(5), 633-636.

Schoenbaum, G., Chiba, A., and Gallagher, M. (1998) Orbitofrontal cortex and basolateral amygdala encode expected outcomes during learning. *Nature Neuroscience*, 1:155-159.

Seamans, J.K., Lapish, C.C., Durstewitz, D. (2008). Comparing the prefrontal cortex of rats and primates: insights from electrophysiology. *Neurotoxicity Research*, 14, 249-262.

Semendeferi, K., Armstrong, E., Schleicher, A., Zilles, K., and Van Hoesen, G.W. (1998) Limbic frontal cortex in hominoids: A comparative study of area 13. *American Journal of Physical Anthropology*, 106:129-155.

Sereno, M.I., Pitzalis, S and Martinez, A. (2001). Mapping of contralateral space in retinotopic coordinates by a parietal cortical area in humans. *Science*, 294, 1350-1354.

Sereno, M. I., and Huang, R. S. (2006). A human parietal face area contains aligned head-centered visual and tactile maps. *Nature Neuroscience*, 9(10), 1337-1343.

Sesack, S.R., Deutch, A.Y., Roth, R.H., Bunney, B.S. (1989) Topographical organization of the efferent projections of the medial prefrontal cortex in the rat: an anterograde tract-tracing study with Phaseolus vulgaris leucoagglutinin. *Journal of Comparative Neurology*, 290, 213-242.

Shimamura AP (2000). The role of the prefrontal cortex in dynamic filtering. *Psychobiology* 28: 207–218

Sidman, R. L., and Rakic, P. (1973). Neuronal migration, with special reference to developing human brain: A review. *Brain Research*, 62(1), 1-35.

Silver, M. A., and Kastner, S. (2009). Topographic maps in human frontal and parietal cortex. *Trends in Cognitive Sciences*, 13(11), 488-495.

Spatz, W.B. (1977). Topographically organized reciprocal connections between areas 17 and MT (visual area of superior temporal sulcus) in the marmoset callithrix jacchus. *Experimental Brain Research*, 27, 559-572.

Sporns, O., Honey, C.J. and Kotter, R. (2007) Identification and classification of hubs in brain networks. *PLoS ONE* 2: e1049.

Stuss, D. T., Benson, D. F., Clermont, R., Della Malva, C. L., Kaplan, E. F., and Weir, W. S. (1986). Language functioning after bilateral prefrontal leukotomy. *Brain and Language*, 28(1), 66-70.

- Stuss, D. T., Benson, D. F., Kaplan, E. F., Della Malva, C. L., and Weir, W. S. (1984). The effects of prefrontal leucotomy on visuoperceptive and visuoconstructive tests. *Bulletin of Clinical Neurosciences*, 49, 43-51.
- Stuss, D. T., and Levine, B. (2002). Adult clinical neuropsychology: Lessons from studies of the frontal lobes. *Annual Review of Psychology*, 53, 401-433.
- Suzuki, W. A., and Amaral, D. G. (1994). Topographic organization of the reciprocal connections between the monkey entorhinal cortex and the perirhinal and parahippocampal cortices. *The Journal of Neuroscience : The Official Journal of the Society for Neuroscience*, 14(3 Pt 2), 1856-1877.
- Takahara, D., Inoue, K., Hirata, Y., Miyachi, S., Nambu, A., Takada, M., Hoshi, E. (2012). Multisynaptic projection from the ventrolateral prefrontal cortex to the dorsal premotor cortex in macaques – anatomical substrate for conditional visuomotor behaviour. *European Journal of Neuroscience*, 36, 3365-3375.
- Taren, A. A., Venkatraman, V., and Huettel, S. A. (2011). A parallel functional topography between medial and lateral prefrontal cortex: Evidence and implications for cognitive control. *The Journal of Neuroscience : The Official Journal of the Society for Neuroscience*, 31(13), 5026-5031.
- Thivierge, J. P., and Marcus, G. F. (2007). The topographic brain: From neural connectivity to cognition. *Trends in Neurosciences*, 30(6), 251-259.
- Tigges, J., Spatz, W. B., and Tigges, M. (1973). Reciprocal point-to-point connections between parastriate and striate cortex in the squirrel monkey (saimiri). *The Journal of Comparative Neurology*, 148(4), 481-489.
- Tootell, R. B., Hadjikhani, N., Hall, E. K., Marrett, S., Vanduffel, W., Vaughan, J. T., and Dale, A. M. (1998). The retinotopy of visual spatial attention. *Neuron*, 21(6), 1409-1422.
- Triplett, J. W., Owens, M. T., Yamada, J., Lemke, G., Cang, J., Stryker, M. P., and Feldheim, D. A. (2009). Retinal input instructs alignment of visual topographic maps. *Cell*, 139(1), 175-185.
- Ungerleider, L. G., and Desimone, R. (1986). Cortical connections of visual area MT in the macaque. *The Journal of Comparative Neurology*, 248(2), 190-222.
- Uylings, H. B., Groenewegen, H. J., and Kolb, B. (2003). Do rats have a prefrontal cortex? *Behavioural Brain Research*, 146(1-2), 3-17.
- Uylings, H. B., and van Eden, C. G. (1990). Qualitative and quantitative comparison of the prefrontal cortex in rat and in primates, including humans. *Progress in Brain Research*, 85, 31-62.
- Van De Werd, H. J., and Uylings, H. B. (2008). The rat orbital and agranular insular prefrontal cortical areas: A cytoarchitectonic and chemoarchitectonic study. *Brain Structure and Function*, 212(5), 387-401.

- Van Essen, D.C., Anderson, C.H. and Felleman, D.J. (1992). Information processing in the primate visual system: An integrated systems perspective. *Science*, 255, 419-423.
- Van Groen, T., Kadish, I. and Wyss, J.M. (1999). Efferent connections of the anteromedial nucleus of the thalamus of the rat. *Brain Research Reviews*, 30, 1-26.
- Vertes, R. P. (2004). Differential projections of the infralimbic and prelimbic cortex in the rat. *Synapse*, 51, 32–58.
- Vertes, R. P. (2006). Interactions among the medial prefrontal cortex, hippocampus and midline thalamus in emotional and cognitive processing in the rat. *Neuroscience*, 142(1), 1-20.
- Walker, A.E. (1940). A cytoarchitectural study of the prefrontal area of the macaque monkey. *Journal of Comparative Neurology*, Volume 73, Issue 1, pages 59–86.
- Wandell, B. A., Dumoulin, S. O., and Brewer, A. A. (2007). Visual field maps in human cortex. *Neuron*, 56(2), 366-383.
- Welker, C. (1971). Microelectrode delineation of fine grain somatotopic organization of (SmI) cerebral neocortex in albino rat. *Brain Research*, 26(2), 259-275.
- Woolsey, T. A. (1967). Somatosensory, auditory and visual cortical areas of the mouse. *The Johns Hopkins Medical Journal*, 121(2), 91-112.
- Young, M.P. (1992). Objective analysis of the topological organisation of the primate cortical visual system. *Nature*, 358, 152-155.
- Zeki, S. (1980). A direct projection from area V1 to area V3A of rhesus monkey visual cortex. *Proceedings of the Royal Society of London. Series B, Containing Papers of a Biological Character. Royal Society (Great Britain)*, 207(1169), 499-506.
- Zeki, S. and Shipp, S. (1988). The functional logic of cortical connections. *Nature*, 335, 335, 311-7.

Table of Contents (Appendices)

Appendix A: Preliminary Experiments	242
Appendix B: Organisation of Prefrontal Cortex – Temporal Cortex Connections, Resultant from Separate Retrograde and Anterograde Injections	248
Appendix C: Hemispheric Effect of Injection Site and Resultant Labelling in Temporal Cortex.....	254
Appendix D: Anterograde Properties of Biotinylated Dextran Amines	256
Appendix E: Comparison of Labelling in Temporal Cortex from Single and Co-injections of Fluoro-Gold and BDA	257
Appendix F: Analysis of Biotinylated Dextran Amines using Darkfield Microscopy	258
Appendix G: Anterograde Properties of Fluoro-Ruby.....	262
Appendix H: Statistical Evidence for Organisation of Input and Output Connections Resultant from Separate Injections of Fluoro-Gold and Fluoro-ruby in Central Prefrontal Cortex.....	269
Appendix I: Labelling in Temporal Cortex from Co-injection of Fluoro-Gold and Fluoro-Ruby in Central Prefrontal Cortex.....	271
Appendix J: Organisation of Connections from Central Prefrontal Cortex – Temporal Cortex, using Fluoro-Gold and Fluoro-Emerald	276
Appendix K: Statistical Comparison Between Central Prefrontal Cortex Connections to Temporal Cortex using BDA & Fluoro-Gold and Fluoro-Ruby & Fluoro-Gold	279
Appendix L: Preliminary Small (2030nl) Tracer Injection Volumes.....	280
Appendix M: Organisation of Connections from Prefrontal Cortex – Sensory-Motor Cortex Resultant from Separate Injections of Fluoro-Gold and BDA	282
Appendix N: Hemispheric Effect of Injection Site and Resultant Labelling in Sensory-Motor Cortex	289
Appendix O: Comparison of Labelling in Sensory-Motor Cortex from Single and Co-injections of Fluoro-Gold and BDA	291
Appendix P: Statistical Evidence for Organisation of Input and Output Connections Resultant from Separate Injections of Fluoro-Gold and Fluoro-Ruby in Central Prefrontal Cortex.....	292
Appendix Q: Labelling in Sensory-Motor Cortex from Co-Injection of Fluoro-Gold and Fluoro-Ruby in Central Prefrontal Cortex.....	294
Appendix R: Statistical Comparison Between Central Prefrontal Cortex Connections to Sensory-Motor Cortex using BDA & Fluoro-Gold and Fluoro-Ruby & Fluoro-Gold	298

Table of Figures (Appendices)

Figure A.1. (i) Coronal section of prefrontal cortex showing the fluorescent visualisation of Fluoro-Gold (100nl) injection site (blue). (ii) Coronal section of prefrontal cortex showing the fluorescent visualisation of BDA (100nl fluorescein) injection site (green). (iii) Coronal section of temporal cortex showing the fluorescent visualisation of retrogradely labelled (Fluoro-Gold) cells (blue). (iv) Coronal section of sensorimotor cortex showing the bright-field visualisation of anterogradely labelled (BDA) axon terminals (brown). Scale bars = 200µm. 244

Figure A.2. (i) Coronal section of PFC depicting the spread of tracer (200nl BDA; Fluorescein) at the injection site. (ii) Coronal section of PFC depicting the spread of tracer (100nl BDA; Fluorescein) at the injection site (VO). Scale bars = 200µm. 245

Figure A.3. (i) Coronal section of PFC depicting the intensity of fluorescence (fluorescein) following direct mounting onto gelatin coated slides. (ii) Coronal section of PFC depicting the intensity of fluorescence (fluorescein) following mounting onto slides via PBS. Scale bars = 200µm. 247

Figure B.1 (i) Coronal section of PFC (AP 4.2mm from Bregma) showing the cytoarchitectural boundaries of the prelimbic (PL), medial orbital (MO), ventral orbital (VO), ventrolateral orbital (VLO), lateral orbital (LO) and dorsolateral orbital (DLO1, DLO2) cortices (according to Van De Werd and Uylings, 2008), depicting sites of injections; Prelimbic: A, Ventral Orbital: B, Ventrolateral Orbital: C and Dorsal Lateral Orbital: D, with 1mm spread. (ii) Coronal section of prefrontal cortex showing location and spread of (100nl) fluorescein (green) at injection site in VLO. (iii) Coronal section of prefrontal cortex showing location and spread of (100nl) Fluoro-Gold (blue) at injection site in VO/MO. (iv) Representations of Fluoro-Gold (100nl) (R4, R5, R6, R7 (solid line)) and BDA (100nl) (R1, R3, R8 (broken line)) injection sites in DLO (R5, R8), VLO (R1, R4), VO/MO (R6) and PL (R5, R8), in the right hemisphere. (v) Representation of BDA injection site (R7) in VO/MO, in the left hemisphere. BDA injection sites were consistently within the boundaries of corresponding Fluoro-Gold injection sites. There is minimal overlap between Fluoro-Gold injection sites (R4 and R5). Fluoro-Gold injection sites are mostly limited to the cytoarchitectural boundaries of PFC regions, and span the whole region (PL, VO/MO, VLO, DLO), injections into VO spread into MO. BDA injection sites are consistently within cytoarchitectural boundaries and span layers II – VI (PL, VO/MO, VLO, DLO).. Scale bars = 200µm. **Error! Bookmark not defined.**249

Figure B.2. (i, ii) Coronal sections showing retrogradely labelled cells (blue) in temporal cortex produced by injection of Fluoro-Gold (100nl) into VO (R6); (i) Fluoro-Gold labelled cells in PRh, Ect, TeA (x4) (ii) Fluoro-Gold labelled cells in PRh (x10). (iii, iv) Coronal sections showing retrogradely labelled cells (blue) in temporal cortex produced by injection of Fluoro-Gold (100nl) into DLO (R5); (iv) PRh, Ect (x4) (v) PRh (x10). (v) Coronal section showing anterogradely labelled areas (brown) in temporal cortex produced by injection of BDA (100nl) into PL (R3) (vi) Coronal section showing anterogradely labelled areas (brown) in temporal cortex produced by injection of BDA (100nl) into VO. Arrows denote the location of the rhinal sulcus. Scale bars = 200µm. **Error! Bookmark not defined.**250

Figure B.3. The mean effect of injection site on the (i)dorsal-ventral, (ii) anterior-posterior and (iii) medial-lateral location of retrogradely labelled cells (n=1412 arising from 4 rats: PL = 253, VO=677, VLO=131, DLO=351) and anterogradely labelled areas (n= 24 PL=4, VO=8, VLO=4, DLO=8) within temporal cortex. Error bars = standard error (iv) Coronal cross section of PFC showing the position of 4 injection sites; Prelimbic (A), ventral orbital (B), ventrolateral orbital (C), dorsolateral orbital (D). Coronal cross section of temporal cortex showing the three dimensions in which the locations of labels were recorded. 253

Figure C.1 Representations of four comparative Fluoro-Gold injection sites made into the left hemisphere; in PL (R13), PL/IL/MO (R19), VLO/LO (R16) and DLO2 (R9), used to ascertain whether hemispheric differences affected projections. R13 is positioned higher than the corresponding right hemisphere PL

injection (R7), however the majority of the injection site is confined to PL and covers the dorsal aspect of the R7 injection site.....	254
Figure C.2. The effect of injection site location on the 3-dimensional location of retrograde labelling in temporal cortex, between left (n=1122 from 7 rats) and right (n=1412, from 4 rats) hemisphere injections of Fluoro-Gold. Error bars = standard error.	255
Figure D.1. Fluorescent images showing labelling in temporal (i & ii) and sensory-motor cortex (iii) produced by co-injections of (100nl) injections of BDA (Fluorescein) (green) and (100nl) Fluoro-Gold (blue). Scales bars = 100µm. Red = Propidium iodide labelled cell bodies. Arrows denote location of Fluorescein labelling.	256
Figure F.1. Darkfield images showing labelling in temporal cortex produced by (100nl) injections of BDA (Fluorescein) into (i) VLO (R41) (ii & iii) PL (R42). Counterstained with thionin. Scale bars = 100µm.	258
Figure F.2. The mean effect of injection site on the (i) dorsal-ventral, (ii) anterior-posterior and (iii) medial-lateral location of retrogradely labelled cells (n=425 arising from 4 rats: PL=77, VO=160, VLO=89, DLO=99 (R37, R38, R41, R42)) and anterogradely labelled areas (derived from darkfield images) (n=36 arising from 4 rats: PL=4, VO=12, VLO=16, DLO=4 (R37, R38, R41, R42)) within temporal cortex. Error bars = standard error. (iv) Coronal cross section of PFC showing the position of 4 injection sites; PL (A), VO (B), VLO (C) and DLO (D). Coronal cross section of temporal cortex showing the three dimensions in which the locations of labels were recorded.	260
Figure G.1. (i, ii & iii) Confocal images of temporal cortex depicting fluorescently (fluorescein) labelled alpha tubulin (green) and Fluoro-Ruby labelling (red) resultant from (100nl) injection into PFC. (iv) Confocal image of temporal cortex depicting fluorescently labelled alpha tubulin (green), DAPI labelled nuclei (blue) and Fluoro-Ruby labelling (red) resultant from (100nl) injection into PFC. Note the large proportion of separate red (Fluoro-Ruby) and green (cell bodies) labelling. Co-labelling of Fluoro-Ruby and Fluorescein (alpha tubulin) is shown by yellow fluorescence. Scale bars = 20µm.....	265
Figure G.2. Comparison of labelling in temporal cortex produced by injections of (100nl) Fluoro-Gold, Fluoro-Ruby, Fluoro-Emerald and Biotinylated dextran amines (BDA).	266
Figure G.3. Labelling in temporal cortex resultant from co-injections of (100nl) Fluoro-Ruby (red) and (100nl) Fluoro-Gold (blue) made into (i & ii) VO (R39), (iii) DLO (R40) and (iv) VLO (R43). Co-labelling of Fluoro-Gold and Fluoro-Ruby = purple. Scale bars = 100 µm.	267
Figure I.1. (i) Coronal section of PFC showing location and spread of (100nl) Fluoro-Gold and (100nl) Fluoro-Ruby at injection site in DLO (R40). (ii) Coronal section of PFC showing location and spread of (100nl) Fluoro-Gold and (100nl) Fluoro-Ruby at injection site in VLO (R43). (iii) Representations of Fluoro-Gold and Fluoro-Ruby co-injection sites in PL (R44), VO (R39), VLO (R43) and DLO (R40). Scale bars = 100µm.	271
Figure I.2. The mean effect of PFC co-injection site on the (i) dorsal-ventral, (ii) anterior-posterior and (iii) medial-lateral location of retrogradely labelled cells (n=606 arising from 4 rats: PL=183, VO=136, VLO=158, DLO=129) and anterogradely labelled axon terminals (n=289 arising from 4 rats: PL=93, VO=66, VLO=59, DLO=71) within temporal cortex. Error bars=standard error. (iv) Coronal cross section of prefrontal cortex showing the position of 4 co-injection sites; prelimbic (A), ventral-orbital (B), ventrolateral orbital (C) and dorsolateral orbital (D). Coronal cross section of temporal cortex showing the three dimensions in which the locations of labels were recorded.	274
Figure J.1. Coronal sections of temporal cortex showing Fluoro-Emerald labelling (green) resultant from (100nl) injections into (i) VLO (R33) and (ii) VO (R34). Arrows denote the location of the rhinal sulcus. Scale bars = 100µm.	276
Figure J.2. The mean effect of PFC injection site on the (i) dorsal-ventral, (ii) anterior-posterior and (iii) medial-lateral location of Fluoro-Gold labelled cells (n=1412 arising from 4 rats: PL=253, VO=677, VLO=131, DLO=351) and Fluoro-Emerald labelling (n=401 arising from 4 rats: PL=66, VO=64, VLO=147, DLO=124) within temporal cortex. Error bars=standard error. (iv) Coronal cross section of prefrontal cortex	

showing the position of 4 injection sites; prelimbic (A), ventral-orbital (B), ventrolateral orbital (C) and dorsolateral orbital (D). Coronal cross section of temporal cortex showing the three dimensions in which the locations of labels were recorded. 278

Figure L.1.(i) Retrograde labelling (blue) in temporal cortex produced by 30nl injection of Fluoro-Gold into DLO (R7). (ii) Labelling (red) in temporal cortex produced by 20nl injection of Fluoro-Ruby into DLO (R8). Arrows denote the location of the rhinal sulcus. Scale bars = 100µm. 281

Figure M.1. (i) Coronal section of PFC (AP 4.2mm from Bregma) showing the cytoarchitectural boundaries of the prelimbic (PL), medial orbital (MO), ventral orbital (VO), ventrolateral orbital (VLO), lateral orbital (LO) and dorsolateral orbital (DLO1, DLO2) cortices (according to Van De Werd and Uylings, 2008), depicting sites of injections; Prelimbic: A, Ventral Orbital: B, Ventrolateral Orbital: C and Dorsal Lateral Orbital: D, with 1mm spread. (ii) Coronal section of prefrontal cortex showing location and spread of (100nl) fluorescein (green) at injection site in VLO. (iii) Coronal section of prefrontal cortex showing location and spread of (100nl) Fluoro-Gold (blue) at injection site in VO/MO. (iv) Representations of Fluoro-Gold (100nl) (R4, R5, R6, R7 (solid line)) and BDA (100nl) (R1, R3, R8 (broken line)) injection sites in DLO (R3, R7), VLO (R1, R6), VO/MO (R4) and PL (R5, R8), in the right hemisphere. (v) Representation of BDA injection site (R7) in VO/MO, in the left hemisphere. BDA injection sites were consistently within the boundaries of corresponding Fluoro-Gold injection sites. There is minimal overlap between Fluoro-Gold injection sites (R4 and R5). Fluoro-Gold injection sites are mostly limited to the cytoarchitectural boundaries of PFC regions, and span the whole region (PL, VO/MO, VLO, DLO), injections into VO spread into MO. BDA injection sites are consistently within cytoarchitectural boundaries and span layers II – VI (PL, VO/MO, VLO, DLO). Scale bars = 200µm. 283

Figure M.2. (i) Coronal section showing retrogradely labelled cells (blue) in cingulate cortex produced by 100nl injection of Fluoro-gold into VLO (injection C). (ii) Coronal section showing retrogradely labelled cells (blue) in cingulate cortex produced by 100nl injection of Fluoro-gold into VO (injection B). (iii) Coronal section showing anterograde labelling (brown) produced by injection of BDA (100nl Fluorescein) into DLO (injection D). Arrow shows area of intense anterograde labelling of axon terminals. Other brown staining indicates less intense anterograde labelling, as well as some artifactual staining. Note the ordered location of labelled neurons within the dorsal-ventral axis. (iv) Coronal section showing retrogradely labelled cells (blue) in sensory cortex produced by injections of Fluoro-Gold (100nl) into VLO (injection C). (v) Coronal section showing retrogradely labelled cells (blue) in sensory cortex produced by injections of Fluoro-Gold (100nl) into and VO (injection B). (vi) Coronal section of sensory-motor cortex showing locations of anterograde labelling (brown) produced by injection of BDA (100nl Texas red) into VLO (injection B). Arrow shows area of intense anterograde labelling of axon terminals. Other brown staining indicates less intense anterograde labelling, as well as some artifactual staining. Scale bars = 200µm. 284

Figure M.3. Diagram representing amalgamated injection sites within prefrontal cortex and subsequent projection sites to sensory-motor cortex for both anterograde (BDA) and retrograde (FG) tracer injections in several rats. Coronal sections depict the injection site and projecting site. (i) The positions of 4 injection sites within prefrontal cortex; PL (injection A: R5(FG), R8(BDA)), VO (injection B: R4(FG), R7(BDA)), VLO (injection C: R6(FG), R1(BDA)) and DLO (injection D: R7(FG), R3(BDA)). (ii) Anterograde labelling of axon terminals (PFC output connections) following injections into 4 PFC sites (A-D BDA: R1, R3, R7, R8). (iii) Retrograde labelling (PFC input connections) following injections into 3 PFC sites (A-D, FG: R4, R5, R6, R7). Note the ordered location of labeled areas/neurons within the dorsal-ventral and medial-lateral axes. . 285

Figure M.4. The mean effect of injection site on the (i) dorsal-ventral, (ii) anterior-posterior and (iii) medial-lateral location of retrogradely cells (n=494 cells arising from 4 rats) and anterogradely labelled areas (n=40 points from 4 rats) within the sensory-motor cortex. Error bars = standard error. (iv) Coronal cross section of PFC indicating the position of 4 injection sites within prefrontal cortex: Prelimbic (injection A), Ventral Orbital (injection B), Ventrolateral Orbital (injection C) and Dorsal Lateral Orbital (injection D), Coronal cross section of sensory-motor cortex, depicting the three dimensions in which the locations of labelled cells were recorded. 288

Figure N.1 Representations of four comparative Fluoro-Gold injection sites made into the left hemisphere; in PL (R13), PL/IL/MO (R19), VLO/LO (R16) and DLO2 (R9), used to ascertain whether hemispheric differences affected projections. R13 is positioned higher than the corresponding right hemisphere PL injection (R7), however the majority of the injection site is confined to PL and covers the dorsal aspect of the R7 injection site..... 289

Figure N.2. The effect of injection site location on the 3-dimensional location of retrograde labelling in sensory-motor cortex, between left and right hemisphere injections of Fluoro-Gold. Error bars = standard error..... 290

Figure Q.1. The mean effect of injection site on the (i) dorsal-ventral, (ii) anterior-posterior and (iii) medial-lateral location of Fluoro-Gold labeled cells (n=282 resultant from 4 rats, PL=48, VO=119, VLO=57, DLO=58) and Fluoro-Ruby labels (n=180 resultant from 4 rats, PL=92, VO=27, VLO=31, DLO=30) within sensory-motor cortex. Error bars = standard error. (iv) Coronal cross section of PFC indicating the position of four co-injection sites within PFC: Prelimbic (injection A), Ventral Orbital (injection B), Ventrolateral Orbital (injection C) and Dorsal Lateral Orbital (injection D), coronal cross section of sensory-motor cortex, depicting the three dimensions in which the locations of labelled cells were recorded. 296

Appendix A.

Preliminary Experiments

Preliminary experiments were carried out in order to determine the spread, accuracy of location and visualisation capabilities of our chosen anterograde and retrograde tracers (Fluorescein, Texas red, Fluoro-Gold and Fluoro-Ruby) in the rat brain. These preliminary experiments enabled the optimisation of our methodology before studies began, ensuring the reliability of the data we produced. Testing the experimental design and tracer solutions beforehand enabled us to make informed decisions about the ideal tracer injection volume and to ensure craniotomies would be made at the precise desired location. Preliminary investigations into the optimum processing and visualisation techniques also ensured that the best possible data would be obtained and analysed, therefore ensuring the reliability and reproducibility of our findings.

Fluorescent vs. Brightfield Imaging for Visualisation of Tracers

Several parallel series of sections were taken from the 1st brains in order to establish the optimum visualisation method for the different tracers being used. One series was coverslipped with vectashield mounting medium (with DAPI) for fluorescent imaging, a second series was processed for bright field imaging of BDA and or/Fluoro-Gold. All tracers used (Fluoro-Gold, Fluorescein and Texas Red) were visualised with both methods initially, in order to determine the best way to process and visualise each tracer to its maximum potential.

Fluorescein, Texas red and Fluoro-Gold injection sites and labelling were examined using both brightfield and fluorescent imaging. Fluoro-Ruby, when introduced later on in the experiments, was also initially visualised with both fluorescent and brightfield imaging to establish the best method. Injections sites of Fluorescein, Texas Red, Fluoro-Gold and Fluoro-Ruby were consistently more easily and more clearly

visualised with fluorescent imaging. Fluorescent imaging allowed for more detailed visualisation of injection sites of all tracers used.

Anterograde labelling from injections of BDA (Fluorescein and Texas Red) throughout the brain was difficult to identify with fluorescent imaging. Fluorescein could be more easily identified with fluorescence than Texas-Red. Areas of anterograde labelling produced by BDA (both Texas Red and Fluorescein) could be more easily identified with brightfield imaging after DAB staining. However, anterograde labelling throughout the brain produced by injections of Fluoro-Ruby were easily identified with fluorescent imaging. Fluorescent imaging of Fluoro-Ruby labelling allowed for more precise and accurate analysis of anterograde labelling in our later studies.

Fluoro-Gold labelled cells throughout the brain were easily and clearly visualised with fluorescent imaging . Fluorescent imaging of Fluoro-Gold was clearer and more easily identified than brightfield imaging, allowing the visualisation of individually labelled cells (Fig. A.1).

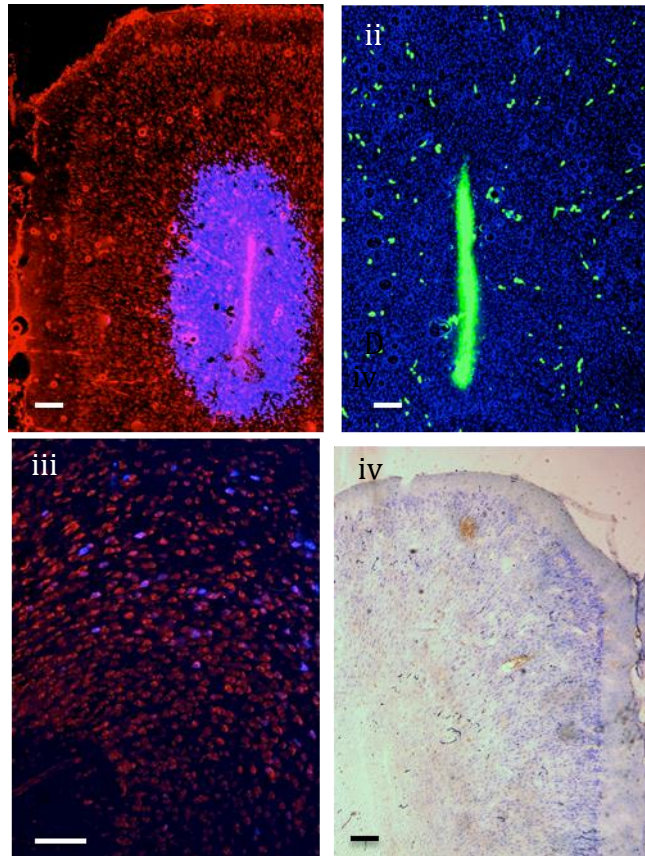


Figure A.1. (i) Coronal section of prefrontal cortex showing the fluorescent visualisation of Fluoro-Gold (100nl) injection site (blue). (ii) Coronal section of prefrontal cortex showing the fluorescent visualisation of BDA (100nl fluorescein) injection site (green). (iii) Coronal section of temporal cortex showing the fluorescent visualisation of retrogradely labelled (Fluoro-Gold) cells (blue). (iv) Coronal section of sensorimotor cortex showing the bright-field visualisation of anterogradely labelled (BDA) axon terminals (brown). Scale bars = 200 μ m.

The results indicated that fluorescent imaging was more accurate and allowed for clearer visualisation of labelling where it was possible to be used. All injection sites, from Fluorescein, Texas Red, Fluoro-Gold and Fluoro-Ruby could be easily and clearly visualised with fluorescent microscopy. Visualisation of cell body labelling at target areas was clear for Fluoro-Gold, as was the visualisation of individually labelled axon terminals with Fluoro-Ruby. However, axonal terminal labelling at target areas from Fluorescein and Texas Red (BDA) could not be seen with fluorescent imaging. Fluorescent imaging was determined to be more accurate for visualisation of labelled cells than DAB staining, due to the fact that fluorescence allows for the visualisation of individually labelled cells or axon terminals whereas with DAB labelling only an area of staining (not individual cells) could be seen. This

had an effect on the detail in the level of analysis which could be applied, however our statistical analysis allowed for this limitation. Based on these findings, Fluoro-Gold labelling was visualised with fluorescence and BDA labelling was visualised with brightfield imaging. All injection sites were visualised with fluorescence. In later studies, where BDA is replaced with Fluoro-Ruby, all labelled cells and axon terminals are visualised and analysed using fluorescent imaging.

Spread of tracers at injection site and tracer injection volume

Tracer injections were initially made at 200nl. Visualisation and analysis of the injection site spread revealed that a volume of 200nl produced too large of a spread (~2mm) for our intended study. The initial study positioned injection sites separated by 1mm, therefore the spread of tracer when injected could not exceed 1mm in order to prevent overlap. We therefore reduced the tracer injection volume to 100nl, which produced our desired injection site spread of tracer to <1mm (Fig. A.2).

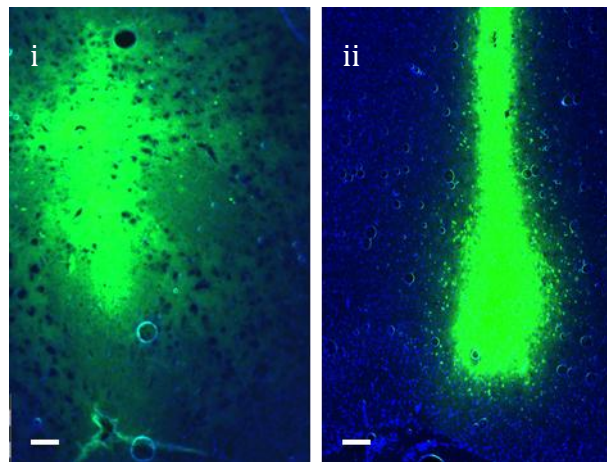


Figure A.2. (i) Coronal section of PFC depicting the spread of tracer (200nl BDA; Fluorescein) at the injection site. (ii) Coronal section of PFC depicting the spread of tracer (100nl BDA; Fluorescein) at the injection site (VO). Scale bars = 200 μ m.

Accuracy of tracer injection location

A vital aspect of the preliminary experiments was to test the accuracy of injection site co-ordinates. Stereo-taxic co-ordinates of injection sites were pre-determined based

on the co-ordinates of Paxinos & Watson (1998). The accuracy of co-ordinates from Paxinos & Watson (1998) was tested using our surgical apparatus. Resultant PFC injection locations were compared to the intended PFC co-ordinate using fluorescent and brightfield images. Results indicated that the location of injection sites was consistently inaccurate in terms of the anterior-posterior location, the co-ordinates consistently placed the injection site 0.5mm further anterior than intended. The medial-lateral co-ordinate and distance below the cortical surface (dorsal-ventral) were found to be accurate. This inaccuracy in the anterior-posterior co-ordinate of injection sites was accounted for in subsequent experiments. All PFC injection sites were planned 0.5mm further posterior than they were expected to be positioned in the brain.

Anatomical Processing

Several parallel series of sections were taken in early studies in order to establish an optimum processing method. Sections floated in PBS prior to being mounted onto gelatin-coated slides were compared with sections mounted directly onto gelatin coated slides. These two series were compared for the quality of imaging and visibility of tracers. Visual inspection of comparable sections (injection sites and areas of labelling) determined that mounting sections directly onto slides produced more clearly visible fluorescently labelled cells and axon terminals, as higher quality images for analysis. Fluorescent visualisation proved that when collected in PBS the mounted sections had a tendency to produce a much greater number of air bubbles in the mounting medium, making clear fluorescent photography, and subsequently numerical analysis of the location of labelled cells, more difficult. In addition to this, we found that the intensity of fluorescent labelling was greater when sections had been mounted directly onto slides (Fig. A.3). Therefore, in all subsequent studies, sections were mounted directly onto slides.

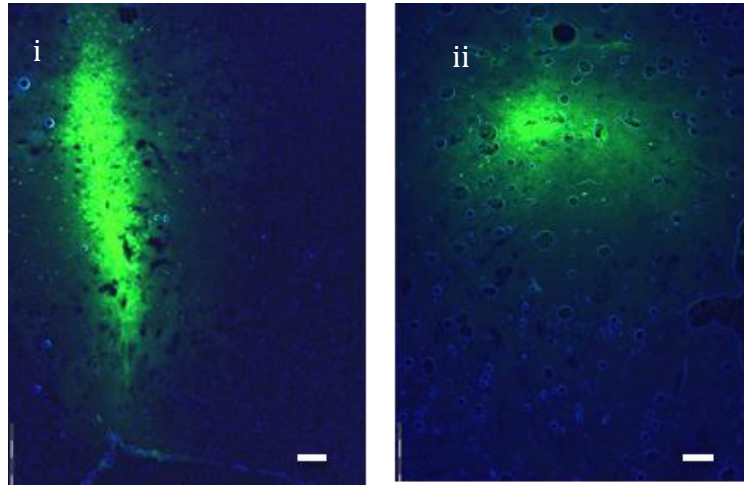


Figure A.3. (i) Coronal section of PFC depicting the intensity of fluorescence (fluorescein) following direct mounting onto gelatin coated slides. (ii) Coronal section of PFC depicting the intensity of fluorescence (fluorescein) following mounting onto slides via PBS. Scale bars = 200 μ m.

Appendix B.

Organisation of Prefrontal Cortex – Temporal Cortex Connections, Resultant from Separate Retrograde and Anterograde Injections

Methodology

All Fluoro-Gold injections were made in the right hemisphere in the initial experiment (Chapter 2) and biotinylated dextran amine injections were made in the left hemisphere, with the exception of injection B (VO) (right hemisphere).

For analysis of Fluoro-Gold labelled retrograde connections, a parallel series of 40µm coronal sections was taken (1 in 6 sections), mounted onto gelatin coated slides, then cover slipped with Vectashield® mounting medium (with propidium iodide) for fluorescent imaging.

Sections were examined using either brightfield (BDA) or fluorescent microscopy (BDA, Fluoro-Gold). Fluorescent photos were captured of BDA and Fluoro-Gold injection sites, retrogradely labelled cells (Fluoro-Gold). Brightfield photos were captured of anterogradely (BDA) labelled areas (Fluorescein and Texas red). All photos were captured using an Olympus DP-11 system microscope with a x4, x10 and x20 objective lens.

Results

Retrograde injections made into PL, VO, VLO and DLO (R4, R5, R6, R7) occurred in the intended PFC regions (Fig. B.1 iv). The majority of retrograde injection sites spanned layers I-VI, covered most of the cytoarchitectural region and were principally confined to cytoarchitectural boundaries of PFC sub-regions. The retrograde injection made into VO covered both VO and MO. There was some overlap between PL and VO injection sites and some spread into infralimbic cortex (IL) (Fig. B.1 iv). Anterograde injections made into PL, VO, VLO and DLO (R1, R3, R7, R8) occurred within the same cytoarchitectural regions as the retrograde equivalents, spanning a

smaller area. Anterograde injection sites were largely within the cytoarchitectural boundaries of PFC sub-regions (the injection into VO occurred in both VO and MO), covering layers II-VI (Fig. B.1 iv, v).

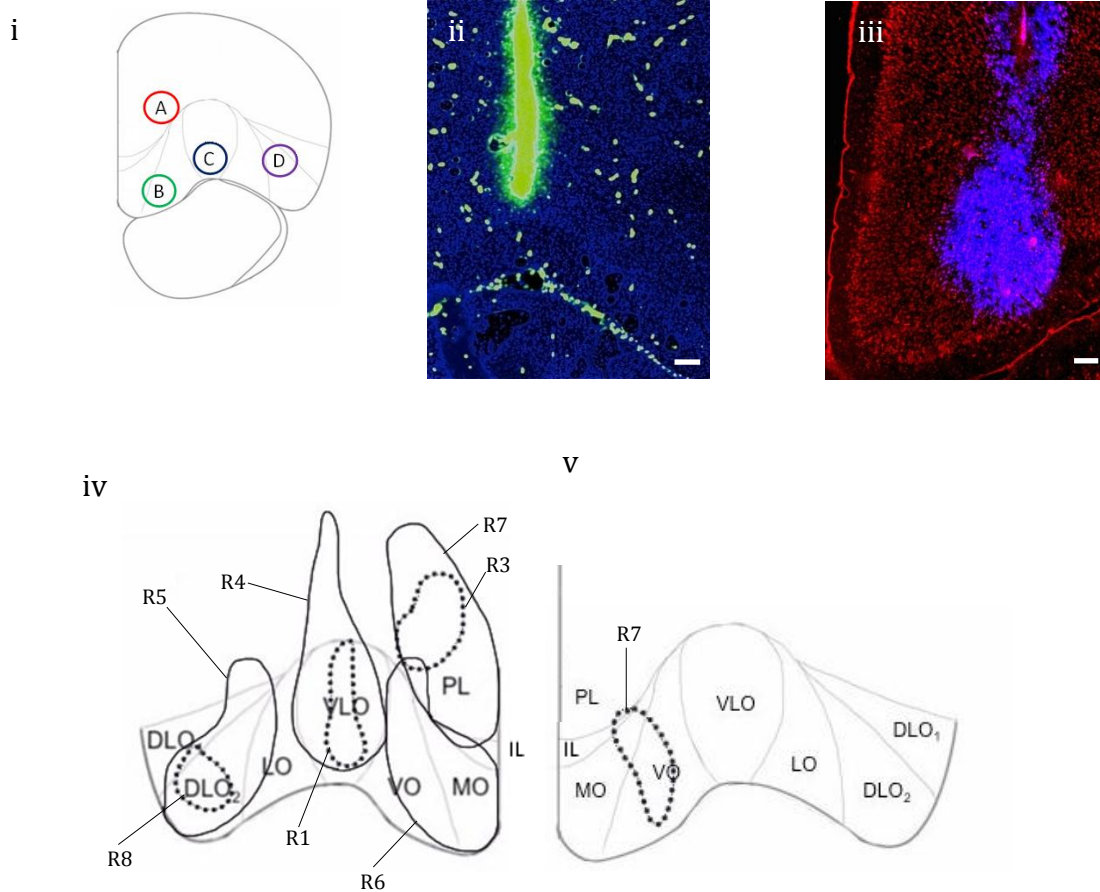


Figure B.1 (i) Coronal section of PFC (AP 4.2mm from Bregma) showing the cytoarchitectural boundaries of the prelimbic (PL), medial orbital (MO), ventral orbital (VO), ventrolateral orbital (VLO), lateral orbital (LO) and dorsolateral orbital (DLO₁, DLO₂) cortices (according to Van De Werd and Uylings, 2008), depicting sites of injections; Prelimbic: A, Ventral Orbital: B, Ventrolateral Orbital: C and Dorsal Lateral Orbital: D, with 1mm spread. (ii) Coronal section of prefrontal cortex showing location and spread of (100nl) fluorescein (green) at injection site in VLO. (iii) Coronal section of prefrontal cortex showing location and spread of (100nl) Fluoro-Gold (blue) at injection site in VO/MO. (iv) Representations of Fluoro-Gold (100nl) (R4, R5, R6, R7 (solid line)) and BDA (100nl) (R1, R3, R8 (broken line)) injection sites in DLO (R5, R8), VLO (R1, R4), VO/MO (R6) and PL (R5, R8), in the right hemisphere. (v) Representation of BDA injection site (R7) in VO/MO, in the left hemisphere. BDA injection sites were consistently within the boundaries of corresponding Fluoro-Gold injection sites. There is minimal overlap between Fluoro-Gold injection sites (R4 and R5). Fluoro-Gold injection sites are mostly limited to the cytoarchitectural boundaries of PFC regions, and span the whole region (PL, VO/MO, VLO, DLO), injections into VO spread into MO. BDA injection sites are consistently within cytoarchitectural boundaries and span layers II – VI (PL, VO/MO, VLO, DLO).. Scale bars = 200µm.

Organisation of Input and Output Connections from Prefrontal Cortex to Temporal Cortex

Retrogradely labelled cells and anterogradely labelled axon terminals were found in the same locations as with the described co-injections of Fluoro-Gold and BDA (Chapter 2, Fig.B.2).

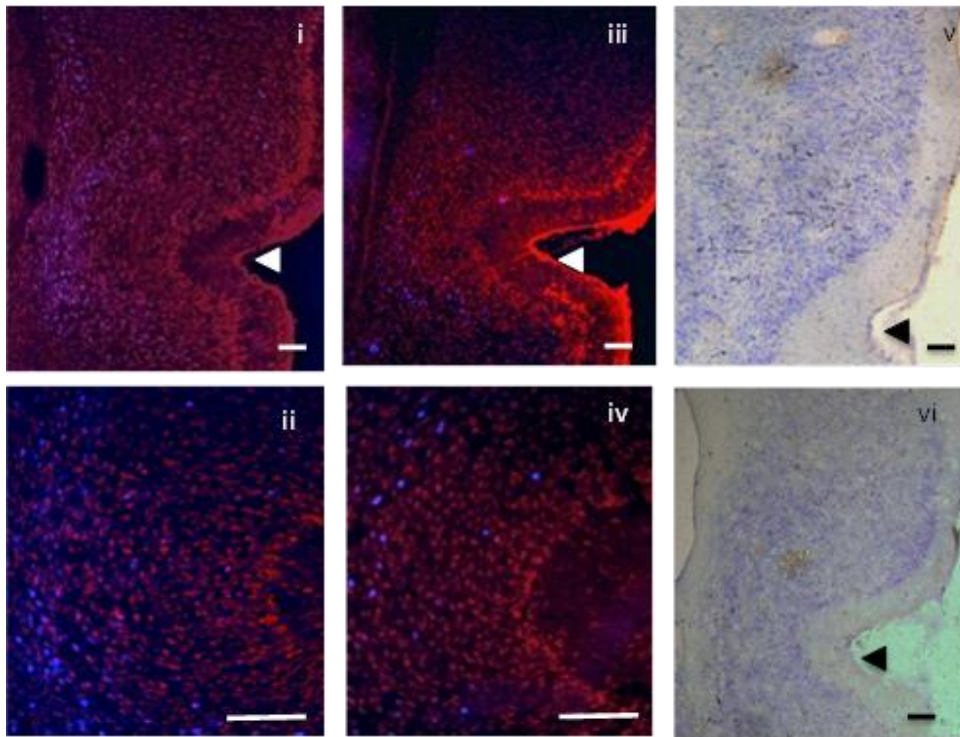


Figure B.2. (i, ii) Coronal sections showing retrogradely labelled cells (blue) in temporal cortex produced by injection of Fluoro-Gold (100nl) into VO (R6); (i) Fluoro-Gold labelled cells in PRh, Ect, TeA (x4) (ii) Fluoro-Gold labelled cells in PRh (x10). (iii, iv) Coronal sections showing retrogradely labelled cells (blue) in temporal cortex produced by injection of Fluoro-Gold (100nl) into DLO (R5); (iv) PRh, Ect (x4) (v) PRh (x10). (v) Coronal section showing anterogradely labelled areas (brown) in temporal cortex produced by injection of BDA (100nl) into PL (R3) (vi) Coronal section showing anterogradely labelled areas (brown) in temporal cortex produced by injection of BDA (100nl) into VO. Arrows denote the location of the rhinal sulcus. Scale bars = 200 μ m.

Statistical evidence for this ordered arrangement came from the following analysis.

For the dorsal-ventral axis: A factorial ANOVA revealed a significant main effect of PFC injection site location on the dorsal-ventral distance of retrogradely labelled cells from the rhinal sulcus ($F_{(3,1408)}=66.967$ $p<0.001$ $r=0.213$) and the dorsal-ventral distance of anterogradely labelled axon terminals from the rhinal sulcus ($F_{(3,20)}=1635.804$ $p<0.001$ $r=0.994$). Post hoc comparisons (Tukey HSD) between the four groups indicate significant differences between all retrograde injection sites (DLO, VO, VLO, PL) ($p<0.001$), with an exception of DLO*VLO ($p=0.997$). Post hoc comparisons (Tukey HSD) indicated significant differences between all anterograde injection sites ($p<0.001$). Three of the PFC regions tested (VLO, VO and DLO) exhibited an ordered arrangement in terms of dorsoventral location of retrograde labels (Fig. B.3.i). Distance of retrograde labelled cells from the rhinal sulcus increases as the injection site moves from lateral (DLO) to medial (VO) and decreases when the injection site reaches PL, indicating a change in pattern. Anterograde labels from VO, VLO and DLO display an ordered arrangement (Fig.B.3.i).

A 2 factor ANOVA revealed no significant interaction effect of PFC injection site location between input and output connections to temporal cortex in the dorsal-ventral axis ($F_{(3,1428)}=2.490$ $p=0.059$). These results indicate some difference in the ordering of input and output connections in this axis of orientation.

For the anterior-posterior axis: A factorial ANOVA revealed a significant main effect of injection site on the anterior-posterior location of retrogradely labelled cells ($F_{(3,1408)}=2911.16$ $p<0.001$ $r=0.821$) and anterogradely labelled axon terminals in temporal cortex ($F_{(3,20)}=6.157$ $p=0.004$ $r=0.485$). Post hoc comparisons (Tukey HSD) indicate significant differences between all retrograde injection sites ($p<0.001$). Post hoc comparisons (Tukey HSD) indicated significant differences between anterograde injection sites B*D (VO*DLO) and A*B (PL*VO) ($p<0.001$). No significant differences were found between anterograde injection sites B*C ($p=0.213$), B*D ($p=0.423$), A*C ($p=0.423$) or A*D ($p=1.00$). Fig.B.3.ii shows the anterior-posterior

ordered arrangement of projections from VLO, DLO and VO. The mean location of retrogradely labelled cells becomes more anterior as the PFC injection site is moved from lateral (DLO) to medial (VO). Similarly, as injection sites move from lateral (DLO) to medial (VO) PFC, the mean location of anterograde labels becomes more posterior (Fig.B.3.ii).

A 2 factor ANOVA revealed a significant interaction effect of PFC injection site location between input and output connections to temporal cortex in the anterior-posterior axis ($F_{(3,1428)}=77.136$ $p<0.001$). These results replicate the clear non-alignment of input and output connections in this axis of orientation identified by our co-injection results (Chapter 2).

For the medial-lateral axis: A factorial ANOVA revealed a significant main effect of injection site on medial-lateral location of retrogradely labelled cells in temporal cortex ($F_{(3,1408)}=16.805$ $p<0.001$ $r=0.109$) and anterogradely labelled axon terminals in temporal cortex ($F_{(3,20)}=886.578$ $p<0.001$ $r=0.989$). Post-hoc comparisons (Tukey HSD) revealed significant differences between retrograde injections into PL(A)*VO(B) ($p<0.001$), PL(A)*VLO(C) ($p<0.001$), PL*DLO(D) ($p<0.001$) and VO(B)*DLO(D) ($p=0.022$). Projections to DLO do not appear to follow the same pattern. Post hoc comparisons (Tukey HSD) indicate significant differences between anterograde injection sites VLO*DLO, VO*DLO and DLO*PL ($p<0.001$). There was no significant difference found between VLO*VO ($p=0.193$), VLO*PL ($p=0.75$) and VO*PL ($p=0.936$). These findings are consistent with those from co-injections of retrograde and anterograde tracer (Chapter 2).

A 2 factor ANOVA revealed a significant interaction effect of PFC injection site location between input and output connections to temporal cortex in the medial-lateral axis ($F_{(3,1428)}=598.485$ $p<0.001$). These results indicate clear non-alignment of input and output connections in this axis of orientation.

The anterograde and retrograde labelling found in areas of temporal cortex resultant from co-injections of BDA and Fluoro-Gold was very similar to the equivalent labelling shown here, produced by separate tracer injections.

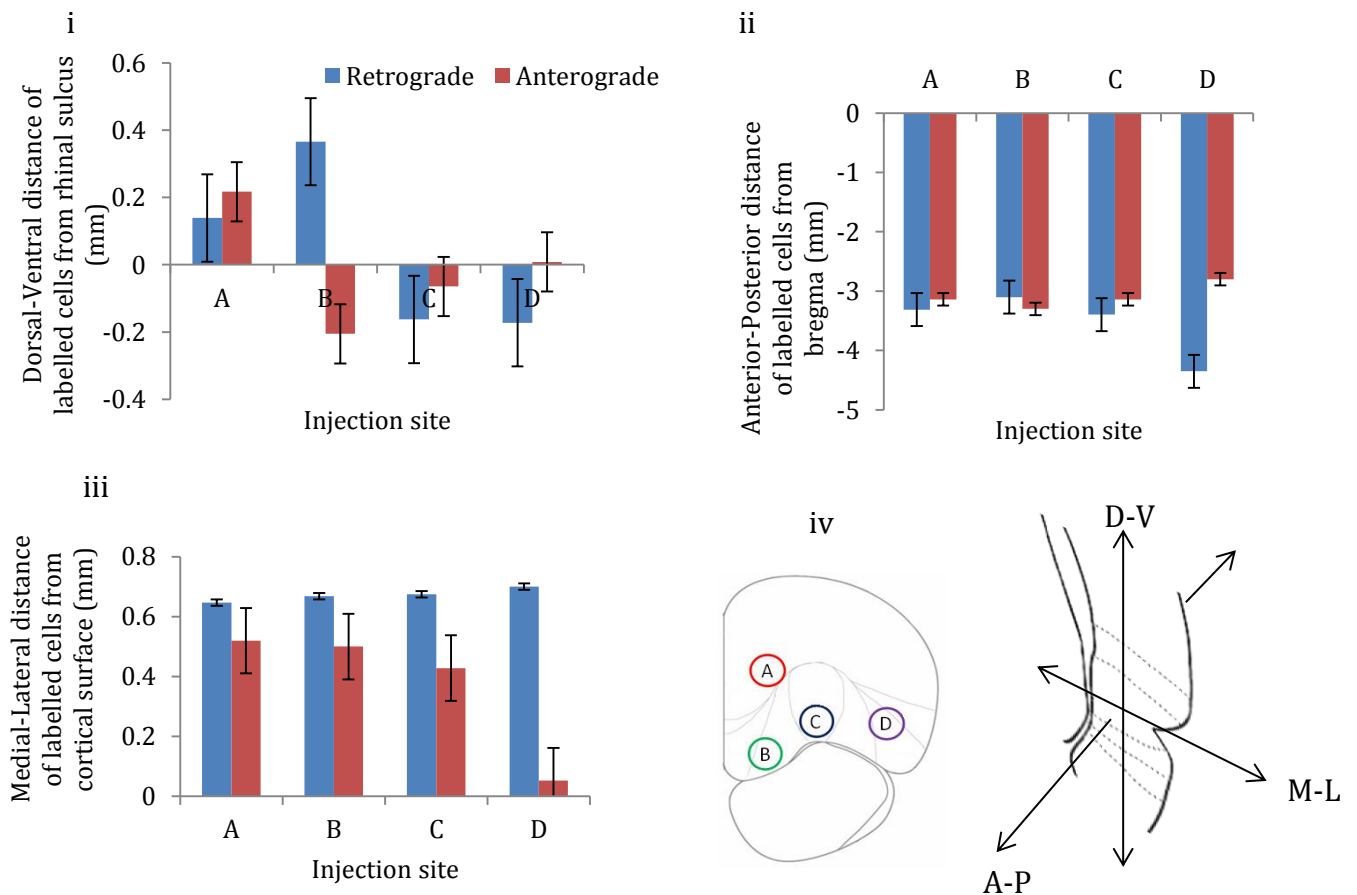


Figure B.3. The mean effect of injection site on the (i)dorsal-ventral, (ii) anterior-posterior and (iii) medial-lateral location of retrogradely labelled cells (n=1412 arising from 4 rats: PL = 253, VO=677, VLO=131, DLO=351) and anterogradely labelled areas (n= 24 PL=4, VO=8, VLO=4, DLO=8) within temporal cortex. Error bars = standard error (iv) Coronal cross section of PFC showing the position of 4 injection sites; Prelimbic (A), ventral orbital (B), ventrolateral orbital (C), dorsolateral orbital (D). Coronal cross section of temporal cortex showing the three dimensions in which the locations of labels were recorded.

Appendix C.

Hemispheric Effect of Injection Site and Resultant Labelling in Temporal Cortex

In the study described in Chapter 2, all of the FG injections were made into the right hemisphere and the majority of BDA injections were made into the left hemisphere. In order to control for possible effects of laterality in the analysis of label locations, the labelling produced by right hemisphere FG injections was compared to labelling produced by additional left hemisphere FG injections which were made later (Fig. C.1).

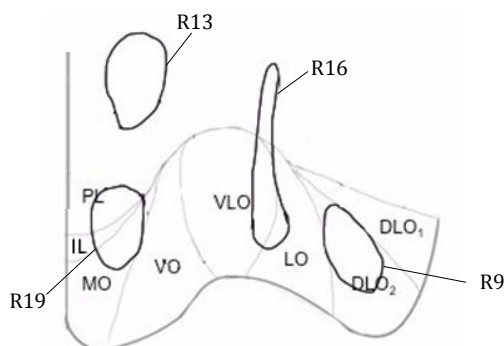


Figure C.1 Representations of four comparative Fluoro-Gold injection sites made into the left hemisphere; in PL (R13), PL/IL/MO (R19), VLO/LO (R16) and DLO₂ (R9), used to ascertain whether hemispheric differences affected projections. R13 is positioned higher than the corresponding right hemisphere PL injection (R7), however the majority of the injection site is confined to PL and covers the dorsal aspect of the R7 injection site.

Retrograde labelling in temporal cortex produced by comparable right and left hemisphere FG injections were compared by applying a paired samples t-test to the mean locations of retrogradely labelled regions in three axes of orientation.

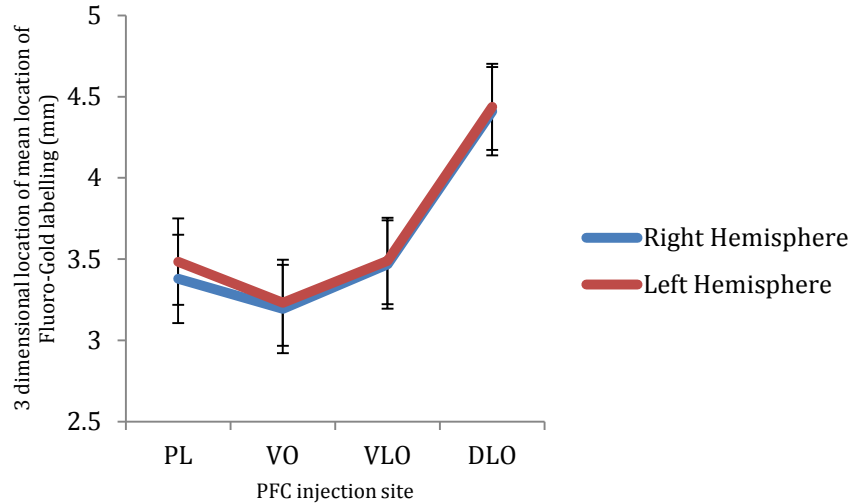


Figure C.2. The effect of injection site location on the 3-dimensional location of retrograde labelling in temporal cortex, between left (n=1122 from 7 rats) and right (n=1412, from 4 rats) hemisphere injections of Fluoro-Gold. Error bars = standard error.

Paired-samples t-tests revealed no significant differences in the mean location of retrograde labelling in temporal cortex resultant from Fluoro-Gold injections into the left and right hemispheres (Fig.C.2); in the dorsoventral axis ($t(3)=1.853$ $p=0.161$), in the anterior-posterior axis ($t(3)=-.471$ $p=0.670$) and in the mediolateral axis ($t(3)=-.701$ $p=0.534$). The analysis also showed no significant difference in the 3-dimensional mean location of retrograde labelling in temporal cortex ($t(3)=-2.454$ $p=0.091$). These findings demonstrate that there is no observable hemispheric difference in PFC – temporal cortex connections.

Appendix D.

Anterograde Properties of Biotinylated Dextran Amines (BDA)

Our observations of BDA fluorescent labelling confirm primarily anterograde properties; we found no co-labelling of Fluoro-Gold and BDA from co-injections (Fig.D.1) and BDA labelling (Fluorescein) was consistently found to be outside of the cell body when examined at high resolution.

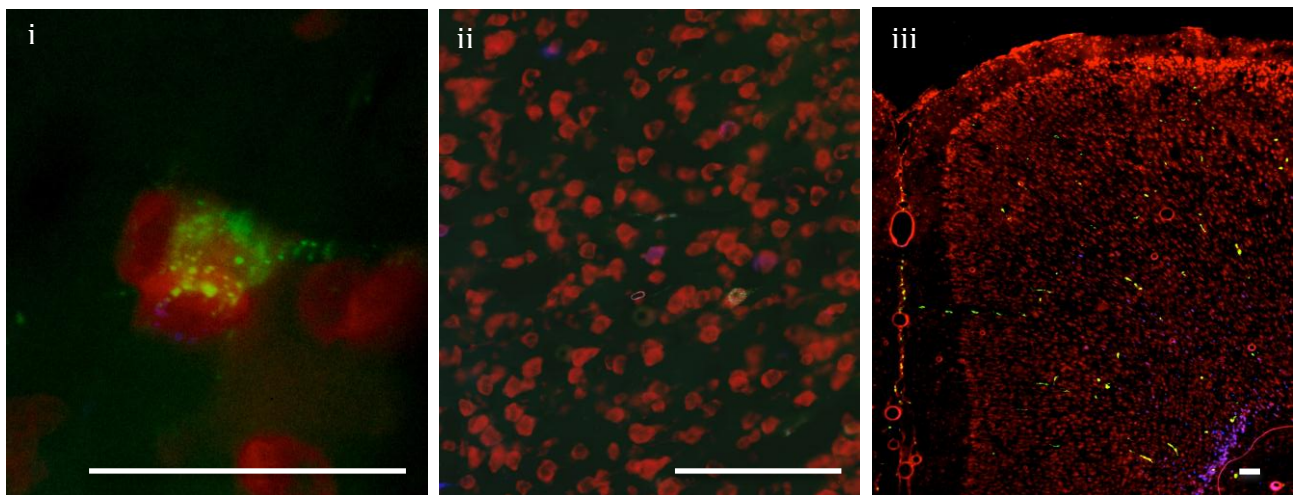


Figure D.1. Fluorescent images showing labelling in temporal (i & ii) and sensory-motor cortex (iii) produced by co-injections of (100nl) injections of BDA (Fluorescein) (green) and (100nl) Fluoro-Gold (blue). Scales bars = 100µm. Red = Propidium iodide labelled cell bodies. Arrows denote location of Fluorescein labelling.

Appendix E.

Comparison of Labelling in Temporal Cortex from Single and Co-injections of Fluoro-Gold and BDA

To further compare the labelling from co-injections and separate injections of BDA (100nl) and Fluoro-Gold (100nl), a statistical analysis was applied to clarify any difference between the input-output relationships, thus confirming the reliability of comparative labelling from separate injection sites.

In order to produce a single numerical comparison between the two types of injection, a Euclidean distance between mean retrograde and anterograde labels was calculated to produce a single 3-dimensional value for labelling from each PFC injection site:

$$E = \sqrt{(\langle DVr \rangle - \langle DVa \rangle)^2 + (\langle APr \rangle - \langle APa \rangle)^2 + (\langle MLr \rangle - \langle MLa \rangle)^2}$$

Paired samples T-tests revealed no significant difference in labelling between co-injections and separate injections ($t(3)=-.1540$ $p=0.221$). This indicates that there is no quantifiable difference in the relationship between input and output projections from PFC to temporal cortex when examined using either co-injections of anterograde and retrograde tracers or separate injections.

Appendix F.

Analysis of Biotinylated Dextran Amine Labelling using Darkfield Microscopy

DAB stained labelling produced by injections of (100nl) BDA was visualized using brightfield and darkfield microscopy. Darkfield microscopy showed areas of BDA labelling similar to that seen with brightfield imaging (Fig.F.1). Darkfield images of labelling in temporal cortex were analysed using the same methodology as that applied to brightfield images (Chapter 2).

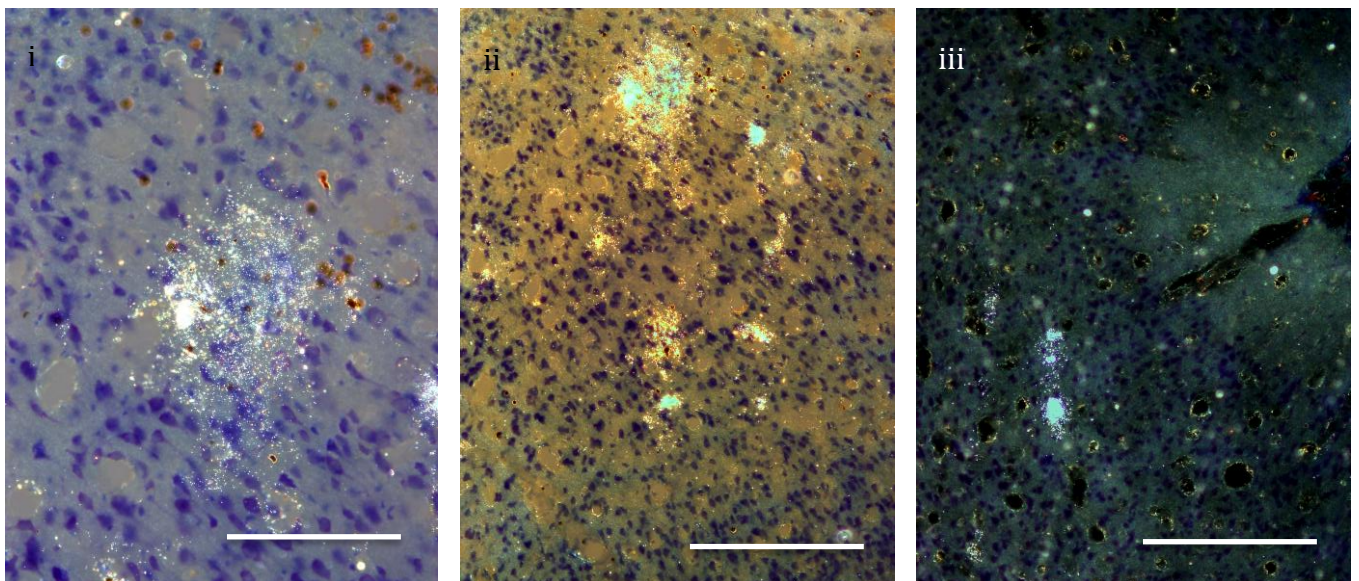


Figure F.1. Darkfield images showing labelling in temporal cortex produced by (100nl) injections of BDA (Fluorescein) into (i) VLO (R41) (ii & iii) PL (R42). Counterstained with thionin. Scale bars = 100 μ m.

Four data points were obtained from the perimeter of each labeled area. Analysis of darkfield images produced evidence for ordered connections between PFC and temporal cortex, comparable to that identified from brightfield images. Darkfield images of BDA labelling in temporal cortex were obtained from co-injections of BDA and Fluoro-Gold (Fig.F.2).

Statistical evidence for this ordered arrangement came from the following analysis:

For the dorsal-ventral axis: A factorial ANOVA revealed a significant main effect of PFC injection site location on the distance of anterograde labelling from the rhinal sulcus ($F_{(3,32)}=7.169$ $p=0.001$ $r=0.428$). A 2 factor ANOVA revealed no significant interaction effect between input and output connections ($F_{(3,453)}=1.892$ $p=0.130$ $r=0.064$).

For the anterior-posterior axis: A factorial ANOVA revealed a significant main effect of PFC injection site location on the distance of anterograde labelling from Bregma. ($F_{(3,32)}=115.556$ $p<0.001$ $r=0.885$). A 2 factor ANOVA revealed a significant interaction effect between input and output connections ($F_{(3,453)}=56.590$ $p<0.001$ $r= .333$).

For the medial-lateral axis: A factorial ANOVA revealed a significant main effect of PFC injection site location on the distance of anterograde labelling from the cortical surface ($F_{(3,32)}=7.275$ $p=0.001$ $r=0.430$). A 2 factor ANOVA revealed a significant interaction effect between input and output connections ($F_{(3,453)}=4.481$ $p=0.004$ $r=0.099$).

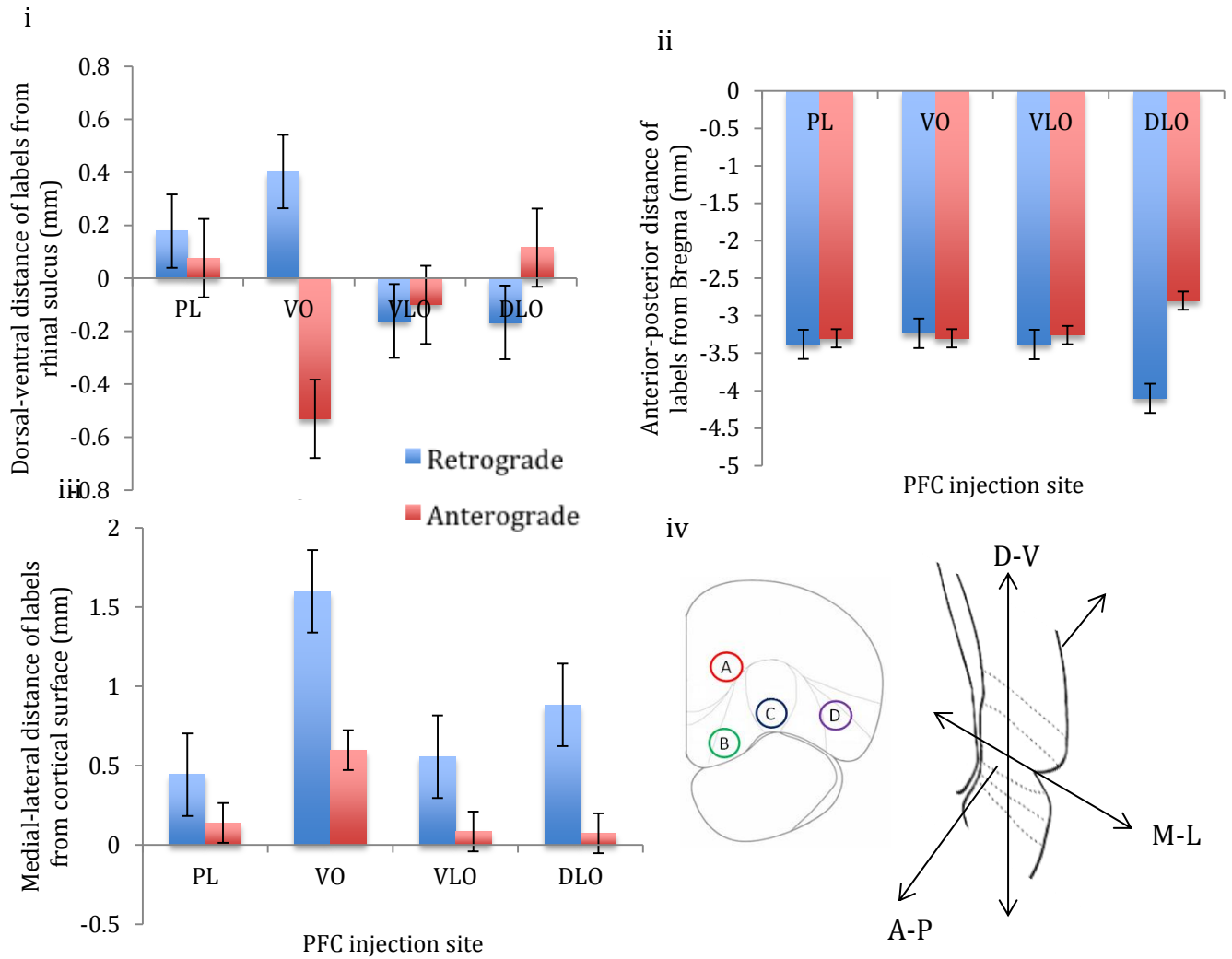


Figure F.2. The mean effect of injection site on the (i) dorsal-ventral, (ii) anterior-posterior and (iii) medial-lateral location of retrogradely labelled cells ($n=425$ arising from 4 rats: PL=77, VO=160, VLO=89, DLO=99 (R37, R38, R41, R42)) and anterogradely labelled areas (derived from darkfield images) ($n=36$ arising from 4 rats: PL=4, VO=12, VLO=16, DLO=4 (R37, R38, R41, R42)) within temporal cortex. Error bars = standard error. (iv) Coronal cross section of PFC showing the position of 4 injection sites; PL (A), VO (B), VLO (C) and DLO (D). Coronal cross section of temporal cortex showing the three dimensions in which the locations of labels were recorded.

Independent samples t-tests showed a consistent significant difference between Fluoro-Gold and BDA labelling in temporal cortex from VO with darkfield ($t(38.129)=4.474$ $p<0.001$) and brightfield ($t(170)=2.411$ $p=0.017$) imaging of BDA. This indicates a consistent difference in location of anterograde and retrograde connections.

No significant difference between the 3 dimensional mean location of darkfield and brightfield labelling was found ($t(3)=1.449$ $p=0.243$), indicating consistency of anterograde labelling across visualization methods.

Appendix G.

Anterograde Properties of Fluoro-Ruby

The anterograde tracer used in this study, Fluoro-Ruby, is known to hold some retrograde properties and in some instances has been described as a bi-directional tracer. To enable a clear understanding of the results and the labelling produced by Fluoro-Ruby injections it was necessary to clarify the properties of the labelling it produced.

Initially, a comparison between the previously used anterograde tracer, BDA was made. BDA is more widely accepted as an anterograde tracer than Fluoro-Ruby. Our own observations of BDA labelling confirm primarily anterograde labelling; we found no co-labelling of Fluoro-Gold and BDA from co-injections. Additionally, BDA labelling (Fluorescein) was consistently found to be outside of the cell body when examined at high resolution (see Appendix D).

In order to directly compare anterogradely labelled connections from our early studies using Biotinylated dextran amines (100nl Texas red and Fluorescein) with anterogradely labelled connections from our later studies using Fluoro-ruby (100nl), it was necessary to verify their consistency with one another in terms of injection site spread and pathway labelling.

We aimed to establish whether the two anterograde tracers used in our experiments, BDA and Fluoro-Ruby, were reliably comparable with one another, thus ensuring the validity of our findings, enabling us to directly compare results from BDA and Fluoro-Ruby studies and confirming Fluoro-Ruby as a reliable anterograde tracer.

In order to compare the locations of individually Fluoro-Ruby labelled axon terminals with BDA labelled areas, a Euclidean calculation was applied to produce a single 3-dimensional location value for temporal cortex labelling from each injection site:

$$E = \sqrt{(\langle DVr \rangle - \langle DVa \rangle)^2 + (\langle APr \rangle - \langle APa \rangle)^2 + (\langle MLr \rangle - \langle MLa \rangle)^2}$$

From the distance (E) values, the difference (x, y, z) between injection sites was calculated:

$$x = D [\textit{injection A}] - D [\textit{injection B}]$$

$$y = D [\textit{injection B}] - D [\textit{injection C}]$$

$$z = D [\textit{injection C}] - D [\textit{injection D}]$$

A paired samples T-test was applied to determine if there was a significant difference between Fluoro-Ruby and BDA labelling from the same PFC injection sites. In addition, paired samples T-tests were applied to each axis of orientation.

To compare the midpoint location of labelling in temporal cortex for Fluoro-Ruby and BDA, first the midpoint location of labelling from each injection site was determined:

$$\frac{\textit{Maximum} - \textit{Minimum}}{2}$$

Distance from Retrograde Labels

The paired samples T-test revealed no significant difference between the 3 dimensional distance between retrograde and anterograde labelling with 100nl Fluoro-Ruby and 100nl BDA in temporal cortex ($t(2)=-1.855$ $p=0.205$). This result indicates that there is not any substantial difference in the labelling produced by the two anterograde tracers in comparison to retrograde labelling, showing that our findings from BDA injections and Fluoro-Ruby injections are comparable with one another. Similar locations of labelling produced by both Fluoro-Ruby and BDA injections also gives strong evidence to support Fluoro-Ruby as an anterograde (not retrograde) tracer.

Midpoint Location of labels

To compare the midpoint location of labelling in temporal cortex for Fluoro-Ruby and BDA, first the midpoint location of labelling from each injection site was determined. A Euclidean value was calculated to determine a 3 dimensional value for the midpoint location of labelling from each injection site.

A paired samples T-test revealed no significant difference between the 3 dimensional midpoint locations of Fluoro-Ruby and BDA labelling from PFC injection sites A, B, C and D ($t(3)=-2.009$ $p=0.138$). This indicates consistency between the labelling we have produced using BDA and Fluoro-Ruby.

Immunofluorescence

Immunofluorescent imaging of alpha tubulin alongside Fluoro-Ruby labelling in temporal cortex indicated that the majority (70%) of Fluoro-Ruby labelling we observed in temporal cortex, as a result of injections into prefrontal cortex, was separate from the fluorescein labeled cell bodies (Fig.G.1). There was some evidence of double labelling of alpha tubulin and Fluoro-Ruby (Fig.G.1.iv), however approximately 30% of cases were found to have possible retrograde properties (Fluorescein and Fluoro-Ruby labelling was seen in the same place). This indicates that the labelling produced by Fluoro-Ruby is for the most part reliably anterograde.

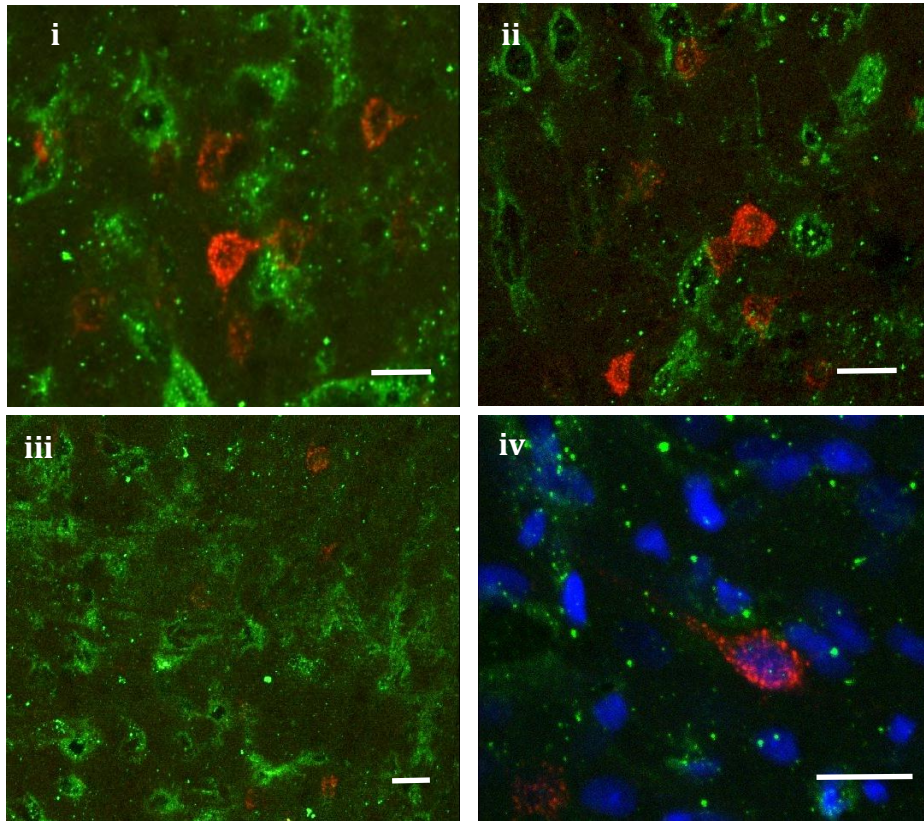


Figure G.1. (i, ii & iii) Confocal images of temporal cortex depicting fluorescently (fluorescein) labelled alpha tubulin (green) and Fluoro-Ruby labelling (red) resultant from (100nl) injection into PFC. (iv) Confocal image of temporal cortex depicting fluorescently labelled alpha tubulin (green), DAPI labelled nuclei (blue) and Fluoro-Ruby labelling (red) resultant from (100nl) injection into PFC. Note the large proportion of separate red (Fluoro-Ruby) and green (cell bodies) labelling. Co-labelling of Fluoro-Ruby and Fluorescein (alpha tubulin) is shown by yellow fluorescence. Scale bars = 20µm.

Comparison of Multiple Tracers

Additionally, we compared the labelling produced by the anterograde tracers Fluoro-Ruby, Fluoro-Emerald and BDA with that produced by the retrograde tracer Fluoro-Gold. Results show that the 3-dimensional organisation of labelling follows a similar pattern for all 3 anterograde tracers (Fluoro-Emerald, Fluoro-Ruby and BDA), the order of labelling produced by Fluoro-Gold is considerably different to all of the tracers considered to be anterograde (Fig.G.2). These findings show that the labelling produced by Fluoro-Ruby in this study is consistent with that of other tracers

considered to be primarily anterograde in nature (notably BDA) and is clearly produces different labelling to a tracer known to be retrograde (Fluoro-Gold), this provides evidence for Fluoro-Ruby being primarily anterograde.

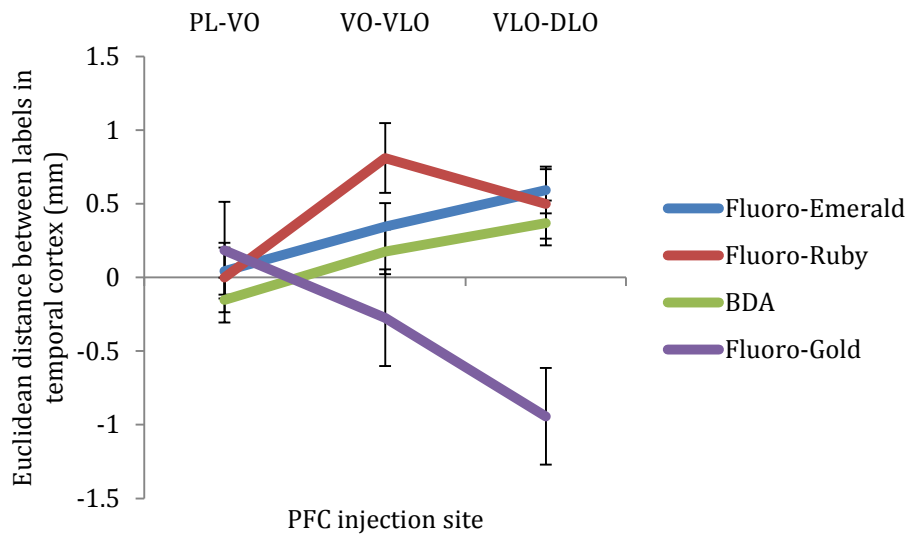


Figure. G.2. Comparison of labelling in temporal cortex produced by injections of (100nl) Fluoro-Gold, Fluoro-Ruby, Fluoro-Emerald and Biotinylated dextran amines (BDA).

Co-injection of Fluoro-Gold and Fluoro-Ruby

Co-injections of (100nl) Fluoro-Gold and (100nl) Fluoro-Ruby were made in 4 rats (R39, R40, R43, R44). Details of the methodology and results of this experiment are described further in Appendix I.

Co-injection of Fluoro-Gold and Fluoro-Ruby, whereby 100nl of Fluoro-Gold was injected, followed by 100nl Fluoro-Ruby into the same injection site, allowed us to ensure labeled connections in temporal and sensory-motor cortex originated from the same location in PFC.

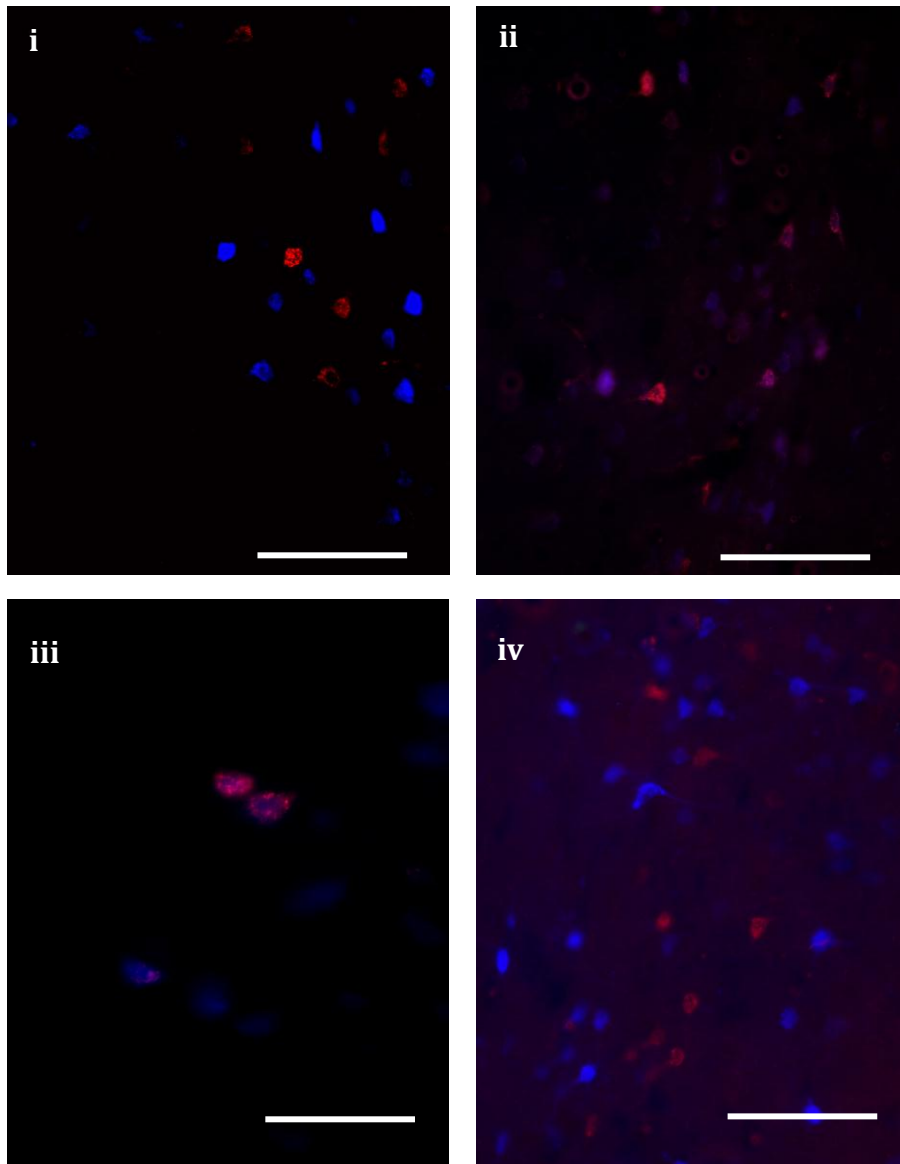


Figure G.3. Labelling in temporal cortex resultant from co-injections of (100nl) Fluoro-Ruby (red) and (100nl) Fluoro-Gold (blue) made into (i & ii) VO (R39), (iii) DLO (R40) and (iv) VLO (R43). Co-labelling of Fluoro-Gold and Fluoro-Ruby = purple. Scale bars = 100 μm .

Fluoro-Gold and Fluoro-Ruby labelling resultant from co-injections showed that the majority of labels were separate to one another (Fig.G.3). The majority of Fluoro-Gold labelling was seen outside of the cell body, whereas Fluoro-Gold was seen inside the cell body. There was minimal co-labelling of Fluoro-Gold and Fluoro-Ruby, in which Fluoro-Ruby was also concluded to be inside the cell body. The extent of co-labelling was estimated by calculating the percentage of co-labelled/cell body versus separate/non-cell body labelling of Fluoro-Rub, across 10 fluorescent

images of temporal cortex. The mean percentage of anterograde (outside of cell body) labelling was found to be 69% (31% retrograde).

Appendix H.

Statistical Evidence for Organisation of Input and Output Connections Resultant from Separate Injections of Fluoro-Gold and Fluoro-Ruby in Central Prefrontal Cortex

Statistical evidence for this ordered arrangement came from the following analysis:

In the dorsal ventral axis: A Factorial ANOVA revealed a significant main effect of central PFC injection site location on the dorsal-ventral distance from the rhinal sulcus of retrogradely labelled cells in temporal cortex ($F_{(3,1408)}=66.967$ $p<0.001$ $r=0.21$) and anterogradely labelled axon terminals in temporal cortex ($F_{(3,440)}=14.457$ $p<0.001$ $r=0.18$). Post hoc comparisons (Tukey HSD) revealed significant differences between injection sites A*B ($p=0.010$), A*C, A*D, B*C and B*D ($p<0.001$). Post hoc comparisons (Tukey HSD) revealed significant differences between anterograde injection sites A*D ($p=0.002$), B*C ($p=0.020$), B*D ($p<0.001$) and C*D ($p=0.019$). These findings indicate ordered arrangements of input and output connections from central PFC to temporal cortex in this axis of orientation.

A 2 factor ANOVA revealed a significant interaction effect of input and output connections ($F_{(3,1848)}=65.523$ $p<0.001$ $r=0.034$). These results show evidence for non-alignment of input and output connections in this axis of orientation.

In the anterior-posterior axis: A Factorial ANOVA revealed a significant main effect of central PFC injection site location on the anterior-posterior location of retrogradely labelled cells in temporal cortex ($F_{(3,1408)}=2911.159$ $p<0.001$ $r=0.82$) and anterogradely labelled axon terminals in temporal cortex ($F_{(3,440)}=1145.478$ $p<0.001$ $r=0.85$). Post hoc comparisons (Tukey HSD) revealed significant differences between all injection sites ($p<0.001$). Post hoc comparisons (Tukey HSD) revealed significant differences between all anterograde injection sites ($p<0.001$). These findings show ordered arrangements of input and output connections from central PFC to temporal cortex in this axis of orientation.

A 2 factor ANOVA revealed a significant interaction effect of input and output connections ($F_{(3,1848)}=2869.926$ $p<0.001$ $r=0.608$). These results provide evidence for clear non-alignment of inputs and outputs in this axis of orientation.

In the medial-lateral axis: A Factorial ANOVA revealed a significant main effect of central PFC injection site location on the medial-lateral distance from the cortical surface of retrogradely labelled cells in temporal cortex ($F_{(3, 1408)}=16.805$ $p<0.001$ $r=0.11$) and anterogradely labelled axon terminals in temporal cortex ($F_{(3,440)}=288.022$ $p<0.001$ $r=0.63$). Post hoc comparisons (Tukey HSD) revealed significant differences between injection sites A*B, A*C, A*D ($p<0.001$) and B*D ($p=0.022$). Post hoc comparisons (Tukey HSD) revealed significant differences between anterograde injection sites A*B, A*D, B*C, B*D and C*D ($p<0.001$). These findings show ordered arrangements of input and output connections in this axis of orientation.

A 2 factor ANOVA revealed a significant interaction effect of input and output connections ($F_{(3,1848)}=147.850$ $p<0.001$ $r=0.074$). These findings show evidence for non-alignment of input and output projections from central PFC to temporal cortex.

Appendix I.

Labelling in Temporal Cortex from Co-injection of Retrograde (Fluoro-Gold) and Anterograde (Fluoro-Ruby) Tracers in Central Prefrontal Cortex

Injection sites in central PFC from co-injections of Fluoro-Gold (100nl) and Fluoro-Ruby (100nl) were positioned in the intended regions, comparable to separate Fluoro-Gold and Fluoro-Ruby injection sites (Fig.I.1), as well as Fluoro-Gold and BDA injection sites (chapter 2). A similar spread of both Fluoro-Gold and Fluoro-Ruby was seen at co-injection sites to that which had been observed at single injection sites (Fig.I.1). Co-injection sites of Fluoro-Gold and Fluoro-Ruby.

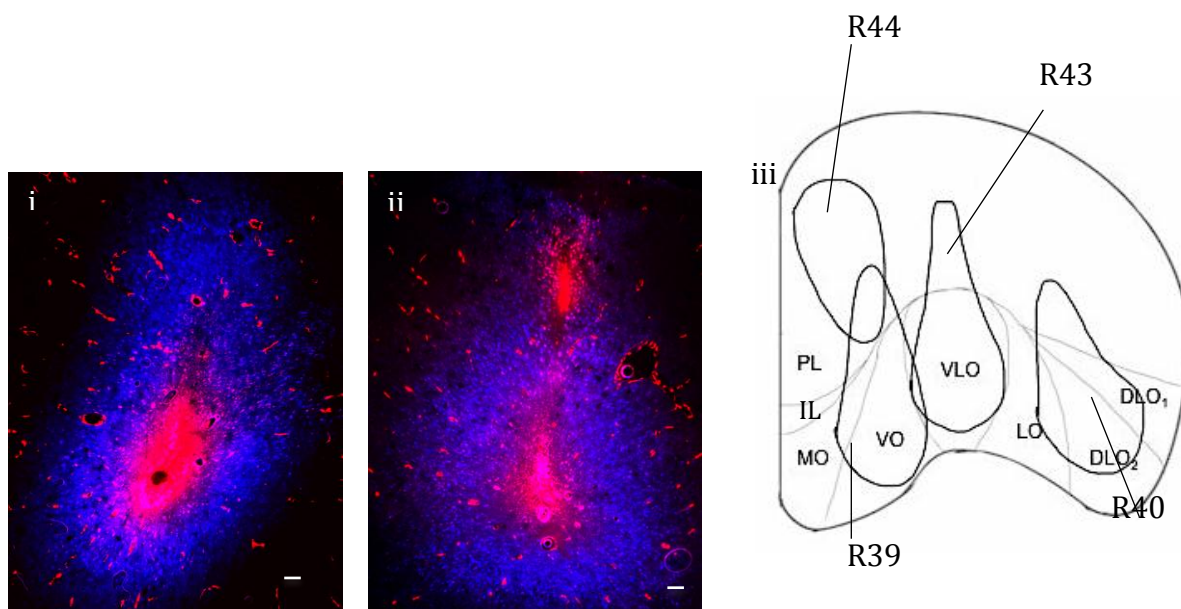


Figure I.1. (i) Coronal section of PFC showing location and spread of (100nl) Fluoro-Gold and (100nl) Fluoro-Ruby at injection site in DLO (R40). (ii) Coronal section of PFC showing location and spread of (100nl) Fluoro-Gold and (100nl) Fluoro-Ruby at injection site in VLO (R43). (iii) Representations of Fluoro-Gold and Fluoro-Ruby co-injection sites in PL (R44), VO (R39), VLO (R43) and DLO (R40). Scale bars = 100 μ m.

Results

The co-injection of retrograde (100nl Fluoro-Gold) and anterograde (100nl Fluoro-Ruby) tracers produced similar results to those produced from separate retrograde and anterograde injections (Fig. I.1). Retrogradely labelled cells and anterogradely labelled axon terminals were found in the same temporal cortex areas as with the previously described separate injections, and those described in chapter 2. The labelling shown here from co-injections of Fluoro-Gold and Fluoro-Ruby shows clear evidence for the ordered arrangement of both input and output connections from PFC to temporal cortex. Additionally, the findings from co-injections of retrograde and anterograde tracer injections provide additional evidence to support the non-alignment of input and output connections.

The results showed that the majority (>50%) of Fluoro-Gold and Fluoro-Ruby labelling in temporal cortex was separate from one another. High power imaging revealed some instance of co-labelling (Fluoro-Gold and Fluoro-Ruby), indicating evidence for some retrograde labelling resultant from Fluoro-Ruby injections. The majority of Fluoro-Ruby labelling was anterograde.

Statistical evidence for this ordered arrangement came from the following analysis:

In the dorsal-ventral axis: A factorial ANOVA revealed a significant main effect of central PFC injection site location on the distance of retrogradely labeled cells ($F_{(3,602)}= 20.625$ $p<0.001$ $r=0.182$) and anterogradely labeled axon terminals ($F_{(3,285)}= 2.736$ $p=0.044$ $r=0.975$) from the rhinal sulcus. These findings show evidence for ordering of input and output connections from central PFC to temporal cortex in this axis of orientation.

A 2 factor ANOVA revealed a significant interaction effect between input and output connections ($F_{(3,894)}=13.083$ $p<0.001$ $r=0.120$). These results show clear evidence of non-alignment of input and output connections, consistent with that found from separate injections.

In the anterior-posterior axis: A factorial ANOVA revealed a significant main effect of central PFC injection site location on the distance of retrogradely labeled cells ($F_{(3,602)} = 206.367$ $p < 0.001$ $r = 0.505$) and anterogradely labeled axon terminals ($F_{(3,285)} = 92.486$ $p < 0.001$ $r = .495$) from Bregma. These results indicate ordered arrangements of input and output connections in this axis of orientation.

A 2 factor ANOVA revealed a significant interaction effect between input and output connections ($F_{(3,894)} = 204.754$ $p < 0.001$ $r = 0.432$). These results show clear evidence of non-alignment of input and output connections, consistent with that found from separate injections.

In the medial-lateral axis: A factorial ANOVA revealed a significant main effect of central PFC injection site location on the distance of retrogradely labeled cells ($F_{(3,602)} = 503.443$ $p < 0.001$ $r = 0.675$) and anterogradely labeled axon terminals ($F_{(3,285)} = 61.004$ $p < 0.001$ $r = 0.420$) from the cortical surface.

A 2 factor ANOVA revealed a significant interaction effect between input and output connections ($F_{(3,894)} = 25.156$ $p < 0.001$ $r = 0.165$). These results show evidence for differential ordering of input and output connections, consistent with that found from separate injections.

This analysis of labelling produced by co-injections demonstrated an ordered organisation of connections between central PFC and temporal cortex. As the PFC source region is moved from medial to lateral (VO to DLO; B to D), the pattern of input projections from temporal cortex moves in anterior-posterior direction across temporal cortex, as well as moving in a dorsal-ventral direction (Fig.I.2).

As anterograde injection sites move from medial to lateral in central PFC, labelled output projections in temporal cortex move from posterior to anterior and from ventral to dorsal, additionally, output projections can be seen moving from medial to lateral in a clear order. From comparing the organisation of connections, these results

clearly show that the input and output projections from central PFC to temporal cortex follow different organisational patterns and are therefore not aligned with one another.

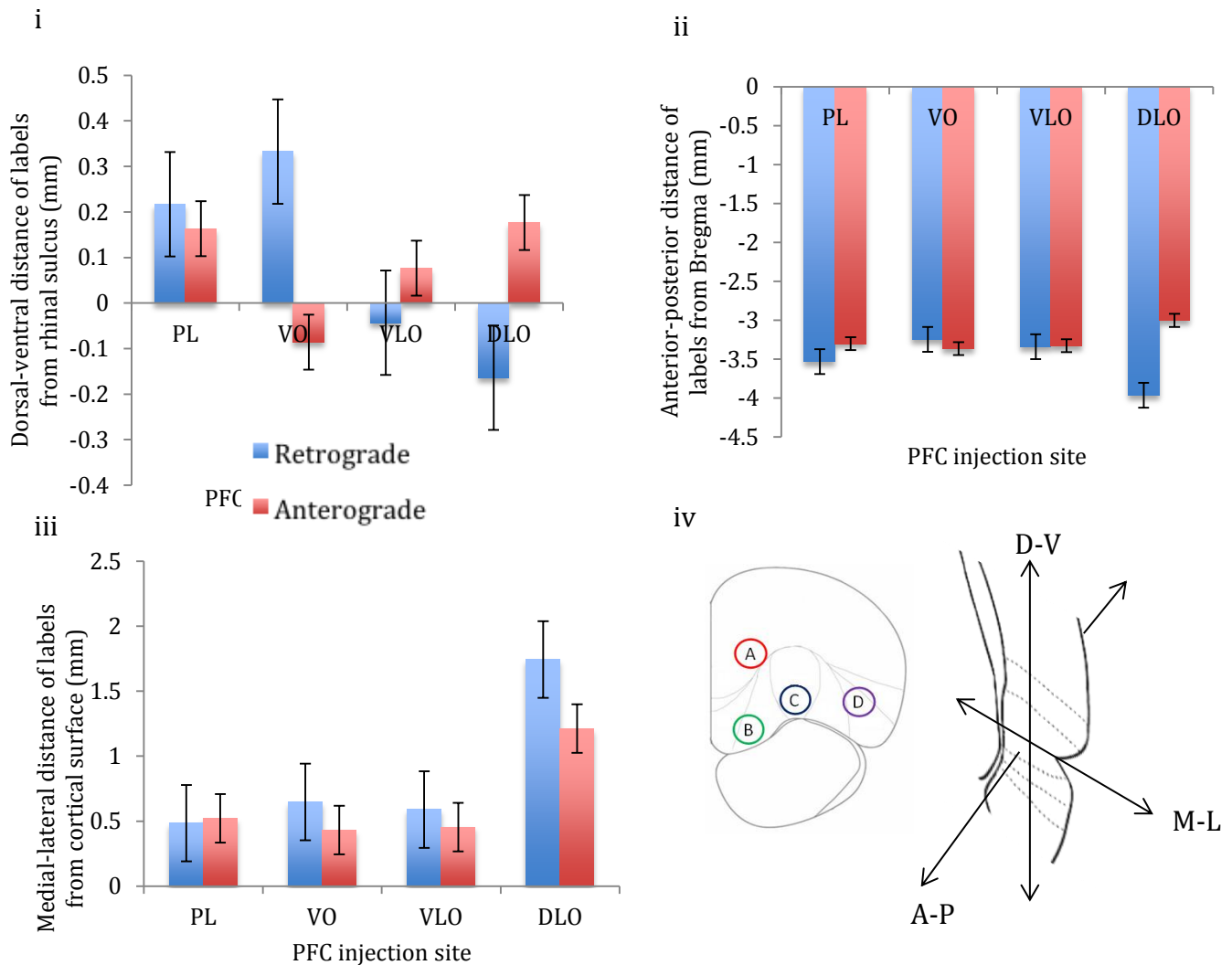


Figure I.2. The mean effect of PFC co-injection site on the (i) dorsal-ventral, (ii) anterior-posterior and (iii) medial-lateral location of retrogradely labelled cells ($n=606$ arising from 4 rats: PL=183, VO=136, VLO=158, DLO=129) and anterogradely labelled axon terminals ($n=289$ arising from 4 rats: PL=93, VO=66, VLO=59, DLO=71) within temporal cortex. Error bars=standard error. (iv) Coronal cross section of prefrontal cortex showing the position of 4 co-injection sites; prelimbic (A), ventral-orbital (B), ventrolateral orbital (C) and dorsolateral orbital (D). Coronal cross section of temporal cortex showing the three dimensions in which the locations of labels were recorded.

The results from co-injections of retrograde (Fluoro-Gold) and anterograde (Fluoro-Ruby) tracers showed no difference in the location of temporal cortex labelling in comparison to separate injections. Statistical evidence for this is provided by paired samples T-tests. No significant difference in the mean location of retrograde labelling in temporal cortex was found: in the dorsal-ventral axis ($t(3)=1.262$ $p=0.296$), in the anterior-posterior axis ($t(3)=.156$ $p=0.886$) and in the medial-lateral axis ($t(3)=.679$ $p=0.546$). No significant difference in the mean location of anterograde labelling in temporal cortex was found: in the dorsal-ventral axis ($t(3)=.887$ $p=0.440$), in the anterior-posterior axis ($t(3)=2.444$ $p=0.092$) and in the medial-lateral axis ($t(3)=.088$ $p=0.936$). These findings demonstrate the consistency of labelling produced by separate and co-injections of retrograde and anterograde tracers (Fluoro-Gold and Fluoro-Ruby) as well as the reproducibility of our findings. This is further supported by our findings from BDA and Fluoro-Gold co-injections (chapter 2).

To further clarify the consistency of results from co-injections and separate injections of tracers, thus clarifying the reliability of our single injection findings, a single numerical comparison was made. A euclidean distance between mean retrograde and anterograde label location was calculated (as was applied to BDA and Fluoro-Gold labelling in chapter 2):

$$E = \sqrt{(\langle DVr \rangle - \langle DVa \rangle)^2 + (\langle APr \rangle - \langle APa \rangle)^2 + (\langle MLr \rangle - \langle MLa \rangle)^2}$$

A paired samples t-test revealed no significant difference in labelling between co-injections and separate injections of Fluoro-Gold and Fluoro-Ruby ($t(3)= -2.523$ $p=0.086$). This shows that there is no quantifiable difference in the labelled connections seen when co-injecting an anterograde and retrograde tracer and when injecting them separately.

Appendix J.

Organisation of Connections from Central Prefrontal Cortex – Temporal Cortex, using Fluoro-Gold and Fluoro-Emerald

Anterograde labelling resultant from injections of (100nl) Fluoro-Emerald (R33, R34, R35, R36) was seen in the same temporal cortex locations as those labelled by Fluoro-Ruby from the same PFC injection site locations. The results of Fluoro-Emerald labelling were consistent with those of Fluoro-Ruby, identifying an ordered arrangement of output connections from PFC to temporal cortex, showing evidence for non-alignment with equivalent input connections (Fluoro-Gold).

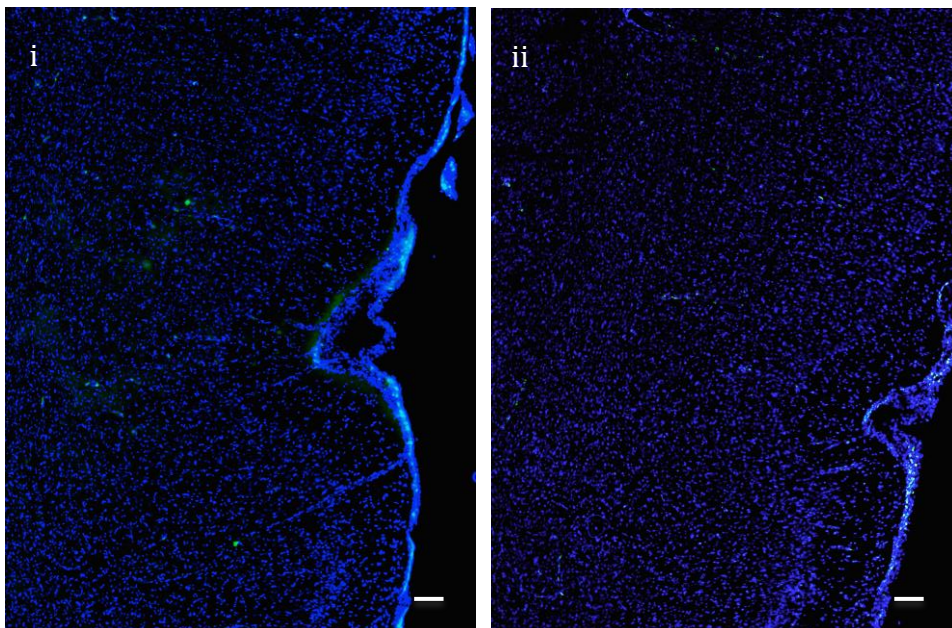


Figure J.1. Coronal sections of temporal cortex showing Fluoro-Emerald labelling (green) resultant from (100nl) injections into (i) VLO (R33) and (ii) VO (R34). Arrows denote the location of the rhinal sulcus. Scale bars = 100µm.

Statistical evidence for this ordered arrangement came from the following analysis:

In the dorsal-ventral axis: A factorial ANOVA revealed a significant main effect of PFC injection site location on the distance of anterogradely labeled axon terminals in temporal cortex from the rhinal sulcus ($F_{(3,397)}=3.081$ $p=0.027$ $r=0.088$). A 2 factor ANOVA revealed a significant interaction effect of input (Fluoro-Gold) and output (Fluoro-Emerald) connections ($F_{(3, 1805)}=23.099$ $p<0.001$ $r=0.112$). These findings show evidence for ordering of output connections from central PFC to temporal cortex in this axis of orientation and non-alignment of input and output connections, consistent with that seen with Fluoro-Ruby labelling.

In the anterior-posterior axis: A factorial ANOVA revealed a significant main effect of PFC injection site location on the distance of anterogradely labeled axon terminals from bregma ($F_{(3,397)}=335.675$ $p<0.001$ $r=0.677$). A 2 factor ANOVA revealed a significant interaction effect of input (Fluoro-Gold) and output (Fluoro-Emerald) connections ($F_{(3, 1805)}=1549.748$ $p<0.001$ $r=0.680$). These findings show evidence for ordering of output connections from central PFC to temporal cortex in this axis of orientation and non-alignment of input and output connections, consistent with that seen with Fluoro-Ruby labelling.

In the medial-lateral axis: A factorial ANOVA revealed a significant main effect of PFC injection site location on the distance of anterogradely labeled axon terminals from the cortical surface ($F_{(3,397)}=23.068$ $p<0.001$ $r=0.234$). A 2 factor ANOVA revealed a significant interaction effect of input (Fluoro-Gold) and output (Fluoro-Emerald) connections ($F_{(3, 1805)}=51.888$ $p<0.001$ $r=0.167$). These findings show evidence for ordering of output connections from central PFC to temporal cortex in this axis of orientation and non-alignment of input and output connections, consistent with that seen with Fluoro-Ruby labelling.

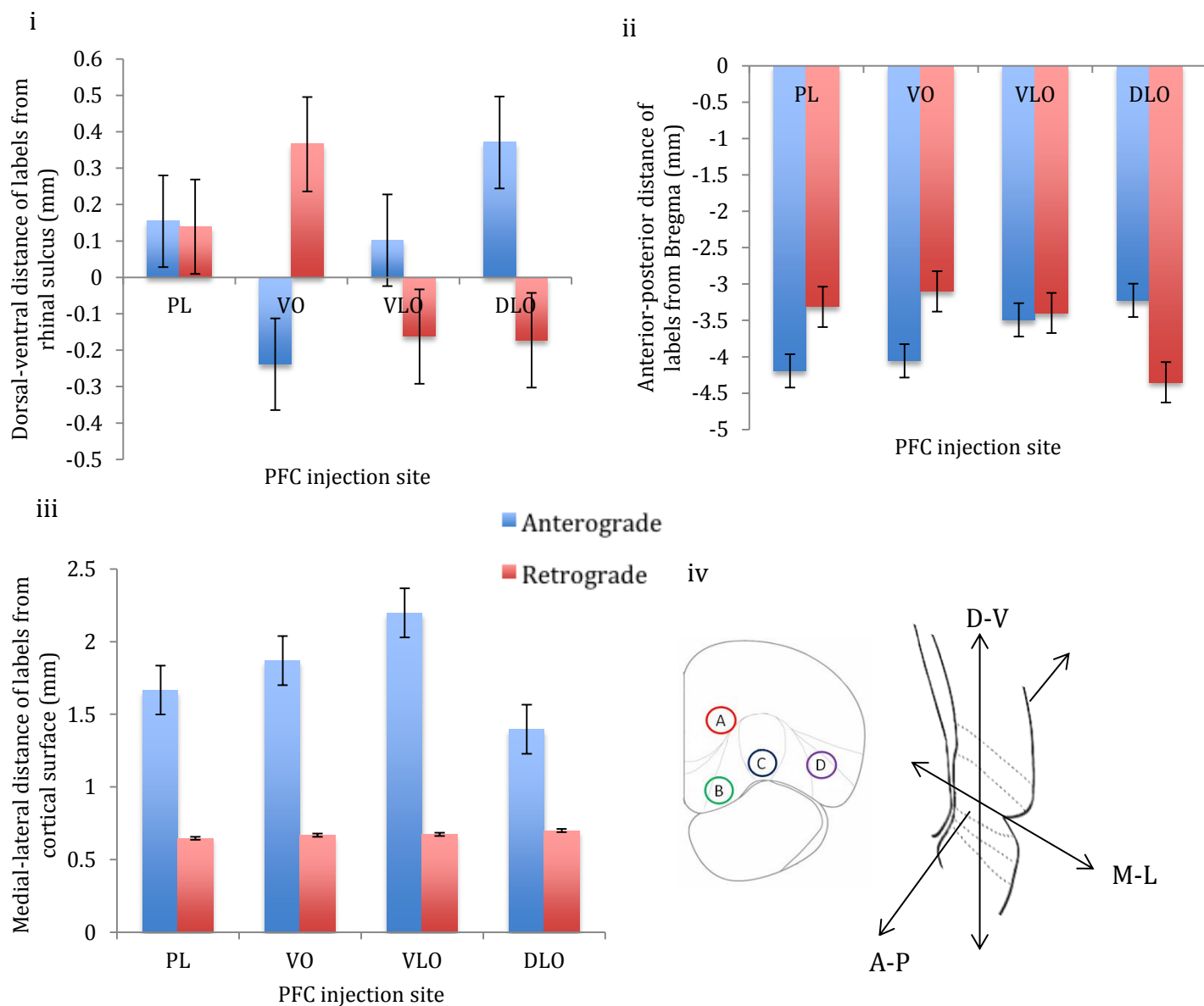


Figure J.2. The mean effect of PFC injection site on the (i) dorsal-ventral, (ii) anterior-posterior and (iii) medial-lateral location of Fluoro-Gold labelled cells (n=1412 arising from 4 rats: PL=253, VO=677, VLO=131, DLO=351) and Fluoro-Emerald labelling (n=401 arising from 4 rats: PL=66, VO=64, VLO=147, DLO=124) within temporal cortex. Error bars=standard error. (iv) Coronal cross section of prefrontal cortex showing the position of 4 injection sites; prelimbic (A), ventral-orbital (B), ventrolateral orbital (C) and dorsolateral orbital (D). Coronal cross section of temporal cortex showing the three dimensions in which the locations of labels were recorded.

Appendix K.

Statistical Comparison Between Central Prefrontal Cortex Connections to Temporal Cortex using BDA & Fluoro-Gold and Fluoro-Ruby & Fluoro-Gold

A statistical comparison of the findings from injections of Fluoro-Gold and Fluoro-Ruby (central PFC) with our findings from the previous experiments (chapter 2), in which retrograde and anterograde tracer injections were made in identical places (Fluoro-Gold and BDA) was carried out

T-tests revealed no significant difference in the patterns of labelling identified in the two experiments, notably no significant difference was identified in the relationship between labelled input and output projections, no significant difference was found in the distance between the FG and BDA labels in the first experiments and the distance between FG and FR labels in this experiment ($t(3)=-1.341$ $p=0.272$). This finding shows the reproducibility of our findings, particularly in regards to the relationship between input and output connections.

Appendix L.

Preliminary Small (20-30nl) Tracer Injection Volumes

Preliminary experiments were carried out in order to determine the spread, accuracy and visualization of small volumes of Fluoro-Gold and Fluoro-Ruby injected into PFC in the rat brain. These preliminary experiments allowed the optimization of injection volumes to enable the smallest possible injections, whilst maintaining visibility of labelling.

Tracer injections were initially made at 20nl for both Fluoro-Gold and Fluoro-Ruby. Labelling from 20nl injections could be easily visualized with Fluoro-Ruby, however could not be easily detected with Fluoro-Gold. Fluoro-Gold injection volume was increased to 30nl, where visibility was similar to that of 20nl Fluoro-Ruby (Fig.L.1). The spread of tracers at the injection sites in PFC was similar for 20nl Fluoro-Ruby and 30nl Fluoro-Gold (~0.5mm).

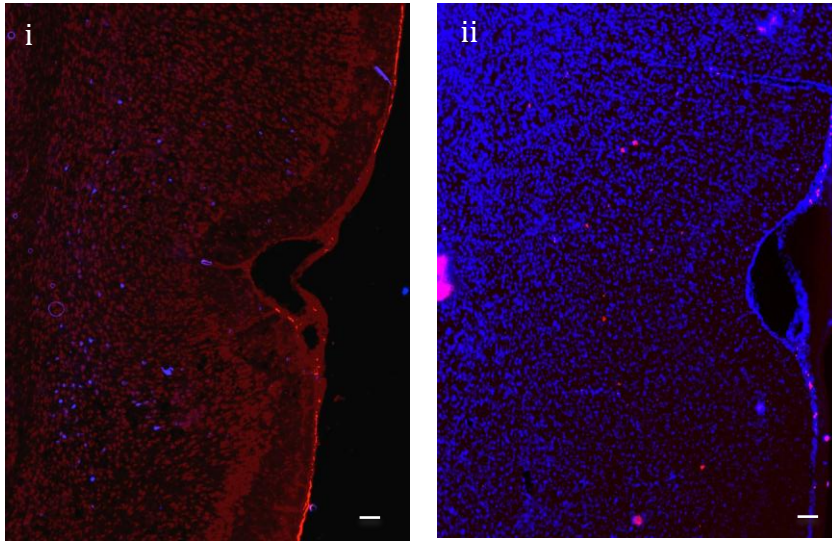


Figure L.1.(i) Retrograde labelling (blue) in temporal cortex produced by 30nl injection of Fluoro-Gold into DLO (R7). (ii) Labelling (red) in temporal cortex produced by 20nl injection of Fluoro-Ruby into DLO (R8). Arrows denote the location of the rhinal sulcus. Scale bars = 100 μ m.

Appendix M.

Organisation of Connections from Prefrontal Cortex - Sensory-Motor Cortex Resultant from Separate Injections of Fluoro-Gold (100nl) and BDA (100nl)

Data was collected from 14 male CD rats (314–358 g, Charles River, UK). Animal procedures were carried out in accordance with the UK Animals scientific procedures act (1986), EU directive 2010/63 and were approved by the Nottingham Trent University Animal Welfare and Ethical Review Body. For detailed methodology and surgical procedures see Chapters 2 and 5.

Results

The findings from this study are published in Bedwell et al (2014). Retrograde injections made into PL, VO, VLO and DLO (R4, R5, R6, R7) occurred in the intended PFC regions (Fig. M.1 iv, v). The majority of retrograde injection sites spanned layers I-VI, covered most of the cytoarchitectural region and were principally confined to cytoarchitectural boundaries of PFC sub-regions. The retrograde injection made into VO covered both VO and MO. There was some overlap between PL and VO injection sites and some spread into infralimbic cortex (IL) (Fig. M.1 iv). Anterograde injections made into PL, VO, VLO and DLO (R1, R3, R7, R8) occurred within the same cytoarchitectural regions as the retrograde equivalents, spanning a smaller area. Anterograde injection sites were largely within the cytoarchitectural boundaries of PFC sub-regions (the injection into VO occurred in both VO and MO), covering layers II-VI (Fig. M.iv, v). The injection sites from single tracer injections resembled those produced by co-injections of Fluoro-Gold and BDA.

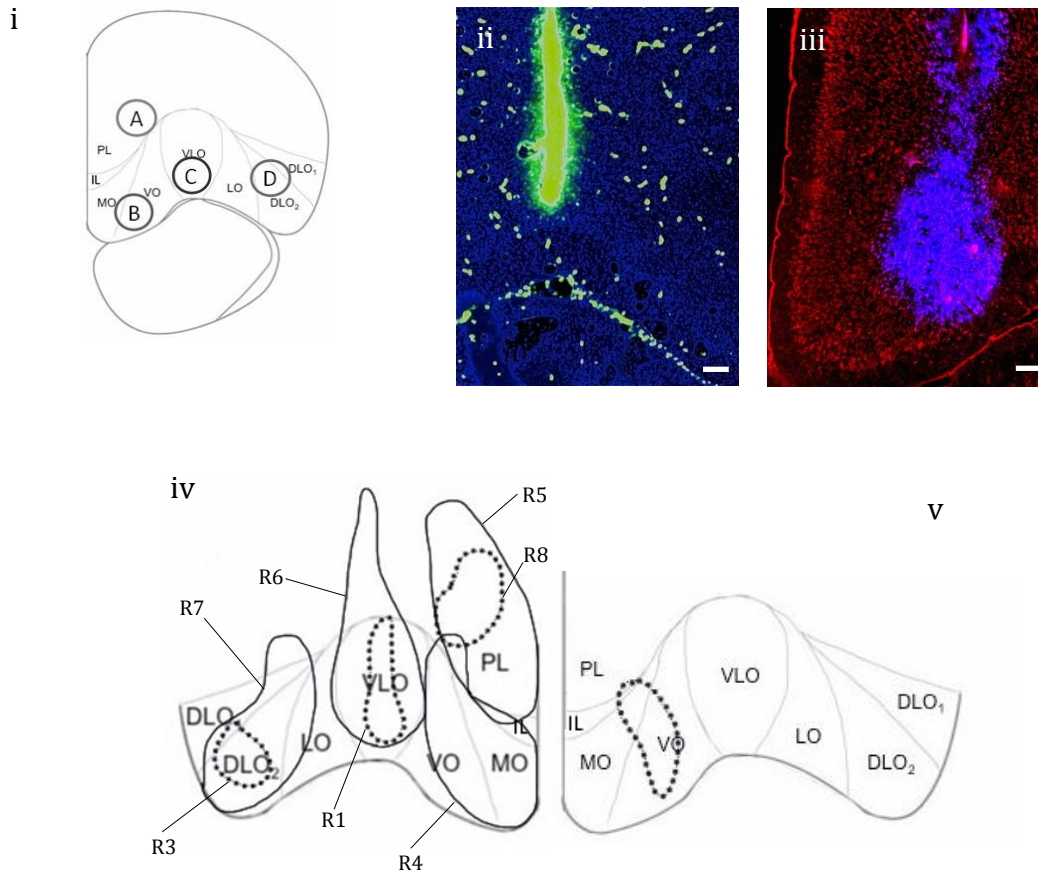


Figure M.1. (i) Coronal section of PFC (AP 4.2mm from Bregma) showing the cytoarchitectural boundaries of the prelimbic (PL), medial orbital (MO), ventral orbital (VO), ventrolateral orbital (VLO), lateral orbital (LO) and dorsolateral orbital (DLO₁, DLO₂) cortices (according to Van De Werd and Uylings, 2008), depicting sites of injections; Prelimbic: A, Ventral Orbital: B, Ventrolateral Orbital: C and Dorsal Lateral Orbital: D, with 1mm spread. (ii) Coronal section of prefrontal cortex showing location and spread of (100nl) fluorescein (green) at injection site in VLO. (iii) Coronal section of prefrontal cortex showing location and spread of (100nl) Fluoro-Gold (blue) at injection site in VO/MO. (iv) Representations of Fluoro-Gold (100nl) (R4, R5, R6, R7 (solid line)) and BDA (100nl) (R1, R3, R8 (broken line)) injection sites in DLO (R3, R7), VLO (R1, R6), VO/MO (R4) and PL (R5, R8), in the right hemisphere. (v) Representation of BDA injection site (R7) in VO/MO, in the left hemisphere. BDA injection sites were consistently within the boundaries of corresponding Fluoro-Gold injection sites. There is minimal overlap between Fluoro-Gold injection sites (R4 and R5). Fluoro-Gold injection sites are mostly limited to the cytoarchitectural boundaries of PFC regions, and span the whole region (PL, VO/MO, VLO, DLO), injections into VO spread into MO. BDA injection sites are consistently within cytoarchitectural boundaries and span layers II – VI (PL, VO/MO, VLO, DLO). Scale bars = 200µm.

The labelling from Fluoro-Gold and BDA (Fig.M.2, Fig.M.3) was similar to that observed from co-injections of BDA and Fluoro-Gold (Chapter 5) and showed evidence for ordering in the PFC – sensory-motor cortex pathway.

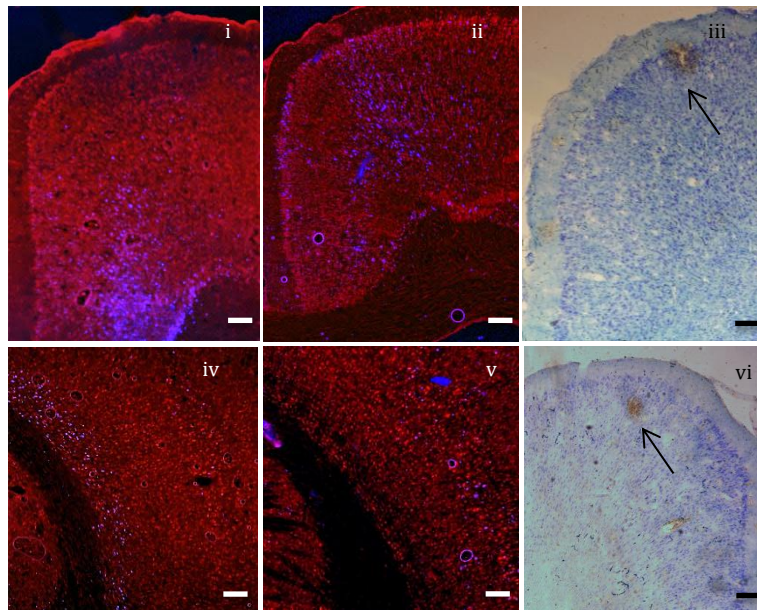


Figure M.2. (i) Coronal section showing retrogradely labelled cells (blue) in cingulate cortex produced by 100nl injection of Fluoro-gold into VLO (injection C). (ii) Coronal section showing retrogradely labelled cells (blue) in cingulate cortex produced by 100nl injection of Fluoro-gold into VO (injection B). (iii) Coronal section showing anterograde labelling (brown) produced by injection of BDA (100nl Fluorescein) into DLO (injection D). Arrow shows area of intense anterograde labelling of axon terminals. Other brown staining indicates less intense anterograde labelling, as well as some artifactual staining. Note the ordered location of labelled neurons within the dorsal-ventral axis. (iv) Coronal section showing retrogradely labelled cells (blue) in sensory cortex produced by injections of Fluoro-Gold (100nl) into VLO (injection C). (v) Coronal section showing retrogradely labelled cells (blue) in sensory cortex produced by injections of Fluoro-Gold (100nl) into and VO (injection B). (vi) Coronal section of sensory-motor cortex showing locations of anterograde labelling (brown) produced by injection of BDA (100nl Texas red) into VLO (injection B). Arrow shows area of intense anterograde labelling of axon terminals. Other brown staining indicates less intense anterograde labelling, as well as some artifactual staining. Scale bars = 200 μ m.

Retrogradely labelled cells were seen in secondary motor (M2), primary motor (M1) and primary somatosensory cortex (S1J). Anterogradely labelled areas were seen in M1, M2 and cingulate cortex (cg1).

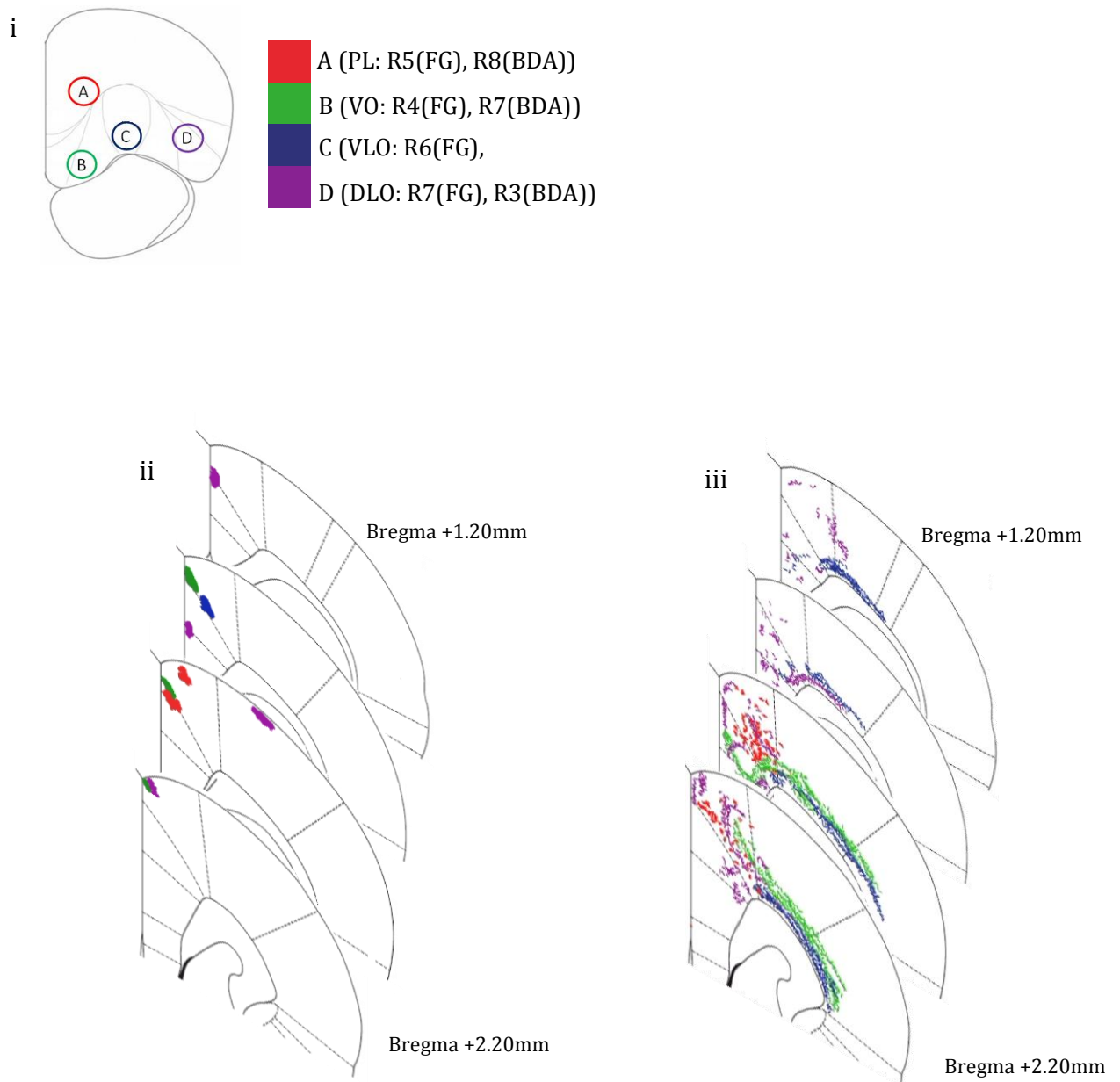


Figure M.3. Diagram representing amalgamated injection sites within prefrontal cortex and subsequent projection sites to sensory-motor cortex for both anterograde (BDA) and retrograde (FG) tracer injections in several rats. Coronal sections depict the injection site and projecting site. (i) The positions of 4 injection sites within prefrontal cortex; PL (injection A: R5(FG), R8(BDA)), VO (injection B: R4(FG), R7(BDA)), VLO (injection C: R6(FG), R1(BDA)) and DLO (injection D: R7(FG), R3(BDA)). (ii) Anterograde labelling of axon terminals (PFC output connections) following injections into 4 PFC sites (A-D BDA: R1, R3, R7, R8). (iii) Retrograde labelling (PFC input connections) following injections into 3 PFC sites (A-D, FG: R4, R5, R6, R7). Note the ordered location of labeled areas/neurons within the dorsal-ventral and medial-lateral axes.

Statistical evidence for this ordering came from the following analysis:

For the dorsal-ventral axis: The factorial ANOVA revealed a significant main effect of injection site on dorsoventral (i.e., laminar) location of retrogradely ($F_{(3,490)} = 380.578, p < 0.001$) and anterogradely ($F_{(3,36)} = 23.719, p < 0.001$) labelled cells in sensory-motor cortex. *Post hoc* comparisons (Tukey HSD) between the four retrograde groups indicate significant differences between PL*VO, PL*VLO, PL*DLO ($p < 0.001$). *Post hoc* comparisons (Tukey HSD) between the four anterograde groups indicated significant differences between PL*DLO, VO*DLO ($p < 0.001$) and VLO*DLO ($p = 0.028$). This indicates an ordered arrangement from sensory-motor areas to medial sub-regions of PFC (PL, VO, VLO; Fig.M.4.i). The 2 factor ANOVA revealed a significant interaction effect between input and output connections ($F_{(3,526)} = 45.709, p < 0.001$). This shows that the dorsoventral location of anterogradely and retrogradely labelled cells vary in respect to one another. The statistical analysis revealed a significant ordering of retrograde and anterograde connections. The 2 factor ANOVA indicated that the input and output connections (anterograde and retrograde label) occurred in different locations in this axis of orientation.

For the anterior-posterior axis: A factorial ANOVA revealed a significant main effect of injection site on anterior-posterior location of retrogradely labelled cells ($F_{(3,490)} = 82.090, p < 0.001$) and anterogradely labelled cells ($F_{(3,36)} = 6.029, p = 0.002$) in sensory-motor cortex. *Post hoc* comparisons (Tukey HSD) between the four retrograde groups indicated significant differences between PL*VO, PL*VLO, PL*DLO, VO*VLO, VO*DLO ($p < 0.001$). *Post hoc* comparisons (Tukey HSD) between the four anterograde groups indicated significant differences between PL*DLO and VO*DLO ($p < 0.006$). The 2 factor ANOVA revealed no significant interaction effect between input and output connections ($F_{(3,526)} = 2.415, p = 0.066$). This indicates an ordered arrangement of input and output connections within the anterior-posterior axis (Fig.M.4.ii). This analysis shows strong evidence for ordering of anterograde connections as well as evidence for ordering of retrograde connections. There is no clear statistical evidence for differential location of inputs and outputs in this axis of orientation.

For the medial-lateral axis: A factorial ANOVA revealed a significant main effect of injection site on medial-lateral location of retrogradely ($F_{(3,490)}=385.767, p<0.001$) and anterogradely ($F_{(3,36)}=24.102, p<0.001$) labelled cells in sensory-motor cortex. *Post hoc* comparisons (Tukey HSD) between the four retrograde groups indicated significant differences between PL*VO, PL*VLO, PL*DLO ($p<0.001$). *Post hoc* comparisons (Tukey HSD) between the four anterograde groups indicated significant differences between all injection sites; PL*VLO, PL*DLO, VO*VLO and VO*DLO ($p<0.001$). Figure M.4.iii shows that no clear ordered arrangement is seen in the medial-lateral axis. The 2 factor ANOVA revealed a significant interaction effect between input and output connections ($F_{(3,526)}=24.695, p<0.001$). This shows that the medial-lateral location of anterogradely and retrogradely labelled cells vary in relation to one another. The statistical analysis revealed a significant ordering of retrograde and anterograde connections. The 2 factor ANOVA indicated that the input and output connections (anterograde and retrograde label) occurred in different locations in this axis of orientation.

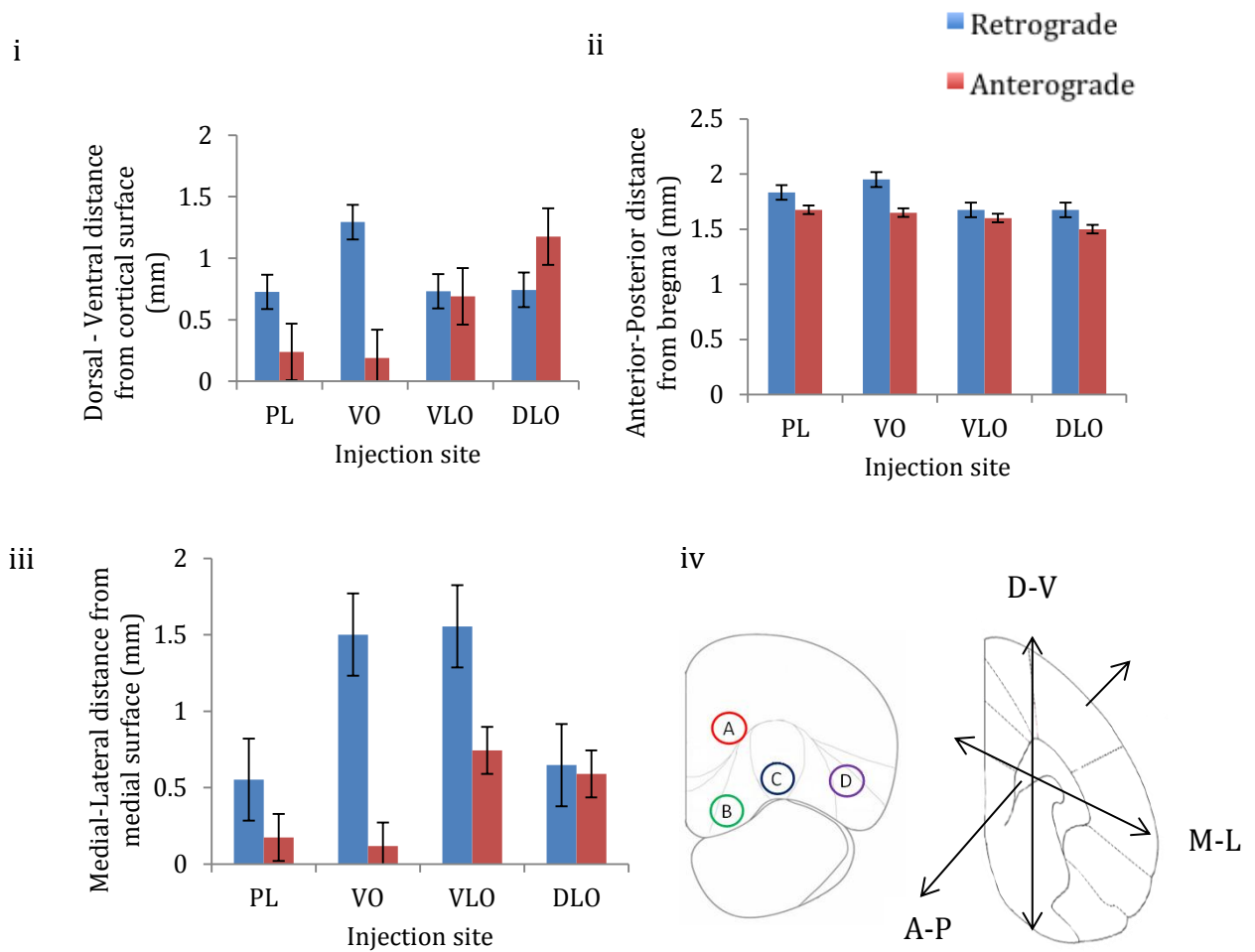


Figure M.4. The mean effect of injection site on the (i) dorsal-ventral, (ii) anterior-posterior and (iii) medial-lateral location of retrogradely cells (n=494 cells arising from 4 rats) and anterogradely labelled areas (n=40 points from 4 rats) within the sensory-motor cortex. Error bars = standard error. (iv) Coronal cross section of PFC indicating the position of 4 injection sites within prefrontal cortex: Prelimbic (injection A), Ventral Orbital (injection B), Ventrolateral Orbital (injection C) and Dorsal Lateral Orbital (injection D), Coronal cross section of sensory-motor cortex, depicting the three dimensions in which the locations of labelled cells were recorded.

Appendix N.

Hemispheric Effect of Injection Site and Resultant Labelling in Sensory-Motor Cortex

In the study described in Chapter 5, all of the FG injections were made into the right hemisphere and the majority of BDA injections were made into the left hemisphere. In order to control for possible effects of laterality in the analysis of label locations, the labelling produced by right hemisphere FG injections was compared to labelling produced by additional left hemisphere FG injections which were made later (Fig. N.1).

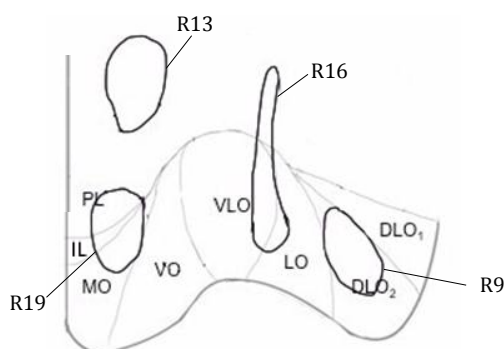


Figure N.1 Representations of four comparative Fluoro-Gold injection sites made into the left hemisphere; in PL (R13), PL/IL/MO (R19), VLO/LO (R16) and DLO₂ (R9), used to ascertain whether hemispheric differences affected projections. R13 is positioned higher than the corresponding right hemisphere PL injection (R7), however the majority of the injection site is confined to PL and covers the dorsal aspect of the R7 injection site.

Retrograde labelling in sensory-motor cortex produced by comparable right and left hemisphere FG injections were compared by applying a paired samples t-test to the mean locations of retrogradely labelled regions in three axes of orientation.

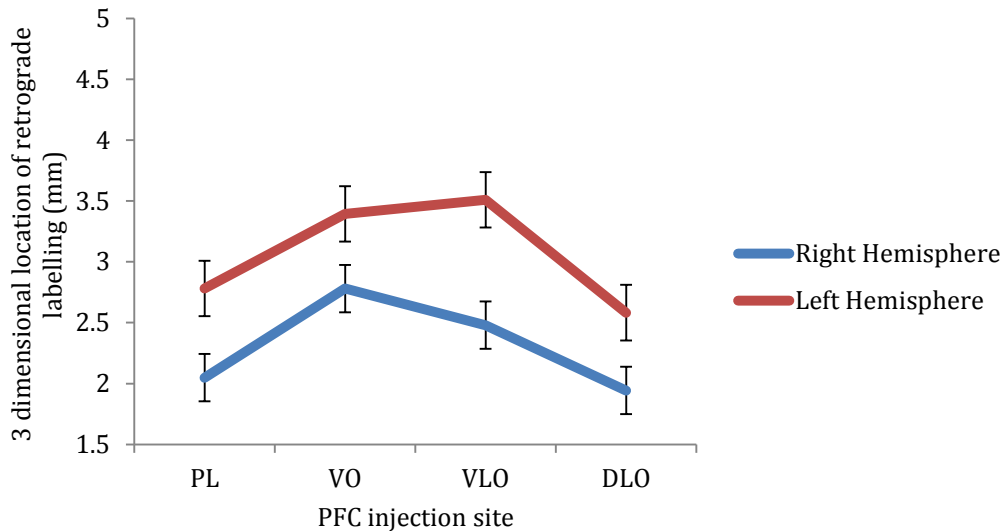


Figure N.2. The effect of injection site location on the 3-dimensional location of retrograde labelling in sensory-motor cortex, between left and right hemisphere injections of Fluoro-Gold. Error bars = standard error.

Paired-samples t-tests revealed no significant differences in the mean location of retrograde labelling in sensory-motor cortex resultant from Fluoro-Gold injections into the left and right hemispheres (Fig.N.2); in the dorsoventral axis ($t(3)=0.415$ $p=0.706$) and in the anterior-posterior axis ($t(3)=0.582$ $p=0.601$). The analysis also showed no significant difference in the 3-dimensional organisation of retrograde labelling in sensory-motor cortex ($t(2)=-.131$ $p=0.908$). These findings demonstrate that there is no observable hemispheric difference in PFC – sensory-motor cortex connections.

Appendix O.

Comparison of Labelling in Sensory-Motor Cortex from Single and Co-injections of Fluoro-Gold and BDA

To further compare the labelling from co-injections and separate injections of BDA (100nl) and Fluoro-Gold (100nl), a statistical analysis was applied to clarify any difference between the input-output relationships, thus confirming the reliability of comparative labelling from separate injection sites.

In order to produce a single numerical comparison between the two types of injection, a Euclidean distance between mean retrograde and anterograde labels was calculated to produce a single 3-dimensional value for labelling from each PFC injection site:

$$E = \sqrt{(\langle DVr \rangle - \langle DVa \rangle)^2 + (\langle APr \rangle - \langle APa \rangle)^2 + (\langle MLr \rangle - \langle MLa \rangle)^2}$$

Paired samples t-tests revealed no significant difference in labelling between co-injections and separate injections ($t(3)=0.982$ $p=0.399$). This indicates that there is no quantifiable difference in the relationship between input and output projections from PFC to temporal cortex when examined using either co-injections of anterograde and retrograde tracers or separate injections.

Appendix P.

Statistical Evidence for Organisation of Input and Output Connections Resultant from Separate Injections of Fluoro-Gold and Fluoro-Ruby in Central Prefrontal Cortex

Statistical evidence for this ordered arrangement came from the following analysis:

In the dorsal-ventral axis: A factorial ANOVA revealed a significant main effect of central PFC injection site location on the dorsal-ventral distance from the cortical surface of retrogradely labelled cells in medial-frontal cortex ($F_{(3,493)}=380.578$ $p<0.001$ $r=0.66$) and anterogradely labelled axon terminals in medial-frontal cortex ($F_{(3,223)}=57.891$ $p<0.001$ $r=0.46$). Post hoc comparisons (Tukey HSD) revealed significant differences between PFC injection sites A*B, A*C and A*D ($p<0.001$). Post hoc comparisons (Tukey HSD) revealed significant differences between anterograde injection sites A*D, B*D and C*D ($p<0.001$). No significant difference was found between anterograde injection sites A*B ($p=0.213$), A*C ($p=0.942$) and B*C ($p=0.818$). Calculation of Pearson's r revealed a significant negative correlation between retrograde labelling in medial-frontal cortex and location of injection site in PFC ($r=-.635$ $p<0.001$) and a significant positive correlation between anterograde labelling in medial-frontal cortex and location of injection site in PFC ($r=0.596$ $p<0.001$).

In the anterior-posterior axis: A factorial ANOVA revealed a significant main effect of central PFC injection site location on the anterior-posterior location of retrogradely labelled cells in medial-frontal cortex ($F_{(3,493)}=82.090$ $p<0.001$ $r=0.38$) and anterogradely labelled axon terminals in medial-frontal cortex ($F_{(3,223)}=41.058$ $p<0.001$ $r=0.40$). Post hoc comparisons (Tukey HSD) revealed significant differences between PFC injection sites A*B, A*C, A*D, B*C and B*D ($p<0.001$). Post hoc comparisons (Tukey HSD) revealed significant differences between anterograde injection sites A*B, A*C, A*D and B*D ($p<0.001$). No significant difference was found between anterograde injection sites B*C ($p=0.194$) and C*D ($p=0.197$).

Calculation of Pearson's r revealed a significant negative correlation between retrograde labelling in medial-frontal cortex and location of injection site in PFC ($r=-.406$ $p<0.001$) and a significant positive correlation between anterograde labelling in medial-frontal cortex and location of injection site in PFC ($r=0.363$ $p<0.001$).

In the medial-lateral axis: A factorial ANOVA revealed a significant main effect of central PFC injection site location on the medial-lateral distance from the medial cortical surface of retrogradely labelled cells in medial-frontal cortex ($F_{(3,493)}=385.767$ $p<0.001$ $r=0.66$) and anterogradely labelled axon terminals in medial-frontal cortex ($F_{(3,223)}=47.123$ $p<0.001$ $r=0.42$). Post hoc comparisons (Tukey HSD) revealed significant differences between PFC injection sites A*B, A*C and A*D ($p<0.001$). Post hoc comparisons (Tukey HSD) revealed significant differences between anterograde injection sites A*D, B*D and C*D ($p<0.001$). No significant difference was found between anterograde injection sites A*B ($p=0.423$), A*C ($p=0.996$), and B*C ($p=0.601$). Calculation of Pearson's r revealed a significant negative correlation between retrograde labelling in medial-frontal cortex and location of injection site in PFC ($r=-.637$ $p<0.001$) and a significant positive correlation between anterograde labelling in medial-frontal cortex and location of injection site in PFC ($r=0.518$ $p<0.001$).

Appendix Q.

Labelling in Sensory-Motor Cortex from Co-injection of Retrograde (Fluoro-Gold) and Anterograde (Fluoro-Ruby) Tracers in Central Prefrontal Cortex

Injection sites in central PFC from co-injections of Fluoro-Gold (100nl) and Fluoro-Ruby (100nl) (R39, R40, R43, R44) were positioned in the intended regions (for details see Appendix I).

Results

The co-injection of retrograde (100nl Fluoro-Gold) and anterograde (100nl Fluoro-Ruby) tracers produced similar results to those produced from separate retrograde and anterograde injections (Chapter 6). Retrogradely labelled cells and anterogradely labelled axon terminals were found in the same sensory and motor cortex areas as with the previously described separate injections (Chapter 6). The labelling shown here from co-injections of Fluoro-Gold and Fluoro-Ruby shows clear evidence for the ordered arrangement of both input and output connections from PFC to sensory-motor cortex. Additionally, the findings from co-injections of retrograde and anterograde tracer injections provide additional evidence to support the differential ordering of input and output connections.

The results showed that the majority (>50%) of Fluoro-Gold and Fluoro-Ruby labelling in temporal cortex was separate from one another. High power imaging revealed some instance of co-labelling (Fluoro-Gold and Fluoro-Ruby), indicating evidence for some retrograde labelling resultant from Fluoro-Ruby injections. The majority of Fluoro-Ruby labelling was anterograde (70%).

Statistical evidence for this ordered arrangement came from the following analysis:

In the dorsal-ventral axis: A factorial ANOVA revealed a significant main effect of central PFC injection site location on the distance of retrogradely labeled cells

($F_{(3,278)}= 13.381$ $p<0.001$ $r=0.214$) and anterogradely labeled axon terminals ($F_{(3,176)}= 40.806$ $p<0.001$ $r=0.434$) from the dorsal surface. These findings show evidence for ordering of input and output connections from central PFC to sensory-motor cortex in this axis of orientation.

A 2 factor ANOVA revealed a significant interaction effect between input and output connections ($F_{(3,454)}=39.755$ $p<0.001$ $r=0.284$). These results show clear evidence of non-alignment of input and output connections, consistent with that found from separate injections.

In the anterior-posterior axis: A factorial ANOVA revealed a significant main effect of central PFC injection site location on the distance of retrogradely labeled cells ($F_{(3,278)}= 42.865$ $p<0.001$ $r=0.366$) and anterogradely labeled axon terminals ($F_{(3,176)}= 24.227$ $p<0.001$ $r=0.348$) from Bregma. These results indicate ordered arrangements of input and output connections in this axis of orientation.

A 2 factor ANOVA revealed a significant interaction effect between input and output connections ($F_{(3,454)}=20.979$ $p<0.001$ $r=0.210$). These results show clear evidence of non-alignment of input and output connections, consistent with that found from separate injections.

In the medial-lateral axis: A factorial ANOVA revealed a significant main effect of central PFC injection site location on the distance of retrogradely labeled cells ($F_{(3,278)}= 47.210$ $p<0.001$ $r=0.381$) and anterogradely labeled axon terminals ($F_{(3,176)}= 51.759$ $p<0.001$ $r=0.477$) from the medial cortical surface.

A 2 factor ANOVA revealed a significant interaction effect between input and output connections ($F_{(3,454)}=50.995$ $p<0.001$ $r=0.318$). These results show evidence for differential ordering of input and output connections, consistent with that found from separate injections.

This analysis of labelling produced by co-injections demonstrated an ordered organisation of connections between central PFC and sensory-motor cortex. As the PFC source region is moved from medial to lateral (PL – DLO: Injection site A-D), retrograde labelling becomes more ventral and posterior whereas anterograde labelling becomes more lateral and posterior.

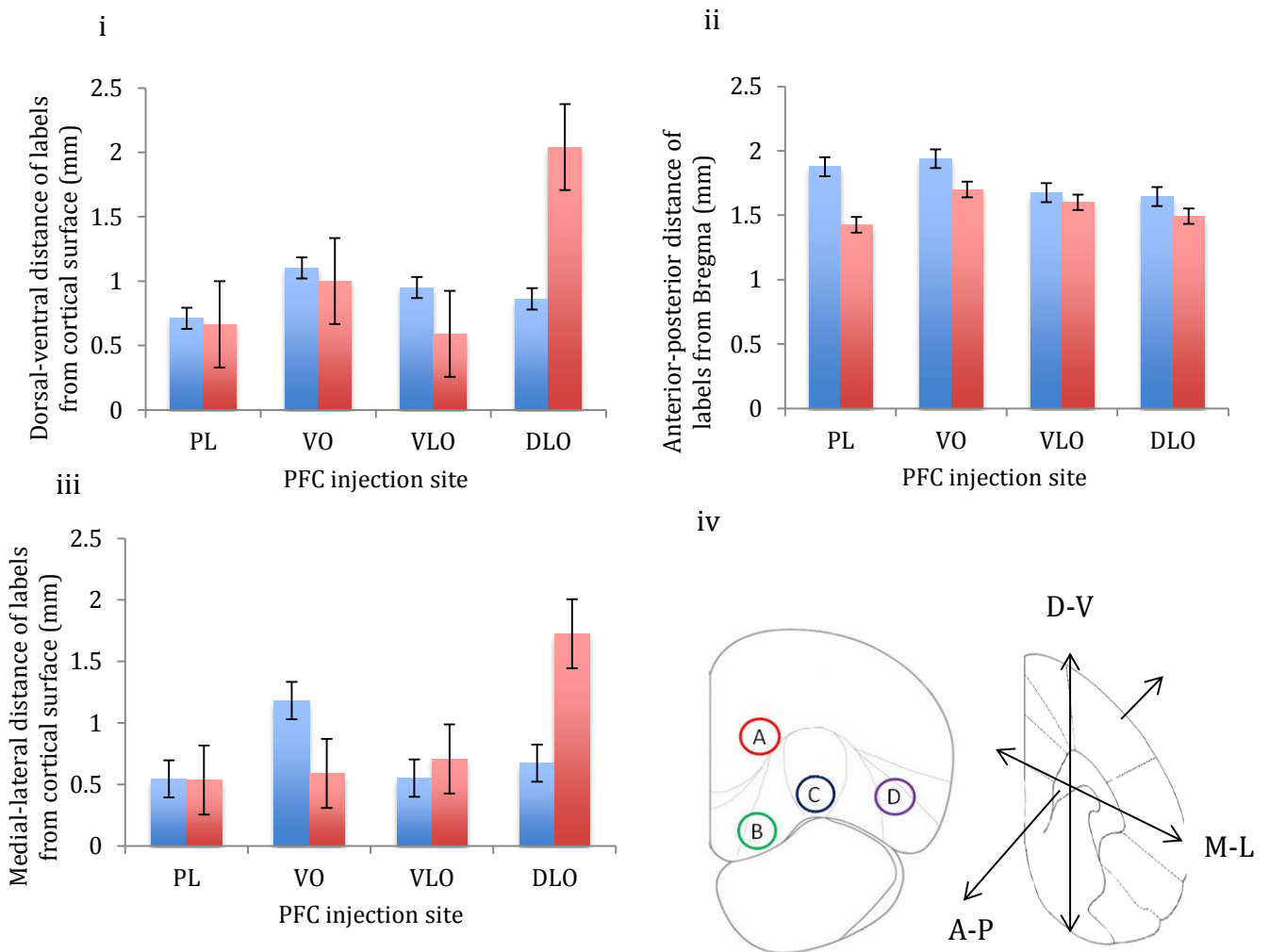


Figure Q.1. The mean effect of injection site on the (i) dorsal-ventral, (ii) anterior-posterior and (iii) medial-lateral location of Fluoro-Gold labeled cells (n=282 resultant from 4 rats, PL=48, VO=119, VLO=57, DLO=58) and Fluoro-Ruby labels (n=180 resultant from 4 rats, PL=92, VO=27, VLO=31, DLO=30) within sensory-motor cortex. Error bars = standard error. (iv) Coronal cross section of PFC indicating the position of four co-injection sites within PFC: Prelimbic (injection A), Ventral Orbital (injection B), Ventrolateral Orbital (injection C) and Dorsal Lateral Orbital (injection D), coronal cross section of sensory-motor

cortex, depicting the three dimensions in which the locations of labelled cells were recorded.

The results from co-injections of retrograde (Fluoro-Gold) and anterograde (Fluoro-Ruby) tracers showed no difference in the location of sensory-motor cortex labelling in comparison to separate injections. Statistical evidence for this is provided by paired samples T-tests. No significant difference in the mean location of retrograde labelling in sensory-motor cortex was found: in the dorsal-ventral axis ($t(3)=0.766$ $p=0.499$), in the anterior-posterior axis ($t(3)=-.057$ $p=0.958$) and in the medial-lateral axis ($t(3)=2.170$ $p=0.118$). No significant difference in the mean location of anterograde labelling in sensory-motor cortex was found: in the dorsal-ventral axis ($t(3)=-.923$ $p=0.424$), in the anterior-posterior axis ($t(3)=-.775$ $p=0.495$) and in the medial-lateral axis ($t(3)=0.062$ $p=0.954$). These findings demonstrate the consistency of labelling produced by separate and co-injections of retrograde and anterograde tracers (Fluoro-Gold and Fluoro-Ruby) as well as the reproducibility of our findings. This is further supported by our findings from BDA and Fluoro-Gold co-injections (Chapter 5).

Appendix R.

Statistical Comparison between Central Prefrontal cortex connections to Sensory-Motor Cortex using BDA & Fluoro-Gold and Fluoro-Ruby & Fluoro-Gold

A statistical comparison of the findings from injections of Fluoro-Gold and Fluoro-Ruby (central PFC) with our findings from the previous experiments (Chapter 6), in which retrograde and anterograde tracer injections were made in identical places (Fluoro-Gold and BDA) was carried out.

T-tests revealed no significant difference in the patterns of sensory-motor cortex labelling identified in the two experiments, notably no significant difference was identified in the relationship between labelled input and output projections, no significant difference was found in the distance between the FG and BDA labels in the earlier experiments and the distance between FG and FR labels in later experiments ($t(3)=-.532$ $p=0.632$). This finding shows the reproducibility of our findings, particularly in regards to the relationship between input and output connections.



The topology of connections between rat prefrontal, motor and sensory cortices

Stacey A. Bedwell, E. Ellen Billelt, Jonathan J. Crofts and Chris J. Tinsley*

School of Science and Technology, Nottingham Trent University, Nottingham, UK

Edited by:

Mikhail Lebedev, Duke University, USA

Reviewed by:

Matthew Jones, University of Bristol, UK

Nandakumar Narayanan, Yale University, USA

***Correspondence:**

Chris J. Tinsley, School of Science and Technology, Nottingham Trent University, Clifton Lane, Nottingham NG11 8NS, UK
e-mail: chris.tinsley@ntu.ac.uk

The connections of prefrontal cortex (PFC) were investigated in the rat brain to determine the order and location of input and output connections to motor and somatosensory cortex. Retrograde (100 nl Fluoro-Gold) and anterograde (100 nl Biotinylated Dextran Amines, BDA; Fluorescein and Texas Red) neuronanatomical tracers were injected into the subdivisions of the PFC (prelimbic, ventral orbital, ventrolateral orbital, dorsolateral orbital) and their projections studied. We found clear evidence for organized input projections from the motor and somatosensory cortices to the PFC, with distinct areas of motor and cingulate cortex projecting in an ordered arrangement to the subdivisions of PFC. As injection location of retrograde tracer was moved from medial to lateral in PFC, we observed an ordered arrangement of projections occurring in sensory-motor cortex. There was a significant effect of retrograde injection location on the position of labelled cells occurring in sensory-motor cortex (dorsoventral, anterior-posterior and mediolateral axes $p < 0.001$). The arrangement of output projections from PFC also displayed a significant ordered projection to sensory-motor cortex (dorsoventral $p < 0.001$, anterior-posterior $p = 0.002$ and mediolateral axes $p < 0.001$). Statistical analysis also showed that the locations of input and output labels vary with respect to one another (in the dorsal-ventral and medial-lateral axes, $p < 0.001$). Taken together, the findings show that regions of PFC display an ordered arrangement of connections with sensory-motor cortex, with clear laminar organization of input connections. These results also show that input and output connections to PFC are not located in exactly the same sites and reveal a circuit between sensory-motor and PFC.

Keywords: prefrontal cortex, sensory-motor cortex, connections, organization

INTRODUCTION

Prefrontal cortex (PFC) has been strongly associated with executive function, temporal ordering, cognitive processes and autonomic functions (Kolb, 1984; Neafsey, 1990; Alvarez and Emory, 2006; Schoenbaum and Esber, 2010). Prefrontal cortex has also been implicated in a number of neurological abnormalities such as autism and psychosis (Goldman-Rakic, 1991; Perlstein et al., 2001; Courchesne et al., 2011). Rodent PFC contains medial PFC (mPFC), orbital and agranular insular regions (Van De Werd and Uylings, 2008) which are thought to be functionally distinct. Dorsal mPFC has functional links to motor cortex and is involved in motor and temporal processing (Narayanan and Laubach, 2006; Vertes, 2006; Kim et al., 2013). Ventral mPFC has a functional role in cognitive and emotional processing (Fryszak and Neafsey, 1994; Vertes, 2006). Rat orbital cortex has been proposed to be involved in associative learning and making predictions about the external environment (Schoenbaum and Roesch, 2005; Schoenbaum and Esber, 2010). Agranular insular cortex has a greater functional role in the processing of sensory information including gustation (Gallagher et al., 1999; Fujita et al., 2011).

Despite the advances in our understanding of PFC function in the rat, the precise neuronal circuitry of PFC regions remains

largely undefined, meaning the functional connectivity cannot yet be fully understood. Topographic organization has been described as a hallmark feature of cortical organization among vertebrates (Thivierge and Marcus, 2007) and is widely regarded as a necessary feature for complex brain function. Ordered structural and physiological organization has been described for several regions of cerebral cortex, including motor, sensory, auditory, visual and entorhinal cortex (Woolsey, 1967; Welker, 1971; Hafting et al., 2005). Connectivity studies of these regions have often indicated that ordered functional organization is based upon an underlying topographically ordered organization of anatomical projections (Porter and White, 1983; Henry and Catania, 2006; Aronoff et al., 2010).

Recent studies into PFC connectivity broadly indicate an ordered structural organization (Hoover and Vertes, 2011; Kondo and Witter, 2014). Kondo and Witter (2014) described a topographic organization of the projection from orbitofrontal cortex to the parahippocampal region in rats. They demonstrated an ordered arrangement of output connections from PFC sub-regions (medial orbital (MO), ventral orbital (VO), lateral orbital (LO)) to areas of perirhinal, postrhinal and entorhinal cortex. This ordered arrangement was reported only for the output projection.

Parallel arrangement of input and output connections, resulting in reciprocal connections is a widely accepted occurrence in cortical organization, and has been described in multiple regions, including perirhinal, postrhinal, entorhinal, piriform, frontal, insular, temporal, cingulate, parietal and areas of occipital cortex (Canto et al., 2008; Agster and Burwell, 2009).

Studies of rat PFC outputs have shown that they also project widely to subcortical (such as the thalamus, striatum, brainstem and amygdala) and cortical targets (such as perirhinal and entorhinal cortex) (Vertes, 2004; Gabbott et al., 2005; Hoover and Vertes, 2007). Such studies have also shown that rat PFC displays gross-level topologically organized connections in rats. Ordered projections from lateral and posterior PFC regions to the posterior cingulate area have been reported (Olson and Musil, 1992). Recent anatomical studies report a topologically organized projection from rat lateral PFC to perirhinal cortex and area TE (Hoover and Vertes, 2011). Tracer studies have demonstrated a broad medial-lateral topographic organization of connections from PFC sub-regions to sub-cortical structures (Berendse et al., 1992; Schilman et al., 2008): a medial-lateral shift in injection sites in PFC produced a corresponding medial-lateral shift in anterogradely labeled projections in striatum and caudate putamen. However, this ordered arrangement has only been reported in subcortical PFC projections, and is described only between cytoarchitecturally distinct PFC sub-regions.

In order to clearly establish the nature of physiological organization within PFC, it is necessary to first gain a more detailed picture of the underlying anatomical organization. Anterograde tract tracing findings have revealed spatially ordered projections from the posterior PFC (mPFC), both within and across different cytoarchitectural areas (Sesack et al., 1989). Further to this, retrograde tracers reveal projections of MO and VO cortices in the rat (Berendse et al., 1992; Schilman et al., 2008). The prominent cortical targets (orbital fields) of MO and VO were found to be adjacent (Berendse et al., 1992), demonstrating a topographic organization of MO and VO projections to medial dorsal striatum.

The following study aimed to establish the ordered organization of connections within PFC. Retrograde and anterograde neuronal tracers were injected into regions of medial and lateral PFC (prelimbic (PL), VO, ventrolateral orbital (VLO) and dorso-lateral orbital cortex (DLO)). We established that PFC contains extensive reciprocal connections with areas of sensory-motor cortex. Further, our findings show a clearly ordered arrangement of input and output connections and evidence for a circuit linking sensory-motor cortex with PFC.

MATERIAL AND METHODS

ANIMALS

Data was collected from 14 male CD rats (314–358 g, Charles River, UK). Animal procedures were carried out in accordance with the UK Animals scientific procedures act (1986), EU directive 2010/63 and were approved by the Nottingham Trent University Animal Welfare and Ethical Review Body. On receipt the animals were examined for signs of ill-health or injury. The animals were acclimatized for 10 days during which time their

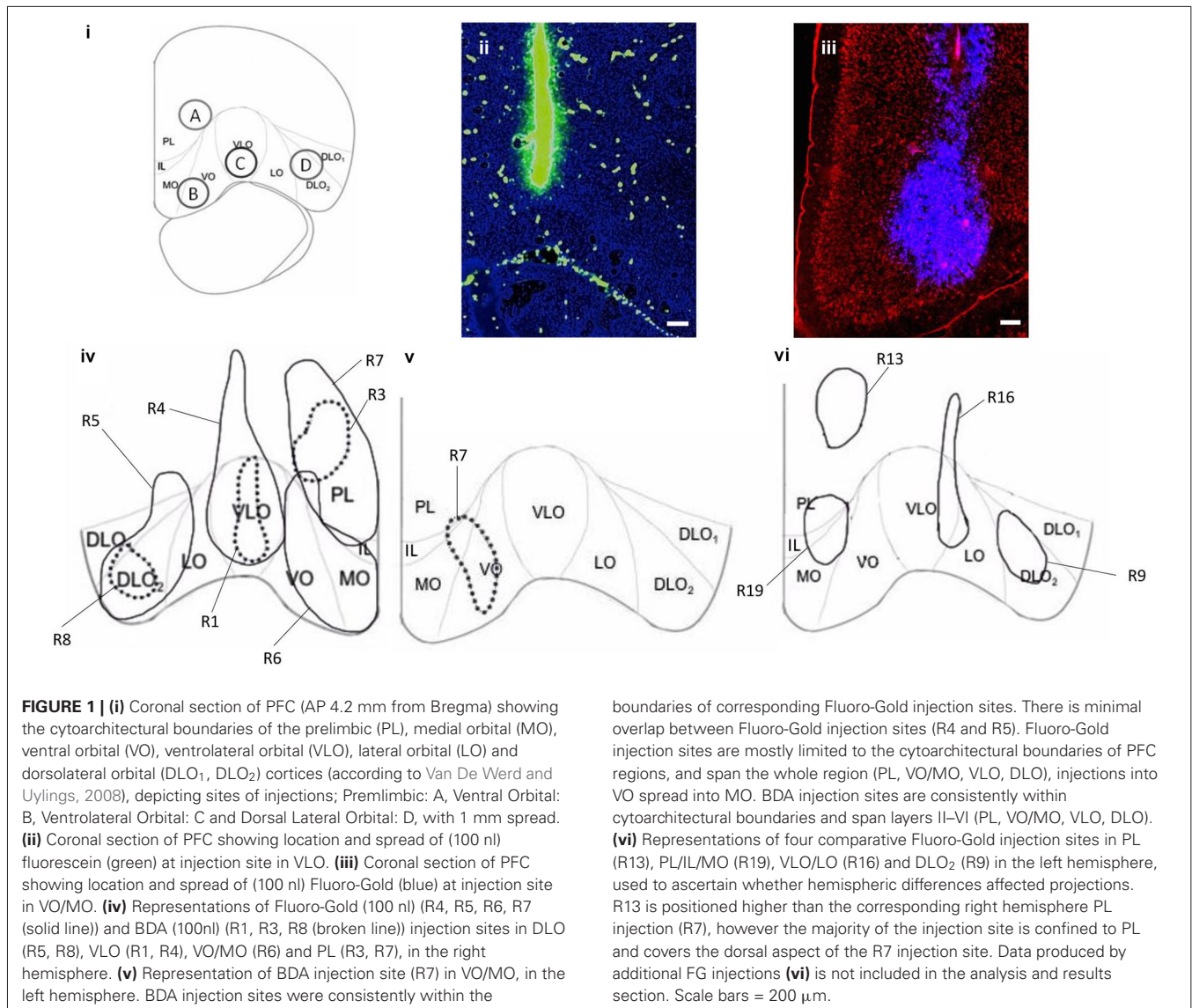
health status was assessed. Prior to surgery the animals were housed together in individually ventilated cages (IVC; Techniplast double decker Greenline rat cages). The animals were allowed free access to food and water. Mains drinking water was supplied from polycarbonate bottles attached to the cage. The diet and drinking water were considered not to contain any contaminant at a level that might have affected the purpose or integrity of the study. Bedding was supplied by IPS Product Supplies Ltd in form of 8/10 corncob. Environmental enrichment was provided in the form of wooden chew blocks and cardboard fun tunnels (Datesand Ltd., Cheshire, UK). Post-surgery the animals were individually housed in the same conditions. The animals were housed in a single air-conditioned room within the Biological support facilities barrier unit. The rate of air exchange was at least fifteen air changes per hour and the low intensity fluorescent lighting was controlled to give 12 h continuous light and 12 h darkness. The temperature and relative humidity controls were set to achieve target values of $21 \pm 2^\circ\text{C}$ and $55 \pm 15\%$ respectively.

Individual bodyweights were recorded on Day - 10 (prior to the start of dosing) and daily thereafter. All animals were examined for overt signs of ill-health or behavioral change immediately prior to surgery dosing, during surgery and the period following surgery. There were no observed clinical signs/symptoms of toxicity or infection. There was no significant effect on body weight development detected.

SURGICAL PROCEDURES

Rats were anesthetized with isoflurane (Merial, Harlow, UK) and placed in a stereotaxic frame with the incisor bar set so as to achieve a flat skull. Buprenorphine (0.05 mg/kg i.m./s.c) and Meloxicam (up to 1 mg/kg s.c/orally) analgesia were provided peri-operatively and for several days post-operatively. Body temperature was monitored during and immediately after surgery using a rectal thermometer. Craniotomies (<1 mm) were made at predetermined stereotaxic coordinates. Sterile tracer solution was deposited into the PFC via a 0.5 μl neuro-syringe (Hamilton, Germany). Injections of anterograde (biotinylated dextran amines, BDA; Fluorescein [SP-1130] and Texas red [SP-1140], Vector laboratories CA) and retrograde tracer (4% Fluoro-Gold in distilled water, Fluorochrome, Denver, Colorado) were made into the PL, VO, VLO or DLO (100 nl/min, 2 min diffusion time), with the intention of revealing the anatomical connections of prefrontal regions. The distance between craniotomy co-ordinates (1 mm) was based on the measured spread of tracers in preliminary and the present studies (<1 mm in diameter). Injections were made at AP 3.7 mm from Bregma (A) ML 1.2 mm, 2.4 mm below cortical surface, (B) ML 1.2 mm, 3.2 mm below cortical surface, (C) ML 2.2 mm, 3.2 mm below cortical surface (D) ML 3.2 mm, 3.2 mm below cortical surface. The injection needle was positioned vertically for all tracer injections. Tracer injections were excluded (1 injection) from the study where the injection site was found to be in a different co-ordinate to that which was intended.

Each rat received injections of Fluorescein (100 nl), Texas red (100 nl) and/or Fluoro-Gold (100 nl) into various subdivisions of PFC, separated by 1 mm (Figure 1). Rats received either



one injection of tracer or an injection of retrograde tracer into one hemisphere and an injection of anterograde tracer into the other hemisphere to allow accurate identification of the tracers injected. All Fluoro-Gold injections were made in the right hemisphere in this experiment (Figure 1iv) and BDA injections were also made in the right hemisphere except in the case of injection B (left hemisphere; Figures 1iv,v). Seven additional and equivalent Fluoro-Gold injections were made into the left hemisphere to verify whether the location and ordering of projections differed on the either side of the brain (four of these are shown in Figure 1vi). The same overall order and positioning of Fluoro-Gold labeling was observed on both sides of the brain.

Following a survival time of 7–8 days, the rats were deeply anesthetized with pentobarbital (Sigma-Aldrich, UK), and transcardially perfused with phosphate buffered saline (PBS) (pH 7.4) (~200 ml) followed by 4% paraformaldehyde (PFA) (pH 7.4)

(~200 ml). The brain was subsequently removed and stored for 24 h in 4% PFA in PBS (pH 7.4), followed by cryoprotection in 30% sucrose in PBS.

ANATOMICAL PROCESSING AND IMAGING

For analysis of anterograde connections, two series of 40 μm coronal sections were taken (two in six sections) on a freezing microtome (CM 1900, Leica, Germany). Sections were mounted onto gelatin coated slides. One series of sections was cover slipped with Vectashield® (Vector laboratories, CA) mounting medium (with DAPI), for fluorescent imaging of Fluorescein and Texas red injection sites. A second series was processed by implementing the avidin-biotin method (Vectastain®ABC, Vector laboratories), for bright field imaging of Fluorescein and Texas red labeled cells. This series of sections was counterstained with thionin. For analysis of retrograde connections, a parallel series of 40 μm coronal sections was taken (one in six sections), mounted onto

gelatin coated slides, then cover slipped with Vectashield® (Vector laboratories, CA) mounting medium (with propidium iodide) for fluorescent imaging of Fluoro-Gold.

Sections were examined using either bright field (Fluorescein and Texas red) or fluorescent microscopy (Fluorescein, Texas red and Fluoro-Gold). Injection sites were determined according to the cytoarchitecture of PFC sub-regions (Van De Werd and Uylings, 2008) and labelled cells were plotted on representative coronal diagrams (Paxinos and Watson, 1998). Fluorescent photos were captured of injection sites and retrogradely labelled cells (Fluoro-Gold). Brightfield photos were captured of anterogradely labelled areas (Fluorescein and Texas red) using an Olympus DP-11 system microscope with a $\times 4$ and $\times 10$ objective lens.

MICROSCOPIC ANALYSIS

Initially, the entire forebrain was examined for labeling. Areas of sensory-motor cortex were found to contain some of the strongest and most consistent labeling of connections; therefore a more detailed analysis was carried out on this region to examine the organization of prefrontal to sensory-motor cortex connections. Prominent labeling was also found in areas of temporal cortex, PFC—temporal cortex connections were investigated in a separate study (Bedwell et al., in preparation).

STATISTICAL ANALYSIS OF THE ARRANGEMENT OF CONNECTIONS BETWEEN PREFRONTAL AND SENSORY-MOTOR CORTEX

We implemented a statistical analysis to determine whether connections between PFC and sensory-motor cortex displayed an ordered arrangement. ImageJ (Wayne Rasband, NIH) was used to determine numerical values representing the three dimensional location of retrogradely labelled cells in sensory-motor cortex. The dorsoventral distance from the dorsal aspect of the cortical surface (mm) and the medial-lateral distance from the midline (mm) were measured from each retrogradely labelled cell. The anterior-posterior location of each retrogradely labelled cell was also recorded in terms of distance (mm) from Bregma (according to Paxinos and Watson, 1998). A similar acquisition of data was implemented for the anterograde data, whereby four equally spaced data points were recorded from the perimeter (i.e., at the perimeter of four quadrants) of each anterogradely labelled area of axon terminals. The dorsoventral location of each of the four data points was measured from the dorsal aspect of the cortical surface (mm) and the medial-lateral location (mm) of each data point was measured from the midline. The anterior-posterior location of each labelled area was also recorded, in terms of distance (mm) from Bregma (according to Paxinos and Watson, 1998). This resulted in four individual three-dimensional locations being recorded for each concentrated area of anterograde labeling.

Labelled cells were grouped according to injection site location. The data was analyzed in SPSS by way of a factorial ANOVA, in order to establish the existence of an effect of injection location on the positioning of labelled cells in anterior-posterior, dorsal-ventral and medial-lateral dimensions. This was followed by *post hoc* analyses of comparisons (Tukey HSD) to further investigate significant differences between four PFC injection locations. The

relationship between anterograde and retrograde label locations was examined by means of a 2 way ANOVA. All statistical tests were applied at a significance level of 0.05 and confidence intervals of 95%.

RESULTS

Retrograde injections made into PL, VO, VLO and DLO (R4, R5, R6, R7) occurred in the intended PFC regions (**Figures 1iv,v**). The majority of retrograde injection sites spanned layers I–VI, covered most of the cytoarchitectural region and were principally confined to cytoarchitectural boundaries of PFC sub-regions. The retrograde injection made into VO covered both VO and MO. There was some overlap between PL and VO injection sites and some spread into infralimbic cortex (IL; **Figure 1iv**). Anterograde injections made into PL, VO, VLO and DLO (R1, R3, R7, R8) occurred within the same cytoarchitectural regions as the retrograde equivalents, spanning a smaller area. Anterograde injection sites were largely within the cytoarchitectural boundaries of PFC sub-regions (the injection into VO occurred in both VO and MO), covering layers II–VI (**Figures 1iv,v**).

We observed the patterns of labeling throughout the brain following injections of anterograde and retrograde tracer into PFC (PL, VO, VLO and DLO) using light/fluorescent microscopy. Retrogradely labelled cells were seen in secondary motor cortex (M2), primary motor cortex (M1), primary somatosensory cortex (S1J, S1BF), cingulate cortex (Cg1), piriform cortex (Pir), perirhinal cortex (PRh), entorhinal cortex (Ect), lateral entorhinal cortex (LEnt), secondary auditory cortex (AuV) and primary auditory cortex (Au1). Anterograde labeling was seen in M2, S1J, secondary somatosensory cortex (S2), Cg1, PRh, Ect, LEnt, agranular insular cortex (AID) and PFC regions. Labeling was stronger in several regions, including sensory-motor areas (M1, M2, S1J; **Figure 2**). Therefore a statistical analysis was applied to this region to determine whether there was evidence for an ordered arrangement of prefrontal to sensory-motor cortex connections.

ORGANIZATION OF INPUT AND OUTPUT CONNECTIONS FROM SENSORY-MOTOR TO PREFRONTAL CORTEX

Retrogradely labelled cells were seen in secondary motor (M2), primary motor (M1) and primary somatosensory cortex (S1J). Labelled cells in the sensory-motor region showed an ordered arrangement in terms of cortical layers (**Figure 3**). Labelled cells produced by an injection of retrograde tracer into DLO appear in layer VI, whereas those produced by an injection of tracer into VLO appear in layer V in the same region. Cells labelled following an injection of tracer into VO appear across layers II to VI. In addition, retrogradely labelled cells were consistently seen in deeper cortical layers (VI, V) than anterogradely labelled areas (I, II; **Figure 3**).

Anterogradely labelled areas were seen in M1, M2 and cingulate cortex (cg1). Anterogradely labelled areas found in motor cortex (M1, M2) maintain a relatively clear spatial order in correspondence to BDA tracer injections in VO, VLO and DLO. As injection sites move from lateral (DLO) to medial (VO), labelled areas become more dorsal. A convergent organization can be seen here; injections into separate PFC regions (separated by 1 mm) produced labeling in the same motor region (M2). Labelled areas

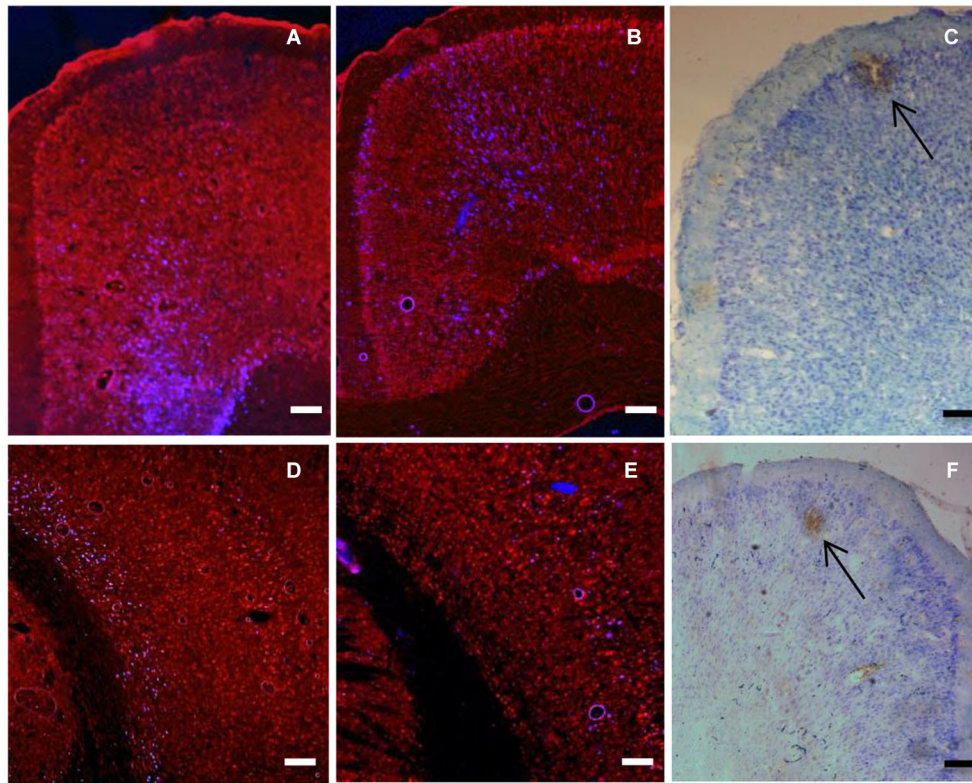


FIGURE 2 | (A) Coronal section showing retrogradely labelled cells (blue) in cingulate cortex produced by 100 nl injection of Fluoro-gold into VLO (injection C). (B) Coronal section showing retrogradely labelled cells (blue) in cingulate cortex produced by 100 nl injection of Fluoro-gold into VO (injection B). (C) Coronal section showing anterograde labeling (brown) produced by injection of BDA (100 nl Fluorescein) into DLO (injection D). Arrow shows area of intense anterograde labeling of axon terminals. Other brown staining indicates less intense anterograde labeling, as well as some artifactual staining. Note the ordered location of labelled neurons within the dorsal-ventral axis. (D) Coronal section

showing retrogradely labelled cells (blue) in sensory cortex produced by injections of Fluoro-Gold (100 nl) into VLO (injection C). (E) Coronal section showing retrogradely labelled cells (blue) in sensory cortex produced by injections of Fluoro-Gold (100 nl) into and VO (injection B). (F) Coronal section of sensory-motor cortex showing locations of anterograde labeling (brown) produced by injection of BDA (100 nl Texas red) into VLO (injection B). Arrow shows area of intense anterograde labeling of axon terminals. Other brown staining indicates less intense anterograde labeling, as well as some artifactual staining. Scale bars = 200 μ m.

were physically closer to one another than their corresponding injection locations (Figure 3).

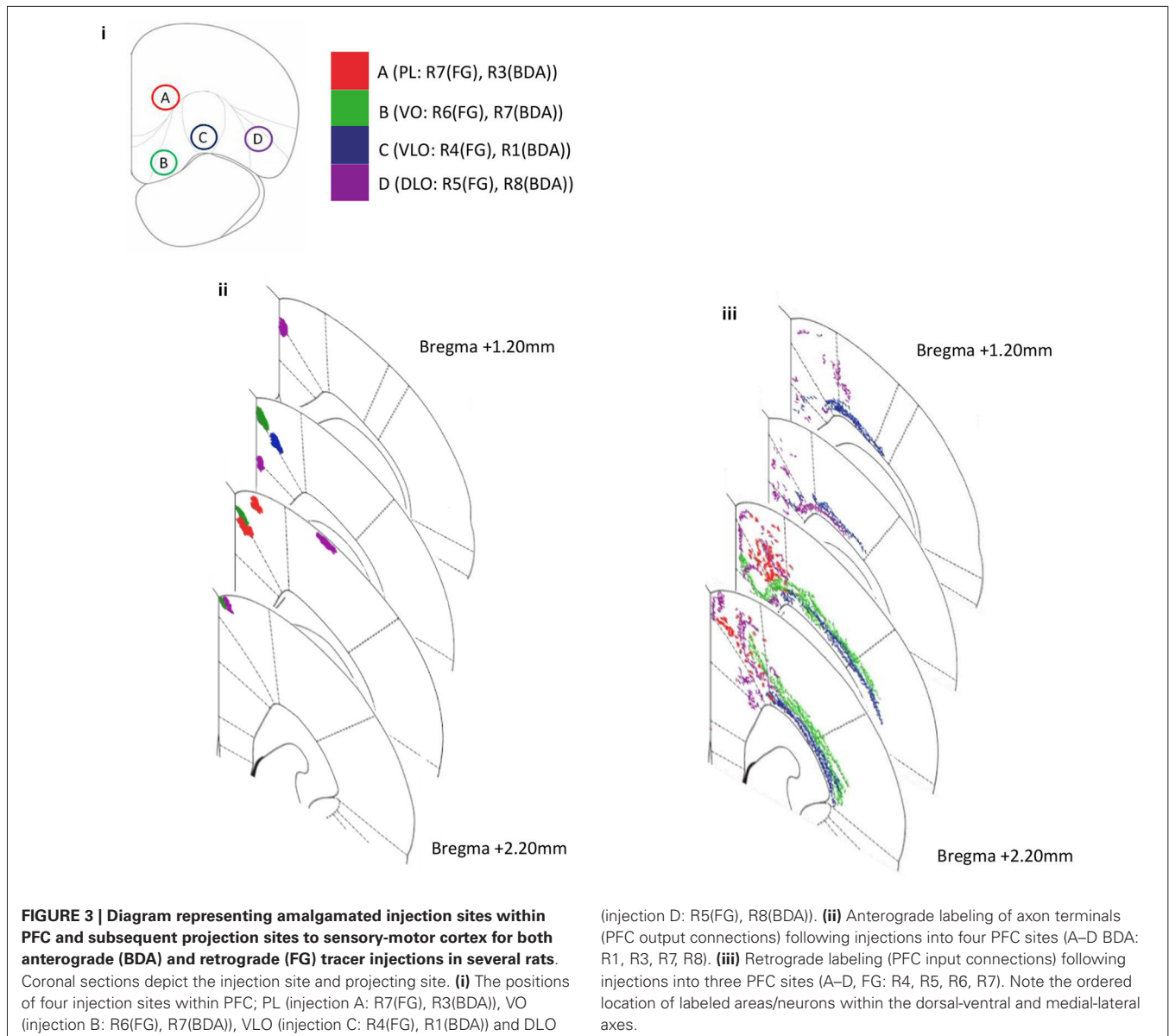
We observed evidence of reciprocal connectivity in the PFC—sensory-motor cortex pathway; anterogradely labelled output connections were consistently found in the same regions of motor cortex (M2) as retrogradely labelled input connections from identical PFC injection sites. This was the case for injections into PL, VO, VLO and DLO. Retrogradely labelled cells were found in additional regions to those in which corresponding anterograde labels were seen. The level of reciprocity appeared to be greater for PL than for VO, VLO and DLO, anterograde labeling from PL was found mostly in the same regions of M2 and Cg1 as retrograde labeling from PL.

STATISTICAL EVIDENCE FOR THE ORDERED ARRANGEMENT AND LOCATION OF INPUT AND OUTPUT CONNECTIONS CAME FROM THE FOLLOWING ANALYSES

A factorial ANOVA was applied to the locations of retrogradely labelled cells in each axis of orientation. This was repeated

for the locations of anterogradely labelled areas. A 2 factor ANOVA (injection type[anterograde, retrograde], injection location [A,B,C,D]) was applied in order to establish the relationship between input and output connections.

For the dorsal-ventral axis: The factorial ANOVA revealed a significant main effect of injection site on dorsoventral (i.e., laminar) location of retrogradely ($F_{(3,490)} = 380.578, p < 0.001$) and anterogradely ($F_{(3,36)} = 23.719, p < 0.001$) labelled cells in sensory-motor cortex. *Post hoc* comparisons (Tukey HSD) between the four retrograde groups indicate significant differences between PL*VO, PL*VLO, PL*DLO ($p < 0.001$). *Post hoc* comparisons (Tukey HSD) between the four anterograde groups indicated significant differences between PL*DLO, VO*DLO ($p < 0.001$) and VLO*DLO ($p = 0.028$). This indicates an ordered arrangement from sensory-motor areas to medial sub-regions of PFC (PL, VO, VLO; Figure 4i). The 2 factor ANOVA revealed a significant interaction effect between input and output connections ($F_{(3,526)} = 45.709, p < 0.001$). This shows that the dorsoventral location of anterogradely and retrogradely labelled cells vary

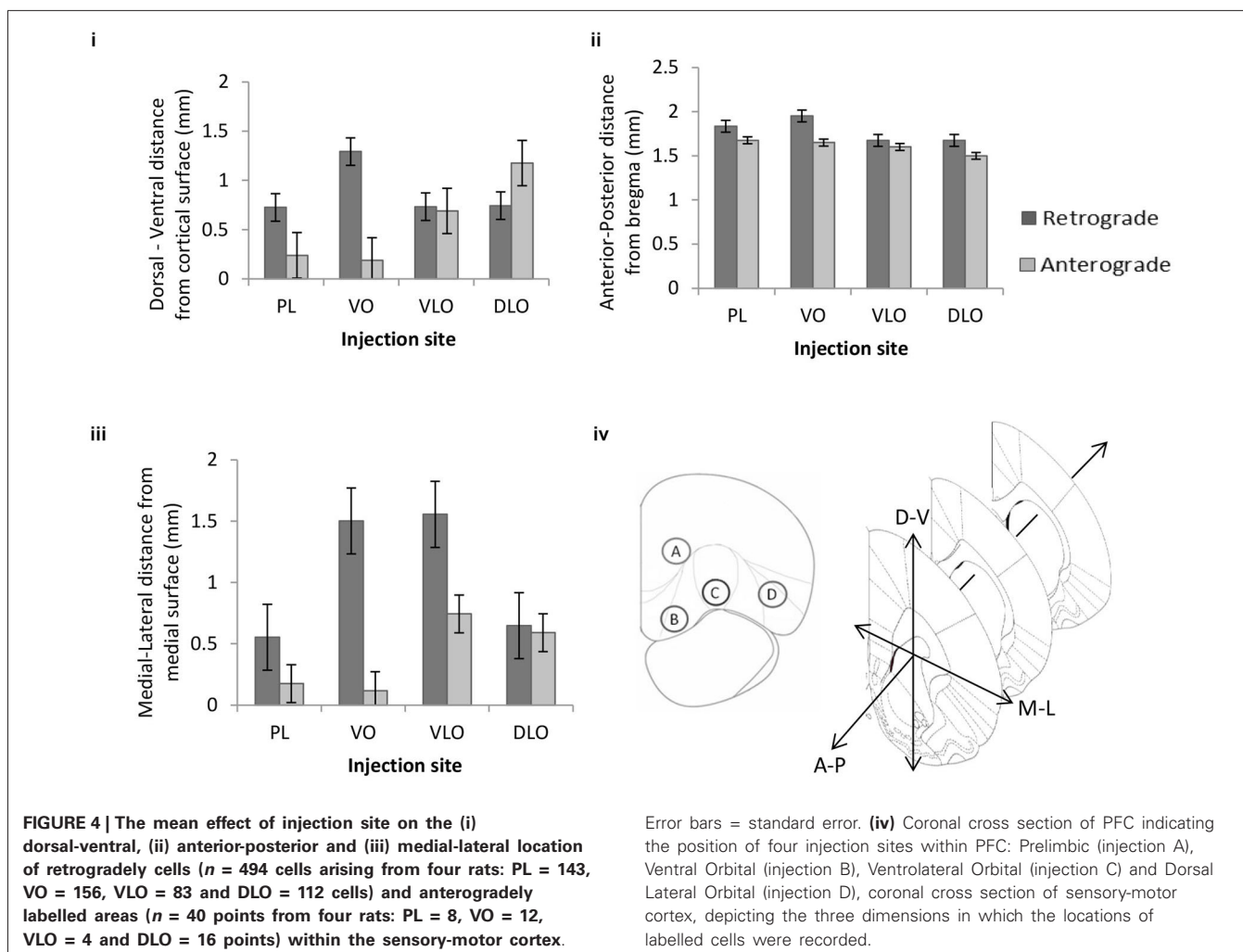


in respect to one another. The statistical analysis revealed a significant ordering of retrograde and anterograde connections. The 2 factor ANOVA indicated that the input and output connections (anterograde and retrograde label) occurred in different locations in this axis of orientation.

For the anterior-posterior axis: A factorial ANOVA revealed a significant main effect of injection site on anterior-posterior location of retrogradely labelled cells ($F_{(3,490)} = 82.090, p < 0.001$) and anterogradely labelled cells ($F_{(3,36)} = 6.029, p = 0.002$) in sensory-motor cortex. *Post hoc* comparisons (Tukey HSD) between the four retrograde groups indicated significant differences between PL*VO, PL*VLO, PL*DLO, VO*VLO, VO*DLO ($p < 0.001$). *Post hoc* comparisons (Tukey HSD) between the four anterograde groups indicated significant differences between PL*DLO and VO*DLO ($p < 0.006$). The 2 factor ANOVA

revealed no significant interaction effect between input and output connections ($F_{(3,526)} = 2.415, p = 0.066$). This indicates an ordered arrangement of input and output connections within the anterior-posterior axis (Figure 4ii). This analysis shows strong evidence for ordering of anterograde connections as well as evidence for ordering of retrograde connections. There is no clear statistical evidence for differential location of inputs and outputs in this axis of orientation.

For the medial-lateral axis: A factorial ANOVA revealed a significant main effect of injection site on medial-lateral location of retrogradely ($F_{(3,490)} = 385.767, p < 0.001$) and anterogradely ($F_{(3,36)} = 24.102, p < 0.001$) labelled cells in sensory-motor cortex. *Post hoc* comparisons (Tukey HSD) between the four retrograde groups indicated significant differences between PL*VO, PL*VLO, PL*DLO ($p < 0.001$). *Post hoc* comparisons



(Tukey HSD) between the four anterograde groups indicated significant differences between all injection sites; PL*VLO, PL*DLO, VO*VLO and VO*DLO ($p < 0.001$). **Figure 4iii** shows that no clear ordered arrangement is seen in the medial-lateral axis. The 2 factor ANOVA revealed a significant interaction effect between input and output connections ($F_{(3,526)} = 24.695$, $p < 0.001$). This shows that the medial-lateral location of anterogradely and retrogradely labelled cells vary in relation to one another. The statistical analysis revealed a significant ordering of retrograde and anterograde connections. The 2 factor ANOVA indicated that the input and output connections (anterograde and retrograde label) occurred in different locations in this axis of orientation. **Figure 4iv** summarizes the approximate position of injection sites and shows the orientations shown in **Figures 4i–iii**.

DISCUSSION

We investigated the organization of connections from adjacent prefrontal regions with the use of neuroanatomical tracers. This study revealed evidence for an ordered arrangement within the projections from PFC to sensory-motor cortex. We revealed a clear ordered arrangement of PFC connections, most prominently

arising from significant portions of sensory-motor cortex. In addition we found evidence of a differential ordering of input and output locations between PFC and sensory-motor regions, in the dorsoventral and mediolateral axes.

INPUT CONNECTIONS FROM SENSORY-MOTOR CORTEX TO PREFRONTAL CORTEX

Following the administration of the retrograde tracer, Fluoro-Gold, to the prefrontal cortical areas PL, VO, VLO and DLO, we found labeling of neuronal cell bodies in areas of motor cortex, temporal cortex, auditory cortex, somatosensory cortex, cingulate cortex and piriform cortex. Projections arising from the motor cortex were amongst those displaying the most labelled cells. These findings are comparable with previous studies (Sesack et al., 1989) which outlined projections from prefrontal to areas of sensory-motor cortex in the rat.

OUTPUT CONNECTIONS FROM SENSORY-MOTOR CORTEX TO SENSORY-MOTOR CORTEX

Following the administration of the anterograde tracers, BDA to the prefrontal cortical areas PL, VO, VLO and, DLO we found

labeling of axon terminals in motor cortex, temporal cortex, auditory cortex, somatosensory cortex, agranular insular cortex, cingulate cortex and PFC regions. The projections arising from the motor and cingulate cortex (M1, M2 and cg1) were amongst those displaying the most labeling. This was broadly consistent with previous studies which outlined prefrontal connections to medial-frontal cortex (Sesack et al., 1989; Vertes, 2004), in that anterograde labels were found in the same regions of cingulate, motor and somatosensory cortex in the rat.

THE ORGANIZATION OF CONNECTIONS BETWEEN PREFRONTAL AND SENSORY-MOTOR CORTEX CORTEX

Our analysis of the location of input and output connections to and from prefrontal regions shows an ordered arrangement of connections occurring in and across three axes of orientation, most significantly so in the anterior-posterior and medial-lateral axes. The analysis of sensory-motor cortex connections revealed an ordered arrangement of input and output connections to PFC occurring in the dorsal-ventral (i.e., laminar) axis (**Figure 4i**). For the dorsal-ventral axis, injections in sites B (VO), C (VLO) and D (DLO) produced an ordered arrangement of PFC output connections to sensory-motor cortex. There was some striking ordering in terms of the input connections from sensory-motor cortex (notably M1 and S1) to PFC. Here specific layers of V and VI differentially project to injection sites B (VO) and C (VLO). Similar laminar organization has been described elsewhere in the same or neighboring circuit: projections from rat medial PFC to striatum, amygdala and thalamus occur in distinct layers of mPFC (Gabbott et al., 2005). This may be of particular significance to PFC function because both of these regions (M1 and S1) contain somatotopic maps. It appears that the same regions implicated in these maps (in layers V and VI) project to distinct regions of PFC (i.e., VO and VLO). It could be functionally useful for the same ordered arrangement to be maintained within sensory-motor to PFC connections.

Our results show a projection from M1, M2 and S1 to PFC and on to M2. This circuit is not typical of the connective organization we might expect to see. Based on a traditional model of cortical function and hierarchical organization of functional connectivity, PFC is positioned at the top of a processing hierarchy (Fuster, 2001; Botvinick, 2008). Subsequently connections would travel from primary sensory cortex, followed by secondary sensory cortex and association areas such as perirhinal cortex before reaching PFC. Finally, return connections would travel to secondary motor cortex (M2) followed by primary motor cortex (e.g., S1 → S2 → Association areas → PFC → M2 → M1), following an order of hierarchical organization from primary cortical regions through secondary regions up to a high order area, then back through secondary regions to a primary region. The connections we have identified from PFC → M2 and M2 → PFC are consistent with what would be expected, based on the model of hierarchical organization. However, the direct connection from S1 → PFC we have observed is unexpected, connecting a primary cortical region directly to the high order PFC. This provides an insight into the complex functional organization of the PFC—sensory-motor cortex pathway.

Our findings show evidence of reciprocal connections between PFC and M2. Anterogradely labelled axon terminals and retrogradely labelled neuronal cells from identical PFC injection sites were consistently found in the same cytoarchitectural regions of M2. This indicates a broad reciprocal organization. However, labeling from retrograde injections was considerably more widespread than that from anterograde injections, resulting in retrograde labels in areas of M1 and S1J. No anterograde labels were seen in these regions, resulting in connections which are not reciprocal. Labeling from PL (injection site A) was found to be more reciprocal than VO, VLO and DLO. These results show that the PFC—sensory-motor cortex pathways contain aspects of reciprocity but is not entirely reciprocal in its organization.

The current findings may be of significance for functional studies of the prefrontal and motor cortex. Prefrontal cortex has long been known to have important inputs to premotor and motor cortices. Recent studies have investigated the functional similarity of medial PFC and motor cortex in the coding of temporal aspects of motor behavior. Neurons in medial PFC and motor cortex display modulated activity during simple reaction time tasks (Narayanan and Laubach, 2009) and neuronal responses in dorsal mPFC are also modulated following errors in similar tasks (Narayanan and Laubach, 2008). Such functional studies highlight the connective links between PFC and motor cortex, a similar functional study has shown that motor cortex delay-related activity is dependent upon activity within mPFC (Narayanan and Laubach, 2006). In the present study our findings add another level of complexity to this area by highlighting the connections of orbital cortex to motor cortex and the significant, indirect input of somatosensory cortex to motor cortex (via the orbital PFC).

SIGNIFICANCE OF ORDERED ARRANGEMENTS AND DIFFERENTIAL ORDERING OF INPUT AND OUTPUT CONNECTIONS FROM PFC TO SENSORY-MOTOR CORTEX

The results presented here outline that PFC displays an ordered arrangement of connections to sensory-motor cortex. The input connections to PFC arise from distinct regions of sensory-motor cortex, notably different layers within motor and S1 somatosensory cortex. In terms of outputs from PFC the projections are to distinct regions of sensory-motor cortex, notably M2 and M1. Therefore there appears to be a broad similarity in location between PFC inputs and outputs to sensory-motor cortex. However, at a more detailed level there is a separation in the location of inputs and outputs to PFC. Labelled input connections can be seen spreading significantly more laterally into regions of motor (M1) and sensory (S1J) cortex in comparison to the consistently medial (Cg1, M2) output labels (**Figure 3**). This provides clear evidence of different locations of input and output connections revealed by differential ordering of anterograde and retrograde labels. Such a differential ordering of inputs and outputs has not been previously described in PFC. A similar differential ordering of input and output connections was also seen in our study of the temporal cortex—PFC pathway (Bedwell et al., in preparation). Previous observations in organization suggest reciprocity of inputs and outputs to be a common attribute in

perirhinal, postrhinal, entorhinal and parahippocampal regions in rats (Agster and Burwell, 2009). In addition, recent dual tracer studies have given no indication that the locations of input and output connections to ventrolateral and medial PFC from premotor cortex, as well as subcortical regions, differ (Kim and Lee, 2012). However, these findings report PFC connectivity on a relatively large scale and from specific sub-regions.

Few studies of rodent PFC have addressed the subject of whether finescale input and output connections occupy the same location (Agster and Burwell, 2009). However, connectional studies of primary sensory (S1) and primary motor cortex (M1) often report reciprocity of connections (Dinopoulos, 1994; Lee et al., 2011). Further, detailed studies of somatosensory and motor cortex in rodent species have shown that inputs and outputs occupy the same, precise locations in the connections between S1 and S2 (Henry and Catania, 2006; Aronoff et al., 2010), M1 and S1 (Porter and White, 1983; Aronoff et al., 2010) and between M1 and S2 (Porter and White, 1983). The study by Porter and White also reported non-reciprocal connections from M1 to the striatum, indicating that motor cortex input and output connections do not always occupy the same location.

An interesting aspect of our results is the finding that the input and output connections from Prelimbic cortex to Cg1 and M2 are largely reciprocal and occur in the same locations (if laminar differences are ignored). This is a very different pattern to that produced after the other injections (notably VO and VLO) which existed in different locations. The significance of this difference in the finescale reciprocity of connections across PFC divisions is not clear but it may relate to the function and organization of the connected regions involved.

Taken together our results indicate that the prefrontal to sensory-motor cortex inputs and outputs display differential ordering and occupy different locations, this differs to the organization displayed between visual and sensorimotor cortical areas (where inputs and outputs display the same ordering and exist in the same locations). It is too early to say whether this differential ordering of input and output locations is a common feature of PFC connections. However, in our laboratory we have found evidence for it in two PFC pathways, i.e., between PFC and sensory-motor cortex (presented here) and between PFC and the temporal cortex.

ACKNOWLEDGMENTS

This work was supported by a Nottingham Trent University studentship awarded to Stacey Bedwell. We would like to thank Danielle MacDonald and Andrew Marr for their technical assistance.

REFERENCES

- Agster, K. L., and Burwell, R. D. (2009). Cortical efferents of the perirhinal, postrhinal and entorhinal cortices of the rat. *Hippocampus* 19, 1159–1186. doi: 10.1002/hipo.20578
- Alvarez, J. A., and Emory, E. (2006). Executive function and the frontal lobes: a meta-analytic review. *Neuropsychol. Rev.* 16, 17–42. doi: 10.1007/s11065-006-9002-x
- Aronoff, R., Matyas, F., Mateo, C., Ciron, C., Schneider, B., and Petersen, C. C. (2010). Long-range connectivity of mouse primary somatosensory barrel cortex. *Eur. J. Neurosci.* 31, 2221–2233. doi: 10.1111/j.1460-9568.2010.07264.x
- Berendse, H. W., Galis-de Graaf, Y., and Groenewegen, H. J. (1992). Topographical organization and relationship with ventral striatal compartments of prefrontal corticostriatal projections in the rat. *J. Comp. Neurol.* 316, 314–347. doi: 10.1002/cne.903160305
- Botvinick, M. M. (2008). Hierarchical models of behavior and prefrontal function. *Trends Cogn. Sci.* 12, 201–208. doi: 10.1016/j.tics.2008.02.009
- Canto, C. B., Wouterlood, F. G., and Witter, M. P. (2008). What does the anatomical organization of the entorhinal cortex tell us? *Neural Plast.* 2008:381243. doi: 10.1155/2008/381243
- Courchesne, E., Mouton, P. R., Calhoun, M. E., Semendeferi, K., Ahrens-Barbeau, C., Hallet, M. J., et al. (2011). Neuron number and size in prefrontal cortex of children with autism. *JAMA* 306, 2001–2010. doi: 10.1001/jama.2011.1638
- Dinopoulos, A. (1994). Reciprocal connections of the motor neocortical area with the contralateral thalamus in the hedgehog (*Erinaceus europaeus*) brain. *Eur. J. Neurosci.* 6, 374–380. doi: 10.1111/j.1460-9568.1994.tb00280.x
- Fryszak, R. J., and Neafsey, E. J. (1994). The effect of medial frontal cortex lesions on cardiovascular conditioned emotional responses in the rat. *Brain Res.* 643, 181–193. doi: 10.1016/0006-8993(94)90024-8
- Fujita, S., Koshikawa, N., and Kobayashi, M. (2011). GABA(B) receptors accentuate neural excitation contrast in rat insular cortex. *Neuroscience* 199, 259–271. doi: 10.1016/j.neuroscience.2011.09.043
- Fuster, J. M. (2001). The prefrontal cortex—an update: time is of the essence. *Neuron* 30, 319–333. doi: 10.1016/s0896-6273(01)00285-9
- Gabbott, P. L., Warner, T. A., Jays, P. R., Salway, P., and Busby, S. J. (2005). Prefrontal cortex in the rat: projections to subcortical autonomic, motor and limbic centers. *J. Comp. Neurol.* 492, 145–177. doi: 10.1002/cne.20738
- Gallagher, M., McMahan, R. W., and Schoenbaum, G. (1999). Orbitofrontal cortex and representation of incentive value in associative learning. *J. Neurosci.* 19, 6610–6614.
- Goldman-Rakic, P. S. (1991). “Prefrontal cortical dysfunction in schizophrenia: the relevance of working memory,” in *Psychopathology and the Brain*. Anonymous, (New York: Raven Press), 1–23.
- Hafting, T., Fyhn, M., Molden, S., Moser, M. B., and Moser, E. I. (2005). Microstructure of a spatial map in the entorhinal cortex. *Nature* 436, 801–806. doi: 10.3410/f.1026484.326461
- Henry, E. C., and Catania, K. C. (2006). Cortical, callosal and thalamic connections from primary somatosensory cortex in the naked mole-rat (*Heterocephalus glaber*), with special emphasis on the connectivity of the incisor representation. *Anat. Rec. A Discov. Mol. Cell. Evol. Biol.* 288, 626–645. doi: 10.1002/ar.a.20328
- Hoover, W. B., and Vertes, R. P. (2007). Anatomical analysis of afferent projections to the medial prefrontal cortex in the rat. *Brain Struct. Funct.* 212, 149–179. doi: 10.1007/s00429-007-0150-4
- Hoover, W. B., and Vertes, R. P. (2011). Projections of the medial orbital and ventral orbital cortex in the rat. *J. Comp. Neurol.* 519, 3766–3801. doi: 10.1002/cne.22733
- Kim, J., Ghim, J. W., Lee, J. H., and Jung, M. W. (2013). Neural correlates of interval timing in rodent prefrontal cortex. *J. Neurosci.* 33, 13834–13847. doi: 10.1523/jneurosci.1443-13.2013
- Kim, U., and Lee, T. (2012). Topography of descending projections from anterior insular and medial prefrontal regions to the lateral habenula of the epithalamus in the rat. *Eur. J. Neurosci.* 35, 1253–1269. doi: 10.1111/j.1460-9568.2012.08030.x
- Kolb, B. (1984). Functions of the frontal cortex of the rat: a comparative review. *Brain Res.* 320, 65–98.
- Kondo, H., and Witter, M. P. (2014). Topographic organization of orbitofrontal projections to the parahippocampal region in rats. *J. Comp. Neurol.* 522, 772–793. doi: 10.1002/cne.23442
- Lee, T., Alloway, K. D., and Kim, U. (2011). Interconnected cortical networks between primary somatosensory cortex septal columns and posterior parietal cortex in rat. *J. Comp. Neurol.* 519, 405–419. doi: 10.1002/cne.22505
- Narayanan, N. S., and Laubach, M. (2006). Top-down control of motor cortex ensembles by dorsomedial prefrontal cortex. *Neuron* 52, 921–931. doi: 10.1016/j.neuron.2006.10.021
- Narayanan, N. S., and Laubach, M. (2008). Neuronal correlates of post-error slowing in the rat dorsomedial prefrontal cortex. *J. Neurophysiol.* 100, 520–525. doi: 10.1152/jn.00035.2008
- Narayanan, N. S., and Laubach, M. (2009). Delay activity in rodent frontal cortex during a simple reaction time task. *J. Neurophysiol.* 101, 2859–2871. doi: 10.1152/jn.90615.2008

- Neafsey, E. J. (1990). Prefrontal cortical control of the autonomic nervous system: anatomical and physiological observations. *Prog. Brain Res.* 85, 147–165; discussion 165–166.
- Olson, C. R., and Musil, S. Y. (1992). Topographic organization of cortical and subcortical projections to posterior cingulate cortex in the cat: evidence for somatic, ocular and complex subregions. *J. Comp. Neurol.* 324, 237–260. doi: 10.1002/cne.903240207
- Paxinos, G., and Watson, C. (1998). *The Rat Brain in Stereotaxic Coordinates*. San Diego, CA: Academic Press.
- Perlstein, W. M., Carter, C. S., Noll, D. C., and Cohen, J. D. (2001). Relation of prefrontal cortex dysfunction to working memory and symptoms in schizophrenia. *Am. J. Psychiatry* 158, 1105–1113. doi: 10.1176/appi.ajp.158.7.1105
- Porter, L. L., and White, E. L. (1983). Afferent and efferent pathways of the vibrissal region of primary motor cortex in the mouse. *J. Comp. Neurol.* 214, 279–289. doi: 10.1002/cne.902140306
- Schilman, E. A., Uylings, H. B., Galis-de Graaf, Y., Joel, D., and Groenewegen, H. J. (2008). The orbital cortex in rats topographically projects to central parts of the caudate-putamen complex. *Neurosci. Lett.* 432, 40–45. doi: 10.1016/j.neulet.2007.12.024
- Schoenbaum, G., and Esber, G. R. (2010). How do you (estimate you will) like them apples? Integration as a defining trait of orbitofrontal function. *Curr. Opin. Neurobiol.* 20, 205–211. doi: 10.1016/j.conb.2010.01.009
- Schoenbaum, G., and Roesch, M. (2005). Orbitofrontal cortex, associative learning and expectancies. *Neuron* 47, 633–636. doi: 10.1016/j.neuron.2005.07.018
- Sesack, S. R., Deutch, A. Y., Roth, R. H., and Bunney, B. S. (1989). Topographical organization of the efferent projections of the medial prefrontal cortex in the rat: an anterograde tract-tracing study with phaseolus vulgaris leucoagglutinin. *J. Comp. Neurol.* 290, 213–242. doi: 10.1002/cne.902900205
- Thivierge, J. P., and Marcus, G. E. (2007). The topographic brain: from neural connectivity to cognition. *Trends Neurosci.* 30, 251–259. doi: 10.1016/j.tins.2007.04.004
- Van De Werd, H. J., and Uylings, H. B. (2008). The rat orbital and agranular insular prefrontal cortical areas: a cytoarchitectonic and chemoarchitectonic study. *Brain Struct. Funct.* 212, 387–401. doi: 10.1007/s00429-007-0164-y
- Vertes, R. P. (2004). Differential projections of the infralimbic and prelimbic cortex in the rat. *Synapse* 51, 32–58. doi: 10.1002/syn.10279
- Vertes, R. P. (2006). Interactions among the medial prefrontal cortex, hippocampus and midline thalamus in emotional and cognitive processing in the rat. *Neuroscience* 142, 1–20. doi: 10.3410/f.1046859.496884
- Welker, C. (1971). Microelectrode delineation of fine grain somatotopic organization of (Sml) cerebral neocortex in albino rat. *Brain Res.* 26, 259–275. doi: 10.1016/s0006-8993(71)80004-5
- Woolsey, T. A. (1967). Somatosensory, auditory and visual cortical areas of the mouse. *Johns Hopkins Med. J.* 121, 91–112.

Conflict of Interest Statement: The authors declare that the research was conducted in the absence of any commercial or financial relationships that could be construed as a potential conflict of interest.

Received: 24 June 2014; accepted: 01 September 2014; published online: 17 September 2014.

Citation: Bedwell SA, Billett EE, Crofts JJ and Tinsley CJ (2014) The topology of connections between rat prefrontal, motor and sensory cortices. *Front. Syst. Neurosci.* 8:177. doi: 10.3389/fnsys.2014.00177

This article was submitted to the journal *Frontiers in Systems Neuroscience*.

Copyright © 2014 Bedwell, Billett, Crofts and Tinsley. This is an open-access article distributed under the terms of the Creative Commons Attribution License (CC BY). The use, distribution or reproduction in other forums is permitted, provided the original author(s) or licensor are credited and that the original publication in this journal is cited, in accordance with accepted academic practice. No use, distribution or reproduction is permitted which does not comply with these terms.

The topology of connections between rat prefrontal and temporal cortices

Stacey A. Bedwell, E. Ellen Billett, Jonathan J. Crofts, Danielle M. MacDonald and Chris J. Tinsley*

Division of Biosciences, School of Science and Technology, Nottingham Trent University, Nottingham, UK

Understanding the structural organization of the prefrontal cortex (PFC) is an important step toward determining its functional organization. Here we investigated the organization of PFC using different neuronal tracers. We injected retrograde (Fluoro-Gold, 100 nl) and anterograde [Biotinylated dextran amine (BDA) or Fluoro-Ruby, 100 nl] tracers into sites within PFC subdivisions (prelimbic, ventral orbital, ventrolateral orbital, dorsolateral orbital) along a coronal axis within PFC. At each injection site one injection was made of the anterograde tracer and one injection was made of the retrograde tracer. The projection locations of retrogradely labeled neurons and anterogradely labeled axon terminals were then analyzed in the temporal cortex: area Te, entorhinal and perirhinal cortex. We found evidence for an ordering of both the anterograde (anterior-posterior, dorsal-ventral, and medial-lateral axes: $p < 0.001$) and retrograde (anterior-posterior, dorsal-ventral, and medial-lateral axes: $p < 0.001$) connections of PFC. We observed that anterograde and retrograde labeling in ipsilateral temporal cortex (i.e., PFC inputs and outputs) often occurred reciprocally (i.e., the same brain region, such as area 35d in perirhinal cortex, contained anterograde and retrograde labeling). However, often the same specific columnar temporal cortex regions contained only either labeling of retrograde or anterograde tracer, indicating that PFC inputs and outputs are frequently non-matched.

Keywords: prefrontal cortex, ordering, connections, temporal cortex, rat

OPEN ACCESS

Edited by:

Mikhail Lebedev,
Duke University, USA

Reviewed by:

Alessandro E. P. Villa,
University of Lausanne, Switzerland
Nandakumar Narayanan,
Yale University, USA
Elizabeth Warburton,
University of Bristol, UK

*Correspondence:

Chris J. Tinsley,
Division of Biosciences, School of
Science and Technology, Nottingham
Trent University, Clifton Lane,
Nottingham NG11 8NS, UK
chris.tinsley@ntu.ac.uk

Received: 20 November 2014

Accepted: 06 May 2015

Published: 20 May 2015

Citation:

Bedwell SA, Billett EE, Crofts JJ,
MacDonald DM and Tinsley CJ (2015)
The topology of connections between
rat prefrontal and temporal cortices.
Front. Syst. Neurosci. 9:80.
doi: 10.3389/fnsys.2015.00080

Introduction

Prefrontal cortex (PFC) is known to have a role in cognitive (Kolb, 1984; Fuster, 2001; Schoenbaum and Roesch, 2005), executive (Alvarez and Emory, 2006), emotional (Frysztak and Neafsey, 1991), and autonomic functions (Neafsey, 1990; Frysztak and Neafsey, 1991). Abnormalities of cortical connections have been linked to neurological/psychiatric disorders such as autism and schizophrenia (Kleinmans et al., 2008; Fornito and Bullmore, 2015). Anatomically, rat PFC includes the medial PFC, orbital frontal cortex and the agranular insular cortex. Rat medial PFC includes the prelimbic, infralimbic medial agranular, and anterior cingulate regions (Vertes, 2004, 2006). Orbital PFC regions include the medial orbital (MO), ventral orbital (VO), ventrolateral orbital (VLO), and lateral orbital (LO) areas (Krettek and Price, 1977; van de Werd and Uylings, 2008). Adjacent to these regions and on the lateral edge of the PFC lies the dorsolateral orbital area (DLO) and the agranular insular area (van de Werd and Uylings, 2008). Functionally, medial PFC (mPFC) has strong links to motor cortex and mPFC is thought to be involved in temporal processing

(Narayanan and Laubach, 2006, 2008, 2009; Smith et al., 2010; Kim et al., 2013). Orbital PFC has a role in the prediction of future outcomes and is proposed to have an analogous functional role in rodents and primates (Schoenbaum and Roesch, 2005; Schoenbaum and Esber, 2010). Functionally, the agranular insular cortex and DLO have connections to neighboring gustatory insular cortex and have a putative sensory role (Gallagher et al., 1999; Fujita et al., 2011). Unlike other regions of the cerebral cortex there is currently little evidence for functional mapping of responses in rodent PFC, however there are topological distinctions to the functional characteristics of PFC regions (Cassaday et al., 2014).

PFC is known to have substantial connections to temporal cortex (Delatour and Witter, 2002; Hoover and Vertes, 2007, 2011; Agster and Burwell, 2009; Kondo and Witter, 2014). Studies have shown that there are projections from PFC to area Te, perirhinal cortex, and entorhinal cortex. In addition there is evidence that there are substantial projections from these temporal cortex regions back to PFC sites (Agster and Burwell, 2009).

There is evidence for topographical ordering in the projections from PFC to temporal cortex (Kondo and Witter, 2014), the projections from PFC to the striatum (Sesack et al., 1989; Berendse et al., 1992; Schilman et al., 2008), the projections from PFC to the epithalamus (Kim and Lee, 2012) and for topographical ordering in the projections from PFC to motor cortex (Bedwell et al., 2014b). In addition at least two studies describe lamina-specific projections to and from the rat PFC. Lamina-specific projections are reported in the projection from sensory-motor cortex to different subdivisions of rat PFC (Bedwell et al., 2014b) and in the projections from mPFC to striatum in the rat (Gabbott et al., 2005).

Although, there is substantial evidence for the ordering of PFC connections, there is conflicting evidence concerning the fine-scale reciprocity of these connections. Reciprocal connections are thought to occur widely throughout the cerebral cortex and there is evidence for their occurrence in rat PFC (Cinelli et al., 1987; Datiche and Cattarelli, 1996; Little et al., 2009), temporal (Vaudano et al., 1991; Pitkanen et al., 2000; Kealy and Commins, 2011), somatosensory (Aronoff et al., 2010; Lee et al., 2011), and visual cortices (Olavarria and Montero, 1981; Miller and Vogt, 1984). Previous studies have reported evidence for both reciprocal (Ishikawa and Nakamura, 2003) and non-reciprocal (Agster and Burwell, 2009) connections of both PFC and temporal cortex. Reciprocal connections have been reported in the connections between perirhinal and pyriform cortex (Agster and Burwell, 2009). Additionally, the connections between lateral entorhinal cortex and secondary motor cortex and between postrhinal cortex and anterior cingulate cortex appear to be non-reciprocal (Agster and Burwell, 2009; Kealy and Commins, 2011). In the connections between sensory-motor cortex and PFC, reciprocal connections are recorded between mPFC and motor cortex however the somatosensory cortex provides an input to PFC that is not reciprocated in many columnar regions of cortex (Bedwell et al., 2014b). One of the problems with interpreting these studies is that most have not sought to address the question of fine-scale reciprocity.

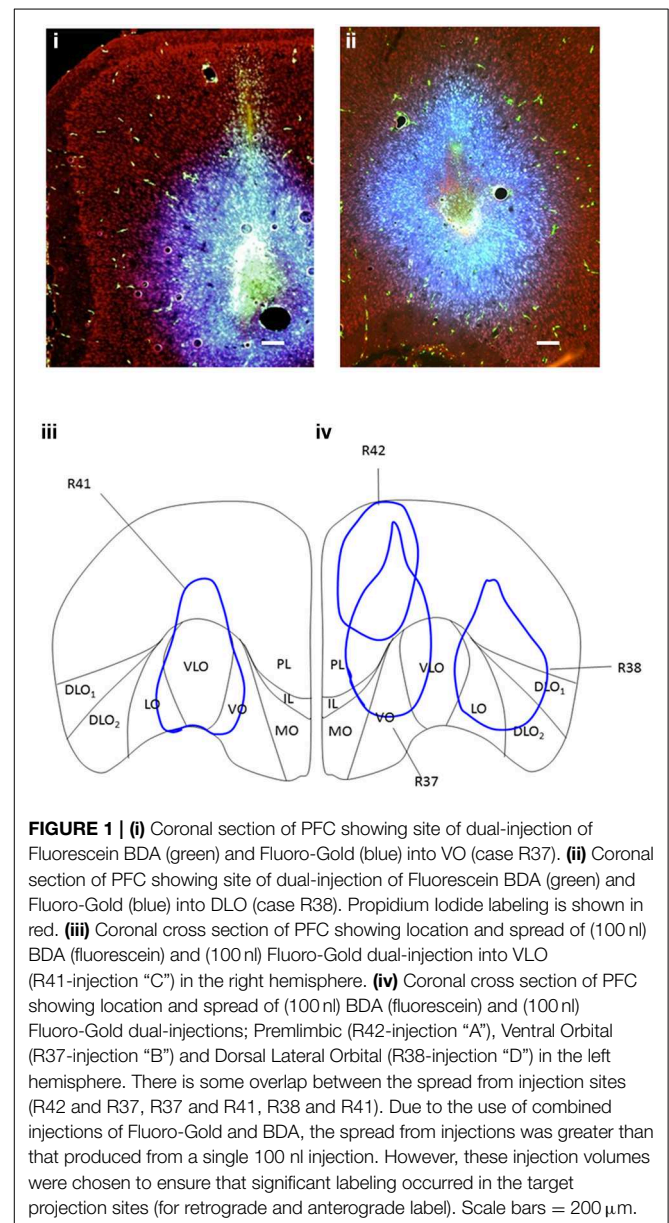
Here we sought to investigate the fine-scale reciprocity of PFC connections through an analysis of the ordering of input and output connections. We performed dual injections of anterograde and retrograde tracer into identical sites within the rat PFC and investigated the location of the associated connected sites (see **Figure 1**). A preliminary version of this report was previously published in abstract form (Bedwell et al., 2014a).

Materials and Methods

Animals

Ethical Statement

All Animal procedures were carried out in accordance with the UK Animals Scientific Procedures Act (1986), EU directive



2010/63 and were approved by the Nottingham Trent University Animal Welfare and Ethical Review Body.

Experimental Animals

Twenty four male CD rats were obtained from Charles River, UK. On receipt the animals were examined for signs of ill-health or injury. The animals were acclimatized for 10 days during which time their health status was assessed. At the start of the surgery the animals weight range was 294–371 g.

Prior to surgery the animals were housed together in Individually Ventilated Cages (IVC) (Techniplast double decker Greenline rat cages). The animals were allowed free access to food and water. Mains drinking water was supplied from polycarbonate bottles attached to the cage. The diet and drinking water were considered not to contain any contaminant at a level that might have affected the purpose or integrity of the study. Bedding was supplied by IPS Product Supplies Ltd in form of 8/10 corncob. Environmental enrichment was provided in the form of wooden chew blocks and cardboard fun tunnels (Datesand Ltd., Cheshire, UK). Post-surgery the animals were individually housed in the same conditions. The animals were housed in a single air-conditioned room within a barrier unit. The rate of air exchange was at least 15 air changes per hour and the low intensity fluorescent lighting was controlled to give 12 h continuous light and 12 h darkness. The temperature and relative humidity controls were set to achieve target values of $21 \pm 2^\circ\text{C}$ and $55 \pm 15\%$, respectively.

In vivo Observations

Individual bodyweights were recorded on Day-10 (prior to the start of dosing) and daily thereafter. All animals were examined for overt signs of ill-health or behavioral change immediately prior to surgery dosing, during surgery and the period following surgery. There were no observed clinical signs/symptoms of toxicity or infection. There was no significant effect on body weight development detected.

Surgical and Experimental Procedures

Rats were anesthetized with isoflurane (Merial, Harlow, UK) and placed in a stereotaxic frame with the incisor bar set so as to achieve a flat skull. Buprenorphine (0.05 mg/kg i.m./s.c) and Meloxicam (up to 1 mg/kg s.c/orally) analgesia were provided peri-operatively and for several days post-operatively. Body temperature was monitored during and immediately after surgery using a rectal thermometer. Craniotomies (<1 mm diameter) were made at predetermined stereotaxic coordinates. Sterile tracer solution was deposited into the PFC cortex by injection, via a 0.5 μl Neuro-syringe (Hamilton, Germany) and delivery was controlled via use of a manual microsyringe injection holder (World Precision Instruments, catalog# 502245). Dual-injections of anterograde (2.5% (w/v) Fluorescein biotinylated dextran amine (BDA); catalog #: SP-1130 or 10% FluoroRuby in distilled water, Fluorochrome, Denver, Colorado) and retrograde tracer (4% (w/v) Fluoro-Gold in distilled water, Fluorochrome) were made into the prelimbic (PL), VO, VLO, or dorsolateral orbital cortex (DLO), with the intention of revealing the anatomical connections of PFC regions (this was

performed via a first injection of Fluoro-Gold followed by a second injection of BDA into the same injection site). The distance between craniotomy co-ordinates (usually 1 mm) was based on the measured spread of tracers in preliminary and the present studies (~1 mm in diameter). The tracer injections were all made with the injection needle orientated vertically. Injections were made at AP 3.7 mm from Bregma (A) ML 1.2, 2.4 mm below cortical surface, (B) ML 1.2, 3.2 mm below cortical surface, (C) ML 2.2, 3.2 mm below cortical surface (D) ML 3.2, 3.2 mm below cortical surface and targeted with the use of a stereotaxic atlas (Paxinos and Watson, 1998).

Each rat received dual-injections of retrograde tracer and anterograde tracer into the same injection site. Rats received injections of (1) Fluoro-Gold (100 nl) at a rate of 100 nl/min and (2) BDA-Fluorescein (100 nl) at a rate of 100 nl/min or Fluoro-Ruby at a rate of 10 nl/min into various subdivisions of PFC, separated by 1 mm (**Figure 1**; Separate labeling of the Fluoro-Gold and BDA-Fluorescein at these injection sites is shown Figure S1 of the Supplementary Material). Three of the dual-injections of Fluoro-Gold and BDA-Fluorescein were made into the left hemisphere of separate rats (rats R37, R38, and R42) and one dual-injection was made in the right hemisphere in another rat (R41). The dual-injections of Fluoro-Gold and Fluoro-Ruby were made into the left hemisphere of separate rats (rats R39, R40, R43, and R44; Sites for these injections are shown in Figure S2 of the Supplementary Material). Additional separate injections of Fluoro-Gold (left hemisphere: rat R15; right hemisphere: rats R4, R5, R6, R7), BDA-Fluorescein (left hemisphere: rat R7; right hemisphere: rats R1, R3, R8) and Fluoro-Ruby (right hemisphere: rats R9, R19, R20, R29) were also made. Eight additional and equivalent Fluoro-Gold injections were made into the left (animal labels: R9, R12, R13, R16, R19, R20, R21) and right (R5) hemisphere of different animals to verify whether the location and ordering of projections differed on the either side of the brain (the results of this analysis are not included in the Results Section). The same overall order and positioning of Fluoro-Gold labeling was observed on both sides of the brain. Some of these animals (R1, R3, R4, R5, R6, R7, R8, R9, R13, R16, R19) were used in a previous study that investigated the connections between the same PFC injection sites and sensory-motor cortex (Bedwell et al., 2014b). The size of spread from injections was very consistent between injections of the same volume and tracer, the diameter of spread resulting from dual injections was larger than that produced from single injections (dual injections were 26% larger).

Following a survival time of 7–9 days, the rats were deeply anesthetised with pentobarbital (Sigma-Aldrich, UK), and transcardially perfused with 0.1 M phosphate buffered saline (PBS, pH7.4) (~200 ml) followed by 4% paraformaldehyde (PFA) (~200 ml) in PBS, pH7.4. The brain was subsequently removed and stored for 24 h in 4% PFA in 0.1 M PBS, followed by cryoprotection in 30% sucrose in 0.1 M PBS.

Anatomical Processing and Microscopy

Anatomical Processing

For analysis of connections, two series of 40 μm coronal sections were taken (2 in 6 sections) on a freezing microtome (CM 1900,

Leica, Germany). Sections were mounted onto gelatin coated slides. One series was processed by implementing the avidin-biotin method (Vectastain[®] ABC, Vector Laboratories, CA), for bright field imaging of Fluorescein labeled axon terminals. This series of sections was counterstained with thionin. For analysis of Fluoro-Gold labeled cells and the fluorescently labeled injection sites, a parallel series of 40 μ m coronal sections was taken, mounted onto gelatin coated slides, then cover slipped with Vectashield[®] mounting medium (with propidium iodide) for fluorescent imaging of Fluoro-Gold (for the injection site and labeled cells), Vectashield with 4',6-Diamidino-2-phenylindole (DAPI) for fluorescent imaging of the Fluoro-Ruby injection site and labeled axon terminals and Fluorescein BDA (for the injection site).

Sections were examined using either bright field (Fluorescein) or fluorescent microscopy (Fluorescein, Fluoro-Gold, and Fluoro-Ruby). Fluorescent photos were captured of the injection sites and retrogradely labeled cells (Fluoro-Gold, see **Figures 2A,B**) and axon terminals labeled by Fluoro-Ruby (see **Figure 2D**). Brightfield photos were captured of anterogradely DAB labeled areas (Fluorescein BDA tracer, see **Figure 2C**), using an Olympus DP-11 system microscope with a x4 and x10 objective lens. We also used dark field microscopy to visualize the anterograde labeling of the BDA. The brightfield and darkfield microscopy of the BDA revealed a very similar pattern of labeling, however the brightfield images produced the clearest and most localized distribution of label. Therefore, the bright field photomicrographs were used for the analysis of anterograde labeling.

Microscopic Analysis

Initially, the entire forebrain was examined for labeling. Areas of temporal and sensory-motor cortex were found to contain the strongest and most consistent labeling of connections; therefore a more detailed analysis was carried out on these regions to examine the organization of connections. Some results of the sensory-motor cortex analysis were reported previously (Bedwell et al., 2014b) and none of the sensory-motor cortex connections are reported in the present paper.

Statistical Analysis of the Arrangement of Connections between PFC and Temporal cortex

We implemented a statistical analysis to determine whether connections between PFC and temporal cortex displayed an ordered arrangement. ImageJ (Wayne Rasband, NIH) was used to determine numerical values representing the location of retrogradely labeled cells in temporal cortex. The dorsoventral and medial-lateral distance (i.e., laminar location) of each retrogradely labeled (Fluoro-Gold) cell was measured from the rhinal sulcus and cortical surface respectively. The anterior-posterior location of each retrogradely labeled cell was also recorded, in terms of distance (mm) from Bregma according to a stereotaxic atlas (Paxinos and Watson, 1998). A similar acquisition was implemented for the anterograde data (DAB visualized BDA projections). Anterogradely labeled areas were defined by intense labeling where a clearly visible area of DAB staining could be seen that covered a grouping of

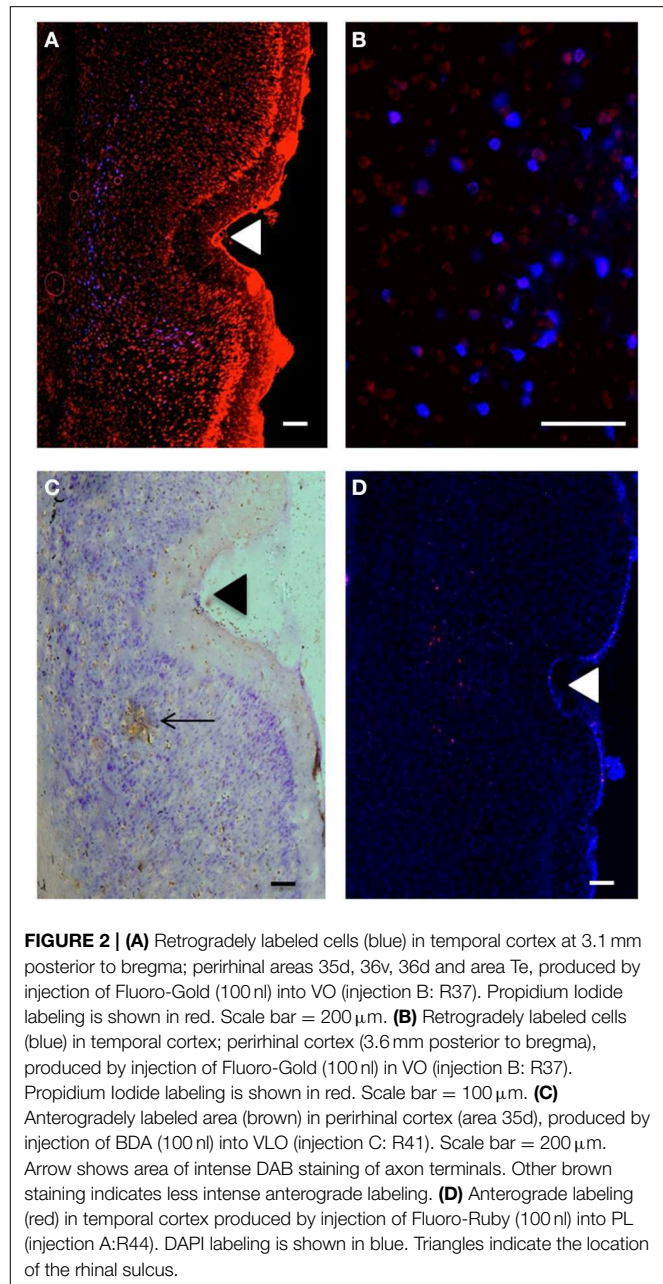
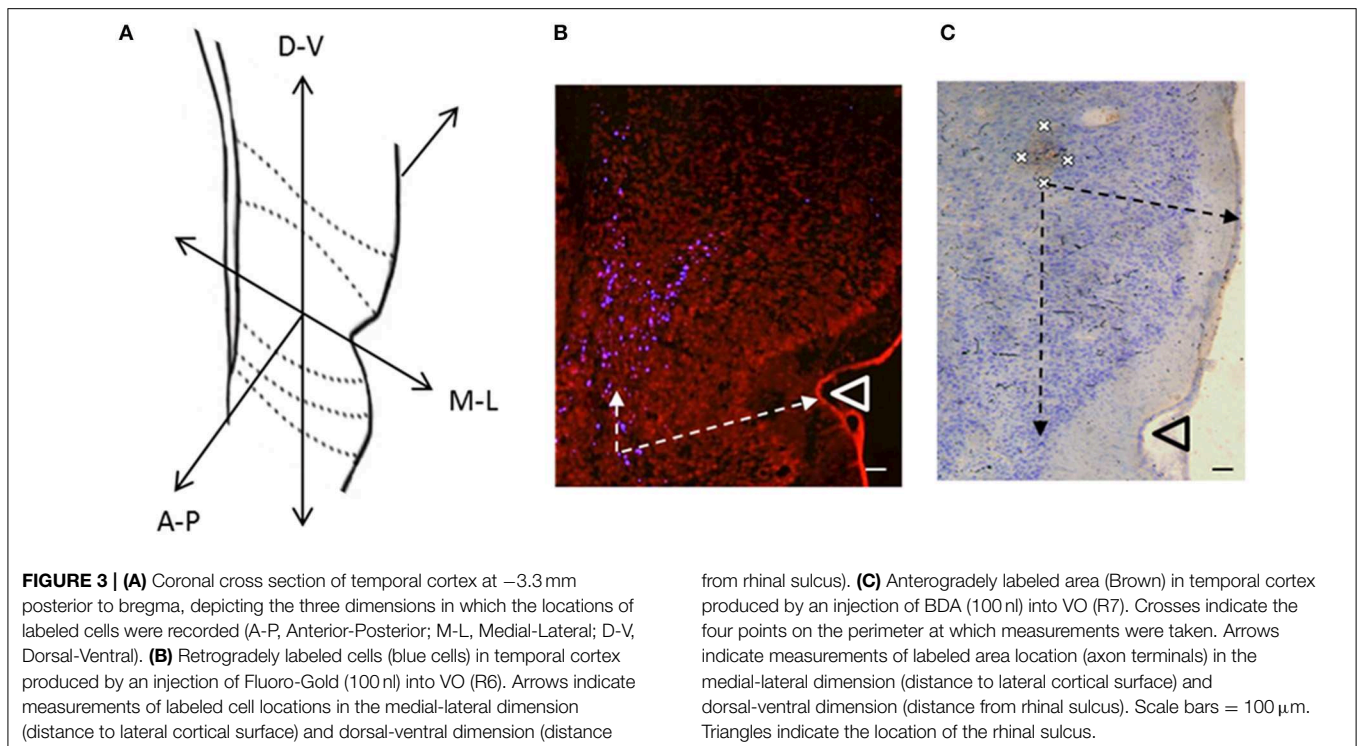


FIGURE 2 | (A) Retrogradely labeled cells (blue) in temporal cortex at 3.1 mm posterior to bregma; perirhinal areas 35d, 36v, 36d and area Te, produced by injection of Fluoro-Gold (100 nl) into VO (injection B: R37). Propidium iodide labeling is shown in red. Scale bar = 200 μ m. **(B)** Retrogradely labeled cells (blue) in temporal cortex; perirhinal cortex (3.6 mm posterior to bregma), produced by injection of Fluoro-Gold (100 nl) in VO (injection B: R37). Propidium iodide labeling is shown in red. Scale bar = 100 μ m. **(C)** Anterogradely labeled area (brown) in perirhinal cortex (area 35d), produced by injection of BDA (100 nl) into VLO (injection C: R41). Scale bar = 200 μ m. Arrow shows area of intense DAB staining of axon terminals. Other brown staining indicates less intense anterograde labeling. **(D)** Anterograde labeling (red) in temporal cortex produced by injection of Fluoro-Ruby (100 nl) into PL (injection A:R44). DAPI labeling is shown in blue. Triangles indicate the location of the rhinal sulcus.

cortical cells (see marked areas in **Figures 2C, 3C**), isolated DAB labeling in proximity with individual cells was not included (see lower portion of **Figure 2C**; See Figure S3 of the Supplementary Material for examples of cortical sections where BDA labeling was weak or absent). Four data points were recorded from quadrants at the perimeter of each anterogradely labeled area, denoting its distance (mm) from the rhinal sulcus in dorsoventral and medial-lateral directions (see **Figure 3**). The anterior-posterior location of each labeled area was also recorded. For the analysis of the location of Fluoro-Ruby axon terminals, which were typically located around the profile of neuronal cell soma, we identified this specific location in terms of x, y, and z coordinates as



described above (i.e., expressed as the average location of the neuron).

Labeled cells were grouped according to injection site location. The positional data was found to be normally distributed. Therefore, these data sets were analyzed in SPSS by way of a factorial ANOVA, in order to establish the existence of an effect of injection location on positioning of labeled cells in anterior-posterior, dorsoventral, and medial-lateral dimensions. The relationship between anterograde and retrograde label locations was examined by means of a Two Factor ANOVA. This allowed us to establish the difference between input and output connectivity patterns. All statistical tests were applied with a significance level of 0.05 and confidence intervals of 95%. Within temporal cortex the statistical analysis was applied to (1) 2443 Fluoro-Gold labeled cells arising from 12 rats: PL($n = 3$), VO($n = 3$), VLO($n = 3$), DLO($n = 3$); (2) 56 BDA labeled points arising from 8 rats: PL($n = 2$), VO($n = 2$), VLO($n = 2$), DLO($n = 2$) and (3) 733 Fluoro-Ruby labeled points arising from 8 rats: PL($n = 2$), VO($n = 2$), VLO($n = 2$), DLO($n = 2$). See Table 1 of the Supplementary Material for summary of animals included in the analysis.

Results

Injections of retrograde and anterograde tracers were made into identical sites within a coronal section of the rat PFC at distance of 4.20 mm anterior to bregma according to Paxinos and Watson (1998) (see Figure 1). The injections were made in a line which followed the curvature of the cortical surface and were largely non-overlapping in terms of spread along the medial-lateral axis

(i.e., in terms of injections into orbital cortex), however the dual nature of the injections made the spread larger than would have been expected from the use of single tracers. There was some significant overlap of spread between the injections placed at A and B (albeit in different animals) due to the oval nature of the spread of tracer injection. Using light/fluorescent microscopy, patterns of labeling throughout the temporal cortex region were visualized following the injections of anterograde and retrograde tracer into the PFC cortex (PL, VO, VLO, and DLO—see sites in Figures 1, 2). Following the injections of tracer into the PFC, the anterograde and retrograde labeling observed was largely confined to the ipsilateral hemisphere, thus only the ipsilateral connections are reported.

Retrograde Labeling in the Temporal Cortex Region

The retrograde tracer Fluoro-Gold labeled neuronal cell bodies in the temporal cortex (see Figures 2A,B). Retrograde labeling was seen in regions adjacent to the rhinal sulcus, namely the perirhinal cortex (areas 35 and 36), entorhinal cortex, area Te, and piriform cortex (all areas were defined according to Burwell (2001).

Anterograde Labeling in the Temporal Cortex Region

Biotinylated dextran amines were used to label the axon terminals in the temporal cortex region and is shown by the area visualized by the brown coloration of the DAB-staining (see Figure 2C). Anterograde labeling was seen in the same regions of the temporal cortex as the retrograde labeling, namely the perirhinal

cortex (areas 35 and 36), entorhinal cortex and area Te (all areas were defined according to Burwell (2001)). The anterograde tracer Fluoro-Ruby was also employed to visualize axon terminals. Fluoro-Ruby was injected at four injection sites, both in terms of single injections and also via dual-injections with Fluoro-Gold (see Table 1 of the Supplementary Material). The pattern of labeling observed was slightly more diffuse than that for BDA Fluorescein but followed the same pattern in terms of the distribution of the label produced.

The Position of Anterograde and Retrograde Labels within the Temporal Cortex Region: Location, Ordering, and Reciprocity

The position of anterograde and retrograde labels arising from identical dual-injection sites usually occupied the same cortical region (i.e., entorhinal cortex, perirhinal cortex, piriform, or area Te). Therefore, the connections were largely reciprocal in nature. Retrograde labeling from the injection into PL was found in the same area of PRh as anterograde labeling from the same injection site, indicating reciprocal connections here. Similarly, retrograde labeling produced from the tracer injection into VLO was found in the same region of PRh (35d and 36v) as anterograde labeling from the same injection site, again indicating a reciprocal connection. However, retrograde labeling from the same injection site was not found in the region of PRh (36v) where anterograde labeling from a tracer injection into DLO was found. Retrograde labeling from the tracer injection into DLO was found in regions of PRh (35d, 36v, 36d), but considerably far from the equivalent anterograde labeled area (Figure 4).

Location and Ordering of PFC Inputs and Outputs: An Analysis of the Fine-scale Reciprocity of Connections

To examine the location and ordering of PFC inputs and outputs we needed to analyse the location of retrograde and anterograde label. To do this the location of labeled areas/cells within the temporal cortex was analyzed by first describing in terms of 3D position (in the x, y, and z axes—see Figure 5) and then by analyzing the locations associated with each injection site statistically.

Figure 4 shows the location of anterograde and retrograde labeling in the temporal cortex region following the different injections into the PFC region (data shown from 4 animals—following dual injections of Fluoro-Gold and BDA-Fluorescein). The figure reveals that as injection site was moved laterally from sites B–D the retrograde label occurred increasingly posteriorly within the temporal cortex region. The figure also shows that the retrograde tracer is much broader in its distribution within temporal cortex than the anterograde tracer. This indicates that there is considerable convergence in the feedback circuit projecting from temporal cortex to PFC and returning back to temporal cortex.

The results of the analysis of the location of retrograde and anterograde labels are shown in detail in Figure 5. Figure 5 shows the results for the locations of label following (1) single and dual injections of Fluoro-Gold and BDA and (2) the

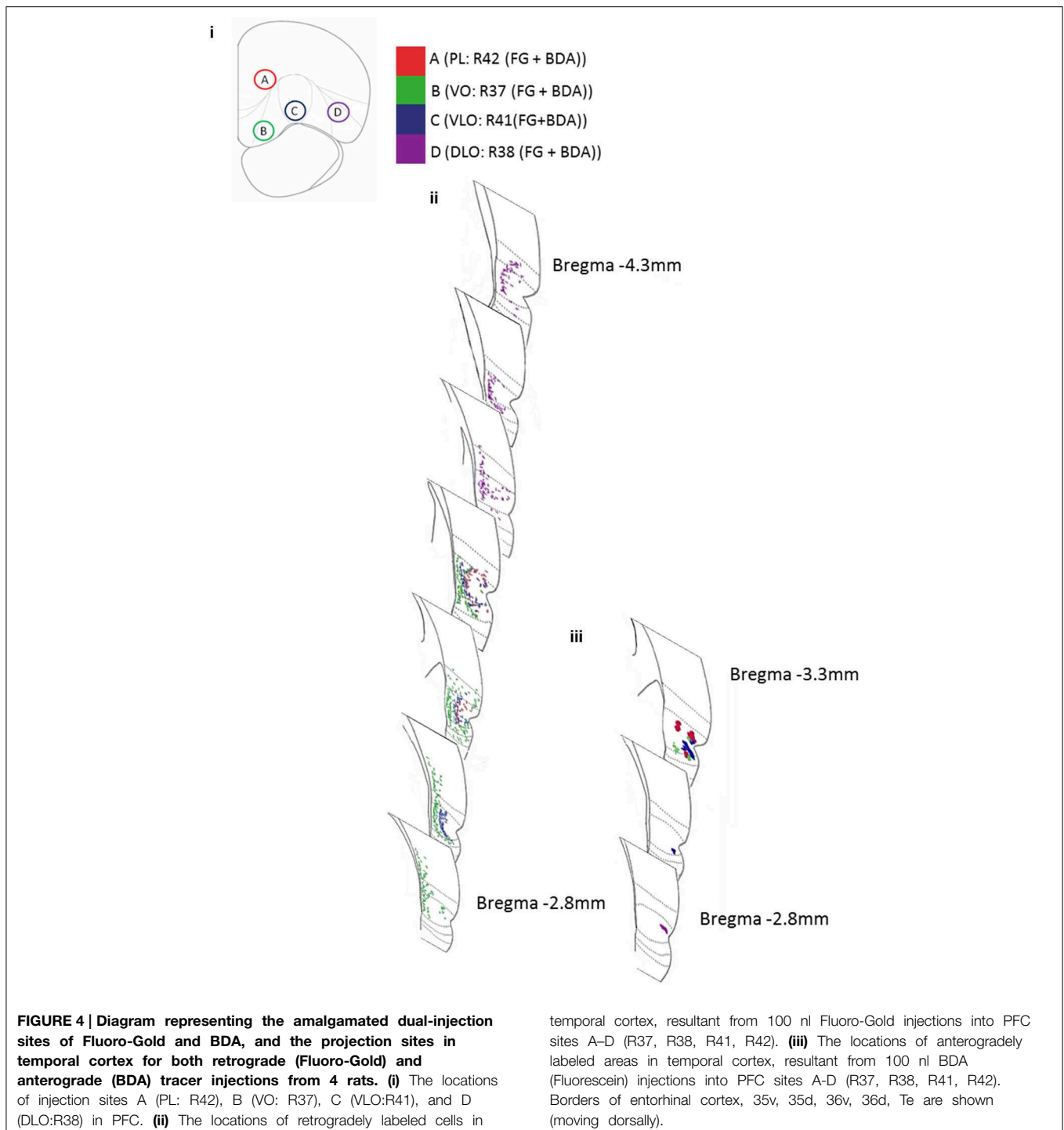
single and dual injections of Fluoro-Gold and Fluoro-Ruby (the data and animals from this figure are detailed in Table 1 of the Supplementary Material). The location of retrograde and anterograde tracer is shown in 3 axes of orientation (dorsal-ventral, anterior-posterior and medial-lateral). In the graphs the mean location of the label is shown by the bar for each axis, the error bars reveal the SEM. The locations of the anterograde Fluoro-Ruby and BDA labeling appeared similar (see Figures 5i–iii) however a statistical analysis shows that there are differences. A Two Factor ANOVA [injection type (anterograde, retrograde), injection location (A,B,C,D)] showed that there is a significant interaction between BDA and Fluoro-Ruby labeling in 2 axes of orientation [anterior-posterior: $F_{(3, 781)} = 3.240$ $p = 0.02$; medial-lateral: $F_{(3, 781)} = 14.057$ $p < 0.001$]. This indicates that the BDA and Fluoro-Ruby labeling is not identical. However, there is a strong similarity between the mean location and ordering of BDA and Fluoro-Ruby labels in all three orientations (Figures 5i–iii).

We also analyzed how the positioning of Fluoro-Gold labeling compared to (1) BDA labeling and (2) Fluoro-Ruby labeling:

The dorsal-ventral graph (Figure 5i) shows prominent and significant ordering of the Fluoro-Gold ($p < 0.001$), BDA ($p < 0.001$) and Fluoro-Ruby ($p < 0.001$) through sites B–D (VO-DLO) [ANOVA injection, location (A,B,C,D)] – a complete outline of the statistical analysis for this study is included in the complementary material section. This panel also shows that the ordering of Fluoro-Gold (moving ventrally across the graph) differs from that of BDA and Fluoro-Ruby [moving dorsally across the graph, excepting PL(A)]. This differential ordering {Two Factor ANOVA [injection type (anterograde, retrograde), injection location (A,B,C,D)]} is present in the comparisons between (1) Fluoro-Gold and BDA ($p < 0.001$) and (2) Fluoro-Gold and Fluoro-Ruby ($p < 0.001$).

The anterior-posterior graph (Figure 5ii) also shows prominent and significant ordering of the Fluoro-Gold ($p < 0.001$), BDA ($p < 0.001$) and Fluoro-Ruby ($p < 0.001$) through sites B–D (VO-DLO) [ANOVA (injection location (A,B,C,D))]. This panel also shows that the ordering of Fluoro-Gold (moving posteriorly across the graph) differs from that of BDA and Fluoro-Ruby (moving anteriorly across the graph, again excepting PL(A)). This differential ordering {Two Factor ANOVA [injection type (anterograde, retrograde), injection location (A,B,C,D)]} is present in the comparisons between (1) Fluoro-Gold and BDA ($p < 0.001$) and (2) Fluoro-Gold and Fluoro-Ruby ($p < 0.001$).

We also found evidence for differential ordering of inputs and outputs in the medial-lateral (i.e., laminar) axis of orientation; this is entirely consistent with the idea that cortical inputs and outputs arise from different cortical layers (Barbas, 1995). Finally it is clear from viewing Figures 4, 5 that although the corresponding anterograde and retrograde tracers do occupy the same approximate cortical regions they do not in general occupy the same intra-areal sites. Table 1 (article) provides a breakdown of the mean locations of retrograde and anterograde labeling in the temporal cortex following *single* and *dual* injections of Fluoro-Gold, BDA and Fluoro-Ruby



into the PFC divisions (this is data that was amalgamated in Figure 5).

To conclude, the results show that the PFC input connections are clearly ordered in the anterior-posterior axis of the temporal cortex. The ordering seen is clear between injection sites B–D, i.e., between the VO and DLO subdivisions of the PFC. Similarly the PFC output connections to the temporal cortex also

displayed clear ordering between VO and DLO in the dorsal-ventral axis. Taken together the results show that there is a generalized reciprocity in terms of PFC inputs and outputs, i.e., that the same cortical regions send and receive projections from the PFC. However, when viewed at a finer resolution we observed that the cortical inputs and outputs to the PFC display different patterns of ordering.

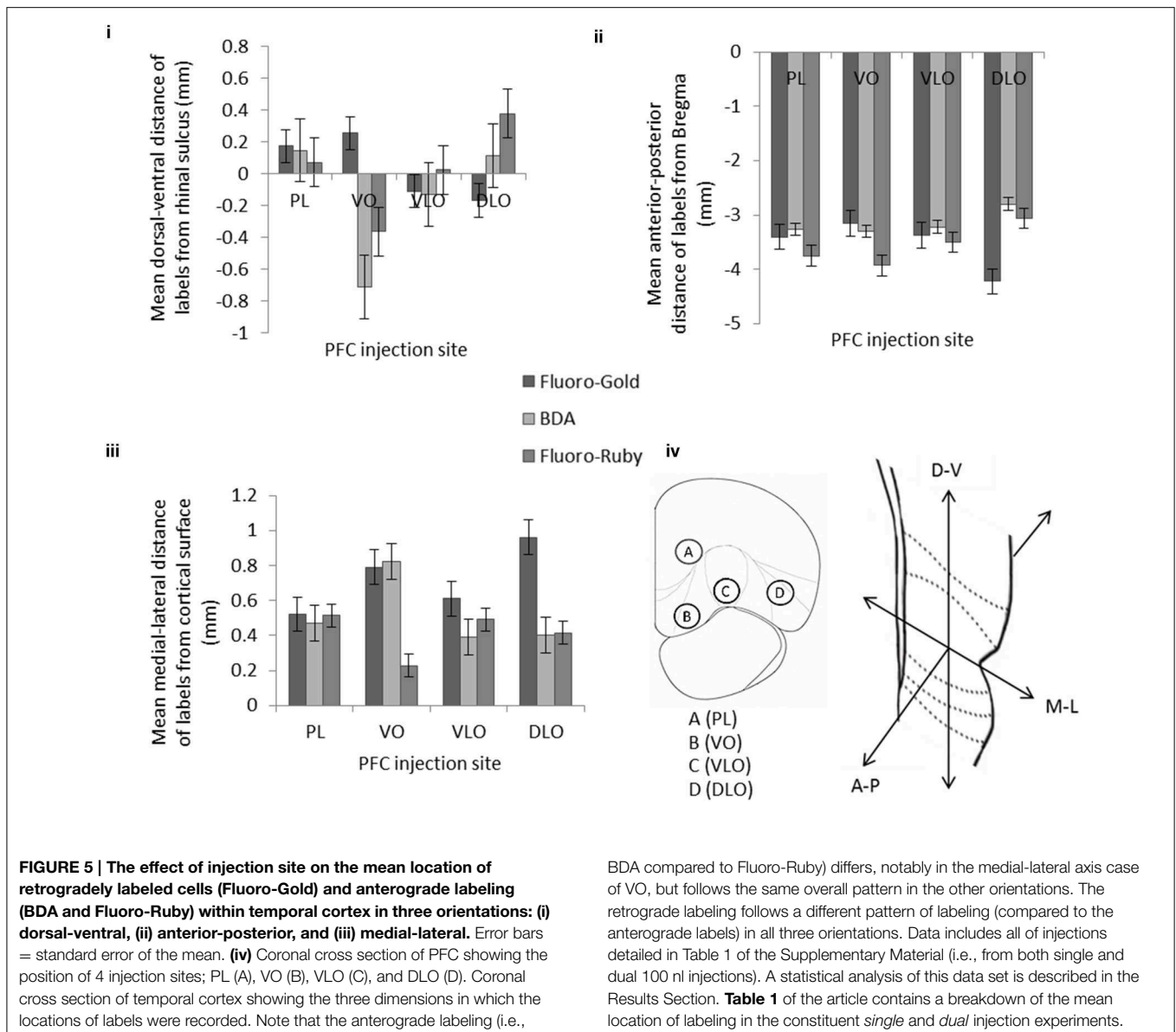


FIGURE 5 | The effect of injection site on the mean location of retrogradely labeled cells (Fluoro-Gold) and anterograde labeling (BDA and Fluoro-Ruby) within temporal cortex in three orientations: (i) dorsal-ventral, (ii) anterior-posterior, and (iii) medial-lateral. Error bars = standard error of the mean. **(iv)** Coronal cross section of PFC showing the position of 4 injection sites; PL (A), VO (B), VLO (C), and DLO (D). Coronal cross section of temporal cortex showing the three dimensions in which the locations of labels were recorded. Note that the anterograde labeling (i.e.,

BDA compared to Fluoro-Ruby) differs, notably in the medial-lateral axis case of VO, but follows the same overall pattern in the other orientations. The retrograde labeling follows a different pattern of labeling (compared to the anterograde labels) in all three orientations. Data includes all of injections detailed in Table 1 of the Supplementary Material (i.e., from both single and dual 100 nl injections). A statistical analysis of this data set is described in the Results Section. **Table 1** of the article contains a breakdown of the mean location of labeling in the constituent *single* and *dual* injection experiments.

Discussion

In summary, we found an ordered arrangement of input and output connections in the PFC. We also found evidence for a differential ordering of input and output connections, indicating that specific PFC inputs and outputs are connected to different columnar regions of temporal cortex.

Methodological Considerations

In this study it should be noted that due to the relatively large volume of tracer injectate and use of pressure injections we cannot entirely exclude the possibility of some uptake of tracers from damaged fibers of passage. The present results are based on dual and single injection of tracers into the same injection site. The dual injection approach is superior to that of single injection studies, however there is always the possibility that different

tracers may be subject to different levels of injection spread and uptake. Injection spread can be relatively easily measured (the spread of our retrograde tracer was larger than that of our anterograde BDA or Fluoro-Ruby tracers) but uptake is more difficult to quantify. A key feature of our results is that, although the location and distribution spread of our projections differed (possibly due to the differences outlined above), they were also centered upon different columnar regions of cortex. It is this key feature (i.e., the different centers of the projection sites) that points to non-reciprocity of fine-scale PFC connections.

Anterograde and Retrograde Labeling following Dual Injections into PFC

Following dual injections of anterograde and retrograde tracer into PFC sites we found significant labeling of anterograde and retrograde connections in temporal cortex. We observed

TABLE 1 | The mean location of labeling in temporal cortex, in three axes of orientation following single and dual tracer injections of Fluoro-Gold, Fluoro-Ruby, and BDA made into PL, VO, VLO, and DLO in prefrontal cortex.

		PL (A)		VO (B)		VLO (C)		DLO (D)	
		Mean	SEM	Mean	SEM	Mean	SEM	Mean	SEM
Dorsal-Ventral	Fluoro-Gold Single Injection	0.14	0.03	0.37	0.02	-0.16	0.05	-0.17	0.03
	Fluoro-Gold Dual Injection (with BDA)	0.18	0.04	0.4	0.14	-0.16	0.04	-0.17	0.07
	Fluoro-Gold Dual Injection (with Fluoro-Ruby)	0.22	0.02	0.33	0.03	-0.04	0.03	-0.16	0.11
	BDA Single Injection	0.22	0.01	-0.21	0.01	-0.06	0.01	0.01	0
	BDA Dual Injection	0.12	0.14	-0.88	0.29	-0.15	0.12	0.21	0.04
	Fluoro-Ruby Single Injection	-0.07	0.05	-0.5	0.14	-0.01	0.05	0.48	0.12
	Fluoro-Ruby Dual Injection	0.16	0.04	-0.09	0.04	0.077	0.05	0.18	0.13
Anterior-Posterior	Fluoro-Gold Single Injection	-3.31	0.02	-3.1	0.01	-3.4	0.02	-4.35	0
	Fluoro-Gold Dual Injection (with BDA)	-3.38	0.02	-3.23	0.02	-3.38	0.02	-4.1	0.02
	Fluoro-Gold Dual Injection (with Fluoro-Ruby)	-3.53	0.03	-3.25	0.01	-3.34	0.02	-3.96	0.02
	BDA Single Injection	-3.14	0	-3.3	0	-3.14	0	-2.8	0
	BDA Dual Injection	-3.3	0	-3.3	0	-3.25	0	-2.8	0
	Fluoro-Ruby Single Injection	-4.41	0.01	-4.21	0.01	-3.6	0.03	-3.1	0.01
	Fluoro-Ruby Dual Injection	-3.3	0	-3.36	0.02	-3.33	0.03	-3	0.02
Medial-Lateral	Fluoro-Gold Single Injection	0.57	0.01	0.66	0.01	0.67	0.02	0.7	0.01
	Fluoro-Gold Dual Injection (with BDA)	0.44	0.01	1.6	0.04	0.56	0.02	0.88	0.06
	Fluoro-Gold Dual Injection (with Fluoro-Ruby)	0.48	0.01	0.65	0.02	0.59	0.02	1.74	0.05
	BDA Single Injection	0.52	0.02	0.5	0.03	0.43	0.03	0.53	0.09
	BDA Dual Injection	0.45	0.04	0.93	0.1	0.38	0.03	0.28	0.06
	Fluoro-Ruby Single Injection	0.5	0.03	0.13	0.01	0.52	0.03	0.01	0
	Fluoro-Ruby Dual Injection	0.52	0.02	0.43	0.03	0.45	0.03	1.21	0.08

The table features the same data as that shown in **Figure 5** but also includes the individual experiments (e.g., in the case of Fluoro-Gold: the results from the single and both dual injection experiments are tabulated here). Note the general agreement between the BDA and Fluoro-Ruby locations (except in the medio-lateral orientation in the case of VO). There are several individual differences between the mean locations of Fluoro-Gold and the anterograde labeling (see the dorso-ventral orientation—VO and the anterior-posterior orientation—DLO). SEM = standard error of the mean.

anterograde label located primarily within the perirhinal cortex. Retrograde label was found to be more widespread: within area Te, perirhinal cortex, entorhinal cortex, and piriform cortex. Previous studies have also reported prominent projections from temporal cortex to PFC and in the return projection.

Ordering of Connections within the Cerebral Cortex

Our findings show that the projections from PFC to temporal cortex and from temporal cortex to PFC are ordered. However, the ordering seen is different for the input and output connections. In a previous study of the PFC projections to temporal cortex the authors reported topographical ordering (Kondo and Witter, 2014). The labeling of anterograde projections that we found was largely confined to the perirhinal cortex region and this is consistent with this previous report by Kondo and Witter. We did not observe a very clear ordering of PFC projections to the perirhinal cortex region but did observe that anterograde label occurred more dorsally in the perirhinal region as PFC injection site traversed from medial-lateral: VO, VLO, DLO. This finding has been reported in the projections from the perirhinal region to MO and VO (in this experiment the retrograde tracer Fluoro-Gold was used) (Hoover and Vertes, 2011). The report by Kondo and colleagues does

not present the same ordering, however we observed similar patterns of labeling to those reported by Kondo and colleagues. Our strongest ordering appeared in the return projections from temporal cortex to PFC (visualized with retrograde labeling).

Previous studies have also reported ordering in the connections from PFC to the striatum (Sesack et al., 1989; Berendse et al., 1992), the thalamus (Groenewegen, 1988) and in the connections between PFC regions (Conde et al., 1995). At a broader level previous studies have reported the topological ordering of rodent PFC to a number of connected cortical and subcortical sites (Sesack et al., 1989; Olsen and Musil, 1992). Topographic ordering of connections is also reported in the connections between PFC and pyriform cortex (Datiche and Cattarelli, 1996). Taken together, there is widespread evidence that PFC connections display clear ordering with both cortical and subcortical sites. This is consistent with other regions of the cerebral cortex where topographically/topologically arranged connections (Henry and Catania, 2006; Thivierge and Marcus, 2007; Aronoff et al., 2010) are hypothesized to support physiological maps (Woolsey, 1967; Welker, 1971; Hafting et al., 2005; Marshel et al., 2011; Dias et al., 2014). To our knowledge this study is the first to simultaneously report on the ordering of anterograde and retrograde labeling in temporal cortex following PFC injections.

Reciprocity of PFC Input and Output Connections to Temporal Cortex

We observed reciprocal connectivity in the pathway between PFC and temporal cortex; anterograde and retrograde label were found in overlapping regions of perirhinal cortex following dual tracer injections into VO and VLO. However, retrograde injections consistently labeled additional regions to their anterograde counterparts. This was most apparent with the labeling from injections into DLO, where anterogradely labeled output connections did not appear in the same cytoarchitectural regions as retrogradely labeled input connections from the same injection site. The labeling displayed areas of reciprocity, but also shows a large number of retrograde labels in temporal cortex that did not have reciprocal anterograde connections. Reciprocity is known to occur widely across the cerebral cortex (Felleman and Van Essen, 1991) and has been reported to occur in temporal cortex connections of rodent cerebral cortex (Agster and Burwell, 2009, 2013).

Fine-scale Reciprocity and the Differential Ordering of Input and Output Connections

The differential ordering of connections described here indicates that retrograde and anterograde labels (and subsequent PFC inputs and outputs) occur in different columnar regions of temporal cortex. This can be compared to similar studies in sensory, motor and association cortex.

In sensory and motor cortex there is strong evidence for both highly ordered reciprocal connections and for weakly reciprocal or non-reciprocal connections. The connections between primary somatosensory cortex (S1) and secondary somatosensory cortex (S2) (Burton and Kopf, 1984; Henry and Catania, 2006), S1 and primary motor cortex (M1) (Porter and White, 1983; Aronoff et al., 2010) and between S2 and M1 (Porter and White, 1983; Burton and Kopf, 1984) are reported to be highly reciprocal in several mammalian species. To qualify this further, the same columnar cortical projection sites contain both input and output connections to the specified target site.

However, if we consider the situation of connections between sensory-motor cortex and other brain sites there is evidence for weaker reciprocal connectivity. In one study, the projection from motor cortex to the ipsilateral striatum did not display a return projection (Porter and White, 1983). Another study involving injections of anterograde tracer or retrograde tracer into PFC subdivisions showed that labeling often occurred in distinct columnar regions of sensory-motor cortex (Bedwell et al., 2014b).

The connections of temporal association cortex appear to show a similar profile (to that of sensory-motor cortex) with some connections displaying tight, parallel-organized input and output connections and others displaying weakly reciprocal or non-reciprocal connections. The connections between pyriform and perirhinal cortex, between lateral entorhinal and perirhinal cortex (Canto et al., 2008) and between pyriform cortex and PFC are reported to be strongly reciprocal (Datiche and Cattarelli, 1996; Agster and Burwell,

2009). The connections between lateral entorhinal cortex and secondary motor cortex (Agster and Burwell, 2009) and some connections between PFC and temporal cortex (Kealy and Commins, 2011) are not reported to be reciprocal at all. A problem with the interpretation of these results is that most studies have not sought to identify the fine-scale reciprocity of cortical inputs and outputs, therefore it is difficult to conclude whether parallel-arranged input and output connections are a feature of specific cortical connections and pathways.

It is noteworthy that in the present study the connections between prelimbic cortex and temporal cortex appeared to be largely reciprocal (see **Figure 4**), unlike the other PFC regions under investigation. A previous study has reported that mPFC connections to PFC regions immediately anterior or posterior are highly reciprocal (Conde et al., 1995). Further, our previous study of PFC connections to the sensory-motor region agreed with this finding, reporting that the connections between prelimbic and secondary motor cortex were reciprocal (Bedwell et al., 2014a). Taken together, these findings suggest that dorsal mPFC displays reciprocal connections between local and long-range cortical sites. By contrast, the orbital PFC shows differential ordering of connections and therefore much weaker reciprocal connections between PFC and sensory-motor (Bedwell et al., 2014b) and temporal cortex connections (present report). The significance of this difference within PFC is not currently clear.

Relevance of the Results to the Subdivisions of Temporal Cortex

Temporal Cortex has been previously defined according to different subdivisions, such as Te1 (primary auditory cortex), Te2, and Te3 (Arnault and Roger, 1990; Shi and Cassell, 1999). Our tracer injections into VO and DLO produced retrograde labeling in Te3. We found no BDA labeling in Te3 from the same PFC injection sites, indicating non-reciprocal connections from Te3 to VO and DLO. None of our tracer injections produced labeling in the other temporal regions: Te1 and Te2. Our finding of non-reciprocal connections between PFC and Te3 adds to the previous findings of non-reciprocal labeling in the brainstem and sub-cortical areas, following tracer injections into Te3 and Te2 (Arnault and Roger, 1990). Arnault and Roger (1990) also reported that Te2 and Te3 have dense reciprocal connections with the medial geniculate complex. There have also been reports of reciprocal connections from ventral Te (Te2 and Te3) to the dorsal aspect of perirhinal cortex (Shi and Cassell, 1999). The same study identified broadly reciprocal connections from perirhinal cortex to multiple cortical regions, these findings are similar to the broad scale reciprocity we have identified between PFC and temporal cortex. Topographic ordering has been described in the connections between Te1 and the medial geniculate complex (Arnault and Roger, 1990). A clear ordering of Te3 labeling cannot be seen from our findings, Arnault and Roger (1990) similarly described no precise topographic ordering of Te2 and Te3 connections to the medial geniculate complex.

Significance of Non-reciprocity for Behavior

Studies of the connections between PFC and the thalamus in primates have described non-reciprocal connections and linked this to feed-forward loops associated with PFC (McFarland and Haber, 2002). It is possible that feed-forward loops could be implicated in the memory functions associated with PFC in a variety of species (Fuster, 2001; Barker and Warburton, 2008).

In conclusion, we found evidence for highly organized topological connections from PFC to temporal connections and in return projections from temporal cortex to PFC. However, the ordering of the input and output connections frequently did not match and reflected a differential ordering of anterograde and retrograde label. In addition we found that following injections into the PFC, anterograde and retrograde labels were not localized within the same columnar regions indicating a mismatch between the organization of PFC inputs and

outputs. The results of this study highlight the need for further investigation into precise ordering, alignment and fine-scale reciprocity of association cortex connections in rodents and higher mammalian species.

Acknowledgments

This work was supported by a Nottingham Trent University studentship awarded to SB. We would like to thank Andrew Marr for his technical support.

Supplementary Material

The Supplementary Material for this article can be found online at: <http://journal.frontiersin.org/article/10.3389/fnsys.2015.00080/abstract>

References

- Agster, K. L., and Burwell, R. D. (2009). Cortical efferents of the perirhinal, postrhinal, and entorhinal cortices of the rat. *Hippocampus* 19, 1159–1186. doi: 10.1002/hipo.20578
- Agster, K. L., and Burwell, R. D. (2013). Hippocampal and subicular efferents and afferents of the perirhinal, postrhinal, and entorhinal cortices of the rat. *Behav. Brain Res.* 254, 50–64. doi: 10.1016/j.bbr.2013.07.005
- Alvarez, J. A., and Emory, E. (2006). Executive function and the frontal lobes: a meta-analytic review. *Neuropsychol. Rev.* 16, 17–42. doi: 10.1007/s11065-006-9002-x
- Arnault, P., and Roger, M. (1990). Ventral temporal cortex in the rat: connections of secondary auditory areas Te2 and Te3. *J. Comp. Neurol.* 302, 110–123. doi: 10.1002/cne.903020109
- Aronoff, R., Matyas, F., Mateo, C., Ciron, C., Schneider, B., and Petersen, C. C. (2010). Long-range connectivity of mouse primary somatosensory barrel cortex. *Eur. J. Neurosci.* 31, 2221–2233. doi: 10.1111/j.1460-9568.2010.02764.x
- Barbas, H. (1995). Anatomic basis of cognitive-emotional interactions in the primate prefrontal cortex. *Neurosci. Biobehav. Rev.* 19, 499–510. doi: 10.1016/0149-7634(94)00053-4
- Barker, G. R., and Warburton, E. C. (2008). NMDA receptor plasticity in the perirhinal and prefrontal cortices is crucial for the acquisition of long-term object-in-place associative memory. *J. Neurosci.* 28, 2837–2844. doi: 10.1523/JNEUROSCI.4447-07.2008
- Bedwell, S. A., Billett, E. E., Crofts, J. J., and Tinsley, C. J. (2014b). The topology of connections between rat prefrontal, motor and sensory cortices. *Front. Syst. Neurosci.* 8:177. doi: 10.3389/fnsys.2014.00177
- Bedwell, S. A., Billett, E. E., Crofts, J. J., and Tinsley, C. J. (2014a). Input and output connections of rat prefrontal cortex display a novel, ordered arrangement [Abstract]. *9th FENS Forum Neurosci.* (inpress).
- Berendse, H. W., Galis-de Graaf, Y., and Groenewegen, H. J. (1992). Topographical organization and relationship with ventral striatal compartments of prefrontal corticostriatal projections in the rat. *J. Comp. Neurol.* 316, 314–347. doi: 10.1002/cne.903160305
- Burton, H., and Kopf, E. M. (1984). Ipsilateral cortical connections from the second and fourth somatic sensory areas in the cat. *J. Comp. Neurol.* 225, 527–553. doi: 10.1002/cne.902250405
- Burwell, R. D. (2001). Borders and cytoarchitecture of the perirhinal and postrhinal cortices in the rat. *J. Comp. Neurol.* 437, 17–41. doi: 10.1002/cne.1267
- Canto, C. B., Wouterlood, F. G., and Witter, M. P. (2008). What does the anatomical organization of the entorhinal cortex tell us? *Neural Plast.* 2008:381243. doi: 10.1155/2008/381243
- Cassaday, H. J., Nelson, A. J., and Pezze, M. A. (2014). From attention to memory along the dorsal-ventral axis of the medial prefrontal cortex: some methodological considerations. *Front. Syst. Neurosci.* 8:160. doi: 10.3389/fnsys.2014.00160
- Cinelli, A. R., Ferreyra-Moyano, H., and Barragan, E. (1987). Reciprocal functional connections of the olfactory bulbs and other olfactory related areas with the prefrontal cortex. *Brain Res. Bull.* 19, 651–661. doi: 10.1016/0361-9230(87)90051-7
- Conde, F., Maire-Lepoivre, E., Audinat, E., and Crepel, F. (1995). Afferent connections of the medial frontal cortex of the rat. II. Cortical and subcortical afferents. *J. Comp. Neurol.* 352, 567–593. doi: 10.1002/cne.903520407
- Datiche, F., and Cattarelli, M. (1996). Reciprocal and topographic connections between the piriform and prefrontal cortices in the rat: a tracing study using the B subunit of the cholera toxin. *Brain Res. Bull.* 41, 391–398. doi: 10.1016/S0361-9230(96)00082-2
- Delatour, B., and Witter, M. P. (2002). Projections from the parahippocampal region to the prefrontal cortex in the rat: evidence of multiple pathways. *Eur. J. Neurosci.* 15, 1400–1407. doi: 10.1046/j.1460-9568.2002.01973.x
- Dias, I. A., Bahia, C. P., Franca, J. G., Houzel, J. C., Lent, R., Mayer, A. O., et al. (2014). Topography and architecture of visual and somatosensory areas of the agouti. *J. Comp. Neurol.* 522, 2576–2593. doi: 10.1002/cne.23550
- Felleman, D. J., and Van Essen, D. C. (1991). Distributed hierarchical processing in the primate cerebral cortex. *Cereb. Cortex* 1, 1–47. doi: 10.1093/cercor/1.1.1
- Fornito, A., and Bullmore, E. T. (2015). Reconciling abnormalities of brain network structure and function in schizophrenia. *Curr. Opin. Neurobiol.* 30, 44–50. doi: 10.1016/j.conb.2014.08.006
- Frysztak, R. J., and Neafsey, E. J. (1991). The effect of medial frontal cortex lesions on respiration, “freezing,” and ultrasonic vocalizations during conditioned emotional responses in rats. *Cereb. Cortex* 1, 418–425. doi: 10.1093/cercor/1.5.418
- Fujita, S., Koshikawa, N., and Kobayashi, M. (2011). GABA(B) receptors accentuate neural excitation contrast in rat insular cortex. *Neuroscience* 199, 259–271. doi: 10.1016/j.neuroscience.2011.09.043
- Fuster, J. M. (2001). The prefrontal cortex—an update: time is of the essence. *Neuron* 30, 319–333. doi: 10.1016/S0896-6273(01)00285-9
- Gabbott, P. L., Warner, T. A., Jays, P. R., Salway, P., and Busby, S. J. (2005). Prefrontal cortex in the rat: projections to subcortical autonomic, motor, and limbic centers. *J. Comp. Neurol.* 492, 145–177. doi: 10.1002/cne.20738
- Gallagher, M., McMahan, R. W., and Schoenbaum, G. (1999). Orbitofrontal cortex and representation of incentive value in associative learning. *J. Neurosci.* 19, 6610–6614.
- Groenewegen, H. J. (1988). Organization of the afferent connections of the mediodorsal thalamic nucleus in the rat, related to the mediodorsal-prefrontal topography. *Neuroscience* 24, 379–431. doi: 10.1016/0306-4522(88)90339-9
- Hafting, T., Fyhn, M., Molden, S., Moser, M. B., and Moser, E. I. (2005). Microstructure of a spatial map in the entorhinal cortex. *Nature* 436, 801–806. doi: 10.1038/nature03721

- Henry, E. C., and Catania, K. C. (2006). Cortical, callosal, and thalamic connections from primary somatosensory cortex in the naked mole-rat (*Heterocephalus glaber*), with special emphasis on the connectivity of the incisor representation. *Anat. Rec. A Discov. Mol. Cell. Evol. Biol.* 288, 626–645. doi: 10.1002/ar.a.20328
- Hoover, W. B., and Vertes, R. P. (2007). Anatomical analysis of afferent projections to the medial prefrontal cortex in the rat. *Brain Struct. Funct.* 212, 149–179. doi: 10.1007/s00429-007-0150-4
- Hoover, W. B., and Vertes, R. P. (2011). Projections of the medial orbital and ventral orbital cortex in the rat. *J. Comp. Neurol.* 519, 3766–3801. doi: 10.1002/cne.22733
- Ishikawa, A., and Nakamura, S. (2003). Convergence and interaction of hippocampal and amygdalar projections within the prefrontal cortex in the rat. *J. Neurosci.* 23, 9987–9995.
- Kealy, J., and Commins, S. (2011). The rat perirhinal cortex: a review of anatomy, physiology, plasticity, and function. *Prog. Neurobiol.* 93, 522–548. doi: 10.1016/j.pneurobio.2011.03.002
- Kim, J., Ghim, J. W., Lee, J. H., and Jung, M. W. (2013). Neural correlates of interval timing in rodent prefrontal cortex. *J. Neurosci.* 33, 13834–13847. doi: 10.1523/JNEUROSCI.1443-13.2013
- Kim, U., and Lee, T. (2012). Topography of descending projections from anterior insular and medial prefrontal regions to the lateral habenula of the epithalamus in the rat. *Eur. J. Neurosci.* 35, 1253–1269. doi: 10.1111/j.1460-9568.2012.08030.x
- Kleinhans, N. M., Richards, T., Sterling, L., Stegbauer, K. C., Mahurin, R., Johnson, L. C., et al. (2008). Abnormal functional connectivity in autism spectrum disorders during face processing. *Brain* 131(Pt 4), 1000–1012. doi: 10.1093/brain/awm334
- Kolb, B. (1984). Functions of the frontal cortex of the rat: a comparative review. *Brain Res.* 320, 65–98. doi: 10.1016/0165-0173(84)90018-3
- Kondo, H., and Witter, M. P. (2014). Topographic organization of orbitofrontal projections to the parahippocampal region in rats. *J. Comp. Neurol.* 522, 772–793. doi: 10.1002/cne.23442
- Krettek, J. E., and Price, J. L. (1977). The cortical projections of the mediodorsal nucleus and adjacent thalamic nuclei in the rat. *J. Comp. Neurol.* 171, 157–191. doi: 10.1002/cne.901710204
- Lee, T., Alloway, K. D., and Kim, U. (2011). Interconnected cortical networks between primary somatosensory cortex septal columns and posterior parietal cortex in rat. *J. Comp. Neurol.* 519, 405–419. doi: 10.1002/cne.22505
- Little, G. E., Lopez-Bendito, G., Runker, A. E., Garcia, N., Pinon, M. C., Chedotal, A., et al. (2009). Specificity and plasticity of thalamocortical connections in Sema6A mutant mice. *PLoS Biol.* 7:e98. doi: 10.1371/journal.pbio.1000098
- Marshel, J. H., Garrett, M. E., Nauhaus, I., and Callaway, E. M. (2011). Functional specialization of seven mouse visual cortical areas. *Neuron* 72, 1040–1054. doi: 10.1016/j.neuron.2011.12.004
- McFarland, N. R., and Haber, S. N. (2002). Thalamic relay nuclei of the basal ganglia form both reciprocal and nonreciprocal cortical connections, linking multiple frontal cortical areas. *J. Neurosci.* 22, 8117–8132.
- Miller, M. W., and Vogt, B. A. (1984). Direct connections of rat visual cortex with sensory, motor, and association cortices. *J. Comp. Neurol.* 226, 184–202. doi: 10.1002/cne.902260204
- Narayanan, N. S., and Laubach, M. (2006). Top-down control of motor cortex ensembles by dorsomedial prefrontal cortex. *Neuron* 52, 921–931. doi: 10.1016/j.neuron.2006.10.021
- Narayanan, N. S., and Laubach, M. (2008). Neuronal correlates of post-error slowing in the rat dorsomedial prefrontal cortex. *J. Neurophysiol.* 100, 520–525. doi: 10.1152/jn.00035.2008
- Narayanan, N. S., and Laubach, M. (2009). Delay activity in rodent frontal cortex during a simple reaction time task. *J. Neurophysiol.* 101, 2859–2871. doi: 10.1152/jn.90615.2008
- Neafsey, E. J. (1990). Prefrontal cortical control of the autonomic nervous system: anatomical and physiological observations. *Prog. Brain Res.* 85, 147–65, Discussion 165–166. doi: 10.1016/S0079-6123(08)62679-5
- Olavarría, J., and Montero, V. M. (1981). Reciprocal connections between the striate cortex and extrastriate cortical visual areas in the rat. *Brain Res.* 217, 358–363. doi: 10.1016/0006-8993(81)90011-1
- Olsen, C. R., and Musil, S. Y. (1992). Topographic organization of cortical and subcortical projections to posterior cingulate cortex in the cat: evidence for somatic, ocular, and complex subregions. *J. Comp. Neurol.* 324, 237–260.
- Paxinos, G., and Watson, C. (1998). *The Rat Brain in Stereotaxic Coordinates*. San Diego, CA: Academic Press.
- Pitkanen, A., Pikkarainen, M., Nurminen, N., and Ylinen, A. (2000). Reciprocal connections between the amygdala and the hippocampal formation, perirhinal cortex, and postrhinal cortex in rat. A review. *Ann. N.Y. Acad. Sci.* 911, 369–391. doi: 10.1111/j.1749-6632.2000.tb06738.x
- Porter, L. L., and White, E. L. (1983). Afferent and efferent pathways of the vibrissal region of primary motor cortex in the mouse. *J. Comp. Neurol.* 214, 279–289. doi: 10.1002/cne.902140306
- Schilman, E. A., Uylings, H. B., Galis-de Graaf, Y., Joel, D., and Groenewegen, H. J. (2008). The orbital cortex in rats topographically projects to central parts of the caudate-putamen complex. *Neurosci. Lett.* 432, 40–45. doi: 10.1016/j.neulet.2007.12.024
- Schoenbaum, G., and Esber, G. R. (2010). How do you (estimate you will) like them apples? Integration as a defining trait of orbitofrontal function. *Curr. Opin. Neurobiol.* 20, 205–211. doi: 10.1016/j.conb.2010.01.009
- Schoenbaum, G., and Roesch, M. (2005). Orbitofrontal cortex, associative learning, and expectancies. *Neuron* 47, 633–636. doi: 10.1016/j.neuron.2005.07.018
- Sesack, S. R., Deutch, A. Y., Roth, R. H., and Bunney, B. S. (1989). Topographical organization of the efferent projections of the medial prefrontal cortex in the rat: an anterograde tract-tracing study with *Phaseolus vulgaris* leucoagglutinin. *J. Comp. Neurol.* 290, 213–242. doi: 10.1002/cne.902900205
- Shi, C. J., and Cassell, M. D. (1999). Perirhinal cortex projections to the amygdaloid complex and hippocampal formation in the rat. *J. Comp. Neurol.* 406, 299–328.
- Smith, N. J., Horst, N. K., Liu, B., Caetano, M. S., and Laubach, M. (2010). Reversible inactivation of rat premotor cortex impairs temporal preparation, but not inhibitory control, during simple reaction-time performance. *Front. Integr. Neurosci.* 4:124. doi: 10.3389/fnint.2010.00124
- Thivierge, J. P., and Marcus, G. F. (2007). The topographic brain: from neural connectivity to cognition. *Trends Neurosci.* 30, 251–259. doi: 10.1016/j.tins.2007.04.004
- van de Werd, H. J., and Uylings, H. B. (2008). The rat orbital and agranular insular prefrontal cortical areas: a cytoarchitectonic and chemoarchitectonic study. *Brain Struct. Funct.* 212, 387–401. doi: 10.1007/s00429-007-0164-y
- Vaudano, E., Legg, C. R., and Glickstein, M. (1991). Afferent and efferent connections of temporal association cortex in the rat: a horseradish peroxidase study. *Eur. J. Neurosci.* 3, 317–330. doi: 10.1111/j.1460-9568.1991.tb00818.x
- Vertes, R. P. (2004). Differential projections of the infralimbic and prelimbic cortex in the rat. *Synapse* 51, 32–58. doi: 10.1002/syn.10279
- Vertes, R. P. (2006). Interactions among the medial prefrontal cortex, hippocampus and midline thalamus in emotional and cognitive processing in the rat. *Neuroscience* 142, 1–20. doi: 10.1016/j.neuroscience.2006.06.027
- Welker, C. (1971). Microelectrode delineation of fine grain somatotopic organization of (SmI) cerebral neocortex in albino rat. *Brain Res.* 26, 259–275. doi: 10.1016/s0006-8993(71)80004-5
- Woolsey, T. A. (1967). Somatosensory, auditory and visual cortical areas of the mouse. *Johns Hopkins Med. J.* 121, 91–112.

Conflict of Interest Statement: The authors declare that the research was conducted in the absence of any commercial or financial relationships that could be construed as a potential conflict of interest.

Copyright © 2015 Bedwell, Billett, Crofts, MacDonald and Tinsley. This is an open-access article distributed under the terms of the Creative Commons Attribution License (CC BY). The use, distribution or reproduction in other forums is permitted, provided the original author(s) or licensor are credited and that the original publication in this journal is cited, in accordance with accepted academic practice. No use, distribution or reproduction is permitted which does not comply with these terms.